The Series of Environmental Radioactivity Measuring Methods

AI-Ge
(No.7)

Gamma-ray Spectrometry using Germanium Semiconductor Detector

Amendment of June 2021
Radiation Monitoring Division
Radiation Protection Department
The Secretariat of
Nuclear Regulation Authority

NRA JAPAN
Nuclear Regulation Authority

Table of Contents

Chapter 1 Introduction

Gamma-ray (γ-ray) spectrometry using a germanium semiconductor detector has been widely used as the main method to analyze radioactivity in γ-ray-emitting nuclides in environmental samples because of its excellent energy resolution and ability for simultaneous quantitative analysis of multiple nuclides without chemical separation.

As a series of methods for radioactivity analysis related to γ-ray spectrometry, the following manuals have been published so far: "Radioiodine Analysis" (No. 4), "Sample Pretreatment for Instrumental Analysis using Germanium Detector, etc." (No. 13), "Radioiodine Analysis in Emergencies" (No. 15), "Sample Pretreatment for Gamma-ray Spectrometry in Emergencies" (No. 24), "Gamma-ray Spectral Analysis Using Germanium Detector in Emergencies" (No. 29), and "In situ Measurement Using Germanium Detector" (No. 33).

The manual "Gamma-ray Spectrometry using a Germanium Detector" was revised in 1992 as Radioactivity Measurement Method Series No. 7, which described the γ-ray analysis method mainly used in normal situations, i.e., not under nuclear emergency conditions. Since then, measurement instruments and their performances have been considerably improved and the analytical methods have progressed. To reflect such progress, the manual was revised for the fourth time in 2020.

The manual revised in 1992 contained many descriptions for developers of analysis software. In contrast, the new version in 2020 was published for those engaging in environmental radioactivity analysis. It consists the description of the basic, significant points for γ-ray spectrometry of environmental samples in normal situations such as radiation monitoring around nuclear facilities. In the text, the basic principles of γ-ray spectrometry, and in the explanation, detailed contents that complement the text are described. Other technical information, including nuclear data and spectral examples; as well as the detailed analytical methods that are described in the 1992-revised manual and still used today, are provided as reference materials.

The main points revised this time are as follows.

- The principles necessary for γ-ray spectrometry of environmental samples aiming for environmental radiation monitoring are described. However, the detailed methods for analysis (including the program codes) are not described.
- The energy region of the measurements is from 50 keV to 2000 keV. (This is because the energy of γ-rays emitted from nuclides in reactors is located in this region.)
- As a premise, spectrum analysis is conducted using a software package commercially supplied by a manufacturer.
- It is the responsibility of the software developer to select the analytical method adopted by the software and confirm its validity. Whereas, it is the responsibility of the users to confirm the validity of the results obtained by a series of analyses, including the operation of the software.
- Considering the present situation, where a method in which peak efficiency is obtained by numerical calculations[*1], such as Monte Carlo simulation, is used and new descriptions have been added.
- In evaluating the errors in the results obtained using γ-ray spectrometry, only counting errors have been conventionally used. However, considering the recent situation where the uncertainty

---

[*1]: A method where an event that a γ-ray enters a germanium semiconductor detector and gives its energy to the detector is reproduced by the numerical calculation using the theoretical formula for the interaction between γ-ray and atom, thereby, the peak efficiency is calculated. As for the Monte Carlo simulation, see Chapter 2.

of measurements[*2] has been widely introduced in many fields, a description of the evaluation of uncertainty of measurements has been newly added.

- As a method to calculate the value of the lower detection limit, the ISO 11929 method, which has recently become internationally used in the field of radiation measurements, has been introduced [1,2].
- A description about quality assurance of the analysis/measurement results has been added.

Currently, most of the procedures for γ-ray spectral measurements and analysis are conducted on the software supplied by the manufacturers of the measurement instruments. However, it should be noted that practical operating procedures concerning the preparation of instruments and analytical software are different depending on the instruments used. Therefore, as to the practical operation, it is necessary to refer to the software manuals and use them after understanding the functions in the instrument.

The nuclides to be measured, described in this manual, are those that are usually detected in normal situations. However, in the case of an emergency, such as an accident at a nuclear facility, various types of nuclides will be detected and the measured spectra will become complex. Therefore, in the case of an emergency, please also refer to the "Gamma-ray Spectral Analysis Using a Germanium Detector in Emergencies" (No. 29).

[*2]: A parameter characterizing the scattering of values that can be rationally linked to the quantity measured, which is accompanied by the measurement results.

Chapter 2 Terms and definitions

[Terms and definitions]

n-type semiconductor

When small quantity (approximately 1 ppm) of pentavalent elements is doped as an impurity into tetravalent elements such as Si and Ge, excess electrons enter the valence band, resulting in the formation of a semiconductor with high electrical conductivity. As doping pentavalent elements, such as P and As, are used, these elements are called “donors” (substances that donate electrons). Also, see “p-type semiconductor.”

energy

In general, the energy of particle beams, such as alpha rays (α-ray) and beta rays (β-ray), is expressed by their kinetic energy. In the case of photons, such as γ- and X-rays, the energy E is expressed in Equation 2.1:

$$E = h\nu = \frac{hc}{\lambda} \tag{2.1}$$

where ν is the frequency, λ is the wavelength, h is the Planck constant, and c is the speed of light. Although the unit of energy is J (joule) in the basic unit system, the energy of ionizing radiation is often expressed by eV (electron volt). One eV is defined as the kinetic energy of a particle having an elementary charge e that is accelerated by a potential difference of 1 V. The relation between joule and electron volt is 1 eV ≈ 1.602 × 10^{-19} J.

energy level

Steady state in which an ato mmolecule, or nucleus can exist, or the energy of this state.

energy resolution

An index of the ability to separate two adjacent spectral lines in the measurement of an energy spectrum using a radiation detector. In general, it is expressed by the half width of the peak (full width at half maximum, FWHM). The energy resolution of a germanium semiconductor detector, which is an index that represents the performance of the detector, is written in the performance specifications or inspection report by the manufacturer. The energy resolution is represented by the FWHM of a peak at 1332.5 keV, γ-rays from ^{60}Co. For the germanium semiconductor detectors used usually, the FWHM is in the range of 1.7–2.2 keV. In other cases, the energy resolution is sometimes expressed by the ratio of half width to energy, as follows:

$$\text{energy resolution (\%)} = \frac{\text{FWHM (keV) of a peak at 1332.5 keV}}{1332.5} \times 100 \tag{2.2}$$

end cap

A part of a cryostat in a germanium semiconductor detector. It is a cap made of aluminum covering the crystal part of the detector. In γ-ray general measurements, an incident window made of a thin aluminum film is used. For the measurements of low-energy photons, a thinner window made of beryllium (Be), etc. is used.

Auger effect

A phenomenon in which an atom in an excited state gives its energy to the orbital electrons, and transitions to a lower-energy state. As a result, an electron is emitted from its orbital.

Auger electron

An Auger electron is an electron emitted by the Auger effect. The energy of the emitted electron is equal to the value obtained by subtracting the binding energy of the emitted electron from the excitation energy (difference between the energy levels). Although the energy of Auger electrons is specific to the element, in the case of compounds, it is influenced by their chemical states. The emissions of Auger electrons and characteristic X-rays are competitive processes.

(radioactive) decay

A phenomenon where a nuclide changes to another nuclide by spontaneously emitting radiation or nuclear fission. There are α decays, β decays, etc. depending on the types of radiation. It is also called (radioactive) disintegration.

decay scheme

Figure 2.1 presents characteristics for radioactive decays of nuclides. The types, intensity, energy, etc. of radiation are shown corresponding to the energy levels of the daughter and granddaughter nuclides.

Gaussian distribution

Probability distribution where the probability density function is expressed in Equation 2.3. It is also called the normal distribution. The probability density function $W(n)$ is expressed in Equation 2.3:

$$W(n) = \frac{1}{\sigma\sqrt{2\pi}} \exp\left\{\frac{-(m-n)^2}{2\sigma^2}\right\} \tag{2.3}$$

where m is the mean value and σ is the standard deviation. Spectral peak shapes obtained in the germanium semiconductor detector agree well with the Gaussian distribution. Please also refer to “Poisson distribution.”

nuclide

Types of individual nuclei with different numbers of protons and neutrons. In general, a nuclide is uniquely determined by its atomic and mass numbers. However, nuclides sometimes include a metastable nucleus (nuclear isomer), which is in an excited state with a relatively long life (μs or more). For example, $^{137\,m}$Ba (half-life: 2.55 min) produced by the β decay of ^{137}Cs is a nuclear isomer of ^{137}Ba.

cascade γ-ray

A γ-ray that is emitted almost simultaneously with the emission of another γ-ray from the same nucleus. When a nucleus in the excited state continuously transitions to lower-energy states one by one, γ-rays with energies corresponding to the difference in the energy levels are emitted continuously. For example, the 1173.2 keV γ-ray emitted from ^{60}Co has a cascade relation with the 1332.5 keV γ-ray. Because the time interval of cascade γ-ray emissions is shorter than the time resolution of a germanium semiconductor detector (approximately μ sec.), each cascade γ-ray cannot be separated even if the cascade γ-rays interact in the detector.

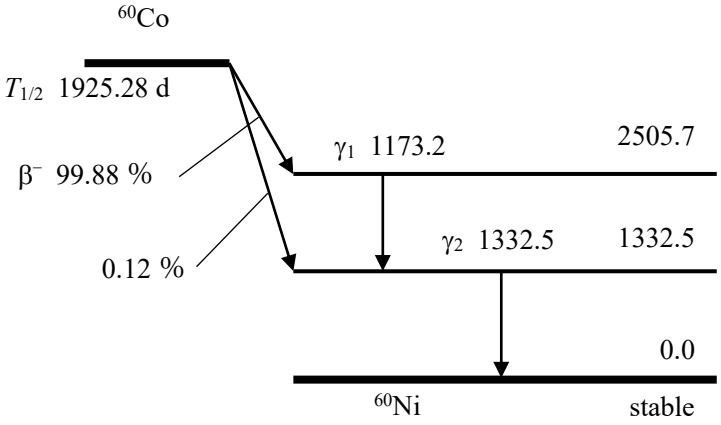

Fig. 2.1 Decay scheme of ^{60}Co

valence band

In a solid, the energy levels in which electrons are allowed to exist are concentrated in a limited energy range like a band (energy band) due to the periodic field of the lattice ions. For semiconductors and insulators, energy bands that are full of electrons in the constituent atoms are called filled bands. Among them, the band with the highest energy level is called the valence band. At a higher level than the valence band, there is a conduction band above the forbidden band.

function fitting method

One of the methods to obtain peak area (net count of the peak) in γ-ray spectral analysis, etc. Assuming a Gaussian function (peak) plus a linear baseline as functions, various parameters such as peak height, peak center, FWHM, and linear baseline are determined. Then, the peak area is obtained by integrating the function. The method is also called the fitting method.

γ-ray

Electromagnetic wave (photons) emitted from a nucleus when the nucleus in an excited state decays to a lower-energy excited level or the ground state. The energy of the γ-ray is almost equal to the energy difference between the two levels. (Strictly, the recoil energy of the nucleus should be subtracted. However, the recoil energy can be neglected because its magnitude is so small.)

γ-ray spectrometry

A technology to measure γ-ray spectra using a germanium semiconductor detector and a method to determine the radioactivity using spectral analysis. It is also called γ-ray spectroscopy.

γ -ray emission ratio

The ratio of γ-rays emitted per one disintegration (Bq), which is specific to the γ-ray. When the nuclide sequentially decays, it is necessary to pay attention to the standard of the decay. For example, the γ-ray emission ratio of 662 keV γ-rays from ^{137}Cs is 0.851 based on the decay of ^{137}Cs as the standard, but it is 0.899 based on that of ^{137m}Ba as the standard.

geometrical efficiency

Counting efficiency, which depends on the geometry (distance, etc.) between a radioactive source (or a sample) and the detector. In the case of a point source, assuming that the solid angle of the detector seen from the source is Ω, the geometrical efficiency is $\Omega/4\pi$. However, because a source and detector generally have some volume and area, it is difficult to determine

quantitatively the geometrical efficiency from a simple calculation.

forbidden band

An energy band between a conduction band and a valence band, where electrons cannot exist. It determines the electrical conductivity of the material. For insulators and pure inorganic crystals, the width of the forbidden band is so large (about 5 eV) that electrons are not excited into the conduction band only by heat at around room temperature (0.05 eV or less). On the other hand, the width of the forbidden band for a germanium semiconductor is 0.665 eV, so electrons are excited into the conduction band at room temperature. This is the reason that the germanium semiconductor detector is cooled to liquid-nitrogen temperature.

depletion layer

A region of a crystal in a semiconductor detector between the p^+ and n^+ electrodes, which is highly pure (sensitive to ionizing radiation) with few charge carriers (electrons and holes). When an ionizing radiation incident on a depletion layer and the energy is absorbed, signals are generated by producing electron–hole pairs, whose quantity is proportional to the energy of the radiation. A depletion layer is also called an intrinsic semiconductor region.

cryostat

A vacuum vessel used at low temperatures. For example, a germanium crystal in a germanium semiconductor detector is placed in a cryostat because the crystal is used at liquid-nitrogen temperature.

counting efficiency

A constant used to determine the radioactivity or intensity of radiation from measured values (counting rate). The counting efficiency ε is expressed in Equation 2.4:

$$\varepsilon = \frac{N}{A \cdot I_\gamma} \tag{2.4}$$

where A (Bq) is the radioactivity, I_γ is the emission rate of radiation to be measured, and N (s^{-1}) is the net counting rate. In this equation, the geometrical efficiency is included. However, when the efficiency of only a detector (detection efficiency) is considered, the equation sometimes does not contain the geometrical efficiency.

uncertainty due to counting statistics

Because the emission of radiation from a source and the detection of radiation are statistically complete random phenomena, the counting value (or counting rate) is influenced by the statistical variation. Since a statistical "fluctuation" of a counting value follows the Poisson's (or Gaussian) distribution, the error expected for a counting value n is expressed as $\sigma = \sqrt{n}$, where σ is the standard deviation. Generally, the measured value is expressed as $n \pm \sigma$. Instead, of "uncertainty due to counting statistics," the term "counting error" is conventionally used.

counting rate

This is the value obtained by dividing a counting value by the measurement time. It has a unit of s^{-1}. In a γ-ray spectrum, the value obtained when a peak area (net count of a peak) is divided by the measurement time (live time) is called the counting rate. The conventional units include cps (count per second) and cpm (count per minute).

detection limit

When a sample and the measurement condition (measurement instrument, measurement time, etc.) are determined, the smallest amount (value) of the analysis objects that can be detected is the detection limit.

detection efficiency

This has the almost the same meaning as "counting efficiency." Occasionally, it indicates the efficiency specific to the detector, without including the geometrical efficiency.

coherent scattering

An interaction between a photon and a substance. It is a phenomenon where an injected photon is scattered by changing only its direction without changing the energy (or wavelength). Even when coherent scattering occurs, no signals are generated in the detector. When the wavelength of a photon is longer than the target substance, it is called Rayleigh scattering. On the other hand, when the wavelength of a photon is shorter than the target substance, it is called Mie scattering.

Covell's method

A method for calculating the peak area (net count value of the peak) in γ-ray spectral analyses. It is also called the "counting value integration method." The count values in a peak are first integrated, then those in the flat region of the peak are subtracted. When there are other peaks with different energies in a peak, this method cannot be directly applied.

scattering

A phenomenon where radiation changes its direction because of the interaction with a substance. When the momentum and kinetic energy of all radiation involved do not change (without nuclear excitation), it is called elastic scattering, and when they change, it is called inelastic (nonelastic) scattering.

mass attenuation coefficient

The cross-sectional area for interaction per unit mass.

single escape peak

It is also called "single-photon escape peak." It is a peak produced by the following phenomenon. First, an incident γ-ray produces a pair of electrons in a detector. Then, one of the two electron pair annihilation photons ($m_0c^2 = 511$ keV) produced by positron annihilation induces the photoelectric effect. Simultaneously, the other photon goes out of the detector without interaction, resulting in the generation of a single escape peak. Assuming the energy of γ-ray is $h\nu$, the observed energy of the escape peak is $h\nu - m_0c^2$. For the peak shape, a single-photon escape peak has a width of about 1 keV due to the influence of the Doppler effect. Also, please refer to the "double escape peak."

spectrum

An energy or pulse height distribution of radiation. In general, the latter definition is used. For α- or β-rays, the spectrum has a similar shape as its energy distribution. In the case of γ-ray, the spectrum basically represents the energy distribution of fast secondary electrons produced by the γ-ray absorption in the effective volume of the detector. However, the actually observed γ-ray spectrum has a wider pulse height distribution due to various "fluctuations," such as statistical fluctuation and noise, produced in the conversion process from the energy of the secondary electrons to the output pulse height.

normal distribution function

A statistical function, also called the "Gaussian distribution function." Refer also "Gaussian distribution."

positive hole

A state where electrons do not exist (hole) in the valence band of a semiconductor, being also called "hole." It is produced by the presence of impurities or the effect of ionization by radiation. Inside a crystal to which an electric field is applied, an atom becomes a neutral atom when an electron moves from the adjacent atom to the hole, and a hole is produced in the adjacent atom that has emitted the electron. Since this process continuously occurs in the direction reverse to the electric field, the hole ostensibly moves in the crystal. In crystals, such as Ge and Si, positive holes contribute to the output signals as charge carriers (carriers) that have similar mobility as that of the free electrons.

total efficiency

In the spectral measurement of γ-rays of certain energy, total efficiency is the counting efficiency for the total count value of the spectrum (total count integrated from the zero to the maximum wave height), including peaks. The total efficiency T is expressed as follows:

$$T = \frac{\varepsilon}{P/T} \tag{2.5}$$

where ε is the peak efficiency, and P/T is the peak-to-total-efficiency ratio. The contribution of scattered radiation may be included. See also "peak total ratio."

relative efficiency

A performance index of germanium semiconductor detectors. It is defined as the ratio of the peak efficiency of a Ge detector to that of 3 inch diameter × 3 inch long NaI(Tl) scintillation detector for 1332.5 keV γ-rays from ^{60}Co. The relative efficiency ε_{rel} (%) is expressed as follows:

$$\varepsilon_{rel} = \frac{\varepsilon_{Ge}}{\varepsilon_{NaI}} \times 100 \tag{2.6}$$

where ε_{Ge} is the peak efficiency of the Ge detector, and ε_{NaI} is the peak efficiency of the NaI(Tl) detector. In the measurement, the distance between the ^{60}Co point source and the surface of the detector is set to 25 cm.

Because $\varepsilon_{NaI} = 1.20 \times 10^{-3}$ in this setup, the relative efficiency ε_{rel} (%) can also be obtained from Equation 2.7:

$$\varepsilon_{rel} = 8.33 \times 10^{4} \times \varepsilon_{Ge} \tag{2.7}$$

Currently, Ge detectors with a relative efficiency of 20%–40% are commonly used, but there are Ge detectors with relative efficiency higher than 100%.

double escape peak

A peak produced when a γ-ray generates electron pair in a detector, and the two electron pair annihilation photons ($m_0c^2 = 511$ keV) generated by the annihilation of the produced positron go out of the detector without interaction. It is also called a double-photon escape peak. Assuming the energy of the γ-ray is $h\nu$, the observed energy is $h\nu - 2m_0c^2$. See also "single escape peak."

dead time

The time used for signal processing for an incident γ-ray. During this time, the signal cannot be processed even when the next γ-ray is newly injected (signal processing is dead). The dead time t_D is expressed in Equation 2.8:

$$t_D = t_R - t_L \tag{2.8}$$

where t_R is the real time (or true time), and t_L is the live time.

internal conversion

A phenomenon where a nucleus in the excited state gives its energy to orbital electrons (orbital electrons in K-shell, etc.) and transitions to the lower-energy level. As a result, orbital electrons are emitted. Internal conversion and γ-ray emission are mutually competitive processes. Generally, internal conversion easily occurs in heavy nuclei and during a small difference in energy levels. When an internal conversion occurs, the characteristic X-rays (or Auger electrons) are emitted.

internal conversion electron

Electrons emitted by internal conversion. Its kinetic energy is the value obtained by subtracting the binding energy of orbital electrons from the difference in the energy levels involved. Therefore, the energy of internal conversion electrons exhibits a line spectrum, which is specific to the nuclide.

pulse pile-up

A phenomenon where two or more pulse signals overlap. The pulse height and waveform for piled-up signals are different depending on the respective pulse height and time difference. Assuming that n (s^{-1}) is the counting rate and τ (s) is the maximum pulse width (the time when the pulse height becomes zero), the number of the pile-up is $n^2\tau$ (s^{-1}). Pulse pile-up becomes a problem in spectral measurements at a high counting rate, which may cause a decrease in the peak counting rate, an increase in the FWHM, or a deterioration of the peak shape.

background

A count value or a spectrum in a measurement without a sample (or radiation source) or measurement of radioactivity-free samples. When a peak area is calculated from a γ-ray spectrum, the flat region included in a peak is sometimes called the background as well.

half-life

The time when radioactivity becomes half that at a reference time. A value of half-life is specific to the nuclide. Specifically, there are nuclides with half-lives of much shorter than one second, whereas nuclides with half-lives of billions of years or more exist. The radioactivity A at a time t is expressed in Equations 2.9:

$$A = A_0 e^{-\lambda t} \quad \text{or} \quad A = A_0 \left(\frac{1}{2}\right)^{t/T} \tag{2.9}$$

where T is the half-life, t is the elapsed time, and A_0 is the radioactivity at the reference time ($t = 0$). Here $\ln(2) \approx 0.693$, and the relationship between half-life and disintegration constant λ is expressed as $T = \ln(2)/\lambda$

full width at half maximum; FWHM

In α- and γ-rays spectra, it is the value that is defined as the width at the half height of the maximum peak height. Assuming that the shape of a peak shows the Gaussian distribution, the relation between the FWHM and standard deviation σ is expressed as $\mathrm{FWHM} = 2\sqrt{2\ln(2)}\,\sigma \fallingdotseq 2.355\sigma$ from Equation 2.3.

p-type semiconductor

When a small concentration (approximately 1 ppm) of trivalent elements is doped as impurities into tetravalent elements such as Si and Ge, holes are generated, resulting in the formation of a semiconductor with high electrical conductivity. As trivalent elements, such as B, Al, Ga, and In, are used, these elements are called acceptors (a substance that accepts electrons). Also, see "n-type semiconductor."

peak efficiency

In the measurements of α-ray and γ-ray spectra, the counting efficiency calculated from the net counting rate of a peak is called the peak efficiency. As a most basic definition, the peak efficiency ε is expressed in Equation 2.10:

$$\varepsilon = \frac{n}{I} \tag{2.10}$$

where n is the net counting rate, and I is the intensity of measured radiation emitted from the source. In γ-ray spectral analysis, it is the most important quantification factor. The peak efficiency depends on the energy of the radiation and the geometry of the sample. Further, it sometimes includes complex correction factors such as self-absorption and the summing effect.

efficiency transfer

A type of semi-experimental calculation method for peak efficiency. It is a method where a peak efficiency obtained at a specific geometry is converted to the peak efficiency obtained from the measurements using the same detector made of different materials and the measurements at a different geometry.

Peak-to-Compton ratio

One of the performance indices for a germanium semiconductor detector. In general, it is defined as the ratio of the peak height (count value) of 1332.5 keV γ-ray from ^{60}Co to the average count value from 1040 keV to 1096 keV in the continuous spectrum. The larger the relative efficiency of a germanium semiconductor detector is, and the better the energy resolution is, the larger the peak-to-Compton ratio is. In normal detectors, the value of the peak-to-Compton ratio is from 30 to 60.

Peak-to-total ratio

In the spectral measurement of a γ-ray of a certain energy, it is defined as the ratio of the peak efficiency to the total efficiency. The total efficiency is the counting efficiency that is calculated from the total count in the whole spectrum including peaks (count value integrated from zero wave height to the maximum wave height). In general, because the larger the germanium crystal is, the larger the probability of a multiple interaction is, the peak-to-total ratio becomes larger. See also "total efficiency."

peak area

Net integrated count value of a peak in the region of the peak. In a γ-ray spectrum, it does not include the count value in the region of the baseline.

peak region

Channel region that is set to calculate the peak area. Although it depends on the analytical methods (Covell's method, function fitting method, etc.), the width of the peak region is generally set to be about 3 × FWHM by referencing the FWHM.

standard source or standard sample

A radiation source (or a sample) whose radioactivity has been precisely determined. Primary standards are determined by the absolute measurement, etc. There are also secondary standards and so forth that are determined by comparing with the primary standard. Standard sources used in radioactivity measurements are called reference sources as well, and they are used for the determination of radioactivity using comparison measurements, or the determination of counting efficiency.

standard deviation

A quantity that indicates the scattering degree of a set of observations or statistical data. It is defined as the positive square root of the dispersion. In the normal distribution function (Gaussian distribution function), the standard deviation represents the spread of the distribution. Assuming that the standard deviation is σ, the integrated value in the $\pm\sigma$ range from the center is about 68.3% of the total integrated value. Further, the integrated values in the $\pm 2\sigma$ and $\pm 3\sigma$ ranges are about 95.0% and about 99.7%, respectively. If the count value follows Poisson's distribution, the relationship between the standard deviation, σ_N, and the count value, N, is expressed by $\sigma_N = \sqrt{N}$.

dead layer

A layer in a semiconductor detector where most of the energy lost by particles cannot contribute to the output signals. For a germanium semiconductor detector whose outer surface of the crystal is an n^+-type, the thickness of the dead layer is about 0.5–0.8 mm. This region does not contribute to the signals of the peak count value. Because low-energy photons of about 100 keV or less are attenuated by this dead layer, the lower the photon energy is, the lower the counting efficiency becomes.

resolution

The resolution of energy. See also "energy resolution."

Bq

A unit for radioactivity, which is defined by the International System of Units (SI). One Bq is defined as one disintegration per second. It is named after French physicist, Henri Becquerel, who won the Nobel Prize for Physics in 1903 for the discovery of radioactivity in uranium.

baseline

Continuous flat area next to the low or high energy sides of a peak in a γ-ray spectrum

Poisson's distribution

A type of a discrete probability distribution. Because a random phenomenon like the decay of a radioactive nuclide follows the Poisson distribution[*1], it is used for the statistical processing of the count value. Assuming that m is the mean count value, the probability $p(n)$ exhibiting the count value n is expressed in Equation 2.11:

$$p(n) = m^n \cdot e^{-m}/n! \tag{2.11}$$

From the relation, $\sigma^2 = \sum(m-n)^2 p(n) = m$

the standard deviation is expressed as, $\sigma = \sqrt{m}$

The value of n is expressed as $n \pm \sqrt{n}$ including the standard deviation σ. Although Poisson's distribution is applied to noncontinuous variables, it almost agrees with the Gaussian distribution function where the value of m is 20 or higher.

interruption peak

In a γ-ray spectrum, when a peak is analyzed by Covell's method (count value integration method) another peak in the analyzed region is called an interruption peak.

radioactive equilibrium

If a nuclide (descendant nuclide) produced by the disintegration of a radioactive nuclide (parent nuclide) is radioactive, and the half-life of the descendant nuclide is shorter than that of the parent nuclide, the radioactivity of the descendant nuclide increases with time. After about eight times the half-life has passed, the ratio of the radioactivity of the descendant nuclide to that of the parent nuclide becomes constant. If the half-life of the descendant nuclide is extremely shorter than that of the parent nuclide, secular equilibrium is realized, thereby, the radioactivity of the descendant and parent nuclides becomes the same. If that is not the case, the radioactivity of the descendant nuclide becomes larger than that of the parent nuclide, so transient equilibrium, where the radioactivity ratio is constant, is realized.

Monte Carlo simulation

A general term for method in which a numerical calculation or simulation is conducted using random numbers. The interaction between γ-rays and substances is the combination of various probabilistic events such as photoelectric effect and scattering. In a Monte Carlo simulation, each behavior of these constituent events is simulated using random numbers. The generation probability of the target event is calculated by repeating these processes enough times. Finally, the peak efficiency can be obtained by calculating the generation probability of the event in which a γ-ray generated from the sample enters the detector and the total energy is given to the detector.

live time

In the measurement using a multichannel pulse height analyzer, live time is a measurement time where the real time (true time) is corrected using the analyzing time (dead time) of the incident pulses. Because measurement time is corrected based on the analyzing time of each input pulse, the live time is shorter than the real time.

[*1]: Except for special cases in which the disintegration probability is close to unity.

random summing

A phenomenon where γ-rays from different nuclides (for example, ^{137}Cs + ^{134}Cs) or γ-rays emitted by different decay events in the same nuclide (for example, ^{137}Cs + ^{137}Cs) are incidentally detected almost simultaneously. This phenomenon generates a pulse pile-up. If the number of incidents γ-rays increases, the generation of pulse pile-up becomes serious, which decreases the count of each γ-ray peak. Peaks generated via this phenomenon strongly depend on the counting rate, so the number of peaks remarkably decreases with the decrease in the counting rate. Whereas, because the summing peaks originating from the cascade transitions do not depend much on the counting rate, they can be distinguished from the peaks originating from random summing by observing the dependence of the peaks on the counting rate. See also "pulse pile-up."

[Abbreviation]

ADC (Analog-to-digital converter)

A part of the multichannel pulse height analyzer; it is an apparatus for converting a wave height value of an input pulse (analog value in volt unit) into a channel number (digital value).

FWHM (Full width at half maximum)

Width at half height. See "half width."

FWTM (Full width at tenth maximum)

A width that is defined as the total width at 1/10 of the maximum peak height. In general, the value of the FWTM is approximately two times that of the FWHM. The symmetry of the peak is mainly determined from the size of the low-energy tail of the peak. The asymmetry of the peak is expressed in Equation 2.12:

$$\text{asymmetry of peak} = \frac{a-b}{b} \tag{2.12}$$

where a and b are the widths at the low- and high-energy sides, respectively, when the FWHM is divided at the peak center.

HV (High voltage)

High voltage that is applied to a detector or high voltage power supply.

MCA (Multichannel pulse height analyzer)

An instrument to analyze the multichannel pulse height.

PA (Preamplifier)

An electronic amplifier that converts a weak electrical signal into a stronger one.

ROI (Region of interest)

A region of interest (concern). In a multichannel pulse height analyzer, it is a channel region designated from a certain channel to another channel.

Chapter 3 Basic principles of Gamma-ray measurement

Gamma-ray (γ-ray) measurement using a germanium semiconductor detector is indirectly conducted by measuring high-energy electrons (secondary electrons) produced by the interaction between the incident γ-rays (photons) and detector. When a γ-ray enters a detector, various types of interactions occur, generating secondary electrons. Owing to the ionization effect of secondary electrons, electron–hole pairs are produced in the germanium crystal. The germanium crystal works as a detector by collecting these charges and converting them into electric signals.

Therefore, the interaction between photons and substances (detector or surrounding materials) is the fundamental of γ-ray spectroscopy. In particular, three types of interactions, which are described hereinafter, are important. An observed energy spectrum (hereinafter "spectrum") obtained using a detector is mainly produced by single or multiple interactions at the sensitive region of the detector. However, in addition to such γ-rays, a spectrum includes other radiations (scattered γ-rays and X-rays) produced by interactions with surrounding materials, such as radiation shields.

3.1 Types and characteristics of the interaction between γ-rays and substances

3.1.1 Photoelectric effect

When a γ-ray enters the sensitive region of a germanium semiconductor detector, it transfers its total energy (E_γ) to the orbital electrons (electrons in K- or L-shell with binding energy I) of a germanium atom. Consequently, fast electrons (photoelectrons) with a kinetic energy of ($E_\gamma - I$) are generated. This phenomenon is called the photoelectric effect.

When E_γ is larger than the binding energy (I_K) of orbital electrons in K-shell, approximately 80 % of the total interaction corresponds to the interaction with orbital electrons in K-shell, whereas approximately 20 % corresponds to the interaction with other orbital electrons.

Because the probability of the photoelectric effect (including all orbital electrons) is proportional to the −3.2th power of the energy of a γ-ray, the photoelectric effect is an interaction predominant in low-energy γ-rays.

When a γ-ray entering a detector causes the photoelectric effect, the entire γ-ray energy is absorbed in the detector; thus, a peak is observed in the spectrum, which is called the photoelectric peak. Spectral analysis is mainly conducted for photoelectric peaks because only photoelectric peaks (total energy absorption peaks) in a γ-ray spectrum have information on the γ-ray energy and radioactivity intensity of the radiation source.

— Relation with energy spectrum —

(1) The sum of the energies of all germanium characteristic X-rays or competitively generated Auger electrons, which are produced following the photoelectric effect, is equal to I. If the total energy is absorbed in the sensitive region of the detector, the sum of this total energy and the photoelectron energy is the energy of the incident γ-ray (E_γ). In most cases of the photoelectric effect, the total γ-ray energy is absorbed in the detector; thus, the generated output signals have accurate information on the energy of the γ-ray. The output signals exhibit single energy distribution, and it is observed as a photoelectric peak in the spectrum (peak PP in Fig. 3.1).

(2) For low γ-ray energy (-100 keV or lower), the probability of the photoelectric effect around the incident surface at the sensitive region of the detector is high. Therefore, the probability that the generated X-rays go out of the detector without being absorbed becomes high. Here, the output signal corresponding to ($E_\gamma - E_X$) obtained by subtracting the Ge X-ray energy (E_X)

(mainly K X-ray; 9.9 keV) from the γ-ray energy is generated. This phenomenon is observed as X-ray escape peaks in the spectrum.

(3) When the photoelectric effect occurs in a surrounding material with a high atomic number, such as a lead shield, characteristic X-rays (for lead, K X-ray: 72.85 keV and L X-ray: -10 keV) generated near the material surface enter the detector, and they are observed in the spectrum (peak marked "KX" in Fig. 3.1). To eliminate these peaks, the inner surface of the lead shield needs to be covered with a cadmium plate of 1 mm thickness and a copper plate of several mm thickness.

3.1.2 Compton scattering

There is a case wherein a part of the energy of an incident γ-ray is transferred to an electron (orbital or free electron), and the γ-ray is not extinguished but scattered with the remaining energy. At that time, the γ-ray gives a part of its energy to an electron in the sensitive region of the detector, generating a fast electron (sometimes called the Compton electron), and the γ-ray changes to the scattered γ-ray with a lower energy ($E_{\gamma}{}'$).

The energy ($E_e = E_{\gamma} - E_{\gamma}{}'$) of the generated fast electron is not constant because the energy differs at each interaction depending on the scattering angle of the γ-ray. Consequently, the energy exhibits a continuous distribution. For a scattering angle of 180°, the Compton electron has the maximum energy, corresponding to the high-energy edge of the continuous distribution called the Compton edge.

The probability of the Compton scattering in germanium is almost constant in the range of the γ-ray energy from dozens of keV to approximately 100 keV. At energies higher than this region, the probability becomes a gradual decreasing function. In an energy range lower than 150 keV, the probability of the photoelectric effect is high. However, at energies higher than 150 keV, the probability of the photoelectric effect significantly decreases with increasing energy. Thus, the probability of the Compton scattering becomes higher than that of the photoelectric effect. Therefore, the Compton scattering is the interaction predominant in γ-rays with energies in hundreds of keV or higher.

In this section, coherent scattering where the energy of a γ-ray does not change is not described because it does not generate any signal in a detector.

— Relation with energy spectrum —

(1) A continuous spectrum (a continuous part at energies lower than the Compton edge (marked "CE" in Fig. 3.1)) is not used for spectral analysis because it has scarcely any information on the γ-ray energy. However, if a scattered γ-ray consecutively causes the photoelectric effect in the sensitive region of the detector, the sum of the energy of the initially generated Compton electron and next generated photoelectron is equal to that of the incident γ-ray. Consequently, an output signal corresponding to the energy of the incident γ-ray is generated. In an actual germanium semiconductor detector, for γ-rays with energies in hundreds of keV or higher, such multiple interactions are the main process that generates a photoelectric peak (marked "PP" in Fig. 3.1). Therefore, the larger the volume of the sensitive region of a detector, the higher the probability of multiple interactions. Consequently, the photoelectric peak in the spectrum relatively increases compared to the Compton continuous region.

(2) When the Compton scattering in materials such as a lead shield is generated by γ-rays, the generated scattering γ-rays entering the detector are detected. The minimum energy of a scattering γ-ray corresponds to the energy at the scattering angle of 180° (peak marked "BS"

in Fig. 3.1). Moreover, the energy exhibits a continuous distribution that continues up to the energy of the incident γ-ray. Although the shape of this continuous distribution depends on the geometry among the γ-ray source, detector, and shield, the back scattering with a scattering angle of 90° or larger is predominant. Therefore, the proportion of the continuous spectrum by the back scattering, including multiple scattering (scattering of two times or more), can be decreased by increasing the inner volume of the shield of a detector.

3.1.3 Electron pair creation

When a γ-ray with an energy of $2m_0c^2$(corresponding to the static mass of the two electrons[*1] = 1.002 MeV) or higher, goes through the Coulomb field near a nucleus, the γ-ray is sometimes extinguished, producing an electron–positron pair. In this case, the nucleus and orbital electron energies do not change.

The sum of the kinetic energy of the generated electron and positron is equal to the value ($E_\gamma - 2m_0c^2$) that the energy corresponding to the static mass of the two electrons is subtracted from the γ-ray energy.

Because an electron pair production is an interaction that occurs for γ-rays with an energy of $2m_0c^2$ or higher, its probability increases with increasing γ-ray energy. However, its probability is only one-hundredth of the total interaction even at 1.5 MeV, implying that an electron pair production is an interaction predominant at further high energy[*2].

The fast positron generated by an electron pair production loses its kinetic energy in the detector. When the positron energy becomes comparable to the thermal energy (-0.1 eV), it is extinguished by combining with the surrounding electrons (electron pair annihilation), being converted to two-electron pair annihilation photons ($E = m_0c^2$).

— Relation with energy spectrum —

Depending on whether the photons generated by the electron pair annihilation in a detector continuously induce the photoelectric effect and Compton scattering, the output signals corresponding to the energy are generated in the spectrum, which are shown below.

(1) A phenomenon where two-electron pair annihilation photons go out of the detector without an interaction is called “double escape.” The following equation expresses the output signal of the double escape:
$E = E_\gamma - 2m_0c^2$ (peak marked “DE” in Fig. 3.1).

(2) A phenomenon where one of the two-electron pair annihilation photons induces the photoelectric effect, and the other photon goes out of the detector is called “single escape.” The following equation expresses the output signal of a single escape:
$E = E_\gamma - m_0c^2$ (peak marked “SE” in Fig. 3.1).

(3) A phenomenon where the two-electron pair annihilation photons induce the photoelectric effect in the detector is the total energy absorption. Here, the output signal is expressed by the following equation:

[*1]: A value where the mass m_0 of a static electron (kinetic energy is zero) is converted to the energy using the equation ($E = m_0c^2$, where c is the light velocity) based on the theory of relativity.

[*2]: Most artificial radioactive nuclides originating from nuclear facilities emit γ-rays with energies less than 1.5 MeV.

$E = E_\gamma$ (peak marked “PP” in Fig. 3.1).

(4) When the Compton scattering is induced by one or two-electron pair annihilation photons in the detector, the output signals exhibit a continuous distribution (a continuous spectral region at the energy lower than CE in Fig. 3.1).

Because the larger the volume of the sensitive region in a detector, the higher the probability mentioned in (3) and larger the peak (peak marked “PP” in Fig. 3.1) in the spectrum. Consequently, the escape peak (peaks marked “DE” and “SE” in Fig. 3.1) and continuous region decrease.

When electron pairs are generated by a γ-ray in the surrounding material, such as a lead shield, the electron pair annihilation photons produced enter the detector, generating peaks of 511 keV (peak marked “511” in Fig. 3.1). Because the kinetic energy of an electron–positron pair at the time of annihilation is nonzero, the energy of the produced electron pair annihilation photons increases or decreases in the range of 511 ± 1 keV influenced by the Doppler effect. Therefore, because a photoelectric or single escape peak originating from electron pair annihilation photons has a wider half width than that generated by the γ-rays of the same energy, it should be carefully considered in spectral analysis.

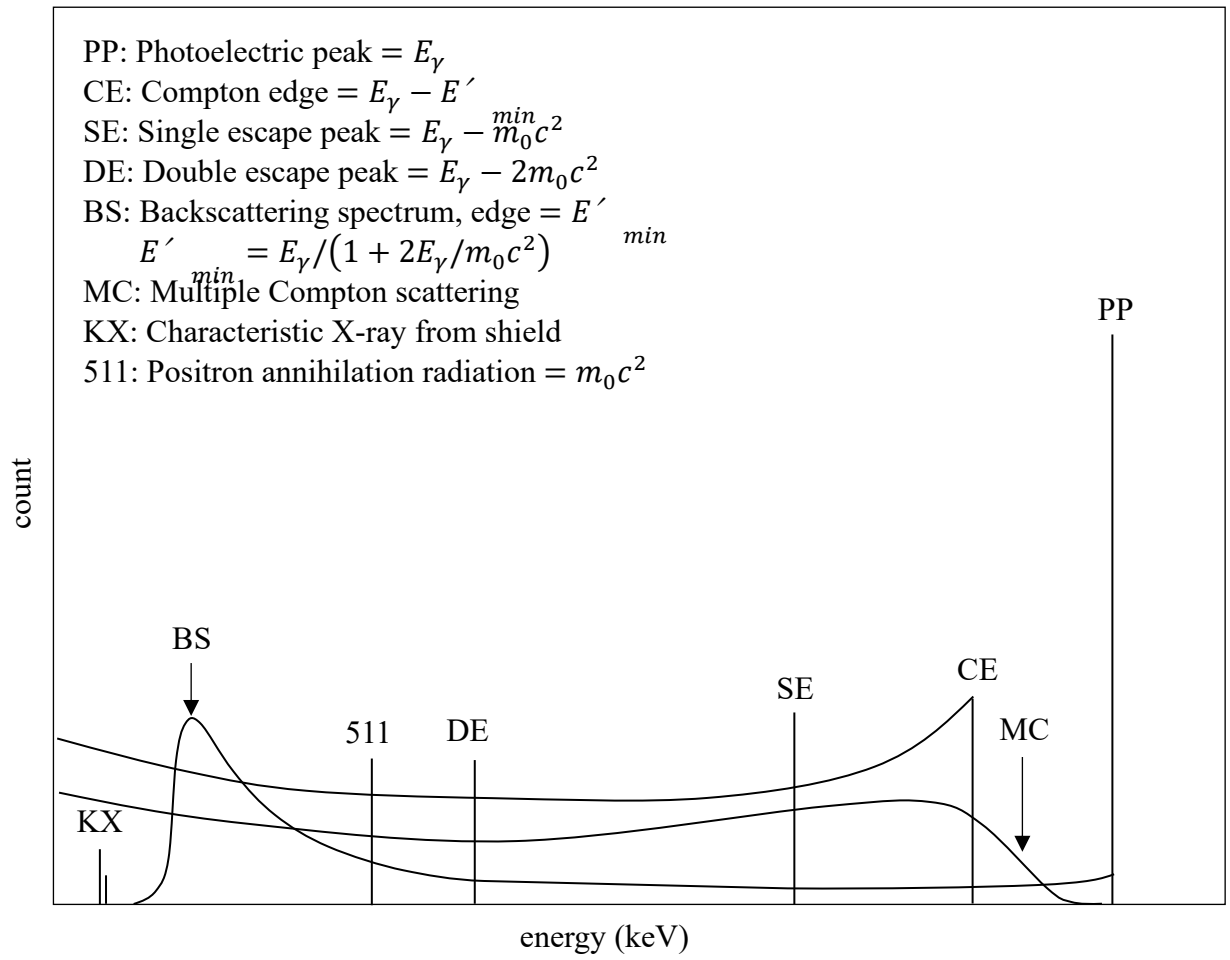

Fig. 3.1 Energy distribution generated in a germanium semiconductor detector by the interaction with γ-rays [3]

3.2 Peak analysis

When the γ-rays of a single energy enter a detector and cause interactions, the energy distribution shown in Fig. 3.1 is obtained. For measuring the γ-ray spectrum from a real sample, because multiple γ-rays with different energy coexist, the spectrum exhibits a complex shape, i.e., the superposition of the energy distributions generated by the interaction between these γ-rays and the detector. However, the peaks to be analyzed are only photoelectric peaks (the absorption peak of the total energy).

Photoelectric peaks are observed as a shape where the peaks are overlapped on the scattering lines or continuous components generated by the Compton scattering due to different energy γ-rays. The peak shape of a photoelectric peak is almost consistent with that of the Gaussian distribution. The reason is that the peak center channel depends on the energy of the detected γ-rays, and the peak area (net area from which the continuous component is subtracted) is proportional to the number of γ-rays that interact with the detector. Therefore, γ-ray emitting nuclides can be identified (qualitatively analyzed) and quantified using these peaks.

Therefore, conducting energy calibration to convert the peak center channel to the energy of the γ-ray is necessary. Furthermore, to convert the peak area to the number of γ-rays, calibrating the peak efficiency (the probability where the γ-rays from a sample entering the detector generate the net count of a photoelectric peak in the observed spectrum) is essential. For the calibration methods, refer to Chapter 5, “Calibration of the detector.”

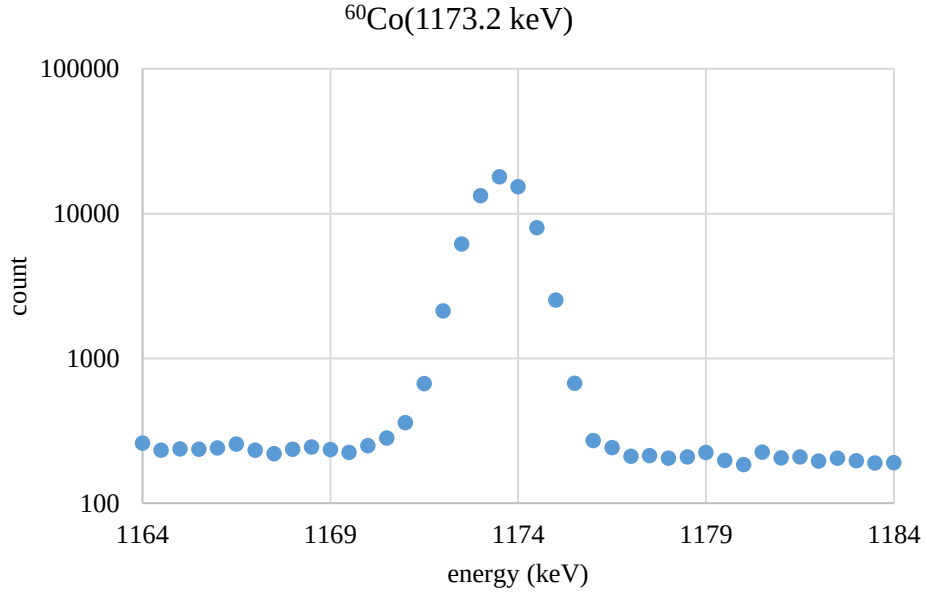

Fig. 3.2 Shape of the photoelectric peak in the γ-ray spectrum obtained using a germanium semiconductor detector

3.3 Various corrections (factors affecting spectral analysis)

3.3.1 Summing・coincidence effect

When nuclides that emit multiple γ-rays simultaneously at the disintegration time are measured, there is a case that multiple photons simultaneously entering the detector are detected. Moreover, the output of the sum of the two-photon signals is generated. This phenomenon is called the summing・coincidence effect or summing effect. If two photons enter a detector simultaneously, the following phenomena are expected to happen.

(1) When both photons lose the total energy in the sensitive region of the detector, the output signal (called the sum peak) corresponding to the sum of the energy of the two photons is generated.

(2) When one of the two photons or both photons cause the Compton scattering, the output signal corresponding to the continuous part in the spectrum is generated.

(3) For a thin incident window of a detector, the summing effect caused by high-energy β-rays or characteristic X-rays generated through EC decays or internal conversion may be generated.

The generation of such a summing effect decreases the counting rate of the total energy absorption peak to be measured. Thus, correcting this effect in the quantitative analysis of the spectrum is necessary. Determined using the mutual relation with the simultaneously emitted γ-rays, the summing effect depends on the decay scheme of the nuclide.

The probability of the summing effect depends on the product of the detection efficiencies for both radiations, implying that the higher the detection efficiency of measurement, the more prominent the summing effect becomes. Therefore, the correction becomes indispensable because the summing effect increases with the crystal size of the germanium semiconductor detector.

3.3.2 Self-absorption

The attenuation of a γ-ray before entering the sensitive region of a detector is one of the correction terms that are indispensable for the quantitative analysis of radioactivity. Absorption by sample supporting materials, such as a sample vessel, and self-absorption (absorption by the sample itself) are such examples. For instance, the latter correction term is indispensable in the measurements of bulk samples like environmental samples.

A γ-ray emitted by nuclear decay has energy specific to the nucleus. For a γ-ray entering a detector with such specific energy, the total energy absorption peak is observed only when the total energy is absorbed in the detector because of the interaction. In the γ-ray spectral analysis, only such peaks are analyzed. However, if a γ-ray loses a part of its energy by self-absorption, it does not generate the total energy absorption peak even if it enters the detector subsequently, thereby decreasing the peak area.

Self-absorption is a complex phenomenon that depends on the γ-ray energy, sample materials, sample shape, shape and size of the detector, and geometry between the detector and sample. Because self-absorption in a bulk sample is sometimes dozens of percentages or more, the correction is indispensable. To correct self-absorption, a method depending on the sample shape and materials is obtained by measuring the standard sources of various media. However, this method is not necessarily realistic because many standard sources with a high precision are required. To precisely correct the self-absorption of γ-rays in a bulk sample when a γ-ray travels in the sample, evaluating the interaction between a γ-ray emitted from a certain position of the sample and the material constituting the sample is necessary. For this purpose, the Monte Carlo simulation is essential, and software for γ-ray spectral analysis equipped with this function is necessary.

However, even when the simulation is not used, practical self-absorption correction is possible by supposing a model where the situation is simplified, although the application of this method is limited. An example of self-absorption correction for environmental samples is shown in document 1.6.

4.1 Construction of instruments

A γ-ray spectrometer using a germanium semiconductor detector comprises a detector (including a main body, preamplifier, and device to cool the detector), measurement instruments (power supplies, linear amplifier, and multichannel pulse-height analyzer), radiation shields, and analyzing equipment (PC and software for spectral analysis). Moreover, a measurement room where the entire instruments are set is essential.

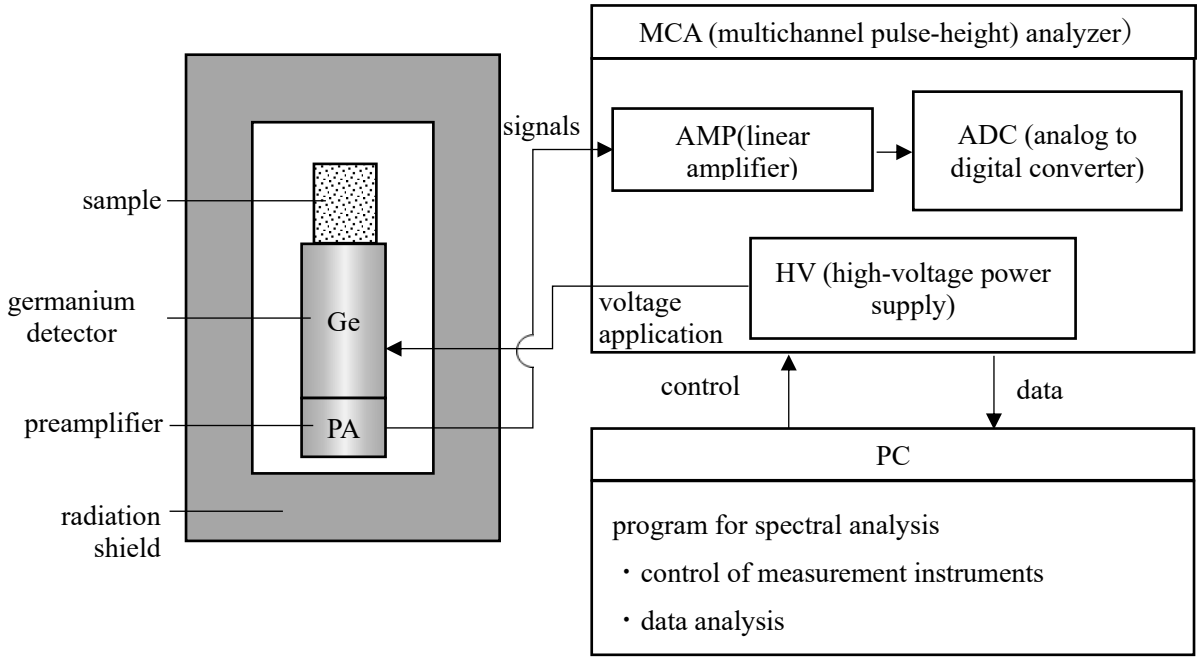

Fig. 4.1 Basic construction of a γ-ray spectrometer using a germanium semiconductor detector

4.1.1 Germanium semiconductor detector

When a γ-ray enters a germanium crystal and interacts with it, the energy of the γ-ray is transferred to the electrons in the crystal. Subsequently, these electrons interact with other electrons one after another, inducing ionization. The initial electron stops by consuming all its kinetic energy on ionization. Therefore, the number of generated electron–hole pairs is proportional to the energy of the γ-ray. If all electron–hole pairs can be collected, the energy analysis (spectrometry) of a γ-ray will become possible.

Therefore, a p-type cylindrical crystal, where the group III elements, such as Ga, are doped as impurities into a high-pure Ge[*1] is used to realize the energy analysis of a γ-ray. At the outer side of a germanium crystal into which γ-rays enter, an electrode (n^+ electrode of approximately 0.5–0.8 mm thickness, which is a dead layer against γ-rays) where Li is doped through thermal diffusion is made. At the cavity produced in the center of the electrode, a p^+ electrode is produced. Therefore, a depletion layer is produced in the crystal by applying the plus potential at the outer

[*1]: For the n-type, the p^+ electrode is produced by doping boron ions into the crystal. Therefore, the dead layer can be made thin (down to approximately 0.3-μm thickness). If a low atomic-number material such as beryllium is used as the incident window, measuring low-energy photons (down to approximately 3 keV) will become possible.

n^+ electrode and minus potential of approximately 3000 V as a reverse bias at the inner p^+ electrode, thereby generating a layer sensitive to γ-rays. The size of this γ-ray sensitive layer is approximately 30–150 mL. With this p-type germanium semiconductor detector, γ-rays in the range of 40–10 MeV can be measured.

To measure further lower-energy γ-rays, using an n-type germanium semiconductor detector is necessary[*2]. Note that for the measurements of the γ-rays of 50 keV or lower, using the efficiency curve is difficult; therefore, quantitative analysis should be conducted by comparing with the measurements of the reference sources of the same shape/materials containing the same nuclides as the sample. Furthermore, for the measurements of γ-rays of 50 keV or higher using the n-type germanium semiconductor detector, care should be taken because the summing effect sometimes occurs between a γ-ray and X-ray (Fig. 4.2). To avoid the summing effect when low-energy γ-rays are not measured, the low-energy X-rays should be shielded by placing a copper plate of approximately 0.5 mm thickness on the end cap to cover the incident window.

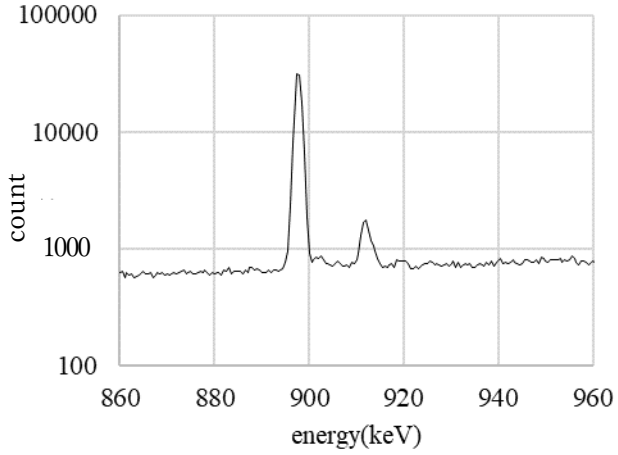

Fig. 4.2 Sum peak of ^{88}Y and X-rays in an n-type germanium semiconductor detector

Figure 4.3 shows the structure of a general coaxial-type germanium semiconductor detector.

[*2]: For the n-type, the p^+ electrode is produced by doping boron ions into the crystal. Therefore, the dead layer can be made thin (down to approximately 0.3-μm thickness). If a low atomic-number material such as beryllium is used as the incident window, measuring low-energy photons (down to approximately 3 keV) will become possible.

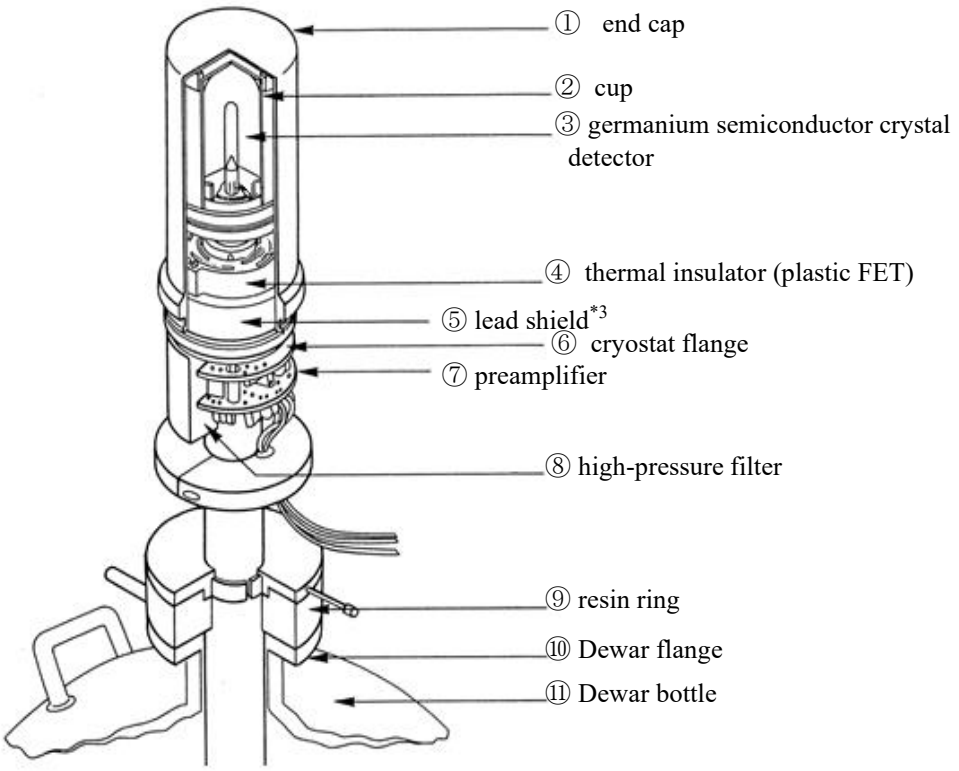

Fig. 4.3 Structure of a germanium semiconductor detector

*3: In a detector for low-background measurements, it is used to shield γ-rays entering from the lower side of the detector.

4.1.2 Cooling equipment

Because a germanium crystal cannot be used at room temperature due to its narrow-forbidden band (0.665 eV), it must be used at the liquid nitrogen temperature (77 K, −196°C). The following systems are used as methods for cooling a crystal (Fig. 4.4).

(1) Cooling using liquid nitrogen

This system uses a liquid nitrogen vessel (Dewar) of approximately 30 L. The consumption of liquid nitrogen is approximately 1–2 L or less per day. Liquid nitrogen must be supplied periodically.

(2) Electric cooling equipment

This system uses a refrigerant gas, such as helium. The refrigerant gas is not needed to be supplied because liquid nitrogen is not used. The resolution of the spectra is a little inferior to that of the liquid nitrogen cooling system due to the noise effect in operation. However, the noise effect on the resolution has been considerably reduced in recent equipment.

(3) Hybrid cooling system

This system combines the liquid nitrogen cooling system with a system in which evaporated nitrogen is collected and returned to the liquid nitrogen. In normal operation, there is scarcely any liquid nitrogen consumption; thus, the supply of liquid nitrogen is not needed for a long time. Furthermore, it has an advantage that the cooling using liquid nitrogen can be continued even if the equipment is out of order.

(1) Cooling using liquid trogen

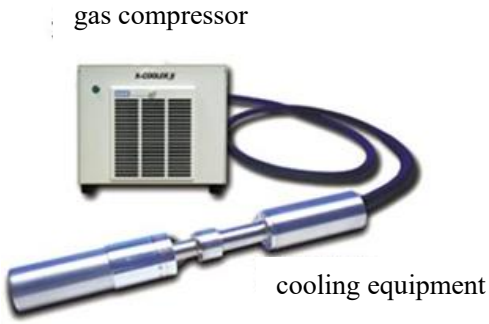

(2) Electric cooling

(3) Hybrid cooling

Fig. 4.4 Cooling systems for a germanium semiconductor detector

4.1.3 Pre-amplifier

This apparatus collects electric charges generated in a detector and converts them to appropriate electric signals (voltage pulses proportional to the amount of charge), then transports the signals to the next linear amplifier. It works as an interface between a detector and an amplifier. Electrically, it works to prevent pulse attenuation, reflection, and noise intrusion.

4.1.4 Linear amplifier (main amplifier)

This apparatus amplifies output pulses from a preamplifier and shapes them to fit the next pulse-height analyzer. The height of the output pulses (pulse height) is proportional to the amount of electric charge generated in the detector.

4.1.5 Multichannel pulse-height analyzer (MCA)

MCA is an instrument where the energy distribution, given to the detector by the interaction between the γ-ray and germanium semiconductor detector, can be obtained by classifying and counting output pulses from a linear amplifier using the wave height (pulse-height analysis). The pulse-height analysis is conducted according to the following process. First, the wave height (analog voltage) of the output pulses from the linear amplifier is converted to a digital value (channel) using an analog to digital converter (ADC). Subsequently, the count values are added to the spectral memory corresponding to the converted channel. A histogram (pulse-height distribution) of the count values at each channel (corresponding to the γ-ray energy) is obtained by conducting this process for many output pulses and integrating the results. This histogram is called the γ-ray spectrum.

Moreover, for the number of channels for memories that accumulate the count values in γ-ray spectral measurements, approximately 4000–8000 channels are widely used. In environmental radiation monitoring, 4000 channels are used.

Recently, the digital signal processing technology using a digital signal processor (DSP) has been widely used. There are also instruments where the pulse-height distribution is obtained using MCA by directly converting output signals from a preamplifier to digital signals. Owing to the digitalization of signals, various performances, such as processing ability at a high counting rate, energy resolution, and stability against temperature changes, have been improved.

4.1.6 Radiation shield

To reduce the radiation from the outside (background), a germanium semiconductor detector for measuring environmental samples must be shielded using a lead of 10–15 cm thickness in the 4π direction (Fig. 4.5).

(1) Materials

Lead is mainly used as a shielding material, but sometimes iron can be used. Moreover, copper or cadmium is sometimes added as a lining material. Therefore, the inside should be lined with thin acrylic plates (approximately 2 mm thickness) to ease the decontamination.

lead : The transmittance of γ-rays from ^{60}Co is 6–7 % for 5 cm thickness. It is worth noting that lead may contain natural radioactive nuclides, such as ^{208}Tl, ^{210}Pb, ^{214}Bi, and ^{228}Ac. If lead contains a large amount of ^{210}Pb, the background becomes high owing to the bremsstrahlung by β-rays from ^{210}Bi, i.e., the descendent nuclide. In such cases, old lead materials should be used without ^{210}Pb (^{210}Bi) or used after inspecting the production lots [4] [5]. Further, when lead is exposed to the inner surface, characteristic KX-rays (approximately 75 keV) from lead are observed. However, the increase in the background because of the backscattering of X-rays from lead is smaller than that from iron.

iron : The transmittance of γ-rays from ^{60}Co is approximately 30 % for 5 cm thickness. When iron is used as a radiation shield, γ-rays (approximately 847 keV) from the excited states of ^{56}Fe may be detected due to the interaction between neutrons derived from cosmic rays and iron. Furthermore, among irons produced in some periods after the Second World War, there is a case that a small amount of ^{60}Co was mixed with iron during the manufacturing process. Therefore, it should be confirmed in advance whether ^{60}Co is mixed.

copper : Copper is sometimes used as an inner lining to reduce lead KX-rays and low-energy γ-rays emitted from uranium- and thorium-series nuclides. However, γ-rays (671 keV) from the excited states of ^{63}Cu produced by the interaction with neutrons derived from cosmic rays are sometimes detected.

cadmium : Although cadmium effectively eliminates lead KX-rays used for an inner lining, cadmium KX-rays (approximately 23 keV) are also emitted. Furthermore, caution should be applied because γ-rays by ^{113}Cd(n,γ) where cadmium reacts with neutrons derived from cosmic rays are sometimes detected.

(2) Inner volume

To reduce the effect of backscattered γ-rays and make a sample in and out easier, an inner volume should be as large as possible. Generally, an inner volume is approximately 20 cm × 20 cm × 20 cm–30 cm × 25 cm × 50 cm[*4].

The inner volume of 30 cm × 25 cm × 50 cm or more is needed to measure samples using a 2 L Marinelli-type vessel.

(3) Weight

The weight of the radiation shield is 1.5–3 tons.

(4) Radioactive materials contained in the shield

In the background measurement for 48 h, any peaks of artificial radioactive nuclides must not be observed.

Table 4.1 presents the counting rates of natural radioactive nuclides in uranium and thorium series for a radiation shield that stops the radiation from the 4π direction using a lead of 15 cm thickness, when measured with a detector of 25 %–30 % relative efficiency.

[*4]: It is convenient to have a space of approximately 27 cm or more on the detector end cap so that the point source can be measured at a distance of 25 cm when measuring the resolution.

Table 4.1 Radioactive nuclides contained in a radiation shield

Nuclide	^{40}K	^{228}Ac	^{214}Bi	^{208}Tl	Continuous region
Energy (keV)	1460.8	911.2	609.3	583.2	120
Counting rate	30–90	50–120	200–500	180–400	150–500

(Note) The unit of the continuous region is (counts/day)/keV, whereas that of the nuclides is (counts/day)/peak. If the counting rate of the continuous region is high, the metal material may contain ^{210}Pb.

(5) Weight scale

This is a piece of equipment to constantly monitor the weight change of a cryostat filled with liquid nitrogen. A weight scale is helpful to judge the liquid nitrogen filling time and the detector's deterioration by heat insulation caused by the decrease in the vacuum pressure of the cryostat. Consequently, it should be installed, and the measured values should be recorded periodically.

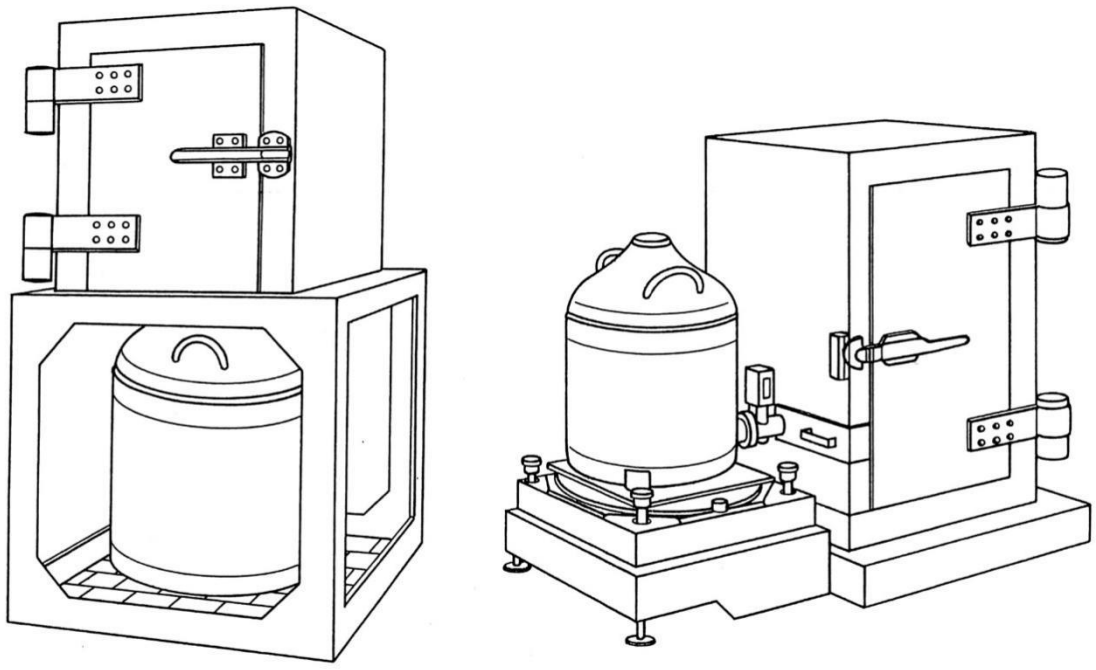

(1) Vertical-type shield for detector (2) L-shaped shield for detector

Fig. 4.5 Examples of radiation shields

4.1.7 Measurement room

The ideal conditions of a measurement room where a germanium semiconductor detector is installed are as follows.

(1) Measurement environment

- Air conditioning should be appropriate so that measurement instruments are stably operated.
- Measurement instruments should not be exposed to wind from an air conditioner or direct sunlight.
- It is desirable to maintain the room temperature at approximately 23°C–25°C, variation in room temperature within ±2°C, and humidity in the range of 50 %–60 %[*5].
- High-level standard sources, for example, should not be stored near the measurement equipment.
- The location of the measurement room should not be near, for example, a γ-ray irradiation facility.

(2) Countermeasures for radioactivity contamination

- Air conditioning systems should be separated from the analysis room where radioisotopes(RI's) are used.
- If the impact on the facility is expected at the time of a nuclear facility accident, it is desirable to block the intake of outside air.
- Cleaning of the measurement room should be easy (the types of floor materials, equipment layout, etc,. should be considered).

(3) Important points in management

- The preparation of samples to be measured should be conducted in a separate room.
- When there is a risk of radioactivity contamination, contamination must not be brought into the measurement room. Consequently, it is desirable to let people change slippers when entering and leaving the room.
- It is desirable to install an adhesive mat at the entrance because it is effective in maintaining cleanliness inside the room.
- It is desirable to periodically collect and measure dust in the measurement room using, for example, a paper carton vacuum cleaner and check the situation of contamination in the room.

(4) Countermeasures to reduce background

- The concentration of radon in the radiation shield should be maintained to be low[*6] (in a normal environment, radon concentration is approximately several Bq/m^3 or lower).
- If a measurement room is in the basement, for example, the high-concentration radon sometimes influences the background count. In this case, sufficient ventilation should be provided to reduce the radon concentration in the air[*7].

[*5]: Changes in the environment of the measurement room may induce peak drifts.

[*6]: In a liquid nitrogen cooling system, radon can be expelled by introducing a nitrogen escape port into the shield. It is also effective to place plastic bags filled with nitrogen gas inside the shield and physically remove the air inside the shield.

[*7]: It is effective to prevent air inflow by filling the gaps in the pipes and use an independent air conditioner working only in the measurement room when radon and thoron flow into the measurement room from the outside environment.

(5) Facility and structure

・The floor should have an allowable load that exceeds the weight of the shield (1.5 to 3 tons).
・The structure should prepare countermeasures for earthquakes. For instance, the instruments should be fixed on the floor, and countermeasures should be taken to prevent damages caused by collisions with other instruments due to vibration in case of earthquakes.
・There should be no noise in power supplies. When the facility is in an industrial area, noise can be reduced using noise filters that fit the location based on the investigation of the frequency component characteristics.
・For a countermeasure against power outages, it is desirable to install an emergency power supply or uninterruptible power supply (UPS).
・It is desirable to prepare power supplies for appliances such as vacuum cleaners separately.
・When liquid nitrogen is used to cool the detector, oxygen meters should be installed.

Chapter 5 Calibration of the detector

By analyzing spectra measured using a germanium semiconductor detector, information on the species and amount of γ-ray emitting nuclides in a sample can be obtained. The analysis of a γ-ray spectrum is conducted for photoelectric peaks (absorption peaks for total energy). To obtain correct analytical results, calibration corresponding to the detector and measurement conditions is required.

In this chapter, only the calibration on software necessary to analyze the measured spectra is described. As to the calibration in hardware, the gain adjustment, for example, is required (see Section 7.1.3) in advance.

The calibration described below is generally performed using special analytical software that has necessary functions. When using the software, the validity of the results obtained using the software should be confirmable (for the validity confirmation, see Chapter 9).

In the following parts, general procedures needed for the analysis using the software are described.

5.1 Energy calibration

Energy calibration aims to obtain a relation between a peak center (channel) in a spectrum and the γ-ray energy corresponding to the peak center. Using this procedure, the γ-ray energy corresponding to the peak center can be obtained and the species of nuclides can be identified. In the energy calibration, the use of spectra measured for multiple γ-ray sources is required so that the entire energy region to be measured is covered. Specifically, the relation between the peak center P and energy of a γ-ray is obtained from the least square method. As an equation to be used, a linear or quadratic equation shown below is enough; thus, a higher-order polynomial is not required.

$$E(\mathrm{keV}) = a \cdot P^2 + b \cdot P + c \ \ (\text{quatrutic equation}) \tag{5.1}$$

5.2 Calibration of half width

When obtaining a relational expression between energy and a channel, the calibration equation between the half width of the peak and energy should also be obtained in advance. Empirically, it is known that the relation between the half width of a peak W (keV) and energy E (keV) is expressed by the following equation that includes the square root of the energy.

$$W = a \cdot E^{1/2} + b \cdot E + c \tag{5.2}$$

The obtained relation between the peak half width and γ-ray energy is used as information to set the peak region in calculating the peak area.

5.3 Calibration of peak efficiency

The purpose of γ-ray spectrometry is to obtain radioactivity (Bq) in a sample. The number of γ-rays emitted from the sample is required, based on the area of the total energy absorption peak in the spectrum, to obtain radioactivity. For this purpose, a peak efficiency ε expressed by the following equation is used:

$$\varepsilon = \frac{N}{A \cdot I_\gamma} \tag{5.3}$$

Where N denotes the counting rate (cps) of the peak, A the radioactivity (Bq), and I_γ the emission rate of the γ-rays to be measured.

A peak efficiency is influenced by the following factors:

- the energy of the γ-ray,
- shape and inner structure of the detector,
- geometry of the measurement sample against the detector,
- shape and material of the sample measurement vessel, and
- shape and material of the measurement sample.

To obtain radioactivity from the γ-ray spectrum of a measurement sample, the peak efficiency value at a certain measurement condition is indispensable. Generally, standard sources are used for the determination of peak efficiency. However, because the peak efficiency changes depending on the conditions such as the energy of γ-rays and shape/material/density of the measurement sample, the applicable scope of the method using standard sources is limited. The peak efficiency is obtained using the following methods.

5.3.1 Measurement of peak efficiency

(1) Actual measurement of standard sources

It would be ideal to obtain the peak efficiency using a standard source containing the same types of nuclides as those in the measurement sample and having the same shape as those of the sample. If multiple types of nuclides are measured, a standard source covering the energy range of the γ-rays from all nuclides is needed. As to the important points in the measurement, refer to Document 1.2, “Examples of obtaining peak efficiency for bulk sources.”

To secure the traceability of measurements, using national standard sources or standard sources that can be traceable to the international standard sources as a standard source for calibration is required. (As to the national standard of Japan, the calibration certificate with additive amounts and the uncertainty of nuclides, issued by an accredited calibration laboratory based on the Japan Calibration Service System formulated by the Measurement Act, should be attached to the source.) (reference Chapter 9).

(2) Calculation of peak efficiency using a simulation or other numerical models

When a γ-ray emitted from a measurement sample enters a detector, the probability that the total energy absorption peak appears can be calculated using the Monte Carlo simulation or other numerical calculation models. In using such numerical models, detailed information about the inner structure of each detector (the shape/size of the crystal, thickness of the dead layer, shape of the other structures, etc.) is required. However, the calculated results are sometimes far from the real values due to slight parameter differences because the calculation process is considerably sensitive to these parameters. Consequently, obtaining the peak efficiency only from the calculation results using numerical models is virtually impossible. Therefore, the results must be verified by measuring at least one standard source that emits γ-rays whose energy covers that of the γ-rays from the samples to be measured. If a difference is observed between the peak efficiencies obtained from the measurement of a standard source and that calculated using a numerical model, the parameters used in the numerical model should be revised as needed while verifying the cause.

5.3.2 Conversion of peak efficiency

The peak efficiency obtained by measuring a standard source can be applied only to the case where a sample of the same shape and materials as the source is measured with the same geometry as that of the source. In the γ-ray spectrometry of environmental samples, bulk samples are often measured. Preparing standard sources corresponding to all assumed shapes and materials for such measurements is unrealistic. Therefore, a method is practically used, where the peak efficiency obtained from the measurements of a standard source under possible limited conditions (shape, material, and γ-ray energy) is converted to that obtained under other conditions. In this case, by obtaining the conversion coefficients from the standard peak efficiency, the quantitative analysis of radioactive nuclides becomes possible even for the samples of different shapes, materials, and nuclides from those of the standard source. The methods shown below are used to convert the peak efficiency.

(1) Energy interpolation of peak efficiency

Using a standard source containing multiple nuclides emitting γ-rays whose energies cover that of the measurement sample (approximately 50–2000 keV)[*1], the obtained peak efficiency is functionalized against the γ-ray energy (the relation between the obtained peak efficiency and γ-ray energy is called the peak efficiency curve). Moreover, using the peak efficiency curve, the peak efficiency for arbitrary γ-ray energy other than that of the standard source can be obtained at least when measured with the same geometry.

(2) Peak efficiency interpolation of bulk sources

The multiple peak efficiency curves obtained are functionalized against filling heights by measuring a standard source containing multiple γ-ray emitting nuclides whose filling heights are set to be different using the cylindrical vessels of the same shape. Thus, the peak efficiency against the arbitrary filling height and γ-ray energy can be obtained using interpolation. For the details, refer to Document 1.2, “Examples of obtaining peak efficiency for bulk source.”

(3) Peak efficiency conversion (efficiency transfer)

This method converts the peak efficiency measured with a certain geometry to that of a sample comprising different materials and measured with different geometry using the same detector. (Because the basic concepts of the methods described in Methods (1) and (2) above are the same as those of the present method, Methods (1) and (2) are included in the present method in a broader sense.) This method uses the numerical model considering the solid angle between the source and detector and the Monte Carlo simulation for the peak efficiency conversion. For the calculation using a numerical model, there is a disadvantage that in the calculation process, the results are strongly affected by the germanium crystal’s shape and inner structure, such as the thickness of the dead layer. However, in the present method, most of the parameters depending on the detector are canceled using the ratio based on the calculation involving the inter structure parameters of the same detector for the standard source and sample. Therefore, the present method has the advantage of having small impact on the calculation results compared with the method described in Section 5.3.1. (2), and the calculation time is short.

For example, by applying the present method, it will be possible to obtain the peak efficiency against a cylindrical sample of arbitrary materials with different diameters and heights. Furthermore, it will be possible to simultaneously evaluate the self-absorption correction

---

[*1]: Realistically, covering the energy range completely is difficult. Specifically, both ends of the energy range are ^{241}Am (59.5keV) and ^{88}Y (1836.1keV). For the energy out of this range, extrapolation is applied in most cases.

considering the sample materials and summing effect. The present method effectively converts the peak efficiency between similar geometries (e.g., a cylindrical vessel→another cylindrical vessel, i.e., the sample position against the detector is similar). However, note that the method is not applicable to the conversion between considerably different geometries (e.g., cylindrical vessel→ Marinelli-type vessel, i.e., the sample position against the detector is different.). Therefore, the applicable scope of the method is limited.

The basic principles of the present method and examples of its application to samples in cylindrical vessels are described in Commentary A, “Peak efficiency conversion (Efficiency transfer).”

In calculating radioactivity values using the conversion coefficients obtained by one of the above methods, the confirmation of the validity of the conversion coefficients in advance is required. For details, refer to Chapter 9, “Quality assurance of analytical results.”

Chapter 6 Nuclear data

Nuclear data (the half-lives of nuclides and energy and emission rate of γ-rays) used for γ-ray spectrometry using a germanium semiconductor detector can be obtained from nuclear data compilations, such as databases and literatures. Recently, some of the nuclear data compilations are published on the Internet. The following is the list of some websites that could be confirmed in 2020.

－Evaluated Nuclear Structure Data File (ENSDF)
https://www.nndc.bnl.gov/ensdf/
－Decay Data Evaluation Project (DDEP)
http://www.lnhb.fr/nuclear-data/
－Evaluated Nuclear Data File (ENDF)
https://www-nds.iaea.org/exfor/endf.htm
－Joint Evaluated Fission and Fusion (JEFF) Library
http://www.oecd-nea.org/dbdata/

In this manual, by referencing the “Radiation Monitoring in Normal Time” (Supplementary Reference Material of the Nuclear Emergency Preparedness Guidance) and the former manual revised in 1992, artificial radioactive nuclides possibly detected in the environment using nuclear accidents and tests and artificial and natural radioactive nuclides are shown in Document 5.

Note that values in nuclear data are different depending on the nuclear data compilation, and values sometimes change by the renewal of the data even in the same nuclear data compilation. This is because the methods for evaluating nuclear data and the data referenced by the nuclear data compilation are different. Consequently, because the calculated results change depending on the nuclear data, the clarification of the types of nuclear data used is required.

In γ-ray spectrometry, the following calculations are performed in the analysis.

(a) Using nuclear data, the intensity of γ-rays (γ/s) is obtained from the certified value (Bq) of the standard source, and the peak efficiency is obtained from the peak counting rate (cps).

(b) Using the peak efficiency, the intensity of γ-rays (γ/s) is obtained from the peak counting rate (cps) of the sample measurement results, and the radioactivity (Bq) is obtained using nuclear data.

The nuclear data are used for converting radioactivity to the intensity of γ-rays (or vice versa). Therefore, the nuclear data used in (a) and (b) above should be cited from the same nuclear data compilation. If the data are cited from the same nuclear data compilation, there is no need to be particular about the latest data because there is no difference in the conversion. From these perspectives, in the renewal of the nuclear data for analysis, caution is required because the re-calculation of the peak efficiency is necessary.

Chapter 7 Measurement and analysis procedure

In this chapter, a series of procedures will be described from the pretreatments of measuring samples to the reporting results, including important points to obtain accurate results in measurements and analysis using a germanium semiconductor detector.

As for the methods of the preparation of measuring samples, please refer to “Sample Pretreatment for Instrumental Analysis using Germanium Detector, etc.” (No.13). For the measurements and analysis in emergency, please also refer to “Gamma-ray Spectral Analysis Using Germanium Detector in Emergencies” (No.29).

7.1 Preparation of measurement instruments

Because the operating procedure of a measurement instrument varies depending on the model, consult the instrument's operation manual for the specific procedure. The following sections describe the critical points required for general γ-ray measuring equipment.

7.1.1 Cooling of detector

- A germanium semiconductor detector needs to be cooled to the liquid-nitrogen temperature during operation.
- Do not apply a high voltage to the detector while it is not cooled, because a large leakage current flows, and the preamplifier may be damaged.
- When allowing an uncooled detector to be the measurable condition, fill it with liquid nitrogen (or turn on the electric cooling system), then wait for approximately 24 h. After the detector has completely cooled, use it.

7.1.2 Application of high voltage

Apply the high voltage specified in the specifications after the detector has been fully cooled. In most cases, the high voltage can be turned on and off using the MCA control software

7.1.3 Gain adjustment

On the hardware, a gain adjustment is performed to adjust the relationship between the horizontal axis (channel) of measuring the γ-ray spectrum and the energy of the γ-ray. The 2000 keV/4000 channel (0.5 keV/channel) setup is commonly used in environmental monitoring.

- Prepare a sealed standard source (^{57}Co 122.1 keV or ^{60}Co 1332.5 keV).
  (Use a source of about 10^4–10^5 Bq, which is not subject to the law.)
- Place the standard radiation source some distance from the end cap of the detector. Then, while collecting the spectrum, set the MCA to the measurement state and make the following adjustments. Adjust the distance between the detector and the source so that the dead time is less than 5 %.
- Adjust the gain of the amplifier so that the peak center position of ^{60}Co (1332.5 keV) is 2665 channel.
- Adjust the zero level of the ADC so that the peak center position of ^{57}Co (122.1 keV) is 244 channel.
- Because the adjustments to the amplifier's gain and the ADC's zero level are mutually influenced, alternately adjust the above two peaks so that they become the respective predetermined position.
- After the two peaks are adjusted to be the predetermined channels, confirm the resolution (Section 9.1).

7.2 Pretreatments of measuring samples

The peak efficiency in γ-ray spectrometry depends on the geometry of measuring samples. As a result, during the pretreatment of measuring samples, it should be noted that the peak efficiency varies due to the sample shape and sample-filling condition in the container, which may influence the quantitative analysis results.

7.2.1 Measurement container

As generally used measurement containers, there are plastic cylindrical containers, Marinelli beakers (2 L, 1 L, and 700 mL), and so forth. Choose appropriate containers considering the amount of measuring samples and required detection limits. To measure a small amount of sample near the detector, a cylindrical container is used. As a result, a measuring sample can be placed close to the detector, resulting in a high peak efficiency but a small maximum amount of sample. A Marinelli beaker, on the other hand, can hold more samples than a cylindrical container, but its peak efficiency per sample amount is lower. For details, refer to Commentary B.

7.2.2 Sample filling

In γ-ray spectrometry using a germanium semiconductor detector, there is no need to separate or purify the nuclides to be measured. As a result, environmental samples can be measured directly or after simple pretreatments (drying, incineration, and precipitation). Nonetheless, because the sample volume grows large, the following items must be checked.

- The sample should be neither coarse nor dense, but it should be homogeneous in the container.
- The sample should keep a constant shape without collapsing in the container.

As to the more specific procedure for the pretreatments of measuring samples, refer to Commentary B.

7.3 Measurement of background

In γ-ray spectrometry, radiation from the surrounding environment and that from the detector itself are simultaneously measured during sample measurements. As a result, it is necessary to measure the detector's background before or after the measurement. That is, by measuring without the sample, the contribution of the background effect must be subtracted from the sample measurement results. More specifically, there are radiation shielding effects of the sample container and matrix, as well as radioactive nuclide effects in the materials. Therefore, the correction should be applied using the measurement results for the blank sample with the same shape and same materials (elemental composition and density) as the measuring sample. It is, however, unrealistic to prepare blank samples for all measuring samples. When the amount of sample is large, such as in a Marinelli beaker, the contribution of shielding effects and radiation becomes significant, and such effects on the quantitative analysis results for the target nuclides cannot be ignored. Therefore, in such cases, it is desirable to grasp the contribution of these effects, and measure the blank samples as needed.

The important points in background measurements are as follows.

- Backgrounds should be measured at least once a month.
- If there was a possibility of contamination, backgrounds should be measured accordingly.
- Backgrounds should be measured at least twice as long as the sample.

As to the methods for background corrections, please refer to Document 1.8.

7.4 Measurement of sample

A series of the measuring procedure, that is, beginning with putting the sample on the end cap of the detector and ending by taking out the sample after the measurement, is described below. It should be noted that the risk of detector contamination can be reduced by placing the sample in a polyethylene double bag and replacing the outer bag with a new polyethylene bag before bringing it into the measurement room. Furthermore, even if the detector is contaminated, the contamination can sometimes be easily eliminated by covering the end cap of the detector with a polyethylene bag.

7.4.1 Procedure for sample measurements

The procedure for sample measurements and the important points are explained below. Also, the example of measurement information that should be recorded is shown in Table 7.1, and the flowchart of the procedure is presented in Fig. 7.1.

(a) Preparation of measuring samples
- Confirm to identify that the sample to be measured is really the target for measurement.
- Confirm the sample by comparing the measurements in the measuring sample container to the descriptions in the sample collection report, ledger, and so on
- Record the information on the measuring sample (sample name, sample number, etc.).

(b) Installation of measuring sample

Put the measuring sample on the end cap of the detector[*1].
- Using a tool etc.[*2], place the measuring sample in the predetermined geometry[*3].
- When a Marinelli beaker is used, confirm the weight change of the liquid-nitrogen weight monitor[*4].
- When the outer bag is not being used in a measurement with an automatic sample changer, care must be taken not to contaminate the detector.

(c) At the beginning of measurement

Before beginning the measurement, the following procedures should be conducted.
- Delete the γ-ray spectra measured before.
  If previously measured γ-ray spectra remain in MCA's memory, delete them after confirming that the spectra have already been saved
- Set measuring time (preset time) as needed.
  Although the measuring time depends on the purpose, it is recommended to be roughly in the range of 3–24 h.

(d) After starting measurement
- Record the measurement information such as the measurement starting time, measurement number, etc. (refer to Table 7.1).

[*1]: Especially an n-type detector is in many cases used always with a detector protection cap in during the measurements including the calibration of the peak efficiency. In this case, the sample should be placed on the protection cap.

[*2]: A special tool with which the geometry can be reproduced is recommended to be used. If there are no such tools, devise something such as making a mark to secure the geometry.

[*3]: A geometry where the peak efficiency has been obtained in advance (refer to Chapter 5).

[*4]: If the air in the bag covering the Marinelli beaker is not adequately evacuated, the pressure of the air will increase the weight of the sample on the cryostat, potentially causing a malfunction. When the value of the liquid nitrogen weight-monitor significantly increases (approximately 0.3 kg as an indication), it is recommended that measures such as removing the sample from the detector and re-bagging it be taken.

・Confirm that the measuring time (real-time or live time[*5]) is increasing.
・Confirm the dead time. If the dead time is significant (roughly 10 %), reduce the sample amount as needed.
・Confirm that in the peak of interest (^{40}K (1460.8keV), ^{137}Cs (661.6keV), etc.), there is no energy drift (deviation) of ±1 keV or larger. This should be confirmed again after a while[*6]. If a peak drift is observed, inspect the experimental room's equipment such as the air conditioner, etc. Then, take the necessary steps, such as adjusting the gain, etc.
・Confirm that no broad peaks of high counting rates are generated in the low-energy region (at dozens of keV or lower)[*7].
・When a peak that can be confirmed is generated in a short time, identify the nuclide corresponding to the peak as much as possible. If this peak is identified as an artificial radioactive nuclide, contact the person in charge of the pretreatment to investigate the possibility that the sample was contaminated during the sample preparation.

(e) At the end of measurement.
・If the preset time was not set, ensure that sufficient measuring time and peak count were obtained before stopping the measurement.
・Record the live time and the measurement end time.
・Save the measured γ-ray spectrum in the PC, etc. In saving the spectrum, be careful not to mistake the measurement number. By reading the γ-ray spectrum again, it can be confirmed that the spectrum was saved correctly.

(f) Taking out of measuring sample
・Confirm that the measurement is ended.
・Confirm that the measuring sample set in the detector is still in the same condition as it was just before the measurement by opening the radiation shield door.
・By collating the taken-out sample with the record, confirm that the sample is correct.

(g) Storage of measuring sample
・After measuring the sample, immediately transport it to a storage location for measured samples, such as a refrigerator. It must be ensured that the sample collected after the measurement is not mixed with samples not yet measured.
・If possible, high-level samples after the measurements should be stored separately from low-level ones after the measurements.
・It is recommended that after measuring high-level samples, the contamination be checked by measuring the background.

[*5] In case the dead time is large, it takes long time for the live time to increase.

[*6]: Check once every 30 min to several hours according to the preset time.

[*7]: The cause of this trouble may be the effects of electric noises. In such a case, the problem is sometimes solved by reconsidering the circuit or changing the LLD (Lower Level Discriminator). If the problem is not solved, it is required to ask the manufacturer of the detector for the countermeasures.

Table 7.1 Examples of measurement information that should be recorded.

Item	Contents to be recorded
(a) Measurement number	Number depending on the measurement instrument (serial number, etc.)
(b) Measurement starting date and time	The date and time when the measurement started (record the date, hour, and minute)
(c) Measurement end date and time	The date and time when the measurement was ended (record the date, hour, and minute) There is no need to record them if the measurement was automatically stopped by the preset time.
(d) Measuring time	The time in which the measurement was conducted Record the preset time, or live time at the end of the measurement.
(e) Person in charge of measurement	Name of the person who conducted the measurement
(f) Measuring sample	The name and number of the sample that was measured Record the measurement container, and amount, filling height, density, and material of the sample as needed.
(g) Data storage location	Filename
(h) Remark	Record the points that were noticed in the measurement.

The flowchart of the sample measuring procedure is shown in Fig. 7.1, and the examples of items to be confirmed by the person in charge of measurement during measurement are listed in Table 7.2.

Measurement

←**(a) Preparation of measuring sample**

- Confirm to identify that the measuring sample is the target sample to be measured.
- Confirm by collating the measurement sample container with the descriptions in the sample collection record sheet, ledger, etc.
- Record the information about the measuring sample (the sample name, sample number, etc.)

←**(b) Installation of measuring sample**

- Confirm that the measuring sample is placed at the predetermined geometry.
- When a Marinelli beaker is used, check the weight change of the liquid-nitrogen weight monitor.
- Be careful not to contaminate the detector.

←**(c) At the beginning of measurement**

- Confirm that the previously measured γ-ray spectrum has been saved.
- Erase the previously measured γ-ray spectrum.
- Set the preset time (3–24 h as an indication).

←**(d) After starting measurement**

- Record the measurement information (refer to Table 7.1)
- Check the measurement starting time in MCA (or PC) and the real-time.
- Confirm that the measuring time (live time) is increasing.
- Confirm that the dead time is not large (rough standard: smaller than 10 %).
- Confirm that the drifts do not occur in the peaks to be measured (^{40}K (1460.8 keV), ^{137}Cs (661.6 keV), etc.).
- Confirm that there are no broad peaks in the low-energy region.
- If a peak is confirmed in a short time, check that the peak does not originate from artificial radioactive nuclides.

←**(e) At the end of measurement**

- Before ending the measurement, confirm that enough measuring time, enough peak counts, etc. are obtained (in the case that the preset time has not been set).
- Record the live time and the measurement end time as needed.
- Save the measured γ-ray spectrum, and record the filename in the save destination.

←**(f) Taking out of measuring sample**

- Confirm that the measurement is ended.
- Check that the sample geometry is the same as that at the beginning of the measurement.
- Collate the taken-out sample with the record.

←**(g) Storage of measuring sample**

- Store the sample in the predetermined place.
- By measuring background, check the contamination of the detector as needed.

Analysis

Fig. 7.1 Flowchart of sample measuring procedure.

Table 7.2 Examples of items to be confirmed by the person in charge of measurement at the time of the measurement.

No.	Checklist	Check column
(a) Preparation of measuring sample		
1	Confirm to identify that the sample to be measured is the measurement target.	
2	Confirm by collating the measurement sample container with the descriptions in the sample collection record sheet, ledger, etc.	
3	Record the information about the measuring sample (the sample name, sample number, etc.)	
(b) Installation of measuring sample		
4	Confirm that the measuring sample is placed in the predetermined geometry.	
5	When a Marinelli beaker is used, check the weight change of the liquid-nitrogen weight monitor.	
6	Be careful not to contaminate the detector.	
(c) At the beginning of measurement		
7	Confirm that the previously measured γ-ray spectrum has been saved.	
8	Erase the previously measured γ-ray spectrum.	
9	Set the preset time as needed (3–24 h as an indication).	
(d) After starting measurement		
10	Record the measurement information (the measurement number, measurement starting date and time, etc.)	
11	Confirm that the measuring time (live time) is increasing.	
12	Confirm that the dead time is not large (rough standard: smaller than 10 %).	
13	Confirm that the drifts do not occur in the peaks to be measured (^{40}K, ^{137}Cs, etc.).	
14	Confirm that there are no broad peaks in the low-energy region.	
15	If a peak is confirmed in a short time, check the peak does not originate from artificial radioactive nuclides.	
(e) At the end of measurement		
16	Before ending the measurement, ensure that sufficient measuring time, peak count, and so on have been obtained (in a case that the preset time has not been set).	
17	Record the live time and measurement end time (as needed).	
18	Save the measured γ-ray spectrum, and record the filename.	
(f) Taking out of measuring sample		
19	Confirm that the measurement is stopped.	
20	Check that the sample geometry is the same as that at the beginning of the measurement.	
21	Confirm that the taken-out sample agrees with the record.	
(g) Storage of measuring sample		
22	Store the sample in the predetermined place.	
23	Check the contamination of the detector as needed.	

7.4.2 Measures when the dead time increases

When measuring samples with high radioactivity, such as ore samples, the number of γ-rays entering the detector skyrockets, causing signal processing in electronic equipment to overload. As a result, the dead time increases.

A sample measurement with increased dead time has the following problems.

- Peaks originating from random summing of γ-rays from different nuclides, etc. are generated.
- It takes a long time to measure (live time does not proceed).
- Peak shapes are deteriorated by pulse pile-up.

Random summing and pulse pile-up may cause the lowering of the net counting rate of γ-ray peaks. As a result, the obtained results sometimes cause underestimation.

If the dead time is found large at the starting of the measurement, it is required to be reduced the number of γ-rays emitted from the sample by decreasing the sample amount[*8].

7.5 Spectral analysis

In spectral analysis, the total energy absorption peaks in the γ-ray spectrum are targeted. The species of nuclides are identified by specifying the γ-ray energy based on the peak position, and the quantitative analyses of nuclides are conducted by the peak area.

The energy of a detected peak is compared to the nuclear data library to identify the nuclide. If there is no appropriate nuclear data, misidentification of the nuclide may happen. In spectra measured at the time of emergency, small γ-ray peaks with low emission rates may be possibly observed. Therefore, by checking not only γ-ray peaks with high emission rates for quantitative analysis but also those with low emission rates, the precision of the nuclide identification can be increased. Furthermore, due to the statistical fluctuation of a baseline, a peak may be deemed analytically detected even if the peak shape is not formed. It is necessary to confirm the spectrum to avoid this misidentification.

As a rule, the output form generated by the software should not be reported in its current state. Instead, the checking by the person in charge of the measurement such as the visually checking of the measured γ-ray spectrum is important in γ-ray spectral analysis.

7.5.1 Procedure for spectral analysis

The procedure for spectral analysis is shown as follows.

(a) Register the information about the measuring samples
- The sample name, sample kind, collection place, date/time of start and end of sample collection, measurement container, sample amount (including unit), filling height, density, the material of the measuring sample, name of the person in charge of measurement, etc.

(b) Register the data files which the software uses in the analysis.
- energy calibration (including half-width calibration) files, peak efficiency calibration files, and the other files necessary for various corrections (self-absorption correction, and coincidence summing correction).

(c) Set analytical conditions
- Select nuclear data library for analysis.
- Select a peak search sensitivity (normally 3).

[*8]: By placing the measuring sample at a distance from the detector, the number of γ -rays entering the detector can be reduced. In this case, it is necessary to have calibrated the peak efficiency in advance so that the peak efficiency in that measuring geometry can be obtained.

Please refer to Document 1.1 “Peak Analysis”.

・Select a condition of attenuation correction
Generally, the date and the time of the sample collection end is the standard.
However, in a case that the period of sample collection is so long that the radioactivity attenuation must be considered, the standard is sometimes set to be the middle[*9] of the sample collection period. It should be noted that there are cases where the attenuation correction is not conducted depending on nuclides. Therefore, select one of the above two cases.

・Select a method to calculate peak area (Covell’s method or fitting method).
Refer to Document 1.1 “Peak analysis”.

・Register the background correction files.Select a background spectrum for subtraction.

(d) Perform analysis

(e) The output of analytical results form

・Output peak search results, peak quantitative results, figures of γ-ray spectra, etc.

(f) Confirmation of analytical results

・Confirm that there is no energy drift (deviation) of ±1 keV or larger for the peak of interest (^{40}K (1460.8 keV), ^{137}Cs (661.6 keV), etc.) in the γ-ray spectrum.

・Confirm the nuclides that were detected.
Confirm the peak shape of γ-ray by expanding the γ-ray spectrum.
(Confirm whether or not the observed peak is the false detection due to the statistical fluctuation of the baseline count in the peak region.)
(Confirm whether or not the peak shape is distorted.)

・In the case of nuclides emitting multiple energy γ-rays, confirm the other γ-ray peaks.
Further, for the nuclide that sequentially decays, check also γ-ray peaks originating from the parent nuclide and the progeny nuclides.

・As to the unknown peaks, identify them referencing the nuclear data (Document 5) aligned in the energy order. Register the nuclear data of the identified nuclides in the nuclear data for analysis if necessary, and repeat the analysis.

The flowchart of the analysis procedure for the measured γ-ray spectrum is shown in Fig.7.2. The examples of items to be confirmed by the person in charge of the measurement at the time of analysis are listed in Table 7.3.

[*9]: If the middle of the collection period cannot be selected, the following procedure is recommended. First, obtain separately the date/time estimated to be the middle, and register this date/time at the time of starting the collection. Then, select the attenuation correction until the registered starting time/date of collection.

Analysis

←**(a) Registration of measuring sample information**

・Resister the sample name, sample kind, collection place, date and time of starting/ending the sample collection, measurement container, sample amount (including units), filling height, density, the material of measuring sample, name of the person in charge of the measurement, etc.

←**(b) Registration of various calibration files**

・Register the energy calibration (including half-width correction) files.

・Register the peak efficiency calibration files.

・If there are files necessary for coincidence summing correction and self-absorption correction, register them.

←**(c) Setting of analyzing conditions**

・Select a nuclear data library for analysis.

・Select a peak search sensitivity (normally 3).

・Select a condition of attenuation correction.

・Select a method for peak area calculation.
Select the method from Covell's method or the fitting method.

・Register the background correction file.
Select a background spectrum for subtraction.

←**(d) Performing analysis**

←**(e) Output of analytical results**

・Output the peak search results, peak quantitative results, figures of γ-ray spectra,etc.

←**(f) Confirmation of analytical results**

・Confirm that there is no drift for the peak of interest (^{40}K, ^{137}Cs, etc.) in the γ-ray spectrum.

・Confirm the nuclides that were detected.
Confirm the peak shape of γ-ray by expanding the γ-ray spectrum.
(Confirm that the observed peak is not false detection that was caused by the statistical fluctuation of the baseline counts.)
(Confirm whether or not the peak shape is distorted.)

・If the nuclides emit multiple energy γ-rays, also confirm the other γ-ray peaks.

・For nuclides that sequentially decay, check also γ-ray peaks originating from the parent nuclide and the progeny nuclides.

・As to the unknown peaks, identify them referencing the nuclear data (Document 5) aligned in the energy order. If necessary, perform the analysis again after registering the nuclear data of the identified nuclides in the nuclear data for analysis.

Evaluation

Fig. 7.2 Flowchart of an analytical procedure for measured γ-ray spectrum.

Table 7.3 Examples of items to be confirmed by the person in charge of measurement at the time of the measurement.

No.	Checklist	Check column
(a) Registration of measuring sample information		
1	The sample name, sample kind, collection place, date and time of starting/ending the sample collection, measurement container, sample amount (including units), filling height, density, the material of measuring sample, name of the person in charge of the measurement, etc. are correctly registered.	
(b) Registration of various calibration files		
2	The energy calibration (including half-width correction) files are correctly registered.	
3	The peak efficiency calibration files are correctly registered.	
4	Files necessary for coincidence summing correction and self-absorption correction are correctly registered.	
(c) Setting of analyzing conditions		
5	The nuclear data library for analysis is correctly selected.	
6	The peak search sensitivity is correctly selected.	
7	The appropriate condition of attenuation correction is selected.	
8	The appropriate method for peak area calculation is selected.	
9	The background correction files are correctly registered.	
(d) Performing analysis		
(e) Output of analytical results		
10	Peak search results, peak quantitative results, and figures of γ-ray spectra are output.	
(f) Confirmation of analytical results		
11	It is confirmed that there are no mistakes in the items described in the analytical result form.	
12	About the detected γ-ray peaks originating from artificial radioactive nuclides ・By expanding the γ-ray spectrum, it is confirmed that there is no abnormality in the peak shape. ・The possibilities of single escape peaks, double escape peaks, and backscattering peaks are considered. ・For nuclides emitting multiple γ-rays, γ-rays with small emitting probability are also confirmed. ・For nuclides decaying sequentially, γ-ray peaks from the parent nuclide as well as those from the progeny nuclides are confirmed.	
13	About unknown γ-ray peaks ・By expanding the γ-ray spectrum, it is confirmed that the unknown peaks are detected not due to the statistical fluctuation of the baseline counts. ・The possibilities of single escape peaks, double escape peaks, sum peak, and backscattering peaks are considered. ・Unknown peaks are identified by referencing the nuclear data aligned in the energy order.	

7.5.2 Treatment of unknown peaks

The nuclear data library is used to collate and analyze the peaks found in the γ-ray spectrum. If there is no corresponding γ-ray energy in the energy range that was identified, the peak is treated as an unknown peak. Although the collation of unknown peaks is expected to be a huge amount of work, peak identification is possible using the nuclear data (refer to Document 5) shown in the energy order[*10].

Before proceeding with the work on peak identification, the following possibilities have to be considered.

- a peak detected in the analytical process due to the statistical fluctuation of the baseline.
- a single escape peak, a double escape peak
- a sum peak
- a backscattering peak

Peaks due to random summing are sometimes detected in high count-rate spectra expected during an emergency. "Gamma-ray Spectral Analysis Using Germanium Detector in Emergencies" has more information (No.29).

7.5.3 Identification of radioactive nuclides

The energies of the peaks detected in a spectrum are compared to the nuclide data library to determine the radioactivity of each nuclide. Therefore, if the γ-ray energy of the nuclide to be identified is not registered in the nuclear data library for analysis, or if the energy of the registered other γ-ray coincides with that of the nuclide to be analyzed within the identifying width, there is a possibility that the nuclide cannot be identified correctly. Single escape peaks, double escape peaks, sum peaks, and backscattering peaks that are not registered in the nuclear data library for analysis cannot be correctly identified.

Furthermore, for samples containing much water, it should be noted that neutrons that are produced secondarily by cosmic rays are decelerated by water, and they become easier to interact with the materials composing the detector. For example, a γ-ray (139.7 keV) emitted from ^{75m}Ge produced by the interaction of the nucleus of germanium used in the detection part of a germanium semiconductor detector with neutrons is possibly misidentified to be a γ-ray (140.5 keV) from ^{99m}Tc, so it should be careful in identifying the peak.

To confirm whether a peak is misidentified or not, there are the following methods.

- For nuclides that emit multiple γ-rays, to confirm the existence of multiple peaks and the consistency of each peak area.
- For the parent nuclide and the progeny nuclides of a nuclide that sequentially decay, to confirm the existence of their peaks and the consistency of the analyzed results.
- To confirm single escape peaks, double escape peaks, sum peaks, and backscattering peaks originating from the other nuclides.
- To check whether or not the half-life of the nuclide is too short compared with the time from the sample collection date/time to the start of the measurement.
- To confirm that the results of the re-measurement decrease in accordance with the half-life of the nuclide.

7.5.4 Treatment of multiple peaks from the same nuclide

Since there are radioactive nuclides that emit multiple γ-rays, it is effective to confirm the detection of multiple γ-rays to improve the precision of identification. In this case, it is necessary

---

[*10]: When the measurement is conducted again to evaluate the validity of the identification results, it is effective to confirm whether the result of the re-measurement decreases in accordance with the half-life of the identified nuclide.

to determine in advance how to treat the γ-rays that are used to report the quantification of radioactivity and the results.

For this purpose, there are generally two methods. One is to focus on the main peak (the first peak of the highest emission rate), and the other is to use the weighted mean of the results obtained from the multiple peaks. Each method's key points are outlined below. It is worth noting that the former measurement method, which focuses on the main peak, is used as the foundation for the current measurement method.

(1) Method focusing on main peak

It is a simple method to focus on the first peak of the highest emission rate[*11].

The results obtained for γ-ray of various energies should not be ignored when confirming the validity of the quantitative results, but rather confirmed. If these two quantitative results are significantly different, the contribution of interference peaks has to be considered (e.g., ^{137}Cs (661.7 keV) against ^{110m}Ag (657.8 keV), etc.). If the contribution of interference peaks is found, it is required to decide to adopt the results for γ-ray peaks with the second-highest emission rate as the quantitative results. Further, when the interference of γ-rays from the other nuclides is expected against the first peak, it is recommended to set the second peak as that of the quantitative analysis in advance on the nuclear data library for analysis.

(2) Method using weighted mean

The weighted mean is calculated for quantitative results of multiple γ-ray peaks by weighting with the reciprocal of the square of the uncertainty. For measurements in normal time, since the quantitative results using γ-rays with a small emission rate have relatively large uncertainty, these results do not make much sense to use in the calculation of the weighted mean. For this reason, it is recommended to determine the γ-ray energy used in weighted mean in advance, considering the emission rate and peak efficiency. It should also be confirmed that, due to interference peaks, the results of each quantitative result of the γ-ray peak used in the weighted mean are not too dissimilar.

When the weighted mean is conducted, the uncertainty surely becomes smaller, thereby the result of the weighted mean becomes larger than $3u$ (u: uncertainty) even if each γ-ray peak is not detected. In this case, it should be careful that the peak may be judged to be seemingly detected in the analysis.

The weighted mean $A \pm u$ for multiple radioactivity values $A_i \pm u_i$ is obtained by the following equations.

$$A = \frac{\sum_i \frac{A_i}{{u_i}^2}}{\sum_i \frac{1}{{u_i}^2}} \tag{7.2}$$

$$\frac{1}{u^2} = \sum_i \frac{1}{{u_i}^2} \tag{7.3}$$

[*11]: Considering the difference in the peak efficiency, the area of a peak with low emission rate possibly becomes larger than that of a photon-induced photoelectric peak with large emission rate.

7.6 Confirming validity of analyzed results

The assumption in evaluating the analyzed results is that the measurement and analysis were done correctly. The analytical results may drastically change if the measurement is conducted in a geometry that differs from that of the calibration source, or if the settings of various corrections (self-absorption correction, coincidence summing correction, and attenuation correction) in the analysis are not appropriate. For example, for the self-absorption correction, the results change depending on the materials and the setting of the filling height/density. Also, for the coincidence summing correction, the results may change depending on whether the correction is conducted or not. Concerning the attenuation correction, it is necessary to confirm that any problem does not happen in the attenuation correction results especially for the progeny nuclides in transient equilibrium.

Even in cases where the measurements and analysis were performed correctly, it is difficult to determine whether the data are valid or not solely based on the obtained measurement results of artificial radioactive nuclides. Based on the consideration of various factors such as the kinds of the accident of nuclear reactor facilities, information on nuclide composition of the emission source, distance from the source, meteorological condition, elapsed time, half-lives, and physical/chemical behaviors (volatile or non-volatile), it is required to evaluate whether the measurement results are valid or not. As to the detected artificial radioactive nuclides, the possibility of the other emission sources (for example, the past atmospheric nuclear explosion tests, medical radioactive materials, etc.) have to be considered as well.

When short-lived nuclides are detected in an emergency, for example, the baseline counts drop as the short half-life nuclides decay. As a result, γ-ray peaks of the other artificial radioactive nuclides that had been hiding are sometimes newly observed.

Furthermore, it is effective that the spectrum is evaluated using the database of the measurement results for the same kind or similar samples. In this case, it follows that the evaluation is focused on the radioactivity concentration of not artificial radioactive nuclides but natural radioactive ones. The concentration of natural radioactive nuclides in the same kind or similar sample is expected to be about the same as that in the sample to be analyzed. By confirming that there is no significant difference based on the comparison of the respective results, it may be sometimes possible to judge the validity of the data.

7.7 Report on analytical results

It is preferable to report together with the values of uncertainty for analytical results where the validity has been confirmed, using the predetermined reporting format. Tables 7.4.1 and 7.4.2 show some examples of reporting formats. In the reporting format, not only the radioactivity concentration of the detected radioactive nuclides but also information on the samples, information on the measurements and analyzing conditions, etc. should be described. When you copy the report's description, compare it to the original to make sure there are not any errors. Refer to Commentary C, "Evaluation of Uncertainty in γ-ray Spectrometry," for more information on how to evaluate uncertainty.

It is possible that a third party evaluating the measurement results will not be able to judge solely on the reported values. In such a case, the output analysis form and the γ-ray spectral chart should be also reported as needed. For detected peaks in γ-ray spectra, Fig. 7.3.1 shows an example for the flowchart from the confirmation of the analytical results shown in Section 7.5.1 (f) to the report on the analysis results described in Section 7.7.

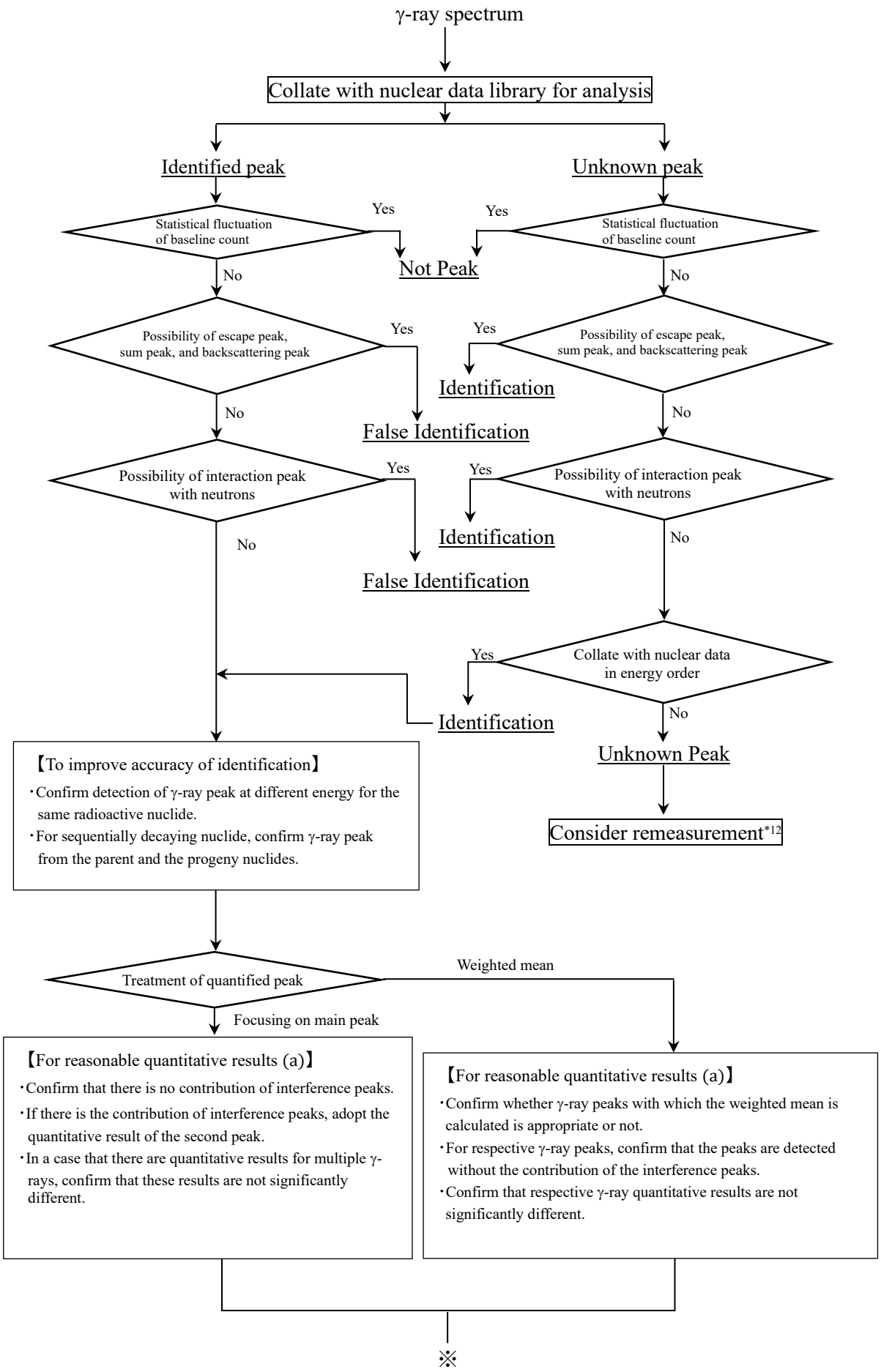
γ-ray spectrum
Collate with nuclear data library for analysis
Identified peak
Unknown peak
Statistical fluctuation of baseline count
Yes
Not Peak
No
Possibility of escape peak, sum peak, and backscattering peak
Identification
False Identification
Possibility of interaction peak with neutrons
Collate with nuclear data in energy order
Unknown Peak
Consider remeasurement*12
【To improve accuracy of identification】
・Confirm detection of γ-ray peak at different energy for the same radioactive nuclide.
・For sequentially decaying nuclide, confirm γ-ray peak from the parent and the progeny nuclides.
Treatment of quantified peak
Weighted mean
Focusing on main peak
【For reasonable quantitative results (a)】
・Confirm that there is no contribution of interference peaks.
・If there is the contribution of interference peaks, adopt the quantitative result of the second peak.
・In a case that there are quantitative results for multiple γ-rays, confirm that these results are not significantly different.
【For reasonable quantitative results (a)】
・Confirm whether γ-ray peaks with which the weighted mean is calculated is appropriate or not.
・For respective γ-ray peaks, confirm that the peaks are detected without the contribution of the interference peaks.
・Confirm that respective γ-ray quantitative results are not significantly different.
※

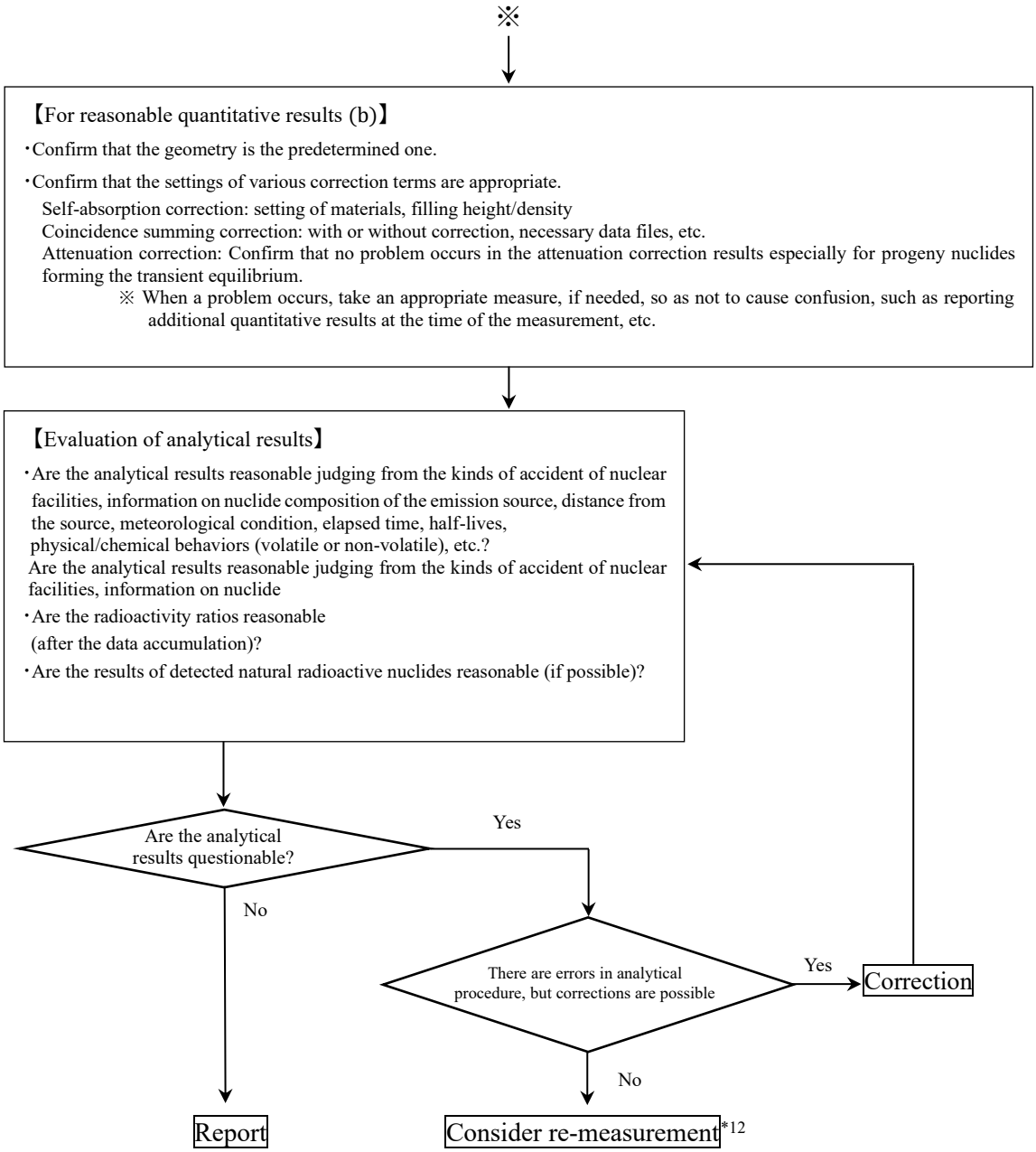

Fig.7.3.1 Example of flowchart until reporting analysis results (continued).

*12: When re-measurement is conducted to evaluate the validity of the identification results, it is effective to confirm whether the re-measured results decrease in accordance with the half-life of the identified nuclide.

Table 7.4.1 Example 1 of reporting form (horizontal form).

Measurement results of nuclides using germanium semiconductor detector

1. Executing institute	
Analyzing institute	
Main person in charge	
Person in charge of measurement	

2. Measuring sample			
Sample name			
Collection place			
Collection year/month/date	/ / : - / / :		
Measurement container		Sample amount*1	
Filling height		Density	

*1: Write unit (g-FW(raw weight), g-DW (dry weight), kg-FW, kg-DW, mL, L, m^2, m^3, etc.) together.

3. Measurement instrument	
Type of detector	
Thickness of shield	
Relative efficiency	
Resolution (1.33MeV)	

4. Measurement and analysis			
(a) Measurement			
Measurement number		Measurement starting date/time	/ / :
Measuring time			
(b) Analysis			
Self-absorption correction	Yes, No		
Attenuation correction	Date of attenuation correction		/ / :
	Attenuation correction of nuclides without considering sequential decay		Yes, No
	Attenuation correction of progeny nuclides in sequential decay*2		No, Inflow consideration, Half-life of parent
Coincidence summing correction	Yes, No	Nuclides with coincidence summing correction n	

*2: Record the attenuation correction method for progeny nuclides in sequential decay (No…without attenuation correction, Inflow consideration…Attenuation correction where the inflow from the parent nuclide is considered, Half-life of parent nuclide…Attenuation correction where the half-life of the parent nuclide was used as that of the progeny nuclide, supposing that the state is in transient equilibrium from the time of the emission.).

5. Measurement result			
Nuclide	Radioactivity concentration ± uncertainty ( )*3	Nuclide	Radioactivity concentration ± uncertainty ( )*3
	±		±
	±		±
	±		±
	±		±
	±		±
	±		±

(Note)

*3: Write down the unit of radioactivity concentration together.

Table 7.4.1 Example 1 of reporting form (vertical form).

Measurement results of nuclides using germanium semiconductor detector

1. Executing institute	
Analyzing institute	
Main person in charge	
Person in charge of measurement	

2. Measuring sample			
Sample name			
Collection place			
Collectiond year/month/date	/ / : - / / :		
Measurement container		Sample amount*1※1	
Filling height		Density	

*1:Write unit (g-FW(raw weight), g-DW (dry weight), kg-FW, kg-DW, mL, L, m^2, m^3, etc.) together.

3. Measurement instrument	
Type of detector	
Thickness of shield	
Relative efficiency	
Resolution (1.33MeV)	

4. Measurement and analysis			
① Measurement			
Measurement number		Measurement starting date/time	/ / :
Measuring time			
② Analysis			
Self-absorption correction	Yes, No		
Attenuation correction	Date of attenuation correction		/ / :
	Attenuation correction of nuclides without considering sequential decay		Yes, No
	Attenuation correction of progeny nuclides in sequential decay*2		No, Inflow consideration, Half-life of parent nuclides
Coincidence summing correction	Yes, No	Nuclide with coincidence summing correction nuclides	

*2:Record the attenuation correction method for progeny nuclides in sequential decay (No…without attenuation correction, Inflow consideration…Attenuation correction where the inflow from the parent nuclide is considered, Half-life of parent nuclide…Attenuation correction where the half-life of the parent nuclide was used as that of the progeny nuclide, supposing that the state is in transient equilibrium from the time of the emission.).

*3:Write down the unit of radioactivity concentration together.

5. Measurement result			
Nuclide	Radioactivity concentration ± uncertainty ( )*3	Nuclide	Radioactivity concentration ± uncertainty ( )*3
	±		±
	±		±
	±		±
	±		±
	±		±
	±		±

(Note)

Table 7.4.2 Example 2 of reporting form.

Measurement results of nuclides using germanium semiconductor detector

1. Executing institute

Analyzing institute	
Main person in charge	
Person in charge of measurement	

2. Measuring sample

Sample name	
Sample species	
Collection place	
Collection year/month/date	/ / : - / / :
Measurement container	U-8 container, Marinelli beaker (2L, 1L, 0.7L), others
Sample amount*1	(g-FW, g-DW, kg-FW, kg-DW, mL, L, m^2, m^3)
Filling height	(mm, cm)
Density	(g cm^3)
(Note)	

*1:Distinguish FW (raw weight) and DW (dry weight).

3. Measurement and analysis

a) Measurement			
Measurement number		Measuring time	(sec)
Measurement starting date/time	/ / :		
b) Analysis			
Self-absorption correction	Yes, No		
Attenuation correction	Attenuation correction date	/ / :	
	Attenuation correction of nuclides without considering sequential decay	Yes, No	
	Attenuation correction of progeny nuclides in sequential decay*2	No, Inflow consideration, Half-life of parent nuclides	
Coincidence summing correction	Yes, No		
Coincidence summing Corrected nuclide			
(Note)			

*2:Record the attenuation correction method for progeny nuclides in sequential decay

(No…without attenuation correction, Inflow consideration…Attenuation correction where the inflow from the parent nuclide is considered, Half-life of parent nuclide…Attenuation correction where the half-life of the parent nuclide was used as that of the progeny nuclide, supposing that the state is in transient equilibrium from the time of the emission.).

Table 7.4.2 Example 2 of reporting form (continued).

4. Information on measurement instrument

Type of detector	
Thickness of shield	(mm)
Relative efficiency	(%)
Resolution(1.33 MeV)	(keV)
(Note)	

5. Measurement result

Nuclide	Radioactivity concentration ± uncertainty ( )*3	Note
	±	
	±	
	±	
	±	
	±	
	±	
	±	
	±	
	±	

*3:Write down the unit of radioactivity concentration together.

6. Note

Chapter 8 Detection limit

The value of a detection limit in radioactivity measurement changes depending on the background of the detector, sample amount, and measurement time, among other factors. Further, since the value of the detection limit in γ-ray spectrometry is calculated considering the various factors involved in spectral analysis, it reflects the performance of the detector. It is important to obtain the value of the detection limit in the peak region of the nuclide to be analyzed for each measurement. The observation of a peak is generally judged by whether the peak area exceeds three times value of the uncertainty related to the counts.

Environmental radioactivity is too weak to be detected in many cases. Therefore, if the value of the detection limit has not been calculated when performing only the spectral analysis based on the peak search, the results cannot be obtained from the measurement. In the case that no peak is observed in a spectrum, it is desirable to have obtained the value of the detection limit in advance by incorporating the program for spectral analysis. If a sample has a radioactivity higher than the detection limit, the radioactivity will in most cases be detected. At the same time, even if the radioactivity in a sample is lower than the detection limit, it is not necessarily the case that the radioactivity will not be detected. In fact, it will possibly be detected as a peak. Furthermore, if the radioactivity coincides with the detection limit, it can be detected with a 50 % probability (the probability with which an existing radioactivity will be judged to be nothing is 50 %).

There are multiple methods to calculate the detection limit value, such as the Cooper's method (described in a former manual, revised in 1992) and the evaluation method by ISO 11929 of the international standard. For details on the various evaluation methods, refer to Commentary D.

Although there are many methods to evaluate the value of the detection limit, it is recommended that a method is selected according to the specifications required by the particular investigation and measurements being conducted. In reporting the detection limit values, it is necessary to specify the adopted evaluation method (including a description of the reliability).

Chapter 9 Quality assurance of analysis results

In this chapter, the requirements necessary to obtain appropriate analytical results using a germanium semiconductor detector will be described.

9.1 Confirming the integrity of instruments

The purpose of quality assurance in radiation monitoring in normal times is to ensure that the quality of the data obtained is objectively maintained at an appropriate level. Thereby, it will for the first time become possible to unifiedly interpret the data among different institutes or those obtained at different times from the same institute. As to the measurement data on the concentration of radioactive materials, it is desirable to guarantee quality according to the concept provided by ISO/IEC 17025. To quantify the concentration of radioactive materials, a quality assurance system has to be established for all steps in a series of actions, from the sample collection to the data evaluation. To guarantee the reliability (quality) of the analytical results, it is required that the appropriate precision management is conducted under the quality assurance system and that a description of the uncertainty is added to the analytical results.

To obtain appropriate analytical results, measurement equipment[*1] that meets the required performance standard must be used, and the equipment must be maintained in properly working condition. To confirm that the equipment is working normally and that there has been no change that could influence the reliability of the analytical results, the following items should be periodically checked.

If an abnormality is found in an instrument, one should stop using it and perform the necessary repairs. After the repair, an operation test should be conducted and the instrument can be used after the equipment integrity is confirmed. If necessary, one should confirm the measurement results obtained before detecting the abnormality and evaluate whether these were affected.

(1) Energy resolution

The γ–rays should be measured from ^{60}Co standard source, and the half-width should be obtained from the shape of a 1,332.5 keV peak.

The frequency of the half-width measurement should be approximately twice per year or more. (If the equipment is stopped due to a power outage or another issue, it should be measured on each occasion.)

If the half-width increases by approximately 10 % or more of the initial value, the cause should be inspected, and the necessary countermeasures should be taken.

(2) Peak efficiency

If the peak efficiency changes, this would seriously influence the analytical results. To avoid this issue, it is required to periodically (about once per year or more) check whether the peak efficiency has changed.

- To check the peak efficiency, one method is to measure γ–rays from the nuclides of long half-life (^{152}Eu, ^{137}Cs, etc.) in the same geometry. In this case, it is confirmed whether the fluctuation of the measurement results (e.g., peak counting rate) exceed a pre-set range.
- If the peak efficiency changes to the extent that a significant effect on the analytical results is observed, the peak efficiency calibration should be performed again. In addition, it should be evaluated whether there was a problem or not by checking the measurement results obtained

---

[*1]: Before beginning the operation of measuring equipment, it is required to have confirmed in advance whether the analysis software adopts a method supported in the academic literature. In addition, it should be confirmed whether or not the measurement test data of a standard source that is traceable to the national or international standard are appropriate.

before the abnormality was found.

(3) Daily inspection of equipment

To maintain the instruments in the normal condition and take countermeasures by finding the abnormality as early as possible, it is recommended that the following daily inspections be performed. Further, it is desirable to create and store an inspection report on these items.

- Confirm whether the equation used for energy calibration is reasonable. For this process, one should measure a standard radiation source and confirm that the deviation of the peak center is within ±1 keV. In contrast to a standard source, in this case it does not matter whether one confirms that the deviation of the center of the peak of interest (e.g., ^{40}K, ^{137}Cs) in the γ-ray spectrum of the measurement sample is within the range of ±1 keV. If the equation for energy calibration is not reasonable, the instrument should be used after readjusting the gain and rebuilding the energy calibration equation.
- Periodically measure the background spectra without a measurement sample and confirm that the measurement instruments are not contaminated. If the instrument is contaminated, the background spectrum should be remeasured after performing the decontamination. Further, one should evaluate whether there was a problem or not by checking the measurement results obtained before finding the contamination. If the contamination cannot be fully eliminated, the measurements of background for subtraction (correction) should be performed at an appropriate frequency.
- Confirm whether the air conditioning is appropriate or not. Overall, it is desirable to maintain room temperature at approximately 23°C–25°C. The fluctuation of room temperature should remain within approximately ±2 °C, and humidity should be maintained in a range of 50 %–60 %.
- Confirm the consumption of liquid nitrogen.
- If an abnormality is observed in the results of the inspection, stop the sample measurement and take the necessary countermeasures, such as conducting repairs based on an investigation of the cause. Further, one should confirm the measurement results obtained before finding the abnormality and evaluate whether these were affected.

9.2 Evaluation of uncertainty

In the international quality system, uncertainties in sample collection, sample treatment, and measurements have to be considered. Among these, the uncertainty in measurements will be described in this section. In radiation monitoring in normal times, since the uncertainty in radioactivity counting is largest, only this uncertainty has been presented so far. However, due to the uncertainty in instrumental calibration and in a series of processes, from sample measurements to the analysis, it is necessary to understand the factors generating the uncertainty in advance. In addition, by evaluating the uncertainty, we can know the uncertainty at each step of a series of analytical work. Thereby, it will become possible to manage and improve the quality of the analytical results. Concerning the evaluation methods for uncertainty in γ-ray spectrometry and examples, please refer to Commentary C.

9.3 Traceability of measurement

The traceability of a measurement is the route from which it is possible to determine what the measurement result was based on. It is used as one of the grounds to exhibit that an analysis was conducted correctly.

Traceability can be secured only for the energy of γ–rays from nuclides contained in a radiation source if the geometry adopted by the measurement is that of a standard source. It cannot be applied to γ–rays with different energies or those measured in different geometries. For this reason, to secure the traceability of measurement results using a germanium semiconductor detector, the user must perform a calibration of the peak efficiency using a standard source that is traceable to the international standard concerning the geometry of the sample to be measured and γ-ray energy.

Standard sources made in Japan are traceable to the national standard and can be obtained together with calibration certificates, which are issued by calibration companies based on the Japan Calibration Service System measurement Act (the added values and uncertainties for nuclides are written in the certification). As an alternative, other radiation sources made in foreign countries that have the agreement of the Mutual Recognition Arrangement (International Committee of Weights and Measures; CIPM-MRA) with Japan may be used.

The peak efficiency obtained by the calibration should be used after setting the expiration date, regular inspection according to the method outlined in Section 9.1, and confirmation that there is no change that affects the analytical results.

9.4 Confirming validity of measurement and analysis method

To obtain accurate analytical results by analyzing γ-ray spectra, it is considered necessary that the calculation method for the analysis and the data (e.g., on the peak efficiency) used in the calculation are reasonable. Furthermore, when measurements are performed under conditions other than those for which the traceability condition outlined in Section 9.3 is secured, conversion factors to measurement conditions with different geometries and energies are required.

To confirm the validity of the measurement and analysis method, the following methods can be used:

(1) Measurement of standard materials

When a standard material with the same nuclides, shape, and material as that of the sample to be measured can be obtained, the validity can be confirmed by the measurement and the analytical results of the standard material.

(2) Comparison with results obtained using other analytical methods

If the standard material cannot be obtained, another method can be used, as follows. First, the same sample is analyzed by two methods: an analytical method by which the validity is to be

confirmed and a method whose validity has been already confirmed. Then, the results obtained by these two methods are compared.

(3) Intercomparison between test institutes

Using the same sample, an intercomparison should be conducted with another test institute (one accredited by the ISO/IEC 17025 is desirable). Then, by confirming that there is no significant difference in the analytical results between the two institutes, the validity of the measurement and analytical process can be confirmed.

(4) Participation in proficiency test

As an external quality control, it is possible to objectively validate the technique of an institute by participating in a proficiency test held by an external organization and comparing the analysis results of the test samples with the assigned values. In the case of the proficiency test based on ISO/IEC 17043, the Z scores and the En values of the participating test institutes are reported. The participating test institutes can compare the submitted results with those obtained by other test institutes.

Explanation

Explanation A Efficiency Transfer

Efficiency transfer is a semi-empirical calculation method that converts a peak efficiency measured for a sample in a specific geometry to that for the sample with a different material in another geometry measured via the same detector.

Methods to expand peak efficiency to other geometries by numerical calculation have long been used. Various evaluations, including the summing and self-absorption effects, have recently become possible using Monte Carlo simulations. These methods to obtain peak efficiency have begun to be applied to various investigations and improvements [6].

A.1 Principle of efficiency transfer

The method of efficiency transfer is based on a principle proposed by Moens et al. [7]. The method is based on a virtual peak-to-total ratio of a detector composed of only a sensitive region without the source, end cap, and dead layer, described by the following equation:

$$(P/T)_V = \frac{4\pi}{\overline{\Omega}} \cdot \varepsilon \tag{A.1}$$

where, $(P/T)_V$ is the virtual peak-to-total ratio, $\overline{\Omega}$ is the effective solid angle, and ε is the peak efficiency.

Under the condition where there is no material causing γ-ray shielding or scattering, including the dead layer between the source and detector, both the peak and total efficiencies are proportional to the effective solid angle toward the detector. For this reason, unlike the peak-to-total ratio observed by real measurement, the virtual peak-to-total ratio does not depend on the geometry but is specific to the detector. Therefore, from equation (A.1), the following relationship holds between the peak efficiency of the radiation source and that of the measurement sample.

$$\varepsilon_2 = \frac{\overline{\Omega}_2}{\overline{\Omega}_1}\varepsilon_1 \tag{A.2}$$

where ε_1 is the peak efficiency at the time of the measurement of the radiation source, $\overline{\Omega}_1$ is the effective solid angle at the time of measurement of the radiation source, ε_2 is the peak efficiency at the time of measurement of the sample, and $\overline{\Omega}_2$ is the effective solid angle at the time of measurement of the sample.

The peak efficiency obtained by the measurement of a standard source is used for ε_1 in the above equation. Since the effective solid angle can be calculated based on the geometry between the sample and the detector and the route of interaction in the detector, it is possible to obtain the peak efficiency ε_2 of the sample from ε_1 of the source by using $\overline{\Omega}_2/\overline{\Omega}_1$ as a conversion coefficient. It should be noted that, in the calculation of ε_2, various effects originating from the inner structure of the detector are cancelled by the term $\overline{\Omega}_2/\overline{\Omega}_1$ and do not particularly influence the calculation results. There are many codes that utilize calculation methods such as the Monte Carlo simulation to perform semi-empirical peak efficiency conversions based on this principle to obtain the effective solid angle. The method described here can be performed using not only the specific software mentioned but also using versatile Monte Carlo simulation codes.

As to the performance of this method, called efficiency transfer, using the versatile Monte Carlo simulation codes (GEANT3, PENELOPE, MCNP, and EGS4), and other specialized software for

γ-ray spectroscopy (ANGLE, DETEFF, GESPECOR, ETNA, and EFFTRAN), the results of a mutual comparison were reported[*1] [8]. The calculation results obtained by multiple codes closely coincide (mostly within 2 %), indicating that there are no practical differences between the various implemented codes. Therefore, it has been shown that the method is effective for γ-ray spectrometry for environmental radiation monitoring. Note that compared with the calculation by versatile Monte Carlo simulation codes, the calculation time using an exclusive software is considerably shortened. Specifically, in most cases, the results can be obtained within several seconds.

A.2 Investigation (examples of application to real detector)

Using EFFTRAN [9], one of the exclusive software programs equipped with efficiency transfer, the peak efficiency conversion for three geometries (U-8 vessel; fill height: 9, 28.4, and 47.6 mm) of agar samples (density: 1.001 g cm^3; additive elements: ^{109}Cd, ^{57}Co, ^{139}Ce, ^{51}Cr, ^{137}Cs, ^{54}Mn, ^{88}Y, ^{59}Fe, and ^{60}Co) was investigated. The peak efficiency obtained from the measurement of the mixed volumetric source in a U-8 vessel (material: alumina; filling height: 30 mm; density: 1.022 g cm^3; nuclides: ^{109}Cd, ^{57}Co, ^{139}Ce, ^{51}Cr, ^{85}Sr, ^{137}Cs, ^{54}Mn, ^{88}Y, and ^{60}Co) was used as a conversion standard.

The information submitted by the manufacturer was used for the inner structure of the detector (the size of the germanium crystal, the thickness of the dead layer, and the structural materials). Using the peak efficiencies A and B, described below, the radioactivity concentration for the additive nuclides was obtained by analyzing the spectra obtained by measuring the samples using a p-type coaxial germanium semiconductor detector with 31 % relative efficiency.

Peak efficiencies used for the analysis:

A: Peak efficiency by EFFTRAN (for agar at each filling height that EFFTRAN converted the standard peak efficiency (mixed volumetric source, fill height 30 mm) to).

B: Peak efficiency from conventional method (interpolation of peak efficiency for volumetric source) (that may be corrected to reflect arbitral fill height and materials (elemental composition and material) obtained from the measurements using a set of mixed volumetric sources (material: alumina) in U-8 vessel with different fill heights.)

[*1]: Testing efficiency transfer codes for equivalence. T. Vidmar, et al. 68, 2010, 355–359.

A.3 Results

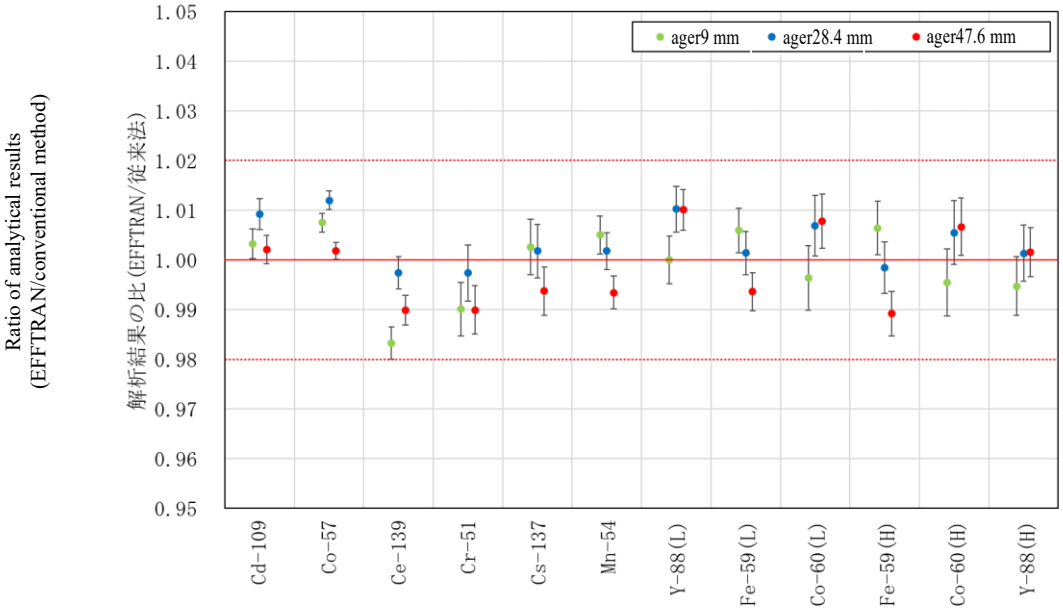

Fig. A.1 Comparison between analytical results using peak efficiency calculated by EFFTRAN and those using peak efficiency obtained from the conventional method.
*Error bars show the uncertainty (k = 1) in the ratio of the analytical results.

The analytical results, based on the peak efficiency from EFFTRAN, agree with those from the conventional method (interpolation of peak efficiency for volumetric source) within a 2 % error. The results show that for the measurements of the samples in the U-8 vessel using a coaxial-type detector, a peak efficiency obtained by the real measurement of one mixed volumetric source can be converted to the peak efficiency for samples of a different material with a different fill height without any practical issue. Additionally, the analytical results from ^{60}Co and ^{88}Y show that there is no problem in the correction of the summing effect.

A.4 Conclusions

Peak efficiency transfer is a semi-empirical method where a peak efficiency obtained for a specific sample geometry is converted to that of another sample geometry using the same detector. As described in A.1, multiple software programs are equipped with a method of calculating peak efficiency, as it is an established method.

Using γ-ray spectrometry, samples with various shapes can be measured. However, given the cost and operational considerations, it is not realistic to prepare standard sources for all sample geometries to be measured. The present method allows the conversion coefficient for multiple geometries to be obtained, making it useful for measurements of samples with various shapes.

It will be necessary to confirm the validity of the method for converting a peak efficiency obtained by the real measurements of mixed volumetric sources to that obtained from a different geometry. However, the present method is effective for obtaining peak efficiencies for volumetric samples in γ-ray spectrometry.

Explanation B Methods for preparation of measurement samples

B.1 Measurement vessel

B.1.1 Type of measurement vessel

Of the many types of vessels used in γ-ray spectrometry, cylindrical plastic vessels and Marinelli-type vessels (700 mL, 1 L, 2 L) are the most common. Marinelli-type vessels are generally used for the direct measurement of samples without pretreatments, including liquids such as milk, sea water, inland water, and severed vegetables. Since the measurement efficiency is high and the quantitative analytical results can to some extent be obtained without pretreatments in a short time, Marinelli-type vessels are used in emergencies when the magnitude of the radioactivity concentration must be known as early as possible.

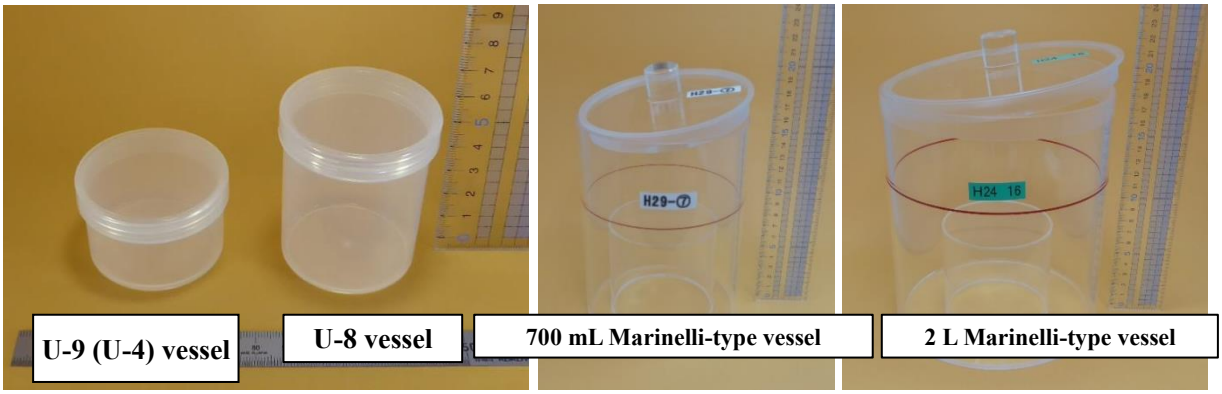

Fig. B.1 Measurement vessels used in γ-ray spectrometry.

B.1.2 Selection of measurement vessel

The peak efficiency and the lower detection limit depend on the shape, volume, bottom area, bottom thickness, etc. of the measurement vessel. Therefore, at some institutes, the measurement vessels are changed depending on the type and amount of the sample and the required lower detection limit. However, it is necessary to obtain the peak efficiency for each vessel. Therefore, it is recommended not to increase the types of vessels unnecessarily. When measurements are conducted on the same amount of a sample (about 100 cm^3, depending on the detector crystal size), the peak efficiency is the highest for the cylindrical vessel with a thin bottom with an area of about 50 cm^2.

When a large amount of a sample can be obtained (especially when multiple samples are to be measured in a short time), a Marinelli-type vessel is better because it has a small lower detection limit. Since Marinelli-type vessels are expensive, they generally are not disposed of after use. Unfortunately, it is not easy to eliminate contamination even after being washed by acid or detergent. Placing the sample in a polyethylene inner bag that can be attached to the inside of the vessel allows the Marinelli-type vessel to be used repeatedly simply by replacing the inner bag. Unlike a Marinelli-type vessel, the inner bags do not occupy a significant volume of space. Even if prepared in advance, hundreds of pieces can be put in one cardboard box. Therefore, inner bags are useful for emergencies and other situations where many samples must be measured.

Table B.1 Examples of various vessels

Vessel	Height mm	Bottom area cm^2	Bottom thickness mm	Material (body)
U-8	61.0	19.6	2.5	polypropylene
U-9 (U-4)	32.0	20.0	2.5	polypropylene
The other cylindrical vessels	35.0	28.3	2.0	polystyrene
	46.0	50.3	2.5	polystyrene
	57.0	70.9	2.5	polystyrene
700 mL Marinelli-type vessel	168.0	-	-	acryl
2 L Marinelli-type vessel	190.0	-	-	acryl

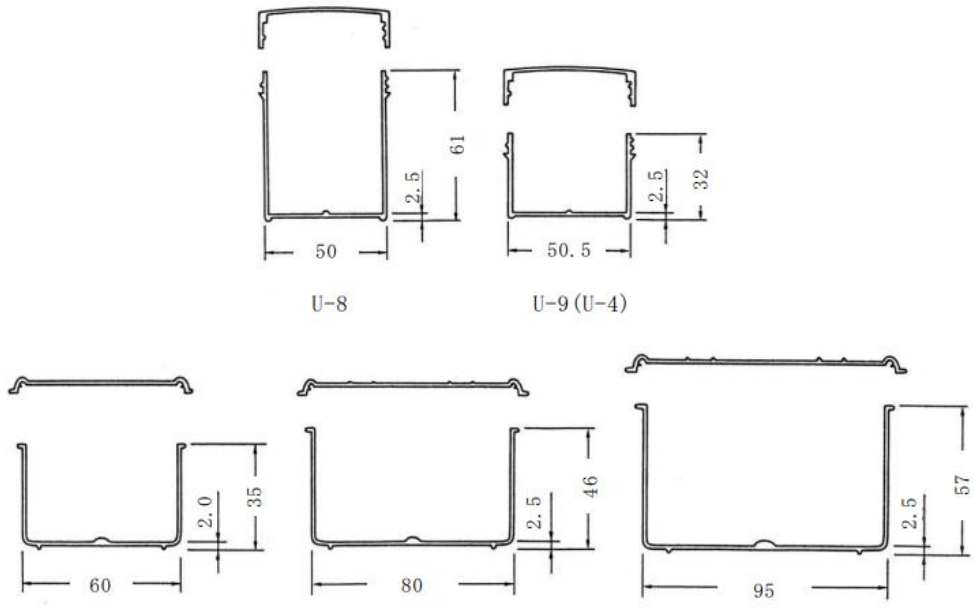

Fig. B.2.1 Cross-section of various cylindrical vessels (all dimensions in mm).

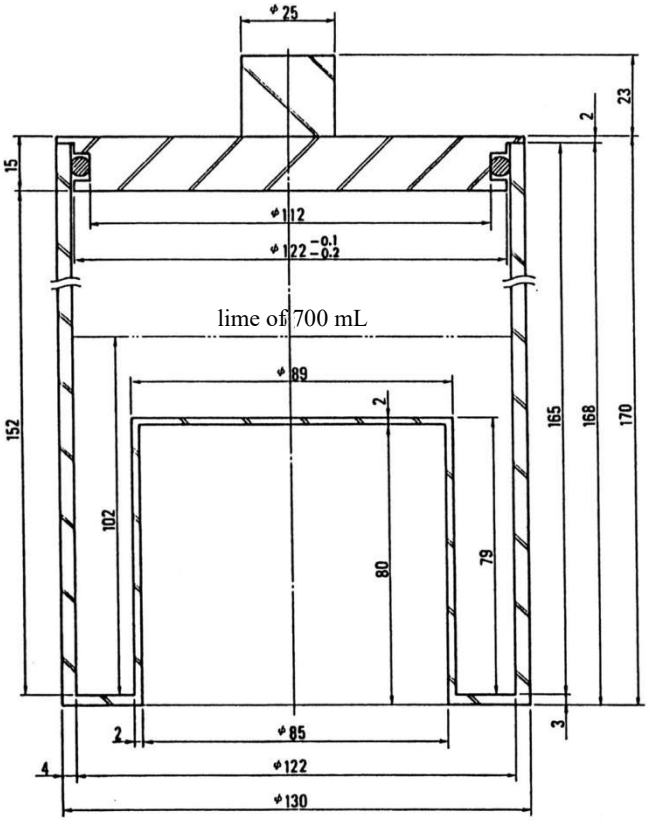

700-mL Marinelli-type vessel

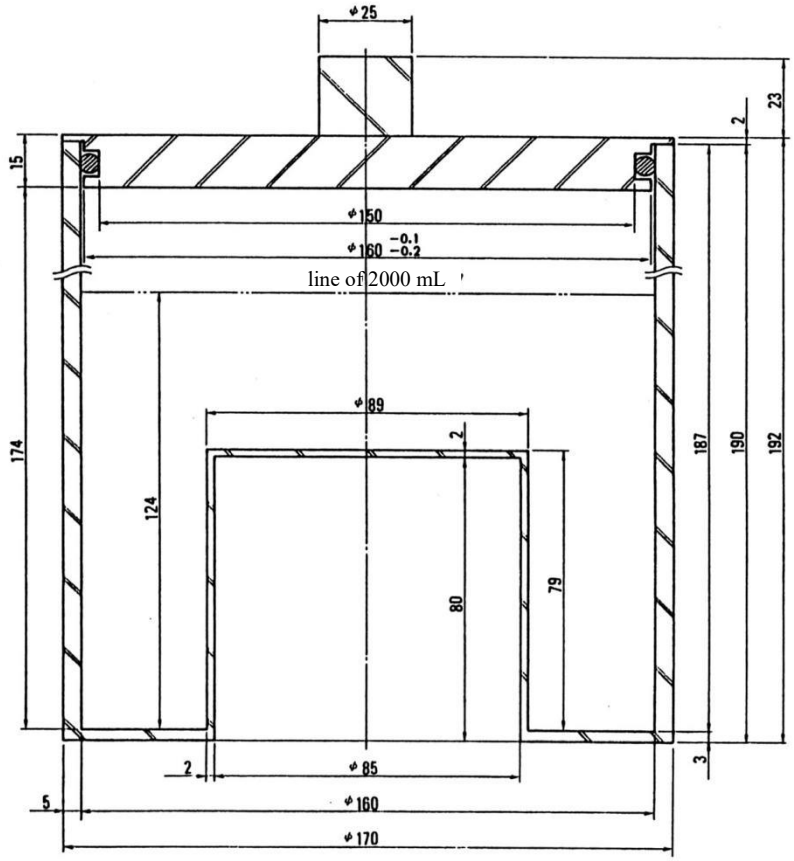

2-L Marinelli-type vessel

Fig. B.2.2 Cross-section of Marinelli-type vessels.

B.2 Sample filling

Using a germanium semiconductor detector, it is possible to quantify the concentration of radioactivity in a sample without separation and purification of the nuclides to be analyzed. Therefore, for environmental samples, the radioactivity is mostly measured as collected (solution or raw sample) or after simple pretreatments (dryness, incineration, precipitation). However, the volume of the measurement sample is larger than ones for which the advanced procedure of concentration is performed. Therefore, the following points should be noted:

- Cross-contamination with other samples should be avoided.
- Sample distribution in the vessel should not be dense nor coarse, but homogeneous.
- The sample should be fixed in the vessel so that it does not crumble down.

In this section the method for sample filling after pretreatment will be described. For sample pretreatments, refer to "Sample Pretreatment for Instrumental Analysis using Germanium Detector, etc." (No.13), and "Method for sampling of Environmental Materials" (No.16). For sample treatments during an emergency, refer to "Sample Pretreatment for γ-ray Spectrometry in Emergencies" (No.24). As a rough indication, when a sample in a U-8 vessel (bottom area: about 20 cm^2, inner volume: about 100 cm^3) is filled up to the boundary of the threaded part (hereafter let this height be the upper limit[*1], 5 cm for a U-8 vessel), the sample weight is about 20–70 g for ash samples, about 60–120 g for soil samples, and about 30g for dry samples. For a Marinelli-type vessel, to make the geometry consistent the sample must be filled up to the line indicated on the vessel. The most common volumes of Marinelli-type vessels are 700 mL and 2 L. For a 700 mL vessel, the net sample weight is in the range of 20–50 g for atmospheric floating dust to about 1000 g for soil. For a 2 L vessel, it is from about 1000 g for seaweed to about 2500 g for liquid or severed biological samples.

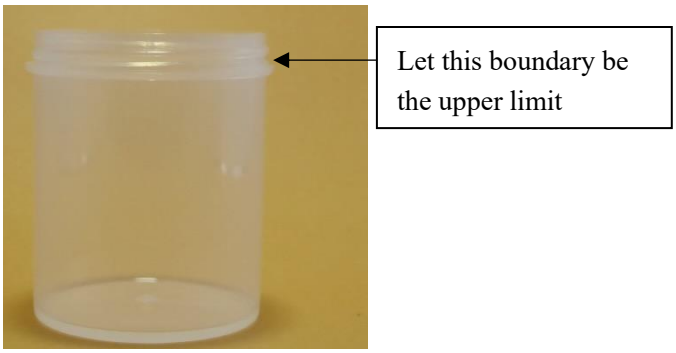

Fig. B.3 Upper height limit of a U-8 vessel.

[*1]: This height is set as the upper limit because if a sample is filled above this level the fill height cannot be precisely measured due to the roughness of the vessel.

B.2.1 Preparation for sample filling

Confirm the measurement sample by collating it with the reports of the collecting situation, etc. Write the information (the sample number, the sample collection date, the type of sample, the collection location, etc.) necessary to identify the sample on the measurement vessel.

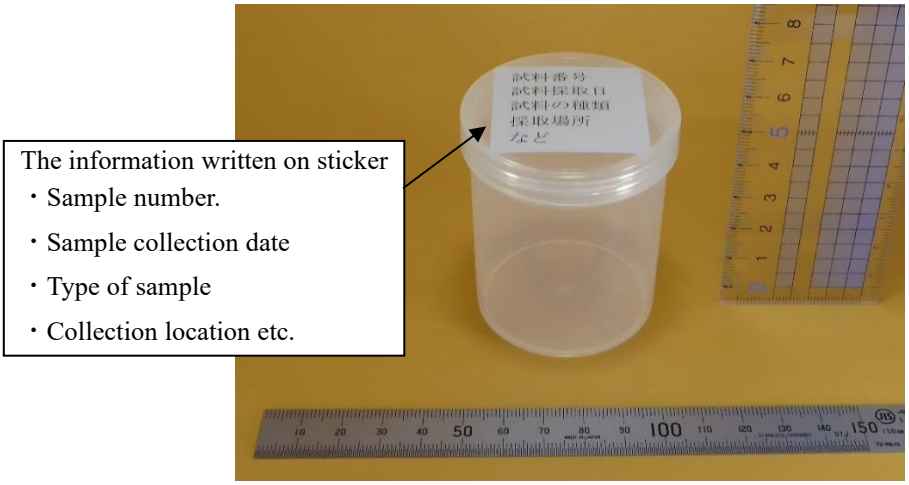

Fig. B.4 Example of a preparation of the sample measurement vessel.

B.2.2 Apparatuses necessary for sample filling:

・apparatuses common to all samples:

precision balance (a function to remove the tare is convenient)
ruler[*2] for the measurement of the sample fill height
acrylic disk (a disk with the same inner diameter as the bottom of the vessel)
thin (0.01–0.05 mm) polyethylene sheet
polyethylene bags for measuring vessel (from small size to large size)
disposable gloves (made of polyethylene, rubber, etc.)
paper towels, scissors, and a cutter

・soil, marine sediment, ash, and dry samples:

measurement vessel (small vessel of about 50–200 mL)
sample filling tool (an acrylic disk that has the same diameter as the inner diameter of the vessel bottom that is glued to a bar about 20 mm in diameter), spatula, etc.

・floating dust samples:

measurement vessel (small vessel of about 50–100 mL)

・water, raw, and dry samples:

measurement vessel (large vessel of about 0.5–2 L, Marinelli-type vessel, etc.)
a kitchen knife, a measuring cylinder (1–2 L), etc.

[*2] When the uncertainty has to be obtained, use tools whose tolerance is known or can be estimated (caliper or metallic straight scale with grade, etc.).

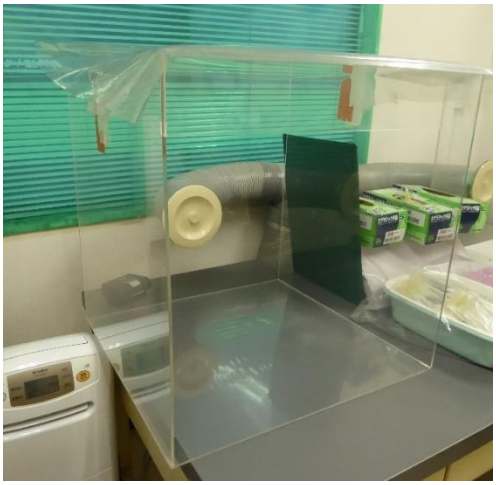

Fig. B.5 Example of a simple fume hood box for sample filling.

B.2.3 Method for filling a sample into a small vessel

Fill the sample at a place where cross-contamination will not happen, such as a fume box or hood. For ease of washing, it is convenient to make a simple transparent fume hood with an air vent out of vinyl chloride.

<Sample filling procedure>

(1) Soil, marine sediment, ash samples

(a) Before use, wipe the work area, for example the inside of the simple fume hood, with a paper towel moistened with pure water[*3].

(b) Wear disposable gloves and lay paper in the simple fume hood to make the clean-up after the procedure easier.

(c) Cover the pressing surface of the sample filling tool with a polyethylene sheet (- 0.01 mm thick).

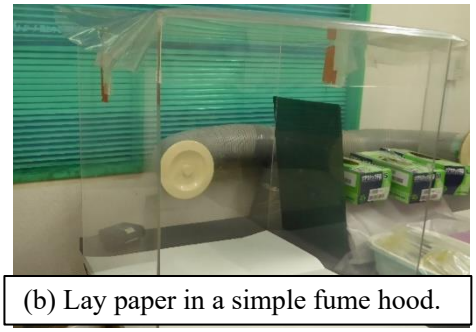

(b) Lay paper in a simple fume hood.

(c) Cover the pressing surface of the sample filling tool with a polyethylene sheet

Fig. B.6.1 Sample filling procedure (1).

(d) Weigh the measurement vessel (including the lid) with the precision balance.

(e) After stirring and thoroughly mixing the sample, put the sample into the measurement vessel in batches of about 1/5 of the total sample volume, being careful to take the batches evenly from the whole sample. If the entire sample is put in at once, the homogeneity of the sample will be reduced; an inhomogeneous distribution may influence the measured values (see Document 2).

[*3]: Organic solvents such as ethanol may cause erosion, depending on the material of the simple fume hood and the vessel.

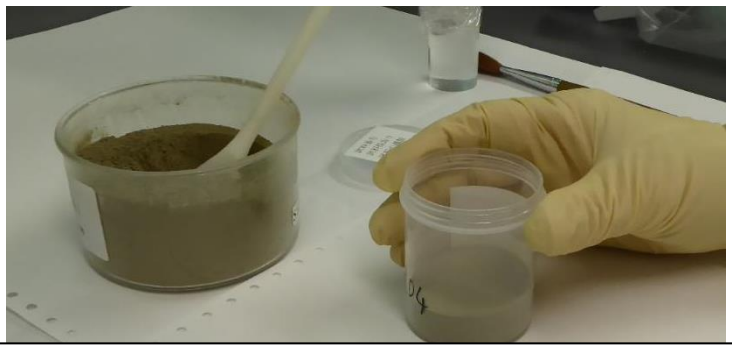

(e) Put the sample in the measuring vessel by dividing into several batches.

Fig. B.6.2 Sample filling procedure (2).

(f) When the first 1/5 of the sample batch is in, compact the sample to some extent by tapping repeatedly against a desk or other surface while keeping the vessel horizontal. Next, press the sample using a sample filling tool.
When using a filling tool, if too much force is used, the bottom of the vessel will break. It is recommended to apply your weight slightly on the vessel while remaining seated.

Soil：Relatively easy to fill into a vessel. Since the pulverized sample is easily dispersed into the air, be careful to avoid cross-contamination.

Marine sediment：Since a sandy sample is not hardened even when pressed, just reduce the number of voids by poking with a spatula or similar instrument. A pulverized sludge sample is not easily hardened, because the sample leaks from the edge of the vessel even when pressed by a filling tool. In this case, press the sample after it is fully compacted by increasing the initial tapping time. Also, be careful to avoid cross-contamination.

Ash sample：Easy to harden by pressing. However, when it is pressed with too much force, “cracks” will be introduced in the solidified sample. Apply an appropriate force. If cracks are introduced, pulverize with a spatula and press again (with less force).

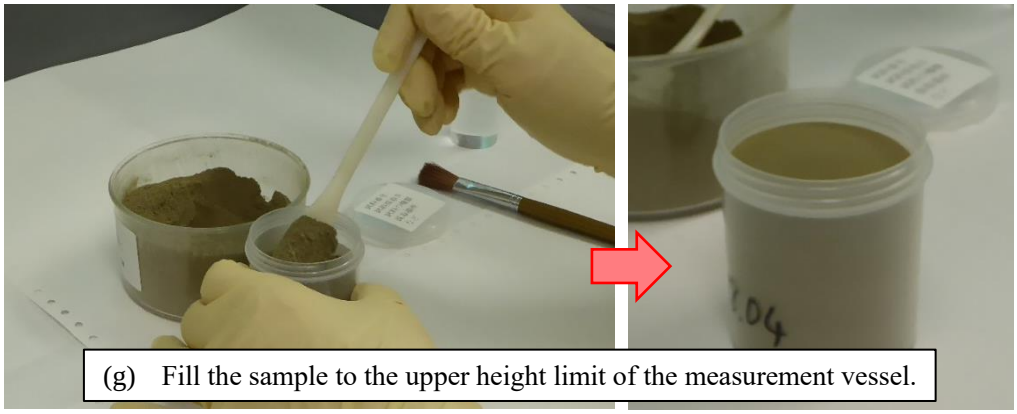

(g) Fill the sample to the upper height limit of the measurement vessel.

Fig. B.6.3 Sample filling procedure (3).

(g) Repeat steps (e)–(f), filling with all of the sample or to the upper height limit of the vessel. Be careful to avoid filling the sample to a height where the sample cannot be accurately measured.

(h) Flatten the top surface of the sample in the measurement vessel and remove any of the sample present on the screw thread and grooves of the vessel with a brush or other tool.

(i) Cover and weigh the vessel, and write the tare sample weight on the vessel. At this time, read to an accuracy of about 0.01g.

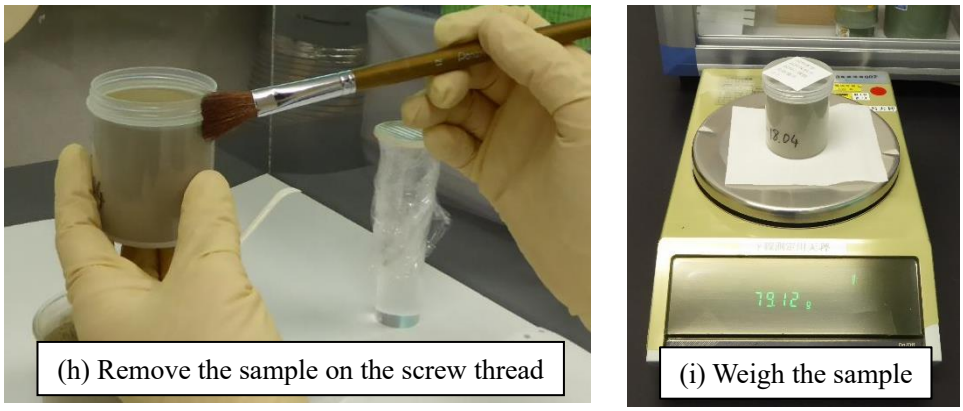

(h) Remove the sample on the screw thread

(i) Weigh the sample

Fig. B.6.4 Sample filling procedure (4).

(j) Measure the sample fill height from the inside of the vessel bottom and write it on the measurement vessel. At this time, measure it to an accuracy of about 0.05 mm by averaging values measured at about three or four sites.

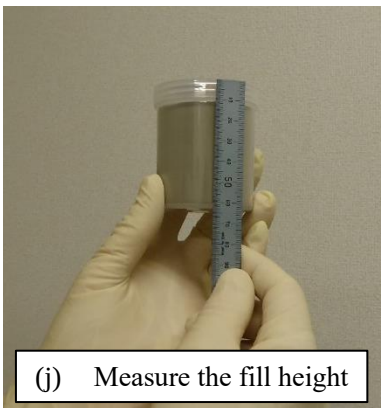

(j) Measure the fill height

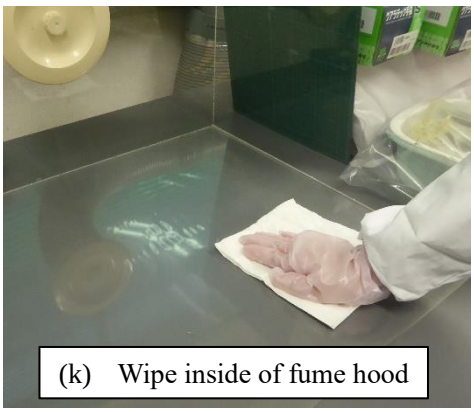

(k) Wipe inside of fume hood

Fig. B.6.5 Sample filling procedure (5).

(k) Wrap the polyethylene sheet covering the filling tool with the paper laid in the work area and throw it away. After removing and discarding the disposable gloves, put on new disposable gloves. Next, wipe the inside of the simple fume hood with a paper towel moistened with pure water.

(l) Remove and discard the disposable gloves, and wash the spatula, filling tool, ruler, brush, and hands, and then wipe off the water.

(If there are multiple samples, repeat steps (b)–(l) for each sample.)

(m) After filling the sample, put on disposable gloves. Then, carefully wipe the measurement vessel with a wet paper towel while taking care to avoid contamination and put it in a polyethylene bag. Do not directly touch the measurement vessel that has been wiped with a paper towel with a hand. Next, grab the sample with a hand inserted in the polyethylene bag and put it into the measurement vessel by turning the bag inside out. While leaving the bag inside out, evacuate the air and tie the inlet of the bag, and be careful to not cause wrinkling at the bottom of the measurement vessel.

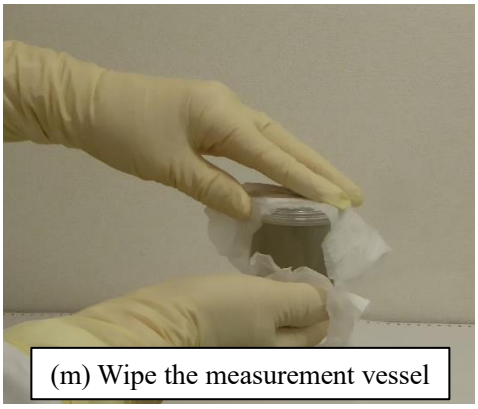

(m) Wipe the measurement vessel

(n) Put it in the bag

Fig. B.6.6 Sample filling procedure (6).

(n) After putting the sample in the polyethylene bag, remove and discard the disposable gloves and bring the sample to the measurement room.

(2) Dry sample

(a) Before use, wipe the work area, such as the inside of the simple fume hood, with a paper towel moistened with pure water.

(b) To make the clean-up after the procedure easier, lay a paper in the fume hood while wearing disposable gloves.

(c) Cover the pressing surface of the sample filling tool with a polyethylene sheet with a thickness of about 0.01 mm.

(d) Measure the weight of the measurement vessel (with the lid) with a precision balance.

(e) Finely pulverize the sample. If the sample is hard, use scissors or a similar tool. Then, ensure that the sample is well stirred and mixed.

(f) Fill with the entire sample or until the upper height limit is reached, whichever is first. If voids remain, it will not be possible to obtain accurate values due to the effects of inhomogeneous distribution of the sample (see Document 2).

(g) Flatten the upper surface of the sample in the measurement vessel. Next, cover and weigh it and write the tare sample weight on the measurement vessel. At this time, read to an accuracy of about 0.01g.

(h) Remove the lid, place an acrylic disk on the sample, press it down, then cover it again. At this time, it is recommended to roll a soft polyethylene sheet and put it onto the acrylic disk to fill the gap.

(i) Measure the sample fill height from the inside of the vessel bottom and write it on the measurement vessel. At this time, average the measured results from about three to four sites to an accuracy of approximately 0.5 mm.

(j) Wrap the polyethylene sheet covering the filling tool with the paper laid in the working area and throw it away. Next, remove and discard the disposable gloves. Then, after putting on new disposable gloves, wipe the inside of the simple fume hood with a paper towel moistened with pure water.

(k) Remove and discard the disposable gloves, and wash the spatula, filling tool, ruler, brush, and hands, and then wipe off the water. If there are multiple samples, repeat steps (b)–(k) for all samples.

(l) After filling the sample, put on disposable gloves. Then, carefully wipe the measurement vessel with a wet paper towel while taking care to avoid contamination, and place it in a polyethylene bag. Do not directly touch the measurement vessel after it has been wiped with a paper towel with a hand. Next, grab the sample with a hand inserted in the polyethylene bag and put it into the measurement vessel by turning the bag inside out. Leaving the bag inside out, evacuate the air and tie the inlet of the bag, and be careful to not cause wrinkles at the bottom of the measurement vessel.

(m) After putting the sample in the polyethylene bag, remove and discard the disposable gloves and bring the sample to the measurement room.

(3) Floating dust sample (for measuring filter papers)

(a) Wipe the work area, such as the inside of the simple fume hood, with a paper towel moistened with pure water.

(b) To make the clean-up process after the procedure easier, lay a paper in the fume hood.

(c) Measure the weight of the measurement vessel (with the lid) with a precision balance.

(d) Cut the filter paper with floating dust using scissors or a cutter according to the inner diameter of the bottom of the measurement vessel. For a large filter paper, cut out as much as possible from the same sample and evenly from the whole. For the method of folding a large filter paper refer to “Sample Pretreatment for Instrumental Analysis using

Germanium Detector, etc." (No.13), "Method for sampling of Environmental Materials" (No.16), and "Sample Pretreatment for γ-ray Spectrometry in Emergencies" (No.24).

(e) With the surface with floating dust facing the bottom, fill with all of the sample or to the upper height limit.

(f) Flatten the upper surface of the sample in the measurement vessel, cover and weigh, then write the tare sample weight on the measurement vessel. At this time, read to an accuracy of about 0.01 g.

(g) Remove the lid, place an acrylic disk on the sample and press it down, then cover again. At this time, it is recommended to roll a soft polyethylene sheet and put it onto the acrylic disk to fill the gap.

(h) Measure the sample fill height from the inside of the vessel bottom and write it on the measurement vessel. At this time, average the measured results at about 3 to 4 points, and measure at an accuracy of about 0.5 mm.

(i) Discard the paper laid in the work area and remove and discard the disposable gloves. Then, after putting on new disposable gloves, wipe the inside of the simple fume hood with a paper towel moistened with pure water.

(j) Remove and discard the disposable gloves. Wash the scissors, cutter knife, ruler, and hands, and wipe all water of them. If there are multiple samples, repeat steps (b)–(j) for all samples.

(k) After filling the sample, put on disposable gloves. Then, carefully wipe the measurement vessel with a wet paper towel while taking care to avoid contamination, and place it in a polyethylene bag. Do not directly touch the measurement vessel after it has been wiped with a paper towel with a hand. Next, grab the sample with a hand inserted in the polyethylene bag and put it into the measurement vessel by turning the bag inside out. While leaving the bag inside out, evacuate the air and tie the inlet of the bag, and be careful to not cause wrinkles at the bottom of the measurement vessel.

(l) After putting the sample in the polyethylene bag, remove and discard the disposable gloves and bring the sample to the measurement room.

B.2.4 Method to fill the sample in a Marinelli-type vessel

For liquid samples such as land water, rainwater, river water, seawater, and milk, directly place them into a measurement vessel. For raw samples containing lots of water such as vegetables and fruits, chop them finely with a kitchen knife or other tool. For non-fibrous samples, a mixer may be used; however, when there are multiple samples, cleaning will be hard work, so this situation should be avoided. For dry samples, chop finely as described in Section B.2.3.

<Sample filling procedure>

(a) Before use, wipe the work area, such as the inside of the simple fume hood, with a paper towel moistened with pure water.

(b) To make the clean-up process after the procedure easier, lay a paper in the simple fume hood while wearing disposable gloves.

(c) Set an inner bag inside of the Marinelli-type vessel and measure the weight. For a dry sample, include the acrylic disk in the weight measurement.

(d) Stir and mix the sample well before placing it in the inner bag. If voids remain, it will not be possible to obtain accurate measurement values due to the effects of inhomogeneous distribution of the sample (see Document 2). Therefore, take care to avoid creating voids while filling the sample.

Solution and raw samples: Fill the sample up to the marked line on the Marinelli-type vessel.

Dry sample: Fill the sample to the top of the marked line on the Marinelli-type vessel, then press the upper surface using an acrylic disk. Push the disk, and confirm that the sample thickness is on the same level with the marked line on the vessel.

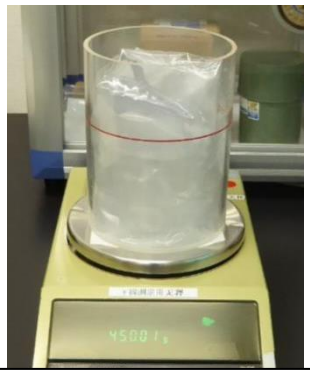

(c) Measure weight of the vessel.

(d) Fill the sample up to the scale on the Marinelli-type vessel.

Fig. B.7.1 Sample filling procedure (Marinelli-type vessel 1).

(e) After filling the sample, measure the weight. Then, write the tare sample weight on a piece of plastic tape attached to the vessel. At this time, read to an accuracy of about 0.01 g.

(f) Close the inlet of the inner bag with plastic tape. Next, secure the lid with plastic tape so that the liquid does not leak. For dry samples, it is recommended to roll a soft polyethylene sheet and put it onto the acrylic disk. Then, press it from the upper side down to the scale on the vessel.

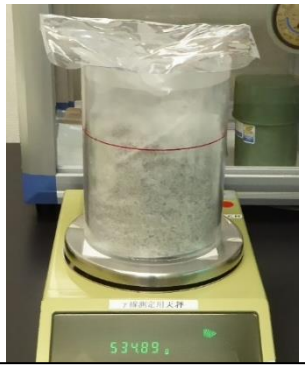

(e) Measure the weight of the sample.

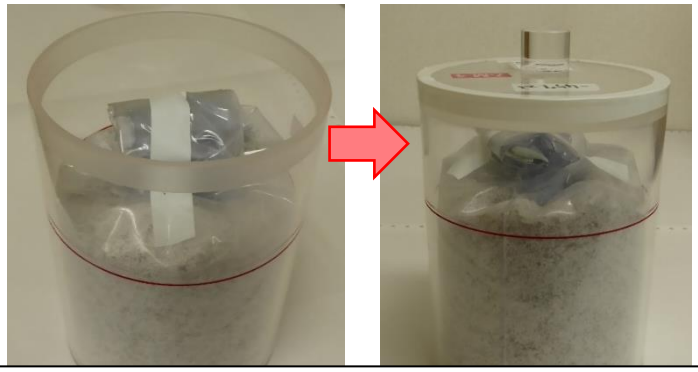

(f) Close the inlet of the inner bag and cover it with the lid.

Fig. B.7.2 Sample filling procedure (Marinelli-type vessel 2).

(g) After discarding the paper laid in the working area, remove and discard the disposable gloves. Then, put on new disposable gloves and wipe the inside of the simple fume hood with a paper towel moistened with pure water.

(h) Remove and discard the disposable gloves and wash the spatula, ruler, brush, and hands, then wipe off all of the water. If there are multiple samples, repeat steps (b)–(h) for all samples.

(i) Wearing disposable gloves, wipe the Marinelli-type vessel with a paper towel moistened with pure water while being careful to avoid contamination. Do not directly touch the Marinelli-type vessel after it has been wiped by the paper towel.

(j) Put the Marinelli-type vessel in a polyethylene bag, remove the air inside, and close the inlet of the bag with plastic tape. Considering that the detector enters the concave part at the bottom of the vessel, close the inlet while pressing the bag onto the concave part, so that enough space can be made from the top of the polyethylene bag to the concave part.

(k) After sealing the polyethylene bag, remove and discard the disposable gloves and bring it to the measurement room.

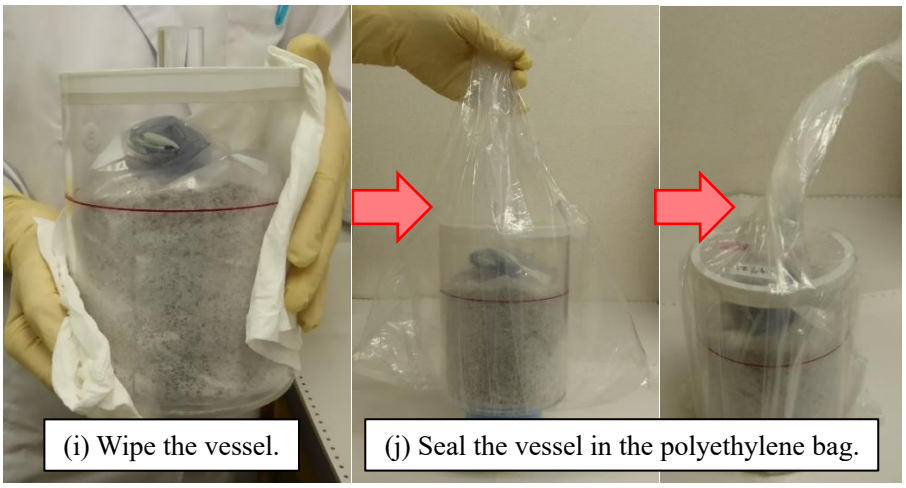

Fig. B.7.3 Sample filling procedure (Marinelli-type vessel 3).

B.2.5 Other sample filling methods

In addition to the samples discussed above, there are samples where special pretreatments were conducted. For example, there are samples that were solidified by machine pressing and samples that were precipitated by chemical treatments. These samples required different filling methods depending on the pretreatments. For similar samples, please refer to “Sample Pretreatment for Instrumental Analysis using Germanium Detector, etc.” (No.13), “Method for sampling of Environmental Materials” (No.16), and “Sample Pretreatment for γ-ray Spectrometry in Emergencies” (No.24). Even in these cases, the abovementioned procedures (e.g., filling samples in as large amounts as possible so that no voids are generated and writing the information necessary for the sample identification on the vessel) are important.

Explanation C Evaluation of uncertainty in Gamma-ray spectrometry

Uncertainty of measurement is one indication of the reliability of measurement results. The definition of measurement uncertainty is "a parameter accompanied by a measurement, which characterizes the scattering of the values that can be rationally connected to the amount to be measured." [10]. Here, notably, a measurement uncertainty is not the scatter in respective measurement results, but the value representing potential fluctuation in a series of measurements.

For measurements of environmental samples using γ-ray spectrometry, the quantity being measured is the radioactivity per unit amount (e.g. weight and volume) of the measured sample (hereafter "radioactivity concentration"). Perfectly defining the measurement uncertainty through identifying all conditions that may influence the radioactivity concentration is difficult. In addition, because the generation of radiation is a statistical phenomenon, there are always statistical fluctuations in the counts obtained using a measurement. Considering these facts, it is almost impossible to obtain true values of radioactivity concentrations. No matter how precisely the measurements and analyzes are performed in the course of a series of measurements, in general the obtained results will be only an approximation or an estimation of the true values of the radioactivity concentration. Furthermore, owing to such imperfection in the measurement, the obtained final results contain errors in a certain range.

In γ-ray spectrometry, a detector does not directly measure the radioactivity concentration, but counts the number of γ-rays, whose total energy is absorbed by interacting with the detector, among γ-rays emitted from nuclides to be measured. For this reason, the radioactivity concentration is obtained not only from the detected count values, but from other information, such as various correction factors (summing-effect, self-absorption, and radioactivity decay), amount of measured sample, γ-ray emission rate, counting efficiency of the detector, and measuring time. In other words, the radioactivity concentration can be thought of as a function of these input amounts, which is expressed by the following equation,

$$A = f(x_1, x_2, x_3, \cdots, x_n) = f(N, m, t, \varepsilon, \gamma, \cdots) \tag{C.1}$$

where A is the radioactivity concentration, $f(x_1, x_2, x_3, \cdots, x_n)$ is the function expressing the calculation from which the radioactivity concentration is derived, and $N, m, t, \varepsilon, \gamma, \cdots$ are the input amounts necessary to obtain the radioactivity concentration.

The standard uncertainty of radioactivity concentrations can be obtained by combining the uncertainties of all the input amounts related to the derived radioactivity concentration, considering the respective sensitivity coefficients. If all input values are independent (no correlation), the uncertainty in the respective input amounts is combined according to the following equation,

$$u(A) = \sqrt{\sum_{i=1}^{n} \left\{ \frac{\partial f}{\partial x_i} u(x_i) \right\}^2} \tag{C.2}$$

where $u(A)$ is the combined standard uncertainty of radioactivity concentration, and $u(x_i)$ are the standard uncertainties of the input amounts $x_1, x_2, x_3, \cdots, x_n$.

In equation (C.2), the derivative coefficient $\partial f / \partial x_i$ is termed the sensitivity factor, which describes how the output amount A changes with respective changes in the input amounts $x_1, x_2, x_3, \cdots, x_n$. For example, the change in the output amount A generated by a small change Δx_i in the input amount x_i is given by $(\Delta A)_i = (\partial f / \partial x_i)(\Delta x_i)$. If this change is generated by the

standard uncertainty of the input amount, x_i, the change in the corresponding output amount A is $(\partial f/\partial x_i)u(x_i)$. Note that a standard uncertainty refers to scattering and is expressed by the standard deviation. The evaluation of standard uncertainty for the respective input amounts is performed by classifying them into types A and B, as described later.

Furthermore, if the output amount A can be expressed by multiplying/dividing the input amounts, $x_1, x_2, x_3, \cdots, x_n$, the relative standard uncertainty for the output amount can be obtained by the square root of the sum of squares for the relative standard uncertainty of the respective input amount. Therefore, equation (C.2) can be rewritten as the following,

$$\frac{u(A)}{A} = \sqrt{\sum_{i=1}^{n} \left\{ \frac{u(x_i)}{x_i} \right\}^2} \qquad \text{(C.3)}$$

where $u(A)/A$ is the relative combined standard uncertainty of radioactivity concentration and $u(x_i)/x_i$ is the relative standard uncertainty of the input amounts $x_1, x_2, x_3, \cdots, x_n$.

In this commentary, the uncertainty will be evaluated using equation (C.3).

C.1 Procedure to evaluate uncertainty

Generally, the measurement uncertainty is evaluated using the following procedure.

(a) Choose factors that will influence the measurement results, and arrange them into a model formula for the measurement.
(b) On the basis of the model formula, consider the factors of the uncertainty.
(c) The uncertainty is evaluated for the factor of each uncertainty.
(d) Combine all individual uncertainties to obtain the uncertainty on the measurement results.

The outline below follows the procedure above for uncertainty evaluation.

(a) Choose the factors that will influence the measurement results, and arrange them into a model formula.

From the measurement procedure and the tolerance criteria by accuracy control etc., fully choose the factors that will influence the final measurement results, and arrange them into a model formula.

(b) On the basis of the model formula, determine the uncertainty factors.

The uncertainty factors in quantifying radioactivity concentrations by γ-ray spectrometry are roughly divided into three types:

i Uncertainty related to the sample to be measured.
ii Uncertainty related to the peak efficiency calibration.
iii Uncertainty related to the sample measurement.

For each item, further detailed factors are considered. Fig. C.1 shows a example diagram of uncertainty factors, which was drawn to specify certain factors. It should be noted that there may be other factors that can influence the measurement results in addition to those factors shown in Fig. C.1.

(c) Evaluate uncertainty for each uncertainty factor

The method to evaluate uncertainty is divided into two types; type A evaluation and type B evaluation.

Type A evaluation is a method for evaluating uncertainty based on statistical analysis for a series of measurement values. Specifically, the standard uncertainty is determined for each factor by obtaining an experimental standard deviation value from repeated measurements.

Type B evaluation is based on procedures other than statistical analysis of a series of measurement values. Specifically, evaluation is performed using scientific judgment based on all obtainable information for fluctuations that may possibly happen. Examples of such obtainable information areg:

— Previously measured data, such as the characteristics of the measuring instrument determined by oneself prior to the sample measurement and temporal changes in peak efficiency.
— General knowledge or experience about the material involved and the behavior or properties of the measurement instrument.
— Specifications from the manufacturer
— Data provided in certificates, such as calibration certificates
— Uncertainty assigned to reference data cited from a handbook

Not all factors of each uncertainty contribute significantly to the uncertainty of the measurement results to be evaluated. The procedure involves each uncertainty being evaluated, and then combining the uncertainties to obtain their contributions to the overall uncertainty. In this procedure, evaluating items that make little or no contribution is not always necessary.

(d) Combine all individual uncertainties to obtain the measurement uncertainty results.

Combine all individual uncertainties obtained in the abovementioned procedure (c) to obtain the combined standard uncertainty.

The combined standard uncertainty obtained in procedure (d) above represents the standard deviation associated with the measurement results. If it is necessary to determine a region in which the real value is likely to be contained, multiply the combined standard uncertainty by the inclusion factor k to obtain the extended uncertainty. The value of k, which is determined by the reliability level and the t-distribution, is generally selected in the range 2–3. In γ-ray spectrometry, because the measurement results can be regarded as following a normal distribution, a value of $k = 2$ is obtained when the reliability level is about 95 %. When reporting the measurement results, an explanation of the meaning of the measured uncertainty value given is often required (statement of whether it is the combined standard uncertainty, or the extended uncertainty ($k = 2–3$)).

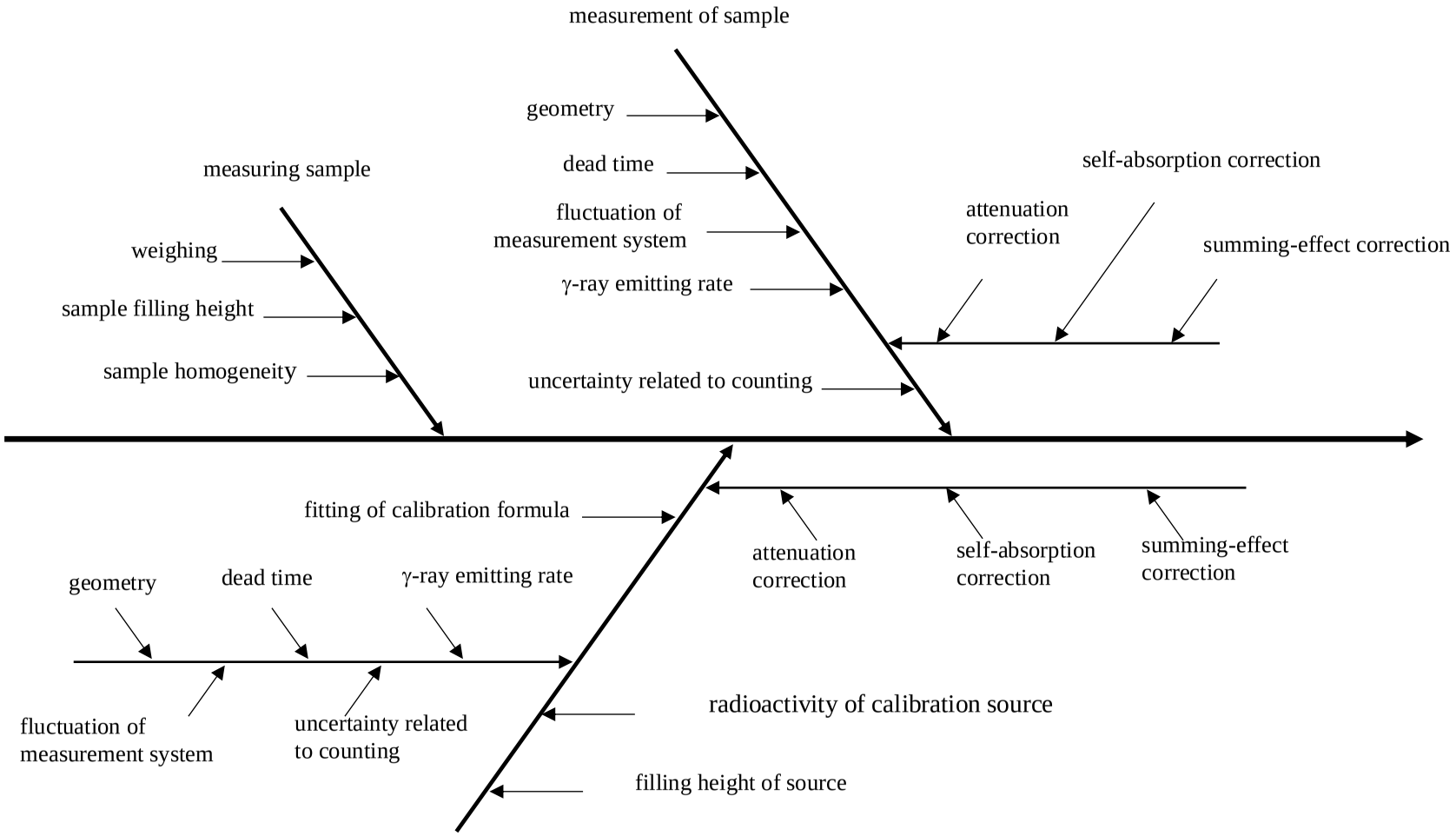

Fig. C.1 Diagram for uncertainty factors in γ-ray spectrometry.

C.2 Uncertainty calculation procedure

C.2.1 Uncertainty related to the measured sample

C.2.1.1 Weighing (u_1)

Use the uncertainty (equation for uncertainty) described in the calibration certificate. If the described uncertainty is not the relative value, calculate the relative standard uncertainty using the following formula,

$$u_1 = \frac{u(w)}{w} \tag{C.4}$$

where $u(w)$ is the uncertainty of the weighed value (g), and w is the weighed value (g).

If there is no description in the calibration certificate, evaluate the uncertainty owing to rounding errors of the indicated values of the measurement instrument and the uncertainty owing to the accuracy of repeated measurements, by referencing the following explanations. Then, obtain the uncertainty of weighing by combining these two uncertainty types.

(1) Uncertainty owing to rounding error of indicated values

Assuming the read limit (minimum scale) of the electronic balance to be l, the uncertainty exhibits a rectangular distribution, where both at the zero point and at the weighed value, the upper and lower limits are $\pm l/2$, respectively. Calculate the relative standard uncertainty from the triangular distribution where the upper and lower limits are $\pm l$, respectively, obtained by combining the two distributions. Note that the standard deviation of a triangular distribution can be obtained by dividing the half-width of the distribution by $\sqrt{6}$ as follows,

$$u_{1a} = \frac{l}{\sqrt{6}w} \tag{C.5}$$

where l is the read limit (g), and w is the weighed value (g).

(2) Uncertainty owing to the accuracy of repeated measurements

The uncertainty related to one weighing can be obtained as a relative value against the average value of the standard deviations by repeatedly measuring a weight close to that of the sample to be measured many times (approximately 10 times), which is represented in the following equation,

$$\frac{w_{STD}}{\bar{w}} \tag{C.6}$$

where $\bar{w}$ is the average value (g) of the repeated measurements, and w_{STD} is the standard deviation (g) of the repeated measurements.

In weighing a real sample, when the measurement is performed only once, the uncertainty is given by the above equation. However, when an average value is adopted as a weighed value by measuring multiple times, the relative standard uncertainty of the weighed value is given by the following equation, assuming the number of the measurements to be n. Note that in the case of a single measurement, equations (C.6) and (C.7) coincide, because $n = 1$.

$$u_{1b} = \frac{w_{STD}}{\bar{w}} \times \frac{1}{\sqrt{n}} \tag{C.7}$$

(3) Uncertainty related to weighing

The relative standard uncertainty is obtained by combining u_{1a} with u_{1b}, as follows,

$$u_1 = \sqrt{(u_{1a})^2 + (u_{1b})^2} \tag{C.8}$$

【Calculation example】

In the case there is no description in the calibration certificate, when the weighed value of an electronic balance with a 0.01 g read limit is 20.06 g, the following equation holds.

$$u_{1a} = \frac{0.01}{\sqrt{6} \times 20.06} = 0.0002035$$

Let us consider the case where the results shown in Table C.1 were obtained using repeated measurements.

Table C.1 Results for repeated measurements of weight.

number	1	2	3	4	5	6	7	8	9	10
Measured value (g)	20.05	20.05	20.06	20.05	20.07	20.06	20.07	20.06	20.05	20.06

Average of measured values：20.06g

Standard deviation ：0.007888g

From equation (C.6), the uncertainty related to one weighing is obtained as follows.

$$\frac{0.007888}{20.06} = 0.0003932$$

When weighing a sample, the value from one measurement is generally adopted, so the following equation holds.

$$u_{1b} = 0.0003932 \times \frac{1}{\sqrt{1}} = 0.0003932$$

Therefore, the weighing uncertainty is obtained by the following equation.

$$u_1 = \sqrt{0.0002035^2 + 0.0003932^2} = 0.0004427\ (0.04427\%)$$

C.2.1.2 Sample filling height (u_2)

A sample filling height is not a direct input value in equation (C.1). Therefore, the uncertainty for the filling height of a sample is evaluated not by the uncertainty value for the measurement of the filling height itself, but by the amount of fluctuation in the peak efficiency against the amount of fluctuation in the filing height. The evaluation procedure is to first determine the uncertainty owing to the accuracy of the measurement instruments and that owing to the accuracy of the repeated measurements. Then, combining these uncertainties provides the uncertainty in the filling height measurement. Next, the fluctuation in the peak efficiency against that of the filling height is evaluated to obtain the uncertainty (u_2) in the sample filling height. In this procedure, the standard energy of the evaluation is set to be 661.7 keV[*1].

[*1]: Since a peak efficiency curve moves nearly in parallel with changes in filling height (see Document 1.2), there is no difference in the evaluation with different energy values.

(1) Uncertainty owing to accuracy of the measurement instrument

The uncertainty is calculated by assuming a rectangular distribution, using the tolerance of the measuring instrument as the upper and lower limits. Note that the standard deviation of a rectangular distribution can be obtained by the half-width of the distribution divided by $\sqrt{3}$, as follows,

$$u_{2a} = \frac{l}{\sqrt{3}h} \tag{C.9}$$

where l (mm) is the tolerance of the measurement instrument and h (mm) is the filling height of the sample being measured.

The tolerances of a caliper and a metallic straight scale are shown in Tables C.2 and C.3, respectively.

Table C.2 Tolerance of caliper (JIS B7507:2016).

Measured length (mm)	Scale, minimum display value or read limit (mm)	
	0.1 or 0.05	0.02 or 0.01
less than 50	±0.05	±0.02
50－100	±0.06	±0.03

Table C.3 Tolerance of metallic straight scale (JIS B7516:2005).

grade	Tolerance length (mm)
1st grade	$\pm[0.10 + 0.05(L/0.5)]$
2nd grade	$\pm[0.10 + 0.10(L/0.5)]$

(Note 1) L is a value where the measured length is represented in meters, and so does not have a unit.

(Note 2) For calculated values of L/0.5, fractions less than 1 are rounded up to an integer value.

(2) Uncertainty owing to the accuracy of repeated measurements

The uncertainty related to one measurement can be obtained as a relative value against the average value of the standard deviation, by performing repeated measurements (approximately 10) for a sample that has nearly the same filling height as the sample to be measured.

$$\frac{h_{STD}}{\bar{h}} \tag{C.10}$$

where $\bar{h}$ is the average value (mm) of repeated measurements, and h_{STD} is the standard deviation (mm) of the repeated measurements.

In the filling height measurement for a real sample, the uncertainty of one measurement is given by the above equation. On the other hand, when the average value for multiple measurements is adopted as a filling height, the relative standard uncertainty on the filling height is given by the following equation, assuming n to be the number of the measurements. Here, note that in the case where only one measurement is performed, equations (C.10) and (C.11) coincide because $n = 1$.

$$u_{2b} = \frac{h_{STD}}{\bar{h}} \times \frac{1}{\sqrt{n}} \tag{C.11}$$

(3) Measurement uncertainty for sample filling height

The relative standard measurement uncertainty of the filling height is obtained by combining u_{2a} and u_{2b}.

$$u_{2c} = \sqrt{{u_{2a}}^2 + {u_{2b}}^2} \tag{C.12}$$

(4) Fluctuation in efficiency against the fluctuation of filling height

Here, substitute the filling height h and the "filling height + uncertainty" term, $h + h \cdot u_{2c}$, respectively, into the following equations, calculate the peak efficiency, and evaluate the fluctuation in peak efficiency with respect to the fluctuation of the sample filling height (the energy of the evaluation standard is set to be 661.7 keV).

$$\frac{1}{\varepsilon} = a + bh + ch^2 \tag{C.13}$$

$$u_2 = \frac{|\varepsilon_2 - \varepsilon_1|}{\varepsilon_1} \tag{C.14}$$

Where ε is the peak efficiency, a, b, c are the constants, h is the filling height (mm) of the sample being measured, ε_1 is the value of ε at the filling height h, and ε_2 is the value of ε at the filling height $h + h \cdot u_{2c}$.

【Example calculation】

When a filling height of 10 mm is measured with a metallic straight scale (1st grade), the tolerance is calculated to be ±0.15 from Table C.3. Therefore, the following relation is obtained.

$$u_{2a} = \frac{0.15}{\sqrt{3} \times 10} = 0.008660$$

Let's consider the case where the results shown in Table C.4 were obtained by repeated measurements.

Table C.4 Results for the repeated measurements of filling height.

Number of times	1	2	3	4	5	6	7	8	9	10
Measured value (mm)	10.0	10.0	10.0	10.5	10.0	10.5	10.5	10.0	10.0	10.0

Average of the measured values：10.15 mm

Standard deviation：0.2415 mm

From equation (C.6), the uncertainty related to one weighing is obtained as follow:.

$$\frac{0.2415}{10.15} = 0.02379$$

Because the average of three measurement values is generally adopted for the sample filling height, the following equation is obtained:

$$u_{2b} = 0.02379 \times \frac{1}{\sqrt{3}} = 0.01374$$

Thus, the measurement uncertainty for the sample filling height is obtained by:

$$u_{2c} = \sqrt{0.008660^2 + 0.01374^2} = 0.01624$$

Next, calculate the effect of the filling height measurement uncertainty on the peak efficiency. When the filling height is 10 mm, substituting $h_1 = 10$ and $h_2 = 10 + 10 \times 0.01624 = 10.1624$ into the following height calibration formula at 661.7 keV (this can be confirmed using an analysis program),

$$1/\varepsilon = 25.96624 + 0.7599944 \times h + 0.0005517124 \times h^2$$

yields the following values:

$$\varepsilon_1 = 0.029743$$
$$\varepsilon_2 = 0.029683$$

Therefore, the uncertainty of the sample filling height is obtained by the following equation.

$$u_2 = \frac{|0.029683 - 0.029743|}{0.029743} = 0.002017\ (0.2017\%)$$

C.2.1.3 Homogeneity of sample

This quantity does not need to be evaluated.

An uneven distribution of radioactive nuclides in a measurement vessel significantly affects the measurement values, so estimating the uncertainty is difficult (see Document 2.1). Therefore, fully mixing the measured sample is necessary during the sample preparation, and to homogeneously fill the measuring vessel with it. Nevertheless, it is possible to estimate the uncertainty owing to sample homogeneity via changing the distribution of radioactive nuclides in a measurement vessel using a Monte Carlo simulation [11] (see Document 2.2).

C.2.2 Uncertainty related to calibration of peak efficiency

A peak efficiency is generally obtained by the following method. First, the peak efficiency obtained by measuring a calibration source (measured value) is expressed as a function of the energy (peak efficiency curve). Then, the peak efficiency is calculated from this peak efficiency curve. To obtain the uncertainty related to the peak efficiency calibration, the uncertainty of the peak efficiency curve must be calculated, including the function fitting. However, at present, a precise evaluation of this is considered difficult[*2]. Therefore, in this commentary, the uncertainty will be evaluated under the following conditions[*3].

(a) First, a peak efficiency curve is divided into two regions: a highly curved low-energy region, and a high-energy region where the curve is approximately linear. Then, the uncertainties for each respective region are evaluated by fitting using two functions. Note that for the calculation example given in this commentary, the energy that divides the respective regions is set to be in the range 166–320 keV.
(b) For various factors, such as the uncertainty of the nuclide concentration in a calibration source, the maximum value in the respective divided region is adopted as the uncertainty in the respective energy regions.
(c) The uncertainty owing to fitting of a function is evaluated based on information about the deviation between the measured value and fitted values. Note that at least three or more γ-ray energies are used for fitting.

[*2]: There are examples where the uncertainties in peak efficiency curves were strictly evaluated [25] [26].

[*3]: This evaluation method was adopted as "Radioactivity Analysis Confirmation Survey, FY2007", entrusted by the Energy Measures Special Account Consignment Business, Ministry of Education, Culture, Sports, Science and Technology. Thereafter, it has been continuously used for mutual comparison analysis among prefectures [28] [29].

C.2.2.1 Filling height of radiation source (u_3)

Similar to C.2.1.2 filling height of sample

$$u_3 = \frac{|\varepsilon_2 - \varepsilon_1|}{\varepsilon_1} \quad \text{(C.15)}$$

C.2.2.2 Radioactivity of calibration source (u_{4L}、 u_{4H})

For each nuclide contained in a calibration source, the relative standard uncertainties are obtained from the uncertainties described in the calibration certificate by division into low- and high-energy regions. The maximum value of these uncertainties is used as the relative standard uncertainty.

【Example calculation】

When the uncertainty for each nuclide concentration, described in the calibration certificate of a calibration source, is the value shown in Table C.5, the following values are obtained.

Table C.5 Uncertainty described in the calibration certificate of a calibration source.

Nuclide	^{109}Cd	^{57}Co	^{139}Ce	^{51}Cr	^{137}Cs	^{54}Mn	^{88}Y	^{60}Co
Standard deviation Uncertainty (%)	2.75	2.6	2.6	2.65	2.6	2.55	2.55	2.55

Low-energy region: $u_{4L} = 2.75\ \%$

High-energy region: $u_{4H} = 2.65\ \%$

(Note 1) If the relative extended uncertainty ($k = 2$) is described in the calibration certificate, the value of the uncertainty is divided by 2 to obtain the relative standard uncertainty.

(Note 2) When multiple sources are used for calibration, the relative standard uncertainties for all nuclides in the calibration sources are obtained in the respective low-energy and high-energy regions. Then, the maximum value of the obtained uncertainties is used as the relative standard uncertainty.

C.2.2.3 Geometry (positional relationship between detector and source)

This factor does not need to be evaluated.

If an instrument is designed so that a source can be set at a predetermined position using tools, such as a specific holder, the uncertainty owing to the geometry would be small and considered negligible compared to other factors, so it is omitted. An example of peak area changes owing to geometry is shown in Table C.6. In this case, using a coaxial p-type detector with a relative efficiency of 31% and a multi-nuclide mixed volumetric source (U-8 vessel, made of alumina, filling height of 4.7 cm), the source was moved horizontally from the center of the detector to a 1 mm offset position. From Table C.6, it is evident that even when the position of the source moves by 1 mm from the center, no significant difference is found in the peak area; thus, the uncertainty can be determined to be sufficiently small.

Table C.6 Comparison of peak areas caused by differences in position setting.

Setting position	Energy of γ-ray		
	88.0 keV	661.7 keV	1332.5 keV
Center	28628.7 ± 196.2	54974.4 ± 241.6	32707.8 ± 182.2
1 mm form the center	28964.3 ± 197.1	54318.7 ± 240.5	32984.7 ± 182.7
Ratio to the center	1.012 ± 0.010	0.988 ± 0.006	1.008 ± 0.008

C.2.2.4 Dead time

Uncertainty originating from dead time (a period when the detector circuit is not operating) is small and insignificant compared with other factors, so it is omitted.

C.2.2.5 Fluctuation in measurement system

Uncertainty originating from the fluctuations in a measurement system within the time of calibration is small and considered insignificant compared with other factors, so it is omitted.

C.2.2.6 Uncertainty related to counting (u_{5L}, u_{5H})

The relative standard uncertainty is calculated from the uncertainty related to the peak area and counting. In this calculation, of the relative standard uncertainty calculated for each nuclide, the maximum value in the low-energy and high-energy regions are each used as the relative standard uncertainty in that region. Thus, the uncertainty is calculated from the following equation,

$$u_5 = \frac{\sigma_N}{N} \tag{C.16}$$

where N is the peak area and σ_N is the uncertainty related to counting.

【Example calculation】

For the results shown in Table C.7 obtained by measurements of a calibration source, the following values are obtained.

Table C.7 Results for measurements of calibration source.

Nuclide (energy)	Peak area (count)	Uncertainty related to counting	Relative standard uncertainty (%)
^{109}Cd (88.0 keV)	159954.7	455.3	0.2846
^{57}Co (122.1 keV)	240783.0	541.1	0.2247
^{139}Ce (165.9 keV)	178768.4	475.8	0.2662
^{51}Cr (320.1 keV)	280192.4	548.5	0.1958
^{137}Cs (661.7 keV)	73158.2	294.3	0.4023
^{54}Mn (834.8 keV)	76776.8	291.4	0.3795
^{88}Y (898.0 keV)	62889.9	268.0	0.4261
^{60}Co (1173.2 keV)	59521.3	253.3	0.4256
^{60}Co (1332.5 keV)	52916.9	237.6	0.4490
^{88}Y (1836.1 keV)	34687.4	189.0	0.5449

Low-energy region: $u_{5L} = 0.2846$ %

High-energy region: $u_{5H} = 0.5449$ %

(Note) If multiple sources are used in the calibration, the maximum value of the relative standard uncertainty for all nuclides is used in both the low-energy and the high-energy region.

C.2.2.7 γ-ray emission rate (u_{6L}, u_{6H})

The relative standard uncertainty to be used is obtained by calculating the relative uncertainty in reference to the nuclear data used in the analysis. Note that of the calculated relative uncertainty, the maximum values in both low-energy and high-energy regions are used as the relative standard uncertainty in the respective regions.

【Example calculation】

γ-ray emission rates and uncertainty for the nuclides used in the analysis are shown in Table C.8.

Table C.8 γ-ray emission rate and uncertainty for each nuclide.

Nuclide (energy)	γ-ray emission rate (%)	Uncertainty of γ-ray emission rate	Relative standard uncertainty (%)
^{109}Cd (88.0 keV)	3.644	0.016	0.4391
^{57}Co (122.1 keV)	85.60	0.17	0.1986
^{139}Ce (165.9 keV)	79.90	—	—
^{51}Cr (320.1 keV)	9.910	0.010	0.1009
^{137}Cs (661.7 keV)	85.10	0.20	0.2350
^{54}Mn (834.8 keV)	99.9760	0.0010	0.0010
^{88}Y (898.0 keV)	93.7	0.3	0.3202
^{60}Co (1173.2 keV)	99.85	0.03	0.0300
^{60}Co (1332.5 keV)	99.9826	0.0006	0.0006
^{88}Y (1836.1 keV)	99.2	0.3	0.3024

Low-energy region: $u_{6L} = 0.4391$ %

High-energy region: $u_{6H} = 0.3202$ %

C.2.2.8 Fitting of calibration formula (u_{7L}, u_{7H})

The calibration data of each nuclide (γ-ray) is used to calculate the [fitting value/measured value]. Then, the fluctuation coefficient of the [fitting value/measured value] in each divided region is chosen as the relative standard uncertainty of the fitting for the calibration formula in each respective region. Thus, the following equation holds,

$$u_7 = \frac{f_{STD}}{\bar{f}} \tag{C.17}$$

where $\bar{f}$ is the average of the [fitting value/measured value] in each divided region and f_{STD} is the standard deviation of the [fitting value/measured value] in each divided region.

【Example calculation】

When the peak efficiency calibration is conducted using a calibration source, leading to the results shown in Table C.9, the following values are obtained.

Table C.9 Calibration data for each nuclide

Nuclide (energy)	Fitting value	Measured value	Fitting value/ Measured value
^{109}Cd (88.0 keV)	0.141720	0.141242	1.003388
^{57}Co (122.1 keV)	0.138644	0.140522	0.986636
^{139}Ce (165.9 keV)	0.115227	0.113012	1.019600
^{51}Cr (320.1 keV)	0.063601	0.064534	0.985549
^{137}Cs (661.7 keV)	0.032975	0.032503	1.014506
^{54}Mn (834.8 keV)	0.026721	0.026740	0.999283
^{88}Y (898.0 keV)	0.025014	0.024792	1.008961
^{60}Co (1173.2 keV)	0.019642	0.019650	0.999584
^{60}Co (1332.5 keV)	0.017506	0.017529	0.998650
^{88}Y (1836.1 keV)	0.013100	0.013151	0.996117

Energy region	Respective value of [fitting value/measured value]	
Low-energy region	Average	1.003208
	Standard deviation	0.016483
	Fluctuation coefficient	1.643 %
High-energy region	Average	1.000379
	Standard deviation	0.009275
	Fluctuation coefficient	0.9271 %

Low-energy region: $u_{7L} = 1.643\ \%$

High-energy region: $u_{7H} = 0.9271\ \%$

(Note) If multiple sources are used in the calibration, the evaluation is conducted for each source and the maximum values among each source are used each in the low-energy region and the high-energy region.

C.2.2.9 Summing-effect correction

For detectors with a small relative efficiency, the uncertainty included in the summing effect does not have as great an influence as the uncertainty related to counting or to radioactivity in the calibration source. Moreover, it is difficult to estimate the uncertainty owing to summing effects, so that it does not necessarily need to be evaluated[*4]. However, using a Monte Carlo simulation, it can be estimated by varying parameters such as geometry, energy of the γ-rays, and the γ-ray emission rate [11].

C.2.2.10 Self-absorption correction

This factor does not need to be evaluated.

The uncertainty related to the self-absorption correction while measuring a standard sample assumes that the composition and homogeneity of the calibration source are sufficiently ensured, so it is omitted.

[*4]: There is an example where the uncertainty owing to summing effects was uniformly evaluated [27].

C.2.2.11 Attenuation correction (u_{8L}, u_{8H})

When referencing the nuclear data used for analysis, the attenuation correction coefficients for the time elapsed from the calibration date/time to the measurement date/time are calculated for the half-life and [half-life + uncertainty], respectively. Then, the relative value of the difference is taken as the relative standard uncertainty[*5] Note that of the calculated relative standard uncertainties, the maximum value in each divided region is used as the relative standard uncertainty in that respective region, which is expressed by the following equations,

$$DF_1 = \left(\frac{1}{2}\right)^{\frac{t}{T}} \tag{C.18}$$

$$DF_2 = \left(\frac{1}{2}\right)^{\frac{t}{T+\sigma}} \tag{C.19}$$

$$u_8 = \frac{|DF_2 - DF_1|}{DF_1} \tag{C.20}$$

where T is the half-life, $T + \sigma$ is the half-life + uncertainty, t is the elapsed time, DF_1 is the attenuation correction coefficient at T, and DF_2 is the attenuation correction coefficient at $T +$.

【Example calculation】

Table C.10 shows the half-lives and uncertainties for nuclides used in the analysis, and the values of DF_1 and DF_2, supposing that the measurement is performed 60 days after the calibration date.

Table C.10 Half-life and uncertainty for each nuclide.

Nuclide	Half-live	Uncertainty of half-life	DF_1	DF_2	Relative standard uncertainty (%)
^{109}Cd	461.9 (days)	0.4 (days)	0.9139	0.9140	0.007791
^{57}Co	271.74 (days)	0.06 (days)	0.8581	0.8581	0.003379
^{139}Ce	137.641 (days)	0.02 (days)	0.7392	0.7393	0.004390
^{51}Cr	27.704 (days)	0.003 (days)	0.2229	0.2229	0.016256
^{137}Cs	30.08 (years)	0.09 (years)	0.9962	0.9962	0.001130
^{54}Mn	312.2 (days)	0.2 (days)	0.8753	0.8754	0.008529
^{88}Y	106.627 (days)	0.021 (days)	0.6770	0.6771	0.007681
^{60}Co	1925.28 (days)	0.14 (days)	0.9786	0.9786	0.000157

Low-energy region: $u_{8L} = 0.007791$ %

High-energy region: $u_{8H} = 0.01626$ %

[*5]: If the elapsed time from the calibration date/time to the measurement date/time is short, this evaluation may be omitted, because the uncertainty related to the attenuation correction is small.

C.2.3 Uncertainty related to sample measurement

C.2.3.1 Geometry (positional relationship between detector and sample)

This uncertainty is the same as for C.2.2.3 the geometry factor mentioned earlier. (positional relationship between detector and sample)

C.2.3.2 Dead time

This uncertainty is the same as that for C.2.2.4 the dead time factor mentioned earlier.

C.2.3.3 Fluctuations in measurement system (u_9)

The fluctuation in the measurement system is taken to be a rectangular distribution, where the upper and lower limits are the permissible standard (relative value) of the fluctuation range set by the accuracy control, as follows,

$$u_9 = \frac{Ac}{\sqrt{3}} \tag{C.21}$$

where Ac is the upper limit of the permissible standard of the fluctuation range.

In the case where fluctuation in the measurement system has been obtained by accuracy controls (trend chart), the value is taken to be the uncertainty. Note that in that case, care must be taken to avoid overlap because the uncertainty related to the geometry between the detector and the sample, described in C.2.3.1, is already included.

【Example calculation】

When accuracy controls are conducted by measurement of standard sources, and the permissible standard is $\pm 5\%$, the following equation holds.

$$u_9 = \frac{0.05}{\sqrt{3}} = 0.02887\ (2.887\%)$$

C.2.3.4 Summing-effect correction

This uncertainty is the same as C.2.2.9 the summing-effect correction mentioned earlier.

C.2.3.5 Self-absorption correction

This factor does not need to be evaluated[*6].

The uncertainty related to the self-absorption correction at the time of sample measurement is difficult to estimate because it originates from the composition and homogeneity of the sample. Thus, the self-absorption correction is omitted here. Nevertheless, using a Monte Carlo simulation, it may be possible to estimate it by varying parameters such as geometry, density of the source, and energy of the γ-rays [11].

C.2.3.6 γ-ray emission rate (u_{10})

This uncertainty is the same as C.2.2.7 the γ-ray emission rate mentioned earlier.

Note that it is evaluated for the nuclides to be measured in each measurement.

[*6]: There have been examples in which the self-absorption correction was uniformly evaluated [27].

C.2.3.7 Attenuation correction (u_{11})

This uncertainty is the same as the as C.2.2.11 the attenuation correction mentioned earlier.

Here, the elapsed time is taken as period from the standard date/time related to sample collection to the measurement date/time.

$$u_{11} = \frac{|DF_2 - DF_1|}{DF_1} \tag{C.22}$$

Note that the evaluation is conducted for the nuclides to be measured in each measurement.

C.2.3.8 Uncertainty related to counting (u_{12})

This uncertainty is the same as the as C.2.2.6 the uncertainty related to counting mentioned earlier.

$$u_{12} = \frac{\sigma_N}{N} \tag{C.23}$$

Note that the evaluation is conducted for the nuclides to be measured in each measurement.

Table C.11 Uncertainty budget sheet

Factor of uncertainty	Low-energy region	High-energy region
C.2.1 Measuring sample		
C.2.1.1 Weighing	u_1	
C.2.1.2 Filling height of sample	u_2	
C.2.1.3 Homogeneity of sample	No need to be evaluated	
C.2.2 Calibration of peak efficiency		
C.2.2.1 Filling heigh of source	u_3	
C.2.2.2 Radioactivity of calibration source	u_{4L}	u_{4H}
C.2.2.3 Geometry	No need to be evaluated	
C.2.2.4 Dead time	No need to be evaluated	
C.2.2.5 Fluctuation of measurement system	No need to be evaluated	
C.2.2.6 Uncertainty related to counting	u_{5L}	u_{5H}
C.2.2.7 γ-ray emission rate	u_{6L}	u_{6H}
C.2.2.8 Fitting of calibration formula	u_{7L}	u_{7H}
C.2.2.9 Summing-effect correction	No need to be evaluated	
C.2.2.10 Self-absorption correction	No need to be evaluated	
C.2.2.11 Attenuation correction	u_{8L}	u_{8H}
C.2.3 Measurement of sample		
C.2.3.1 Geometry	No need to be evaluated	
C.2.3.2 Dead time	No need to be evaluated	
C.2.3.3 Fluctuation of measurement system	u_9	
C.2.3.4 Summing-effect correction	No need to be evaluated	
C.2.3.5 Self-absorption correction	No need to be evaluated	
C.2.3.6 γ-ray emission rate	u_{10}	
C.2.3.7 Attenuation correction	u_{11}	
C.2.3.8 Uncertainty related to counting	u_{12}	
Relative combined standard uncertainty	u_{relL}	u_{relH}

Table C.12 Uncertainty budget sheet (example calculation)

Factor of uncertainty	Low-energy region	High-energy region
C.2.1 Measuring sample		
C.2.1.1 Weighing	0.0443%	
C.2.1.2 Filling height of sample	0.202%	
C.2.1.3 Homogeneity of sample	No need to be evaluated	
C.2.2 Calibration of peak efficiency		
C.2.2.1 Filling height of source	0.202%	
C.2.2.2 Radioactivity of calibration source	2.75%	2.65%
C.2.2.3 Geometry	No need to be evaluated	
C.2.2.4 Dead time	No need to be evaluated	
C.2.2.5 Fluctuation of measurement system	No need to be evaluated	
C.2.2.6 Uncertainty related to counting	0.285%	0.545%
C.2.2.7 γ-ray emission rate	0.439%	0.320%
C.2.2.8 Fitting of calibration formula	1.64%	0.927%
C.2.2.9 Summing-effect correction	No need to be evaluated	
C.2.2.10 Self-absorption correction	No need to be evaluated	
C.2.2.11 Attenuation correction	0.00779%	0.0163%
C.2.3 Measurement of sample		
C.2.3.1 Geometry	No need to be evaluated	
C.2.3.2 Dead time	No need to be evaluated	
C.2.3.3 Fluctuation of measurement system	2.89%	
C.2.3.4 Summing-effect correction	No need to be evaluated	
C.2.3.5 Self-absorption correction	need to be evaluated	
Relative combined standard uncertainty, except for the uncertainties of γ-ray emission rate, attenuation correction, and the uncertainty related to counting in the sample measurement.	4.35%	4.09%
C.2.3.6 γ-ray emission rate	Evaluated in every measurement	
C.2.3.7 Attenuation correction	Evaluated in every measurement	
C.2.3.8 Uncertainty related to counting	Evaluated in every measurement	
Relative combined standard uncertainty	Evaluated in every measurement	

C.2.4 Example calculation of measurement uncertainty in real environmental samples

In this section, measurement results from environmental samples are used as an example showing the comparative magnitude of the effect of each uncertainty factor on the uncertainty of the final measurement.

For a measured soil sample, the radioactivity concentration of ^{137}Cs was 1.87 Bq/kg (peak area: 426.4±38.6), and the uncertainty related to counting (relative standard uncertainty) is obtained from the peak area as follows.

$$\frac{38.6}{426.4} = 0.09053$$

Further, the uncertainty in the γ-ray emission rate (relative standard uncertainty) of ^{137}Cs is obtained from Table C.8, as follows.

$$0.2350\%$$

Note that the elapsed time between the standard date/time related to the sample collection and the measurement date/time is significantly shorter than the half-life of the nuclide (^{137}Cs) to be measured. Therefore, the uncertainty related to the attenuation correction in the sample measurement can be omitted. From Table C.12, the relative combined standard uncertainty that excludes the uncertainty related to the γ-ray emission rate in the sample measurement, the attenuation correction and counting is 4.09%, so the relative combined standard uncertainty of the measured value is given by the following equation.

$$\sqrt{0.04087^2 + 0.09053^2 + 0.002350^2} = 0.09936 \quad (9.936\%)$$

Therefore, the standard uncertainty of the measured value is obtained as follows.

$$1.87 \times 0.09936 = 0.1858 \simeq 0.19 \ \text{(Bq/kg)}$$

Next, the magnitude of the contribution of each uncertainty factor relative to the uncertainty of the measured value was evaluated using the following equation.

$$S_j = \frac{\{u(x_j)/x_j\}^2}{\sum_{i=1}^{n}\{u(x_i)/x_i\}^2} \times 100 \qquad \text{(C.24)}$$

where S_j is the contribution of each uncertainty factor (%) and $u(x_i)/x_i$ are the relative standard uncertainties of the input values $x_1, x_2, x_3, \cdots, x_n$.

The result of this evaluation yields the magnitude of the contributions from each uncertainty factor, which is shown in Fig. C.2.

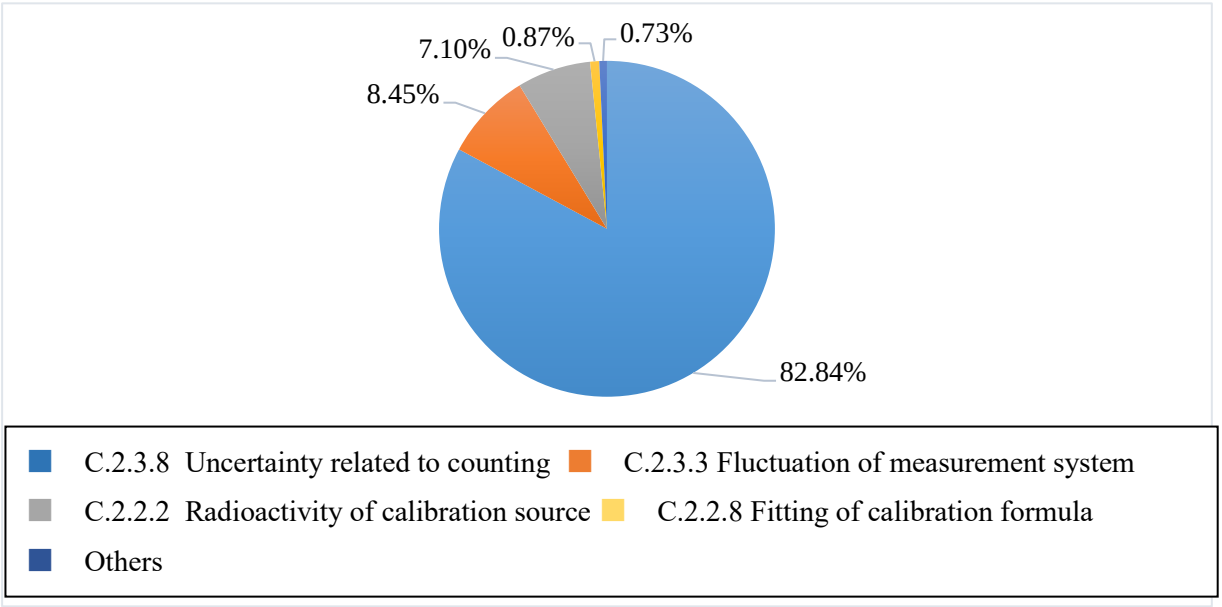

Fig. C.2 Magnitude of contributions from each uncertainty factor.

Fig. C.2 indicates that among the uncertainty factors, the largest contributions came from the uncertainty related to counting, the uncertainty owing to fluctuations in the measurement system, and uncertainty in the radioactivity of calibration source. When measuring environmental samples, the often (but not always) low concentration of nuclides to be detected leads to many cases in which the uncertainty related to counting has the largest contribution.

After comparing the magnitude of contributions from each uncertainty factor, it is desirable to investigate whether or not the uncertainty can be reduced by reviewing the measurement procedures and evaluation methods for the factors with the largest contributions. In the case of this example, where the uncertainty related to counting has the largest contribution, the uncertainty can be reduced by increasing the measurement time.

Explanation D Example calculation of lower detection limit

Methods for calculating the lower detection limit include Cooper's method [12], Kaiser's method [13], Currie's method [14], and the ISO 11929 evaluation method [15]. This commentary presents the respective concepts of the detection limit and example calculations using Currie's method and the ISO 11929 evaluation method.

The concept of the detection limit involves considering the distribution of the measured values. When an object to be measured is repeatedly and fully measured many times, the measured values are represented by the distribution shown in Fig. D.1, which is described using a mathematical model termed a normal or Gaussian distribution, in which the average value is the maximum.

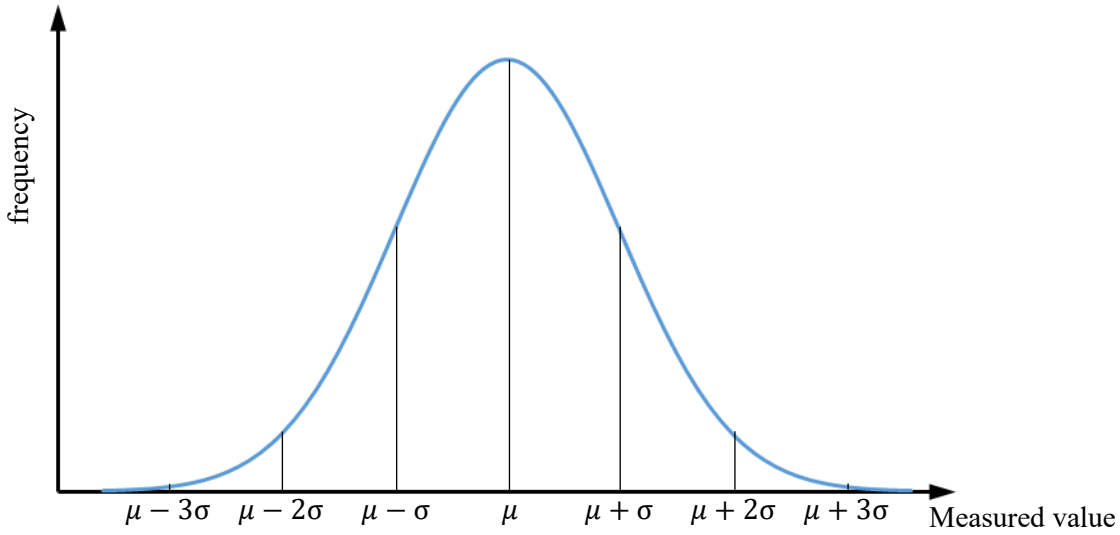

μ : Average of measured values
σ : Standard deviation for distribution of measured values

Fig. D.1 Distribution of measured values.

In the distribution shown in Fig. D.1, about 68% of the measured values fall into the range of $\mu \pm \sigma$, while about 95% fall in the range of $\mu \pm 2\sigma$, and about 99.7% are in the range of $\mu \pm 3\sigma$.

D.1 Lower detection limit by Cooper's method

D.1.1 Concept

For a sample measurement in which the nuclides to be measured are not present, the net count in the peak region of the nuclides to be measured, i.e., the peak area, exhibits the distribution shown in Fig. D.2. In this case, the lower detection limit is the lowest detection count value, defined by the peak area corresponding to $N_m = k\sigma$, where N_m represents the peak area and σ is the uncertainty related to counting (standard uncertainty).

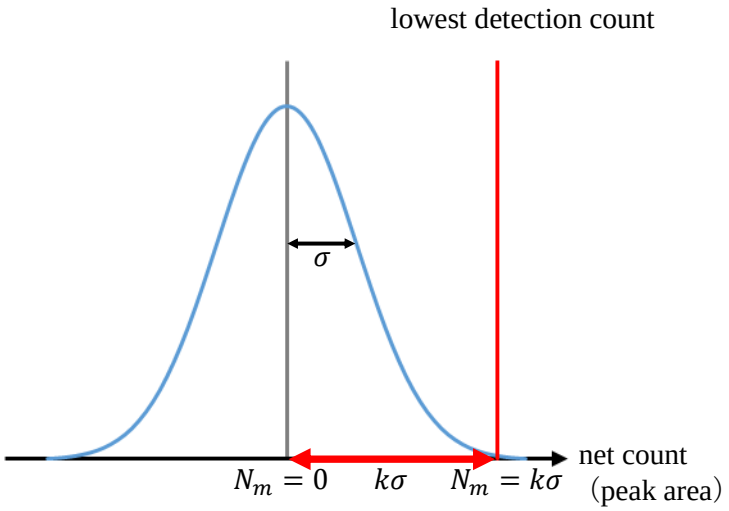

Fig. D.2 Conceptual diagram of the lower detection limit determined by Cooper's method.

D.1.2 Calculation of lower detection limit

The lowest detection count N_m is defined by the following equation,

$$N_m = k\sigma \qquad \text{(D.1)}$$

where σ is the uncertainty related to counting and k is the inclusion coefficient (typically, k=3).

In case of a peak for which the baseline has no slope, as in Fig. D.3, we let the count value at channel i be n_i, and obtain the following equations (refer to Document 1.1):

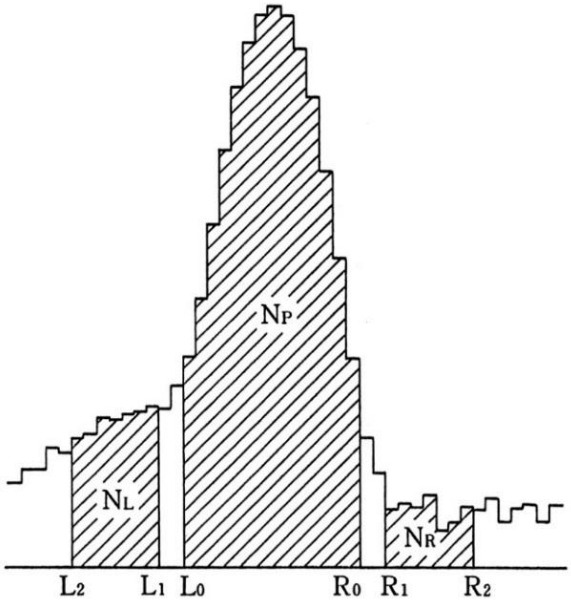

Fig. D.3 Peak with a baseline that has no slope.

$$N_P = \sum_{i=L_0}^{R_0} n_i \quad 、 \quad N_L = \sum_{i=L_2}^{L_1} n_i \quad 、 \quad N_R = \sum_{i=R_1}^{R_2} n_i$$

$$\beta_L = \frac{R_0 - L_0 + 1}{2(L_1 - L_2 + 1)} \quad 、 \quad \beta_R = \frac{R_0 - L_0 + 1}{2(R_2 - R_1 + 1)}$$

Because the area of the portion of the baseline in the peak region is $\beta_L N_L + \beta_R N_R$, the peak area is given by the equation:

$$N_m = N_P - \beta_L N_L - \beta_R N_R$$

Within this time, the uncertainty σ related to counting in the peak area is given by the following equation:

$$\begin{aligned}\sigma^2 &= \left(\sqrt{N_P}\right)^2 + \left(\beta_L\sqrt{N_L}\right)^2 + \left(\beta_R\sqrt{N_R}\right)^2 \\ &= N_m + \beta_L N_L + \beta_R N_R + {\beta_L}^2 N_L + {\beta_R}^2 N_R \\ &= N_m + \beta_L(1+\beta_L)N_L + \beta_R(1+\beta_R)N_R\end{aligned}$$

Substituting the above equation into equation (D.1) yields the following relation:

$$N_m = k\sqrt{N_m + \beta_L(1+\beta_L)N_L + \beta_R(1+\beta_R)N_R}$$

Solving this equation provides the lowest detection count value, as follows:

$$N_m = \frac{k^2 + k\sqrt{k^2 + 4\{\beta_L(1+\beta_L)N_L + \beta_R(1+\beta_R)N_R\}}}{2} \quad \text{(D.2)}$$

The more generalized form of this equation is given by the following equation. This generalized equation corresponds to the case, in which peaks from interference and background sources must be subtracted,

$$N_m = N_P - (N_1 + N_2 + \cdots + N_n)$$
$$= \frac{k^2 + k\sqrt{k^2 + 4\{(N_1 + {\sigma_1}^2) + (N_2 + {\sigma_2}^2) + \cdots + (N_n + {\sigma_n}^2)\}}}{2} \quad \text{(D.3)}$$

where N_P is the area in the peak region, N_i is the area to be subtracted, and σ_i is the uncertainty related to counting in the area to be subtracted.

The value obtained for the lowest detection count is converted to radioactivity or a radioactivity concentration, and the converted values are considered the lowest detection limit value.

D.2 Lower detection limit by ISO 11929

D.2.1 Concept

The concept behind the lower detection limit by ISO 11929 is an extension of the conventional Currie's method, and provides a value that incorporates uncertainties related to factors other than counting.

In the ISO 11929 method, when uncertainties related to factors other than counting is not considered, the calculation results coincide with those obtained by Cooper's method (k=3.29)[*1].

・Decision threshold: $y^* = k_{1-\alpha} \times \tilde{u}(0)$

※ $\tilde{u}(0)$: Standard uncertainty of the measured value when the true value is 0.

A decision threshold is a value that is determined in the presence of physical effects and is defined by the distribution of blank measurements, as explained below.

When measuring a blank that does not contain any nuclides to be measured, the measured values exhibit the distribution ($\mu = 0$) shown in Fig. D.4. For this distribution, when the probability (risk rate) of a type I error is α, the measured values that exceed the point of 100α% on the upper side are taken as the decision threshold, which are values where physical effects exist, considerably unlike the blank.

[*1]: As in the uncertainty related to counting, the calculation results do not coincide unless the considered factors (peak area, baseline area, interfering peak area, peak background area, etc.) are exactly the same.

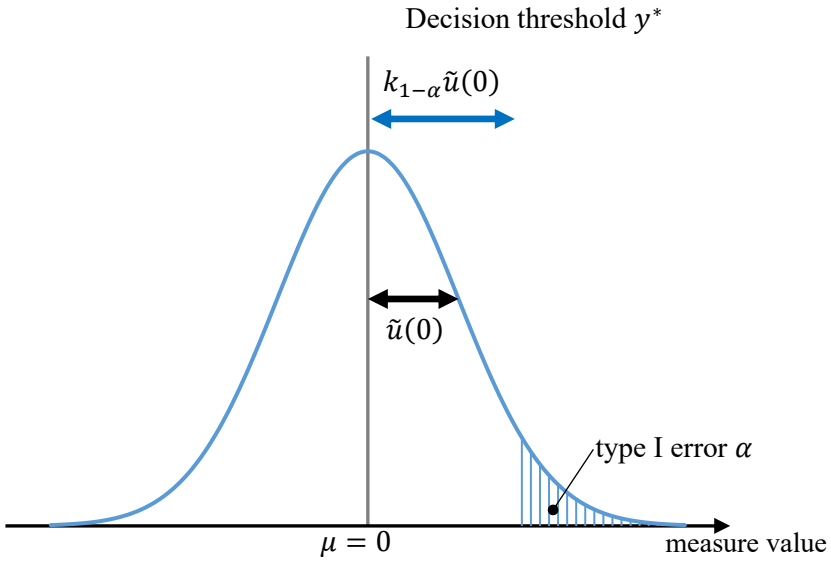

$\tilde{u}(0)$: Standard uncertainty of the measured value when the true value is 0
$k_{1-\alpha}$: Inclusion coefficient when the probability of a type I error becomes α

Fig. D.4 Decision threshold by the ISO 11929 method.

・Lower detection limit: $y^{\#} = y^* + k_{1-\beta} \times \tilde{u}(y^{\#})$
※ $\tilde{u}(y^{\#})$: Standard uncertainty of a measured value when the true value is $y^{\#}$.

Here, the measured value is assumed to originate not only from the blank, but also from the sample, which is defined as follows.

During a sample measurement, when the true value of the measured amount is larger than and also near the decision threshold, the measured value exhibits the distribution shown in Fig. D.5, which overlaps with the blank measurement distribution.

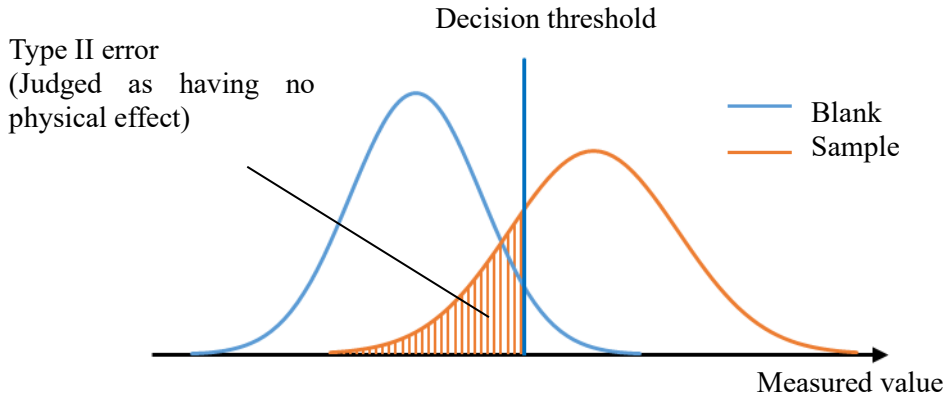

Fig. D.5 Distribution of measured values when the true value of the measured amount is close to the decision threshold.

In this case, the measured values in the shaded area in Fig. D.5 are lower than the decision threshold, so physical effects are judged not to exist. Then, if the probability of a Type II error is called β, the lower detection limit is considered the true value of the measured amount when the lower 100β% point in the sample measurement distribution agrees with the decision threshold value, as shown in Fig. D.6.

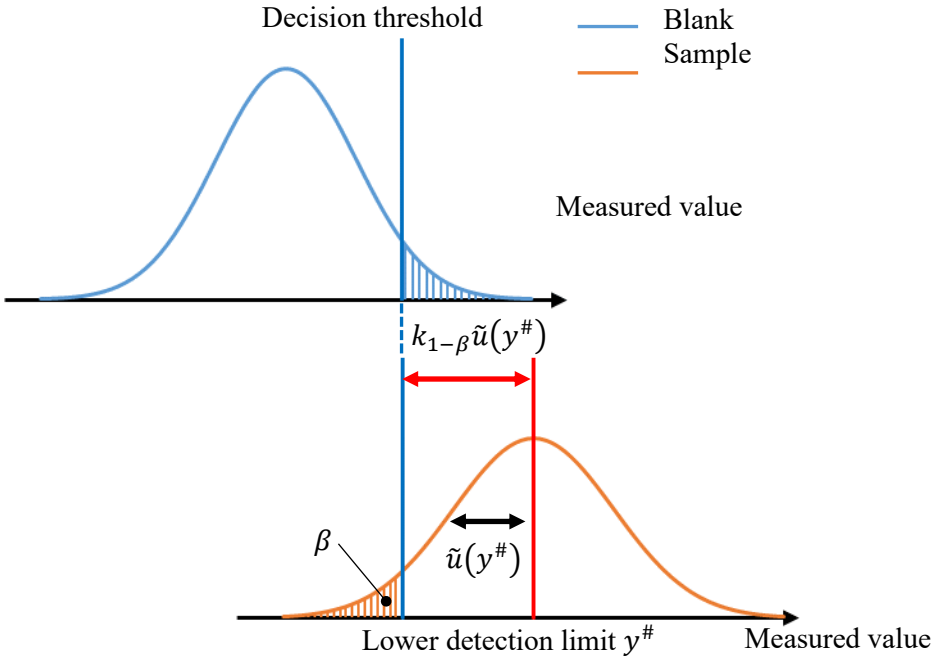

$\tilde{u}(y^{\#})$: Standard uncertainty of the measured value when the true value is $y^{\#}$.
$k_{1-\beta}$: Inclusion coefficient when the probability of a Type II error becomes β.

Fig. D.6 Lower detection limit by the ISO 11929 method.

The lower detection limit is used to evaluate the measurement procedures by comparison with the guideline value y_r.
(If $y^{\#} < y_r$, the measurement procedure is considered to be appropriate.)
Here, the guideline value y_r determined by ISO 11929-1:2019 is as follows:
A value that corresponds to scientific, legal, and other requirements for the lower detection limit, and is intended for evaluating the measurement procedure by comparison with the lower detection limit.

Note 1: The guideline values are determined by properties such as radioactivity, specific radioactivity, concentration and surface density of radioactivity, and dose rate.
Note 2: A lower detection limit is compared with the guideline value to determine whether the measurement procedure meets the requirement defined by the guideline value, that is, whether it fits the measurement purpose. If the lower detection limit is lower than the guideline value, the measurement procedure meets that requirement.
Note 3: The guideline value is not to be confused with the values specified by compliance requirements and regulatory limits.

Furthermore, in the case where $\alpha = \beta = 0.05$ (5%), the inclusion coefficients are given by the relation, $k_{1-\alpha} = k_{1-\beta} \fallingdotseq 1.645$.
Fig. D.7 summarizes the concept of the decision threshold and the lower detection limit in a single diagram.

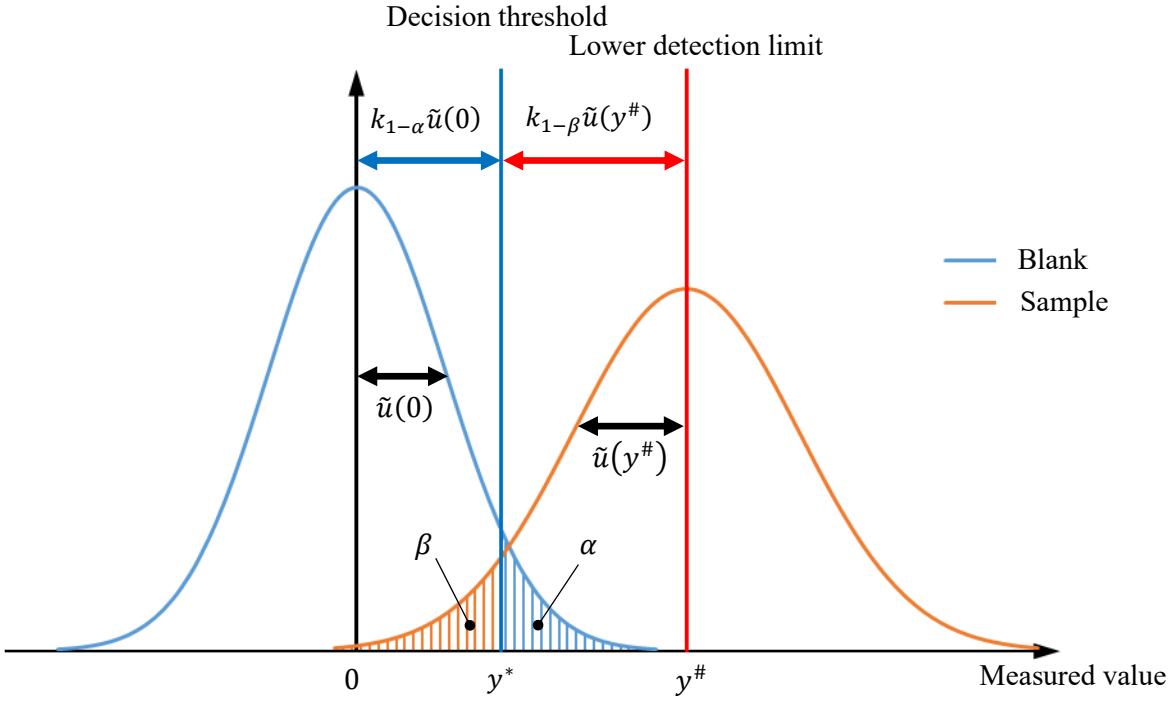

Fig. D.7 Concept of lower detection limit from ISO 11929.

<Definition> Excerpted from the ISO 11929-1:2019

The definition of the decision threshold and the detection limit according to ISO 11929-1:2019 are shown below.

3.12 Decision threshold

Value of the estimator of the measurand, which when exceeded by the result of an actual measurement using a given measurement procedure of a measurand quantifying a physical effect, is used to decide that the physical effect is present.

Note 1 to entry: The decision threshold is defined such that in cases where the measurement result, y, exceeds the decision threshold, y^{*}, the probability of a wrong decision, namely that the true value of the measurand is not zero if in fact it is zero, is less or equal to a chosen probability α.

Note 2 to entry: If the result, y, is below the decision threshold, y^{*}, it is decided to conclude that the result cannot be attributed to the physical effect; nevertheless, it cannot be concluded that it is absent.

3.13 Detection limit

Smallest true value of the measurand which ensures a specified probability of being detectable by the measurement procedure

Note 1 to entry: With the decision threshold according to 4.13, the detection limit is the smallest true value of the measurand for which the probability of wrongly deciding that the true value of the measurand is zero is equal to a specified value, β, when, in fact, the true value of the measurand is not zero. The probability of being detectable is consequently $(1 - \beta)$.

Note 2 to entry: The terms detection limit and decision threshold are used in an ambiguous way in different standards (e.g. standards related to chemical analysis or quality assurance). If these terms are referred to one has to state according to which standard they are used.

D.2.2 Calculation of lower detection limit

An example calculation of the lower detection limit is described below. This example uses the model formula described in Analytical Quality in Nuclear Applications Series No. 48 "Determination and Interpretation of Characteristic Limits for Radioactivity Measurements" published by IAEA, to calculate the lower detection limit when peaks do not exist or are not present in the analyzed regions.

The spectral data used in this calculation were obtained in the following manner. A soil sample of 0.1054 kg was placed in a polypropylene cylindrical vessel (U-8 vessel) at a height of 50 mm and was measured for about 70,000 sec. The nuclides used for the calculation were selected only in consideration of the spectral shape, and for no other particular reasons.

D.2.2.1 General formula to obtain radioactivity from count values

$$A = n_n \cdot w \tag{D.4}$$

The variables used are shown below.

A: radioactivity (Bq) or radioactivity concentration (Bq/kg, Bq/L, etc.)
n_n: net count of peak region
w: conversion coefficient from peak area to radioactivity or radioactivity concentration

$$w = \frac{1}{t \cdot \varepsilon_E \cdot a \cdot m \cdot f_1 \cdot f_2 \cdot f_3}$$

t: measurement time (s)
ε_E: detection efficiency at energy E
a: γ-ray emission rate
m: sample amount (kg, L, etc.)
If A is obtained as radioactivity, this is not necessary.
f_1: attenuation correction coefficient
f_2: self-absorption correction coefficient
f_3: summing-effect correction coefficient

D.2.2.2 Decision threshold

$$A^* = k_{1-\alpha} \cdot w \cdot \sqrt{n_0 \cdot \frac{x_g}{x_0} \cdot \left(1 + \frac{x_g}{x_0}\right)} \tag{D.5}$$

The variables are shown below.

A^*: decision threshold (Bq or Bq/kg, Bq/L, etc.)
$k_{1-\alpha}$: inclusion coefficient where a Type I error becomes α
n_0: sum of count in baseline region
x_g: channel number in peak region
x_0: sum of channel number in baseline region

Note: $n_0 \cdot \frac{x_g}{x_0}$ in equation (D.5) represents the area of the baseline portion in the peak region.

Concerning more general cases, such as in the presence of interfering peaks, see reference [16] (5.4.6.5 Continuous background, the specified activity of the value is not zero, there are overlapping peaks).

D.2.2.3 Lower detection limit

$$A^{\#} = \frac{2 \cdot A^* + k^2 \cdot w}{1 - k^2 \cdot u_{rel}(w)^2} \tag{D.6}$$

The variables are as shown below.

$A^{\#}$: lower detection limit (Bq or Bq/kg, Bq/L, etc.)
k : inclusion coefficient

$$k = k_{1-\alpha} = k_{1-\beta}$$

$k_{1-\beta}$: inclusion coefficient where a Type II error becomes β
$u_{rel}(w)$: relative standard uncertainty of conversion coefficient w
Except for the uncertainty related to the counts of the measured sample, use the relative standard uncertainty where all uncertainties related to the measurements are summed.

D.3 Example calculation of lower detection limit

D.3.1 Case of no peaks in the analyzed region

^{59}Fe（1291.6 keV）

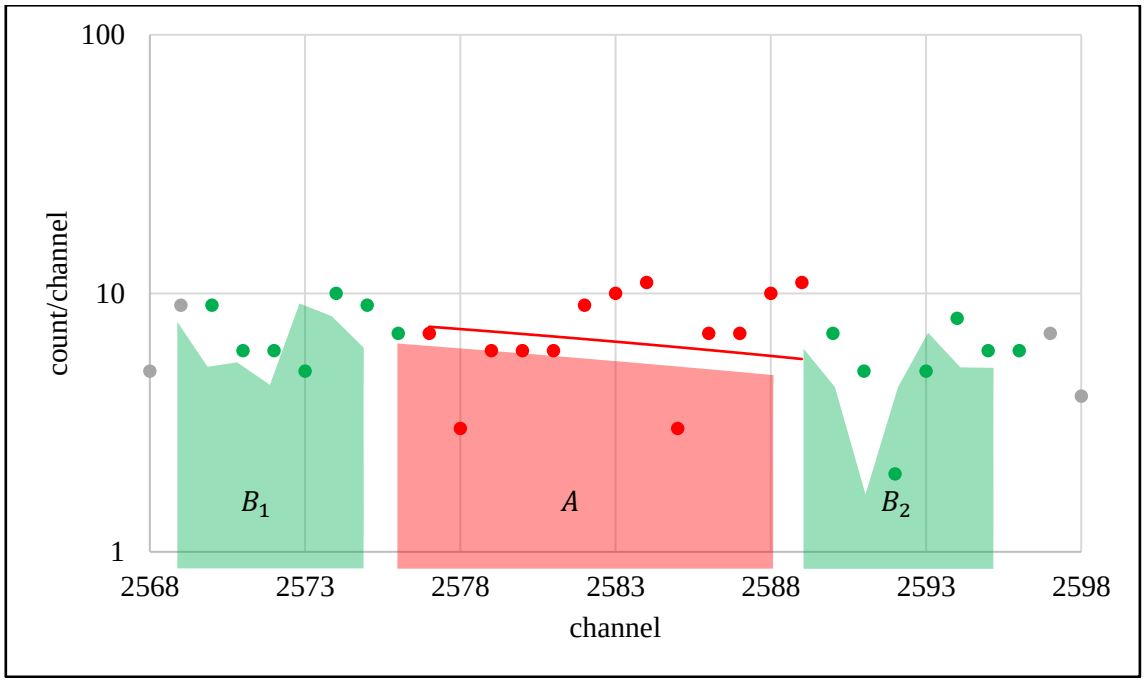

Fig. D.8 Analysis region for ^{59}Fe.

Table D.1 Channel and count data in each region.

Region B_1		Region A		Region B_2	
Channel	Count	Channel	Count	Channel	Count
2570	9	2577	7	2590	7
2571	6	2578	3	2591	5
2572	6	2579	6	2592	2
2573	5	2580	6	2593	5
2574	10	2581	6	2594	8
2575	9	2582	9	2595	6
2576	7	2583	10	2596	6
		2584	11		
		2585	3		
		2586	7		
		2587	7		
		2588	10		
		2589	11		

・Lower detection limit by Cooper's method

Table D.2 Values of each parameter, decision threshold, and lower detection limit.

Parameter	Value
β_L	0.9286
β_R	0.9286
N_L (area of baseline at low-energy side)	52
N_R (area of baseline at high-energy side)	39
k	3
N_m (lowest detection count)	43.06
Lower detection limit (Bq/kg)	1.654

・Lower detection limit by the ISO 11929 method

Table D.3 Values of each parameter, decision threshold, and lower detection limit.

Parameter	Value
x_g (channel number in peak region)	13
x_0 (sum of channel number in baseline regions 1 and 2)	14
$n_0 \frac{x_g}{x_0}$	84.50
$\sqrt{n_0 \frac{x_g}{x_0}\left(1+\frac{x_g}{x_0}\right)}$	12.77
w	0.03840
$u_{rel}(w)$ (refer to the 5th row from the bottom of Table C.12 in Commentary C)	0.04087
$k\ (\alpha = \beta = 0.05(5\%))$	1.645
Decision threshold A^* (Bq/kg)	0.8064
Lower detection limit $A^{\#}$ (Bq/kg)	1.725

D.3.2 Case of peaks present in the analyzed region

^{228}Ac (911.2 keV)

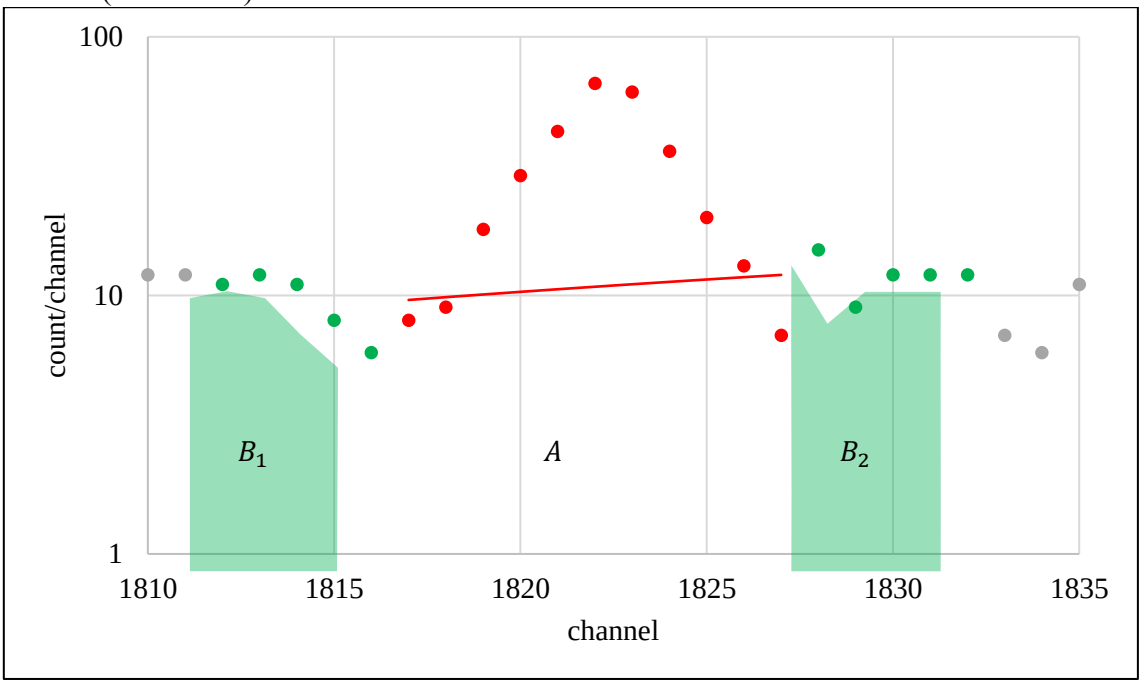

Fig.D.9 Analysis region for ^{228}Ac.

Table D.4 Channel and count data in each region.

Region B_1		Region A		Region B_2	
Channel	Count	Channel	Channel	Count	Channel
1812	11	1817	8	1828	15
1813	12	1818	9	1829	9
1814	11	1819	18	1830	12
1815	8	1820	29	1831	12
1816	6	1821	43	1832	12
		1822	66		
		1823	61		
		1824	36		
		1825	20		
		1826	13		
		1827	7		

・Lower detection limit by Cooper's method

Table D.5 Values of each parameter, decision threshold, and lower detection limit.

Parameter	Value
β_L	1.100
β_R	1.100
N_L (area of baseline at low-energy side)	48
N_R (area of baseline at high-energy side)	60
k	3
N_m (the lowest detection count)	52.10
lower detection limit（Bq/kg）	2.509

・Lower detection limit by the ISO 11929 method

Table D.6 Values of each parameter, decision threshold, and lower detection limit.

Parameter	Value
x_g (channel number in peak region)	11
x_0 (sum of channel number in baseline regions 1 and 2)	10
$n_0 \frac{x_g}{x_0}$	118.8
$\sqrt{n_0 \frac{x_g}{x_0}\left(1+\frac{x_g}{x_0}\right)}$	15.79
w	0.04816
$u_{rel}(w)$(refer to the 5th row from the bottom of Table C.12 in Commentary C)	0.04087
$k\left(\alpha=\beta=0.05(5\%)\right)$	1.645
Decision threshold A^* (Bq/kg)	1.251
Lower detection limit $A^\#$ (Bq/kg)	2.645

Document

Document 1 Calculation method used in Gamma-ray spectral analysis

The manual revised in 1992 was structured to include a lot of content for analytical software developers; conversely, the present manual is written for people who are taking charge of environmental radioactivity analysis. Its structure describes fundamental items in the γ-ray spectrometry of environmental samples conducted in real time, such as radiation monitoring around nuclear facilities.

Therefore, the details of the analytical methods described in the manual revised in 1992 are not mentioned in this text. However, it should be noted that such analytical methods are currently being used, so it is required to describe them in this manual. Further, it is necessary to deal with such references by citing the manual revised in 1992. Considering these circumstances, the details of the calculation methods used for analysis and technical information are described in Document 1.

Document 1.1 Peak analysis

After investigation, spectral peaks were obtained through sample measurement, nuclides were identified, and radioactivity was calculated from the areas of the photoelectric peaks (peaks in all energy ranges). It is difficult to analyze γ-ray spectra obtained by measuring environmental samples due to low counting rate, poor peak shape, and existence of interfering peaks. There are two methods to quantify radioactivity:

- A peak detected as a result of the investigation is identified, then the peak area is calculated, and the radioactivity is quantified.
- Depending on the detection of peaks, an area corresponding to the peak of the nuclide to be analyzed is calculated, and the radioactivity is quantified.

In the former, the analytical results for nuclides of interest sometimes cannot be obtained, while the latter cannot correspond to unexpectedly existing nuclides. Therefore, it is necessary to use both methods in an appropriate manner.

Document 1.1.1 Peak search and full width at half maximum

For setting a peak region, etc., search peaks in the spectrum, and make formulas of the FWHM (full width at half maximum, i.e., the width at the half height of a peak) and channel as a function of energy.

(1) Procedure for calculation processing

(a) Obtain a tentative FWHM from the past measurement data and generate a Gaussian smoothed second derivative filter (If possible, it is recommended to change the filter width depending on the FWHM of the peak, count value, and neighboring peaks).

(b) Perform a smoothed secondary differentiation, and search peaks by comparing with the uncertainty related to the counting.
For the smoothed second derivative spectrum, calculate the center of the detected peak by the three-point calculation method or the first derivative coefficient zero-cross method, and obtain the initial value of the peak center for the sake of (d) described later.

(c) Among the detected peaks, consider the peaks where there are no neighboring peaks (within three times of the FWHM) to create relational expressions between the FWHM/channel and energy. The possible peaks to be picked up are Pb-Kα X-ray (although there is another X-ray peak right next to it.), and γ-rays from ^{214}Pb, ^{208}Tl, ^{214}Bi, and ^{40}K.

(d) The picked-up peaks are function-fitted by "linear expression + Gaussian function." Then, list the uncertainties of the obtained peak center, FWHM, peak area, and other parameters.

(e) Function-fit the FWHM to $a + b \times \sqrt{(\text{energy})}$, and perform the X^2 test.

- Since electron pair annihilation radiation (511.0 keV) and single escape peaks do not adhere to the above equation, they are used for making the channel-energy formula[*1].
- If the value of the investigated X^2 is not within the reliable range, the peaks are excluded one by one in descending order of the values in the formula below, and the function fitting and X^2 test are repeated.

[*1]: Some analytical software uses a common peak in the creation of the FWHM formula and the channel-energy formula, and cannot be used to create just one of the formulas.

$$|W_i - W(E_i)|/\sqrt{\sigma_i{}^2 + \sigma(E_i)^2} \qquad \text{(D1.1.1)}$$

W_i : half width for each peak
$W(E_i)$: half width obtained from the half width-energy formula
σ_i : uncertainty of half width for each peak
$\sigma(E_i)$: uncertainty of half width-energy formula

(f) If the result of (e) is different from the FWHM used in (a) by more than the statistical fluctuation, then it is to be corrected. Then, return to (a), and start over from the filter creation.

(2) Gaussian smoothed second derivative filter for peak search

(a) Differentiate twice a Gaussian function that has 1–2 times the width kW (at this time, $k = 1-2$) of the FWHM in a spectrum, and make a numeric filter.

$$F(x) = \exp\left\{-\frac{2.773}{(kW)^2}(x-P)^2\right\} \qquad \text{(D1.1.2)}$$

P : peak center

After replacing with $x - P = j$, differentiate the above equation twice for j, and the following relationship is obtained.

$$F''(j) = -\left\{\frac{5.546}{(kW)^2}\left(1 - \frac{5.546j^2}{(kW)^2}\right)\exp\left(-\frac{5.546j^2}{2\cdot(kW)^2}\right)\right\} \qquad \text{(D1.1.3)}$$

(b) Change j by 1 from $-3 \times (kW)$ to $3 \times (kW)$ to obtain $F''(j)$, and let the results be the Gaussian smoothed second derivative filter. This range of j is sufficient, and no more change is required because $F''(j)$ will decrease.

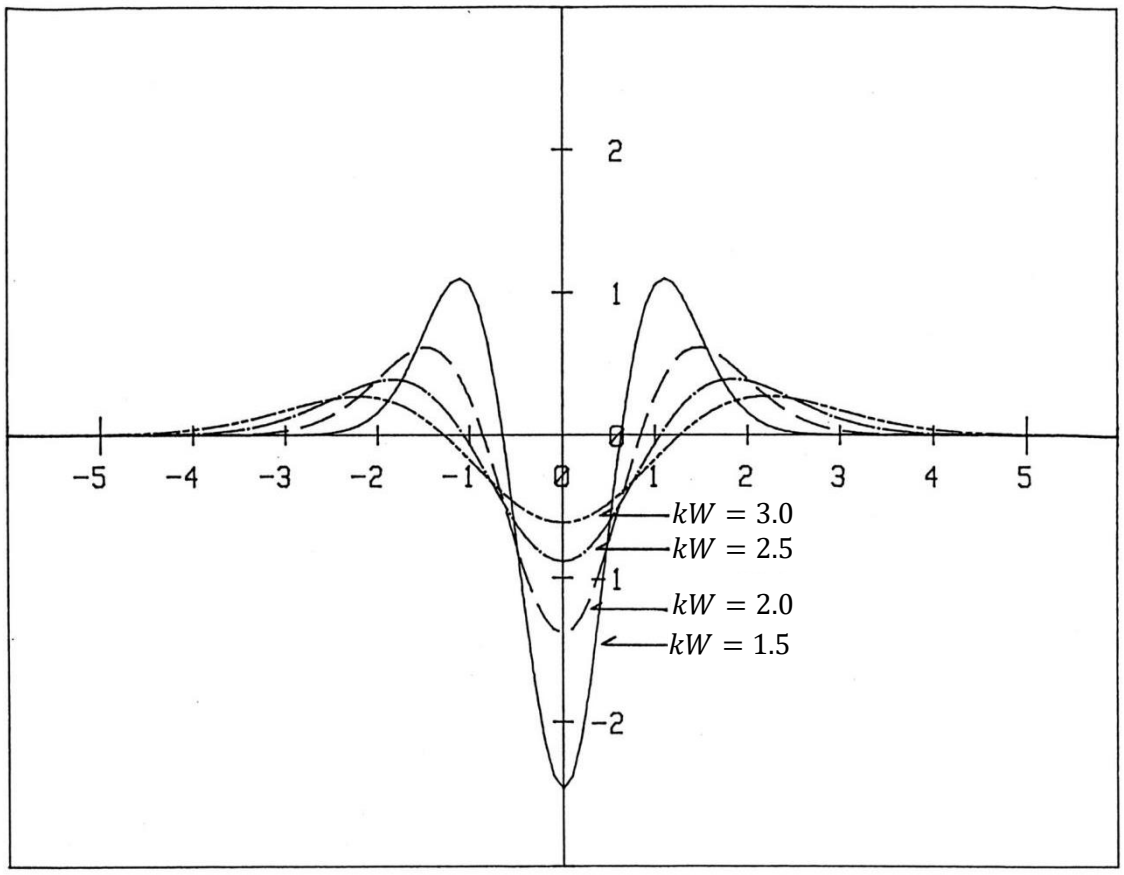

Fig. D1.1.1 Gaussian smoothed second derivative filter

(3) Calculation of the smoothed second derivative and uncertainty related to the counting

Obtain the uncertainty related to smoothed second derivative value and it's counting by using the filter obtained in the above item (b). The smoothed second derivative value is calculated by the following equation.

$$N''(i) = \sum_{j=-K}^{K} F''(j) \cdot N(i+j) \qquad \text{(D1.1.4)}$$

$N(i+j)$ ：count value of $(i+j)$ channel
$F''(j)$ ：Gaussian smoothed second derivative filter
K ：$3 \times (kW)$

The uncertainty related to the counting of $N''(i)$ is calculated by the following equation.

$$\sigma''(i) = \sqrt{\sum_{j=-K}^{K} F''(j)^2 \cdot N(i+j)} \qquad \text{(D1.1.5)}$$

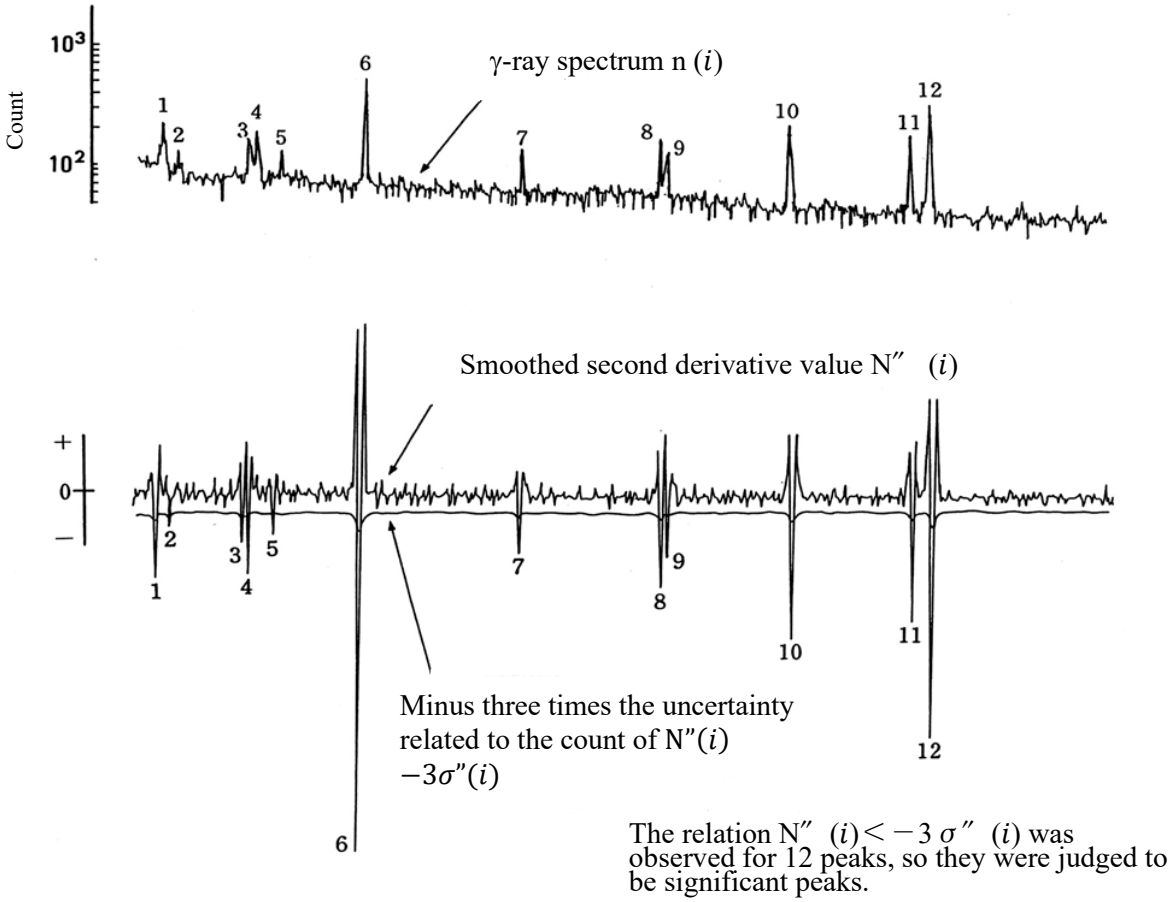

Fig. D1.1.2 Smoothed second derivative and its uncertainty

(4) Judgement of peak

Calculate the smoothed second derivative and its uncertainty for the count value in all channels, put them in pairs and arrange them in a channel order. Compare the smoothed second derivative with its uncertainty in the same channel. Seek the position where the smoothed second derivative is smaller than 2–3 times the uncertainty, and set this point as the peak.

The peaks that are not real ones may be picked up if the criterion to judge the existence of a peak is too sensitive. Therefore, it is reasonable to let the part where the smoothed second derivative is less than minus 2–3 times the uncertainty, be the candidate of the peak. The variable s in the following equation is the peak search sensitivity. In the γ-ray spectrum for the environmental sample, an s value of about three is generally used.

$$N''(i) < -s \times \sigma''(i) \qquad \text{(D1.1.6)}$$

It is sufficient to increase $-s$ in the above equation (within a range that does not become positive) to search for small peaks so as to reduce overlook as much as possible. However, the number of peaks will still increase not due to the fluctuation of radioactivity but simply due to statistical fluctuations in the count value. By calculating the peak area and identifying the nuclide it can be determined whether the searched peak represents the existence of radioactivity.

(5) Calculation of peak center channel

The following two calculation methods are used to calculate the initial value of the fitting function or to conduct manual calculations.

(a) Obtain peak center channel P by the three-point count value method.

Among the peaks, let the channel with the highest count value be h; the count at this channel be N_h; and the count at $h-1$ and $h+1$ channels be N_{h-1} and N_{h+1}, respectively. Then, it can be approximated as follows.

a) Here, the peak center is approximated by a parabola

$$P = h + \frac{1}{2}\left\{\frac{N_{h+1} - N_{h-1}}{2N_h - N_{h-1} - N_{h+1}}\right\} \tag{D1.1.7}$$

b) In this case, the peak center is approximated by a Gaussian function

$$P = h + \frac{1}{2} \cdot \frac{\ln(N_{h+1}/N_{h-1})}{\ln\{{N_h}^2/(N_{h-1} \cdot N_{h+1})\}} \tag{D1.1.8}$$

(b) A peak center channel can also be obtained by the first derivative coefficient zero-cross method.

a) Consider a peak center between the highest count channel and the second one.

b) Let the adjacent channels across the peak center be m and $m+1$, and let the first derivative coefficients against the count value of these peaks be ΔN_m and ΔN_{m+1}, respectively.

c) The values of ΔN_m and ΔN_{m+1} are obtained by substituting m and $m+1$ for i in the following equation as follows:

$$\Delta N_i = \sum_{j=-k}^{k} j \cdot N_{i+j} \tag{D1.1.9}$$

where N_q is the number of counts for channel q.

Determine the value of k depending on the width and symmetry of the peak.

The value of k equivalent to 1–1.5 keV is sufficient. For $k=2$ and $k=3$, the following relationships are obtained.

$$k = 2: \ \Delta N_i = 2(N_{i+2} - N_{i-2}) + N_{i+1} - N_{i-1}$$

$$k = 3: \ \Delta N_i = 3(N_{i+3} - N_{i-3}) + 2(N_{i+2} - N_{i-2}) + N_{i+1} - N_{i-1}$$

d) Obtain the peak center channel from the relationship,

$P = m + \Delta N_m/(\Delta N_m - \Delta N_{m+1})$.
However, if the conditions $\Delta N_m > 0$ and $\Delta N_{m+1} \leqq 0$ are not satisfied, then repeat the calculation by shifting the front and back channels by one unit (channel).

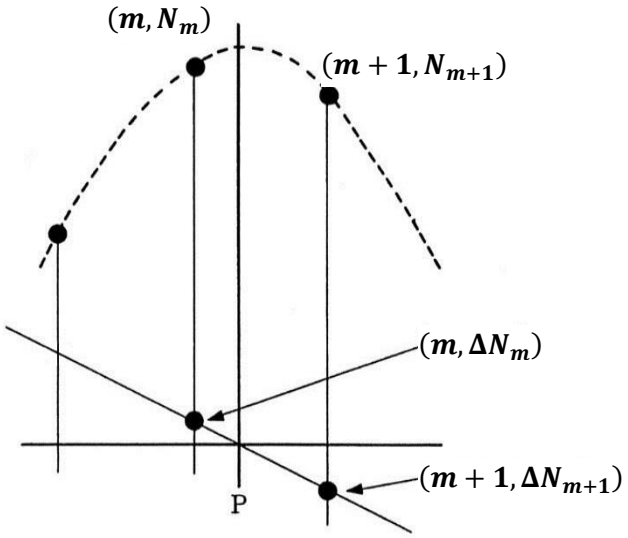

Fig. D1.1.3 First derivative coefficient zero-cross method.

(6) Calculation method for peak FWHM (For the specific calculation methods, refer to the Document 1.1.3)

Function-fit the picked-up peaks by "linear function + Gaussian function." The equations related to the "linear function + Gaussian function" are listed below.

$$F(i, C_k) = C_1 + C_2(i - P) + C_3 \exp\{C_4(i - P)^2\} \quad \text{(D1.1.10)}$$

C_1, C_2, C_3, and C_4 : constant

P : peak center channel

The FWHM obtained here is used for peak search, determination of peak region, and so forth.

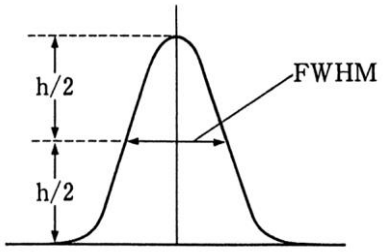

Fig. D1.1.4 Definition of half width

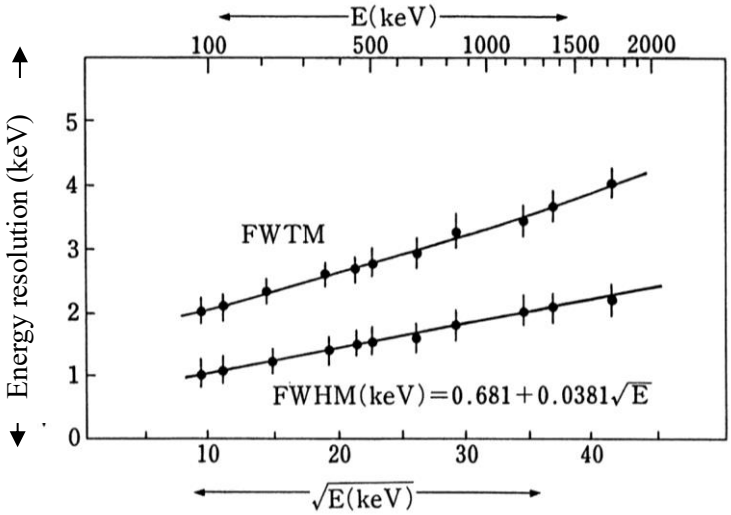

Fig. D1.1.4 Example of energy resolution

Document 1.1.2 Channel-energy relational expression

Since the channel-energy relational expression varies slightly from measurement to measurement, it is desirable to make it using the peaks in the analyzed spectrum, such as the sample and background. An example of the calculation procedure is shown below.

(1) Among the results of peak search (D1.1.1 (1) (c)), determine the peak for calculating the equations for the channel and energy.

(a) Referencing the previous calculation results and nuclear data table, identify the nuclides corresponding to the picked-up peaks and investigate their energy.

(b) Obtain the channel-energy relational expression by the least-squares method.

(c) Investigate the value of X^2. If the value is not within the set interval, exclude the peaks one by one in descending order of the values in the formula below, and repeat the function fitting and the X^2 test.

$$|\{P_i - P(E_i)\}|/\sqrt{\{\sigma_i{}^2 + \sigma(E_i)^2\}} \qquad \text{(D.1.1.11)}$$

P_i	: center of each peak
$P(E_i)$	: peak center obtained from channel-energy relational expression
σ_i	: uncertainty of each peak center
$\sigma(E_i)$	: uncertainty of channel-energy relational expression

(2) Calculate the channel-energy relational expression and its uncertainty

・If there are three clear peaks at appropriate intervals, it is sufficient for the calculation.

・If three peaks are used for the calculation, then use the quadratic equation.

・Even if there are many peaks, do not use equations higher than the quadratic equation.

・Two parabolas may be used by connecting them at the vertices.

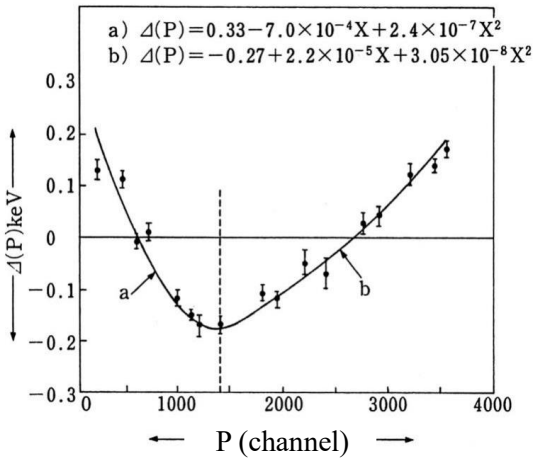

$\Delta(P)$：equation for channel obtained by linear regression; energy difference between the energy obtained from ($E = a + bP$：where a and b are constants) and true γ-ray energy.

Fig. D1.1.5 Example of deviation $\Delta(P)$ obtained from the linear relationship of the channel-energy relational expression

Document 1.1.3 Peak analysis

When a γ-ray enters a detector and its total energy is absorbed by the detector, a photoelectric peak (total energy absorption peak) is observed in the spectrum. The peak center channel depends on the energy of the detected γ-ray, and the peak area (net area where the continuous component is subtracted from the raw area) is proportional to the number of γ-rays that interact with the detector. Therefore, using the peaks in the γ-ray spectrum, it is possible to identify (qualitatively analyze) and quantitatively analyze the γ-ray emitting nuclides.

For quantitative analysis, it is necessary to obtain the area of the peak in a spectrum. To calculate the peak area, the function fitting method or the Covell method (described later) is used.

Document 1.1.3.1 Function fitting

Let the fitting region be about eight times the FWHM on each left and right side from the peak center. Since the peak shapes are slightly different depending on the detector, it is difficult to determine only one peak function. Therefore, it is desirable to make the peak function according to each detector. An example of the function that can be applied to the spectra with small uncertainty related to counting will be described below.

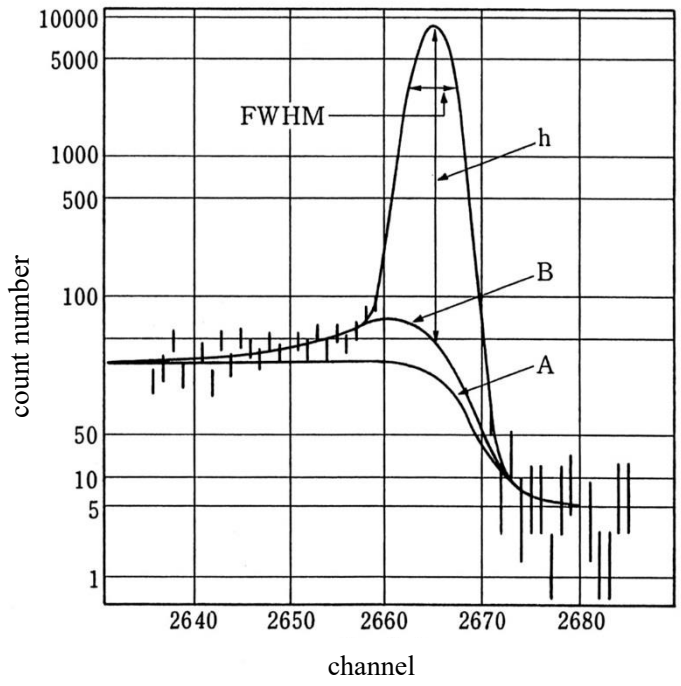

Fig. D1.1.6 Exploded view of function curve

Connect Gaussian curves, where the left and right sides of the FWHM's (W_l, W_r) are different, at their vertices.

Let x_0 be the peak center, and express the step-wise shape A on the low-energy side with the following equation.

$$\frac{a}{1+\exp\{(x-x_0)/(1.5W_l)\}}$$

Then, express the hem shape B[*2] on the low-energy side with the following equation.

$$\frac{b}{1+c(x-x_0)^2}\times\frac{1}{1+\exp\{(x-x_0)/(1.5W_l)\}}$$

By combining the above relations, the following equations are obtained.

$$P(x)=h\times\exp\{-2.7726(x-x_0)^2/(W_l \text{ or } W_r)^2\}+\frac{1}{1+\exp\{(x-x_0)/(1.5W_l)\}}\times\left\{a+\frac{b}{1+c(x-x_0)^2}\right\}+g \qquad \text{(D1.1.12)}$$

h : peak height
W_l: width applied to the left side of the peak
W_r: width applied to the right side of the peak
a: step height
b: height of tailing
c: width of tailing
g: height of baseline

The fitting parameters are h, a, b, c, W_l, W_r, and g, and the peak center x_0. Determine some of the values of these parameters based on the following points, and then perform the function fitting.

- In case a specific nuclide is not considered, calculate the peak center by applying the three-point counting value method or the first derivative coefficient zero-cross method to the smoothed second derivative spectrum.
- In case a specific nuclide is considered, calculate the peak center by applying the channel-energy relational expression. Unless the count number is high, do not set the peak center as the fitting parameter.
- Let the peak height and baseline be the fitting parameters obtained by function fitting. When performing function fitting, make the parameters such as the steps, asymmetry, tailing, and FWHM functional in advance by measuring the energy dependencies. It is recommended that they be set as fixed parameters.

After the fitting calculation, calculate the uncertainty of the fitting parameters. Next, it is recommended to calculate X^2 to check the goodness of fit.

Furthermore, a composite peak is calculated in the following way.

- If there is a dimple between the peaks even when the peaks are overlapping, the fitting calculation is possible.
- Even if the peaks are overlapping to the extent that the dimple cannot be seen, calculating the composite peak is possible when the distance of the peak center is fixed (i.e., the nuclide is

---

[*2]: There are two types shown below for the shapes of tailing B on the low-energy side for the peaks, because they are different depending on the detector.

1.A shape where the slope of the rise of a peak is gentler on the low-energy side than that on the high-energy side.

2.A shape where the baseline of a peak is higher on the low-energy side than that on the high-energy side.

assumed).

- If the peaks are virtually overlapping completely, calculate the composite peak using the data on different peaks of the same nuclide. The contribution coefficient method is one of them.

An example in Document Fig. 1.1.8 shows the results where the function fitting was actually conducted for a composite peak.

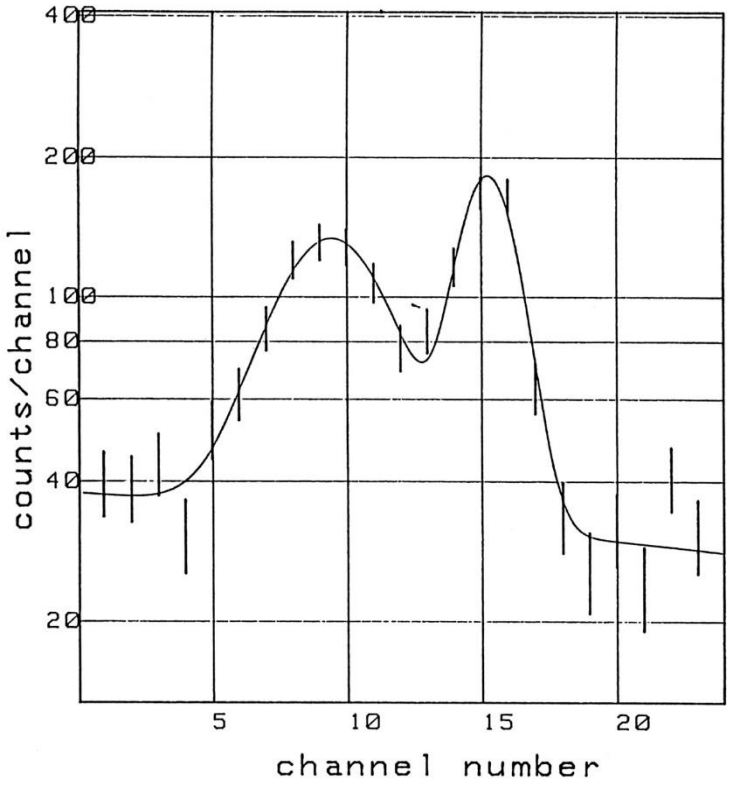

Cl: 3.785E＋1 ± 3.84E＋0
C2: －4.036E－1 ± 2.23E－1
C3: 1.00lE＋2 ± 7.16E＋0
C4: －1.097E－1 ± 1.86E－2
C5: 9.421E＋0 ± 1.63E－1
C6: 1.491E＋2 ± 1.11E＋1
C7: －4.343E－1 ± 6.34E－2
C8: 1.525E＋1 ± 8.66E－2

Chi Sq. by Weighted LSF：
1.58E＋0I
Fitting Accuracy: 1.00

Fig. D1.1.7 Function fitting for composite peak.

The fitting function Y is given by the following equation,

$$Y = C_1 + C_2X + C_3\exp\{C_4(X - C_5)(X - C_5)\} + C_6\exp\{C_7(X - C_8)(X - C_8)\} \quad \text{(D1.1.13)}$$

where X is the channel number.

- The term $C_1 + C_2X$ is the linear function of the baseline.
- The term $C_3\exp\{C_4(X - C_5)(X - C_5)\}$ is the peak function (Gaussian function) at height C_3, center C_5, and half width $\sqrt{(4\ln 2)/-C_4}$
- The term $C_6\exp\{C_7(X - C_8)(X - C_8)\}$ is the peak function (Gaussian function) at height C_6, center C_8, and half width $\sqrt{(4\ln 2)/-C_7}$

The calculation results in this example were as follows.

Baseline: $37.8 - 0.404X$
Peak function on the left side: $100.1\exp\{-0.1097(X - 9.42)(X - 9.42)\}$
Height: 100.1
Center: 9.42 channel
Half width: 5.03 channel
Peak function on the right side: $149.1\exp\{-0.4343(X - 15.25)(X - 15.25)\}$
Height: 149.1
Center: 15.25 channel
Half width: 2.53 channel

Document 1.1.3.2 Calculation of FWHM and using those results for function fitting
(1) Calculation of FWHM

To obtain the FWHM, calculate the channel where the value of the peak function is half the value at the peak center. In other words, when the function value was given, the "reverse function program" that obtains the variables to realize the function value will be required.

By letting the peak function be $Y = P(X)$, the relation $X = P^{-1}(Y)$ is obtained. Here let $Y_{1/2}$ be the half height on both sides of the height at the peak center. When the two X values at $\mathrm{P_L}^{-1}(Y_{1/2})$ and $\mathrm{P}_H{}^{-1}(Y_{1/2})$ are X_l and X_r, respectively, the relation FWHM$= X_r - X_l$ is obtained.

Next, calculate the square of the uncertainty for each X_r and X_l.

$$\sigma_X{}^2 = \sum_{i,j} \frac{\partial P^{-1}}{\partial C_i} \sigma(C_i, C_j) \frac{\partial P^{-1}}{\partial C_j} \quad \text{(D1.1.14)}$$

C_i : Fitting parameter of peak function obtained by the least-squares method
$\sigma(C_i, C_j)$: covariance of C_i and C_j (If $i = j$, it corresponds to dispersion)

Since the FWHM is expressed as the reverse function of the peak function, "partial differential of the reverse function" is required to calculate the uncertainty. For this purpose, the principle "partial differential of a reverse function is equal to the reciprocal of the partial differential" can be used

($\frac{\partial P^{-1}}{\partial C_i} = \frac{1}{\frac{\partial P(X_{l\,or\,r})}{\partial C_i}}$).

Calculate the square root of the sum of squares of each uncertainty X_r and X_l, and let the results be the uncertainty of FWHM.

(2) Peak asymmetry

Generally, a peak has different widths on the left and right sides of the center. Therefore, a peak is expressed using the peak center P and the width at one-tenth height of the maximum count. When the full width tenth maximum (FWTM) is divided at the peak center, then the width on the low-energy and high-energy sides are considered to be a and b, respectively; the peak asymmetry is given by the following equation.

$$\text{Preak asymmetry} = \frac{a - b}{b} \quad \text{(D1.1.15)}$$

(3) Calculation method for FWHM etc.

The FWHM can be calculated by the following method. By using this method, it is possible to infer whether the function fitting is properly performed.

(a) Obtain the peak center with the smoothed first derivative coefficient zero-cross method (refer to (5) (b) of Document 1.1.1).
(b) Obtain the baseline by averaging the count values of about 30 channels on the high-energy side.
(c) Calculate the FWHM and FWTM. Connect the count values by a linear line, and calculate the proportional distribution.
(d) Calculate the asymmetry at the FWTM.

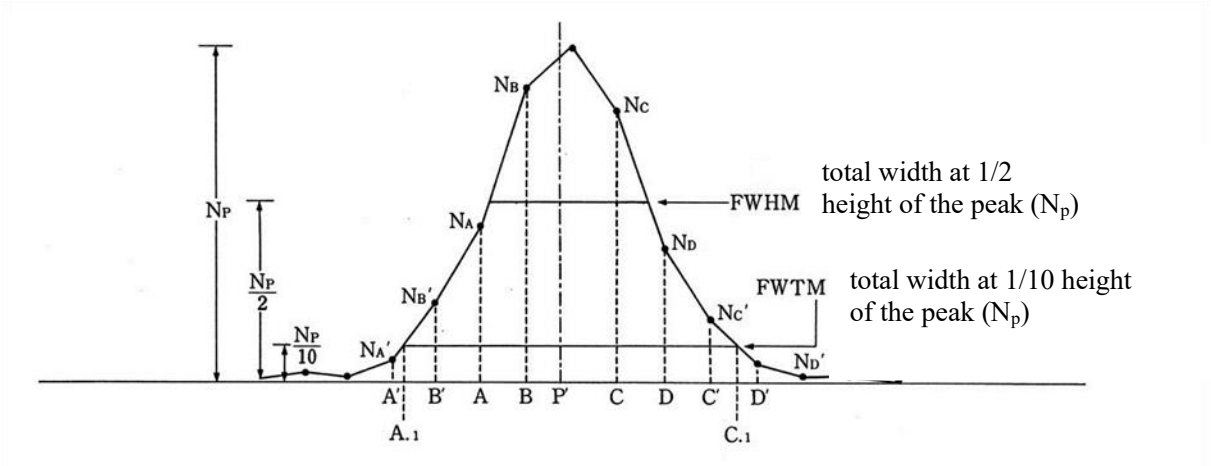

Fig. D1.1.9 Half width and peak asymmetry.

$$W(\mathrm{ch}) = \left[C + \frac{N_C - N_P/2}{N_C - N_D}\right] - \left[A + \frac{N_P/2 - N_A}{N_B - N_A}\right] \quad \text{(D1.1.16)}$$

$$W(\mathrm{ch}) = \left[C' + \frac{N_{C'} - N_P/10}{N_{C'} - N_{D'}}\right] - \left[A' + \frac{N_P/10 - N_{A'}}{N_{B'} - N_{A'}}\right] \quad \text{(D1.1.17)}$$

$$C' \rightarrow C_{.1} \qquad A' \rightarrow A_{.1}$$

$$\text{asymmetry} = \frac{\left(P' - A_{.1}\right) - \left(C_{.1} - P'\right)}{\left(C_{.1} - P'\right)} \times 100 \quad (\%) \quad \text{(D1.1.18)}$$

W	: FWHM
$A, B, C, D, P, A', B', C',$ and D'	: channel
$N_A, N_B, N_C, N_D,$ and N_P ・・・	: count value
P'	: peak center channel

If the zero-cross point in the first derivative coefficient and the uncertainty related to the count for the FWTM have been calculated, then it will be possible to calculate the uncertainty of the asymmetry.

Document 1.1.3.3 Method to obtain peak area by function fitting

In principle, the peak area is calculated by function fitting. Let the region represented by the Gaussian function be the area. It should be noted that the peak area does not include the tailing parts or the steps.

Some differences in the area may be generated between the Covell method (described later) and function fitting, but there is no problem in their practical usage.

It is recommended to investigate in advance how the peak asymmetry, tailing, and step changes depending on energy, and use those results by reflecting the same in the peak function.

Except for cases involving poor conditions, such as a small peak overlapped on a tailing and complex peak, if limited to simple peaks, the linear function and simple Gaussian function can be used for the peak area calculation.

Document 1.1.4 Calculation of peak area by Covell method

The Covell method is a method where a baseline is set based on the region without peaks (hereafter referred to baseline region) on the left and right sides of a peak, and the peak area is obtained by correcting the baseline part in the peak region. Fig. D1.1.10 shows the conceptual diagram of the Covell method.

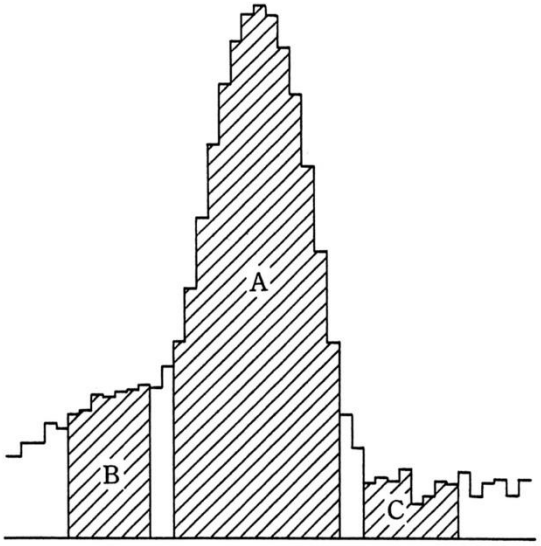

Fig. D1.1.10 Peak area calculation by the Covell method

Example of calculation: Consider a peak to be divided into low energy and high-energy sides from the peak center. Then, letting that all the numbers of the channels used for the calculation of the respective peak region and baseline region be the same, the following relations are obtained.

Peak area: $N_{net} = A - B - C$

Standard deviation of peak area: $\sigma_N = \sqrt{A + B + C}$

Concerning the peaks where the uncertainty related to counting is small and the tailing is known, let the border between the baseline region on the low-energy side and the peak region be the corner of the curve.

Document 1.1.4.1 Setting the peak region and the neighboring baseline

The peak and individual baseline regions of the respective spectrums cannot be determined independently. However, supposing that the peak shape is represented by a simple Gaussian function, and the baseline is linear in a limited range[*3], they will be determined so that the following conditions are satisfied.

(1) Obtain the center channel P of the supposed peaks by the channel-energy relational expression (refer to Document 1.1.2), and set the same channel width u' on the left and right sides of P. When the FWHM is set to be W, the channel width u' is determined in the following way.

$$1.5 \times W \gtrsim u' \gtrsim 1.1 \times W$$

Let the border on the low-energy side be $L_0 = P - u'$, and round off the resulting decimal down to the nearest whole number.

Let the border on the high-energy side be $R_0 = P + u'$, and round off the resulting decimal up to the nearest whole number.

(2) For a complex peak where two peaks overlap, determine the peak center channels P_L and P_H using the channel-energy relational expressions (refer to D1.1.2), for the respective low energy and high-energy γ-rays.

Let the border on the low-energy side be $L_0 = P_L - u'$, and round off the resulting decimal down to the nearest whole number.

Let the border on the high-energy side be $R_0 = P_H + u'$ and round off the resulting decimal up to the nearest whole number.

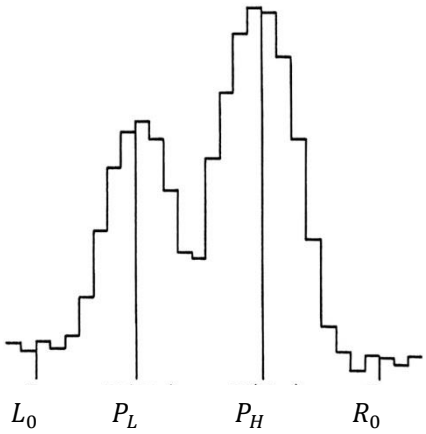

Fig. D1.1.8 Peak region for complex peaks

[*3]: When adopting the least squares method, quadratic equation or higher-order equations can be used for the base.

(3) As a general rule, determine the baseline region as follows.
Border on the low-energy side (from channel L_2 to channel L_1)

$$P - L_1 \gtrsim 1.5 \times W,\ L_1 - L_2 \gtrsim P - L_0$$

Border on the high-energy side (from channel R_1 to channel R_2)

$$R_1 - P \gtrsim 1.5 \times W,\ R_2 - R_1 \gtrsim R_0 - P$$

However, L_2, L_1, R_1, and R_2 are set as integers.

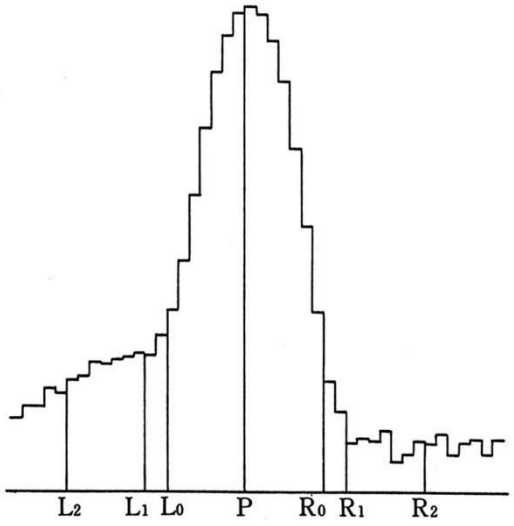

Fig. D1.1.9 Baseline regions (L_2–L_1) and (R_1–R_2)

Document 1.1.4.2 Method to obtain area for a single independent peak

(1) In cases where there is a slope in the baseline

In this section, the peak area is obtained assuming that the baseline in a γ-ray spectrum has a slope. For a baseline without a slope, refer to (2).

First, for the peak region, obtain N_P by determining L_0 and R_0 according to the method described in Document 1.1.4.1.

$$N_P = \sum_{i=L_0}^{R_0} n_i \tag{D1.1.19}$$

where n_i is the count of channel i.

Next, for baseline region, obtain N_L and N_R by determining L_2, L_1, and R_1, R_2 according to the method described in the Document 1.1.4.1.

$$N_L = \sum_{i=L_2}^{L_1} n_i \, , N_R = \sum_{i=R_1}^{R_2} n_i \tag{D1.1.20}$$

From the above equations, calculate the peak area N_{net} and its standard deviation σ_N as follows.

$$N_{net} = N_P - \beta_L N_L - \beta_R N_R \tag{D1.1.21}$$

$$\sigma_N = \sqrt{N_P + {\beta_L}^2 N_L + {\beta_R}^2 N_R} \tag{D1.1.22}$$

In the above equations, β_L and β_R are given by the following equations.

$$\beta_L = \frac{(R_1 + R_2 - L_0 - R_0)(R_0 - L_0 + 1)}{(L_1 - L_2 + 1)(R_1 + R_2 - L_2 - L_1)}$$

$$\beta_R = \frac{(L_0 + R_0 - L_1 - L_2)(R_0 - L_0 + 1)}{(R_2 - R_1 + 1)(R_1 + R_2 - L_2 - L_1)}$$

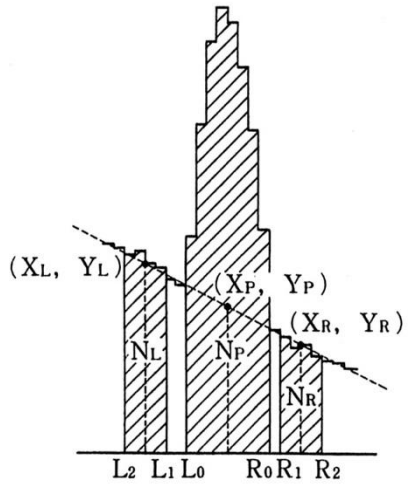

Fig. D1.1.10 Method to obtain area of a peak that includes the baseline with the slope.

Using equations (D1.1.21) and (D1.1.22), β_L and β_R can be obtained as follows. Since the baseline is a linear function $Y = aX + b$ (a and b: constant), letting the midpoints in the baseline regions on the low energy and high-energy sides, respectively, be (X_L, Y_L) and (X_R, Y_R), and letting the midpoint of the baseline in the peak region be (X_P, Y_P); the following relations are obtained.

$$\begin{aligned} Y_P &= \frac{Y_R - Y_L}{X_R - X_L}(X_P - X_L) + Y_L \\ &= \frac{(X_R - X_P)Y_L + (X_P - X_L)Y_R}{X_R - X_L} \end{aligned} \tag{D1.1.23}$$

Further, the midpoint in the respective baseline regions can be expressed by the following equations.

$$X_L = \frac{L_1 + L_2}{2} \qquad Y_L = \frac{N_L}{L_1 - L_2 + 1}$$

$$X_R = \frac{R_1 + R_2}{2} \qquad Y_R = \frac{N_R}{R_2 - R_1 + 1}$$

$$X_P = \frac{L_0 + R_0}{2}$$

Therefore, the area S_{LR} of the baseline region that is subtracted from the peak region is given by the following equation.

$$\begin{aligned} S_{LR} &= Y_P(R_0 - L_0 + 1) \\ &= \frac{(R_1 + R_2 - L_0 - R_0)(R_0 - L_0 + }{(L_1 - L_2 + 1)(R_1 + R_2 - L_2 - L} \cdot \mathrm{N}_L \\ &+ \frac{(L_0 + R_0 - L_1 - L_2)(R_0 - L_0 + }{(R_2 - R_1 + 1)(R_1 + R_2 - L_2 - L} \cdot N_R \\ &= \beta_L N_L + \beta_R N_R \end{aligned} \tag{D1.1.24}$$

(2) In case there is no slope in the baseline

First, for the peak region, obtain N_P by determining L_0 and R_0 according to the method described in the D.1.1.4.1,

$$N_P = \sum_{i=L_0}^{R_0} n_i \qquad \text{(D1.1.25)}$$

where n_i is the count of channel i.

Next, for the baseline region, obtain N_L and N_R by determining L_2, L_1, and R_1, R_2 according to the method described in the Document 1.1.4.1.

$$N_L = \sum_{i=L_2}^{L_1} n_i \,, \qquad N_R = \sum_{i=R_1}^{R_2} n_i \qquad \text{(D1.1.26)}$$

From the above equations, the peak area N_{net} and its standard deviation σ_N are calculated as follows.

$$N_{net} = N_P - \beta_L N_L - \beta_R N_R \qquad \text{(D1.1.27)}$$

$$\sigma_N = \sqrt{N_P + {\beta_L}^2 N_L + {\beta_R}^2 N_R} \qquad \text{(D1.1.28)}$$

In the above equations, β_L and β_R are determined by the following equations.

$$\beta_L = \frac{R_0 - L_0 + 1}{2(L_1 - L_2 + 1)}$$

$$\beta_R = \frac{R_0 - L_0 + 1}{2(R_2 - R_1 + 1)}$$

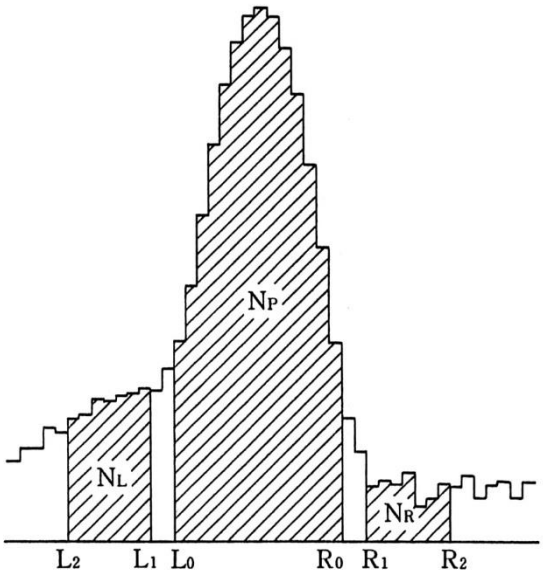

Fig. D1.1.11 Method to obtain the area of a peak that has the baseline without the slope.

At this moment, let half of the channel numbers used for the calculation of the peak area be the channel numbers used for the calculation of the baseline regions on the respective low energy and high-energy sides; this calculation will be simplified because β_L and β_R become 1.

$$L_1 - L_2 + 1 = \frac{1}{2}(R_0 - L_0 + 1) \qquad \therefore \beta_L = 1 \qquad \text{(D1.1.29)}$$

$$R_2 - R_1 + 1 = \frac{1}{2}(R_0 - L_0 + 1) \qquad \therefore \beta_R = 1 \qquad \text{(D1.1.30)}$$

Therefore, the peak area N_{net} and its standard deviation σ_N are calculated as follows.

$$N_{net} = N_P - N_L - N_R \qquad \text{(D1.1.31)}$$

$$\sigma_N = \sqrt{(N_P + N_L + N_R)} \qquad \text{(D1.1.32)}$$

Document 1.1.5 Processing interfering peaks

If interfering peaks are found in a peak search, the following processes should be performed.

- Obtain the peak area by the method where a baseline is set by avoiding the interfering peak, when the count between a peak to be analyzed and the interfering peak drops to the baseline and each peak becomes independent, , which will be described below (Document 1.1.5.1 (1)).
- When the two peaks are almost completely overlapped, the contribution coefficient method is used, which is described below (Document 1.1.5.1 (2)).

  Note that, since the contribution coefficient for the interference from radiation shielding is intrinsically different from that for the interference from the sample, the correction by the contribution coefficient should be performed after subtracting the background. The calculation process will become complicated depending on the method used for the background subtraction.

  Furthermore, it should be noted that, unless the sample has the same shape and same self-absorption as the source by which the contribution coefficient has been measured, accurate correction will not be possible. Due to these circumstances, errors are unavoidable to some extent.
- When the dent between the two peaks does not drop to the baseline (complex peak), function fitting (refer to Document 1.1.3) is used.
- In case the main peak of the nuclide to be analyzed is a complex peak, and if there is an independent sub-peak whose uncertainty related to counting of the peak area is smaller than that of the main peak, then focus on analyzing this independent peak even if its emission rate is small.

Document 1.1.5.1 Processing of the interfering peak in the baseline next to the single independent peak

(1) Method of determining the baseline while avoiding interfering peak

The processing is performed when the following criteria are satisfied[*4].

(a) When it is judged by peak search that interfering peaks exist in the baseline region.

(b) Let P'' be the other prominent single peak emitted from the same nuclide generating the interfering peak (hereafter referred to as the interfering standard peak). When the peak area $N_{net}(P'')$ is larger than twice the uncertainty $\sigma_N(P'')$ related to the counting, that is, when $N_{net}(P'') \geqq 2\sigma_N(P'')$ holds and $N_{net}(P'')$ multiplied by the contribution coefficient ν is two counts or more ($\nu N_{net}(P'') \geqq 2$),

Determine how to select the peak region against the peak to be analyzed by the method described in Document 1.1.4.1. Also, determine the baseline region by avoiding the interfering peaks. In other words, let L_1 or R_1 be the channel 1.5 × FWHM or greater from the interfering peak center P'.

The methods to obtain peak area N_{net} and its standard deviation σ_N follow the method described in Document 1.1.4.2.escribed described in the Document 1.1.4.2.

[*4]: If condition (a) holds, it is safer to take this method even if condition (b) does not hold.

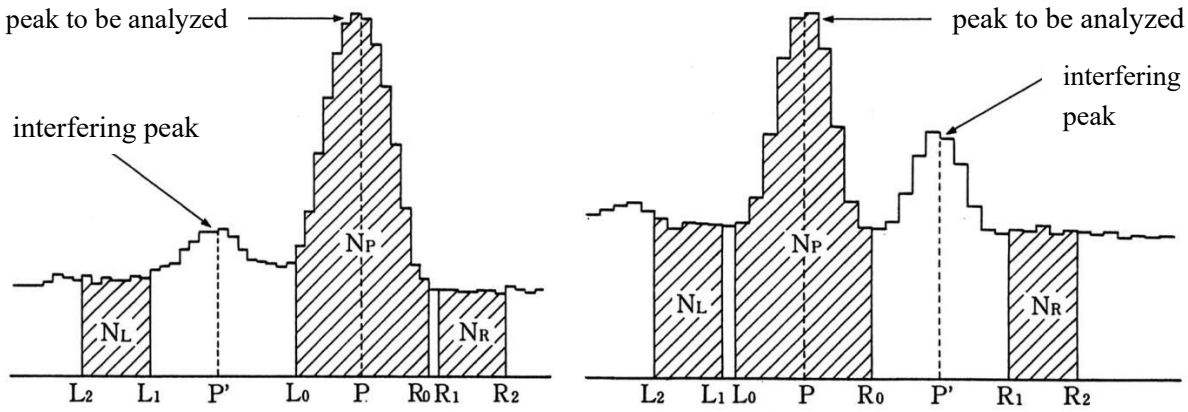

$P' - L_1 \geq 1.5\mathrm{FWHM}$ $R_1 - P' \geq 1.5\mathrm{FWHM}$

Fig. D1.1.12 Method to determine the baseline region avoiding interfering peaks.

(2) Method to correct peak area using contribution coefficient [*5]

For a single independent peak where the interfering peaks exist in the neighboring baseline, a method has been developed to correct the peak area using the contribution coefficient. The correction of interfering peaks is applied when the following criteria are satisfied.

- In the case that the area $N_{net}(P'')$ of the interfering standard peak is larger than twice the uncertainty $\sigma_N(P'')$ related to the counting, that is, $N_{net}(P'') \geqq 2\sigma_N(P'')$.
- In addition to the above criterion, in case that $N_{net}(P'')$ multiplied by the contribution coefficient ν is two counts or more, that is, $\nu N_{net}(P'') \geqq 2$.

(a) Determine the peak region for the analyzed peak by the method described in Document 1.1.4.1.

$$N_P = \sum_{i=L_0}^{R_0} n_i \qquad \text{(D1.1.33)}$$

[*5]: It is desirable to judge the validity of the correction by comparing the uncertainty related to counting increased by the correction contribution with the error generated in the radioactivity value by not making the correction.

(b) Determine the baseline region so that it includes all interfering peaks. That is, letting the center channel of the interfering peak be P', determine L_2, L_1, R_1, and R_2 so that the following conditions are satisfied.

When an interfering peak is on the low-energy side of the peak to be analyzed (Fig. D.1.1.16), the following relationship should hold.

$$L_1 - P' \geqq 1.5 \times \mathrm{FWHM} \text{ and } P' - L_2 \geqq 1.5 \times \mathrm{FWHM}$$

Conversely, when an interfering peak is on the high-energy side of the peak to be analyzed, the following relationship holds.

$$P' - R_1 \geqq 1.5 \times \mathrm{FWHM} \text{ and } R_2 - P' \geqq 1.5 \times \mathrm{FWHM}$$

(c) For an interfering standard peak, determine the peak area $N_{net}\left(P''\right)$ and its uncertainty $\sigma_N\left(P''\right)$ according to the method described in Document 1.1.4.2.

(d) Using $N_{net}\left(P''\right)$, the peak area $N_{net}\left(P'\right)$ of the interfering peak can be estimated as follows.

$$N_{net}\left(P'\right) = \nu N_{net}\left(P''\right) \quad \text{where} \quad \nu = \frac{a'}{a''} \cdot \frac{\varepsilon'}{\varepsilon''} \qquad \text{(D1.1.34)}$$

In the above equation, a' and a'' are the γ-ray emission rates for peaks P' and P'', respectively. The variables ε' and ε'' are the peak efficiencies (including the self-absorption correction) of γ-rays for the peaks P' and P'', respectively. The value of a'/a'' can be obtained from the nuclear data, and that of $\varepsilon'/\varepsilon''$ can be obtained from the peak efficiency calibration formula. Alternatively, an experimental value can be used as a value of ν.

(e) Obtain N_L and N_R in the baseline region determined above.

$$N_L = \sum_{i=L_2}^{L_1} n_i\,, \qquad N_R = \sum_{i=R_1}^{R_2} n_i \qquad \text{(D1.1.35)}$$

(f) The peak area N_{net} of a peak to be analyzed and its standard deviation σ_N can be calculated as follows.

When an interfering peak exists on the low-energy side of a peak to be analyzed, the following relationship is obtained.

$$N_{net} = N_P - \beta_L \left\{ N_L - \nu N_{net}\left(P^{\prime\prime}\right) \right\} - \beta_R N_R \tag{D1.1.36}$$

$$\sigma_N = \sqrt{N_P + {\beta_L}^2 N_L + {\beta_R}^2 N_R + \left\{ \nu \beta_L \sigma_N \left(P^{\prime\prime}\right) \right\}^2} \tag{D1.1.37}$$

In the above equations, β_L and β_R are calculated in the following equations.

$$\beta_L = \frac{(R_1 + R_2 - L_0 - R_0)(R_0 - L_0 + 1)}{(L_1 - L_2 + 1)(R_1 + R_2 - L_2 - L_1)}$$

$$\beta_R = \frac{(L_0 + R_0 - L_1 - L_2)(R_0 - L_0 + 1)}{(R_2 - R_1 + 1)(R_1 + R_2 - L_2 - L_1)}$$

(If there is an interfering peak on the high-energy side of a peak to be analyzed, L and R may be replaced for all of the equations (D1.1.36) and (D1.1.37).)

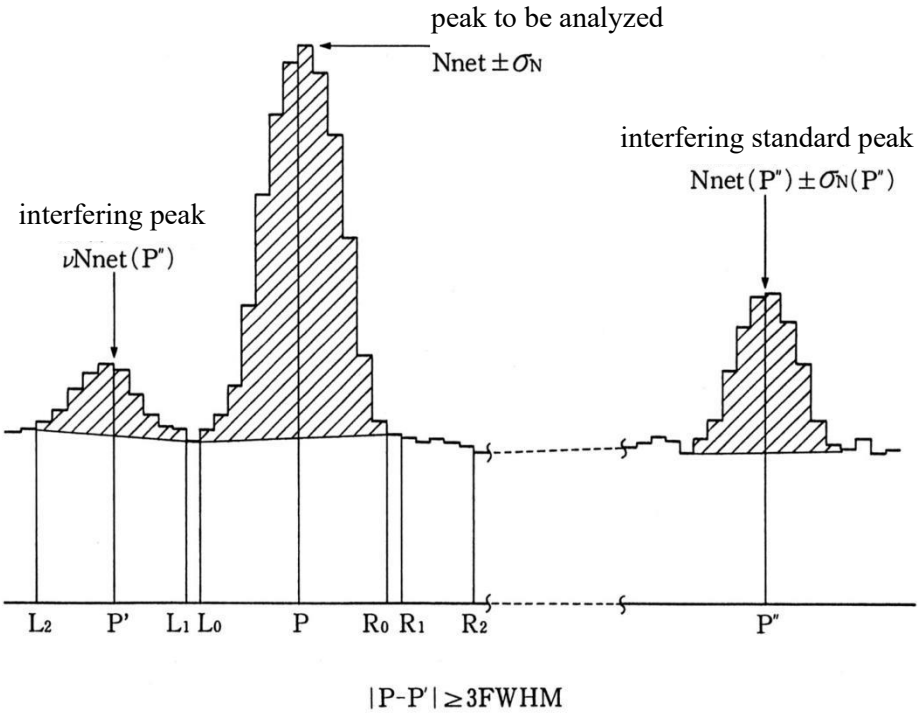

Fig. D1.1.13 Method to subtract the contribution of the interfering peak from the baseline.

Document 1.1.5.2 Analysis of complex peak (peak where other peaks exist within three times the FWHM)

(1) In case two peaks originate from the same nuclide.

(a) Let the peak region be $L_0 = P_L - u'$, $R_0 = P_H + u'$ according to Document 1.1.4.1 (2), where P_L and P_H are the peak center channels on the low energy and the high-energy sides, respectively.

(b) Calculate the baseline region according to equation (Document 1.1.4.2), and obtain the peak area $N_{net}(P_L + P_H)$ including the peaks and standard deviations σ_N.

(c) If the peak efficiencies against energy for P_L and P_H are ε_L and ε_H, respectively, and the γ-ray emission rates for P_L and P_H are a_L and a_H, respectively, the following equations are obtained.

$$N_{net}(P_L) \pm \sigma_L = \frac{\varepsilon_L a_L}{\varepsilon_L a_L + \varepsilon_H a_H}\{N_{net}(P_L + P_H) \pm \sigma_N\} \quad \text{(D1.1.38)}$$

$$N_{net}(P_H) \pm \sigma_H = \frac{\varepsilon_H a_H}{\varepsilon_L a_L + \varepsilon_H a_H}\{N_{net}(P_L + P_H) \pm \sigma_N\} \quad \text{(D1.1.39)}$$

In the above equations, the relation $\varepsilon_L \fallingdotseq \varepsilon_H$ may be set.

(2) In the case where two peaks originate from different nuclides and there are interfering standard peaks.

(a) The correction of the interfering peaks is applied when the same criteria as in D1.1.5.1 (2) are satisfied.

(b) According to Document 1.1.4.1.(2), let the peak region be $L_0 = P_L - u'$ and $R_0 = P_H + u'$ where P_L and P_H are the peak center channels on the low energy and high-energy sides, respectively.

(c) Calculate the baseline region according to Document1.1.4.2, and obtain the peak area $N_{net}(P_L + P_H)$ including both peaks.

Here, let P_L be the analyzed peak and be represented by P, and let P_H be the interfering peak and be represented by P'. In other words, the peak area including the interfering peaks is represented by $N_{net}\left(P + P'\right)$, and its standard deviation is represented by $\sigma_N\left(P + P'\right)$.

(d) Obtain the peak area $N_{net}\left(P''\right)$ and its standard deviation $\sigma_N\left(P''\right)$ for the interfering peak $\left(P''\right)$ according to the method described in Document 1.1.4.2.

(e) Let the ratio (contribution coefficient) of the peak area of the interfering peak to $N_{net}\left(P^{\prime\prime}\right)$ be ν. Letting the γ-ray emission rates for $P^{\prime}$ and $P^{\prime\prime}$ be $a^{\prime}$ and $a^{\prime\prime}$, respectively, and the peak efficiencies for $P^{\prime}$ and $P^{\prime\prime}$ be $\varepsilon^{\prime}$ and $\varepsilon^{\prime\prime}$, respectively. The value of ν is given by the following equation.

$$\nu = \frac{a^{\prime}}{a^{\prime\prime}} \cdot \frac{\varepsilon^{\prime}}{\varepsilon^{\prime\prime}}$$

Here, note that the self-absorption corrections have been performed for $\varepsilon^{\prime}$ and $\varepsilon^{\prime\prime}$.

(f) The peak area $N_{net}(P)$ and the standard deviation σ_N for the peak to be analyzed are expressed by the following equations.

$$N_{net}(P) = N_{net}\left(P + P^{\prime}\right) - \nu N_{net}\left(P^{\prime\prime}\right) \quad \text{(D1.1.40)}$$

$$\sigma_N = \sqrt{\left\{\sigma_N\left(P + P^{\prime}\right)\right\}^2 + \nu^2\left\{\sigma_N\left(P^{\prime\prime}\right)\right\}^2} \quad \text{(D1.1.41)}$$

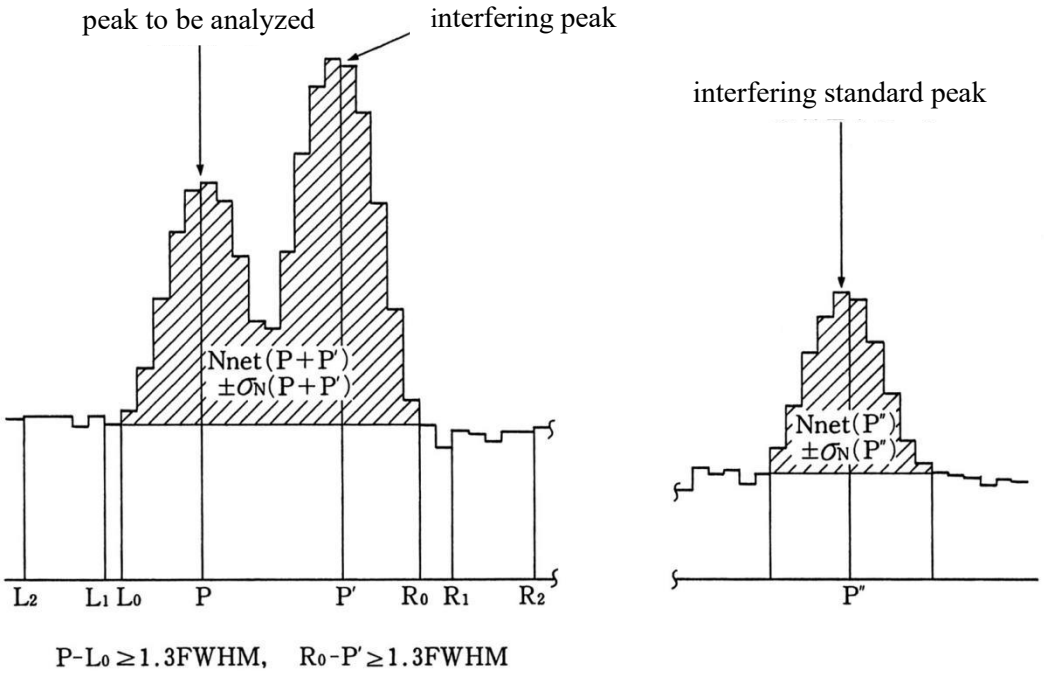

Fig. D1.1.14 Method to subtract an interfering peak from a complex peak.

(3) Analyzing complex peaks using simultaneous equations

This method is only applicable when the peak shape is represented by the Gaussian function, and the center channels P_1 and P_2 and the FWHM can be precisely obtained.

(a) Obtain the peak channel for both peaks accurately from the energy equations (refer to Document1.1.2).

(b) Obtain the FWHM of the peak from the equations (refer to the Document 1.1.1) (The FWHM for both peaks can be considered to be equal).

(c) Determine the channel region for the analysis so that the following conditions are satisfied: L_0, L_1, L_2, R_0, R_1, R_2, and U_0 are integers. U_1 and U_2 are obtained with a precision of two digits after the decimal point.

$$L_0 \approx P_1 - 1.5 \times \mathrm{FWHM} \quad \text{(D1.1.42)}$$

$$R_0 \approx P_2 + 1.5 \times \mathrm{FWHM} \quad \text{(D1.1.43)}$$

$$U_0 \approx \frac{1}{2}(P_1 + P_2) \quad \text{(D1.1.44)}$$

$$U_1 = U_0 - P_1 \quad \text{(D1.1.45)}$$

$$U_2 = P_2 - U_0 \quad \text{(D1.1.46)}$$

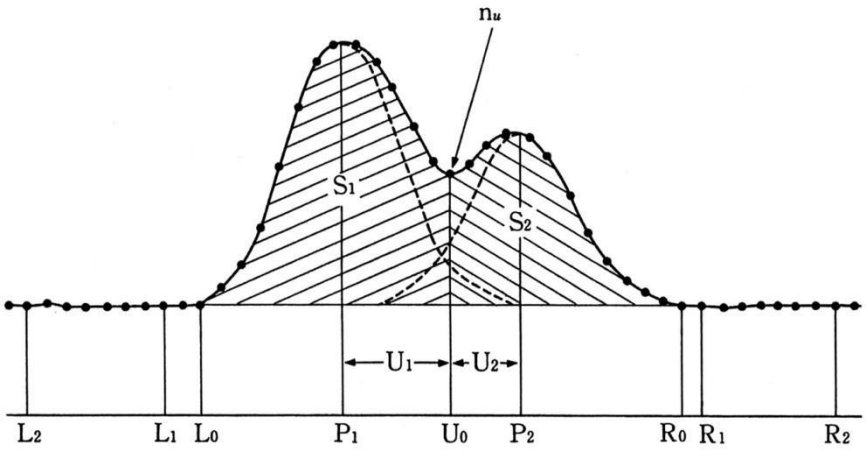

Fig. D1.1.15 Method to determine region by simultaneous equations.

(d) Obtain the peak areas S_1 and S_2, and the standard deviations σ_1 and σ_2 in the regions from L_0 to U_0 and from U_0 to R_0, respectively, as follows.

$$N_P(1) = \sum_{i=L_0}^{U_0-1} n_i \,, \qquad N_P(2) = \sum_{i=U_0+1}^{R_0} n_i \tag{D1.1.47}$$

$$N_L = \sum_{i=L_2}^{L_1} n_i \,, \qquad N_R = \sum_{i=R_1}^{R_2} n_i \tag{D1.1.48}$$

$$S_1 = N_P(1) + \frac{1}{2} n_u - \beta_1 N_L \,, \qquad \sigma_1 = \sqrt{N_P(1) + \frac{1}{4} n_u + {\beta_1}^2 N_L} \tag{D1.1.49}$$

$$S_2 = N_P(2) + \frac{1}{2} n_u - \beta_2 N_R \,, \qquad \sigma_2 = \sqrt{N_P(2) + \frac{1}{4} n_u + {\beta_2}^2 N_R} \tag{D1.1.50}$$

For the above formula,

$$\beta_1 = \frac{U_0 - L_0 + 0.5}{L_1 - L_2 + 1} \qquad \beta_2 = \frac{R_0 - U_0 + 0.5}{R_2 - R_1 + 1}$$

(e) Let the peak areas for peaks P_1 and P_2 be N_1 and N_2, respectively, and let the standard deviations for peaks P_1 and P_2 be σ_{N1} and σ_{N2}, respectively. Then these values are obtained by the following equations.

$$N_1 = \alpha_{11} S_1 + \alpha_{12} S_2 \,, \qquad \sigma_{N1} = \sqrt{(\alpha_{11}\sigma_1)^2 + (\alpha_{12}\sigma_2)^2} \tag{D1.1.51}$$

$$N_2 = \alpha_{21} S_1 + \alpha_{22} S_2 \,, \qquad \sigma_{N2} = \sqrt{(\alpha_{21}\sigma_1)^2 + (\alpha_{22}\sigma_2)^2} \tag{D1.1.52}$$

In the above equations, the values of α_{11}, α_{12}, α_{21}, and α_{22} are obtained as follows.

Let the values of $U_1{}'$ and $U_2{}'$ be $U_1{}' = 2.355 \times U_1/\mathrm{FWHM}$ and $U_2{}' = 2.355 \times U_2/\mathrm{FWHM}$, respectively. Then, calculate the probabilities $P\left(U_1{}'\right)$ and $P\left(U_2{}'\right)$ as follows.

Distribution $$F(x) = \frac{1}{\sqrt{(2\pi)}} \exp(-x^2/2) \tag{D1.1.53}$$

From the relationship $x = u'$, the probability shown on the right side of the above equation can be expressed by integration as follows.

$$P\left(u'\right) = \frac{1}{\sqrt{(2\pi)}} \int_{u'}^{\infty} \exp(-x^2/2)\, dx \tag{D1.1.54}$$

The following equation is used to approximate the integration in the above equation.

$$P\left(u^{'}\right) = F\left(u^{'}\right)(b_1 t + b_2 t^2 + b_3 t^3 + b_4 t^4 + b_5 t^5) + e\left(u^{'}\right) \quad \text{(D1.1.55)}$$

where $r = 0.2316419, t = \dfrac{1}{1 + r u^{'}}$

$b_1 = 0.31938153$, $b_2 = -0.356563782$

$b_3 = 1.781477937$, $b_4 = -1.821255978$

$b_5 = 1.330274429$

For the uncertainties in the approximation, $P\left(U_1^{'}\right)$ and $P\left(U_2^{'}\right)$ are calculated assuming $\left|e\left(u^{'}\right)\right| < 7.5 \times 10^{-8}$, $u^{'} = U_1^{'}$, and $u^{'} = U_2^{'}$.

The values of α_{11}, α_{12}, α_{21}, and α_{22} can be obtained by the following equations.

$$\begin{aligned}
\alpha_{11} &= \frac{1 - P\left(U_2^{'}\right)}{1 - P\left(U_1^{'}\right) - P\left(U_2^{'}\right)}, \alpha_{12} \\
&= \frac{-P\left(U_2^{'}\right)}{1 - P\left(U_1^{'}\right) - P\left(U_2^{'}\right)} \\
\alpha_{21} &= \frac{-P\left(U_1^{'}\right)}{1 - P\left(U_1^{'}\right) - P\left(U_2^{'}\right)}, \ \alpha_{22} \\
&= \frac{1 - P\left(U_1^{'}\right)}{1 - P\left(U_1^{'}\right) - P\left(U_2^{'}\right)}
\end{aligned} \quad \text{(D1.1.56)}$$

Document 1.2 Examples to obtain peak efficiency for volumetric source

Cylindrical measurement vessels are generally used in γ-ray spectrometry for environmental samples. In this case, it is operationally convenient for the peak efficiency to be obtained from the arbitrary sample filling height and γ-ray energy.

In this section, a set of volumetric sources with different heights were used to obtain peak efficiencies from arbitrary heights of volumetric samples. Examples of the same will also be provided.

Document 1.2.1 Standard source[*1]

Prepare a set of multi-nuclide volumetric sources with different filling heights (from 5 to 50 mm with 10 mm intervals). The vessel for the source and samples are the same. The uncertainty for the filling height of a standard volumetric source must be ≤0.5 mm. The set of nuclides and their criteria of radioactivity are set as shown in Table D.1.2.1.

Table D1.2.1 Criteria of radioactivity (Bq) per one standard volumetric source on the day of measurement.

^{109}Cd	^{57}Co	^{139}Ce	^{203}Hg	^{113}Sn	^{85}Sr	^{137}Cs	^{54}Mn	^{59}Fe
3000	200	100	300	300	400	300	600	1000

(Note) The energies of γ-rays emitted from each nuclide are found in Document 5.

Although there has been no problem in using a source with a radioactivity that is several times the value shown in the table above, the dead time should be set to ≤5%.

When low-energy γ-rays around 60 keV are to be measured, add an ^{241}Am source of 300 Bq.

When ^{203}Hg or ^{113}Sn are not suitable (e.g., when the matrix is agar), use ^{51}Cr of 600 Bq instead of these nuclides. To know the state of the energy region at ≥1,500 keV, add ^{60}Co and ^{88}Y. In this case, use the data after performing the corrections because there is a summing-effect.

The matrix materials for a standard volumetric radiation source include agar, alumina, plastic, etc. The standard volumetric sources can be purchased from the Japan Radioisotope Association (in Japan).

[*1]: When measuring a standard volumetric source in solution, care should be taken to avoid the contamination of the germanium semiconductor detector and radiation shield. In addition, care should be taken to ensure that the measurement vessel is sealed and not destroyed and that the polyethylene bag is not broken.

Document 1.2.2 Measurement

For the measurement of a source, note the following points.

- Should be measuring a source until the uncertainty related to the counting of area (3σ) for all peaks become <2% .
- Should measure the standard source at the same position and with the same packaging as the sample. In addition to this, the polyethylene bag covering the source and sample should be the same. If measure samples with using a polyethylene bag or protection cap in order to avoid contamination of the detector, must use the same one when measure a source.
- Since nuclides with short half-lives are included in the set of standard radiation sources, it is required to measure them as early as possible after purchase.
- When a γ-ray emitted from a standard source hits the lead shield, Pb KX-ray ($K_{\beta 1}$ = 84.936 keV) is produced, which may interfere with the ^{109}Cd peak (88.0 keV). In this case, the detector and source surroundings sometimes would be covered by a thick copper plate of approximately 5 mm in order to remove this effect. If it is used in measuring sample that the measurement of peak efficiency which used the shield (e.g., copper plate), need to be covered the detector and sample surroundings for the same way.
- When the X-ray region is not measured with an n-type detector, the summing-effect by X-rays from the source can be reduced by measuring a sample and source with the end cap of the detector covered with a 0.5 mm thick copper plate.
- Care should be taken regarding X-rays emitted by the electron capture in ^{139}Ce, etc.

Document 1.2.3 Preparation of a peak efficiency curve

Obtain the count number per one second (cps) from the net peak area of the nuclide. Attenuation correction of the certified value (Bq) and γ-ray emission number per a unit time (γ/s) is required for a standard source to get those obtained on the measuring date. The radiation decay must be considered in advance. If the measured values are shown in Bq, the unit should be changed to γ/s from the emission rate in advance. Then, obtain the peak efficiency for the energy to be measured by dividing the counting rate (cps) obtained from the measured values by the γ-ray emission number per a unit time (γ/s). Plot the calculated peak efficiency and energy on the vertical and horizontal axis, respectively on a log-log graph. Observe and determine the peak region used to calculate the area by expanding the spectrum or plotting the data.

The procedure for setting the peak and baseline region is described in Fig. D1.2.1. The procedure for setting the region (channel) is shown Fig. D1.2.2. This region is used in calculating the net area by Covell's method. The energy is calibrated to 2000 keV / 4000 channels for a detector with approximately 1.9 keV resolution.

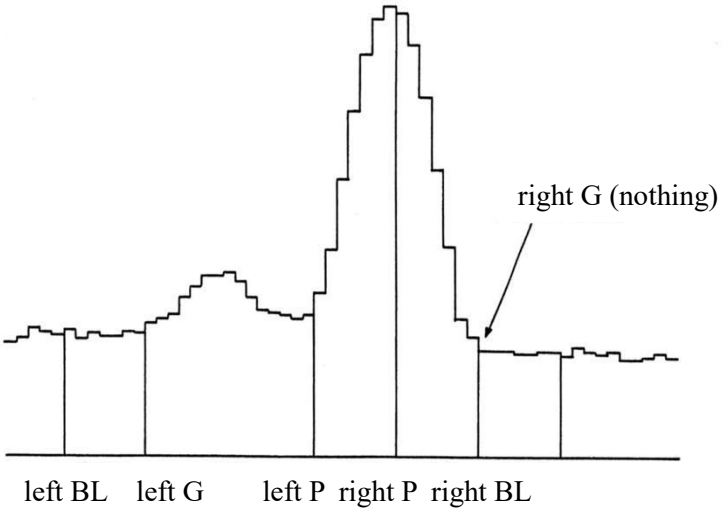

Fig. D1.2.1 Procedure for setting the peak and baseline region.

left BL, right BL: Baseline regions on the low- or high-energy sides to calculate the baseline part of the peak.

left G, right G: Baseline regions on the low- or high-energy sides. Interfering peaks are not used in the calculation.

left P, right P: Peak regions on the low- or high-energy sides.

Set the calculation region (number of channel) according to the energy of γ-rays as shown in Document Table D1.2.2.

Table D1.2.2 Energy of γ-rays and calculation region.

Nuclide	Energy	Left BL	Left G	Left P	Right P	Right G	Right BL
	(keV)	(channel)	(channel)	(channel)	(channel)	(channel)	(channel)
^{109}Cd	88.0	4	14	4	4	0	4
^{57}Co	122.1	4	0	4	4	0	4
^{139}Ce	165.9	4	0	4	4	0	4
^{203}Hg	279.2	4	0	4	4	0	4
^{113}Sn	391.7	4	0	4	4	0	4
^{85}Sr	514.0	5	0	5	5	0	5
^{137}Cs	661.7	5	0	5	5	0	5
^{54}Mn	834.8	5	0	5	5	0	5
^{88}Y	898.0	5	0	5	5	0	5
^{65}Zn	1115.5	5	0	5	5	0	5
^{59}Fe	1099.2	6	0	6	6	0	6
^{60}Co	1173.2	7	0	7	7	0	7
^{59}Fe	1291.6	7	0	7	7	0	7
^{60}Co	1332.5	8	14	8	8	0	8
^{88}Y	1836.1	8	0	8	8	0	8

The measured values of ^{88}Y, ^{60}Co, etc., need to be corrected when they become too low due to a summing-effect[*2]. If correction is not performed, the measured values of ^{88}Y and ^{60}Co are set as reference values to calculate the slope of the peak efficiency curve. However, these values are not used for the calculation of the peak efficiency curve. A peak due to characteristic X-rays from lead, which is typically observed on the low-energy side of ^{109}Cd (88.0 keV) should be excluded. An escape peak originating from ^{88}Y, which is typically observed on the low-energy side of ^{60}Co (1,332.5 keV) should also be excluded.

[*2]: Refer to the Document 1.4 “Summing-effect correction.”

The obtained peak efficiency for each energy is plotted on a log-log graph. The peak efficiency and energy are plotted on the vertical and horizontal axis, respectively, using an efficiency calculation program.

At 300–600 keV and above, the peak efficiency curve approaches a linearly decreasing straight line.

The photoelectric effect that follows the Compton scattering occurs at lower energies. At low energies, the peak efficiency increases while the transmittance of γ-rays decreases. For this reason, a peak efficiency curve for energies ≤200 keV typically exhibits a convex shape with the apex around 120 keV. An example is shown in Fig. D1.2.2.[*3].

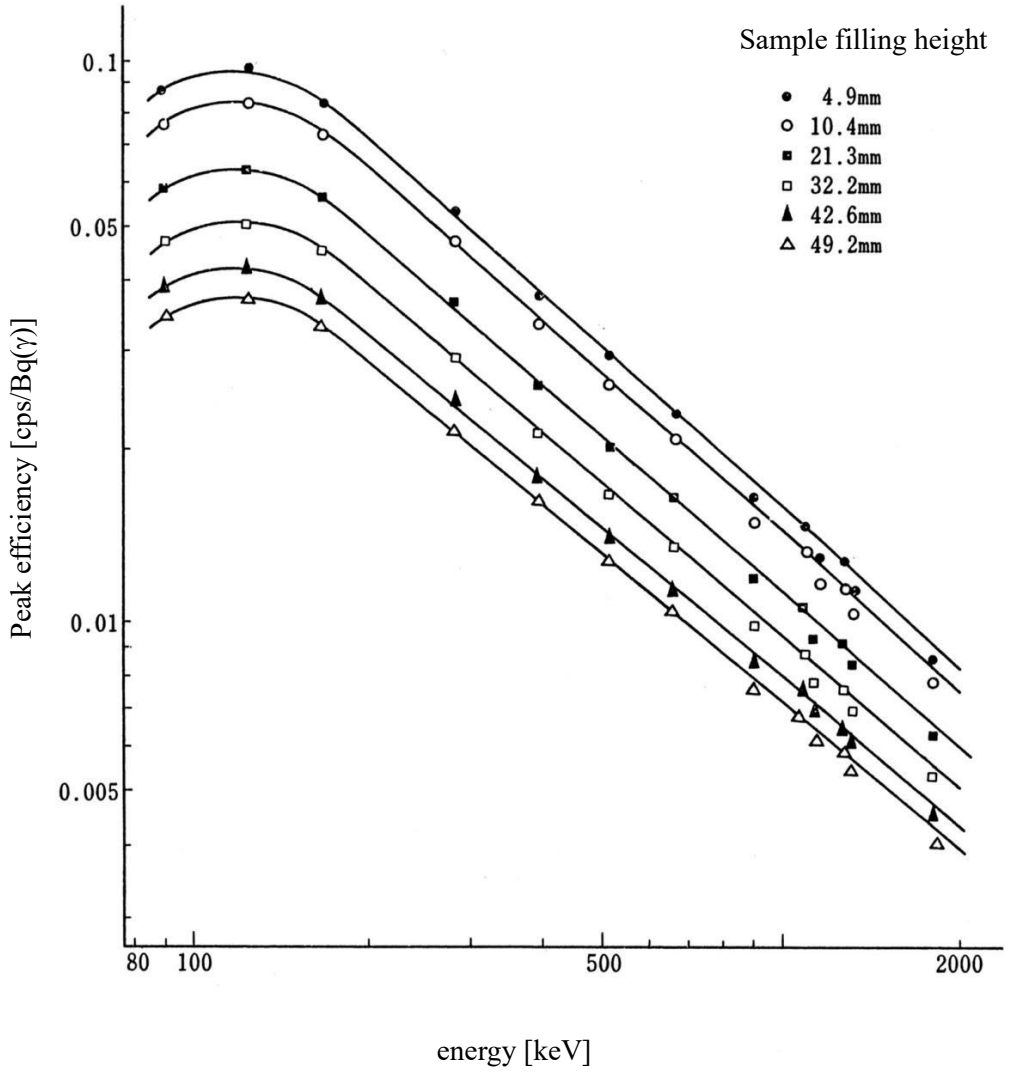

Fig. D1.2.2 Example of peak efficiency curves for each sample filling height.

[*3]: Example for a standard source in aqueous solution. The radioactivity concentration was homogeneous and the measurements were performed by alternatively repeating measurement and dilution. Thus, the radioactivity was unchanged and the measured values exhibited clear peak efficiency curves. Note that for the data of ^{60}Co and ^{88}Y, the corrections of the summing-effect were not performed.

Functionalize the peak efficiency curve of a standard source for each filling height (5, 10, 20, 30, 40, and 50 mm). The function forms are expressed in equation(D.1.2.1) and (D.1.2.2) below, where the peak efficiency is ε, γ-ray energy is E in keV, and $X = \ln(E/E_0)$ (C_1–C_6 are the constants).

$$\ln(\varepsilon) = C_1 + C_2 \mathrm{X} \qquad : E_0 \leqq E \qquad \text{(D1.2.1)}$$

$$\ln(\varepsilon) = C_1 + C_2 \mathrm{X} + C_3 X^2 + C_4 X^3 + C_5 X^4 + C_6 X^5 \qquad : E < E_0 \qquad \text{(D1.2.2)}$$

Select the energy E_0 at the border between the linear and curved regions where the peak efficiency curve became smooth in the range from 300 keV to 600 keV.

The term C_6 is only necessary if the calibration is performed at ≤80 keV. Calculation is performed by the least square method by letting $\ln(\varepsilon)$ and X be variables. (If the function fitting is conducted by separation of the energy regions, determine the values of C_1 and C_2 on the high-energy side first before calculations of C_3–C_6 on the low-energy side.)

In this way, the peak efficiencies at an arbitrary energy (from 80 keV to 2,000 keV) can be obtained for each filling height of the source. From the graph, check whether the curves do not cross and the interval does not unnaturally change. For currently available sets of volumetric sources, a well-aligned curve group generally cannot be obtained due to the uncertainty of the certification and inhomogeneity of the source. However, even when the filling heights are different, the shapes of the curves are essentially similar.

While setting the filling height (h) of the sample as a variable, plot C_1–C_6 obtained for multiple samples with different filling heights and functionalize them as in equation(D1.2.3.)

$$\exp(-C_n) = \alpha_n h^2 + \beta_n h + \gamma_n \qquad \text{(D1.2.3)}$$

Unless a very good source is available, the curve will not be smooth except for C_1. In such case, use the average value of each filling height as C_2–C_6 values.

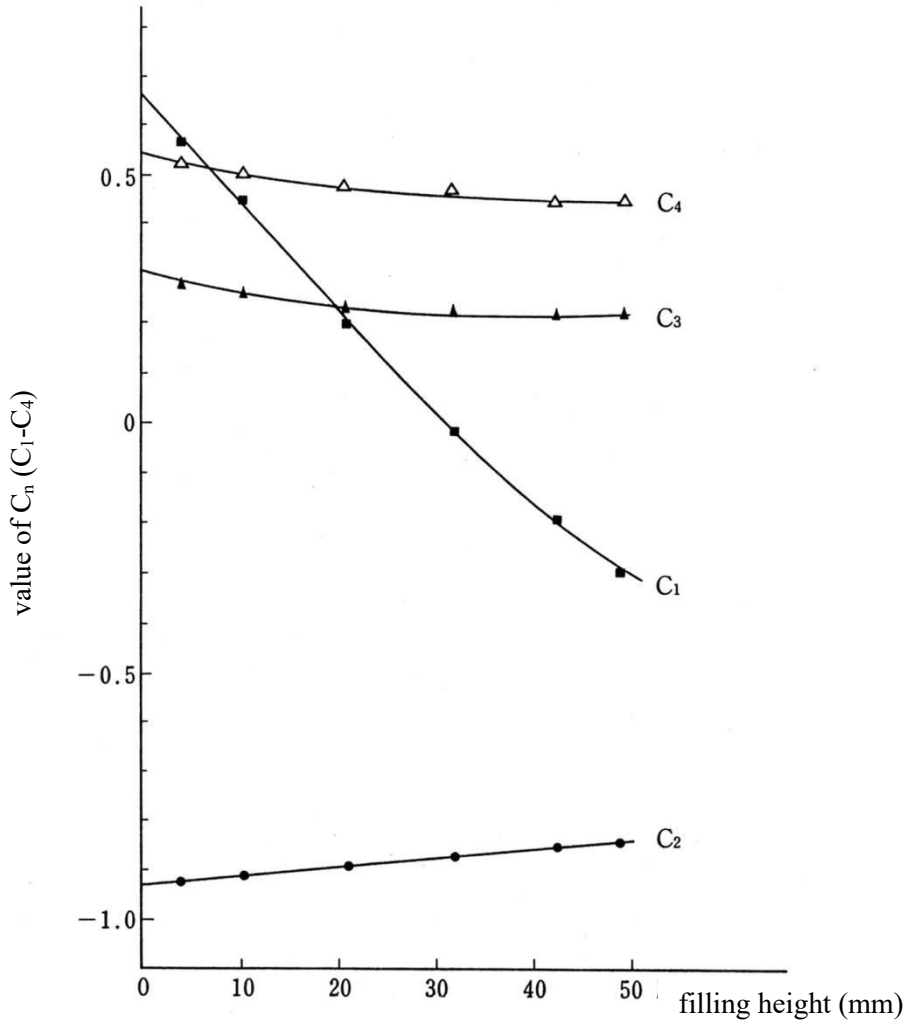

Fig. D1.2.3 Relationship between constants C_1–C_4 and filling height of a volumetric source.

(Note 1) For the example in the above figure, neither C_5 or C_6 was needed.

(Note 2) The values C_1–C_4 on the vertical axis are those where the function fitting was performed for the peak efficiency curve (shown in Fig. D.1.1.2. (unit: cps/nCi))

Using the above results, the parameters C_1–C_4 can be obtained for an arbitrary sample filling height and the peak efficiency curve can be obtained.

Document 1.2.4 Method using relative and standard peak efficiency curves

To obtain the peak efficiency by the methods described so far, a group of peak efficiency curves must be created by measuring several multi-nuclide standard volumetric sources with different filling heights. Here, an alternative method is described. First, obtain a standard peak efficiency curve that represents the relationship between the reciprocal of the peak efficiency for the energy (standard energy) of a γ-ray and the filling height of the standard volumetric source. Next, obtain a relative peak efficiency curve (a peak efficiency curve when the peak efficiency at the standard energy is converted to 1) against the standard energy. Then, substitute the peak efficiency for the value obtained by multiplying the reciprocal of the standard peak efficiency curve by the relative peak efficiency curve. However, a point source is used to obtain the peak efficiency curve, thereby it needs to be assumed that there was no significant difference in the shapes between the peak efficiency curve obtained by the point source and the volumetric source.

The peak efficiency obtained by a standard volumetric source in aqueous solution coincides with the peak efficiency curve with self-absorption correction obtained by the alternative method. The exception is for the low-energy region as shown in Fig. D1.2.4. Therefore, there were no major problems with the above assumptions in this example. However, note that there were some cases where an error of $\geq \pm 15\%$ occurred.

The standard radiation sources and measurement methods are described below.

- Measure a mixed point source (Amersham, QCD-1, etc.) containing ^{109}Cd, ^{57}Co, ^{139}Ce, ^{203}Hg, ^{113}Sn, ^{85}Sr, ^{137}Cs, ^{88}Y, and ^{60}Co, which is placed at a distance of 4 cm from the central axis of the detector end cap. Determine the relative efficiency curve. To reduce the summing-effect of ^{88}Y and ^{60}Co, the distance should be 4 cm.
- The measuring time is set when the uncertainty related to the counting of all relevant peak areas became $\leq$2%.
- Measure the KCl standard volumetric source at 5, 10, 20, 30, 40, and 50 mm height or cesium standard solution source which in a measurement vessel whose shape is same as that of the measuring sample. Thereafter, obtain the standard efficiency curve, which represents the relationship between the reciprocal of the peak efficiency and filling height.

Note that the radioactivity of KCl corresponds to approximately 1.7 Bq per 1 g.

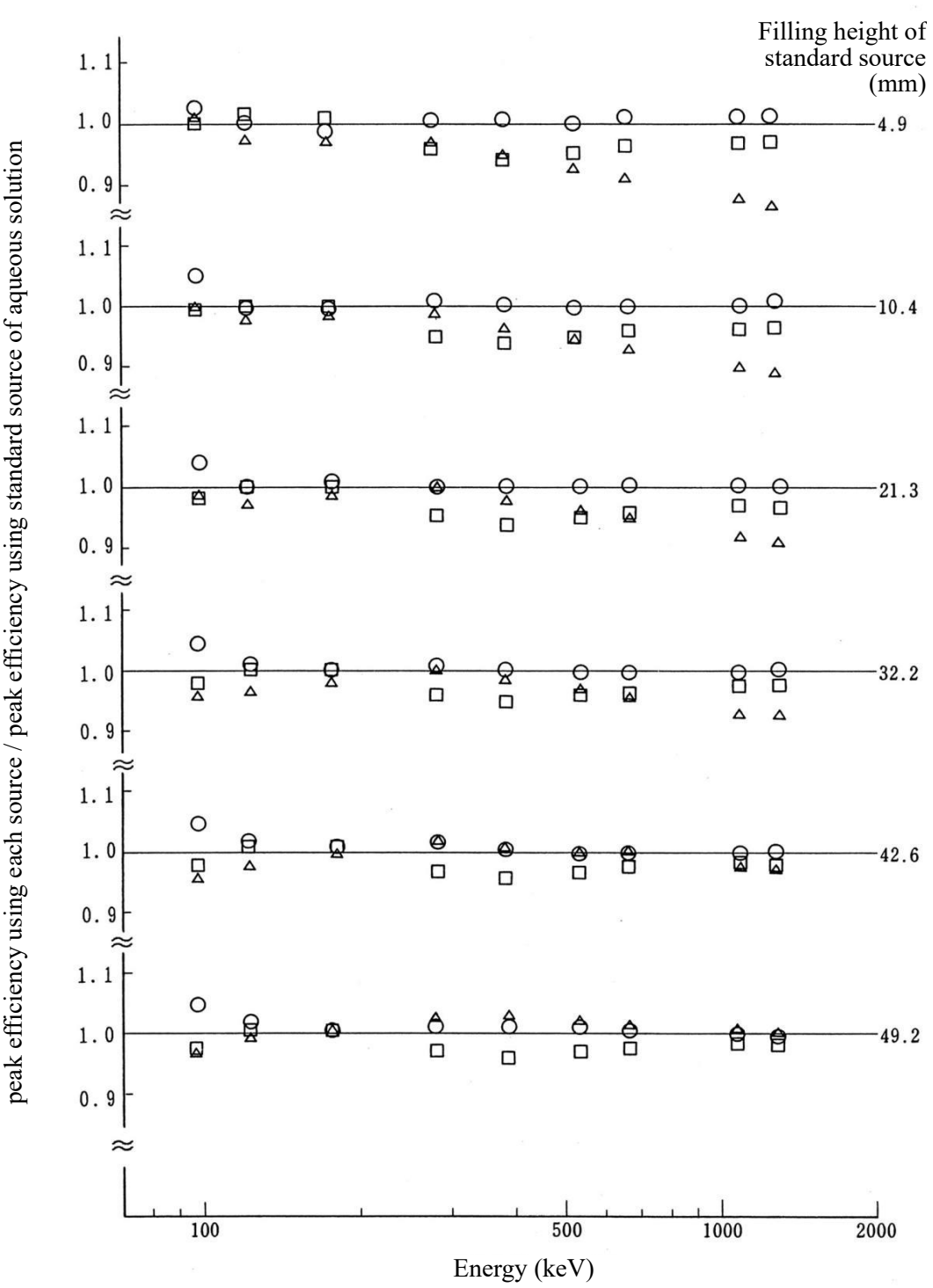

△: Peak efficiency using volumetric source with different specific gravity
□: Peak efficiency using a point source efficiency integration method
○: Peak efficiency using relative and standard peak efficiency curves

Fig. D1.2.4 Comparison of the peak efficiency using a standard source of aqueous solution with the peak efficiencies using 1) volumetric source with different specific gravity (△), 2) point source efficiency integral method (□), and 3) relative and standard peak efficiency curves (○).

Document 1.2.5 Peak efficiency including self-absorption correction for a two-layered sample

Depending on the sample, it may be measured in separated two layers. For example, seawater is sometime measured in the two layers of precipitate: sulfide and ammonium phosphomolybdate. The peak efficiency containing the self-absorption correction for sulfide in the lower layer is obtained in a similar way to that for a single layer. On the other hand, the peak efficiency containing the self-absorption correction for the upper ammonium phosphomolybdate layer is obtained by (D.1.2.4), which considers the absorption of γ-rays in the lower layer.

$$\varepsilon_A = \frac{\exp\{(\mu_A - \mu_S) \times H_1\}}{H_2 - H_1} \times (H_2 \times \varepsilon_2 - H_1 \times \varepsilon_1) \qquad \text{(D1.2.4)}$$

ε_A : peak efficiency containing the self-absorption correction for the upper layer

μ_A : linear attenuation coefficient in the upper layer

μ_S : linear attenuation coefficient in the lower layer

H_2 : filling height of the total sample

H_1 : filling height of the lower layer

ε_2 : peak efficiency including self-absorption correction, assuming that the height is H_2 and the total sample is composed of material from the upper part

ε_1 : peak efficiency including self-absorption correction, assuming that the height is H_1 and the total sample is composed of material from the upper part.

Document 1.3 Peak efficiency of Marinelli-type vessel

A Marinelli-type vessel[*1] is often used to directly measure the radioactivity of liquid samples such as milk, seawater, land water, and shredded vegetables without any pretreatments. The advantages of using such a vessel include high sensitivity and quantitative results that are obtained in a short time. Therefore, it is often used in urgent cases when we want to know quickly whether the radioactivity is high. A Marinelli-type vessel has a complex reverse well-shape that encloses a detector; therefore, it is difficult to functionalize the peak efficiency by the sample filling height (unlike a U-8 vessel). For the measurement of peak efficiency, it is required that the shape of the radiation source is the same as the sample. If the amount of liquid sample is insufficient, the volume should be increased to the standard volume with water or liquid.

Document 1.3.1 Method to obtain peak efficiency for ^{131}I, ^{137}Cs, and ^{40}K

Here, methods to obtain peak efficiency will be explained by using three kinds of nuclides, i.e., ^{131}I, ^{137}Cs, and ^{40}K. ^{131}I and ^{137}Cs are important nuclides that are typically found during emergencies while ^{40}K is in most samples as a natural radioactive nuclide.

Obtain the peak efficiency by measuring a Marinelli standard source containing ^{131}I,^{137}Cs, and ^{40}K until the peak area exceeds 20000 counts. When using a germanium semiconductor detector with a relative efficiency of 25%, the typical peak efficiencies for ^{131}I, ^{137}Cs, and ^{40}K are approximately 0.012, 0.008, and 0.004 count/γ, respectively. These values are dependent on the shape and volume of the Marinelli-type vessel.

If nuclides with γ-ray energy of $\geq$ 200 keV are detected other than ^{131}I, ^{137}Cs, and ^{40}K, the calculations described below are considered.

Plot the measured peak efficiencies on a log-log graph, where the data will become linear at γ-ray energies of $\geq$ 200 keV. The line is expressed by the equation, $\varepsilon = a \cdot E^{-b}$, where ε is the peak efficiency (count/γ), E is the γ-ray energy (keV), and a and b are constants.

Obtain the constants a and b by substituting the peak efficiencies and energies of two nuclides, which are chosen from ^{131}I, ^{137}Cs, and ^{40}K. Calculate the peak efficiency for a target nuclide by substituting the γ-ray energy of the nuclide for $\varepsilon = a \cdot E^{-b}$.

[*1]: For the Marinelli-type vessel, refer to the Commentary B.

Document 1.3.2 Method to obtain peak efficiency in cases where the number of nuclides is ≥ 3

Obtain the peak efficiency curve by measuring standard sources including ^{109}Cd, ^{57}Co, ^{139}Ce, ^{203}Hg, ^{113}Sn, ^{85}Sr, ^{137}Cs, ^{88}Y, ^{59}Fe, and ^{60}Co, which emit γ-rays at appropriately dispersed energies in the range from 80 keV to 2 MeV. ^{88}Y and ^{60}Co typically show lower values due to a summing-effect. However, these values are not so high as when sample vessel is placed directly above the end cap. Thus, a large error does not occur even if these low values are ignored.

Plot the relationship between the measured peak efficiencies and energies on a log-log graph. Perform the functionalization with a procedure similar to that described in Document 1.2.3, while ignoring the C_6 term that is not needed.

Document 1.3.3 Self-absorption correction

When using a Marinelli-type vessel, always fill the sample up to a constant height. The self-absorption corrections have to be performed for sample materials with different linear attenuation coefficients. This is done using a standard volumetric source of a single shape. The method to obtain an equation for self-absorption correction is as follows.

(a) Measure a standard source and obtain the peak efficiency $\varepsilon_s(E, \mu_s)$, where E and μ_s are the energy and linear attenuation coefficient of the standard source, respectively.

(b) Among the peak efficiencies, assuming that the function $f(\mu)$ for the components related to the linear attenuation coefficients are the reciprocal of the quadratic function of μ, $f(\mu)$ is obtained by the following equation using the peak efficiency and linear attenuation coefficient for the standard source.

$$f(\mu) = (1 + a\mu + b\mu^2)^{-1} \quad \text{(D1.3.1)}$$

where a and b are the constants.

The followings are the examples[*2] of calculation for a and b in the Marinelli-type vessel, described in Commentary B.1.2.

For 0.7 L $f(\mu) = (1 + a_{0.7}\mu + b_{0.7}\mu^2)^{-1}$ (D1.3.2)

$a_{0.7} = -0.558435$ $b_{0.7} = 5.58197$

For 2.0 L $f(\mu) = (1 + a_{2.0}\mu + b_{2.0}\mu^2)^{-1}$ (D1.3.3)

$a_{2.0} = 1.71115$ $b_{2.0} = 1.02209$

Obtain $f(\mu_s)$ and $f(\mu_x)$, by substituting μ in D1.3.1 for the linear attenuation coefficient μ_s for the material of the standard source and the linear attenuation coefficient μ_x of the sample, respectively.

Here, the suffix x represents the measuring sample.

(c) Obtain the peak efficiency $\varepsilon_x(E, \mu_x)$ of the sample by equation(D1.3.4).

$$\varepsilon_x(E, \mu_x) = \frac{f(\mu_x)}{f(\mu_s)}\ \varepsilon_s(E, \mu_s) \quad \text{(D1.3.4)}$$

[*2]: For a Marinelli-type vessel of a different volume, a and b are calculated in the following procedure.

As a Marinelli-type vessel has a shape that surrounds the detector, the self-absorption components do not depend much on the detector shape or the peak efficiency. Therefore, the peak efficiency of the detector $\varepsilon(E, G, \mu)$ can be approximated by the following equation,

$$\varepsilon(E, G, \mu) \fallingdotseq \varepsilon(E, G) \cdot f(\mu)$$

where E is the energy, G is the geometry, and μ is the linear attenuation coefficient of the sample. Assuming that $f(\mu)^{-1}$ can be approximated by the quadratic equation, the following relations are derived.

$$\frac{\varepsilon(E, G, \mu_{s1})}{\varepsilon(E, G, \mu_{s2})} = \frac{f(\mu_{s1})}{f(\mu_{s2})} = \frac{1 + a\mu_{s2} + b{\mu_{s2}}^2}{1 + a\mu_{s1} + b{\mu_{s1}}^2}$$

The right side of this equation does not depend on the energy or detector, but only depends on the shape and the material of the vessel. By substituting materials (linear attenuation coefficients) and the peak efficiencies of two standard sources for this equation, calculate the constants a and b.

Document 1.4 Method for summing-effect correction

Many radioactive nuclides emit two or more γ-rays almost at the same time per one decay. This is because the transition from a nuclear excited state after a decay to a lower-energy state happens sequentially in a short time. A γ-ray whose energy corresponds to the energy difference between the two states is emitted almost at the same time. The multiple γ-rays emitted by one nuclear decay are generated within the resolution time of a detector. We note that sequentially emitted multiple γ-rays are called cascade γ-rays. Therefore, when cascade γ-rays are absorbed in a detector, they cannot be divided. In such cases, one signal whose energy corresponds to the sum of the energies of the cascade γ-rays is observed. This leads to a reduction in the counts of γ-rays that should be measured. This phenomenon is called the coincidence-sum effect (summing-effect). Unlike the pile-up phenomenon where pulses are randomly overlapped at a high-count rate, the summing-effect may show up at a low-count rate, too. The summing-effect depends on the detection efficiency and decay scheme of the nuclide, and its values could be as high as tens of a percent[*1].

When a decay scheme is a little complex, the summing-effect becomes considerably complicated. Therefore, if the decay scheme is rewritten, the summing-effect may be easier to understand.

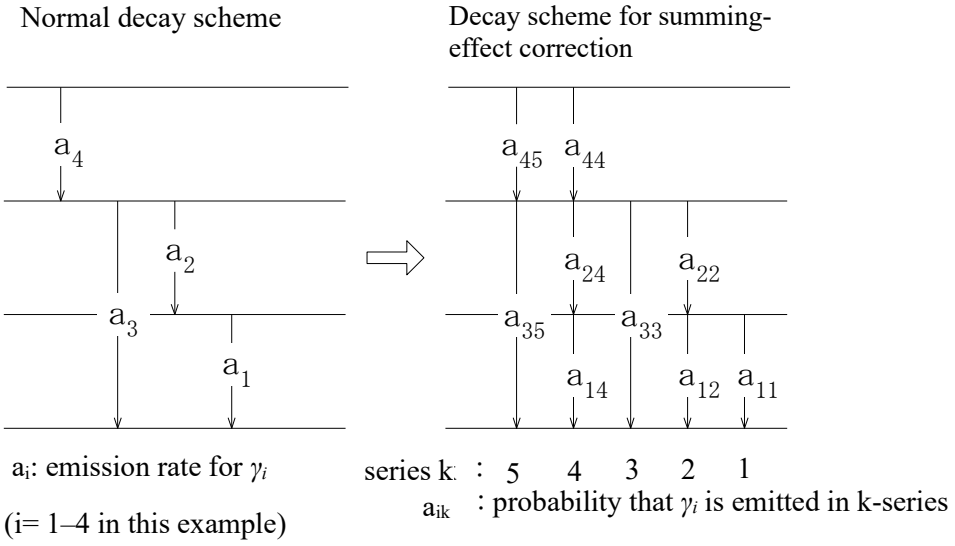

Fig. D1.4.1 Example for a rewrite of a decay scheme.

A usual decay scheme is shown in the left side of Fig. D1.4.1. When considering a summing-effect, rewrite the decay scheme like the right side of Fig. D1.4.1. If multiple γ-rays are emitted from a nuclide, only γ-rays in the cascade will be considered as objects of the summing-effect. If not, the summing-effect is not generated. The right side of Fig. D1.4.1 shows the cascade in the form of a series. The γ_3 causes the summing-effect only in the series 5, that is, the γ_3 causes the summing-effect only with γ_4. To be exact, due to the summing-effect by the series 2 and 4 (γ_1, γ_2), the signals corresponding to γ_3 will increase (crossover), but here these will be ignored[*2].

In deriving the formula for the summing-effect correction, the following are considered.

・If a series are the same, all of the transition probabilities are the same. The transition probability is given by a_{ok}.
The survival rate after a γ-ray emission reduction by an internal conversion is given by f_i for each γ_i and let $f_i a_{ok} = a_{ik}$.

[*1]: Even when a detector with a relative efficiency of 40% is used, the summing-effect could be ≥20%.

[*2]: Gamma-rays that induce the crossover are generally not used for peak efficiency calibration.

・ The total emission rate a_i for γ_i is the sum of the emission probability of γ_i in each series as shown by equation (D1.4.1).

$$a_i = \sum_k a_{ik} \tag{D1.4.1}$$

・ Ignore the angular correlation[*3].

The method to correct the summing-effect is described below.

(1) In a certain series, express a γ-ray that has a cascade relationship with γ_i as γ_j $(i \neq j)$.

(2) In a certain series, the probability that any γ_j is not counted becomes $\prod_j(1 - f_j T_j)$.

T_j : total efficiency against γ_j

$\prod$: multiplication sign

(3) The probability that γ_i in a certain series (k) with an information on the energy of γ_i is counted per one decay is expressed by equation (D.1.4.2).

$$\varepsilon_i f_i a_{ok} \prod_{j \neq i} (1 - f_j T_j) \tag{D1.4.2}$$

ε_i :peak efficiency against γ_i

(4) After summing all series, (D.1.4.3) is obtained.

$$\sum_k \varepsilon_i f_i a_{ok} \prod_{j \neq i} (1 - f_j T_j) \tag{D1.4.3}$$

Consequently, the sum becomes the counts actually measured (energy of γ_i). This is the expected value of the counts (per one decay) for a measured γ_i. Therefore, equation (D1.4.4)–(D1.4.7) hold true.

$$\sum_k \varepsilon_i f_i a_{ok} \prod_{j \neq i} (1 - f_j T_j) = \varepsilon_i^* a_i \tag{D1.4.4}$$

ε_i^* :observed peak efficiency

$$\sum_k \varepsilon_i a_{ik} \prod_{j \neq i} (1 - f_j T_j) = \varepsilon_i^* a_i \tag{D1.4.5}$$

$$\varepsilon_i^* = \varepsilon_i \sum_k \left[\frac{a_{ik}}{a_i} \prod_{j \neq i} (1 - f_j T_j) \right] \tag{D1.4.6}$$

The value of ε_i where a summing-effect correction was conducted is obtained by equation (D.1.4.7).

$$\varepsilon_i = \frac{\varepsilon_i^*}{\sum_k \left[\frac{a_{ik}}{a_i} \prod_{j \neq i} (1 - f_j T_j) \right]} \tag{D1.4.7}$$

(5) To perform a summing-effect correction, it is necessary to know the decay scheme and total efficiency of the other γ-rays, which have a cascade relationship with the measured γ-ray. The total efficiency (T) can be obtained using a standard γ-ray source, but it is more difficult to

---

[*3]: When γ_1 and γ_2 are in a cascade relationship, a value indicating the direction of γ_2 is likely to be emitted against the direction of the γ_1 emission.

obtain T than to obtain the peak efficiency. The is because the appropriate γ-ray source must be a nuclide that emits a single γ-ray only and the treatment of the scattered γ-rays is difficult. The T is generally expressed by equation (D1.4.8) using the peak to total ratio (P/T).

$$T = \frac{\varepsilon}{(P/T)} \tag{D1.4.8}$$

The peak to total ratio $((P/T))$ can be obtained by using a monochromatic γ-ray source, which is expressed by $(P/T) = n_P/n_T$. Where n_P and n_T are the peak area in the spectrum and area of the total spectrum, respectively. Note that the correct value of the radioactivity of the γ-ray source is not needed.

It is ideal to obtain a (P/T) by an actual measurement. However, if the space inside the radiation shield is a cube with a side of approximately 20 cm, the (P/T) can also be calculated by equation (D1.4.9) [17].

$$(P/T) = a \times \ln(\varepsilon_{rel}) + \beta \tag{D1.4.9}$$

$a = e^{(-0.30\times\ln(E)-1.11)}$

$\beta = e^{(-1.82\times\ln(E)+9.15)}$

E :energy of γ-ray (keV)

ε_{rel} :relative efficiency (%)

Next, the case where mainly two γ-rays, including ^{60}Co and ^{88}Y, cause the summing-effect is described. The decay scheme is shown in Fig. D1.4.2.

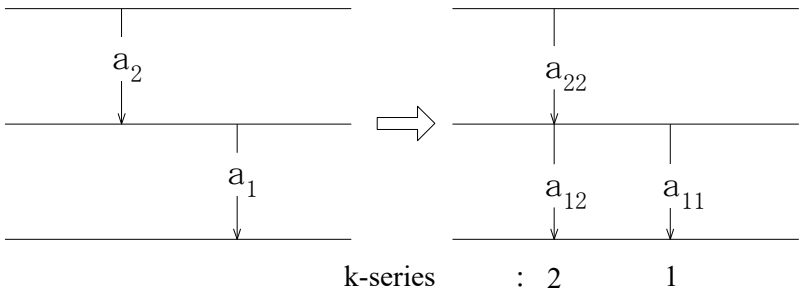

Fig. D1.4.2 Decay scheme for a nuclide that emits two γ-rays.

(1) For γ_1, the equation (D1.4.5) is replaced by equation (D.1.4.10).

$$\varepsilon_1^* a_1 = \varepsilon_1 a_{11} + \varepsilon_1 a_{12}(1 - f_2 T_2) \quad \text{(D1.4.10)}$$

$$\therefore \ \varepsilon_1^* = \varepsilon_1 \left[\frac{a_{11}}{a_1} + \frac{a_{12}}{a_1}(1 - f_2 T_2) \right]$$

$$= \varepsilon_1 \left(\frac{a_{11} + a_{12}}{a_1} - \frac{a_{12}}{a_1} f_2 T_2 \right)$$

As $a_{11} + a_{12} = a_1$, the right side of equation 1.4.10 becomes equation(D1.4.11).

$$= \varepsilon_1 \left(1 - \frac{a_{12}}{a_1} f_2 T_2 \right) \quad \text{(D1.4.11)}$$

For γ_2, the equations below are obtained equation (D1.4.12).

$$\varepsilon_2^* a_2 = \varepsilon_2 a_{22}(1 - f_1 T_1)$$

$$\therefore \ \varepsilon_2^* = \varepsilon_2 \frac{a_{22}}{a_2}(1 - f_1 T_1) \quad \text{(D1.4.12)}$$

(2) For ^{60}Co and ^{88}Y, the internal conversions are ignored, where $f_1 = 1$ and $f_2 = 1$. Thus, $a_{12} = a_{22} = a_2$. In addition, since the total emission rate of γ_1 is regarded as 100%, $a_1 = 1$ holds. (In the case of ^{60}Co, additionally $a_2 = 1$.)
Therefore, the equations (D1.4.11) and (D1.4.12) in (1) are expressed by equations (D1.4.13) and (1.4.14), respectively.

$$\varepsilon_1^* = \varepsilon_1(1 - a_2 T_2) \quad \text{(D1.4.13)}$$

$$\varepsilon_2^* = \varepsilon_2(1 - T_1) \quad \text{(D1.4.14)}$$

(3) To correct a summing-effect and obtain a correct peak efficiency, the equations (D1.4.15) and (D1.4.16) are used.

$$\varepsilon_1 = \frac{\varepsilon_1^*}{1 - a_2 T_2} = \frac{\varepsilon_1^*}{1 - \frac{a_2 \varepsilon_2}{(P/T)_2}} \quad \text{(D1.4.15)}$$

$$\varepsilon_2 = \frac{\varepsilon_2^*}{1 - T_1} = \frac{\varepsilon_2^*}{1 - \frac{\varepsilon_1}{(P/T)_1}} \quad \text{(D1.4.16)}$$

ε : peak efficiency
ε^* : observed peak efficiency
a : emission rate
T : total efficiency
(P/T): peak to total ratio

(4) From the equations (D1.4.15) and (D1.4.16), the value of ε_2 is needed to obtain the correct value of ε_1. However, the true value of ε_2 is unknown at the beginning of a study. Therefore, ε_1 is obtained by substituting ε_2^* instead of ε_2 into (D1.4.15). Meanwhile, ε_2 is obtained by substituting ε_1 into (D1.4.16). This procedure is repeated until the result converges. Usually, two times is sufficient.

Document 1.5 Examples for the calculation of Gamma-ray attenuation coefficients of environmental samples

Except for a forward scattering at extremely small angle in the Compton scattering, a γ-ray loses a lot of energy on only once interaction: Compton scattering, electron pair production or electron pair production. For the quantitation of photoelectric peaks using a germanium semiconductor detector, a γ-ray attenuation coefficient is used for self-absorption correction of a volumetric sample. The coefficient is calculated using the sum of the cross sections (or attenuation coefficients) for the above interactions.

For a coherent scattering where a γ-ray energy is unchanged, an isotropic scattering occurs with a wide scattered beam. Therefore, in the measurement of a volumetric sample, the number of incoming and outgoing scattered γ-rays into a medium are assumed equal. In this case, a coherent scattering was not considered in the presented calculation examples [18].

As a simplified model to evaluate the attenuation of a γ-ray penetrating a substance, consider a γ-ray parallel beam of an intensity of I_0 that vertically enters a substance with a thickness of x. The ratio that the γ-rays transmit to a substance is given by equation (D1.5.1).

$$I/I_0 = \exp(-\mu x) \qquad \text{(D1.5.1)}$$

Here, μ is the called linear attenuation coefficient. When the unit of thickness x is cm, the unit of μ is cm^{-1}. Instead of the thickness x, ρx where x is multiplied by the density of the substance tested is sometimes used. In that case, mass attenuation coefficient μ/ρ (cm^2/g) is used instead of μ.

When the atomic cross section of the interaction and number of atoms in 1 g substance is given by σ (cm^2) and N (g^{-1}), respectively, equation(D.1.5.2) is obtained.

$$\mu/\rho = \sigma \cdot N \qquad \text{(D1.5.2)}$$

The value of μ/ρ is determined by the elemental composition of a tested substance and its γ-ray energy. There is a method to obtain μ/ρ from the approximation function [19] [20] using the atomic number of a substance and energy as variables. As an example, the following shows a method to obtain μ/ρ of the γ-ray energy E from 80 to -2 MeV using a formula [19] for the interaction cross sections. The method is applicable to environmental samples containing elements whose atomic number Z is $\leq$30.

Although this approximate formula may cause an error of several percentages, it is enough to do the correction of self-absorption in environmental samples. The details of this method are shown below.

Note that since samples for actual measurements are mostly volumetric samples, the emissions of γ-rays from a sample into the detector are not a parallel beams. In such a case, in order to evaluate the γ-ray attenuation in a sample, methods such as a numerical calculation considering the solid angle from the geometry between the detector and sample, as well as the Monte Carlo simulation are indispensable.

(a) For the elements in a substance, obtain the cross sections against photons of energy E_1 in the unit of barn ($10^{-24}cm^2$) using a numerical table. The cross section is given by $\sigma(E_1)$.
Note that when the mass attenuation coefficient μ/ρ (cm^2/g) is used, $\sigma(E_1)$ may be replaced with $\mu/\rho(E_1)$ (hereinafter, the same applies).

(b) Similarly, obtain the cross section $\sigma(E_2)$ at an energy E_2 from a numerical table. Determine E_1 and E_2 so that the error becomes a minimum in the applicable energy range.
(example) $E_1 = 100\ keV \quad E_2 = 500\ keV$

(c) Obtain $A(Z)$ and $B(Z)$ by simultaneously solving equation (D1.5.3) using 2 conditions. The first condition is where $\sigma(Z,E)$ is substituted by $\sigma(E_1)$ and E in the right side is substituted by E_1. The other condition is where $\sigma(Z,E)$ is substituted by $\sigma(E_2)$ and E in the right side is substituted by E_2.

$$\sigma(Z,E) = A(Z)\cdot E^{-3.15} + B(Z) \cdot \exp[0.408(\ln E) - 0.066(\ln E)^2] \quad \text{(D1.5.3)}$$

(d) In this way, the approximate formula for the cross section taking the energy E as the variable is obtained for an element. For other elements, perform the procedures from (a) to (c).

(e) The mass attenuation coefficient μ/ρ (cm^2/g) of a compound with the molecular weight of M and elemental composition of AaBbCc…… is calculated by equation (D1.5.4).

$$\mu/\rho = 0.6022(a\cdot\sigma_A + b\cdot\sigma_B + c\cdot\sigma_c + \cdots)/M \quad \text{(D1.5.4)}$$

For the case when the mass attenuation coefficient μ/ρ (cm^2/g) is used instead of the cross section σ, the value of μ/ρ is calculated by equation (D1.5.5).

$$\mu/\rho = a\cdot\mu/\rho_A + b\cdot\mu/\rho_B + c\cdot\mu/\rho_C + \cdots \quad \text{(D1.5.5)}$$

Where, a, b, c, … represent the weight composition ratio.

Example for the calculation of mass attenuation coefficient

The following is an example for obtaining the mass attenuation coefficient for Al_20_3 (alumina) at 134keV (^{144}Ce 11.1%).

(a) Obtain the cross sections ($\sigma(\mathrm{Al}_{100})$) in the unit of barn ($10^{-24}$cm^2) at 100 keV photons for the elements constituting the substance from a numerical table.

aluminum Z = 13

energy (keV)	photoelectric effect	compton scattering	electron pair production	sum
100	0.827	6.22	0	7.047
500	0.0061	3.75	0	3.756

$\sigma(\mathrm{Al}_{100}) = 7.047$

(b) Similarly, obtain the cross sections ($\sigma(\mathrm{Al}_{500})$) for aluminum at 500 keV.

$\sigma(\mathrm{Al}_{500}) = 3.756$

(c) Obtain $A(Z)$ and $B(Z)$ by simultaneously solving equation (D.1.5.3) using 2 conditions. The first condition is where $\sigma(Z,E)$ is substituted by $\sigma(E_1)$ and E in the right side is substituted by 100. The other condition is where $\sigma(Z,E)$ is substituted by $\sigma(E_2)$ and E in the right side is substituted by 500. These are shown below.

$$\sigma(Z,E) = A(Z)\cdot E^{-3.15} + B(Z)\cdot \exp\left[0.408(\ln E) - 0.066(\ln E)^2\right]$$

aluminum

$$7.047 = A(Z)\cdot (100)^{-3.15} + B(Z)\cdot \exp\left[0.408(\ln 100) - 0.066(\ln 100)^2\right]$$
$$3.756 = A(Z)\cdot (500)^{-3.15} + B(Z)\cdot \exp\left[0.408(\ln 500) - 0.066(\ln 500)^2\right]$$

Solve the simultaneous equations.

$$A(Z) = 1.814\times 10^6$$
$$B(Z) = 3.801$$

Then, the following approximate formula is obtained.

$$\sigma(Z,E) = 1.814\times 10^6\cdot E^{-3.15} + 3.801\cdot \exp\left[0.408(\ln E) - 0.066(\ln E)^2\right]$$

(d) Also for oxygen, obtain the approximate formula by performing (a), (b), and (c).

oxygen Z = 8

energy (keV)	photoelectric effect	compton scattering	electron pair production	sum
100	0.0804	3.88	0	3.960
500	0	2.31	0	2.31

$$\sigma(O_{100}) = 3.960$$
$$\sigma(O_{500}) = 2.31$$

$$3.960 = A(Z) \cdot (100)^{-3.15} + B(Z) \cdot \exp\left[0.408\{\ln(100)\} - 0.066\{\ln(100)\}^2\right]$$
$$2.31 = A(Z) \cdot (500)^{-3.15} + B(Z) \cdot \exp\left[0.408\{\ln(500)\} - 0.066\{\ln(500)\}^2\right]$$

Obtain $A(Z)$ and $B(Z)$ by solving the simultaneous equations.

$$A(Z) = 3.615 \times 10^5$$
$$B(Z) = 2.340$$

$$\sigma(Z,E) = 3.615 \times 10^5 \cdot E^{-3.15} + 2.340 \cdot \exp\left[0.408(\ln E) - 0.066(\ln E)^2\right]$$

(e) The mass attenuation coefficient for alumina (Al2O3) with a molecular weight (M) of 102 μ/ρ (cm^2/g) at 134 keV (^{144}Ce 11.1%) is calculated as follows.

Cross section for aluminum at 134 keV is obtained as follows.

$$\sigma(13,134) = 1.814 \times 10^6 \cdot 134^{-3.15} + 3.801 \cdot \exp\left[0.408\{\ln(134)\} - 0.066\{\ln(134)\}^2\right] = 6.118$$

Cross section for oxygen at 134 keV is obtained as follows.

$$\sigma(8,134) = 3.615 \times 10^5 \cdot 134^{-3.15} + 2.340 \cdot \exp\left[0.408\{\ln(134)\} - 0.066\{\ln(134)\}^2\right] = 3.616$$

Then, obtain the mass attenuation coefficient.

$$\mu/\rho = 0.6022(a \cdot \sigma A + b \cdot \sigma B)/M$$
$$= 0.6022(2 \cdot 6.118 + 3 \cdot 3.616)/102$$
$$= 0.136\ (cm^2/g)$$

Document 1.6 Correction for self-absorption

Since a volumetric sample has a thickness, a fraction of the γ-rays emitted from a volumetric sample loses its energy by interacting with the sample itself. This phenomenon is called self-absorption. Since γ-rays that lose energy by this phenomenon are not counted as photoelectric peaks, a correction is necessary.

The thicker a sample is, the easier Self-absorption caused. Also, the larger a sample has linear attenuation coefficient, the easier Self-absorption caused. Since the peak efficiency calculated using the volumetric source contains the effect of the self-absorption by a volumetric source, the peak efficiency cannot be directly applied to a sample whose materials and density are different from the source.

A method to correct only self-absorption is described below. For a correction including a summing-effect, refer to the Document 1.2.

Document 1.6.1 Principles of self-absorption and its correction

Consider a parallel γ-ray beam passing with a unit distance at a certain position in a sample. The number of γ-rays decrease by interaction with the sample material at this position. The number of extinct γ-rays at this position is proportional to the number of γ-rays incident to this position. Here, the proportional constant is the linear attenuation coefficient μ. The decrease in the number is not related to "the position of γ-ray extinction"; however, it only depends on the number of γ-rays. Therefore, a three-dimensional coordinate is considered, such that attenuation can be expressed by the linear differential equations (D1.6.1).

$$\frac{dN}{dx} = -\mu \times N \qquad N = A \cdot \exp(-\mu \cdot X) \qquad \text{(D1.6.1)}$$

where
- N : number of γ-rays at the bottom of a sample vessel
- A : number of γ-rays emitted from the sample
- X : distance from the emitted position to the bottom of the sample vessel

The number of γ-rays emitted from the sample decreases depending on the distances from the emitted position and bottom of the sample vessel.

Slice the sample in a surface parallel to the bottom of the vessel. Then, multiply the peak efficiency for the surface by the rate of decrease due to the self-absorption. Summing up this corrected surface efficiency from the bottom to the top of the vessel.

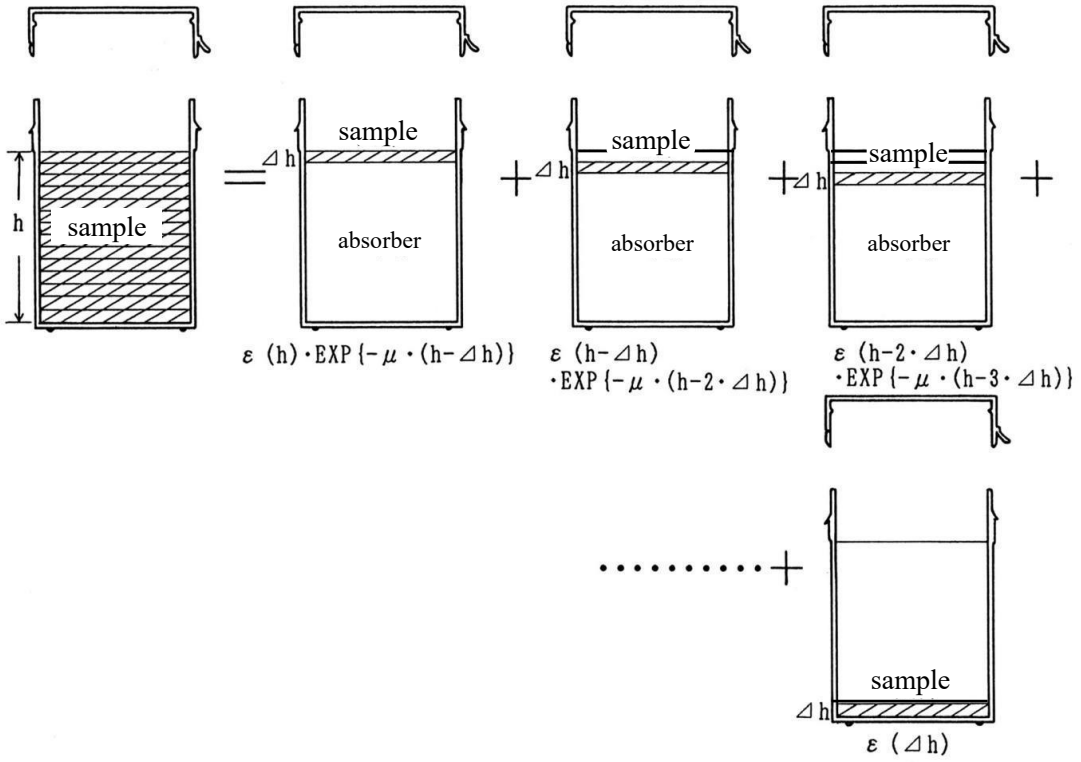

Fig.D1.6.1 Accumulate surface efficiency from bottom to top of vessel while considering with self-absorption.

Document 1.6.2 Liner attenuation coefficient

(1) The linear attenuation coefficients used in self-absorption correction (refer to the Document 1.5) are depending on the energy of γ-rays and materials of the sample. Photoelectric effect, Compton scattering, electron pair production, and so forth causes the loss of energy or disappearance of γ-rays. When the atomic number of a sample is ≤20, the linear attenuation coefficient is expressed by one formula. The coefficient can be calculated if the apparent density and γ-ray energy are known. The apparent density can be calculated from the weight of the measured sample, area at the bottom of the sample vessel, and thickness of the sample. For marine sediment, soil, incinerated materials, etc., the relationship between the mass attenuation coefficient and γ-ray energy is given by equation (D.1.6.2).

$$\mu/\rho\,(cm^2/g) = \exp\left\{-2.361 - 0.3949 \times \ln\frac{E}{400} - 0.06914 \times \left(\ln\frac{E}{400}\right)^2\right\} \quad \text{(D1.6.2)}$$

μ/ρ: mass attenuation coefficient for marine sediment, soil, incinerated materials, etc. (μ : linear attenuation coefficient for a sample)

E : energy of γ-ray (keV)

(2) For ammonium phosphomolybdate and manganese dioxide that are used for the treatment of seawater, the mass attenuation coefficient for soil etc. cannot be applied. This is because the average atomic number is too large. The mass attenuation coefficient for ammonium phosphomolybdate is expressed by equation (D1.6.3.)

$$\mu/\rho\,(cm^2/g) = 1.794 \times (E^{-0.4921}) + 673500 \times (E^{-3.040}) \quad \text{(D1.6.3)}$$

μ/ρ : mass attenuation coefficient for ammonium phosphomolybdate
(μ ： linear attenuation coefficient for ammonium phosphomolybdate)
E : energy of γ-ray (keV)

The mass attenuation coefficient for manganese dioxide is the sums of the mass attenuation coefficient for ammonium phosphomolybdate multiplied by 0.13 and soil multiplied by 0.87, respectively.

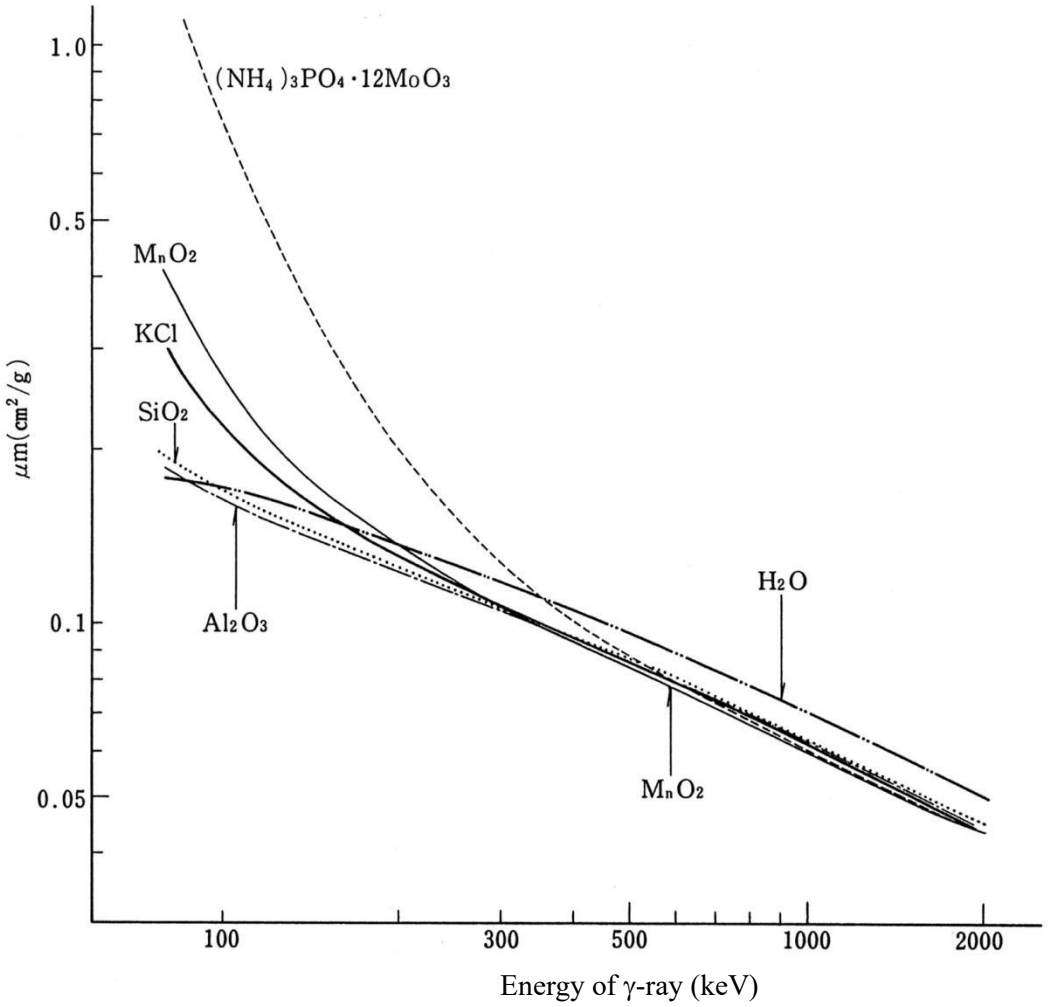

Fig.D1.6.2 Mass attenuation coefficient.

(3) For a sample where ammonium phosphomolybdate is homogenously mixed with hydroxides and sulfides, the following equation is used.

$$\mu_{total} = \left(\mu_1 \times \frac{w_1}{w_{total}} + \mu_2 \times \frac{w_2}{w_{total}}\right) \quad \text{(D1.6.4)}$$

μ_{total} : linear attenuation coefficient for total mixed sample
μ_1 : linear attenuation coefficient for ammonium phosphomolybdate
μ_2 : linear attenuation coefficient for hydroxide and sulfide (same as the linear attenuation coefficient for soil, etc.)
w_{total} : weight of total mixed sample
w_1 : weight of ammonium phosphomolybdate
w_2 : weight of hydroxide and sulfide

Document 1.6.3 Calculation method [21]

When the relationship between the peak efficiency ε and the filling height h for multiple standard sources with the same materials and the different filling height is approximated by the reciprocal of the linear function, the equation (D1.6.5) is obtained

$$\varepsilon \simeq (b \cdot h + c)^{-1} \quad \text{(D1.6.5)}$$

where b and c and constants.

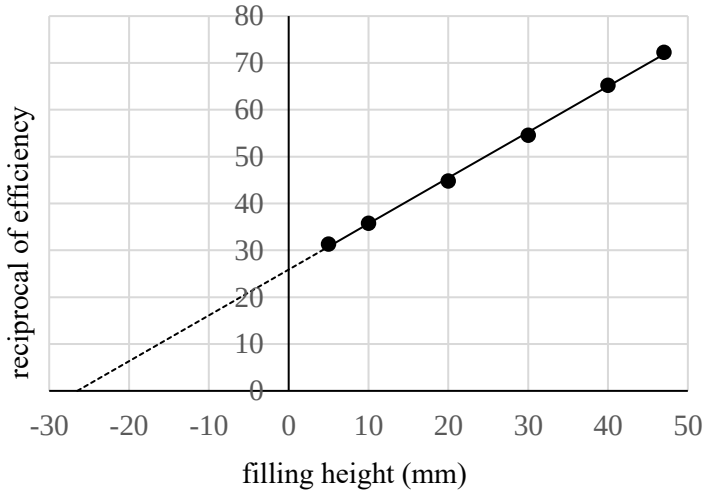

Fig. D1.6.3 Relationship between peak efficiency and filling height.

In the above equation, if $D = c/b$ and $\varepsilon_0 = 1/c$, the equation is reduced to equation (D1.6.6).

$$\varepsilon \simeq D \cdot \varepsilon_0/(h + D) \quad \text{(D1.6.6)}$$

(D1.6.6) only approximates the difference in the self-absorption between the sample and the source; therefore, it cannot be used to obtain the absolute value of the peak efficiency due to the large errors[*1]. As shown in Fig. D1.6.4, D represents the distance from the bottom of a sample to the effective center of the detector.

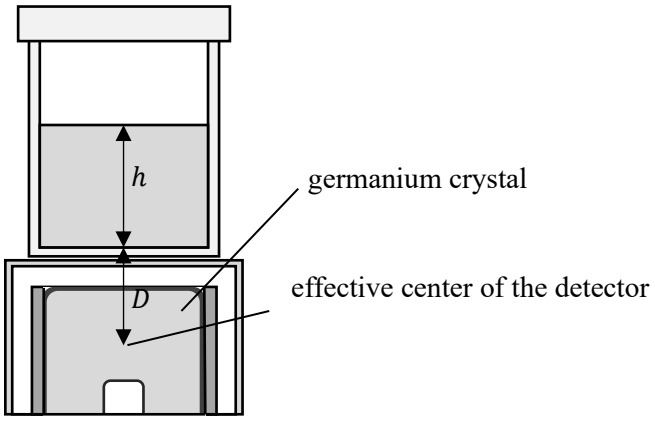

Fig. D1.6.4 Effective center of detector.

Assuming that the γ-rays are emitted as parallel beams, the difference $\Delta\varepsilon$ in the self-absorption between the standard volumetric source and the measuring sample can be calculated. The linear attenuation coefficients for the sample and standard volumetric are μ and μ_s, respectively. The variable in the vertical direction is x. Therefore, equation (D1.6.7) is obtained.

$$\Delta\varepsilon = \frac{D^2 \cdot \varepsilon_0}{h} \int_0^h \frac{1 - \exp\{(\mu_s - \mu) \cdot x\}}{(x + D)^2} dx \qquad \text{(D1.6.7)}$$

The value of D slightly changes depending on the γ-ray energy. However, The value of D slightly changes depending on the γ-ray energy. However, if the difference in the linear attenuation coefficient between the standard volumetric source and measured sample is small, even if the values are not accurate, this doesn't occur much difference in the correction results. There is no problem except for the special cases such as ^{144}Ce (133.5keV) in a manganese dioxide sample which height is as high as 5 cm is quantitatively analyzed. (in case the standard source is water, the difference in the linear attenuation coefficient $\Delta\mu \approx 0.4$) Therefore, there is no need to change the value of D with the energy.

Calculate ε_0 using the functionalized peak efficiency. If $a = (\mu_s - \mu) \cdot D$ and $X = h/D$ are set using the Simpson's rule, the equation (D1.6.8) is obtained.

$$\Delta\varepsilon(h) = \frac{\varepsilon_0}{12}\left\{4 \cdot \frac{1 - e^{aX/4}}{\left(1 + \frac{X}{4}\right)^2} + 2 \cdot \frac{1 - e^{aX/2}}{\left(1 + \frac{X}{2}\right)^2} + 4 \cdot \frac{1 - e^{3aX/4}}{\left(1 + \frac{3 \cdot X}{4}\right)^2} + \frac{1 - e^{a}}{(1 + X} \right. \qquad \text{(D1.6.8)}$$

[*1]:The relationship between the reciprocal of the peak efficiency ε and filling height h was originally expressed by a quadratic equation.

Document 1.7 Example for calculation of attenuation correction

The intensity of radioactivity in a radioactive nuclide decreases with time. The set of measured data represents the radioactivity at the time of the measurement. So, if you want to know the radioactivity in a certain time, need to calculate radioactivity at the time. The calculation is described below.

(1) Calculation for correction of attenuation by decay at the time of measurement

The decease $(-dN/dt)$ in radioactive nuclides with time has a relationship with the decay constant (λ) and number (N) of the radioactive nuclides. This is given by equation (D1.7.1.)

$$-\frac{dN}{dt} = \lambda N \qquad \text{(D1.7.1)}$$

The integration of equation (D1.7.1) yields the relations described below.

If the radioactivity is $A \pm \sigma$ at the time of measurement, the radioactivity $A_0 \pm \sigma_0$ at time t before a measurement (e.g., at the time of the sampling) is given by equations (D1.7.2) and (D1.7.3).

$$A_0 = A \exp(\lambda t) \qquad \text{(D1.7.2)}$$
$$\sigma_0 = \sigma \exp(\lambda t) \qquad \text{(D1.7.3)}$$

Using the half-life T, the above equations are rewritten as equations (D1.7.4) and (D1.7.5), respectively.

$$A_0 = A\ (1/2)^{-(t/T)} \qquad \text{(D1.7.4)}$$
$$\sigma_0 = \sigma\ (1/2)^{-(t/T)} \qquad \text{(D1.7.5)}$$

(2) Calculation of attenuation correction for sequential decay

A radioactive nuclide decays may convert to a stable or another radioactive nuclide. If another nuclide is formed, the original and newly produced nuclide is called “parent nuclide” and “descendent nuclide”, respectively. The decay of a parent nuclide is expressed by the above equation. However, if do the same way for descendent nuclide, it is including the influx of the parent nuclide.In this case, Equation 1 needs to be rewritten as equations (D1.7.6) and (D1.7.7) for the parent and descendent nuclides, respectively.

$$-\frac{dN_p}{dt} = \lambda_p N_p \qquad \text{(D1.7.6)}$$

N_p ： number of parent nuclides λ_p ： decay constant of parent nuclide

$$-\frac{dN_d}{dt} = \lambda_d N_d - \lambda_p N_p \qquad \text{(D1.7.7)}$$

N_d ： number of descendent nuclides λ_d ： decay constant of descendent nuclide

Equations (D1.7.8) to (D1.7.9) are the results of solving the above equations and performing the attenuation correction for time (t) toward the past.

$$A_{p0} = A_p \exp(\lambda_p t) \quad \text{(D1.7.8)}$$

$$\sigma_{p0} = \sigma_p \exp(\lambda_p t) \quad \text{(D1.7.9)}$$

$$A_{d0} = A_d \exp(\lambda_d t) - \frac{\lambda_d}{\lambda_d - \lambda_p}\{\exp(\lambda_d t) - \exp(\lambda_p t)\} A_p \quad \text{(D1.7.10)}$$

$$\sigma_{d0} = \sqrt{\{\sigma_d \exp(\lambda_d t)\}^2 + \frac{{\lambda_p}^2}{(\lambda_d - \lambda_p)^2}\{\exp(\lambda_d t) - \exp(\lambda_p t)\}^2 {\sigma_p}^2} \quad \text{(D1.7.11)}$$

The followings are the explanations regarding a case where a nuclide sequentially decays depending on the parent-descendent relation.

1. A state called transient equilibrium which the half-life of a parent nuclide is not long (but is longer than the half-life of the descendent nuclide), temporal change in the radioactivity is observable. In this time, the radioactivity ratio of the parent to the descendent nuclides is constant.
2. A state called secular equilibrium is reached when the half-life of a parent nuclide is longer than the half-life of the descendent nuclide, radioactivity ratio of the parent to the descendent nuclides is constant, and temporal change is not observed.
3. In case a where a nuclide decays depending on a parent-descendent relation, the descendent nuclide “within 3σ” at the time of measurement may change to “3σ or larger” after the correction.
   a) Consider the case where the radioactivity of descendent nuclides was weak and had a small uncertainty and radioactivity of parent nuclides was strong and had a small uncertainty[*1]. The descendent nuclides will grow with the elapsed time. When the future radioactivity of the descendent nuclides is calculated, “within 3σ” will change to “3σ or higher” with the elapsed time.
   On the other hand, if we consider the past radioactivity of the descendent nuclides, the past radioactivity will become negative and “within 3σ”. This is obtained by drawing a curve that is continuously connected to the present radioactivity according to Fig D1.7.11 and calculating retroactively.
   b) Even if the measured values for both a parent and descendent nuclides are “within 3σ” and not detected, when the positive and the negative signs of the two measured values are opposite, the radioactivity of the descendent nuclide may become “3σ or higher” by the attenuation correction. An example calculation according to equation (D1.7.11) is shown in Fig. D1.7.1.
   The left side of the figure shows an example where the signs of the measured values were the same for the parent and descendent nuclides. These values were always “within 3σ” regardless of the time.
   The right side of the figure represents an example where the sign of the measured values for the parent nuclide was different from the descendent nuclide. Going back to the past, only the descendent nuclides exceeded 3σ in a certain period, and the sign of the lower 3σ for the descendent nuclides became positive.

[*1]:It happens at the time of so-called scavenge.

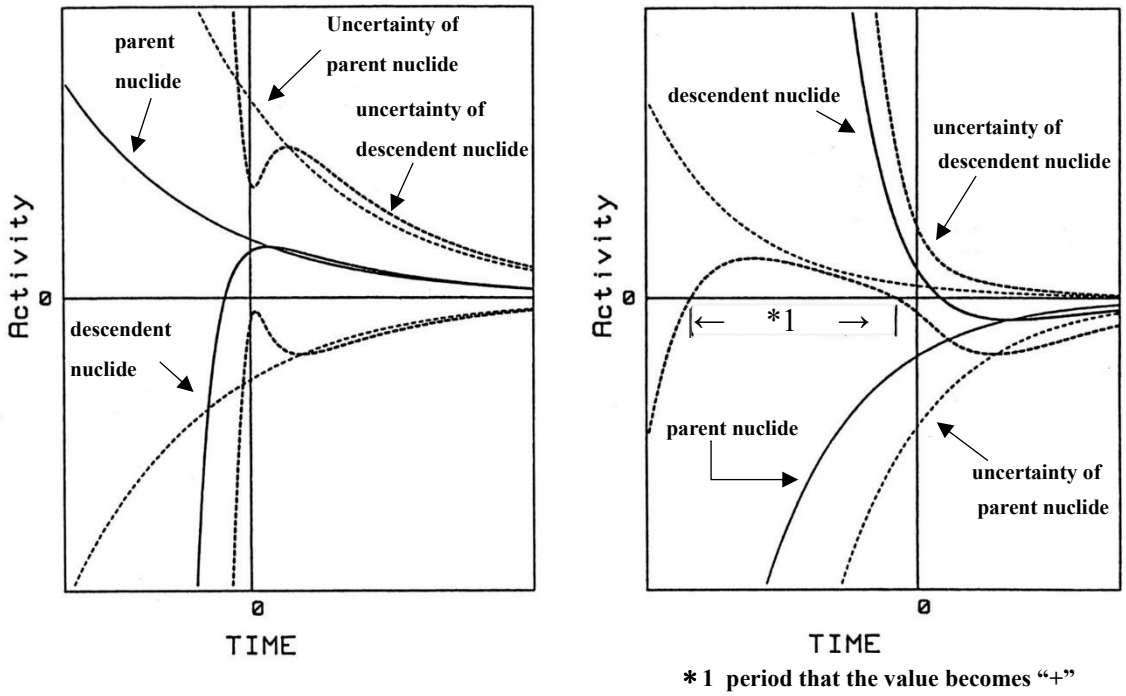

Fig. D1.7.1 Attenuation correction curves for a decay that depends on theparent-descendent relation. The solid and dotted lines show the radioactivity and the scope of 3σ, respectively.

(3) Calculation of attenuation correction for decay during a measurement

For a nuclide with a life not longer than the measuring time, the calculation of the attenuation correction is complicated. The calculation that considers the decay of a radioactive nuclide during the measurement is given by equation (D1.7.12).

$$A_0 = \frac{\lambda t_m}{1 - \exp(-\lambda t_m)} \times \exp(\lambda t) \times (A \pm \sigma) \qquad \text{(D1.7.12)}$$

t_m : measuring time (real time[*2])

t : decay correction time (difference between the standard time of the decay correction and the starting time of the measurement)

[*2]: It is also called true time. Here, it is expressed as real time.

(4) Calculation of decay correction by sequential decay during a measurement

In cases where both parent and descendent nuclides have lives longer than the measuring time, but not for a long time, a calculation that considers the "inflow from the parent nuclide into the descendent nuclide during the measurement" is required.

Examples for such cases is ^{99}Mo (parent nuclide with half-life 66.02 h) and ^{99m}Tc (descendent nuclide with half-life 6.007 h).

t_m	: measuring time (real time)
t	: decay correction time (difference between the standard time of decay correction and the starting time of the measurement)
$A_p \pm \sigma_p$	: radioactivity of parent nuclide at the time of measurement
$A_d \pm \sigma_d$	: radioactivity of descendent nuclide at the time of measurement
$A_{p0} \pm \sigma_{p0}$	: radioactivity of parent nuclide at the standard time of decay correction
$A_{d0} \pm \sigma_{d0}$	: radioactivity of descendent nuclide at the standard time of decay correction

When the variables are set as shown above, the following equations are obtained.

$$A_{p0} \pm \sigma_{p0} = \frac{\lambda_p t_m}{1 - \exp(-\lambda_p t_m)} \times \exp(\lambda_p t) \times (A_p \pm \sigma_p) \quad \text{(D1.7.13)}$$

$$A_{d0} = \frac{A_p \lambda_d t_m}{\lambda_d - \lambda_p} \left\{ \frac{\lambda_p \times \exp(\lambda_p t)}{1 - \exp(-\lambda_p t_m)} - \frac{\lambda_d \times \exp(\lambda_d t)}{1 - \exp(-\lambda_d t_m)} \right\} + \frac{A_d \lambda_d t_m \times \exp(\lambda_d t)}{1 - \exp(-\lambda_d t_m)} \quad \text{(D1.7.14)}$$

$$\sigma_{d0} = \sqrt{{\sigma_p}^2 \frac{(\lambda_d t_m)^2}{(\lambda_d - \lambda_p)^2} \left\{ \frac{\lambda_p \times \exp(\lambda_p t)}{1 - \exp(-\lambda_p t_m)} - \frac{\lambda_d \times \exp(\lambda_d t)}{1 - \exp(-\lambda_d t_m)} \right\}^2 + {\sigma_d}^2 \left\{ \frac{\lambda_d t_m \times \exp(\lambda_d t)}{1 - \exp(-\lambda_d t_m)} \right\}^2} \quad \text{(D1.7.15)}$$

(5) Application of the calculation methods for decay correction

To avoid misunderstanding, decay correction is performed only when radioactivity is detected. This is the right choice, whether or not a nuclide decays sequentially in a parent-descendant relationship.

1. For nuclides in natural decay series, the calculation of the decay correction is difficult and only a little meaning. Therefore, just have to present the values at the time of measurement, not have to do the decay correction.
2. Strictly speaking, when a decay is a continuous series, it is required to solve the linear simultaneous first-order differential equations.
3. For descendent nuclides, wouldn't mind performing the decay correction assuming that the decay is in a transient equilibrium.

Document 1.8 Method for background correction

The counts that are not from sample are excluded in the calculation of the radioactivity. Therefore, the background (blank or absence of a sample) is measured to make the corrections. The correction method is described by equation (D1.8.1).

$$N \pm \sigma_N = S/T_S - B/T_B \pm \sqrt{(\sigma_S/T_S)^2 + (\sigma_B/T_B)^2} \quad \text{(D1.8.1)}$$

N : net peak counting rate
σ_N : uncertainty related to the count of net counting rate
S : sample peak area
σ_S : uncertainty related to the count of sample peak area
B : background peak area
σ_B : uncertainty related to the count of background peak area
T_S : measuring time for sample
T_B : measuring time for background

The points below are considered.

- When the peak area in a background spectrum is 2σ or less, the correction of the applicable sample peak is not necessary.
- For a background used for the correction, data obtained from various measurements are considered including the measurement before the sample, measurement after the sample, and average of multiple measurements. Care should be taken for nuclides in natural series (refer to 4.1.6 (4) and 4.1.7 (4)) since the counting rate significantly changes depending on the measuring date.

Document 1.9 Peak to total ratio

To perform a summing-effect correction, knowledge on the total efficiency of all γ-rays that have a cascade relationship with the target γ-ray is necessary. To determine the total efficiency, first obtain the peak to total ratio, which is the ratio of the peak efficiency to total efficiency as a function of γ-ray energy. A peak to total ratio is influenced by the materials and inner volume of the radiation shield, as well as the relative efficiency of the detector.

Document 1.9.1 Radiation source and measurement

Using a γ-ray point source that is composed of a single nuclide (^{241}Am, ^{109}Cd, ^{57}Co, ^{139}Ce, ^{51}Cr, ^{113}Sn, ^{85}Sr, ^{137}Cs, ^{54}Mn, or ^{65}Zn), measure the nuclide until the uncertainty related to the counts of the target peak area becomes $\leq$ 2%.

As the peak to total ratio changes only approximately 3% even when the position of the point source changes near the position where the measuring sample is set, it is sufficient to measure at one position. For this reason, the measurement position should be at 5 cm on the central axis of the end cap. In the case of an n-type detector, place a copper plate with 0.5 mm thickness on the end cap to eliminate X-rays emitted from the source.

Further, to minimize the γ-ray scattering, the source and supporting tools (Fig. D1.9.1) should be made by as few as possible less materials which are as light as possible (paper, foamed styrol, low density wood, etc.).

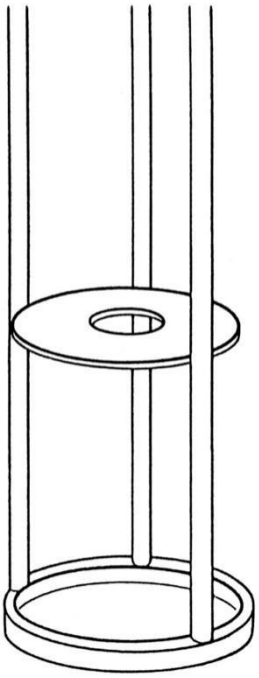

Fig. D1.9.1 Source holder used for the measurement of peak to total ratio.

Document 1.9.2 Method to obtain peak to total ratio

A peak to total ratio is obtained from a peak area divided by the total spectral area.

(1) The net counts, where the baseline is subtracted from the counts of a peak area (the part represented by the vertical lines in Fig. D1.9.2a), is represented by the peak area.

(2) Accumulate the count values from the lower limit of the low-energy side (hereafter referred to as LLD) of the spectrum to those in the 4096 channels. A count number lower than the LLD is obtained by extrapolating from a channel that is higher by dozens of channels than the LLD. This is approximated with a rectangle or trapezoid as shown by the vertical line region in Fig. D1.9.2b. The total counts, including those obtained by the approximation, are then considered as the total spectral area.

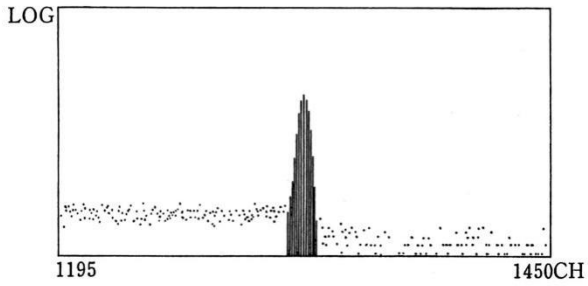

Fig.D1.9.2a γ-ray spectrum for ^{137}Cs (around the total energy peak).

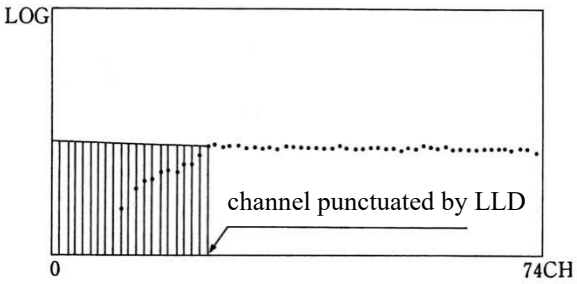

Fig. D1.9.2b γ-ray spectrum for ^{137}Cs (around the LLD).

(3) Plot the relationship between the peak to total ratio and energy of ^{241}Am, ^{109}Cd, ^{139}Ce, ^{51}Cr, ^{85}Sr, ^{137}Cs, and ^{54}Mn (which emit a single peak) in a log-log-graph.

(4) For nuclides generating two peaks like ^{57}Co, ^{113}Sn, and ^{65}Zn, use the value for the larger peak. Obtain the peak to total ratio corresponding to the energy of the smaller peak from the graph. Thereafter, the reciprocal of the peak to the total ratio is multiplied by the area of the smaller peak. Finally, estimate the total spectral area originating from the peak.

(5) Divide the area of the larger peak by the area where the result of (4) is subtracted from the total spectral area (including the two peaks). The result obtained is the peak to total ratio at this energy.

(6) Plot the peak to total ratio from (5) on a graph, and functionalize the relationship between the peak to total ratio and energy.

Document 1.9.3 Functionalization of peak to total ratio

(1) According to the report[*1],the peak to total ratio is calculated by the following formulas if regarding a detector that is housed in a lead shield with an internal volume of approximately 20 cm^3 [17].

$$\ln(\alpha) = -0.30 \times \ln(E) - 1.11$$
$$\ln(\beta) = -1.82 \times \ln(E) + 9.15$$
$$(P/T) = \alpha \times \ln(\varepsilon_{rel}) + \beta \qquad \text{(D1.9.1)}$$

E : energy of γ-ray (keV)
(P/T) : peak to total ratio
ε_{rel} : relative efficiency (%)

(2) When the volume of the space inside the shield is not approximately 20 cm^3, actually measure the peak to total ratio and functionalize according to equation (D1.9.1).

[*1]: Note that if $\ln(\beta)$ is replaced by the equation below, the accuracy is improved. (M. Noguchi, unpublished)
$\ln(\beta) = -7.97 + 3.31 \times \ln(E) - 0.383 \times \ln(E) \times \ln(E)$

Document 1.10 Detectable level of the germanium semiconductor detector

According to “the Nuclear Emergency Preparedness and Response Guidelines” (April, 2018), it is required to set the measurement target values for radioactive materials in the atmosphere and other environmental samples. In this section, for foods and atmospheric floating dust measured for the purpose of “Estimation and Evaluation of Radiation Exposure to Local Residents”, the measurement conditions and the detectable levels of the main nuclides will be described for the reference when setting the measurement target values.

The conditions are found below.

(1) Samples to be measured

・nuclides except for ^{131}I

pretreatment: incineration or evaporation to dryness

vessel : U-8 vessel

・^{131}I

pretreatment: not needed

vessel : 2L Marinelli-type vessel

(2) Measurement conditions

・instrument

coaxial-type germanium semiconductor detector

p-type

relative efficiency

In Table D1.10.1, approximately 20%.

In Table D1.10.2 with a U-8 vessel or Marinelli-type vessel of approximately 40% and 30%, respectively

・measurement time

In Table D1.10.1, approximately 80000 s.

In Table D1.10.2, approximately 70000 s.

Table D1.10.1 Detectable levels with the germanium semiconductor detector

Sample	Amount	^{144}Ce	^{131}I	^{140}Ba	^{134}Cs	^{106}Ru	^{137}Cs	^{95}Zr	^{95}Nb	^{54}Mn	^{60}Co	^{140}La	Unit
Radish, Chinese cabbage	about 2 kg raw	0.44	(0.19)	0.37	0.093	0.74	0.19	0.19	0.19	0.19	0.093	0.28	Bq/kg raw
Spinach	about 2 kg raw	0.48	(0.19)	0.37	0.093	0.74	0.19	0.19	0.19	0.19	0.093	0.28	Bq/kg raw
Rice milling	about 2 kg raw	0.48	(0.19)	0.37	0.093	0.74	0.19	0.19	0.19	0.19	0.093	0.28	Bq/kg raw
Tea	about 1 kg raw	0.93	(0.37)	0.74	0.19	1.5	0.37	0.37	0.37	0.37	0.19	0.56	Bq/kg raw
Tap water	about 20 L	1.9×10^{-2}	(0.19)	1.5×10^{-2}	7.4×10^{-3}	3.7×10^{-2}	7.4×10^{-3}	7.4×10^{-3}	1.1×10^{-2}	1.1×10^{-2}	7.4×10^{-3}	1.5×10^{-2}	Bq/L
Milk	about 2 L	0.44	(0.19)	0.37	0.093	0.74	0.19	0.19	0.19	0.19	0.093	0.28	Bq/L
Horse mackerel, flatfish	about 1 kg raw	0.96	−	0.74	0.19	1.5	0.37	0.37	0.37	0.37	0.19	0.56	Bq/kg raw
Squid	about 1 kg raw	0.93	−	0.74	0.19	1.5	0.37	0.37	0.37	0.37	0.19	0.56	Bq/kg raw
Turban shell (sazae)	about 1 kg raw	0.93	−	0.74	0.19	1.5	0.37	0.37	0.37	0.37	0.19	0.56	Bq/kg raw
Kelp (kombu)	about 1 kg raw	0.96	−	0.74	0.19	1.5	0.37	0.37	0.37	0.37	0.19	0.56	Bq/kg raw
Floating dust	about 10^4 m^3	2.6×10^{-5}	3.7×10^{-6}	1.9×10^{-5}	7.4×10^{-6}	3.7×10^{-5}	7.4×10^{-6}	1.1×10^{-5}	1.1×10^{-5}	1.1×10^{-5}	7.4×10^{-6}	1.9×10^{-5}	Bq/m^3

Relative efficiency is approximately 20%

Measuring time is approximately 80000 s

For ^{131}I, a raw sample is measured in a 2 L Marinelli-type vessel. For other nuclides, a sample after pretreatments is measured in a U-8 vessel.

Table D1.10.2 Detectable levels with the germanium semiconductor detector

Sample	Amount	^{144}Ce	^{131}I	^{140}Ba	^{134}Cs	^{106}Ru	^{137}Cs	^{95}Zr	^{95}Nb	^{54}Mn	^{60}Co	^{140}La	Remark
Land water	about 20 L	0.014	(0.17)	0.011	0.0043	0.030	0.0033	0.0053	0.0031	0.0032	0.0041	0.0041	Bq/L
Soil	about 0.1 kg dry soil	11	—	6.5	2.1	18	2.1	3.6	2.6	2.2	2.6	2.5	Bq/kg dry soil
Incinerated material (agricultural products)	about 5 kg raw	0.13	(0.31)	0.11	0.035	0.28	0.033	0.058	0.032	0.034	0.060	0.043	Bq/kg raw
Incinerated material (marine products)	about 4 kg raw	0.28	(0.21)	0.21	0.070	0.56	0.069	0.12	0.068	0.072	0.14	0.043	Bq/kg raw
Atmospheric floating dust	about 3000 m^3	1.3×10^{-4}	2.7×10^{-5}	9.6×10^{-5}	3.5×10^{-5}	2.7×10^{-4}	3.0×10^{-5}	4.9×10^{-5}	2.9×10^{-5}	2.9×10^{-5}	3.7×10^{-5}	3.9×10^{-5}	Bq/m^3
Fallout	about 0.5 m^2	0.69	—	0.46	0.19	1.3	0.14	0.23	0.14	0.14	0.18	0.18	MBq/km^2

Relative efficiency is approximately 40%

Measurement time is approximately 70000 s

For nuclides other than ^{131}I, a sample after pretreatments is measured in a U-8 vessel.

For ^{131}I, a raw sample is measured in a 2 L Marinelli-type vessel using a detector of about 30% relative efficiency.

Method to calculate the detectable levels

・For typical samples, the average value of the lower detectable values is obtained based on the past data. The past data is obtained by the detector of approximately 40% relative efficiency (for a 2 L Marinelli-type vessel with approximately 30% relative efficiency).

・In actual measurements, the conditions, including the background, are different depending on the radiation shield and setting environment. This is even when the same detector is used. Therefore, the averaged values are multiplied by three with the measurements having a high background. The calculated overestimated values are considered at the detectable levels or “detectable levels even if the condition is bad.”

Document 2 Effect of inhomogeneous distribution of samples in measurement container (example of U-8 container)

One advantage of γ-ray spectrometry using a germanium semiconductor detector is that large samples can be measured without chemical separation and purification due to the characteristics of γ-rays. It is ideal that the radioactive nuclides to be measured should be homogeneously distributed inside the filled sample in a measurement container. However, for liquid samples, radioactive nuclides may be adsorbed on the inner wall of the measurement container or particles containing radioactive nuclides may precipitate. Also, for soil samples, considering the degree of sample mixing and contamination of particles containing high-level radioactivity, another concern is that radioactive nuclides in a measurement container may not be homogeneously distributed.

Thus, in this paper, we investigated the influence of the inhomogeneity of radioactive nuclides in a container on the measurement values using electron gamma shower version5 (EGS5), which is the electromagnetic cascade Monte Carlo simulation code. Table D2.1 and Fig. D2.1 show the information on the detector used for the investigation.

Table D2.1 Detector used for Monte Carlo simulations

Crystal type	Coaxial p-type
Relative efficiency (%)	31
Height of germanium crystal (mm)	50.47
Diameter of germanium crystal (mm)	52.20
Thickness of dead layer (top surface) (mm)	0.40
Thickness of dead layer (side surface) (mm)	0.60
Diameter of core hole (mm)	7.50
Depth of core hole (mm)	35.07
Thickness of crystal holder (mm)	1.90
Thickness of end cap (mm)	1.50
Distance between end cap and crystal (mm)	7.53

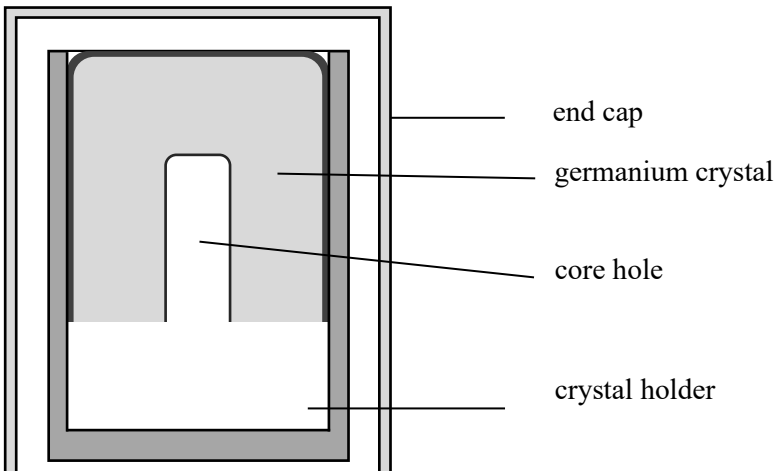

Fig. D2.1 Detector used for the Monte Carlo simulation (schematic diagram).

Document 2.1 Localization of radioactive nuclides

Document 2.1.1 Condition of investigation

We investigated the effects of the localization of radioactive nuclides in a measurement container on the measurement values by performing the Monte Carlo simulation under the following conditions.

Measurement container: Cylindrical container made of polypropylene (U-8 container)

Sample material: Water

Soil composition[22]: O (49.0%), Si (36.5%), Al (7.1%), Fe (4.0%), C (2.0%), K (1.4%)

density: 1.55 g cm^3

Filing height: 5 cm

Energy: 88.0 keV (^{109}Cd), 661.7 keV (^{137}Cs), 1836.1 keV (^{88}Y)

Number of generated photons: 10000000

Condition of localization: refer to Table D2.2 - D2.4

Document 2.1.2 Effects of localization on measurement values

Effects of the localization on measurement values and localization conditions are shown below.

Table D2.2 Conditions of localization for radioactive nuclides(vertical direction)

condition 1	condition 2	condition 3	condition 4
	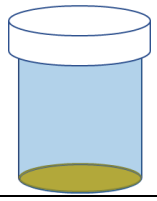	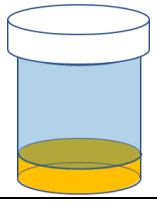	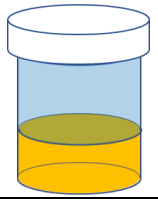
1.0000	0.0000	0.2000	0.4000
condition 5	condition 6	condition 7	condition 8
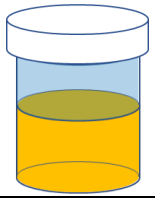	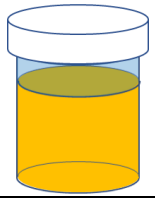	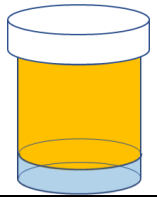	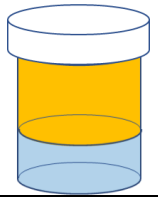
0.6000	0.8000	0.8000	0.6000
condition 9	condition 10	condition 11	condition 12
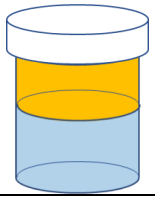	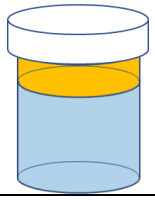	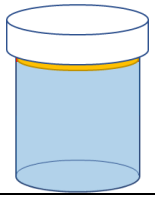	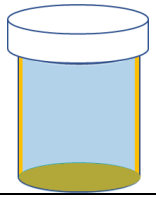
0.4000	0.2000	0.0000	0.0000

(Note) The radioactive nuclides of the same concentration are inhomogeneously distributed in the parts shown in orange. The numerical value represents the volume ratio of each part compared with condition 1.

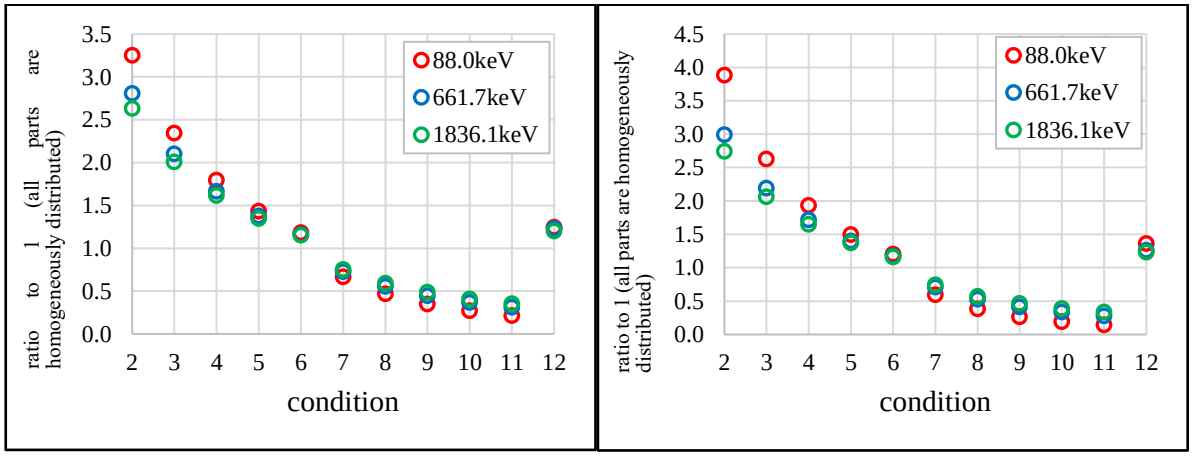

(Note) The left and right figures show the results for water and soil, respectively.

Fig. D2.2 Effects of localization (vertical direction) on the measured values.

Table D2.3 Conditions of localization for radioactive nuclides(horizontal direction)

condition 13	condition 14	condition 15	condition 16	condition 17
	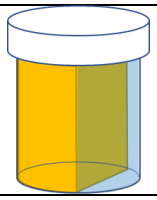	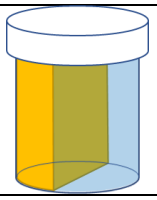	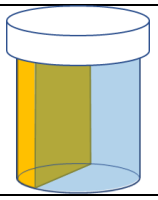	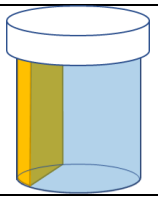
0.8904	0.7082	0.5000	0.2918	0.1096

(Note) radioactive nuclides of the same concentration are localized in the parts shown in orange.
The numerical value represents the volume ratio of each part compared with condition 1.

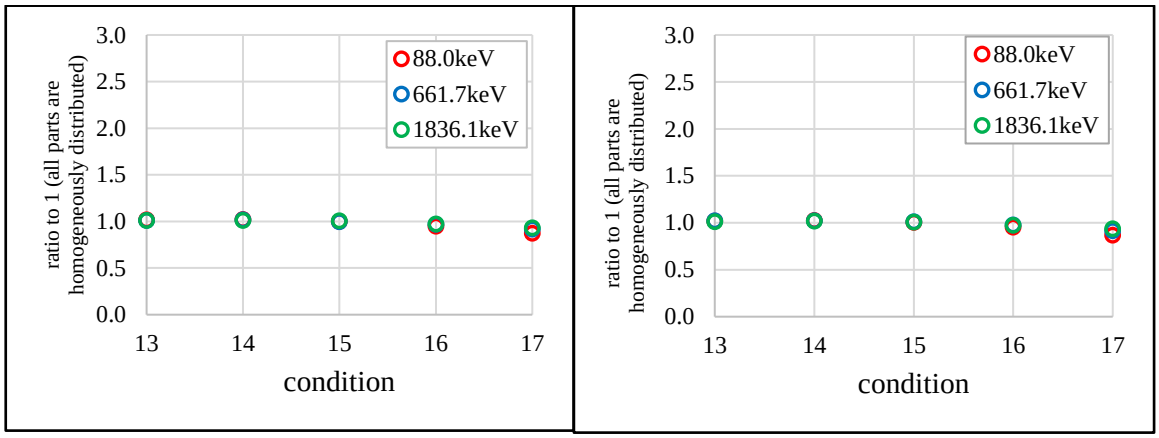

(Note) The left and right figures show the results for water and soil, respectively.
Fig. D2.3 Effects of localization (horizontal direction) on the measured values.

Table D2.4 Conditions of localization for radioactive nuclides
(cylindrical shape of aconcentric circle with the axis)

condition 18	condition 19	condition 20	condition 21	condition 22
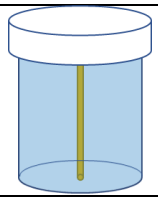	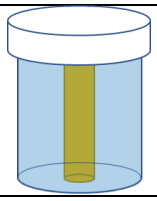	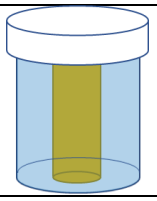	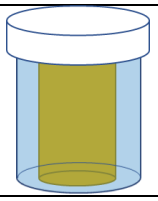	
0.0000	0.0434	0.1736	0.3906	0.6944

(Note) Radioactive nuclides of the same concentration are localized in the parts shown in the ocher.
The numerical value represents the volume ratio of each part compared with condition 1.

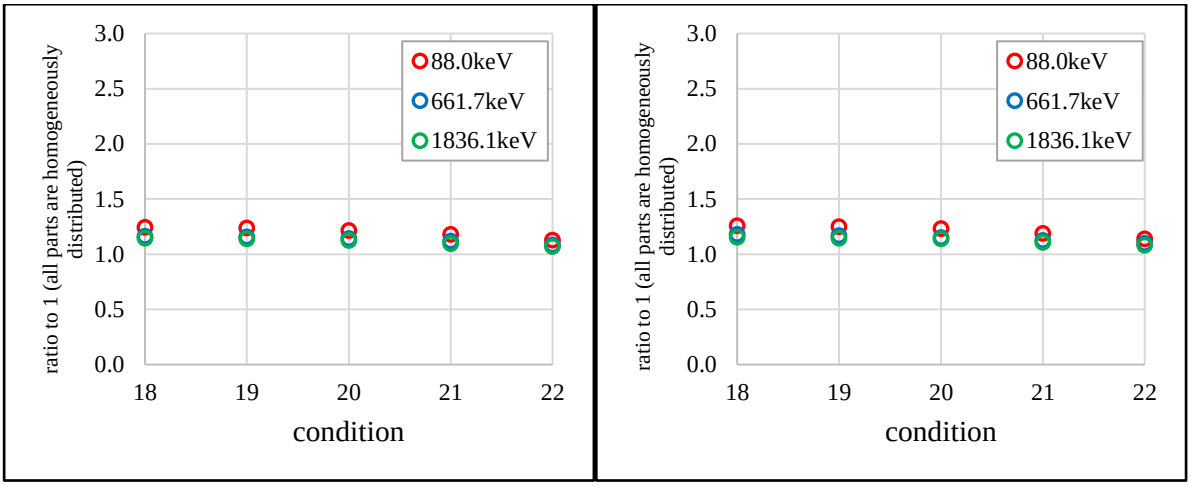

(Note) The left and right figures show the results for water and soil, respectively.

Fig. D2.4 Effects of localization (cylindrical shape of a concentric circle with the axis) on the measured values.

The effects of the localization in a measurement container on the measured values have the same tendency in all conditions, however, differences exist depending on the γ-ray energy. The γ-ray energy with the largest localization effect is 88.0 keV. This is attributed to the large self-absorption. When the material is water and radioactive nuclides were localized in a measurement container in the vertical direction, a 0.21–3.25 times change was recorded compared with condition 1 (all parts are homogeneously distributed). Furthermore, for a sample localized horizontally or in a cylindrical shape of a concentric circle with the axis, 0.87–1.02 or 1.07–1.24 times changes were generated, respectively, compared with condition 1. For the soil sample, 0.14–3.88 times changes were generated compared with condition 1 when radioactive nuclides were localized in a measurement container in the vertical direction. Additionally, for a sample localized horizontally or in a cylindrical shape of a concentric circle with the axis, 0.87–1.02 or 1.08–1.26 times changes were generated, respectively, compared with condition 1. From these results, it was clarified that when a sample is localized in the vertical direction, the effect of the localization on the measured values is large since the distance between the source and detector changes. Furthermore, for radioactive nuclides adsorbed on the container wall (condition 12), the measured values for water and soil samples were 1.24 and 1.36 times, respectively, compared with condition 1, making the measured values overestimated. Such localization happens when a water sample is measured without pretreatments, or mixing of a soil sample is insufficient. To prevent adsorption of radioactive nuclides in water samples on the container wall, please refer to “Sample Pretreatment for γ-ray Spectrometry in Emergencies” (No.24).

Document 2.2 Homogeneity of distribution for radioactive nuclides

Document 2.2.1 Condition of investigation

When radioactive nuclides are in homogeneously distributed in a measurement container, the effects of the distribution on measured values are investigated under the following conditions using the Monte Carlo simulation by EGS5 [11].

Measurement container: Inside dimension; length 4.2 cm, width 4.2 cm, height 6.0 cm, wall thickness 0.1 cm, and a container made of polypropylene (Let the bottom area be about the same as the U-8 container)

Sample material: Alumina

Filling height: 1.0 cm, 2.0 cm, 3.0 cm, 4.0 cm, 5.0 cm

Energy: 88.0 keV (^{109}Cd), 661.7 keV (^{137}Cs), 1836.1 keV (^{88}Y)

Condition of photon generation: The inside of the sample filled in a container was divided into cubes with sides of 0.2 cm. Then, the condition was randomly determined using random numbers so that photons were generated from the 10% cube (For example, for the filling height of 1.0 cm, the sample was divided into $21 \times 21 \times 5 = 2205$ cubes, and approximately 220 cubes were randomly chosen from these cubes, then the photons were generated from selected cubes.).

Placement pattern: 3000 patterns

Number of generated photons: 500000 photons per one pattern

The counting efficiencies (counts/number of generated photons) were calculated for each placement pattern, and the relative standard deviations were obtained from the frequency distribution. From these results, we evaluated the effect of the distribution of radioactive nuclides on the measured values.

In Guide to the Expression of Uncertainty in Measurement supplement 1 [10,23], the number of iterations (number of placement patterns in the above condition) was recommended to be at least 10000. However, it is not realistic to perform 10000 or more iterations in all conditions using a general PC. Therefore, to select a candidate where more than 10000 iterations are performed, the investigation was conducted by setting the placement pattern to 3000 patterns.

Document2.2.2 Effect on measured values

From the investigation, the frequency distribution of the counting efficiency agreed well in all 15 patterns with the normal distribution, as shown in Fig. D2.5. Table D2.5 shows the relative standard deviation obtained from the normal distribution. Results show that for each γ-ray energy, the relative standard deviation tend to increase depending on the filling height. Furthermore, the difference in the relative standard deviation depending on the γ-ray energy was about 0.3% at the maximum for the same filling height .Owing to the effect of the self-absorption ,the maximum energy was 88.0 keV in almost every case.

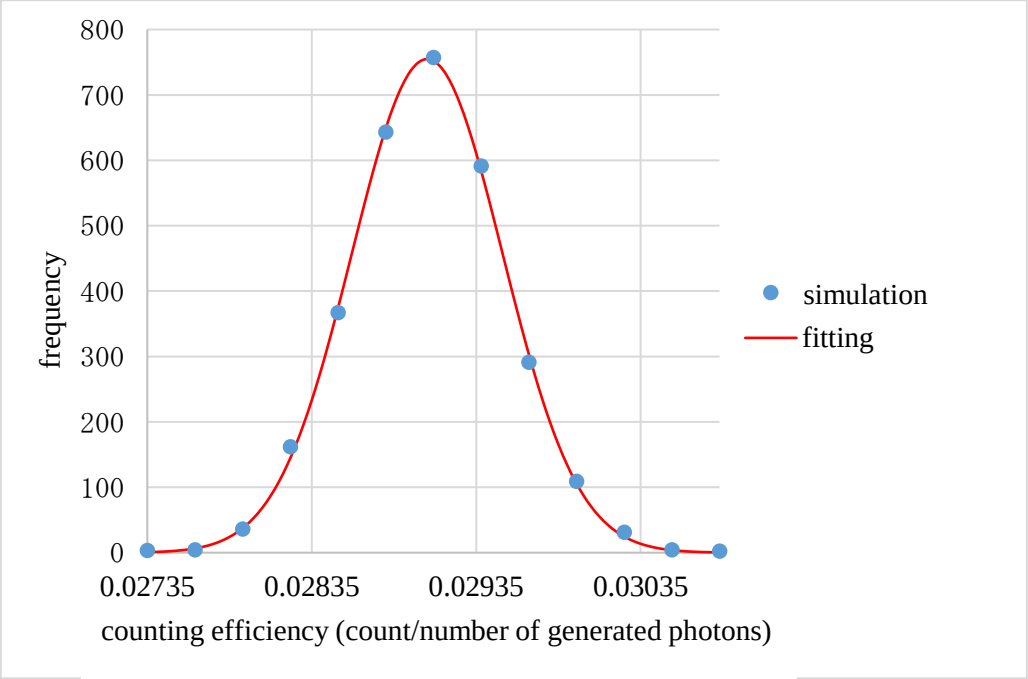

Fig. D2.5 Frequency distribution of counting efficiency for 1.0 cm filling height and 661.7-keV energy.

Table D2.5 Relative standard deviation in respective condition

		γ-ray energy (keV)		
		88.0	661.7	1836.1
Filling height (cm)	1.0	1.75%	1.58%	1.78%
	2.0	1.98%	1.82%	2.01%
	3.0	2.14%	1.96%	2.15%
	4.0	2.25%	2.07%	2.16%
	5.0	2.44%	2.17%	2.29%

The energy of which the relative standard deviations tend to be large and small were 88.0 keV and 661.7 keV, respectively. Similarly, the filling heights which the relative standard deviations were maximum and minimum were 1.0 cm and 5.0 cm, respectively. In four conditions which combined these energy and filling heights, the Monte Carlo simulation was performed setting the placement pattern to 10000 patterns.

To minimize the statistical uncertainty for the count number and become the similar uncertainty among the filling heights, the number of generated photons was set to 1000000 and 2000000 at the filling height of 1.0 cm and 5.0 cm, respectively.

From the investigation, the frequency distribution of the counting efficiency agreed well with the normal distribution in all four conditions, as shown in Fig. D2.6. Table D2.6 presents the relative standard deviations obtained from the normal distribution. Since the relative standard deviation for each filling height and γ-ray energy, almost agrees with that in Table D2.5, the effects of the filling height and γ-ray energy on the relative standard deviation were considered the same as those in Table D.2.5. Furthermore, the effects of the distribution of radioactive nuclides in a measurement container on the measured values were about 1.7%–4% and 1.5%–2.0% at 88.0 keV and 661.7 keV, respectively. Therefore, for 1836.1 keV, shown in Table D.2.5, the effects of the distribution of radioactive nuclides in a measurement container on the measured values when

uniformly evaluated regardless of the filling height and γ-ray energy can be estimated to be about 2.5%. As this result was obtained in the geometrical condition shown in Document 2.2.1, the relative standard deviation remarkably changes if the geometrical condition is changed. For this reason, investigating the setting of the geometrical condition was required. For example, the relative standard deviation when one side of the cube was 0.1 cm, filling height was 1.0 cm, γ-ray energy was 88.0 keV, and the photon generation rate was 10% was 0.74%. Also, when one side of the cube was 0.2 cm, filling height was 1.0 cm, γ-ray energy was 88.0 keV, and the photon generation rate was 20%, the relative standard deviation was 1.23%. Here, one side of the cube was set to 0.2 cm to let the sample both go through a sieve of 2 mm in the pretreatment of environmental samples, such as soil, and be evaluated at the condition where the relative standard deviation becomes maximum. The time consumed for the Monte Carlo simulation using the parallel calculation by the Core i7-7700 K(4.2 GHz) Linux 4 was about 5 days for 15 conditions shown in Document 2.2.1 and about 7 days for 4 conditions shown in Document 2.2.2.

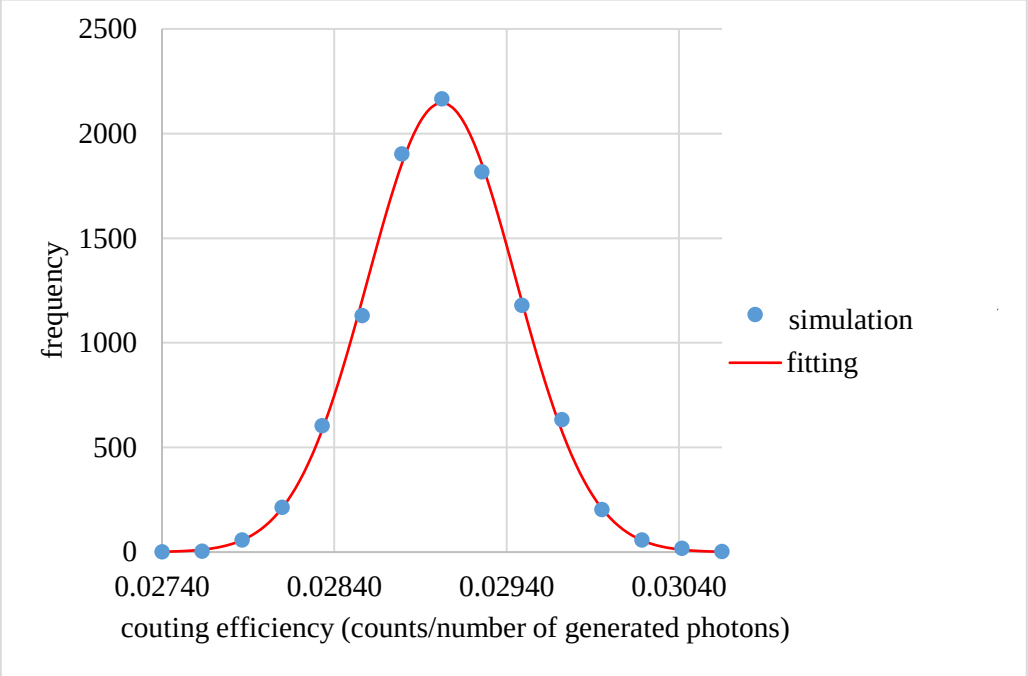

Fig. D2.6 Frequency distribution of the counting efficiency at 1.0 cm filling height and 661.7-keV energy, when the placement patterns and the number of generated photons were increased.

Table D2.6 Relative standard deviation in each condition when the placement patterns and the number of generated photons were increased

		Energy (keV)	
		88.0	661.7
Filling height (cm)	1.0	1.68%	1.48%
	5.0	2.41%	2.03%

Document 3 Investigation on the improvement of peak-to-total ratio used for summing-effect correction

In γ-ray spectrometry using a germanium semiconductor detector, the count value of a peak for nuclides that emit cascade γ-rays decreases due to the summing effect. The degree of a summing effect depends on the detection efficiency and decay scheme of the nuclide. In some cases, the summing effect on the peak count value reaches several tens of percent. Thus, because the measured values may underestimate the radioactivity (concentration) due to the summing effect, performing the correction for the peak count values that are decreased by the summing effect is necessary (Document 1.4).

The total efficiency needed for correcting the summing effect is obtained from the peak-to-total ratio, which is the ratio of the peak efficiency to the total efficiency. Although a peak-to-total ratio can be obtained by measuring γ-rays from multiple sources containing a single nuclide, it can be also obtained from the following empirical equation.

$$(P/T) = \alpha \times \ln(\varepsilon_{rel}) + \beta \qquad \text{(D3.1)}$$

where,

(P/T)	peak-to-total ratio
ε_{rel}	relative efficiency (%)
α	$\ln(\alpha) = -0.30 \times \ln(E) - 1.11$
β	$\ln(\beta) = -7.97 + 3.31 \times \ln(E) - 3.83 \times \{\ln(E)\}^2$
E	energy of γ-ray (keV)

The equation (D3.1) is obtained by measuring a point source [17]. However, since most environmental samples are volumetric ones, the peak-to-total ratio may be different from the real measurement condition. For environmental samples collected after the Fukushima Daiichi nuclear power station accident, although ^{134}Cs was detected, the summing-effect correction was insufficient [24]. A possible cause of this miss assignment was the peak-to-total ratio used for calculating the correction.

In this Document, we presented results where a peak-to-total ratio was obtained semi-experimentally using the conversion equation from the measured values for ^{137}Cs volumetric source and the results of the Monte Carlo simulation using EGSS. Furthermore, we introduced investigated results where the obtained peak-to-total ratio was applied to the summing-effect correction for ^{134}Cs volumetric source.

Document 3.1 Peak-to-total ratio for 661.7 keV γ-rays from ^{137}Cs volumetric source

Using the following two coaxial p-type germanium semiconductor detectors, the peak-to-total ratio was obtained by measuring a ^{137}Cs volumetric source (made of alumina, 6 filling heights of 0.5–4.7 cm) in a polyethylene cylindrical container (U-8 container), and the obtained results were compared with the values obtained using equation (D3.1). The results are presented in Figs. D3.1 and D3.2.

detector A: CANBERRA GC2519-7915-30, relative efficiency 31%

detector B: ORTEC GEM-50195S、relative efficiency 58%

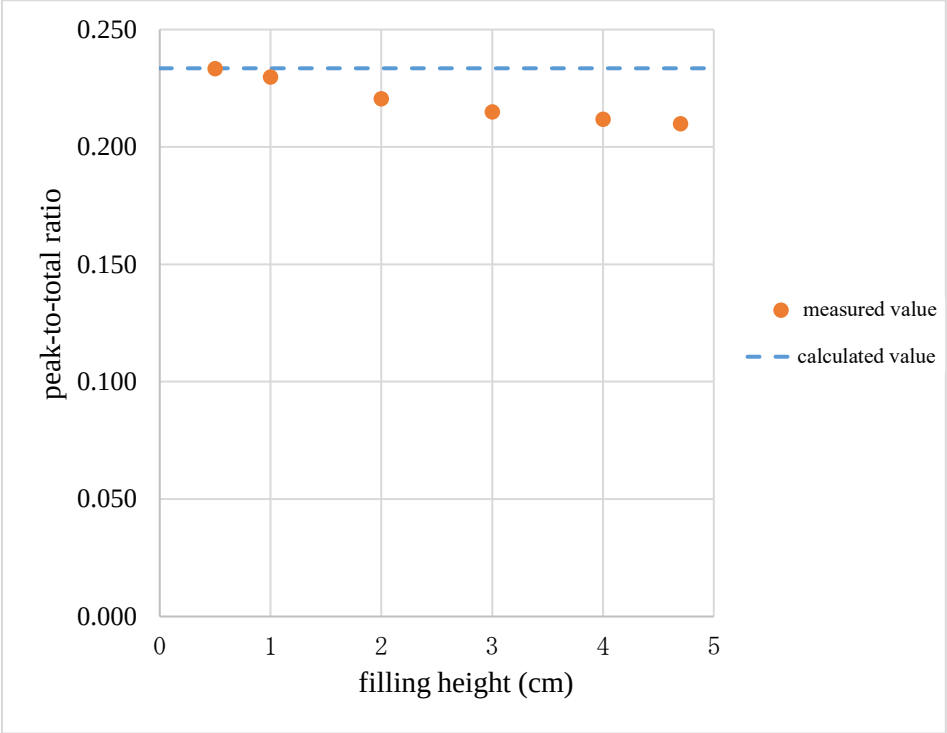

(Note) The calculated values were obtained from the relative efficiency using equation (D3.1).

Fig. D3.1 Peak-to-total ratio for detector A at 661.7 keV.

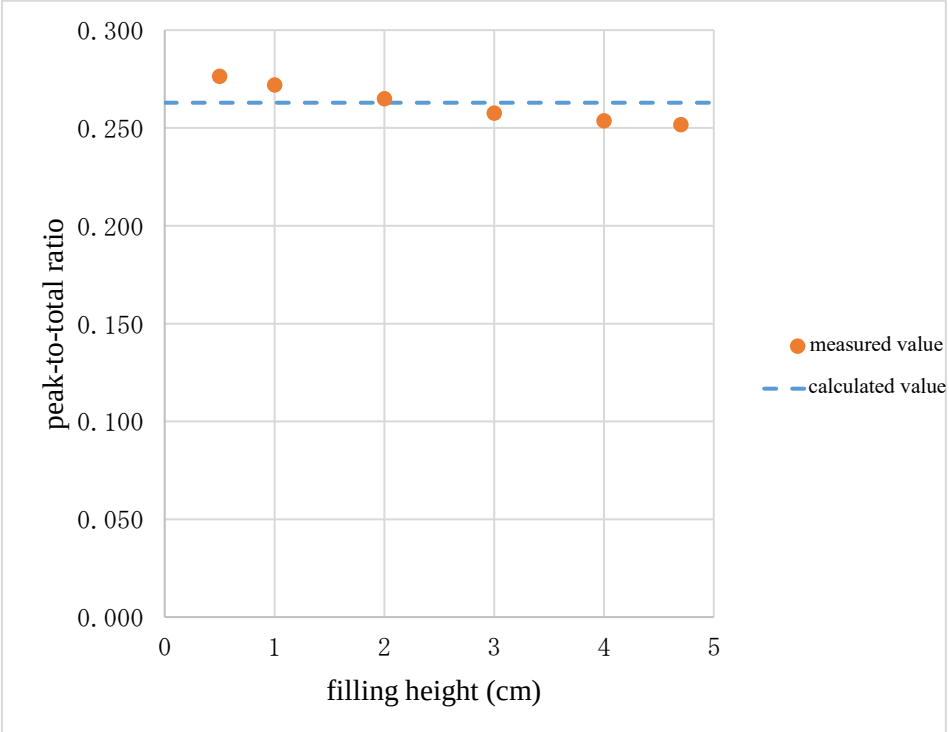

(Note) The calculated values were obtained from the relative efficiency using equation (D3.1)

Fig. D3.2 Peak-to-total ratio for the detector B at 661.7 keV.

From the comparison, the peak-to-total ratio at 661.7 keV obtained using the ^{137}Cs volumetric source almost agreed with the value obtained from equation (D3.1) for detector A at the filling height of 0.5 cm. However, as the filling height increased, the peak-to-total ratio decreased (Fig. D3.1). Similarly, for detector B, the peak-to-total ratio almost agreed with the value obtained from equation (D3.1) at the filling height of 2.0 cm. However, the peak-to-total ratio decreased with the increase in the filling height (Fig. D3.2).

Document 3.2 Conversion of a peak-to-total ratio to that at the other energy

The peak-to-total ratio at 661.7 keV obtained by the procedure described in Document 3.1 was converted to that at the other energy by equation (D3.2) using the peak-to-total ratio obtained from the Monte Carlo simulation by the EGS5. Then, the results obtained were compared with the values from equation (D3.1). The results are presented in Figs. D3.3 and D3.4.

$$\left(\frac{P}{T}\right) = PT(661.7) \times \frac{PT_{MC}(E)}{PT_{MC}(661.7)} \qquad \text{(D3.2)}$$

where,

$PT(661.7)$ peak total ratio at 661.7 keV obtained from the measurements

$PT_{MC}(661.7)$ peak total ratio at 661.7 keV obtained from the Monte Carlo simulation

$PT_{MC}(E)$ peak total ratio at the energy E obtained from the Monte Carlo simulation

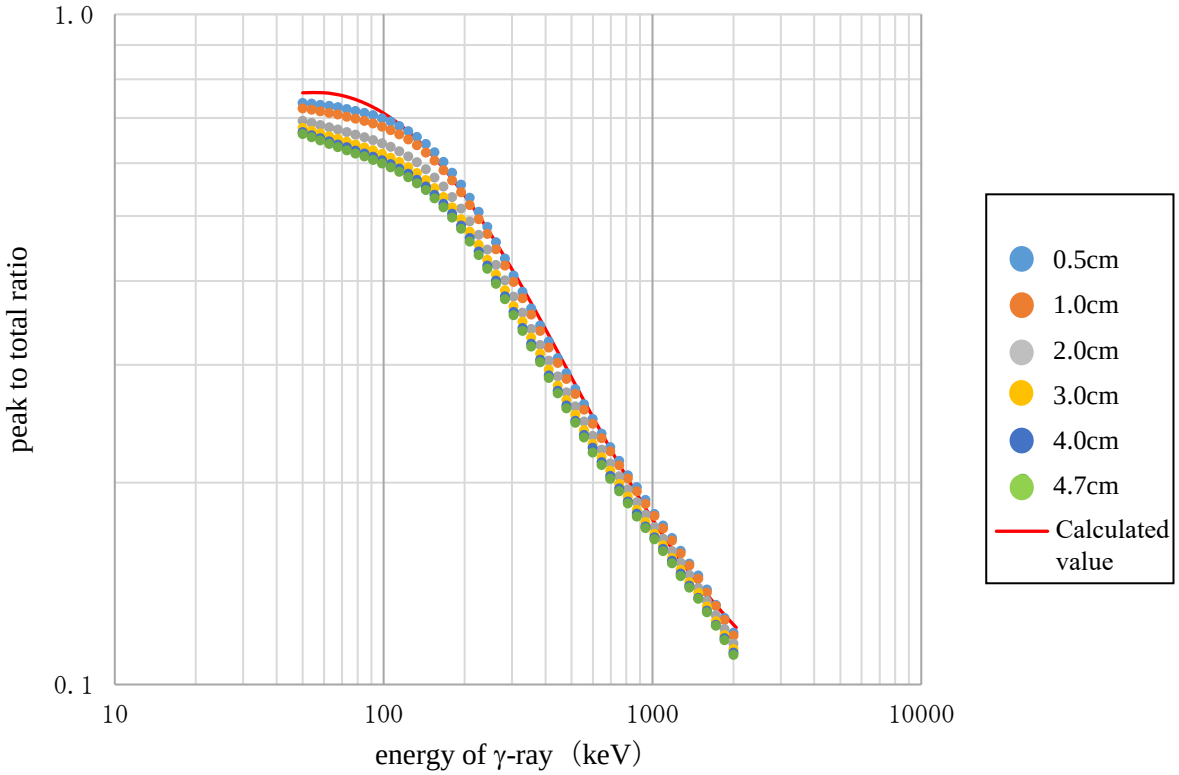

(Note) The calculated values were obtained from the relative efficiency using equation (D3.1)

Fig. D3.3 Peak-to-total ratio converted by the equation (D3.2) for detector A.

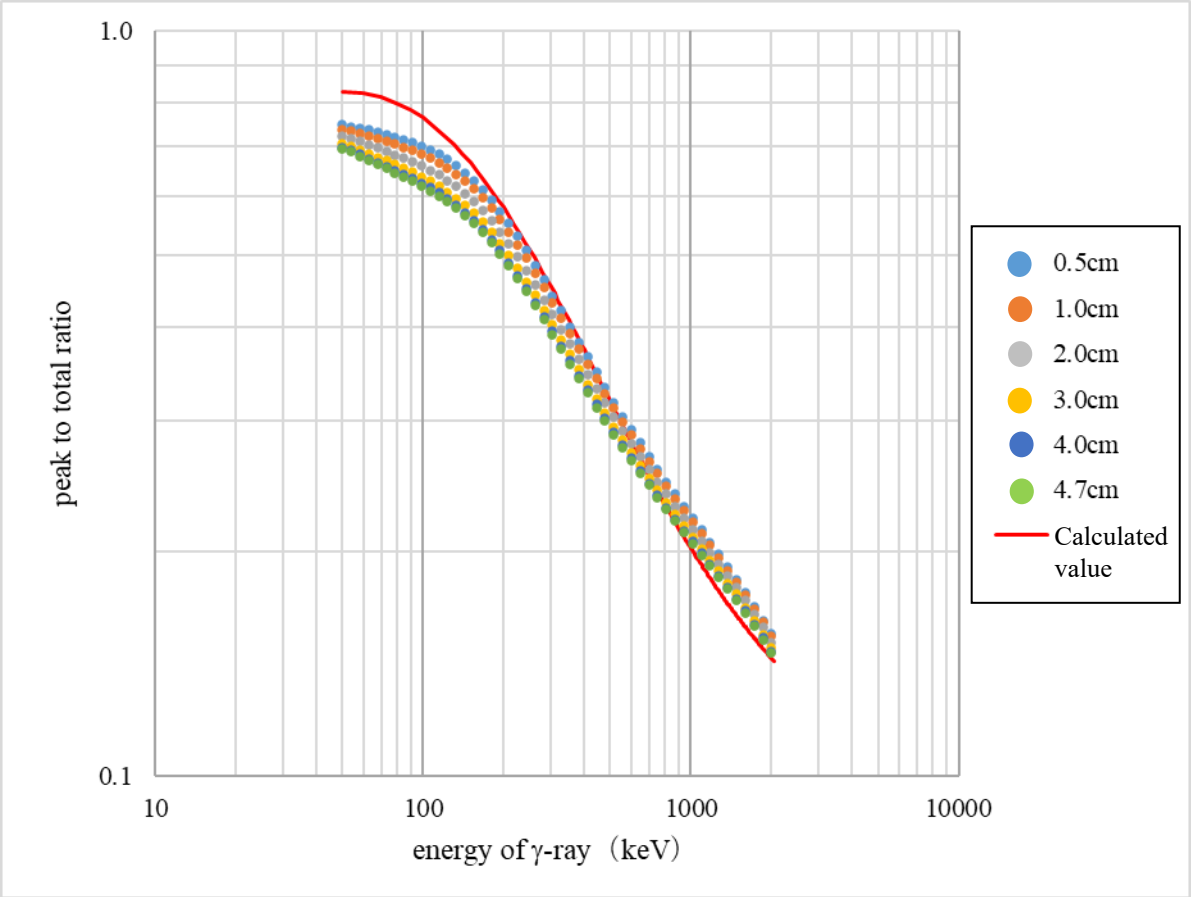

(Note) The calculated values were obtained from the relative efficiency using the equation (D3.1)

Fig. D3.4 Peak-to-total ratio converted by the equation (D3.2) for detector B.

Document 3.3 Analysis of ^{134}Cs volumetric source

Using the peak-to-total ratio obtained using the procedure in Document 3.2, the radioactivity of ^{134}Cs volumetric source in the polypropylene cylindrical container was measured. We obtained the radioactive peaks from 604.7 keV and 795.9 keV[*1], and compared the results with the calibrated values. The results are shown in Figs. D3.5–D3.8 and Table D3.1. For the uncertainties shown in the figures, only the uncertainty related to the counting was considered, and let the uncertainty be the extended uncertainty ($k = 2$). Note that the summing-effect corrections using the peak-to-total ratios obtained from equations (D3.1) and (D3.2) are written as methods Ⅰ and II, respectively.

[*1]: Gamma Studio of the SEIKO EG&G CO. LTD. was used for the analysis.

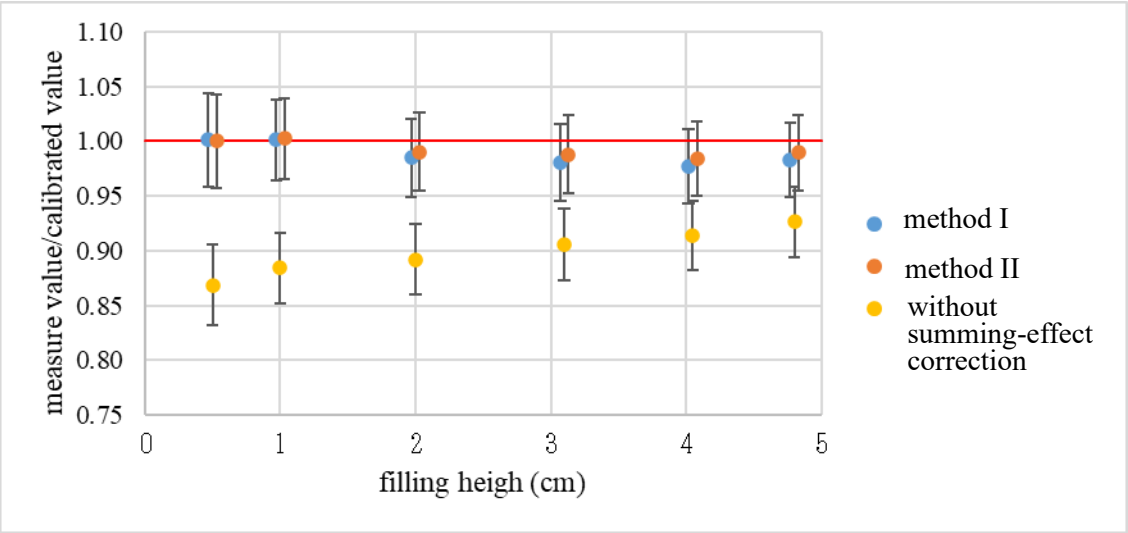

Fig. D3.5 Analytical results of ^{134}Cs volumetric source for detector A. The energy of γ-rays was 604.7 keV.

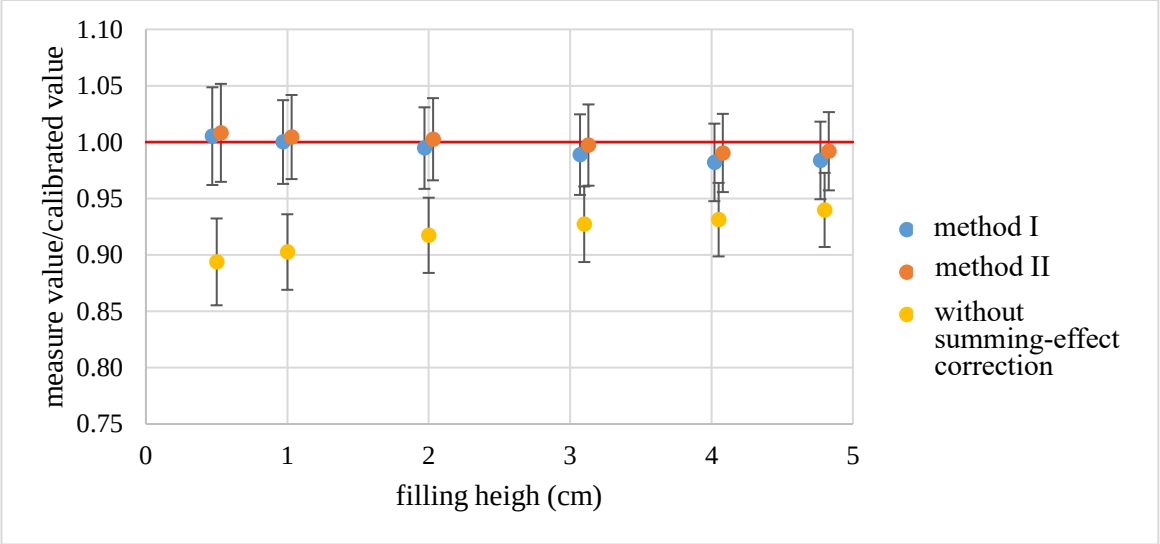

Fig. D3.6 Analytical results of ^{134}Cs volumetric source for detector A. 795.9 keV.

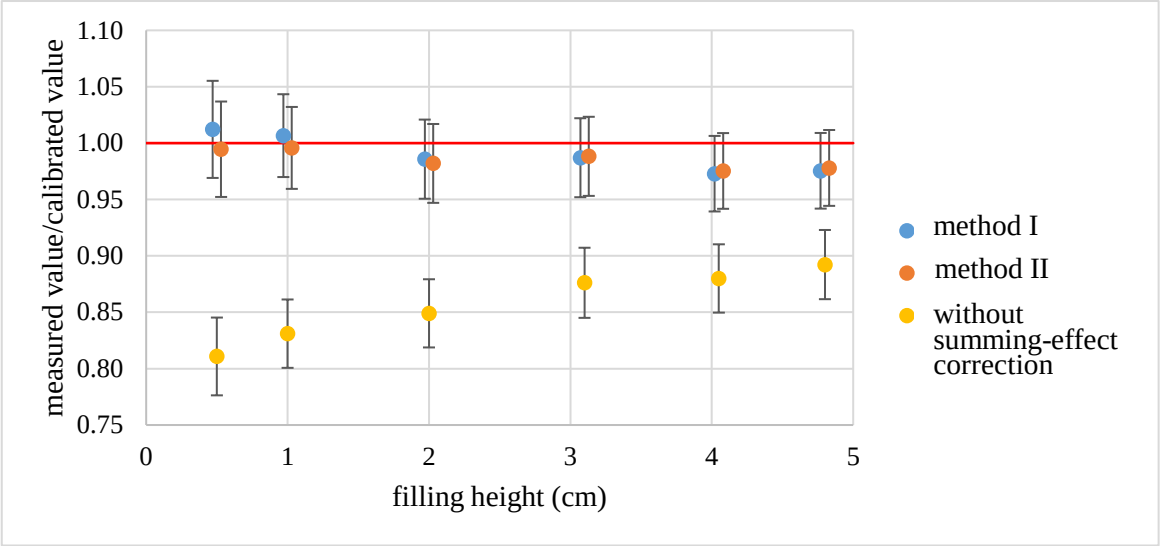

Fig. D3.7 Analytical results of ^{134}Cs volumetric source for detector B. The energy of γ-rays was 604.7 keV.

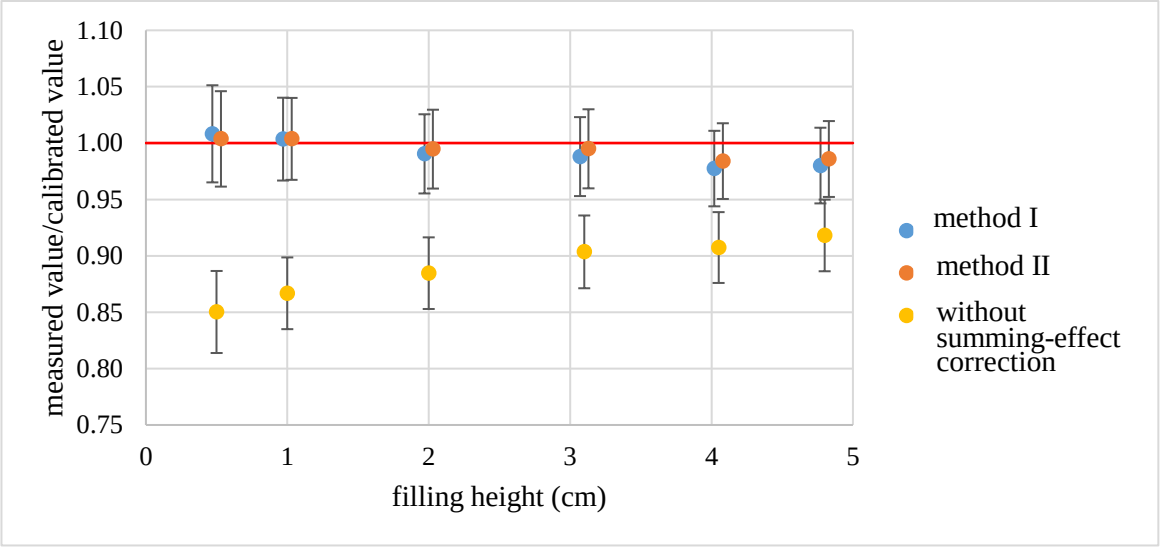

Fig. D3.8 Analytical results of ^{134}Cs volumetric source for detector B. The energy of γ-rays was 795.9 keV.

Table D3.1 Scope of the difference between analytical results and calibration values

detector	analyzed peak (keV)	without summing-effect correction	Method I	Method II
A	604.7	−13.1% – −7.4%	−2.3% – 0.1%	−1.6% – 0.3%
	795.9	−10.6% – −6.0%	−1.8% – 0.5%	−1.0% – 0.8%
B	604.7	−18.9% – −10.8%	−2.7% – 1.2%	−2.5% – −0.4%
	795.9	−15.0% – −8.2%	−2.3% – 0.8%	−1.6% – 0.4%

When the summing-effect correction was not performed, the analytical results of ^{134}Cs for detectors A and B were lower by about 6%–13% and about 8%–19%, respectively, than the calibrated values. Furthermore, the higher the filling height, the closer the results were to the calibration values. For samples with low filling height, since the sample geometry was relatively close to the detector, the contribution of the summing effect was considered to be large.

For method Ⅰ, the analytical results for both detectors almost agreed with the calibration values within the scope of the uncertainty. However, it was observed that the higher the filling height, the

lower the analytical results became, indicating that the coefficient of summing-effect correction coefficient depended on the geometry.

For method II, the analytical results for both detectors got close in most cases to the calibration values, compared with method I. Although the summing-effect correction depended on the geometry, the effect became smaller. This is because the peak-to-total ratio of the volumetric source was not constant but changed depending on its filling height. Thus, it is considered that the summing-effect correction got close to the appropriate values using the peak-to-total ratio for the volumetric source in line with real samples.

From the results above, the following method is proposed for the summing-effect correction. Up to now, peak-to-total ratios obtained using the empirical formulas have been conventionally used for the summing-effect correction. Instead of such empirical formulas, it is recommended to use the conversion formulas obtained from real measurement values for a ^{137}Cs volumetric source and the results of the Monte Carlo simulation using EGS5 since they improved the summing-effect correction to some extent. Although the improvement of the summing-effect correction was observed in this method, the dependence on the geometry remains unknown. Thus, it is not a fundamental solution at present.

In recently used numerical models (including efficiency transfer) such as the Monte Carlo simulation, the interaction between a γ-ray entering a germanium detector and the detector, including the summing-effect, can be reproduced. Thus, the peak-to-total ratio itself is becoming unnecessary.

For these reasons, the summing-effect correction using the peak-to-total ratio obtained in this study has an advantage in the short term that commercially available analytical programs can be applied without major modification. However, since the Monte Carlo simulation is in principle superior to this method, shifting to a simulation-based summing-effect correction method is considered a realistic solution in the medium to long term.

Document 4 Spectra Example

Germanium semiconductor detectors possess excellent resolution, and in a single measurement, can detect numerous peaks from γ–ray spectra. In addition, by properly performing various calibrations, they can correctly identify nuclides corresponding to the peaks.

Nuclides are generally automatically identified using an analytical program. However, when many nuclides species are in a γ-ray spectrum, the nuclides might be misidentified. Therefore, to ensure reliability in the identifying of nuclides, a user must confirm the process.

Knowing the spectral examples of routinely measured samples helps identify the nuclides because the spectral shapes differ depending on the type of the measured samples.

In addition, it should be noted that there are spectral patterns specific to the detector in a background spectrum. For example, different peak shapes are acquired from characteristic X-rays, electron pair annihilation radiation, and radiation from natural radioactive nuclides. Moreover, there are specific spectral patterns in the continuous region. In a measured spectrum of a sample, the peak shape, detected nuclides, and the Compton region shape are almost similar, based on the nuclides species. Therefore, understanding the characteristics of various spectra assists in identifying the nuclides, confirming the error in samples to be measured, and whether the measuring instrument is operating normally.

In the present document, to facilitate the nuclide identification processes, examples will be presented, as follows: one example for a background spectrum, one example for a spectrum obtained by measuring a 2L Marinelli beaker filled with pure water, eight examples for spectra obtained by measuring various environmental samples, and one example for a spectrum of atmospheric floating dust released by the accident at the Fukushima Daiichi Nuclear Power Station. In addition, three examples described in the previous manual revised in 1992, i.e., samples related to the nuclear tests, atmospheric floating dust related to the nuclear accident, and smear samples related to the nuclear accident, are also described because they provide valuable data.

In the spectral examples, the nuclide name and the related γ–ray energy (in keV) are attached to the peak of the detected nuclide.

For the obtained counts (spectrum), the background was not subtracted. Note that for energies of γ–rays, nuclear data in the ENSDF (August 2019) were used, and the spectra step was 1 channel = about 0.5 keV.

Document 4.1 Background (measurement without anything on the detector)

The spectrum was measured on September 13, 2019, using a detector with a relative efficiency of 31% for 140000 sec.

Radiation shield: lead of 15 cm thickness in 4π direction, and inside dimension of 30×30×60cm

- Natural radioactive nuclides in thorium- and uranium-series were detected.
- Characteristic X-rays from the shield were detected.
- By the reaction between cosmic ray-derived neutrons and measuring instruments, γ–rays from ^{71m}Ge, that is, the radioactivation products and γ–rays produced by ^{56}Fe(n,n')^{56}Fe, and ^{74}Ge(n,n')^{74}Ge reactions, were detected (in some cases, they were not detected).

It is recommended that the background spectrum of the measurement instrument is determined by performing measurements over a significant period of time. Note that Fe-56(n,n') and Ge-74(n,n') in Fig.D.4.1 represent γ–rays produced by the ^{56}Fe(n,n')^{56}Fe and the ^{74}Ge(n,n')^{74}Ge reactions, respectively.

Document 4.2 Pure water (2L Marinelli beaker)

The spectrum was measured on July 30, 2016, using the same detector as in Document 4.1 for 140000 sec.

- Similar peaks as those in Document 4.1 were detected.
- By covering the detector with a 2L Marinelli beaker filled with pure water, the reaction between cosmic ray-derived neutrons and the measuring instrument became remarkable. Further, due to the interaction between germanium isotopes and neutrons, γ–rays originating from the radioactivation products ^{71m}Ge and ^{75m}Ge were detected.
  Also, γ–rays produced by the ^{56}Fe(n,n')^{56}Fe, ^{70}Ge(n,γ)^{71}Ge, ^{72}Ge(n,γ)^{73}Ge, ^{73}Ge(n,γ)^{74}Ge and ^{74}Ge(n,n')^{74}Ge reactions were detected (in some cases, they were not detected).

Peaks originating from the interaction between germanium isotopes and neutrons were occasionally detected, when a liquid sample or a sample containing a lot of water in a Marinelli beaker was measured.

In Fig.D4.2, Fe-56(n,n'), Ge-70(n,γ), Ge-72(n,γ), Ge-73(n,γ), and Ge-74(n,n') represent γ–rays produced by the ^{56}Fe(n,n')^{56}Fe, ^{70}Ge(n,γ)^{71}Ge, ^{72}Ge(n,γ)^{73}Ge, ^{73}Ge(n,γ)^{74}Ge, and ^{74}Ge(n,n')^{74}Ge reactions, respectively.

Document 4.3 Atmospheric floating dust-1

The spectrum was measured for a case where floating particulate material in 3,400 m^3 air was collected by the suction filtration (using dust monitor filter paper (HE-40T and CP-20)), and put into a measurement container with 100 mL inner volume (U-8 container), on November 4, 2010, for 70000 sec.

- In addition to nuclides detected in the background, ^{7}Be, ^{40}K, and ^{210}Pb were detected.
- By the reaction between cosmic ray-derived neutrons and the measuring instrument, the radioactivation product ^{75m}Ge was detected (in some cases, it was not detected).

Document 4.4 Atmospheric floating dust-2

The spectrum measured for a case where floating particulate material in 3400 m^3 air was collected by the suction filtration (using dust monitor filter paper (HE-40T and CP-20)), and put into the measurement container of 100 mL inner volume (U-8 container), for 70000 s on November 5, 2018.

- In addition to nuclides detected in the background, ^{7}Be, ^{40}K, and ^{210}Pb were detected.
- ^{137}Cs originating from the accident at the Fukushima Daiichi Nuclear Power Station was detected.
- By the reaction between cosmic ray-derived neutrons and measuring instruments, γ–rays from ^{71m}Ge and ^{75m}Ge that were the radioactivation products and γ–rays produced by the ^{56}Fe(n,n')^{56}Fe, ^{74}Ge(n,n')^{74}Ge, and ^{206}Pb(n,n')^{206}Pb reactions, were detected (in some cases, they were not detected).

In Fig. 4.4, Fe-56(n,n'), Ge-74(n,n'), and Pb-206(n,n') represent γ–rays produced by the ^{56}Fe(n,n')^{56}Fe, ^{74}Ge(n,n')^{74}Ge, and ^{206}Pb(n,n')^{206}Pb reactions, respectively.

Document 4.5 Fallout-1

The spectrum measured for a case where the fallout collected with a large water-basin which has a 5000 cm^2 aperture for one month was evaporated and dried, then put into a measurement container of 100 mL inner volume (U-8 container) for 70000 s on April 15, 2010.

- In addition to nuclides detected in the background, ^{7}Be, ^{40}K, and ^{210}Pb in the dust were detected.
- By the reaction between cosmic ray-derived neutrons and measuring instruments, γ–rays from ^{71m}Ge and ^{75m}Ge that were the radioactivation products and γ–rays produced by the $^{74}Ge(n,n')^{74}Ge$ and $^{206}Pb(n,n')^{206}Pb$ reactions were detected (in some cases, they were not detected).
- If a sample contains a large amount of ^{7}Be, caution should be exercised because the backscattering peaks (about 166 keV) originating from γ–rays from ^{7}Be are overlapped with γ–rays from ^{139}Ce (165.8 keV).

In Fig.D.4.5, Ge-74(n,n') and Pb-206(n,n') represent γ–rays produced by the $^{74}Ge(n,n')^{74}Ge$ and $^{206}Pb(n,n')^{206}Pb$ reactions, respectively.

Document 4.6 Fallout-2

The spectrum measured for a case where the fallout collected with a large water-basin which has 5000 cm^2 aperture for one month was evaporated and dried, then put into a measurement container of 100 mL inner volume (U-8 container), for 70000 s on June 19, 2018.

- In addition to nuclides detected in the background, ^{7}Be, ^{40}K, and ^{210}Pb in the dust were detected.
- ^{134}Cs and ^{137}Cs originating from the accident at the Fukushima Daiichi Nuclear Power Station were detected.
- By the reaction between cosmic ray-derived neutrons and measuring instruments, γ–rays from ^{71m}Ge and ^{75m}Ge that were the radioactivation products and γ–rays produced by the $^{74}Ge(n,n')^{74}Ge$ reaction were detected (in some cases, they were not detected).

In Fig. D.4.6, Ge-74(n,n') represents γ–rays produced by the $^{74}Ge(n,n')^{74}Ge$ reaction.

Document 4.7 Soil-1

The spectrum measured for a case where surface soil was put into a measurement container of 100 mL inner volume (U-8 container), for 70000 s on April 13, 2005.

- ^{228}Ac, ^{212}Pb, ^{212}Bi, and ^{208}Tl of thorium-series nuclides were detected.
- ^{234m}Pa, ^{226}Ra, ^{214}Pb, ^{214}Bi, and ^{210}Pb of uranium-series nuclides were detected.
- ^{235}U of actinium-series nuclide was detected.
- Due to the remaining effect of atmospheric nuclear tests, ^{137}Cs from the fallout was detected.
- By the reaction between cosmic ray-derived neutrons and measuring instruments, γ–rays from ^{71m}Ge that were the radioactivation products, were detected (in some cases, they were not detected).

Document 4.8 Soil-2

The spectrum measured for a case where surface soil was put into a measurement container of 100 mL inner volume (U-8 container), for 70000 s on October 22, 2018.

- ^{228}Ac, ^{212}Pb, ^{212}Bi, and ^{208}Tl of thorium-series nuclides were detected.
- ^{234m}Pa, ^{226}Ra, ^{214}Pb, and ^{214}Bi of uranium-series nuclides were detected.
- ^{235}U of actinium-series nuclide was detected.
- ^{134}Cs and ^{137}Cs originating from the accident at the Fukushima Daiichi Nuclear Power Station were detected.

Document 4.9 Marine products

The spectrum measured for a case where edible parts of the marine product (horse mackerel) were dried, incinerated, and put in a measurement container of 100 mL inner volume (U-8 container), for 70000 s on December 13, 2005. Note that the terms “SE” and “DE” in the figure represent a single escape peak and a double escape peak, respectively.

- Natural radioactive nuclides that were similar to the backgrounds were detected.
- Single escape (SE) peak and double escape (DE) peak for ^{40}K were clearly detected.
- By the reaction between cosmic ray-derived neutrons and measuring instruments, γ–rays from ^{71m}Ge, that was the radioactivation product, and γ–rays produced by the ^{206}Pb(n,n')^{206}Pb reaction, were detected (in some cases, they were not detected).

In Fig. D.4.9, Pb-206(n,n') represents γ–rays produced by the ^{206}Pb(n,n')^{206}Pb reaction.

Document 4.10 Ore (monazite powder)

The spectrum measured for the ore containing a relatively large amount of uranium and thorium that was put in a measurement container of 100 mL inner volume (U-8 container), for 70000 s on October 12, 2010. The term “sum” in the figure represents a sum peak.

- Although nuclides species observed for the ore resembled those observed for the soil, the ore contained a large amount of uranium and thorium. So, the radioactivity concentrations for the isotopes and decay products of these nuclides were high.
  Therefore, the spectrum baseline was high due to the Compton scattering by the interaction between the emitted γ–rays and the detector.
- Since the ore had a high radioactivity concentration of isotopes for uranium and thorium and their decay products, many peaks were observed for the nuclides with a low emission rate. Therefore, the nuclide identification should be performed carefully.
  It should be noted that the peak of ^{228}Ac was observed at 1459.1 keV (emission rate: 0.83%), which should not be misidentified as the peak of ^{40}K at 1460.82 keV (emission rate: 10.66%).
- By the reaction between thorium in the sample and γ–rays, Th X-rays were observed at 89.957 keV ($K\alpha_2$) and 105.604 keV ($K\beta_1$). Note that the peak of Th X-rays at 93.350 keV ($K\alpha_1$) is considered to be overlapped with the peak of ^{234}Th at 92.38 keV (emission rate: 2.13%) and 92.80 keV (emission rate: 2.1%).
- For samples with a high thorium concentration, since the main peak of ^{234m}Pa at 1001.03 keV (emission rate: 0.84%) was overlapped with the sum peak at 1001.157 keV, originating from ^{228}Ac (911.2 keV, emission rate: 25.8%) and Th X-ray (89.957 keV: $K\alpha_2$), the ^{234m}Pa should be quantified with caution. In particular, if a peak is observed at 1004.6 keV (the sum peak originating from γ–rays of ^{228}Ac at 911.2 keV and Th $K\alpha_1$ X-rays at 93.350 keV), Th $K\alpha_2$ X-rays are considered to be detected as well.
  Thereby, there is a high possibility that the main peak of ^{234m}Pa is overlapped with the sum peak originating from γ–rays of ^{228}AckeV and Th $K\alpha_2$ X-rays.

Document 4.11 Atmospheric floating dust related to the accident at the Fukushima Daiichi Nuclear Power Station

The spectrum for a case where the atmospheric floating dust collected in Chiba City, just after the accident at the Fukushima Daiichi Nuclear Power Station, was measured for 30000 s on March 15, 2011. The term "sum" in the figure represents the sum peak.

- Artificial radioactive nuclides such as ^{99}Mo, ^{99m}Tc, ^{129}Te, ^{129m}Te, ^{131}I, ^{132}Te, ^{132}I, ^{133}I, ^{134}Cs, ^{136}Cs, ^{137}Cs, ^{140}Ba, and ^{140}La were detected.
- Among numerous observed peaks, ^{132}I had the largest number of peaks, and about 60 peaks were observed, including the sum peaks.
- The baseline of the spectrum was high in all regions due to the high isotopes concentration of iodin, cesium, etc.
- Although ^{132}I has a short half-life of 2.28 h, ^{132}Te (half-life: 78.2 h) that is the parent nuclide of ^{132}I, was detected. Therefore, ^{132}I that had grown from ^{132}Te was detected at a high concentration at the time of the measurement on March 15, 2011.
- ^{99}Mo－^{99m}Tc, ^{132}Te－^{132}I, and ^{140}Ba－^{140}La, which have the parent-progeny relations, were detected.

Document 4.12 Samples related to nuclear tests

The spectrum for the precipitation collected in Japan, just after the nuclear test in China, that was measured for 35401 s.

- Artificial radioactive nuclides ^{58}Co, ^{91}Sr, ^{91}Y, ^{93}Y, ^{95}Zr, ^{95}Nb, ^{97}Zr, ^{97}Nb, ^{99}Mo, ^{99m}Tc, ^{103}Ru, ^{131}I, ^{132}Te, ^{132}I, ^{136}Cs, ^{140}Ba, ^{140}La, ^{141}Ce, ^{143}Ce, ^{144}Ce, ^{147}Nd, and ^{239}Np were detected.
- Since many fission product nuclides were contained in the sample at high concentrations, the baseline of the spectrum was high in all energy regions.
- ^{91}Sr－^{91}Y, ^{95}Zr－^{95}Nb, ^{97}Zr－^{97}Nb, ^{99}Mo－^{99m}Tc, ^{132}Te－^{132}I, and ^{140}Ba－^{140}La, which have the parent-progeny relations, were detected.

Document 4.13 Floating dust related to the nuclear accident

The spectrum for the atmospheric floating dust collected in the former Soviet Union during the Chernobyl accident, that was measured for 50000 s on May 2, 1986.

- Artificial radioactive nuclides, ^{95}Nb, ^{99}Mo, ^{99m}Tc, ^{103}Ru, ^{106}Ru, ^{110m}Ag, ^{125}Sb, ^{129}Te, ^{129m}Te, ^{131}I, ^{132}Te, ^{132}I, ^{134}Cs, ^{136}Cs, ^{137}Cs, ^{140}Ba, and ^{140}La were detected.
- Among numerous observed peaks, ^{132}I had the largest number of peaks, and about 60 peaks were observed, including the sum peaks.
- The baseline of the spectrum was high in all regions due to the high isotopes concentration of iodin, cesium, etc.
- Although ^{132}I has a short half-life of 2.28 h, ^{132}Te (half-life: 78.2 h) that is the parent nuclide of ^{132}I was detected. Therefore, ^{132}I that had grown from ^{132}Te was detected at a high concentration at the time of the measurement on May 2, 1986.
- ^{99}Mo－^{99m}Tc, ^{132}Te－^{132}I, and ^{140}Ba－^{140}La, which have the parent-progeny relations, were detected.

Document 4.14 Smear samples related to the nuclear accident

The spectrum for the smear sample collected in the former Soviet Union during the Chernobyl accident, that was measured for 1011 s on May 31, 1986.

- Artificial radioactive nuclides, ^{95}Zr, ^{95}Nb, ^{103}Ru, ^{106}Ru, ^{110m}Ag, ^{125}Sb, ^{129m}Te, ^{131}I, ^{132}Te, ^{132}I, ^{134}Cs, ^{136}Cs, ^{137}Cs, ^{140}Ba, ^{140}La, ^{141}Ce, ^{144}Ce, and ^{147}Nd were detected.
- Because 35 days passed since the accident, short half-life nuclides such as isotopes of iodine had decayed. Nevertheless, the spectrum baseline was high due to isotopes of cesium and the other nuclides such as ^{95}Zr, ^{95}Nb, and ^{140}La.
- ^{95}Zr－^{95}Nb,^{132}Te－^{132}I, and ^{140}Ba－^{140}La, which have the parent-progeny relations, were detected.

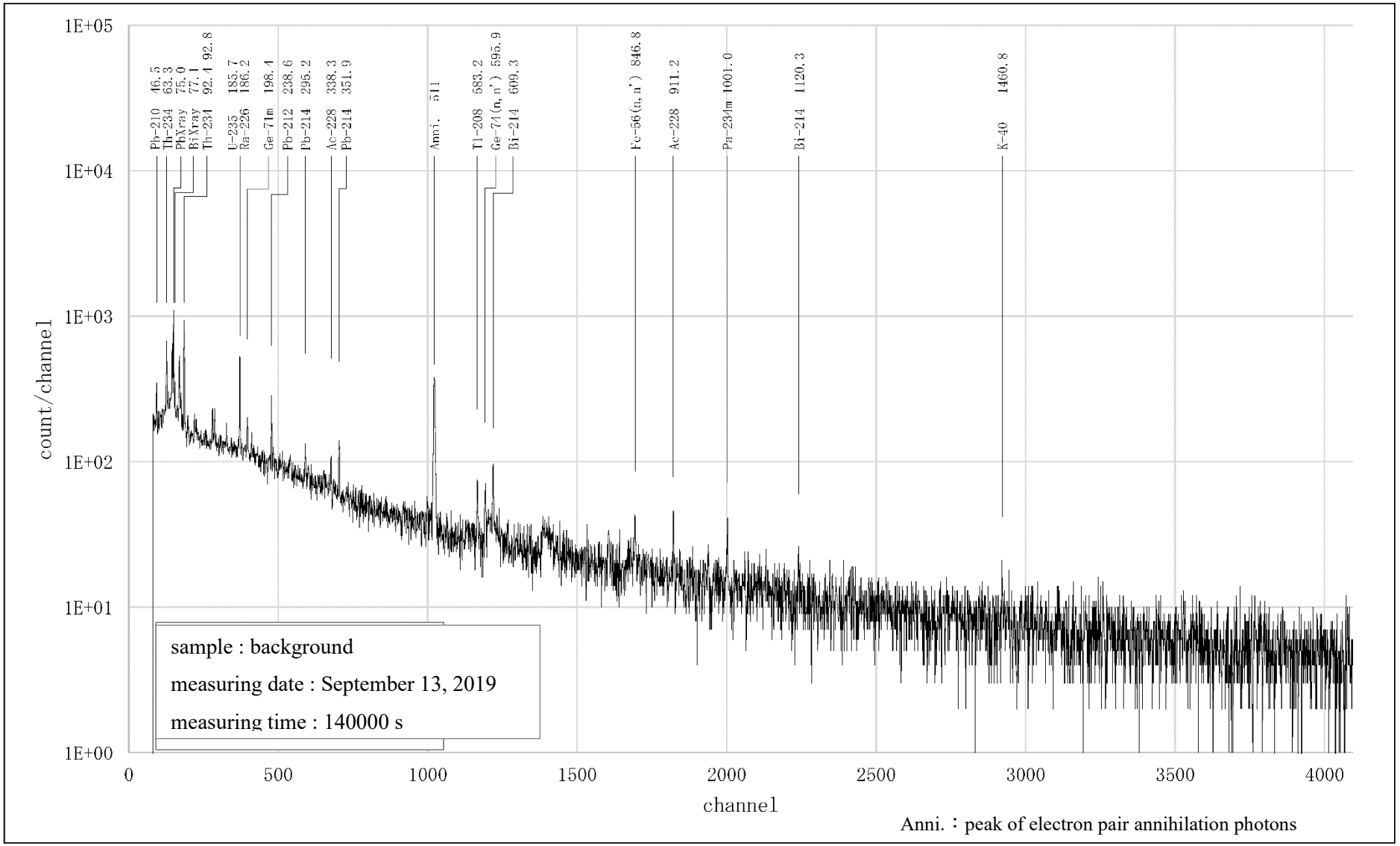

Fig. D4.1 Background (measured without anything on the detector).

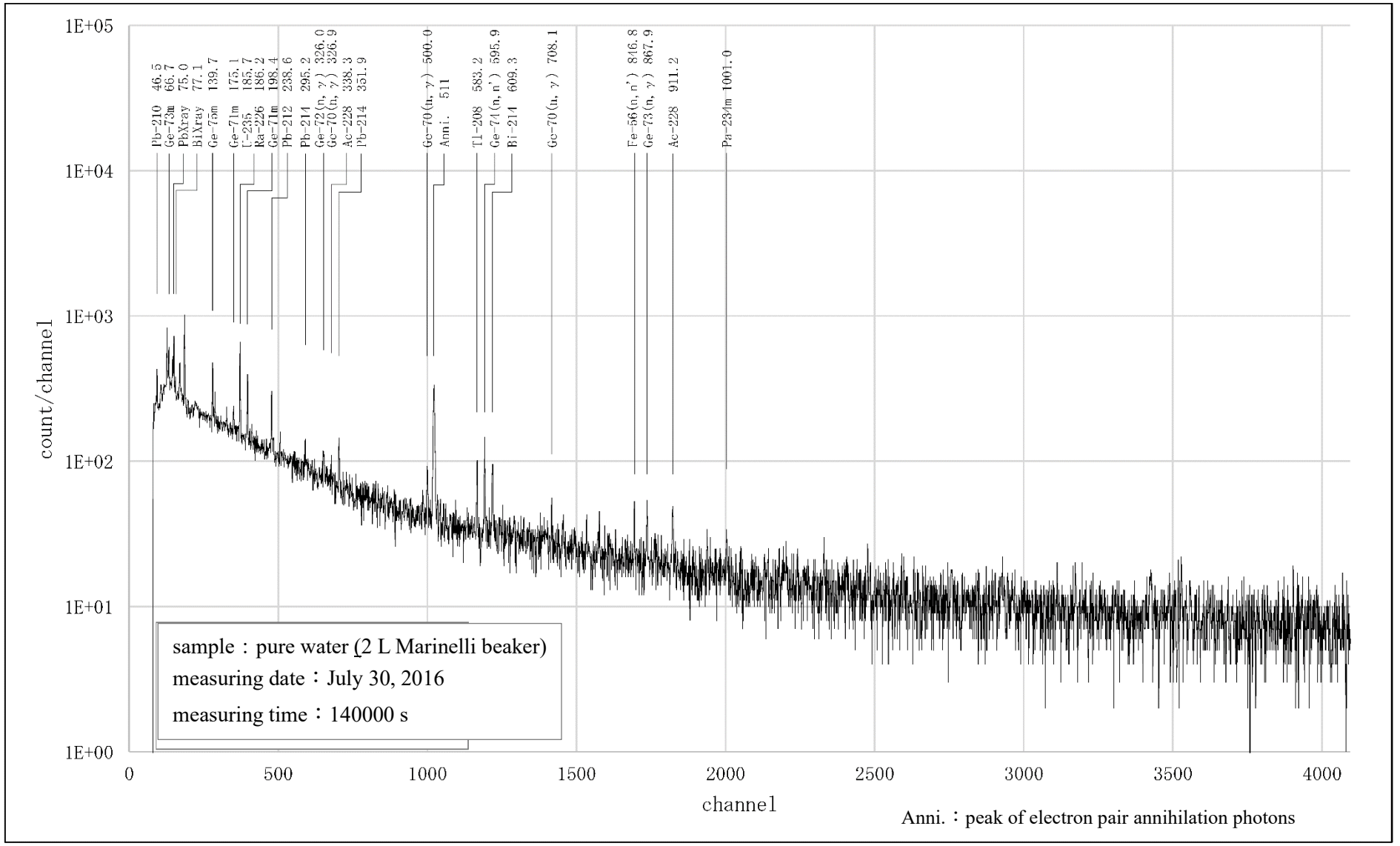

Fig. D4.2 Pure water (2L Marinelli beaker).

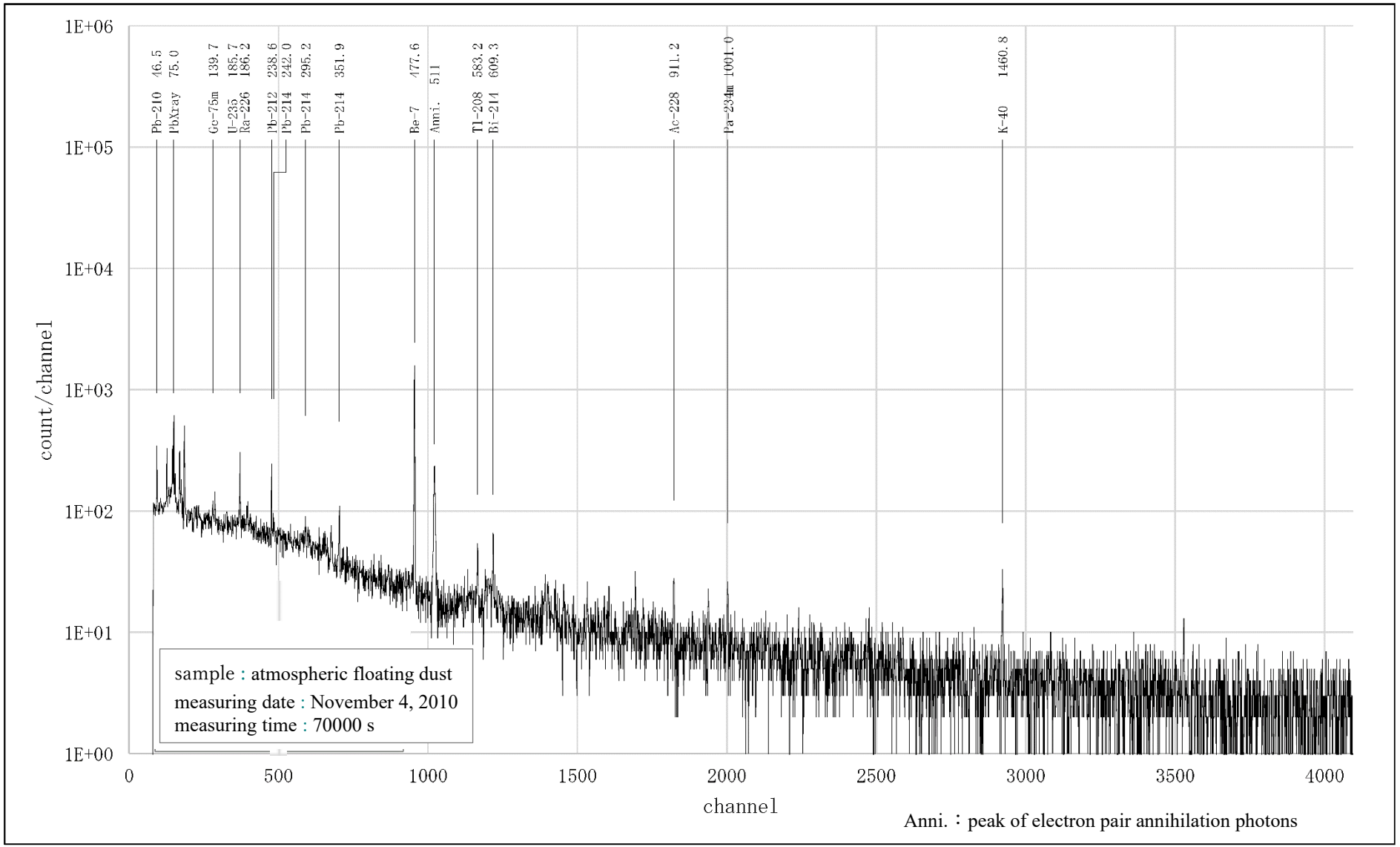

Fig. D4.3 The atmospheric floating dust-1.

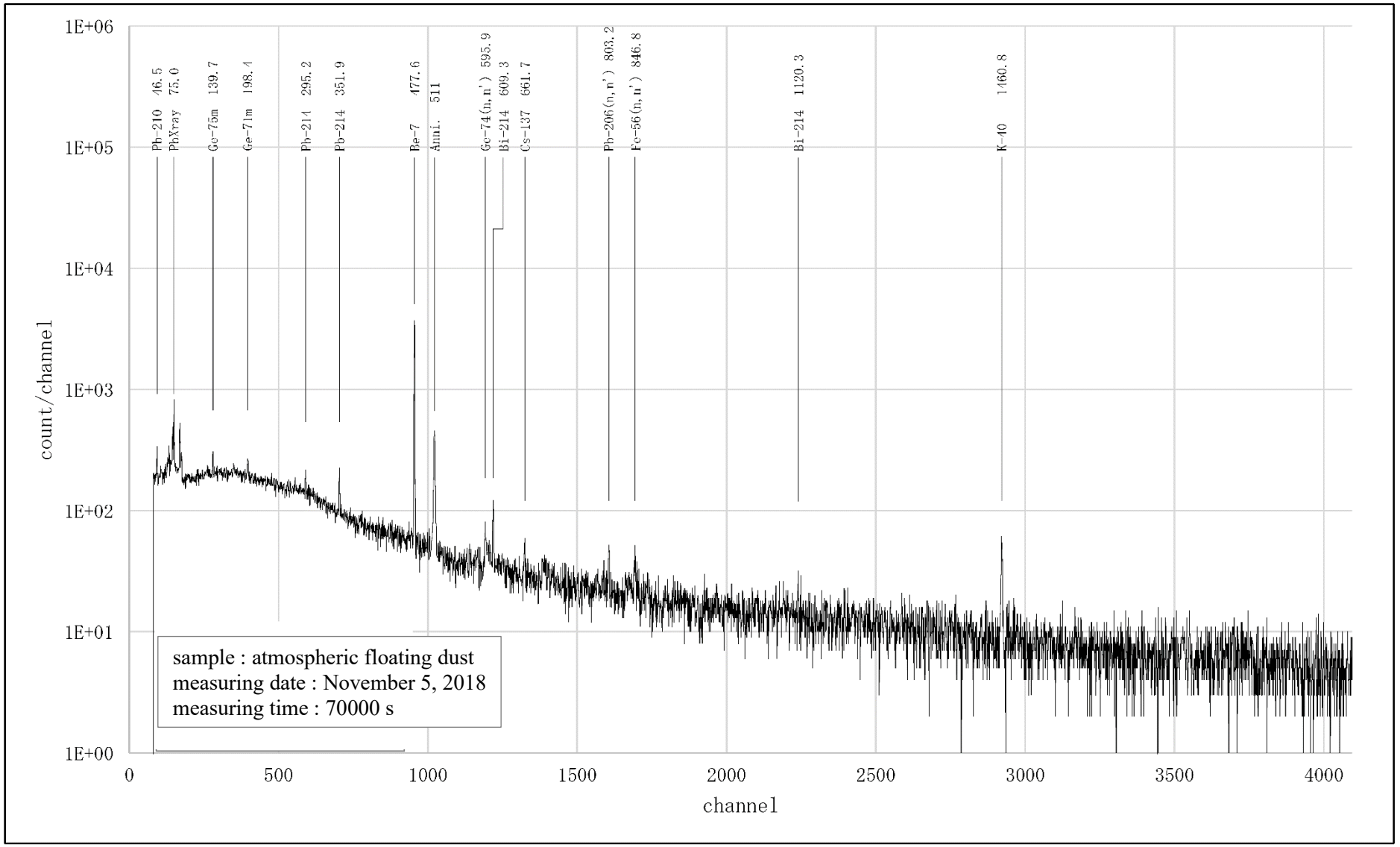

Fig. D4.4 The atmospheric floating dust-2.

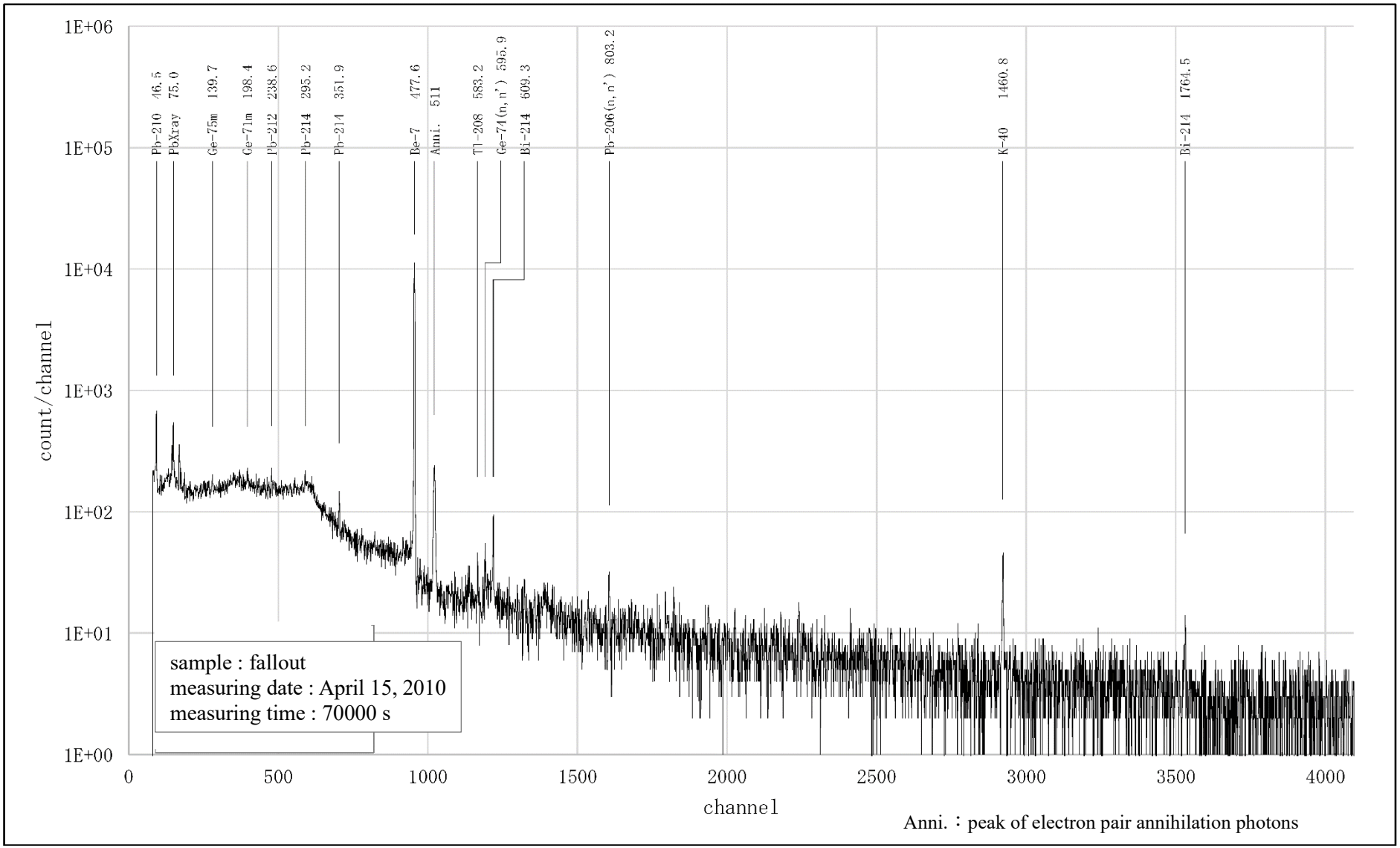

Fig. D4.5 Fallout-1.

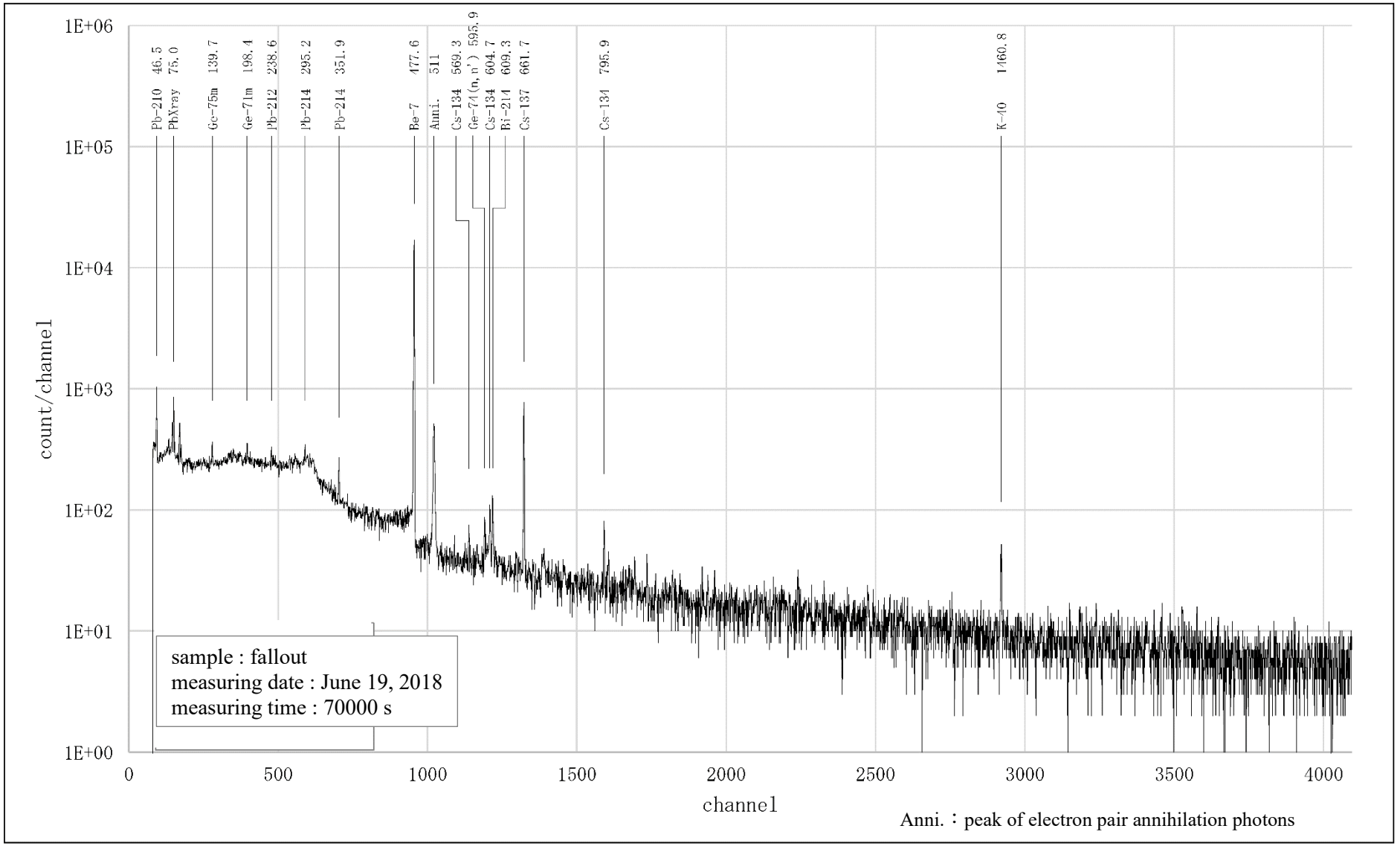

Fig. D4.6 Fallout-2.

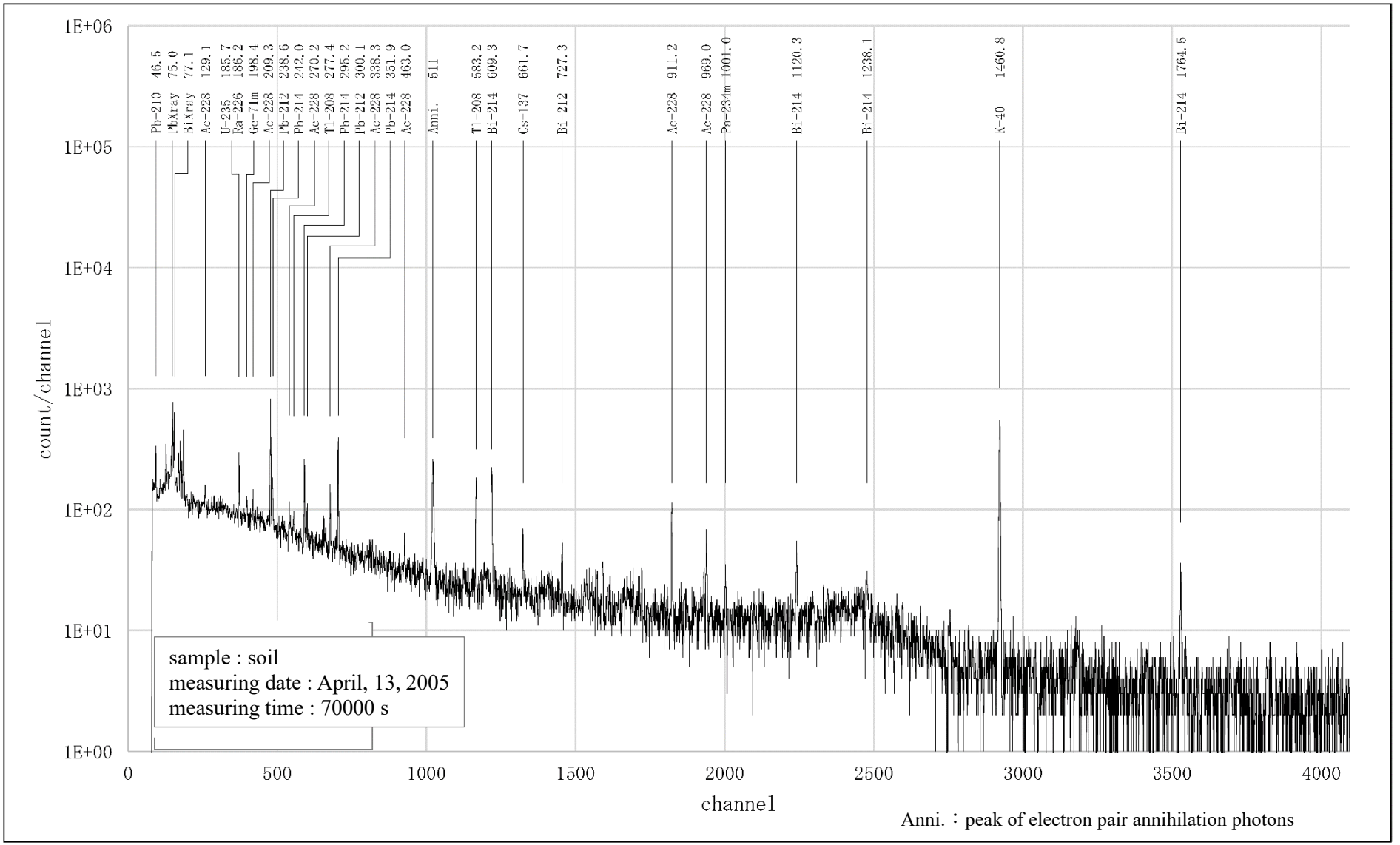

Fig. D4.7 Soil-1.

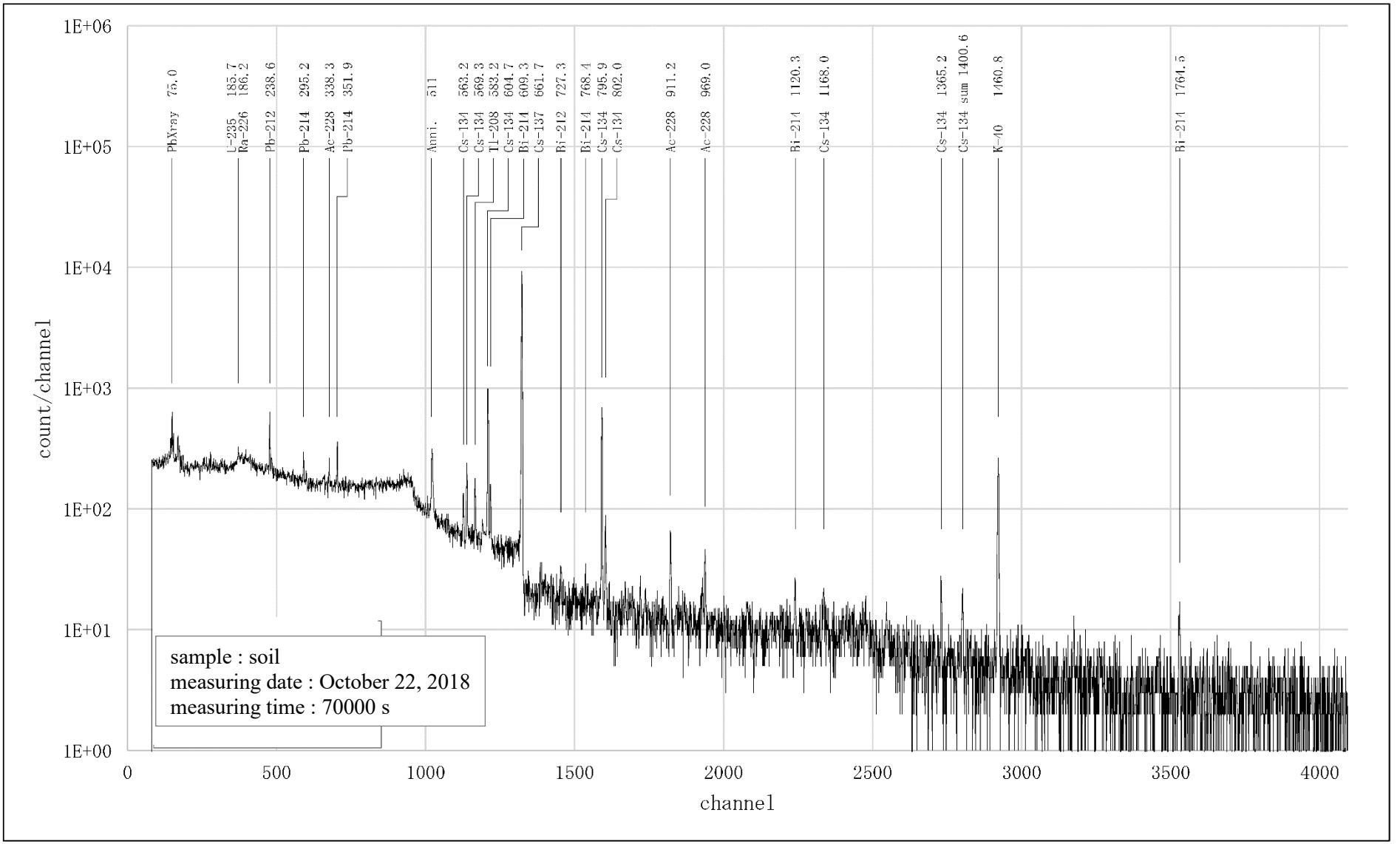

Fig. D4.8 Soil-2.

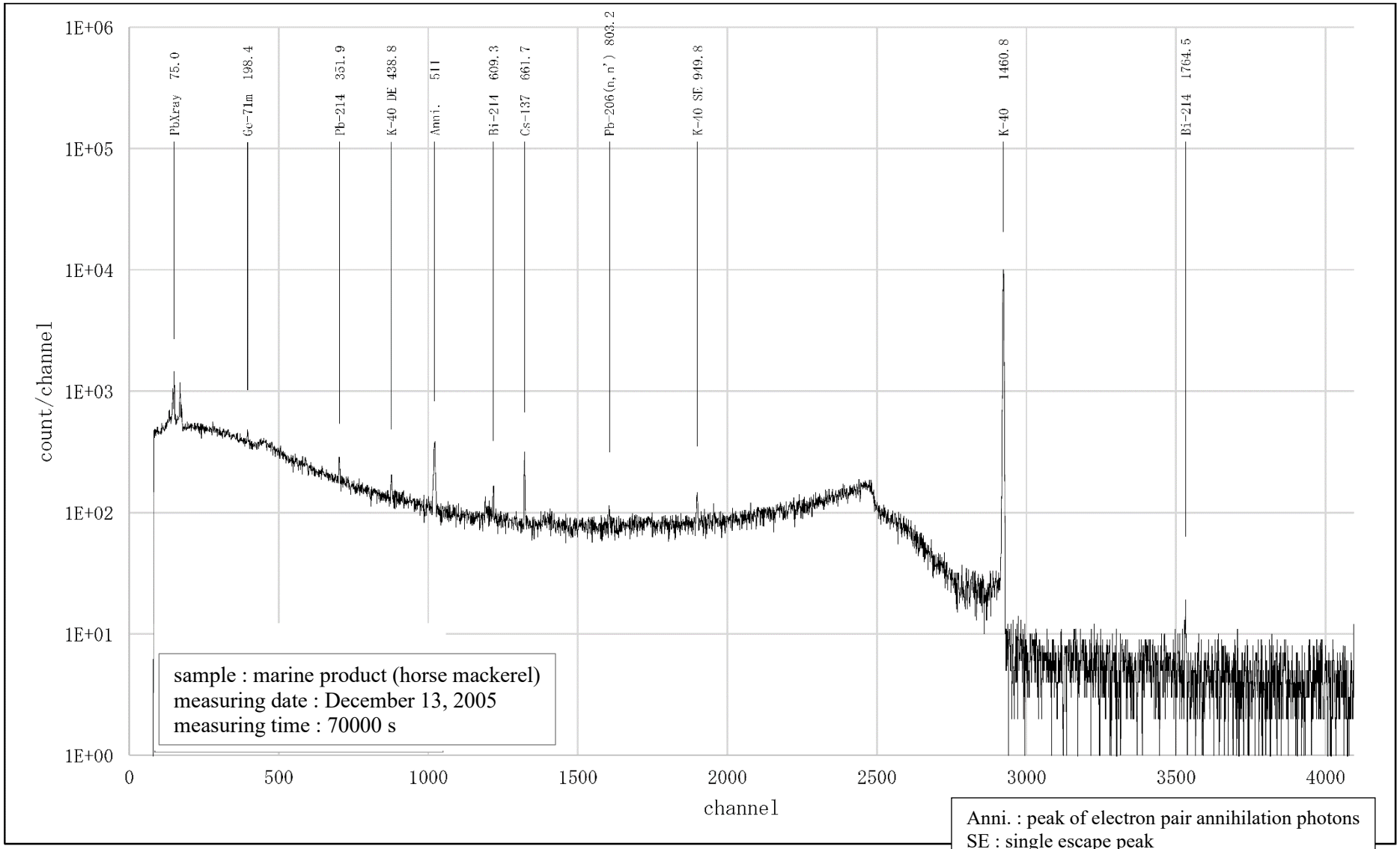

Fig. D4.9 Marine product (horse mackerel).

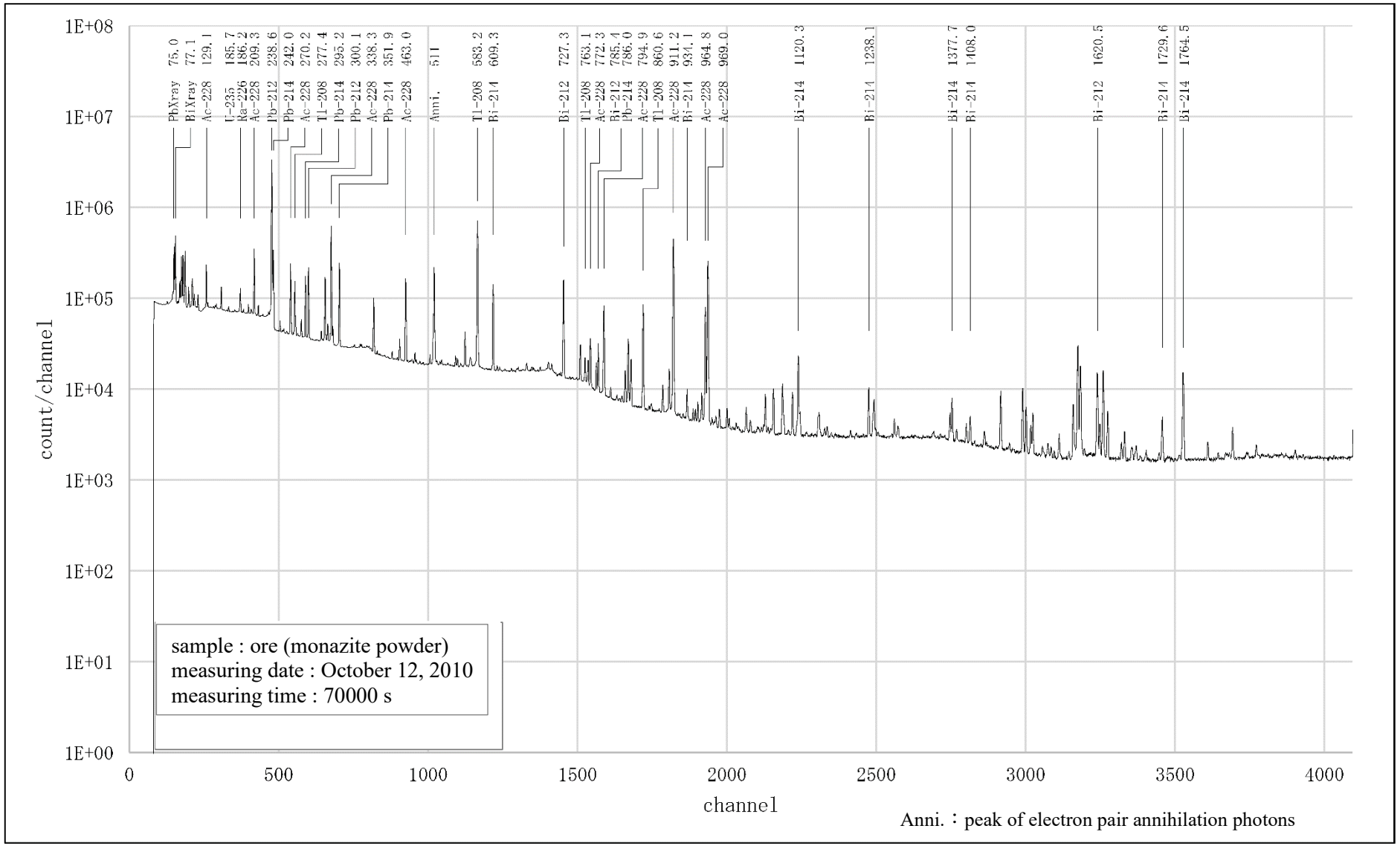

Fig. D4.10 Ore (monazite powder).

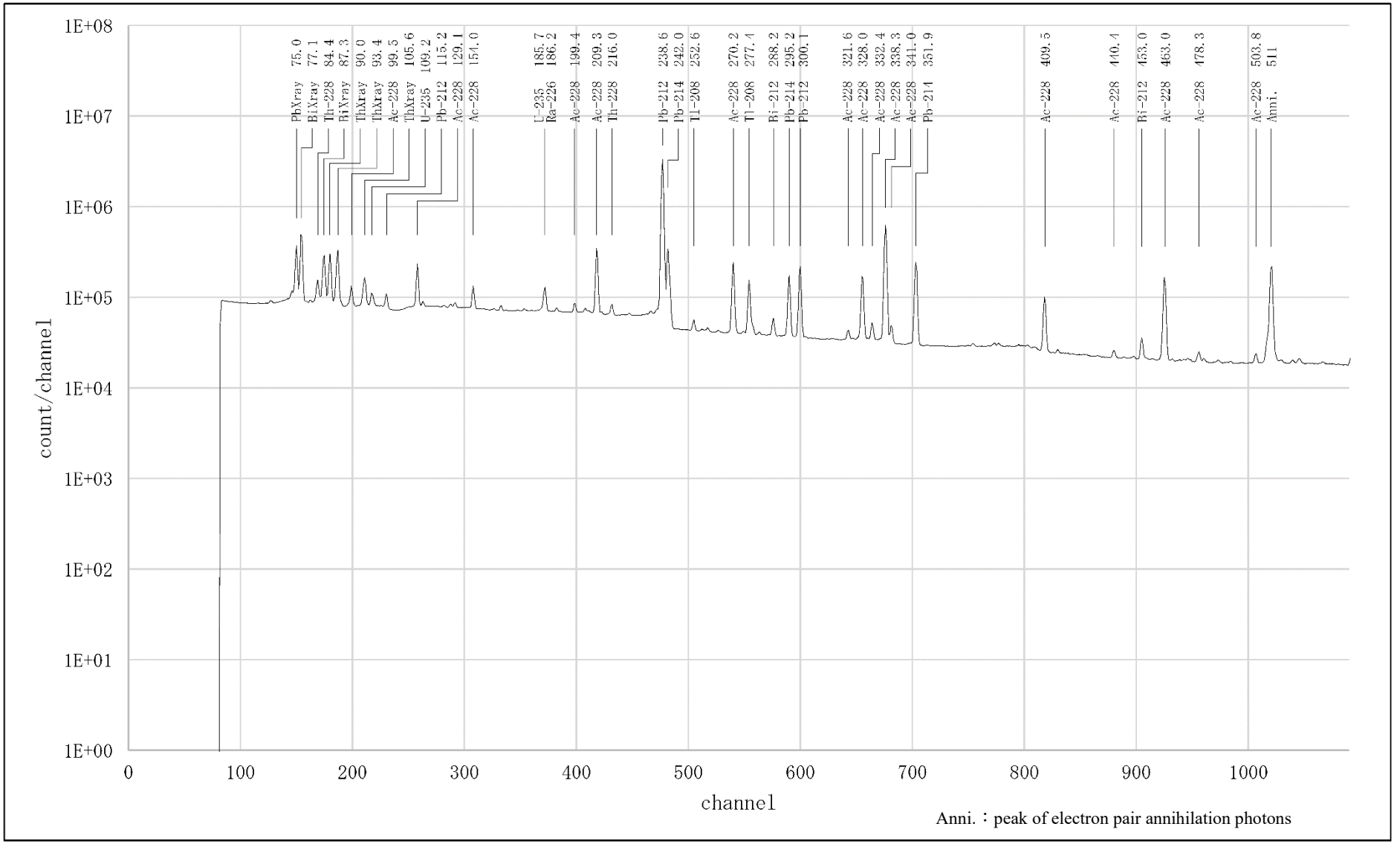

Fig. D4.10.1 Ore (monazite powder) (enlarged view of 1/4 part).

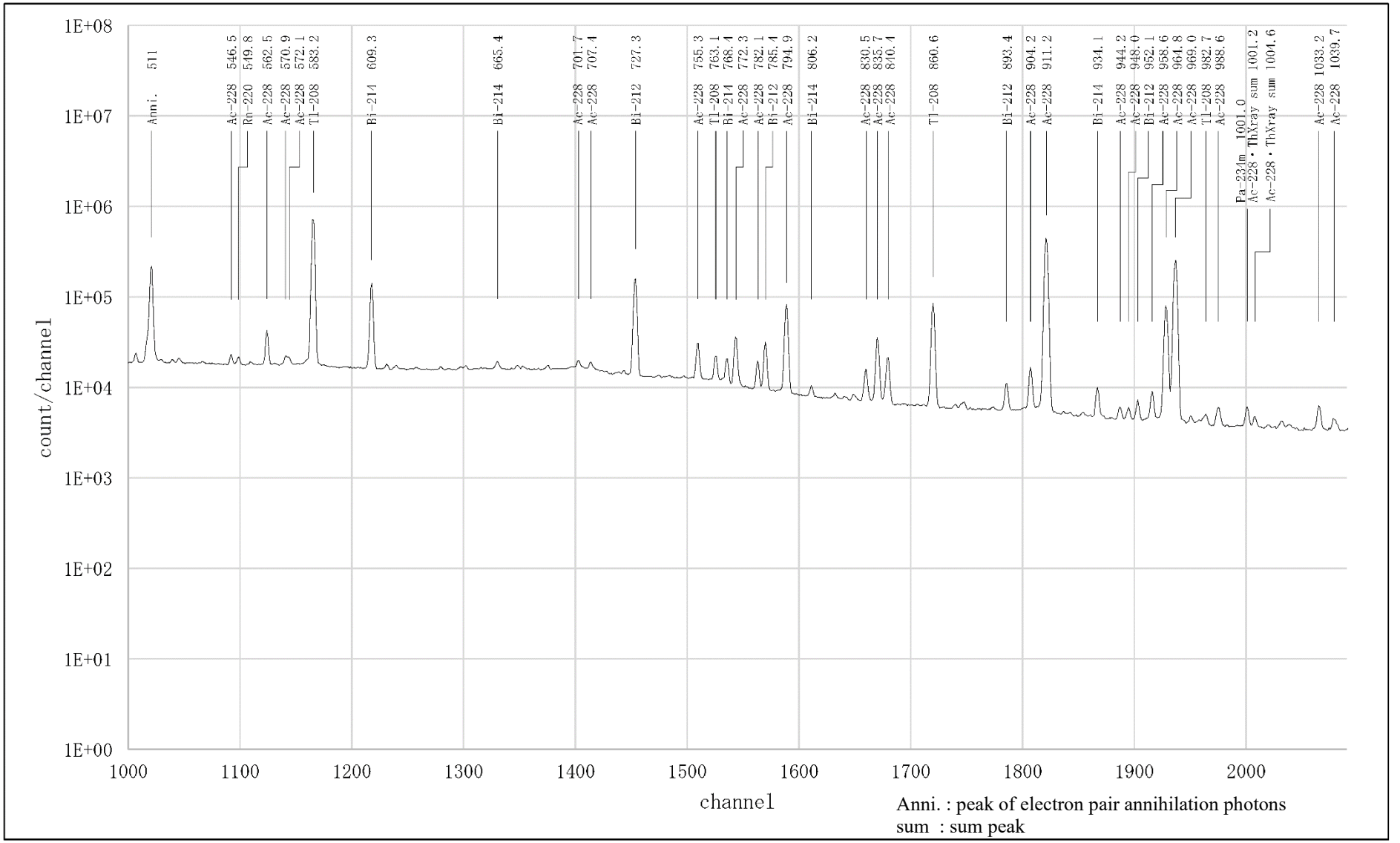

Fig. D4.10.2 Ore (monazite powder) (enlarged view of 2/4 part)

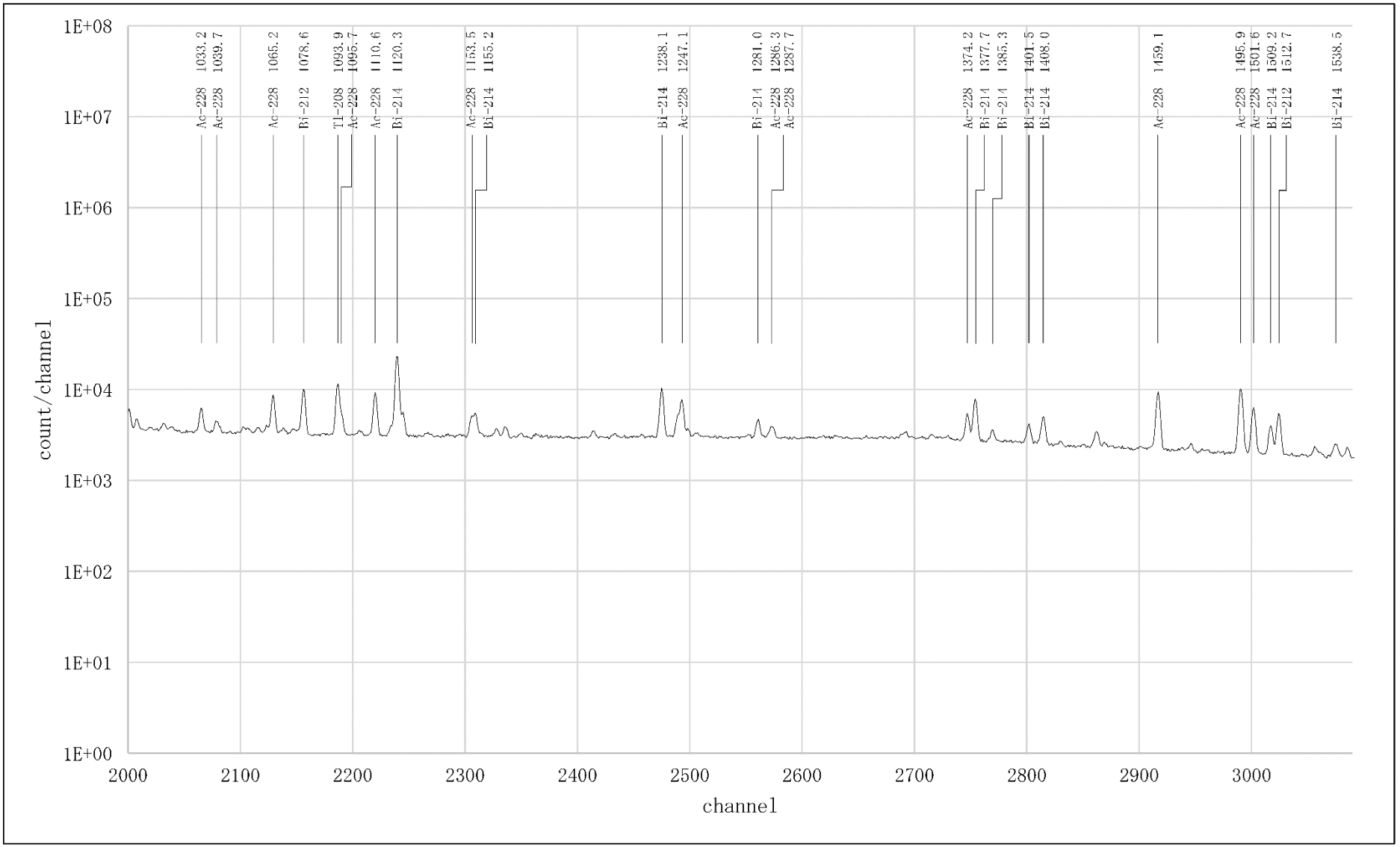

Fig. D4.10.3 Ore (monazite powder) (enlarged view of 3/4 part).

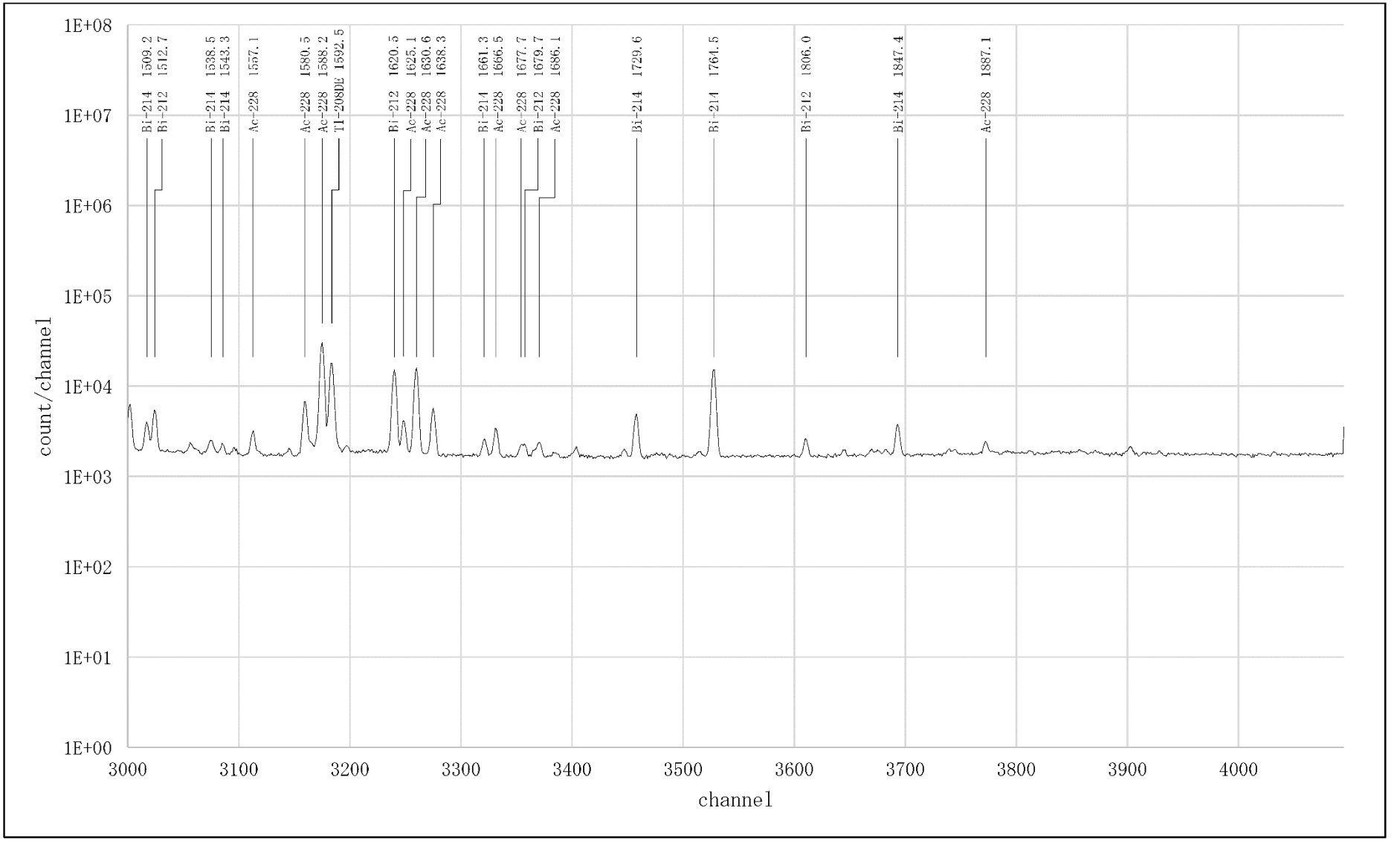

Fig. D4.10.4 Ore (monazite powder) (enlarged view of 4/4 part).

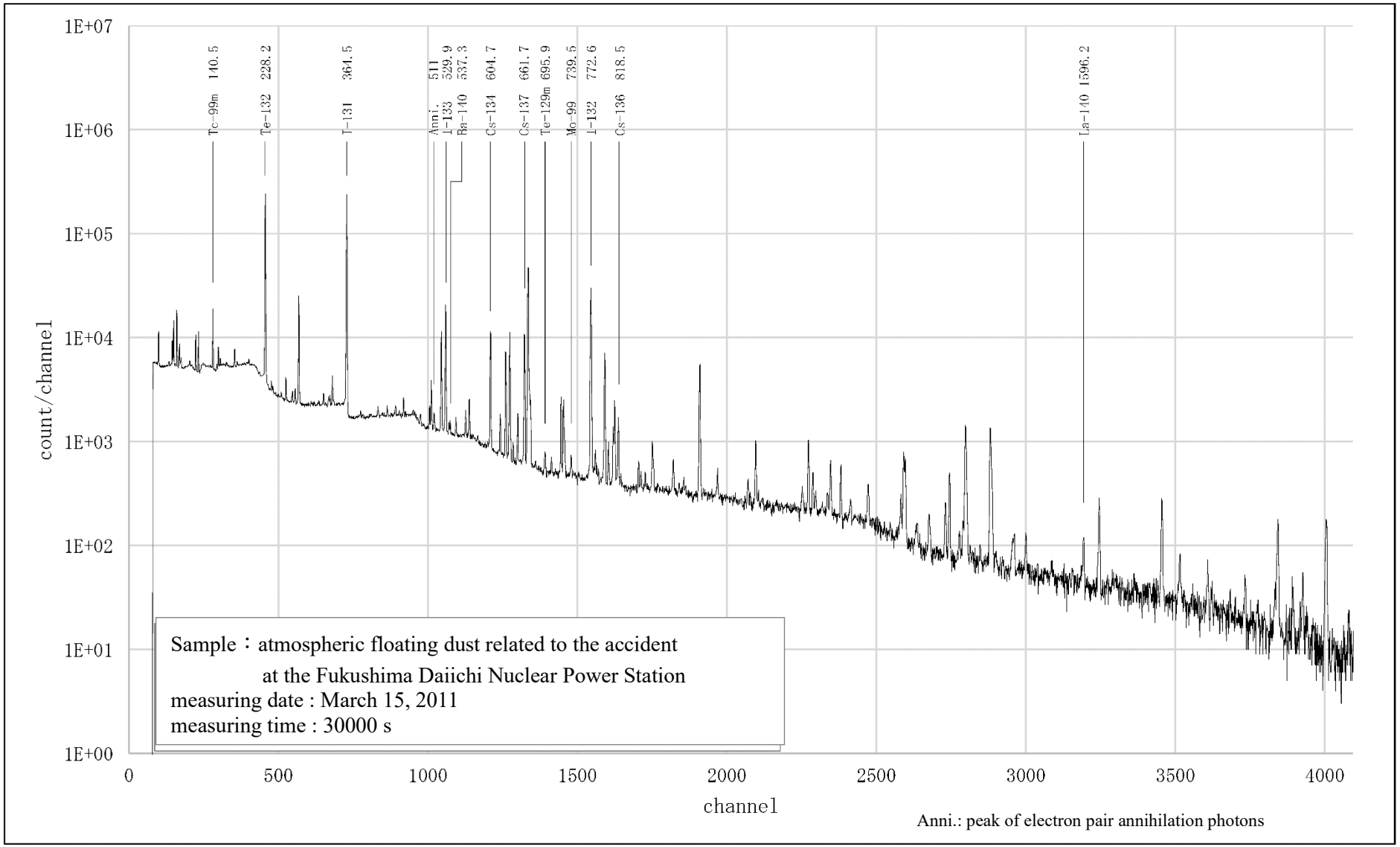

Fig. D4.11 Atmospheric floating dust related to the accident at the Fukushima Daiichi Nuclear Power Station.

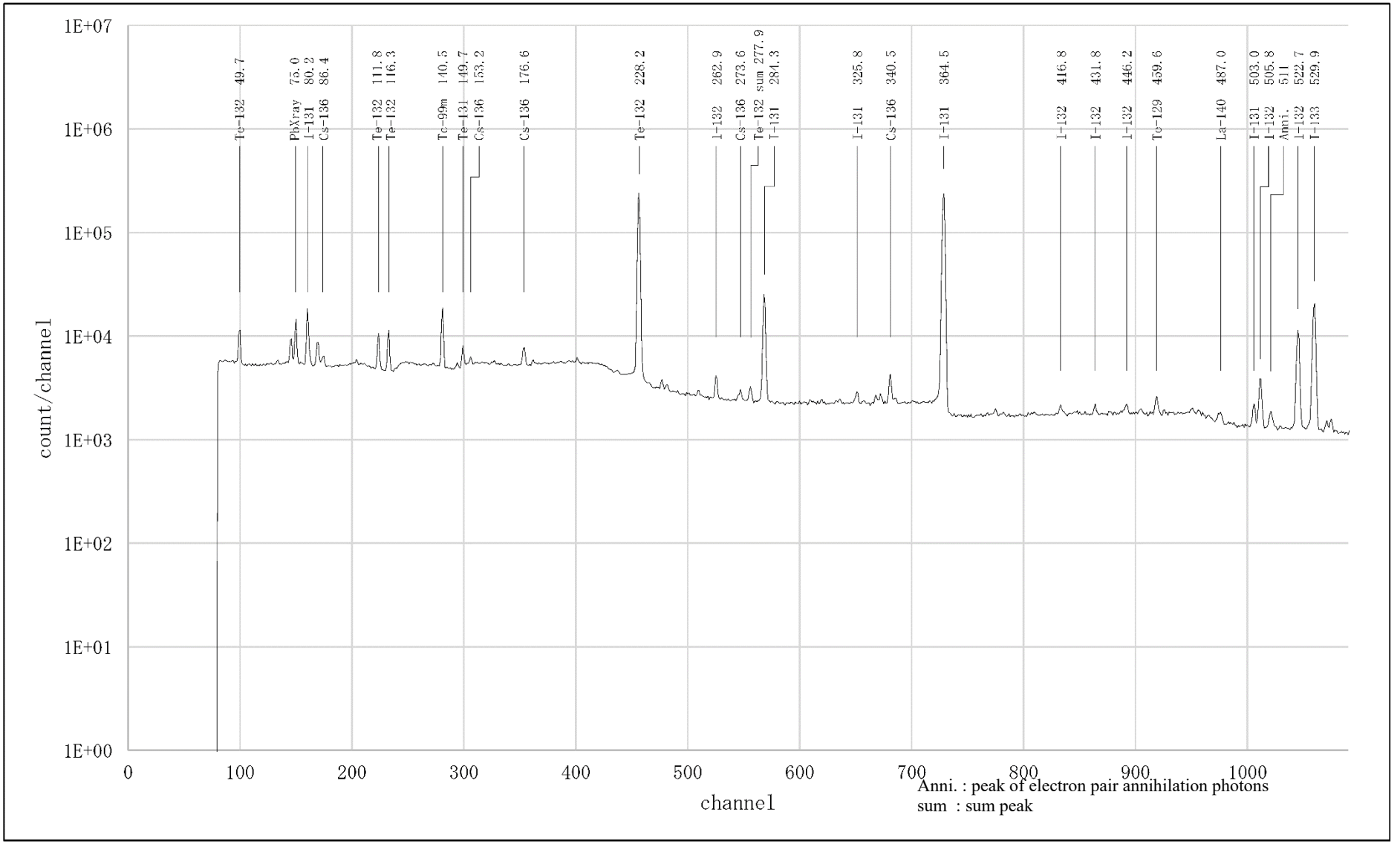

Fig. D4.11.1 Atmospheric floating dust related to the accident at the Fukushima Daiichi Nuclear Power Station (enlarged view of 1/4 part).

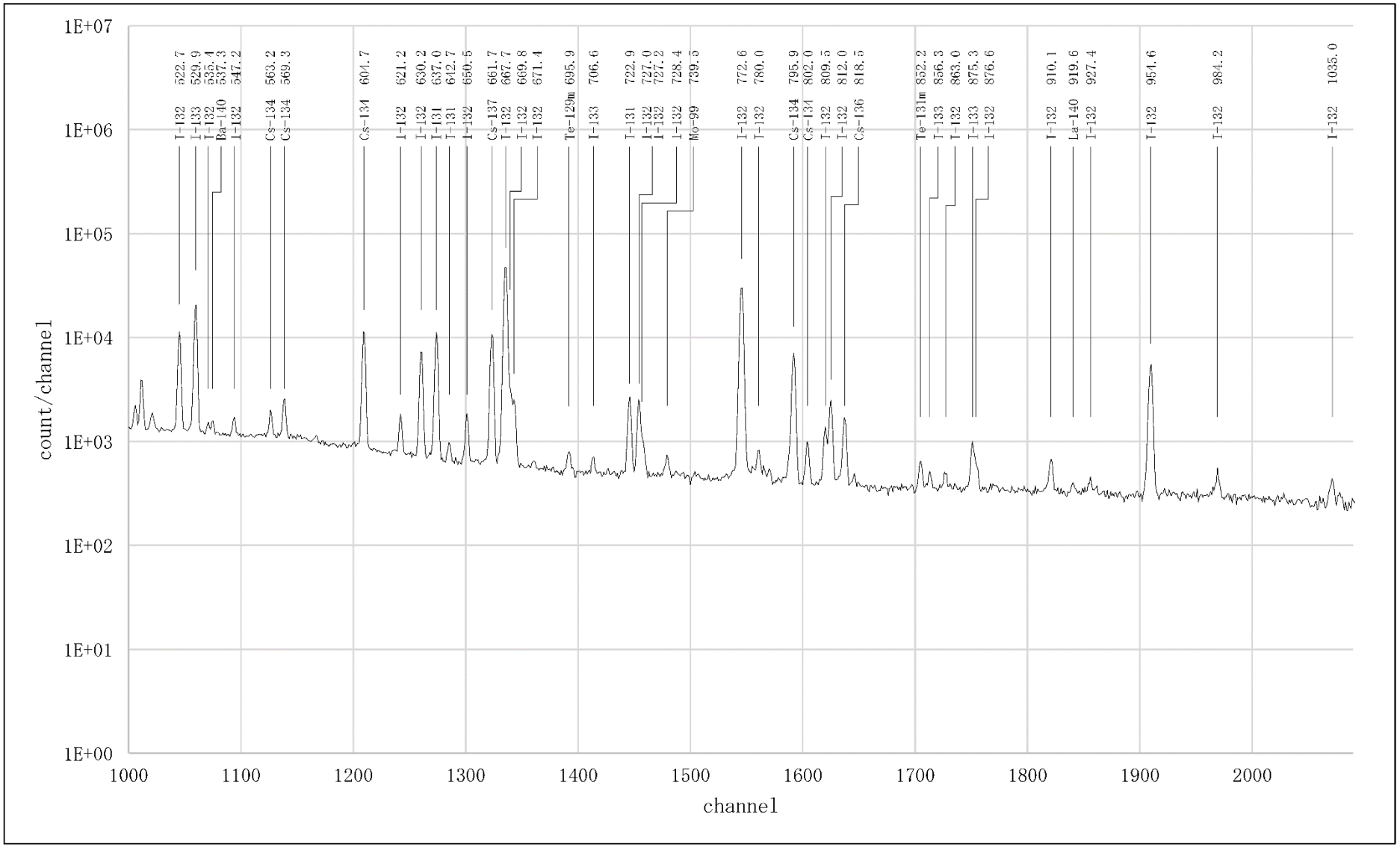

Fig. D4.11.2 Atmospheric floating dust related to the accident at the Fukushima Daiichi Nuclear Power Station (enlarged view of 2/4 part).

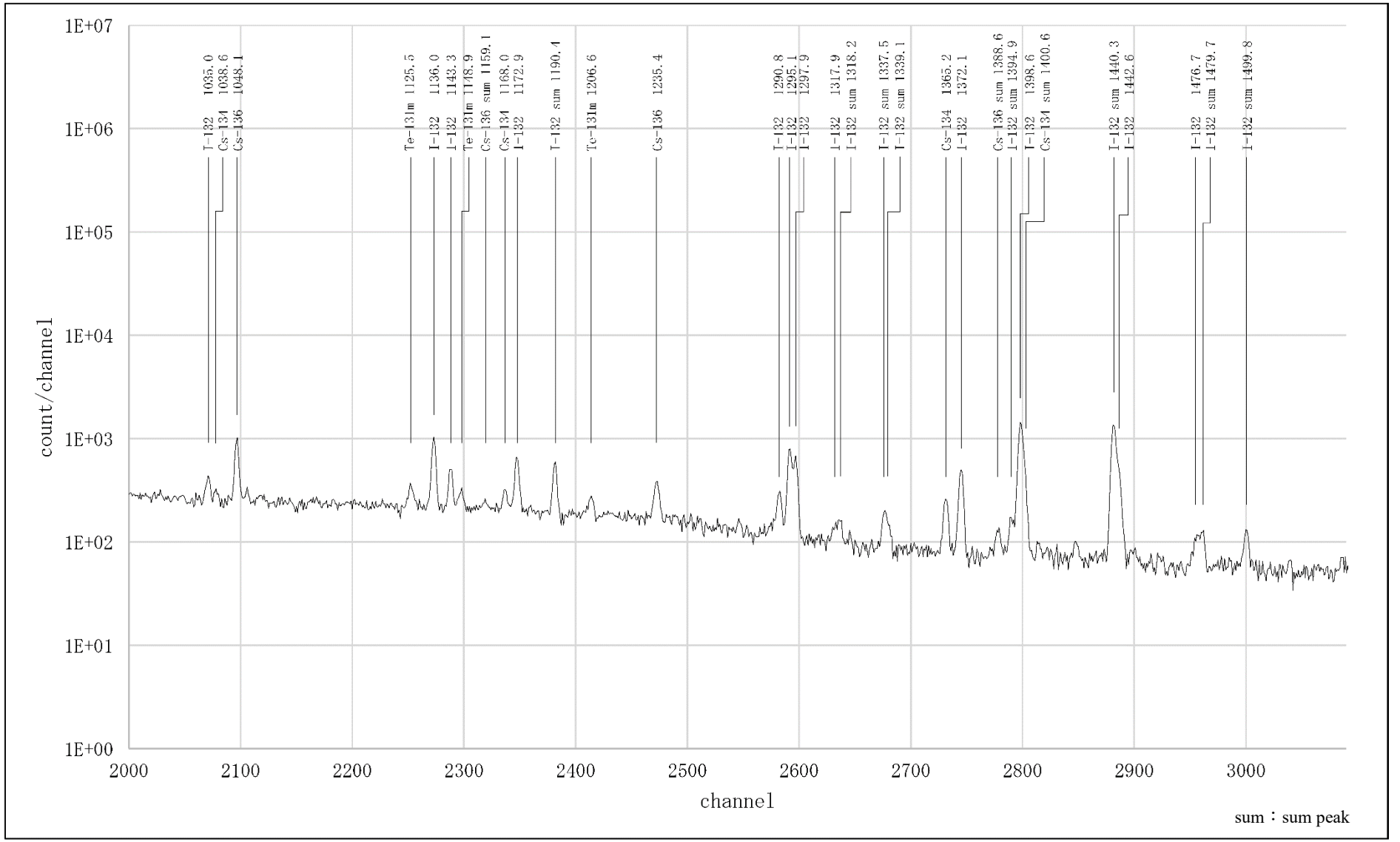

Fig. D4.11.3 Atmospheric floating dust related to the accident at the Fukushima Daiichi Nuclear Power Station (enlarged view of 3/4 part).

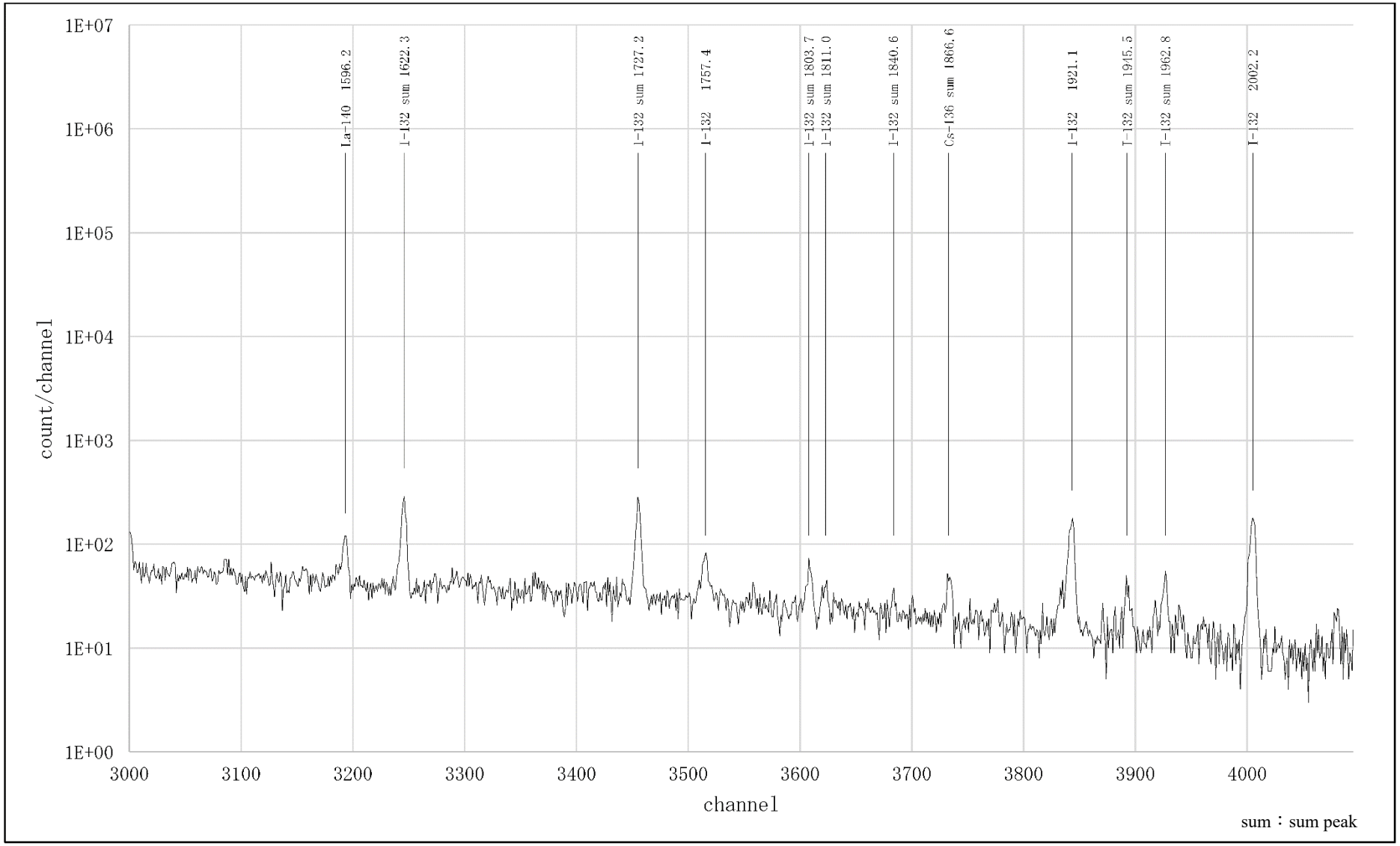

Fig. D4.11.4 Atmospheric floating dust related to the accident at the Fukushima Daiichi Nuclear Power Station (enlarged view of 4/4 part).

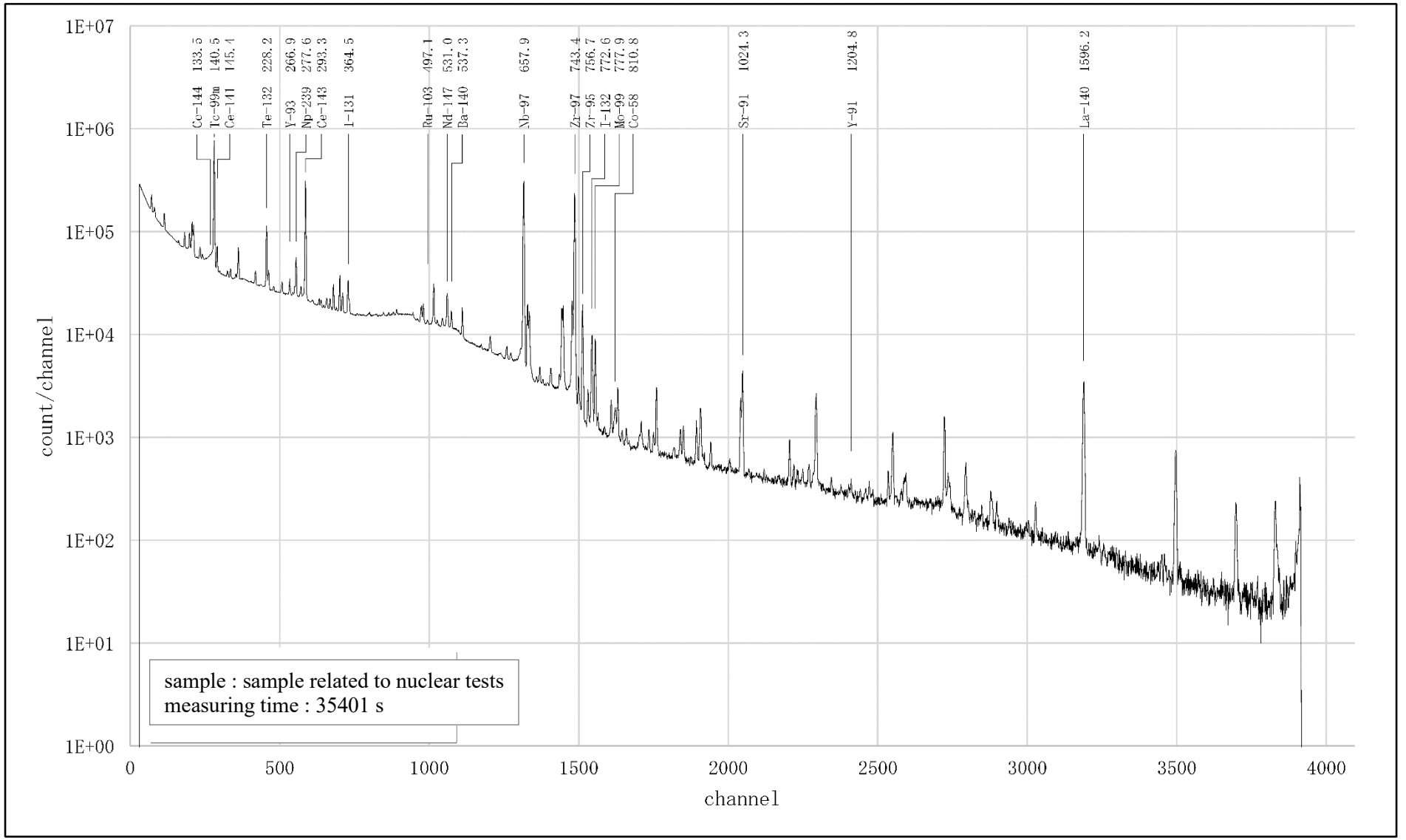

Fig. D4.12 Sample related to nuclear tests.

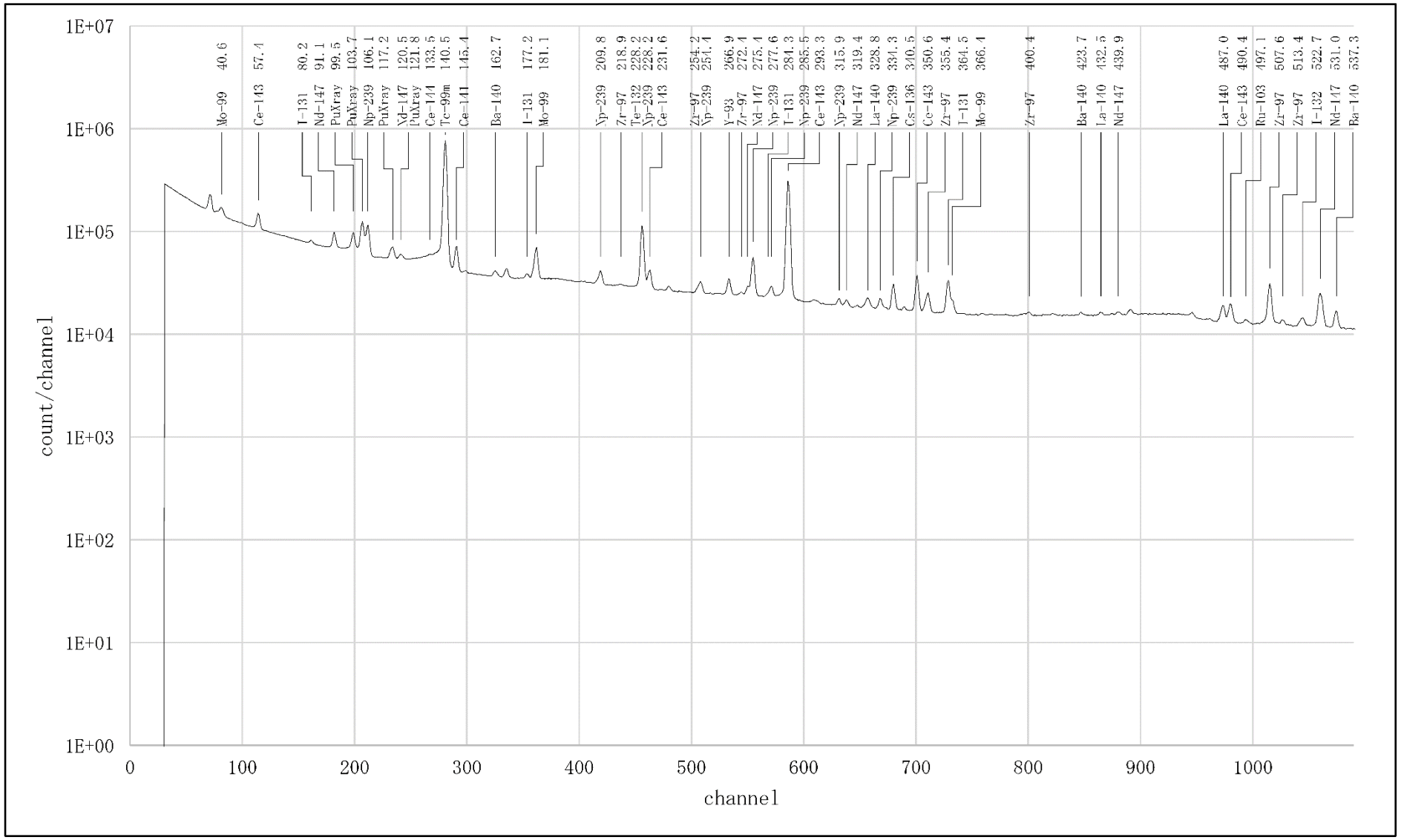

Fig. D4.12.1 Sample related to nuclear tests (enlarged view of 1/4 part).

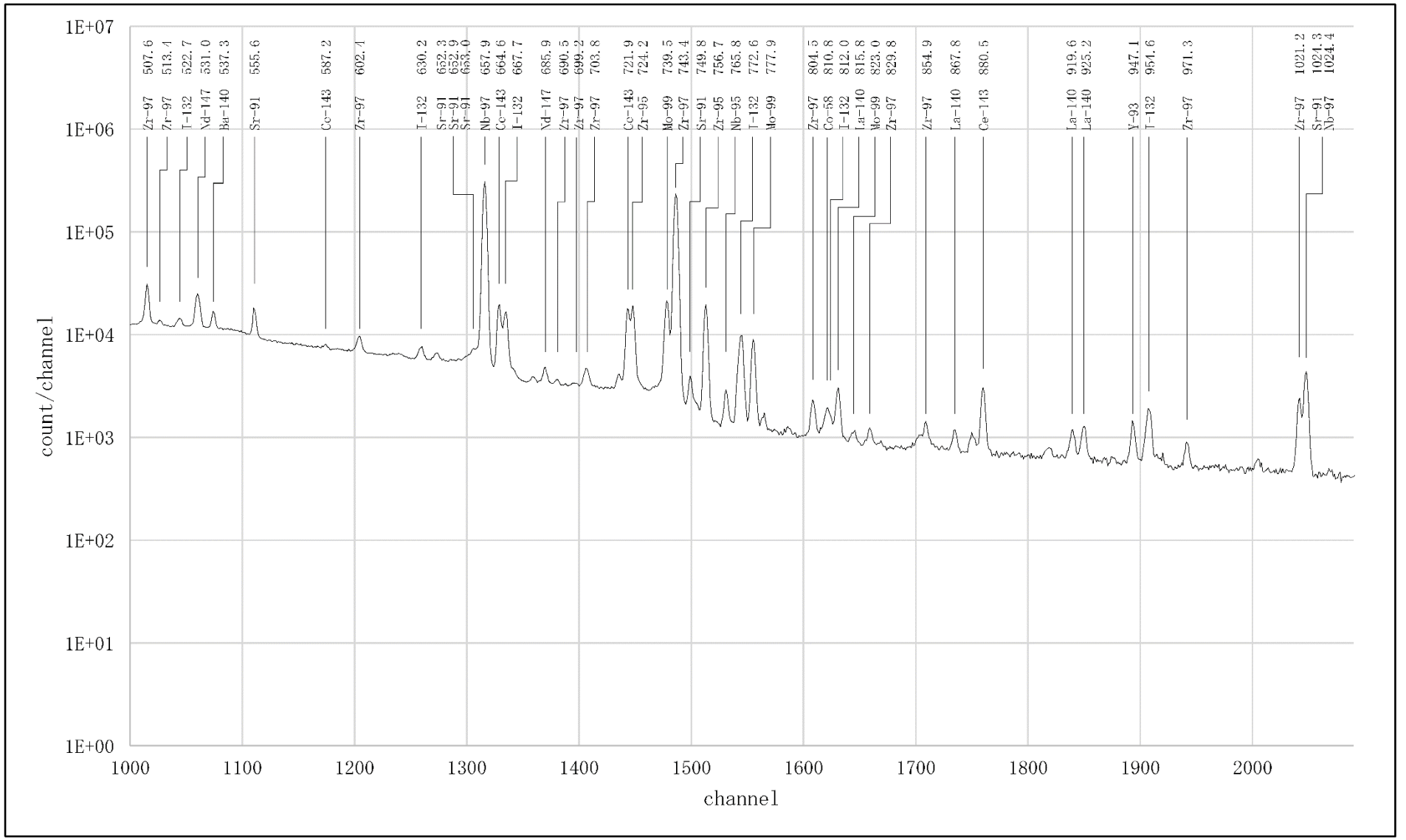

Fig. D4.12.2 Sample related to nuclear tests (enlarged view of 2/4 part).

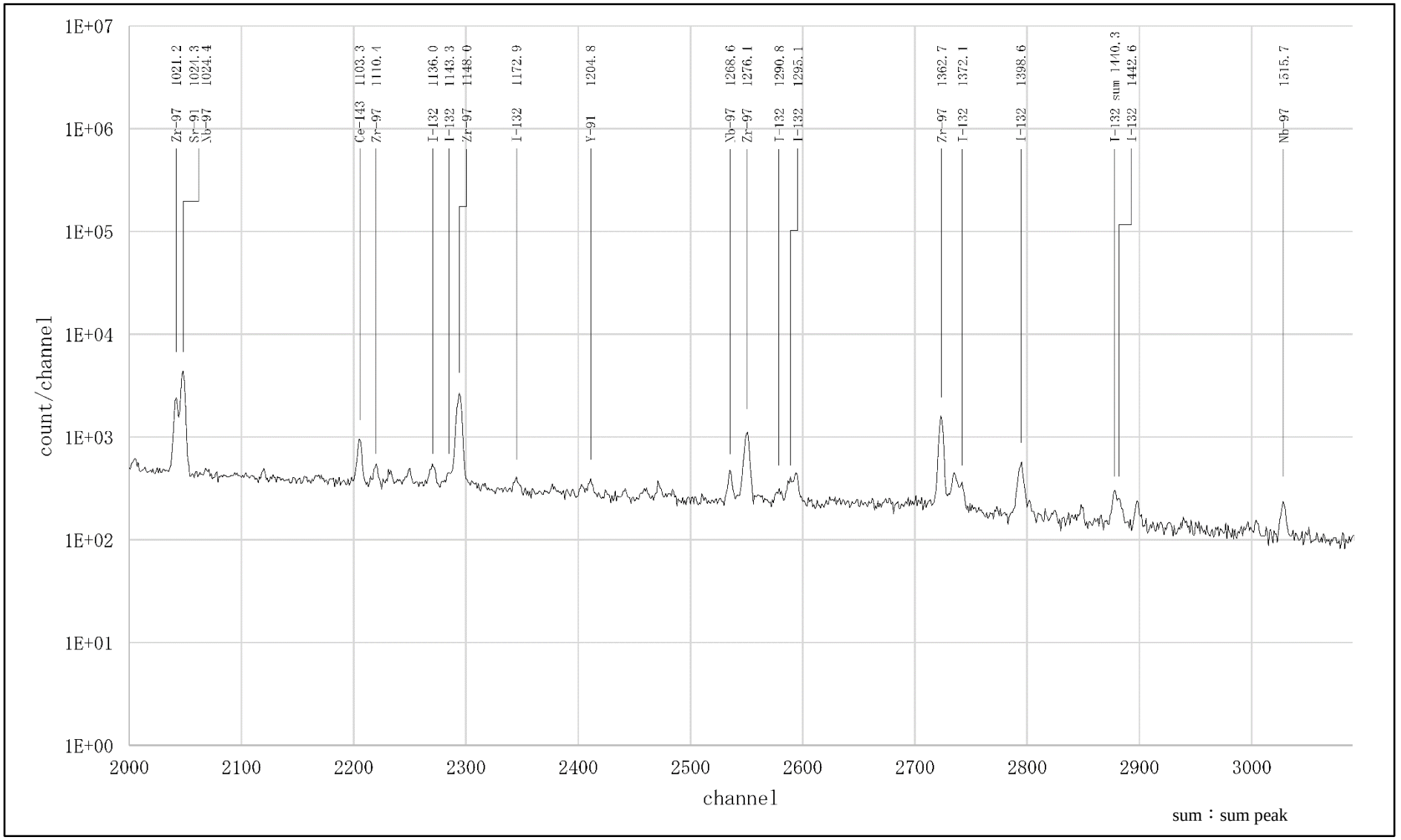

Fig. D4.12.3 Sample related to nuclear tests (enlarged view of 3/4 part).

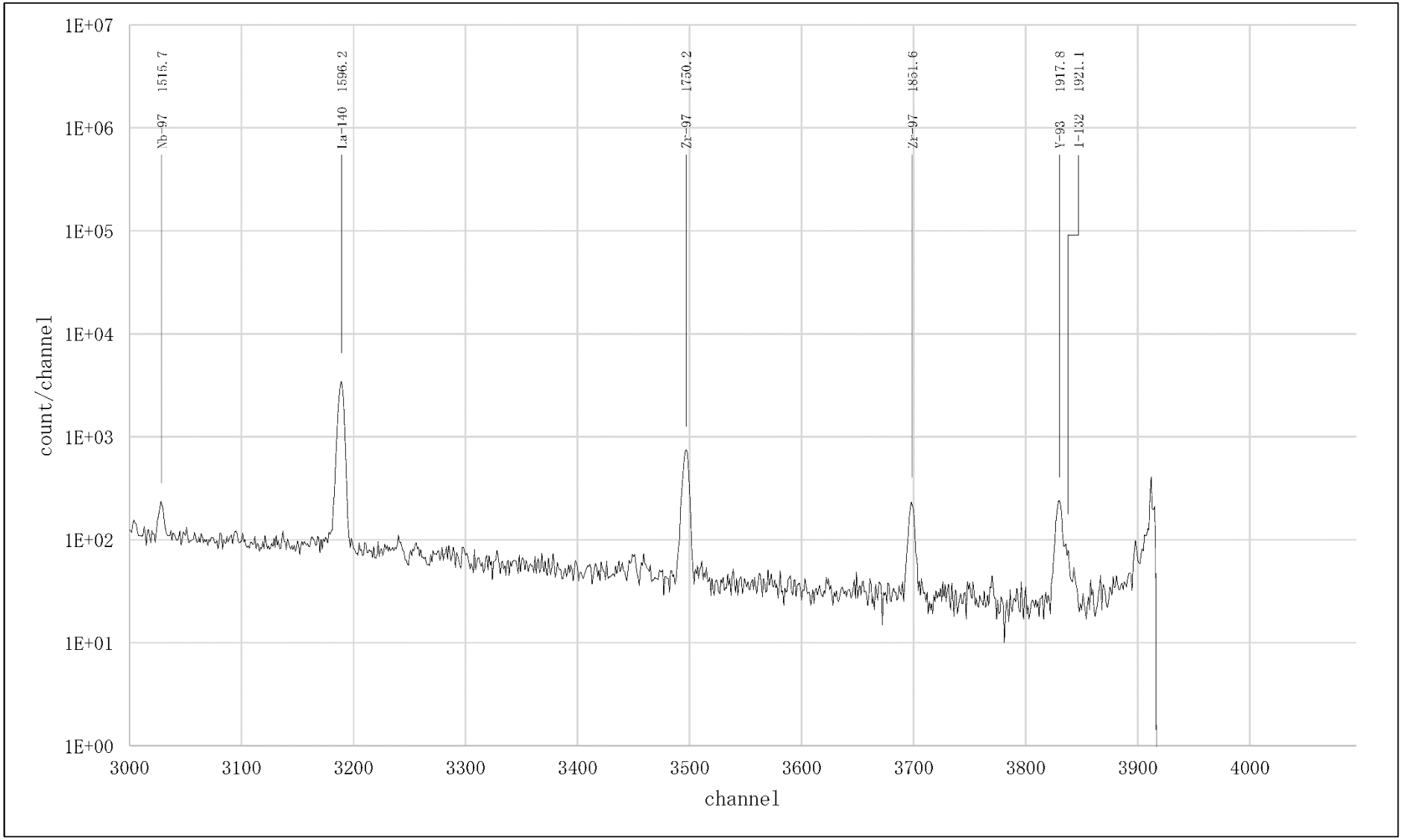

Fig. D4.12.4 Sample related to nuclear tests (enlarged view of 4/4 part)

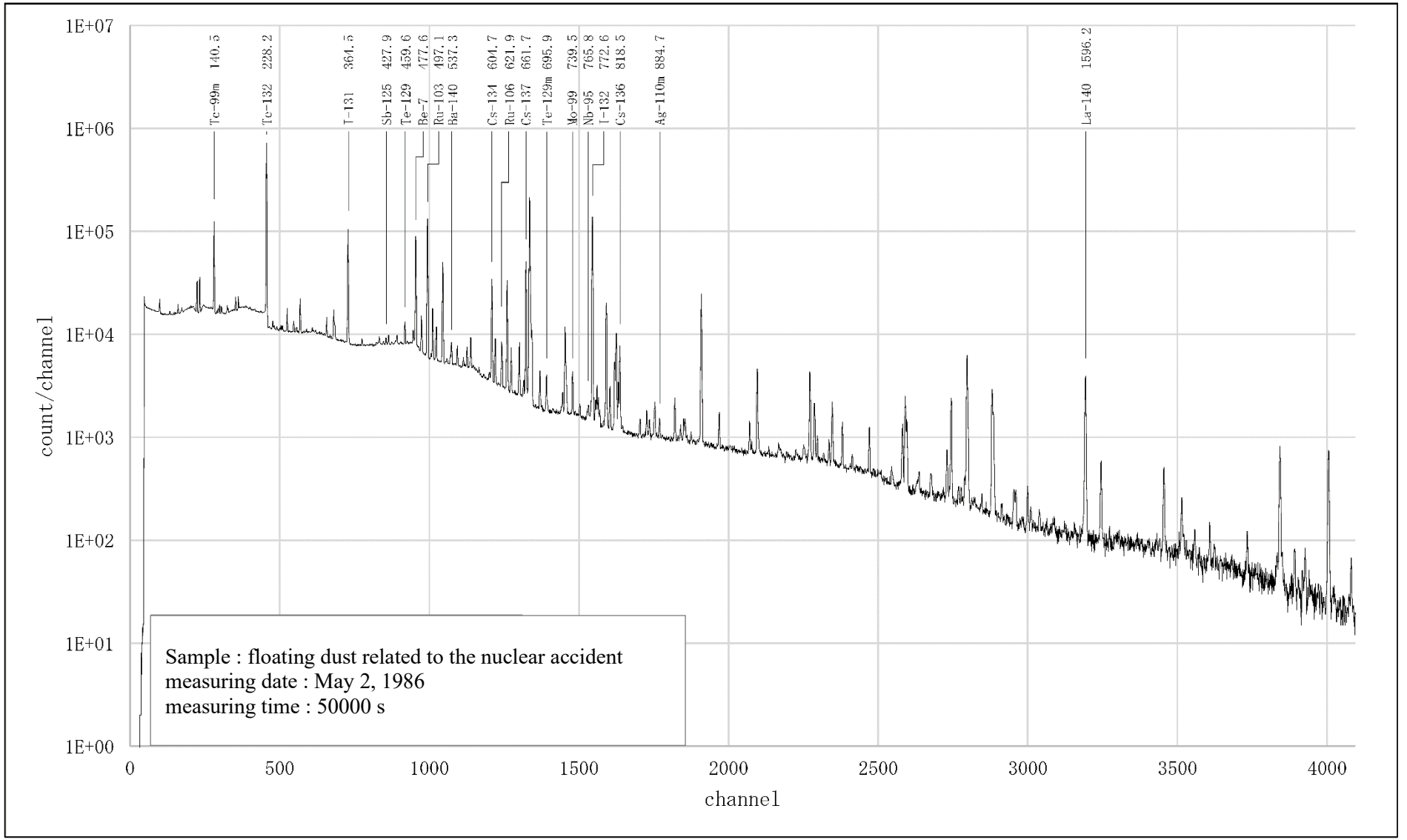

Fig. D4.13 Floating dust related to the nuclear accident.

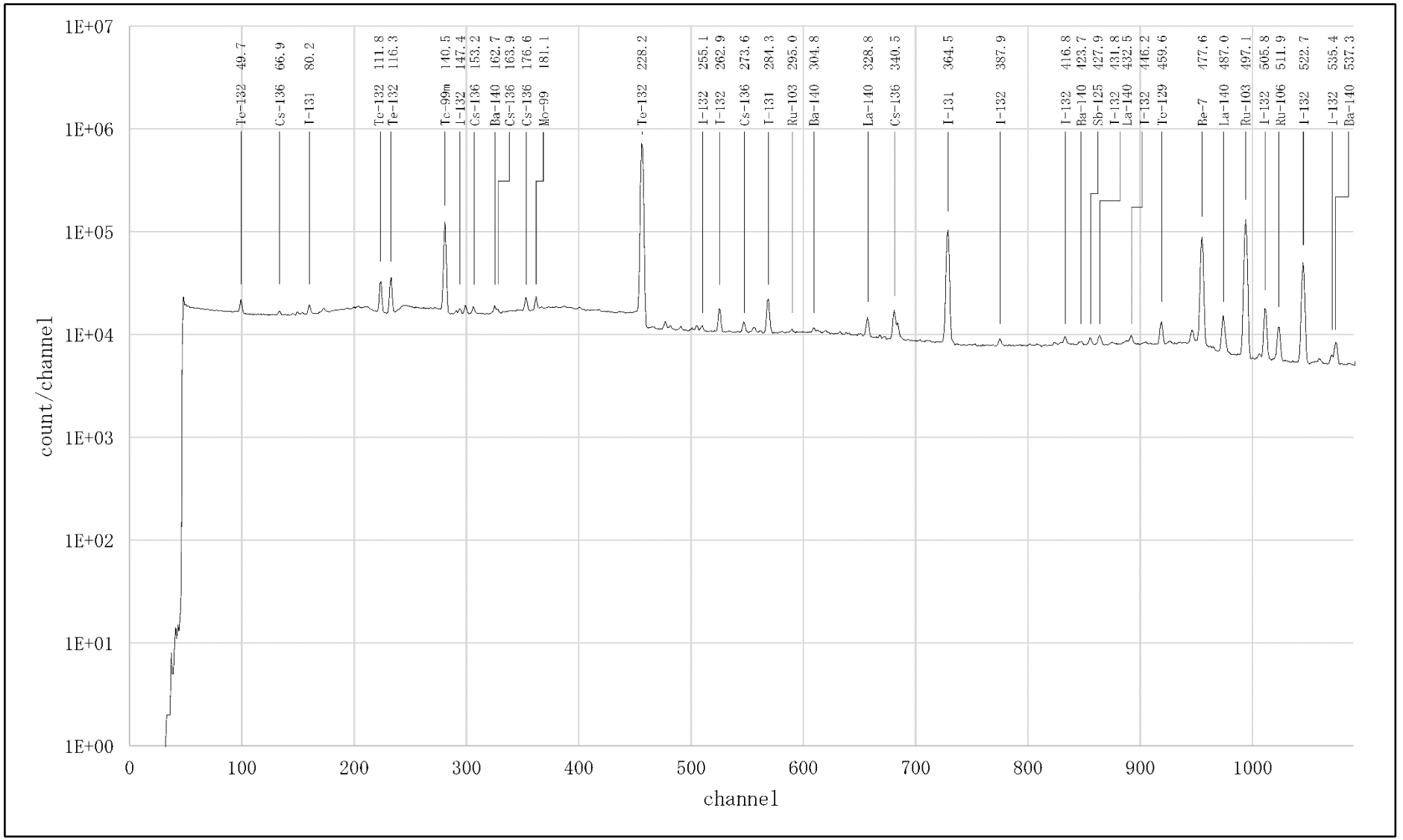

Fig. D4.13.1 Floating dust related to the nuclear accident (enlarged view of 1/4 part).

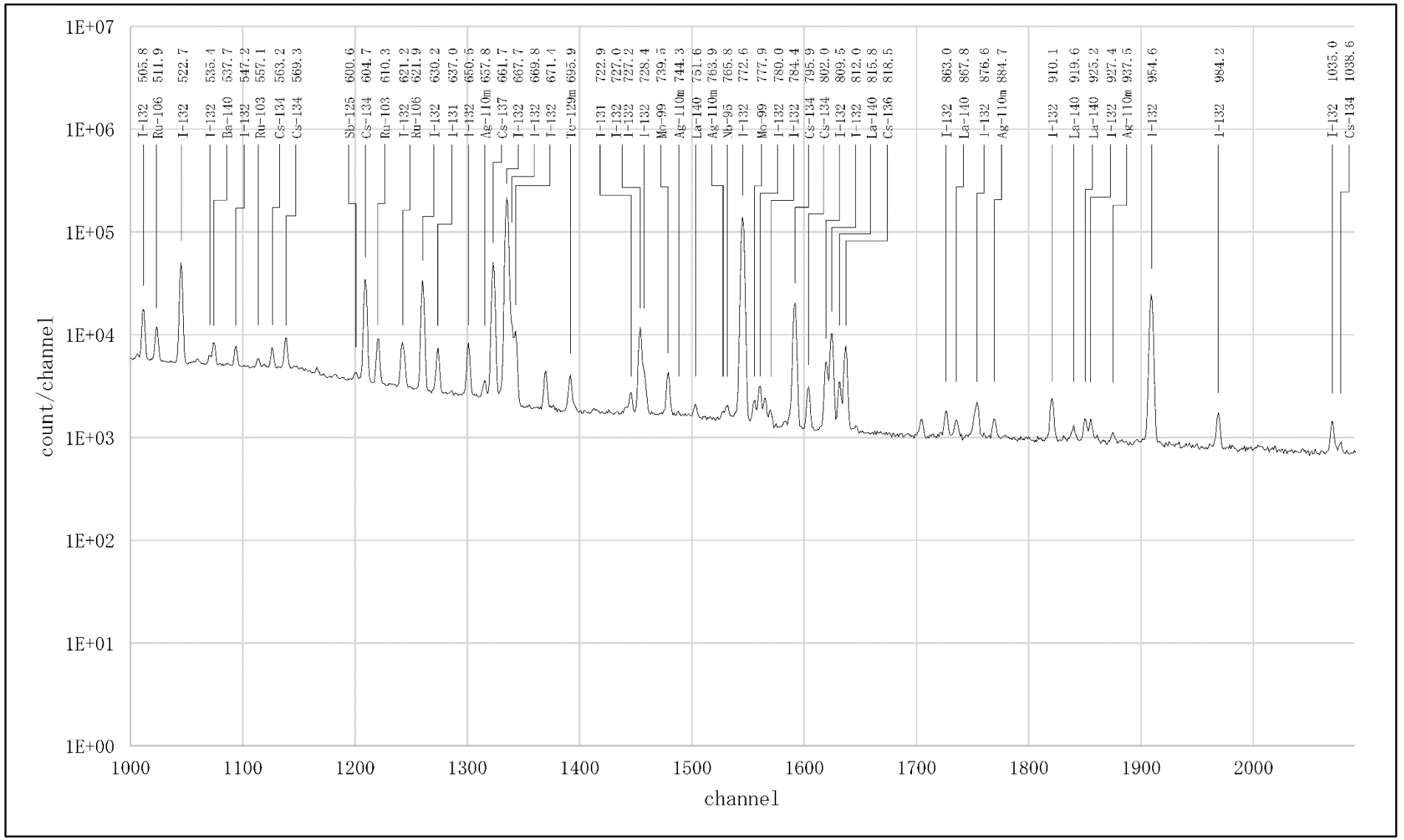

Fig. D4.13.2 Floating dust related to the nuclear accident (enlarged view of 2/4 part).

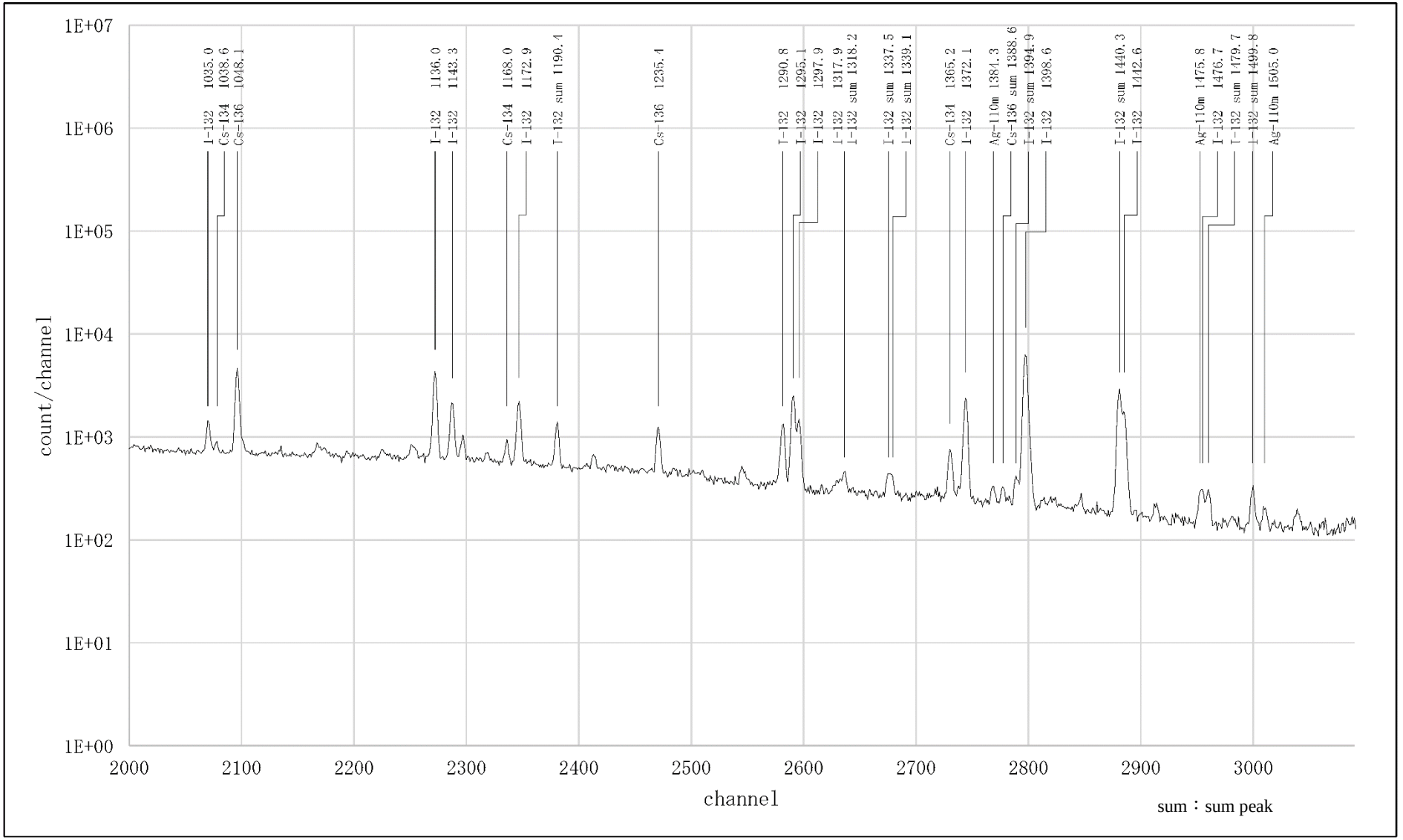

Fig. D4.13.3 Floating dust related to the nuclear accident (enlarged view of 3/4 part).

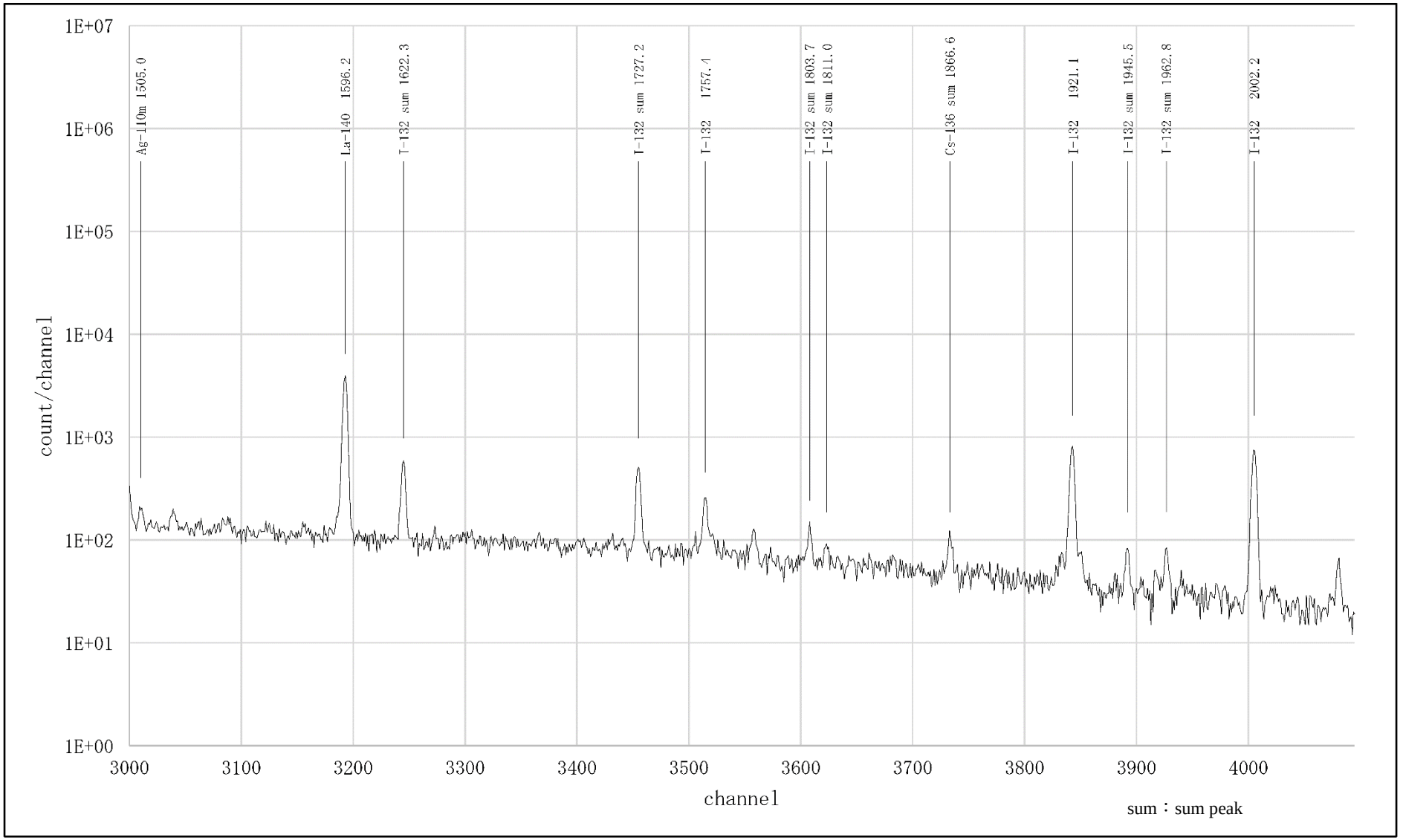

Fig. D4.13.4 Floating dust related to the nuclear accident (enlarged view of 4/4 part).

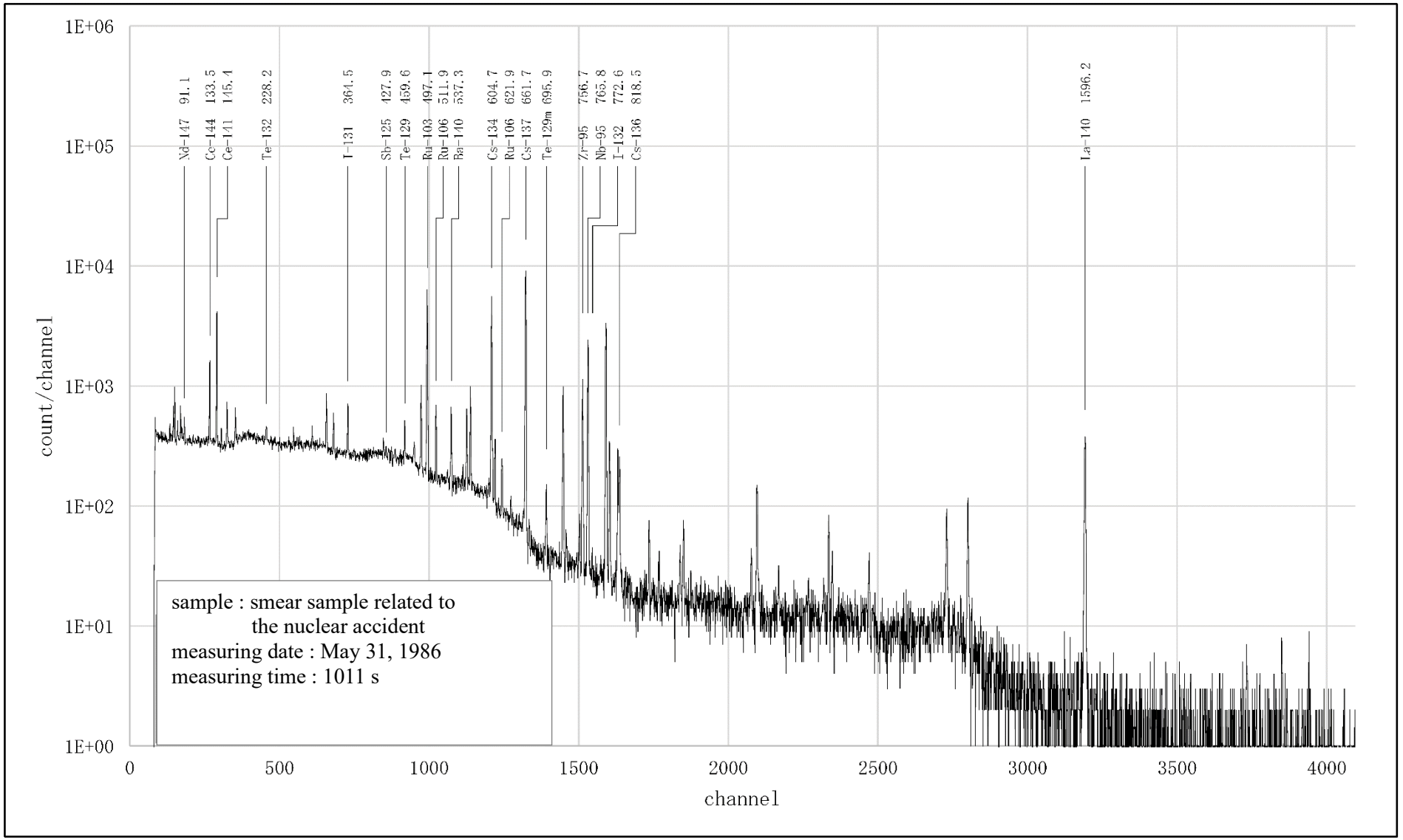

Fig. D4.14 Smear sample related to the nuclear accident.

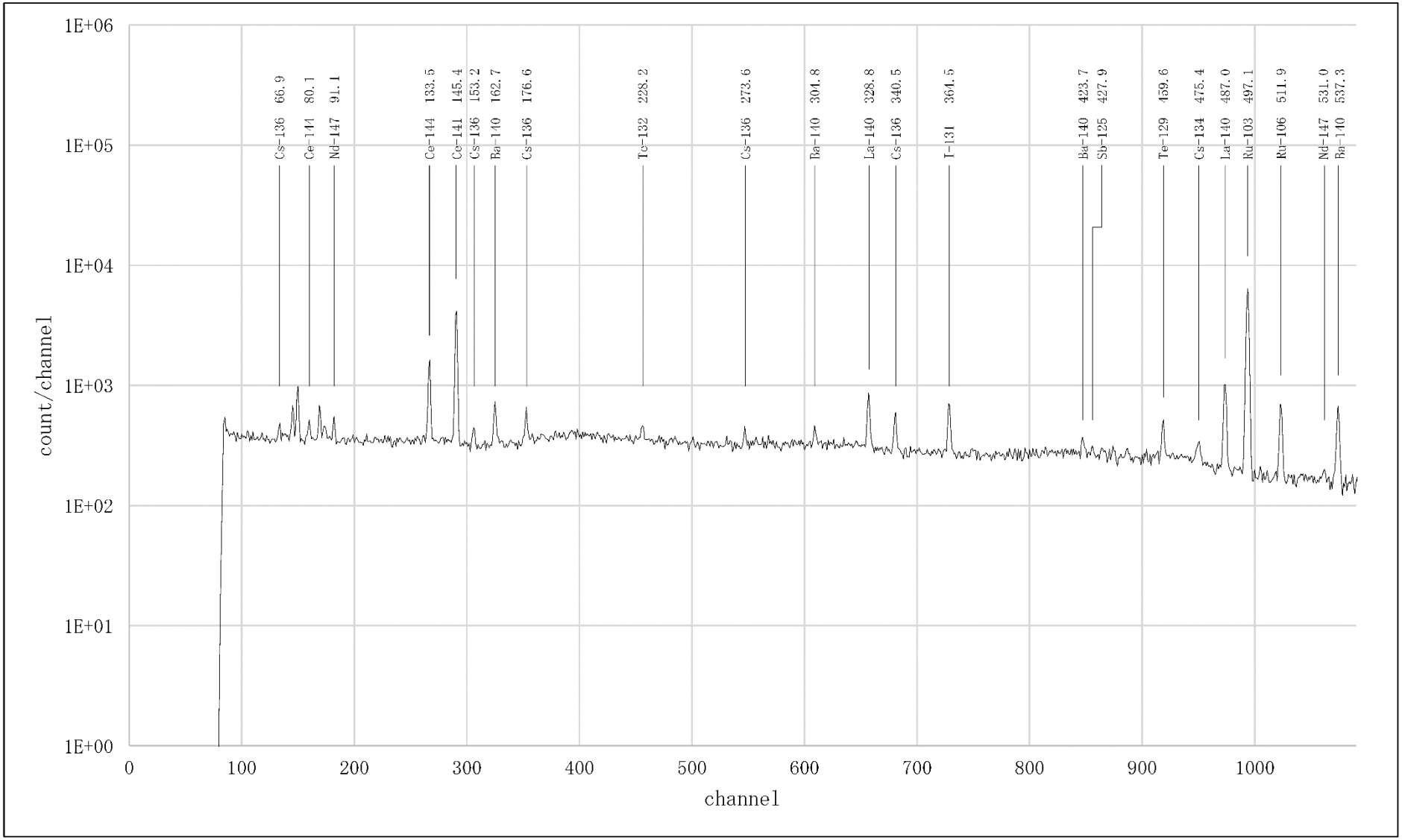

Fig. D4.14.1 Smear sample related to the nuclear accident (enlarged view of 1/4 part).

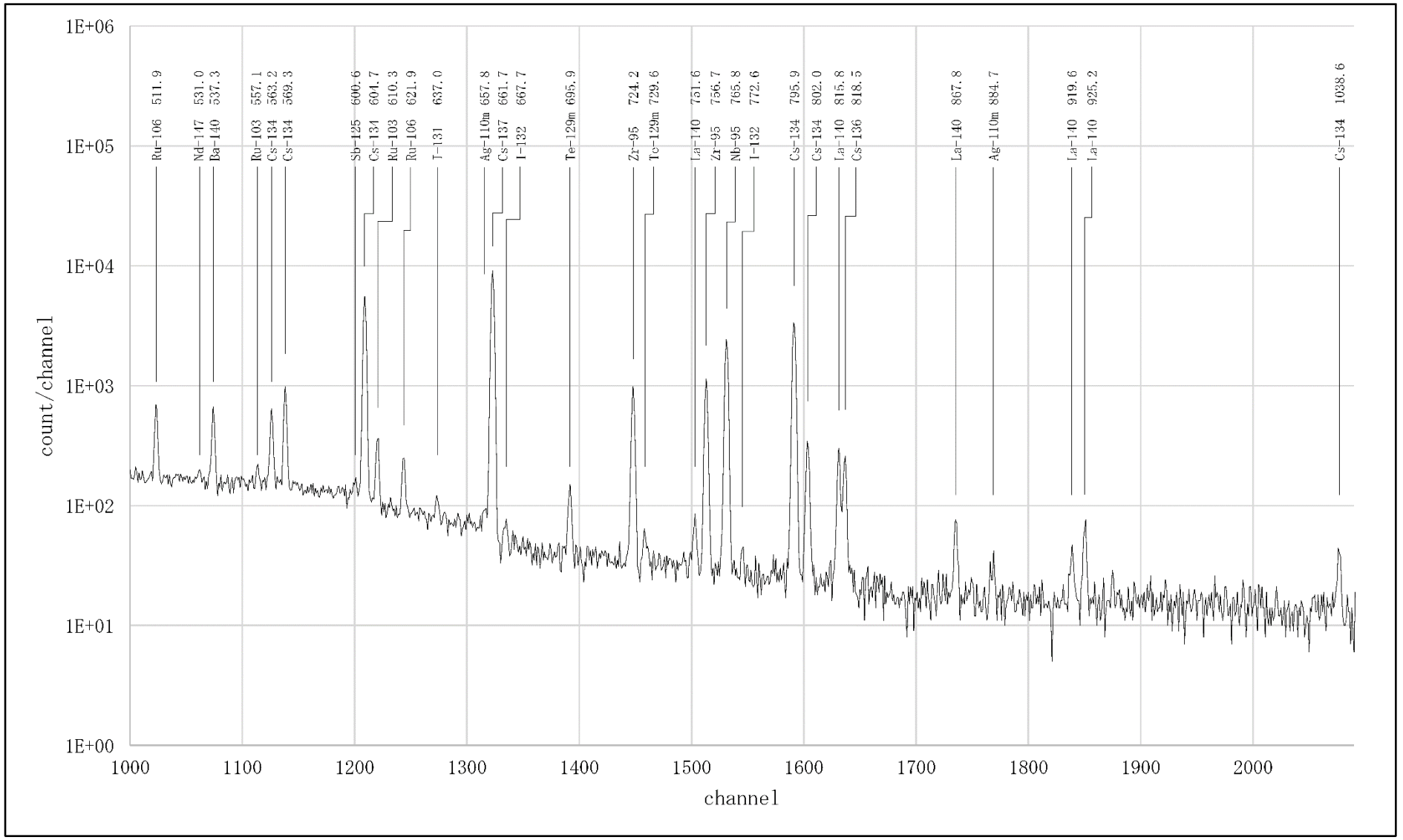

Fig. D4.14.2 Smear sample related to the nuclear accident (enlarged view of 2/4 part).

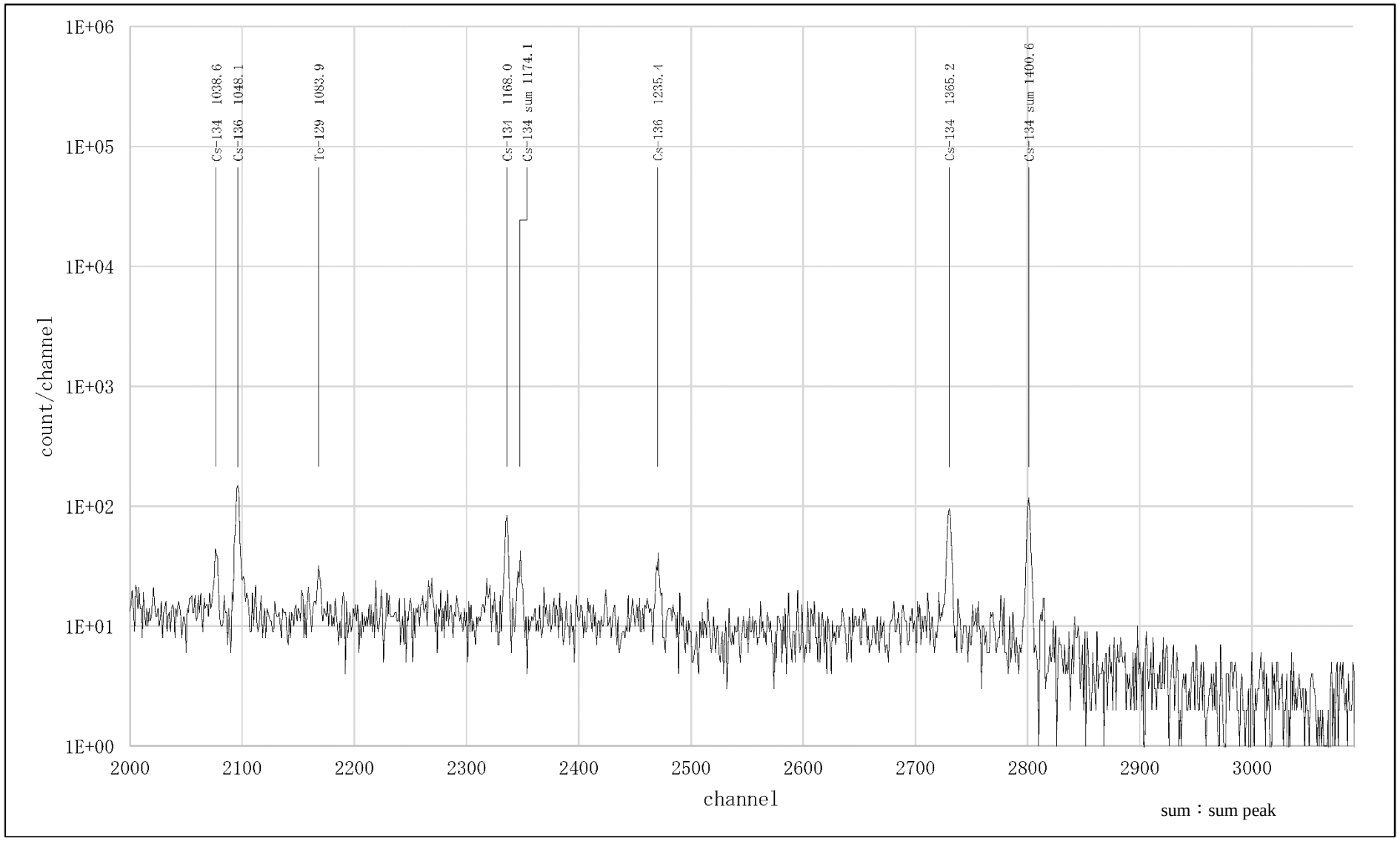

Fig. D4.14.3 Smear sample related to the nuclear accident (enlarged view of 3/4 part).

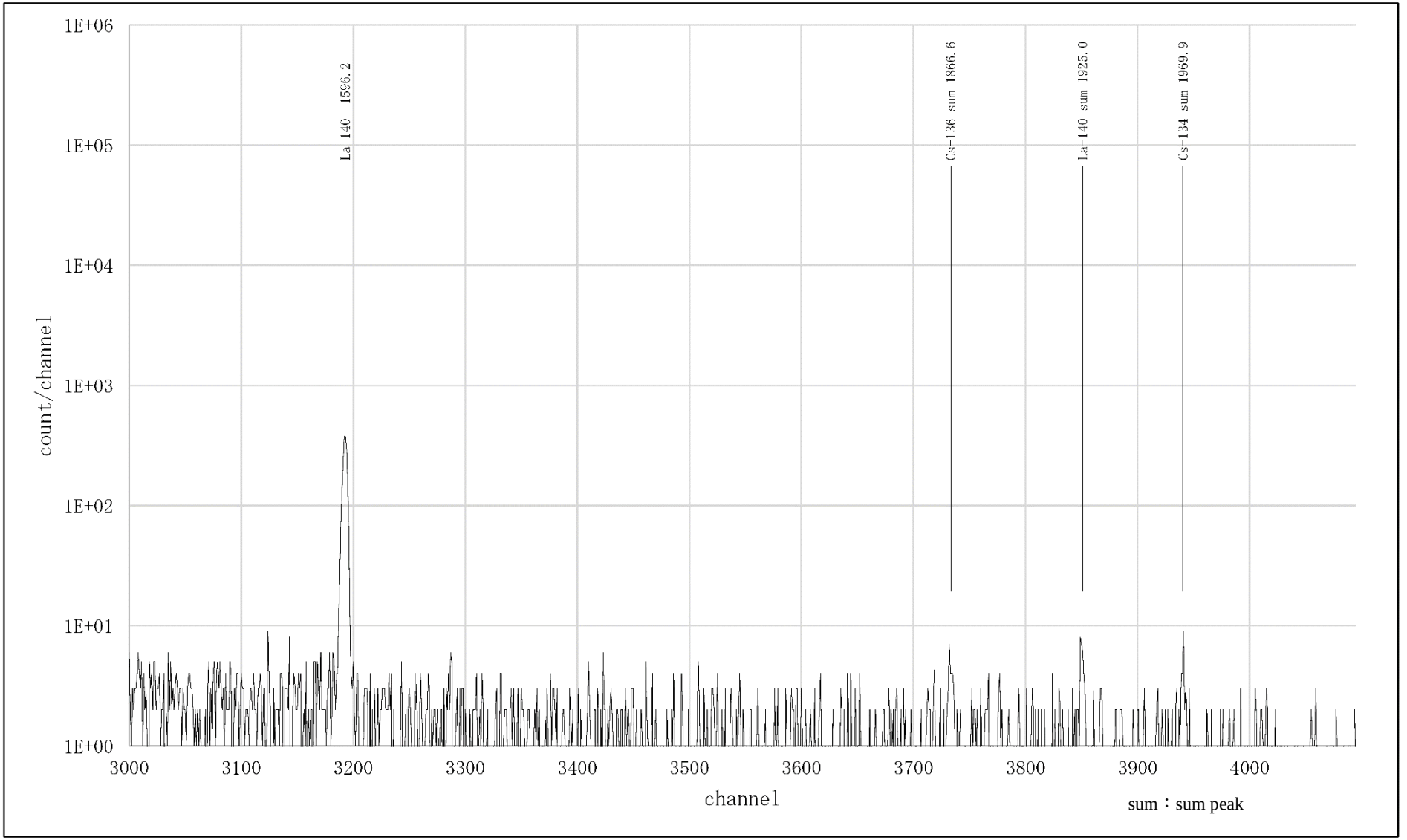

Fig. D4.14.4 Smear sample related to the nuclear accident (enlarged view of 4/4 part).

Document 5 Nuclear data table

Identify one reliable nuclear data collection, and extract the nuclear data on the selected nuclide from the data collection. It will become easy to reconstruct the extracted nuclear data by managing them in the database and electronic files. For the analytical program, select the artificial and natural radioactive nuclides based on the monitoring plan, etc., by the institute to which they belong, and register (or make library files) them. Hereafter, the database, where the data extracted from the nuclear data collection are managed, is called "master nuclear data library." The nuclear data registered (the library files made) in the analytical program and used for the analysis, are called "analytical nuclear data library." To prepare the library for the analysis at the emergency time, please refer to "γ -ray Spectral Analysis Using Germanium Detector in Emergencies" (No.29).

Document 5.1 Acquisition of nuclear data

In this section, the method to acquire the nuclear data on nuclides will be described by letting the basic nuclear data collection be the ENSDF (Evaluated Nuclear Structure Data File) (August, 2019).

Document 5.1.1 Acquisition of basic nuclear data collection

The ENSDF is a nuclear data collection that has been compiled as an electronic file. It can be used freely without the copyright permission of the NNDC (National Nuclear Data Center) that manages the ENSDF. The electronic files of the ENSDF can be obtained from the NNDC through the internet (http://www.nndc.bnl.gov). The file is compiled in multiple files for each mass number.

ENSDF_191004_099.ZIP (Nuclear data for the mass number of 99 or less are compiled.)
ENSDF_191004_199.ZIP (Nuclear data for the mass number from 100 to 199 are compiled.)
ENSDF_191004_300.ZIP (Nuclear data for the mass number from 200 to 300 are compiled.)
※As of November 2019.

The above compilations are files per multiple mass numbers summarized in the ZIP format as one file. Using an expanding (unzipping) program corresponding to the ZIP format, after uncompressing the file, it can be used. For example, when ENSDF_191004_199.ZIP is expanded (unzipped), the files ensdf.100,…, and ensdf.181,… are created. For the nuclide of 181 mass number, refer to the file ensdf.181. It should be noted that the mass number described here is related to the descendent nuclide after the targeted nuclide decay. Furthermore, it is possible to search for each nuclide and obtain the nuclear data on the web page.

Document 5.2 Extraction of nuclear data from nuclear data collection for each nuclide

To extract data on each nuclide from the ENSDF, it is convenient to use the RADLIST, a program for the ENSDF distributed on the NNDS homepage. Although in the ENSDF, data are described according to a special format, the RADLIST makes the text file, in which the special format of ENSDF is converted to the table format. Extract the nuclear data for the targeted nuclides from the text file, converted using the RADLST for each mass number, and register them in the master nuclear data library.

Document 5.3 Creation of nuclear data library for the analysis

In the nuclear data library for the analysis, register the nuclides to be monitored[*1], such as ^{60}Co, ^{131}I, ^{134}Cs, and ^{137}Cs, and ^{7}Be, ^{40}K, and natural radioactive nuclides in uranium and thorium series. In the γ-ray spectrometry of the environmental samples, acquired using a germanium semiconductor detector, in most cases, the artificial radioactive nuclides that are the monitoring targets cannot be not detected, except the ^{137}Cs. It is difficult to evaluate the measurement results only based on the result in which the nuclides were not detected. Therefore, let the measurement results for natural radioactive nuclides be one of the evaluation items. Further, a peak of natural radioactive nuclide detected in the background measurement must be corrected during the sample measurement (Document 1.8). For these reasons, in the nuclear data library for the analysis, it is necessary to register the natural radioactive nuclides that are possibly included in the samples and the natural radioactive nuclides detected in the background measurement. Furthermore, when adding a nuclide in the nuclear data library for the analysis, extract the data from the master nuclear data library, and add it in the library. The nuclear data library for the analysis, to which the new nuclear data have been added, should be stored separately from the previous one.

Document 5.4 Nuclear data table

Nuclear data extracted from Document 5.2 are shown in Tables D5.1–D5.4. Note that Tables D5.1–D5.4 are published according to the following:

(a) The nuclear data source is the ENSDF (as of August 2019).
(b) The half-life units Y, D, H, M, and S correspond to year, day, hour, minute, and second, respectively.
(c) For the power of 10, 1.248E + 9 represents 1.248×10^9.
(d) The value uncertainty in the table overlaps with the minimum digit of that value, as shown below:

Energy	Uncertainty of energy	Energy ± uncertainty
37.2	22	37.2 ± 2.2

Energy	Uncertainty of energy	Energy ± uncertainty
661.657	3	661.657 ± 0.003

Half-life	Uncertainty of half-life	Half-life ± uncertainty
1.248E + 9	3	$(1.248 \pm 0.003) \times 10^9$

Emission rate	Uncertainty of emission rate	Emission rate ± uncertainty
0.270	12	0.270±0.012

(e) In Table D5.1, γ-rays with the emission rate of 0.01% or higher are listed except for ^{206}Tl and ^{210}Po.

[*1]: ^{60}Co and ^{134}Cs are nuclides for which summing-effect correction is necessary. As the nuclide for which the summing-effect correction is performed in the analysis differs depending on the manufacturer of the analysis program, it is necessary to contact the manufacturer of the nuclide for which the used analysis program performs the summing-effect correction and to know it. Nuclides supported by the γ-ray spectra analytical programs in Japan are ^{22}Na, ^{46}Sc, ^{57}Co, ^{58}Co, ^{59}Fe, ^{60}Co, ^{88}Y, ^{133}Ba, ^{134}Cs, and ^{152}Eu.

(f) In Table D5.2, γ-rays with the emission rate of 0.1% or higher are listed with one digit after the decimal point except for ^{206}Tl and ^{210}Po.
(g) In Table D5.2, a letter (K) shown in ［Pb(Kα1)］, etc. represents the X-ray, and a letter s in ［^{132}I　s］, etc., represents the sum peak. In these peaks, only energy is shown.
(h) In Tables D5.1 and D5.2, a symbol ※ such as in ［※^{75}Ge］ in the tables represents the radioactive nuclide originating from the detector and the radiation shield.
(i) In Tables D5.1 and D5.2, a symbol † such as in ［†^{228}Ac］ in the tables represents the natural radioactive nuclide.
(j) Tables D5.3 and D5.4 show the nuclear data of nuclides used for the calibration.

Note that it should be careful about the following points:

Note 1 As ^{106}Ru (half-life: 371.8 D) is a pure γ-ray emitting nuclide (β^-, 100%), γ-ray of ^{106}Rh is registered in the nuclear data library for the analysis, assuming that the radiation equilibrium is established.

Note 2 γ-rays with the same energy emitted from a single nuclide are those generated from the different energy transitions.

Table D5.1 Nuclear data for each nuclide.

Nuclide name	Half-life	Uncertainty of half-life	Half-life unit	γ -ray energy (keV)	Uncertainty of γ-ray energy(keV)	Emission rate (%)	Uncertainty of emission rate(%)
† ^{7}Be	53.22	6	D	477.6035	20	10.44	4
† ^{40}K	1.248E+9	3	Y	1460.820	5	10.66	17
^{51}Cr	27.704	3	D	320.0824	4	9.910	10
^{54}Mn	312.20	20	D	834.848	3	99.9760	10
⁎^{56}Mn	2.5789	1	H	846.7639	19	98.85	3
				1037.8334	24	0.040	5
				1238.2738	22	0.040	4
				1810.726	4	26.9	4
^{58}Co	70.86	6	D	810.7594	20	99.450	10
				863.951	6	0.686	10
				1674.725	7	0.517	10
^{59}Fe	44.490	9	D	142.6510	20	1.02	5
				192.343	5	3.08	12
				334.80	20	0.270	12
				382.0	4	0.018	3
				1099.245	3	56.5	19
				1291.590	6	43.2	14
				1481.70	20	0.059	7
^{60}Co	1925.28	14	D	1173.228	3	99.85	3
				1332.492	4	99.9826	6
⁎^{63}Zn	38.47	5	M	365.2	4	0.0115	25
				443.13	20	0.016	5
				449.93	5	0.236	19
				515.0	10	0.021	9
				584.82	15	0.033	5
				624.3	3	0.014	4
				669.62	5	8.2	3
				675.0	6	0.015	4
				742.25	10	0.067	9
				899.0	4	0.012	3
				962.06	4	6.5	4
				1123.72	7	0.111	13
				1130.7	3	0.013	3
				1149.50	16	0.019	3
				1208.8	3	0.012	3
				1327.03	8	0.069	5
				1374.47	13	0.034	3
				1389.66	8	0.043	6
				1392.55	8	0.097	16
				1412.08	5	0.75	5
				1547.04	6	0.122	7
				1573.71	20	0.0164	18
				1861.3	3	0.0139	21
				1866.1	3	0.020	3
^{65}Zn	243.93	9	D	1115.5391	20	50.04	10
⁎^{74}Ga	8.12	12	M	233.2	5	0.16	3
				258.8	5	0.11	3
				302.0	7	0.11	4
				365.0	7	0.09	3
				444.2	5	0.06	3
				471.1	5	0.39	5
				484.9	3	1.06	6
				492.99	6	5.0	3
				497.56	15	0.96	10
				504.7	5	0.10	3
				521.0	5	0.12	3
				540.9	5	0.16	3
				545.5	5	0.064	19

Nuclide name	Half-life	Uncertainty of half-life	Half-life unit	γ-ray energy (keV)	Uncertainty of γ-ray energy(keV)	Emission rate (%)	Uncertainty of emission rate(%)
*^{74}Ga	8.12	12	M	551.8	5	0.11	3
				595.87	4	91.80	20
				604.21	10	2.85	19
				608.40	5	14.4	8
				639.00	10	0.83	5
				652.5	5	0.06	3
				701.52	10	0.77	11
				715.0	3	0.22	4
				733.9	4	0.110	19
				784.30	20	0.67	7
				809.3	3	0.29	7
				867.83	6	8.7	6
				886.71	15	0.34	8
				942.47	7	1.27	6
				960.99	7	1.62	7
				975.1	3	0.27	3
				993.55	10	0.64	4
				999.90	20	0.13	13
				999.90	20	0.13	13
				1024.3	5	0.07	7
				1024.3	5	0.14	3
				1101.32	6	5.42	19
				1131.52	14	0.87	6
				1134.5	3	0.19	20
				1134.5	3	0.19	20
				1160.33	10	0.63	5
				1177.42	18	0.24	3
				1184.40	20	0.28	3
				1204.22	4	7.62	19
				1293.9	5	0.25	4
				1312.84	11	0.62	9
				1332.1	3	1.74	10
				1337.18	10	0.8	8
				1337.18	10	0.8	8
				1357.90	20	0.16	16
				1417.6	7	0.110	10
				1443.38	7	1.8	19
				1443.38	7	1.8	19
				1471.70	20	0.193	19
				1478.2	3	0.30	3
				1489.37	7	2.88	6
				1510.2	3	0.23	3
				1570.34	10	0.97	4
				1601.97	20	0.29	3
				1617.2	3	0.129	19
				1630.7	10	0.09	8
				1676.77	14	0.73	4
				1744.90	20	4.82	10
				1806.5	3	0.28	5
				1829.75	16	1.90	5
				1940.63	7	5.4	3
				1971.0	4	0.20	5
				1999.30	20	0.40	4
*^{74}As	17.77	2	D	595.83	8	59	4
				608.43	8	0.552	21
				634.78	8	15.4	11
				635.0	20	0.0357	21
				887.00	10	0.0255	15
				993.46	8	0.0184	19
				1204.35	8	0.285	20

Nuclide name	Half-life	Uncertainty of half-life	Half-life unit	γ-ray energy (keV)	Uncertainty of γ-ray energy(keV)	Emission rate (%)	Uncertainty of emission rate(%)
*^{75}Ge	82.78	4		66.00	20	0.114	13
				198.60	10	1.19	12
				264.60	10	11.4	11
				353.0	5	0.021	3
				419.10	20	0.185	19
				468.80	20	0.223	24
				617.70	20	0.114	13
*^{75m}Ge	47.7	5	S	61.92	10	0.0119	24
				136.01	8	0.020	6
				139.68	3	39.5	4
^{85}Kr	10.739	14	Y	513.997	5	0.434	10
^{86}Rb	18.642	18	D	1077.0	4	8.64	4
^{91}Sr	9.65	6	H	118.50	20	0.074	5
				261.20	20	0.449	17
				272.6	6	0.26	4
				274.70	20	1.04	5
				359.10	10	0.050	4
				379.90	10	0.147	6
				393.00	10	0.050	4
				486.50	20	0.080	5
				506.70	10	0.044	4
				520.8	3	0.034	4
				533.90	10	0.077	5
				593.10	10	0.094	5
				620.10	10	1.78	7
				626.80	10	0.044	4
				631.30	10	0.556	21
				652.3	3	2.98	20
				652.90	20	8.0	5
				653.0	20	0.37	14
				660.90	10	0.101	5
				749.80	10	23.7	8
				761.40	10	0.576	22
				793.60	10	0.064	4
				820.80	20	0.161	7
				823.70	10	0.067	4
				879.70	10	0.188	7
				892.90	10	0.070	4
				901.30	20	0.094	5
				925.80	20	3.85	13
				973.90	10	0.040	4
				992.20	10	0.044	4
				1024.30	10	33.5	11
				1054.60	10	0.224	8
				1140.80	10	0.127	6
				1280.9	5	0.93	4
				1305.30	10	0.017	4
				1327.40	10	0.040	4
				1353.50	20	0.023	4
				1413.40	10	0.98	4
				1473.80	10	0.168	7
				1486.40	10	0.013	4
				1545.90	10	0.067	4
				1553.6	3	0.017	4
				1626.8	3	0.013	4
				1651.4	5	0.291	11
				1724.0	5	0.161	7
^{91}Y	58.51	6	D	1204.80	13	0.26	4
^{93}Y	10.18	8	H	266.90	10	7.4	12
				273.0	10	0.072	19
				287.0	10	0.076	16
				341.5	5	0.045	7

Nuclide name	Half-life	Uncertainty of half-life	Half-life unit	γ-ray energy (keV)	Uncertainty of γ-ray energy(keV)	Emission rate (%)	Uncertainty of emission rate(%)
^{93}Y	10.18	8	H	680.20	10	0.67	10
				714.40	20	0.017	4
				947.10	10	2.1	4
				962.30	20	0.0122	24
				987.7	3	0.011	3
				1158.50	20	0.030	6
				1168.61	20	0.011	5
				1183.50	10	0.049	9
				1184.7	6	0.020	5
				1203.30	10	0.109	17
				1237.40	10	0.030	8
				1425.40	10	0.25	4
				1450.50	10	0.33	5
				1470.10	10	0.066	16
				1642.70	10	0.052	9
				1651.70	20	0.024	5
				1827.80	20	0.024	5
				1917.80	10	1.57	23
^{95}Zr	64.032	6	D	235.690	20	0.270	20
				724.192	4	44.27	22
				756.725	12	54.38	22
^{95}Nb	34.991	6	D	204.1161	17	0.028	9
				561.9		0.015	3
				765.803	6	99.808	7
^{97}Zr	16.749	8	H	111.6	3	0.065	10
				182.9	5	0.032	7
				202.5	6	0.029	9
				218.90	20	0.168	19
				254.17	14	1.15	8
				272.40	16	0.23	3
				294.8	4	0.08	3
				297.2	3	0.066	12
				305.1	9	0.028	19
				330.43	19	0.143	15
				355.40	9	2.09	10
				400.42	16	0.245	16
				410.0	10	0.07	5
				473.5	6	0.07	4
				507.64	8	5.03	19
				513.41	18	0.55	5
				558.0	10	0.028	19
				600.6	6	0.09	10
				602.37	14	1.38	8
				690.52	16	0.183	18
				699.2	3	0.101	20
				703.76	5	1.01	5
				707.4	6	0.032	17
				743.36	3	93.09	16
				772	3	0.24	13
				775.0	8	0.1862	4
				804.52	9	0.61	8
				805.6	8	0.2793	5
				829.79	9	0.239	18
				854.89	8	0.357	23
				971.34	15	0.278	17
				1018.1	8	0.3724	7
				1021.2	3	1.01	17
				1026.7	8	0.2793	5
				1110.44	19	0.093	19
				1147.97	8	2.62	11

Nuclide name	Half-life	Uncertainty of half-life	Half-life unit	γ-ray energy (keV)	Uncertainty of γ-ray energy(keV)	Emission rate (%)	Uncertainty of emission rate(%)
^{97}Zr	16.749	8	H	1276.07	9	0.94	6
				1361.0	8	0.6516	12
				1362.68	9	1.02	11
				1750.24	22	1.09	11
				1851.61	9	0.31	3
^{97}Nb	72.1	7	M	178.0	3	0.049	10
				238.4	3	0.049	10
				549.25	20	0.049	10
				657.94	9	98.23	8
				719.53	19	0.090	9
				857.46	21	0.045	7
				909.55	14	0.040	7
				1024.4	3	1.09	7
				1117.02	18	0.085	8
				1148.6	3	0.049	10
				1268.62	10	0.147	20
				1515.66	19	0.122	13
				1629.09	22	0.025	7
^{99}Mo	65.924	6	H	40.58324	17	1.04	4
				158.782	15	0.0176	8
				162.370	15	0.0120	7
				181.068	8	6.05	12
				366.421	15	1.200	25
				380.13	8	0.0105	9
				411.491	15	0.0150	8
				528.788	15	0.0532	20
				620.03	4	0.0279	14
				621.771	24	0.018	4
				739.500	17	12.20	16
				777.921	20	4.31	9
				822.972	15	0.134	3
				960.754	20	0.095	3
^{99m}Tc	6.0072	9	H	140.5110	10	89	4
				142.63	3	0.0222	20
^{103}Ru	39.247	3	D	39.760	10	0.0692	12
				53.286	10	0.443	11
				241.875	10	0.0143	3
				294.964	10	0.288	4
				443.810	10	0.339	5
				497.085	10	91.0	13
				557.057	10	0.841	11
				610.333	10	5.76	7
				612.09	6	0.105	6
^{106}Rh	30.07	35	S	428.40	20	0.071	3
				434.25	21	0.0202	21
				439.2	3	0.0126	21
				511.861	4	20.4	4
				616.22	9	0.75	9
				621.93	6	9.93	23
				680.25	14	0.0110	7
				715.90	20	0.0100	5
				873.49	5	0.439	11
				1045.6	6	0.0133	17
				1050.41	6	1.56	5
				1062.14	5	0.0320	8
				1114.48	5	0.0118	19
				1128.07	5	0.404	10
				1180.73	8	0.0145	4
				1194.54	5	0.0573	12
				1496.33	13	0.0222	8

Nuclide name	Half-life	Uncertainty of half-life	Half-life unit	γ-ray energy (keV)	Uncertainty of γ-ray energy(keV)	Emission rate (%)	Uncertainty of emission rate(%)
^{106}Rh	30.07	35		1562.25	6	0.163	4
				1766.25	5	0.0343	9
				1796.94	9	0.0277	7
				1927.22	9	0.0153	5
				1988.44	8	0.0261	7
^{108m}Ag	438	9	Y	79.131	3	6.6	5
				433.937	4	90.5	6
				614.276	4	89.8	19
				722.907	10	90.8	19
^{110m}Ag	249.83	4	D	120.23	3	0.0171	9
				133.333	7	0.0746	16
				219.348	8	0.073	5
				221.078	10	0.0685	10
				229.420	22	0.0120	14
				266.914	12	0.041	4
				365.448	11	0.094	5
				387.075	9	0.0525	9
				396.894	22	0.037	4
				446.812	3	3.70	5
				467.01	4	0.0252	19
				544.56	4	0.018	3
				572.70	10	0.0175	13
				573.0	4	0.0172	10
				603.08	20	0.011	8
				620.3553	17	2.73	8
				626.256	10	0.217	17
				630.62	5	0.033	5
				647.9	4	0.0177	5
				657.7601	11	95.61	10
				666.90	9	0.029	14
				676.59	7	0.143	10
				677.6218	12	10.70	5
				687.0092	18	6.53	3
				706.6761	15	16.69	7
				708.133	20	0.23	5
				744.2756	18	4.77	3
				763.9425	17	22.60	7
				818.0245	18	7.43	4
				884.6782	13	75.0	12
				937.485	3	35.0	3
				997.246	14	0.130	4
				1018.94	4	0.0142	7
				1085.447	14	0.073	4
				1117.48	3	0.0494	9
				1125.709	20	0.0308	14
				1163.19	5	0.075	23
				1164.98	7	0.044	3
				1251.06	4	0.027	3
				1300.07	7	0.0191	7
				1334.348	16	0.143	5
				1384.2932	20	25.1	5
				1420.29	10	0.027	4
				1475.7794	23	4.08	5
				1505.0282	20	13.33	16
				1562.2942	18	1.22	3
				1592.77	6	0.0209	8
				1783.49	3	0.0102	5
				1903.53	3	0.0162	7
^{113}Ag	5.37	5	H	17.70	20	0.042	5
				96.20	20	0.0370	20

Nuclide name	Half-life	Uncertainty of half-life	Half-life unit	γ-ray energy (keV)	Uncertainty of γ-ray energy(keV)	Emission rate (%)	Uncertainty of emission rate(%)
^{113}Ag	5.37	5	H	133.50	20	0.0660	20
				206.40	20	0.0200	20
				217.20	10	0.0280	20
				258.80	10	1.64	3
				298.60	10	10.00	
				316.30	10	1.343	20
				333.10	10	0.598	9
				339.40	10	0.638	10
				364.40	10	0.140	3
				369.0	10	0.010	5
				374.30	20	0.0250	20
				382.10	10	0.145	3
				392.40	10	0.0200	20
				410.80	10	0.0120	20
				584.00	10	0.21	3
				585.0	10	0.010	5
				611.0	5	0.045	10
				624.00	10	0.0190	10
				672.30	10	0.87	3
				672.30	10	0.030	10
				680.60	10	0.695	16
				734.0	10	0.010	5
				809.90	10	0.0150	20
				816.10	10	0.0110	20
				827.0	10	0.010	5
				878.50	10	0.0520	20
				883.60	10	0.282	7
				896.10	10	0.058	10
				988.40	10	0.423	9
				1049.90	10	0.045	3
				1084.50	10	0.016	3
				1126.10	10	0.061	3
				1180.80	10	0.037	3
				1194.60	10	0.378	10
				1479.20	10	0.068	4
^{113}Sn	115.09	3	D	255.134	10	2.11	8
				391.698	3	64.97	17
^{124}Sb	60.20	3	D	254.49	4	0.0161	10
				336.21	4	0.074	3
				371.00	11	0.038	5
				400.30	6	0.139	7
				444.09	3	0.1889	20
				469.06	7	0.050	3
				481.42	4	0.0237	19
				525.50	21	0.138	4
				530.45	3	0.0421	20
				572.06	6	0.0190	13
				602.7261	23	97.8	4
				632.489	19	0.1046	10
				645.8521	19	7.42	3
				662.42	3	0.029	4
				709.34	5	1.353	13
				713.776	4	2.276	18
				722.782	3	10.76	5
				735.7	7	0.056	6
				735.9	7	0.071	7
				766.32	4	0.01213	20
				790.706	7	0.739	6
				816.8	3	0.0729	18
				856.68	4	0.0238	10

Nuclide name	Half-life	Uncertainty of half-life	Half-life unit	γ-ray energy (keV)	Uncertainty of γ-ray energy(keV)	Emission rate (%)	Uncertainty of emission rate(%)
^{124}Sb	60.20	3	D	899.23	3	0.0172	14
				968.195	4	1.882	10
				976.62	5	0.0832	16
				1045.125	4	1.833	12
				1086.70	8	0.0378	18
				1263.45	7	0.0413	18
				1301.14	9	0.0343	10
				1325.504	4	1.580	15
				1355.20	5	1.038	13
				1368.157	5	2.624	14
				1376.090	9	0.483	5
				1385.33	4	0.063	3
				1436.554	7	1.217	9
				1445.11	4	0.330	4
				1488.887	24	0.672	6
				1526.317	24	0.409	5
				1565.7	5	0.014	3
				1579.82	5	0.38	5
				1622.4	4	0.0409	10
				1690.971	4	47.57	19
				1720.72	3	0.0951	17
				1918.74	6	0.0545	16
^{125}Sb	2.75856	25	Y	19.80	6	0.0204	10
				35.489	5	4.37	5
				58.43	5	0.012	6
				116.955	11	0.263	4
				172.719	8	0.191	8
				176.3140	20	6.84	7
				178.842	5	0.0337	24
				198.654	11	0.0128	6
				204.138	10	0.317	7
				208.077	5	0.248	5
				209.32	9	0.045	3
				227.891	10	0.1311	23
				321.04	4	0.416	5
				380.452	8	1.517	17
				408.065	10	0.184	3
				427.874	4	29.6	3
				443.555	9	0.306	4
				463.365	4	10.49	11
				600.5970	20	17.65	19
				606.713	3	4.98	6
				635.950	3	11.22	15
				671.441	6	1.791	19
^{127}Sb	3.85	5	D	61.10	10	1.44	14
				154.3	5	0.15	8
				252.4	3	8.5	6
				280.4	5	0.66	16
				290.8	5	2.02	16
				293.3	9	0.29	15
				310.0	7	0.26	12
				391.8	5	0.96	9
				412.1	5	3.8	5
				441.0	9	0.7	4
				445.1	5	4.3	3
				451.0	7	0.18	8
				456.0	10	0.11	8
				473.0	4	25.8	16
				502.8	6	0.8	3
				543.3	5	2.9	5

Nuclide name	Half-life	Uncertainty of half-life	Half-life unit	γ-ray energy (keV)	Uncertainty of γ-ray energy(keV)	Emission rate (%)	Uncertainty of emission rate(%)
^{127}Sb	3.85	5	D	584.2	11	0.33	19
				603.5	5	4.5	3
				624.0	10	0.066	23
				637.8	5	0.44	15
				652.3	9	0.37	8
				667.5	9	0.74	9
				682.3	10	0.6	3
				685.7	5	36.8	20
				698.5	5	3.64	22
				722.2	5	1.88	15
				745.9	5	0.15	8
				763.7	8	0.07	4
				783.7	5	15.1	9
				817.0	6	0.40	19
				820.6	6	0.22	12
				924.4	9	0.52	8
				1141.6	8	0.37	8
				1155.2	10	0.040	23
				1290.3	8	0.37	12
				1377.9	9	0.07	4
^{127}Te	9.35	7	H	57.63	8	0.030	5
				202.90	10	0.058	7
				215.10	10	0.039	5
				360.30	10	0.135	14
				417.90	10	0.99	14
^{129}Te	69.6	3	M	27.81	5	16.3	20
				208.96	5	0.180	13
				250.62	5	0.38	3
				278.43	5	0.57	4
				281.26	5	0.165	12
				342.88	5	0.049	4
				459.60	5	7.7	6
				487.39	5	1.42	11
				531.83	5	0.088	7
				624.34	5	0.097	7
				740.96	5	0.037	3
				802.10	5	0.192	14
				804.60	13	0.022	3
				833.28	5	0.045	4
				982.27	5	0.0160	12
				1083.85	5	0.49	4
				1111.64	5	0.191	15
				1260.63	5	0.0112	9
^{129m}Te	33.6	1	D	27.81	5	0.027	6
				105.50	5	0.14	4
				556.65	5	0.118	24
				671.84	5	0.025	5
				695.88	6	3.0	6
				701.7	3	0.025	5
				729.57	5	0.70	14
				740.96	5	0.027	6
				817.04	5	0.091	18
				844.81	5	0.034	7
				1022.43	5	0.017	4
				1050.21	5	0.018	4
^{130}I	12.36	1	H	158.80	18	0.020	7
				227.55	16	0.012	5
				246.306	22	0.047	5
				280.09	11	0.024	7
				302.49	6	0.013	5

Nuclide name	Half-life	Uncertainty of half-life	Half-life unit	γ-ray energy (keV)	Uncertainty of γ-ray energy(keV)	Emission rate (%)	Uncertainty of emission rate(%)
^{130}I	12.36	1	H	363.467	15	0.089	20
				417.932	4	34.2	10
				427.94	4	0.083	11
				429.1		0.034	11
				457.758	21	0.237	15
				510.472	9	0.85	3
				536.066	6	99.00	
				539.053	8	1.40	4
				553.916	10	0.66	3
				586.049	8	1.69	6
				603.548	14	0.61	3
				623.0	3	0.017	11
				668.536	9	96	3
				686.060	14	1.07	4
				729.54	22	0.011	8
				739.512	10	82	3
				749.02	14	0.012	5
				800.23	4	0.101	5
				808.29	3	0.236	10
				814.15	11	0.025	5
				821.15	8	0.043	5
				854.99	10	0.035	5
				867.75	22	0.043	6
				877.35	4	0.191	10
				897.04	16	0.021	5
				944.21	8	0.062	14
				967.02	3	0.88	3
				996.80	16	0.028	5
				1060.07	17	0.017	5
				1094.29	20	0.028	8
				1096.48	4	0.552	20
				1122.15	4	0.253	11
				1157.43	3	11.3	4
				1222.56	3	0.179	8
				1272.12	3	0.748	25
				1403.90	3	0.345	16
				1417.69	13	0.0119	20
				1424.73	15	0.0208	20
				1487.85	15	0.0119	20
				1500.20	9	0.0396	20
				1545.78	23	0.023	4
				1547.75	23	0.018	4
				1607.29	12	0.045	3
^{131m}Te	33.25	25	H	36.83	3	0.0116	15
				62.380	20	0.0351	24
				66.95	5	0.022	4
				73.32	5	0.026	3
				78.57	8	0.015	3
				79.19	3	0.123	5
				81.140	20	3.92	10
				86.430	20	0.142	5
				98.30	10	0.013	3
				100.00	10	0.071	4
				101.6	3	0.164	16
				102.060	10	7.66	20
				103.3	3	0.045	8
				105.00	20	0.026	4
				109.40	20	0.034	8
				111.90	20	0.030	8
				113.50	10	0.011	4

Nuclide name	Half-life	Uncertainty of half-life	Half-life unit	γ-ray energy (keV)	Uncertainty of γ-ray energy(keV)	Emission rate (%)	Uncertainty of emission rate(%)
^{131m}Te	33.25	25	H	127.4	4	0.022	8
				130.50	10	0.067	8
				134.860	20	0.68	3
				137.60	20	0.07	4
				149.3	3	0.075	19
				149.710	10	4.9	7
				151.20	20	0.07	3
				155.90	20	0.037	23
				159.66	4	0.123	15
				169.70	20	0.030	8
				172.00	20	0.011	4
				177.20	20	0.063	12
				182.250	20	0.71	19
				182.250	20	0.992	20
				183.11	8	0.149	19
				188.13	5	0.205	12
				189.76	4	0.49	4
				190.52	6	0.112	15
				200.630	20	7.28	17
				203.4	4	0.019	8
				207.50	10	0.037	12
				210.3	3	0.015	4
				211.9	4	0.011	4
				213.98	3	0.411	20
				227.7	4	0.015	12
				230.65	5	0.187	12
				232.30	10	0.090	12
				235.00	20	0.015	12
				240.930	10	7.32	15
				253.170	20	0.627	16
				255.44	7	0.299	13
				261.40	20	0.015	4
				267.2	3	0.015	12
				269.2	3	0.05	6
				269.2	3	0.05	6
				278.560	20	1.72	5
				281.4	3	0.034	19
				283.20	20	0.37	4
				290.30	20	0.075	12
				296.8	3	0.049	8
				302.70	20	0.037	12
				303.90	20	0.037	8
				309.47	6	0.36	4
				323.7	4	0.015	8
				331.2	6	0.030	12
				334.270	10	9.22	20
				335.44	7	0.131	23
				342.92	5	0.37	12
				342.92	5	0.04	4
				345.9	3	0.09	3
				351.30	10	0.202	19
				353.5	3	0.07	4
				354.70	10	0.220	12
				357.4	3	0.019	8
				362.3	4	0.07	4
				364.98	10	1.16	15
				375.8	3	0.011	4
				377.8	3	0.019	19
				377.8	3	0.019	19
				379.3	3	0.019	8

Nuclide name	Half-life	Uncertainty of half-life	Half-life unit	γ-ray energy (keV)	Uncertainty of γ-ray energy(keV)	Emission rate (%)	Uncertainty of emission rate(%)
^{131m}Te	33.25	25	H	383.90	7	0.19	3
				403.3	4	0.030	12
				408.2	3	0.06	3
				417.40	20	0.269	20
				432.40	7	0.64	3
				452.30	4	1.5	4
				462.92	5	1.76	5
				468.16	9	0.30	3
				492.65	5	0.07	15
				506.80	20	0.086	15
				524.80	10	0.131	16
				530.70	10	0.101	19
				541.40	10	0.108	23
				546.70	20	0.037	8
				558.10	20	0.022	8
				572.70	20	0.041	23
				579.8	3	0.075	23
				586.30	3	1.90	9
				597.00	20	0.049	19
				602.09	4	0.30	12
				609.40	10	0.134	16
				637.3		0.015	15
				657.20	20	0.030	15
				665.05	3	4.18	11
				681.9	3	0.030	8
				685.90	10	0.149	12
				695.62	8	0.38	3
				702.50	7	0.377	20
				713.10	4	1.38	16
				738.80	20	0.063	12
				744.20	4	1.53	5
				749.0	8	0.015	8
				773.67	3	36.8	8
				774.10	10	0.52	8
				782.49	4	7.51	18
				793.75	3	13.4	3
				801.60	20	0.019	8
				822.78	4	5.90	13
				844.90	20	0.15	4
				848.90	20	0.037	12
				852.21	3	19.9	6
				852.21	3	0.37	19
				856.05	6	0.60	4
				865.10	20	0.19	4
				872.3	3	0.097	12
				881.6	3	0.034	12
				910.00	3	3.17	10
				920.62	5	1.16	8
				923.40	20	0.112	23
				930.0	4	0.019	12
				941.27	5	0.75	3
				987.80	10	0.149	12
				995.1	3	0.086	15
				999.20	10	0.164	19
				1003.60	20	0.026	15
				1005.70	20	0.071	15
				1023.60	20	0.060	8
				1035.40	20	0.101	8
				1059.69	4	1.49	5
				1072.30	20	0.022	4

Nuclide name	Half-life	Uncertainty of half-life	Half-life unit	γ-ray energy (keV)	Uncertainty of γ-ray energy(keV)	Emission rate (%)	Uncertainty of emission rate(%)
^{131m}Te	33.25	25	H	1108.3	3	0.022	8
				1114.1	3	0.011	4
				1125.46	4	11.0	3
				1127.96	6	0.93	8
				1148.89	7	1.5	3
				1148.89	7	0.24	25
				1150.90	9	0.63	8
				1162.70	20	0.026	8
				1165.50	10	0.134	12
				1181.4	4	0.011	8
				1206.60	4	9.41	22
				1211.00	20	0.060	12
				1237.32	5	0.63	4
				1254.2	4	0.026	4
				1315.16	8	0.67	8
				1316.20	20	0.09	4
				1318.30	20	0.037	8
				1333.8	3	0.052	8
				1340.60	10	0.097	12
				1376.8	4	0.041	8
				1389.6	3	0.015	4
				1394.83	9	0.105	8
				1403.6	6	0.011	8
				1496.5	4	0.056	8
				1547.75	9	0.067	8
				1646.01	5	1.20	5
				1696.8	5	0.015	4
				1880.1	3	0.060	8
				1887.70	7	1.31	5
				1936.15	9	0.071	8
				1980.3	3	0.030	8
^{131}I	8.0252	6	D	80.1850	20	2.62	4
				163.930	8	0.0211	5
				177.2140	20	0.269	4
				272.498	17	0.0576	12
				284.305	5	6.12	7
				318.088	16	0.0774	17
				324.65	3	0.0212	25
				325.789	4	0.273	22
				358.40	20	0.016	6
				364.489	5	81.5	8
				404.814	4	0.0546	17
				503.004	4	0.359	4
				636.989	4	7.16	10
				642.719	5	0.217	5
				722.911	5	1.77	3
^{131m}Xe	11.86	4	D	163.930	8	1.95	6
^{132}Te	.204	13	D	49.720	10	15.0	6
				111.76	8	1.74	8
				116.30	8	1.96	9
				228.16	6	88	4
^{132}I	2.295	13	H	136.7	4	0.04	5
				136.7	4	0.04	5
				147.40	10	0.237	20
				183.6	3	0.138	20
				194.3	5	0.089	
				234.3	6	0.030	10
				241.2	5	0.049	
				250.8	6	0.011	12
				250.8	6	0.011	12

Nuclide name	Half-life	Uncertainty of half-life	Half-life unit	γ-ray energy (keV)	Uncertainty of γ-ray energy(keV)	Emission rate (%)	Uncertainty of emission rate(%)
^{132}I	2.295	13	H	255.1	3	0.010	10
				255.10	20	0.237	20
				262.90	10	1.28	10
				278.4	4	0.025	25
				278.4	4	0.025	25
				284.90	10	0.71	7
				296.5	6	0.016	
				306.7	4	0.06	6
				306.7	4	0.06	6
				310.1	4	0.05	6
				310.1	4	0.05	6
				316.7	4	0.128	20
				343.7	4	0.089	20
				355.2	4	0.03	4
				355.2	4	0.03	4
				363.34	5	0.49	10
				376.6	4	0.010	5
				387.9	3	0.17	18
				387.9	3	0.17	18
				387.9	3	0.17	18
				402.6	6	0.023	
				416.8	3	0.47	5
				431.8	3	0.47	5
				445.0	6	0.099	
				446.2	3	0.60	5
				473.6	4	0.17	4
				478.2	4	0.17	4
				488.0	4	0.23	24
				488.0	4	0.23	24
				505.79	3	4.94	20
				522.65	9	16.0	5
				535.4	3	0.51	5
				539.7	4	0.06	7
				539.7	4	0.06	7
				547.20	20	1.14	8
				559.7	4	0.089	20
				572.5	4	0.04	4
				572.5	4	0.04	4
				591.1	6	0.05	5
				591.1	6	0.05	5
				600.0	6	0.08	8
				600.0	6	0.08	8
				609.8	5	0.039	10
				620.90	20	0.39	20
				621.2	3	1.58	20
				630.190	20	13.3	4
				642.4	5	0.035	
				650.50	20	2.57	20
				659.0	7	0.10	10
				667.7141	20	98.70	
				669.80	20	4.6	6
				671.40	20	3.5	10
				684.40	20	0.039	10
				687.8	5	0.039	20
				706.4	7	0.020	
				727.0	3	2.2	6
				727.2	3	3.2	6
				728.40	20	1.6	4
				771.7		0.020	20
				772.600	10	75.6	13

Nuclide name	Half-life	Uncertainty of half-life	Half-life unit	γ-ray energy (keV)	Uncertainty of γ-ray energy(keV)	Emission rate (%)	Uncertainty of emission rate(%)
^{132}I	2.295	13	H	780.00	20	1.18	4
				784.4	4	0.38	4
				791.2	4	0.099	20
				809.50	20	2.6	3
				812.00	20	5.5	4
				831.3	5	0.025	10
				847.9	5	0.017	5
				863.00	20	0.56	5
				866.0	6	0.025	25
				866.0	6	0.025	25
				876.60	20	1.04	4
				886.1	5	0.025	8
				888.7	5	0.021	22
				888.7	5	0.021	22
				904.4	5	0.013	4
				910.10	20	0.93	3
				927.4	3	0.41	4
				947.2	6	0.044	14
				954.55	9	17.6	5
				965.8	5	0.035	8
				984.20	20	0.59	4
				995.8	5	0.030	10
				1002.5	6	0.016	17
				1002.5	6	0.016	17
				1005.4	6	0.016	5
				1009.0	4	0.046	7
				1035.00	20	0.51	5
				1049.6	4	0.046	12
				1081.8	4	0.021	22
				1081.8	4	0.021	22
				1086.2	4	0.079	20
				1096.9	4	0.044	8
				1112.4	4	0.065	15
				1126.5	4	0.03	4
				1126.5	4	0.03	4
				1136.000	20	3.01	14
				1143.30	20	1.35	6
				1147.8	5	0.27	5
				1172.90	20	1.09	7
				1206.7	6	0.017	
				1212.3	4	0.012	3
				1242.6	7	0.012	
				1254.1	4	0.059	7
				1263.6	5	0.027	6
				1272.8	4	0.168	20
				1290.80	20	1.13	5
				1295.10	20	1.88	7
				1297.910	20	0.89	7
				1314.0	5	0.059	9
				1317.918	6	0.118	15
				1372.07	13	2.47	10
				1390.7	7	0.015	10
				1398.57	10	7.01	20
				1410.6	3	0.043	7
				1442.56	10	1.40	5
				1456.50	20	0.049	7
				1476.70	20	0.130	9
				1519.60	20	0.079	5
				1542.3	6	0.0158	20
				1592.9	3	0.047	4

Nuclide name	Half-life	Uncertainty of half-life	Half-life unit	γ-ray energy (keV)	Uncertainty of γ-ray energy(keV)	Emission rate (%)	Uncertainty of emission rate(%)
^{132}I	2.295	13	H	1617.90	20	0.010	5
				1644.0	6	0.013	4
				1661.4	5	0.016	3
				1671.3	4	0.022	4
				1715.4	4	0.055	4
				1720.6	5	0.054	4
				1727.2	4	0.067	6
				1752.3	7	0.025	8
				1757.40	20	0.30	3
				1760.4	6	0.059	20
				1768.5	8	0.025	8
				1778.5	4	0.079	8
				1814.0	5	0.016	4
				1830.1	5	0.028	5
				1879.2	5	0.014	3
				1913.7	5	0.030	10
				1921.08	12	1.23	6
				1985.625	6	0.0118	20
^{133}I	20.83	8	H	150.4		0.030	7
				176.97	7	0.078	18
				233.221	15	0.294	9
				245.95	8	0.035	9
				262.702	6	0.359	12
				267.173	19	0.117	7
				345.43	5	0.104	18
				361.09	5	0.11	4
				372.05	15	0.010	6
				381.59	7	0.045	5
				386.85	5	0.059	5
				417.6		0.154	11
				422.910	12	0.311	11
				438.87	8	0.040	5
				510.530	4	1.83	6
				522.4		0.04	5
				529.872	3	87.0	23
				537.73	10	0.036	7
				556.17	8	0.020	3
				617.974	14	0.544	16
				648.76	6	0.057	13
				670.10	8	0.043	6
				678.7	3	0.022	7
				680.247	11	0.650	20
				706.578	8	1.51	5
				768.382	15	0.460	15
				789.59	6	0.050	4
				820.506	22	0.155	6
				856.278	7	1.24	4
				875.329	5	4.51	13
				909.67	3	0.214	9
				911.49	5	0.046	7
				1052.296	18	0.556	17
				1060.07	6	0.138	7
				1087.71	10	0.0122	18
				1236.441	6	1.51	5
				1298.223	5	2.35	7
				1350.38	3	0.150	5
^{133}Xe	5.2475	5	D	79.6142	12	0.44	19
				80.9979	11	36.9	3
				160.6120	16	0.1066	13
^{133m}Xe	2.198	13	D	233.221	15	10.12	15

Nuclide name	Half-life	Uncertainty of half-life	Half-life unit	γ-ray energy (keV)	Uncertainty of γ-ray energy(keV)	Emission rate (%)	Uncertainty of emission rate(%)
^{134}Cs	2.0652	4	Y	242.738	8	0.027	3
				326.589	13	0.0162	10
				475.3650	20	1.477	7
				563.246	5	8.338	14
				569.331	3	15.373	17
				604.7210	20	97.62	11
				795.864	4	85.46	6
				801.953	4	8.688	16
				1038.610	7	0.990	3
				1167.968	5	1.790	5
				1365.185	7	3.017	8
^{135}Xe	9.14	2	H	158.197	18	0.289	14
				200.19	10	0.012	5
				249.794	15	90	3
				358.39	3	0.221	11
				373.13	10	0.015	3
				407.990	20	0.358	17
				608.185	15	2.90	14
				654.432	16	0.0450	24
				731.520	20	0.055	4
				812.63	3	0.070	3
^{136}Cs	13.01	5	D	66.881	17	4.79	20
				86.36	3	5.9	7
				109.681	7	0.409	20
				153.246	4	7.7	5
				163.9200	20	4.69	20
				166.576	6	0.63	3
				176.602	4	13.7	3
				187.285	6	0.54	5
				233.5	4	0.080	10
				273.646	8	12.66	20
				302.4	4	0.030	10
				315.5	5	0.020	18
				319.911	8	0.50	7
				340.547	8	46.8	5
				490.00	20	0.080	20
				507.188	10	1.00	5
				733.0	5	0.01994	
				818.514	12	99.70	10
				1048.073	20	80	3
				1235.362	23	20.0	7
				1321.6	4	0.050	20
				1538.09	20	0.100	20
				1551.30	20	0.015	5
^{137}Cs	30.08	9	Y	661.657	3	85.10	20
^{140}Ba	12.751		D	13.846	15	1.22	18
				29.9660	10	14.1	5
				113.51	3	0.0161	13
				118.837	3	0.061	8
				132.6870	10	0.202	6
				162.6600	10	6.22	10
				304.849	3	4.29	7
				423.7220	10	3.10	4
				437.5750	20	1.929	20
				537.261	9	24.39	24
^{140}La	1.67858	21	D	64.135	10	0.0143	19
				68.916	6	0.0754	19
				109.422	11	0.219	4
				131.117	8	0.467	10
				173.543	9	0.127	4

Nuclide name	Half-life	Uncertainty of half-life	Half-life unit	γ-ray energy (keV)	Uncertainty of γ-ray energy(keV)	Emission rate (%)	Uncertainty of emission rate(%)
^{140}La	1.67858	21	D	241.93	3	0.414	8
				266.543	12	0.466	8
				306.90	20	0.025	7
				328.762	8	20.3	3
				397.52	5	0.073	5
				432.493	12	2.90	3
				438.5	5	0.039	10
				487.021	12	45.5	6
				618.12	5	0.037	4
				751.637	18	4.33	4
				815.772	19	23.28	20
				867.846	20	5.50	7
				919.550	23	2.66	3
				925.189	21	6.90	7
				950.99	3	0.519	7
				992.9	5	0.013	5
				1045.05	24	0.025	15
				1097.20	23	0.023	5
				1303.5	4	0.042	7
				1405.20	17	0.059	7
				1596.21	4	95.4	15
				1877.29	19	0.041	4
				1924.62	13	0.0134	19
^{141}Ce	32.511	13	D	145.4433	14	48.4	3
^{143}Ce	33.039	6	H	57.356	7	11.7	4
				139.742	17	0.077	5
				231.5500	20	2.05	5
				293.2660	20	42.8	5
				350.619	3	3.23	4
				371.29	3	0.025	3
				389.640	20	0.0364	18
				432.999	6	0.159	4
				446.02	9	0.015	3
				447.450	20	0.060	3
				490.368	5	2.16	3
				497.810	20	0.045	3
				556.870	10	0.0317	18
				587.200	20	0.267	4
				614.22	3	0.0120	13
				664.571	15	5.69	7
				721.929	13	5.39	7
				791.070	20	0.0133	5
				806.340	20	0.0287	9
				809.980	20	0.0312	9
				880.460	10	1.031	13
				937.820	10	0.0261	13
				1002.850	10	0.0753	19
				1031.22	3	0.0201	9
				1046.78	4	0.0120	9
				1060.220	20	0.0364	14
				1103.250	20	0.415	6
^{144}Ce	284.91	5	D	33.568	10	0.200	23
				40.98	10	0.257	16
				53.395	5	0.100	8
				80.120	5	1.36	6
				99.961	15	0.040	5
				133.5150	20	11.09	20
^{144}Pr	17.28	5	M	696.510	3	1.342	14
				1489.160	5	0.278	5
^{147}Nd	10.98	1	D	91.1050	20	28.1	8

Nuclide name	Half-life	Uncertainty of half-life	Half-life unit	γ-ray energy (keV)	Uncertainty of γ-ray energy(keV)	Emission rate (%)	Uncertainty of emission rate(%)
^{147}Nd	10.98	1	D	117.98	5	0.0160	14
				120.48	5	0.376	9
				196.64	4	0.190	4
				240.50	20	0.043	3
				271.87	6	0.0132	10
				275.374	15	0.910	19
				319.411	18	2.13	5
				398.155	20	0.912	19
				408.52	6	0.0187	14
				410.48	3	0.150	4
				439.895	22	1.28	3
				489.24	3	0.155	4
				531.016	22	13.4	3
				541.83	7	0.019	3
				589.35	4	0.039	3
				594.80	3	0.283	6
				680.52	15	0.0294	15
				685.90	4	0.886	18
^{152}Eu	13.517	14	Y	121.7817	3	28.53	16
				148.00	5	0.0205	11
				212.43	11	0.0207	6
				244.6974	8	7.55	5
				251.633	9	0.0670	19
				271.08	4	0.0715	19
				275.42	4	0.0346	9
				295.9387	17	0.440	5
				315.10	3	0.0399	11
				316.13	13	0.0101	5
				324.83	3	0.0681	19
				329.41	5	0.1213	25
				340.46	10	0.0266	8
				344.2785	12	26.59	21
				351.66	5	0.0106	8
				367.7892	20	0.859	6
				411.1165	12	2.237	13
				416.02	3	0.1088	20
				443.9607	16	2.827	15
				444.01	17	0.298	11
				482.33	5	0.0247	8
				488.6793	20	0.414	4
				493.54	4	0.0303	14
				503.467	9	0.1524	20
				520.24	4	0.0534	17
				523.13	5	0.0153	7
				526.88	5	0.0120	8
				534.25	5	0.0410	11
				556.48	10	0.0177	7
				562.98	14	0.0202	19
				563.986	5	0.494	5
				566.438	6	0.131	4
				586.265	3	0.455	4
				595.61	12	0.032	11
				656.489	5	0.1441	23
				671.155	14	0.024	5
				674.64	14	0.169	4
				675.0		0.0213	8
				678.623	5	0.473	4
				686.60	5	0.0203	7
				688.670	5	0.856	7
				696.87	19	0.016	8

Nuclide name	Half-life	Uncertainty of half-life	Half-life unit	γ-ray energy (keV)	Uncertainty of γ-ray energy(keV)	Emission rate (%)	Uncertainty of emission rate(%)
^{152}Eu	13.517	14	Y	712.83	5	0.0955	25
				719.346	7	0.250	8
				719.36	14	0.095	4
				728.04	4	0.0111	4
				764.88	4	0.189	5
				768.96	4	0.082	5
				778.9046	24	12.93	9
				794.78	5	0.0263	16
				805.71	9	0.0152	6
				810.451	5	0.317	3
				839.36	4	0.0177	6
				841.574	5	0.168	3
				867.380	3	4.23	3
				896.59	9	0.0670	22
				901.19	5	0.0854	25
				919.337	4	0.419	5
				926.31	5	0.272	4
				930.59	5	0.0729	19
				958.63	5	0.0197	11
				963.367	7	0.140	7
				964.057	5	14.51	7
				974.09	5	0.0136	8
				990.18	5	0.0314	14
				1005.27	5	0.659	11
				1084.0	10	0.245	8
				1084.38	11	0.0106	8
				1085.837	10	10.11	5
				1089.737	5	1.734	12
				1109.18	5	0.189	7
				1112.076	3	13.67	9
				1170.97	9	0.0372	16
				1206.09	16	0.0130	14
				1212.948	11	1.415	9
				1249.94	5	0.187	3
				1261.35	5	0.0335	14
				1292.78	5	0.101	3
				1299.142	8	1.633	11
				1348.10	7	0.0173	8
				1363.78	5	0.0258	6
				1408.013	3	20.87	10
				1457.643	11	0.497	5
				1528.10	4	0.279	4
^{154}Eu	8.601	10	Y	123.0706	9	40.4	5
				131.56	7	0.0131	5
				188.22	7	0.2400	24
				232.12	7	0.0218	5
				247.9290	7	6.89	7
				269.65	8	0.0115	6
				301.38	7	0.0124	4
				305.2		0.0205	4
				312.32	7	0.0182	4
				322.07	7	0.0619	8
				346.70	7	0.0260	5
				397.07	7	0.0276	7
				401.26	7	0.188	3
				403.49	7	0.0223	18
				444.4925	19	0.547	6
				467.92	7	0.0626	9
				478.24	7	0.2250	23
				517.98	7	0.0498	15

Nuclide name	Half-life	Uncertainty of half-life	Half-life unit	γ-ray energy (keV)	Uncertainty of γ-ray energy(keV)	Emission rate (%)	Uncertainty of emission rate(%)
^{154}Eu	8.601	10	Y	533.03	8	0.0185	11
				534.86	7	0.017	7
				557.53	7	0.269	3
				569.50	7	0.0139	21
				581.97	7	0.893	9
				591.755	3	4.95	5
				598.30	7	0.0105	14
				602.68	7	0.0293	11
				613.24	7	0.0931	12
				625.2557	24	0.316	4
				649.52	7	0.0874	19
				664.74	8	0.0261	11
				669.14	8	0.0160	8
				676.60	7	0.1672	18
				692.4206	18	1.777	19
				715.76	7	0.187	6
				723.3015	22	20.06	20
				756.8021	23	4.52	5
				800.61	8	0.0212	11
				815.51	7	0.511	6
				845.416	7	0.568	12
				850.67	7	0.243	3
				873.1835	23	12.08	12
				880.65	7	0.084	6
				892.775	6	0.521	6
				904.064	3	0.889	10
				924.57	7	0.0649	10
				996.29	7	10.48	10
				1004.76	7	18.01	19
				1047.18	18	0.0613	15
				1118.27	7	0.113	4
				1128.552	7	0.300	4
				1140.702	6	0.237	4
				1160.31	7	0.0462	6
				1188.14	7	0.0876	9
				1241.34	7	0.1226	17
				1246.121	4	0.856	11
				1274.429	4	34.8	4
				1289.88	11	0.0210	8
				1291.36	8	0.022	8
				1294.99	8	0.0116	6
				1408.28	7	0.0247	11
				1494.048	4	0.698	8
				1537.81	7	0.0575	12
				1596.481	3	1.797	24
^{203}Pb	51.92	3	H	279.1952	10	80.9	19
				401.320	3	3.35	11
				680.515	3	0.75	3
† ^{206}Tl	4.202	11	M	803.06	3	0.0050	5
^{207}Bi	31.55	4	Y	569.6980	20	97.75	3
				897.77	12	0.128	5
				1063.656	3	74.5	3
				1442.20	20	0.1310	20
				1460.0	15	1.61	6
				1770.228	9	6.87	3
† ^{208}Tl	3.053	4	M	211.40	15	0.180	10
				233.36	15	0.310	10
				252.61	10	0.780	20
				277.371	5	6.6	3
				485.95	15	0.049	4

Nuclide name	Half-life	Uncertainty of half-life	Half-life unit	γ-ray energy (keV)	Uncertainty of γ-ray energy(keV)	Emission rate (%)	Uncertainty of emission rate(%)
† ^{208}Tl	3.053	4	M	510.77	10	22.60	20
				583.1870	20	85.0	3
				587.7		0.060	20
				650.1	3	0.050	20
				705.2	3	0.022	4
				722.04	12	0.24	4
				748.70	20	0.046	3
				763.13	8	1.79	3
				808.30	20	0.030	7
				821.20	20	0.041	4
				835.90	20	0.076	11
				860.557	4	12.50	10
				883.30	20	0.031	3
				927.60	20	0.125	11
				982.70	20	0.205	8
				1093.90	20	0.430	20
				1160.8	3	0.011	3
				1185.2	3	0.017	5
				1282.8	3	0.052	5
† ^{210}Pb	22.20	22	Y	46.5390	10	4.25	4
† ^{210}Po	138.376	2	D	803.06	3	0.00103	0
† ^{211}Pb	36.1	2	M	65.420	14	0.077	6
				81.00	20	0.045	12
				83.80	10	0.058	9
				88.20	20	0.017	4
				94.3	3	0.012	3
				95.00	20	0.018	3
				97.30	20	0.0116	13
				244.0		0.039	13
				313.59	9	0.031	4
				342.91	4	0.035	6
				362.072	17	0.043	3
				404.853	10	3.78	6
				427.088	10	1.76	5
				478.0	4	0.013	3
				481.1	4	0.026	6
				481.92	12	0.0103	13
				500.4	5	0.012	3
				609.38	4	0.043	7
				676.69	7	0.013	4
				704.64	3	0.462	11
				766.51	3	0.617	17
				832.01	3	3.52	6
				951.0		0.022	13
				1014.64	5	0.0173	6
				1080.16	6	0.0123	7
				1109.48	5	0.115	4
				1196.33	5	0.0102	4
† ^{211}Bi	2.14	2	M	351.07	5	13.02	12
† ^{212}Pb	10.64	1		115.183	5	0.596	10
				176.68	5	0.052	7
				238.6320	20	43.6	6
				300.087	10	3.30	5
				415.2		0.0131	22
† ^{212}Bi	60.55	6	M	39.857	4	1.06	9
				288.20	4	0.337	3
				328.03	4	0.125	7
				433.7	5	0.017	4
				452.98	5	0.363	4
				473.0	7	0.050	4

Nuclide name	Half-life	Uncertainty of half-life	Half-life unit	γ-ray energy (keV)	Uncertainty of γ-ray energy(keV)	Emission rate (%)	Uncertainty of emission rate(%)
† ^{212}Bi	60.55	6	M	727.330	9	6.67	9
				785.37	8	1.102	13
				893.408	5	0.378	20
				952.120	11	0.17	4
				1073.60	20	0.0160	20
				1078.62	10	0.564	20
				1512.7	3	0.29	4
				1620.50	10	1.47	4
				1679.7	5	0.058	13
				1806.0	5	0.090	20
† ^{214}Pb	26.8	9	M	53.2284	18	1.075	7
				118.2		0.094	21
				137.5	3	0.053	14
				141.3	6	0.058	18
				170.07	6	0.015	3
				196.19	5	0.067	8
				205.68	9	0.0114	13
				216.47	7	0.0100	23
				241.9950	23	7.251	16
				258.86	3	0.531	4
				274.80	4	0.355	10
				295.2228	18	18.42	4
				298.8		0.026	5
				305.26	3	0.0312	21
				314.33	7	0.078	6
				323.84	4	0.029	3
				351.9321	18	35.60	7
				462.02	6	0.212	5
				470.6	8	0.011	3
				480.432	20	0.337	4
				487.14	6	0.432	5
				511.00	9	0.033	9
				533.660	20	0.181	6
				538.42	8	0.020	3
				543.83	7	0.044	4
				580.14	3	0.370	4
				765.97	19	0.053	4
				785.96	8	1.06	3
				839.07	8	0.583	8
† ^{214}Bi	19.9	4	M	268.80	20	0.0170	20
				273.80	5	0.128	7
				280.97	4	0.067	7
				304.20	20	0.019	19
				304.20	20	0.019	19
				333.37	5	0.065	4
				334.78	8	0.019	19
				334.78	8	0.019	19
				338.5	6	0.11	4
				348.92	6	0.104	12
				351.9	5	0.070	10
				386.78	5	0.295	5
				388.89	5	0.402	10
				394.05	8	0.0126	9
				396.02	6	0.026	4
				405.720	20	0.169	6
				426.5	5	0.012	4
				452.92	10	0.030	4
				454.790	20	0.292	4
				461.08	11	0.051	6
				469.77	4	0.132	5

Nuclide name	Half-life	Uncertainty of half-life	Half-life unit	γ-ray energy (keV)	Uncertainty of γ-ray energy(keV)	Emission rate (%)	Uncertainty of emission rate(%)
† ^{214}Bi	19.9	4	M	474.44	4	0.099	6
				485.92	11	0.022	4
				487.95	13	0.028	9
				494.20	9	0.0104	10
				501.99	14	0.0180	20
				519.90	5	0.0165	17
				524.60	8	0.0168	17
				536.78	4	0.065	6
				542.83	7	0.077	6
				572.78	6	0.078	5
				595.24	7	0.0170	20
				609.320	5	45.49	16
				615.77	5	0.054	7
				617.10	20	0.034	4
				633.10	4	0.056	3
				639.62	8	0.033	3
				649.22	5	0.057	5
				658.70	20	0.0140	20
				660.94	13	0.053	4
				665.447	9	1.531	6
				683.23	5	0.082	5
				697.93	8	0.067	4
				699.82	13	0.016	5
				703.11	4	0.472	9
				704.96	22	0.047	7
				708.87	21	0.0121	12
				710.71	8	0.0740	20
				719.87	3	0.392	8
				723.08	10	0.037	3
				727.0	10	0.036	14
				733.81	7	0.041	3
				740.76	13	0.0430	20
				752.85	3	0.128	7
				768.360	5	4.894	11
				769.7	5	0.030	10
				786.35	14	0.32	4
				788.6	4	0.0130	20
				799.3	3	0.036	7
				806.180	9	1.264	5
				814.96	9	0.039	3
				821.18	3	0.161	8
				826.45	10	0.117	13
				832.36	9	0.0280	20
				840.4	5	0.0100	20
				847.16	11	0.024	3
				873.06	18	0.018	3
				878.03	12	0.012	3
				904.31	8	0.076	7
				915.75	13	0.0230	20
				930.20	20	0.026	4
				934.056	6	3.107	10
				934.10	20	0.050	10
				934.5	5	0.010	3
				938.65	16	0.013	4
				939.6	5	0.017	6
				943.33	11	0.0170	20
				961.62	17	0.0101	13
				964.08	3	0.365	10
				965.00	10	0.011	3
				976.18	12	0.0154	21

Nuclide name	Half-life	Uncertainty of half-life	Half-life unit	γ-ray energy (keV)	Uncertainty of γ-ray energy(keV)	Emission rate (%)	Uncertainty of emission rate(%)
† ^{214}Bi	19.9	4	M	989.34	17	0.010	3
				991.49	19	0.0110	20
				1013.4	7	0.013	4
				1021.36	17	0.0150	23
				1032.38	7	0.063	4
				1033.30	20	0.020	3
				1045.70	20	0.0230	20
				1051.96	3	0.313	7
				1062		0.013	8
				1067.39	24	0.025	6
				1069.96	7	0.272	9
				1087		0.015	7
				1103.70	13	0.098	12
				1104.71	13	0.078	4
				1109		0.015	5
				1118.9	5	0.040	10
				1120.294	6	14.92	3
				1130.45	16	0.036	3
				1133.66	3	0.2512	10
				1155.210	8	1.633	6
				1155.6	5	0.016	4
				1167.30	20	0.0120	20
				1173.00	8	0.055	3
				1207.68	3	0.451	10
				1238.122	7	5.834	15
				1279.0	7	0.0130	20
				1280.976	10	1.434	6
				1284.0	10	0.0110	10
				1285.1	5	0.016	3
				1303.75	7	0.107	5
				1316.99	9	0.081	6
				1329.94	16	0.081	6
				1341.49	13	0.021	3
				1371		0.0100	20
				1377.669	8	3.988	11
				1385.310	13	0.793	5
				1401.515	12	1.330	5
				1407.988	11	2.394	7
				1449		0.018	9
				1479.17	9	0.055	4
				1484		0.013	5
				1509.210	10	2.130	10
				1538.53	5	0.398	11
				1543.34	5	0.303	10
				1583.204	15	0.705	5
				1594.75	7	0.267	12
				1599.37	5	0.324	12
				1636.36	16	0.0115	13
				1657.07	17	0.048	4
				1661.274	16	1.047	6
				1684.012	20	0.214	5
				1729.595	11	2.878	8
				1764.491	10	15.30	3
				1813.72	13	0.0110	10
				1838.36	4	0.350	10
				1847.429	13	2.025	9
				1873.16	5	0.214	8
				1890.32	9	0.084	8
				1896.05	12	0.149	8
				1898.68	14	0.050	7

Nuclide name	Half-life	Uncertainty of half-life	Half-life unit	γ-ray energy (keV)	Uncertainty of γ-ray energy(keV)	Emission rate (%)	Uncertainty of emission rate(%)
†^{214}Bi	19.9	4	M	1935.62	16	0.032	3
†^{219}Rn	3.96	1	S	130.60	3	0.13	9
				221.5	3	0.030	5
				271.230	10	10.8	7
				293.56	4	0.073	6
				401.810	10	6.6	5
				438.2	6	0.015	16
				517.60	6	0.044	4
				676.66	7	0.0173	24
†^{223}Ra	11.43	5	D	10.0	10	0.0139	14
				14.40	10	0.0167	15
				33.6	5	0.10	4
				63.2	5	0.056	16
				104.23	8	0.019	3
				106.78	3	0.0236	15
				110.856	10	0.058	5
				114.70	20	0.010	5
				122.319	10	1.209	23
				136.10	20	0.028	3
				144.235	10	3.27	9
				154.208	10	5.70	17
				158.635	10	0.695	18
				175.65	15	0.019	5
				177.30	10	0.047	5
				179.54	6	0.153	14
				219.0	8	0.014	6
				221.32	24	0.036	6
				247.2	5	0.010	3
				249.30	10	0.039	10
				251.6	3	0.042	14
				255.20	20	0.053	7
				269.463	10	13.9	4
				288.18	3	0.160	5
				293.80	20	0.0667	10
				323.871	10	3.99	9
				328.38	3	0.209	8
				334.01	6	0.101	6
				338.282	10	2.84	7
				342.87	4	0.222	15
				346.8	3	0.181	3
				362.052	17	0.046	3
				362.90	20	0.015	7
				369.5		0.0209	3
				371.676	15	0.487	16
				372.90	10	0.0500	8
				373.3		0.0500	8
				376.0	3	0.012	4
				376.10	20	0.013	5
				382.8	3	0.014	5
				387.70	20	0.015	6
				393.5	5	0.011	4
				430.6	3	0.019	6
				432.12	10	0.035	3
				439.3		0.082	14
				445.033	12	1.29	5
				481.6	5	0.021	6
				487.50	20	0.0111	14
				527.611	13	0.071	5
				598.721	24	0.095	5
				609.31	4	0.057	3

Nuclide name	Half-life	Uncertainty of half-life	Half-life unit	γ-ray energy (keV)	Uncertainty of γ-ray energy(keV)	Emission rate (%)	Uncertainty of emission rate(%)
†^{223}Ra	11.43	5	D	632.0	10	0.031	10
†^{224}Ra	3.66	4	D	240.986	6	4.10	5
†^{226}Ra	1600	7	Y	186.211	13	3.64	4
†^{227}Th	18.68	9	D	6.5	3	0.09	3
				20.25	5	0.24	4
				24.13	5	0.088	10
				27.41	9	0.030	6
				29.860	10	0.076	13
				31.580	10	0.068	12
				40.20	3	0.015	4
				41.93	5	0.028	14
				43.77	5	0.213	23
				43.8	5	0.055	23
				44.22	12	0.053	14
				44.40	5	0.013	9
				48.30	3	0.014	6
				49.82	5	0.43	10
				50.130	10	8.4	9
				50.85	5	0.015	7
				59.6	5	0.010	4
				61.441	20	0.090	13
				62.45	5	0.11	12
				62.45	5	0.11	12
				64.35	10	0.026	5
				68.74	3	0.03	4
				68.74	3	0.03	4
				69.8	3	0.010	4
				72.85	5	0.025	20
				73.63	5	0.014	6
				75.01	5	0.027	11
				77.4	4	0.0103	9
				79.690	20	1.95	18
				93.88	5	1.51	14
				94.97	5	0.019	20
				94.97	5	0.019	20
				96.03	5	0.070	15
				99.58	10	0.026	7
				99.60	20	0.0129	11
				100.27	3	0.084	17
				113.11	5	0.54	5
				113.11	5	0.155	14
				117.20	5	0.199	22
				117.5	5	0.013	4
				123.58	10	0.014	6
				134.60	10	0.034	7
				138.40	10	0.014	3
				140.6	3	0.022	16
				141.42	5	0.07	8
				141.42	5	0.07	8
				150.14	20	0.011	4
				164.52	10	0.015	3
				168.36	10	0.015	3
				173.45	3	0.017	3
				175.8	3	0.021	6
				184.65	5	0.036	5
				197.56	10	0.013	4
				200.50	10	0.013	9
				201.64	10	0.024	4
				204.14	10	0.23	4
				204.98	10	0.16	3

Nuclide name	Half-life	Uncertainty of half-life	Half-life unit	γ-ray energy (keV)	Uncertainty of γ-ray energy(keV)	Emission rate (%)	Uncertainty of emission rate(%)
†^{227}Th	18.68	9	D	206.08	5	0.25	4
				210.62	5	1.25	14
				212.70	4	0.079	12
				212.7	3	0.019	6
				218.90	5	0.06	6
				218.90	5	0.06	6
				219.0	3	0.050	13
				234.76	10	0.45	7
				235.960	20	12.9	12
				246.12	10	0.0123	14
				248.10	10	0.025	6
				250.27	8	0.45	6
				252.50	5	0.111	19
				254.63	3	0.71	15
				256.230	20	7.0	7
				262.87	5	0.107	12
				267.05	20	0.010	3
				270.56	20	0.028	10
				272.91	5	0.51	5
				279.80	5	0.054	14
				281.42	5	0.09	10
				281.42	5	0.09	10
				284.24	10	0.040	14
				285.52	10	0.044	13
				286.09	20	1.74	22
				289.59	10	1.9	5
				289.77	10	0.019	5
				292.41	5	0.066	10
				296.50	5	0.44	6
				299.98	3	2.21	20
				300.50	16	0.014	3
				304.500	20	1.15	17
				306.1	3	0.010	4
				308.40	3	0.017	3
				312.69	3	0.52	6
				314.75	10	0.035	3
				314.85	4	0.3	3
				314.85	4	0.3	3
				319.24	5	0.032	7
				324.88	20	0.010	3
				329.850	20	2.9	3
				334.370	20	1.14	13
				342.55	4	0.35	10
				346.450	10	0.0120	17
				350.54	7	0.110	21
				352.61	10	0.0101	24
				362.63	10	0.051	5
				379.40	10	0.010	3
				383.51	4	0.025	24
				392.4	5	0.010	3
†^{228}Ac	6.15	2	H	18.40		0.014	4
				56.96	5	0.019	4
				57.766	5	0.47	3
				77.34	3	0.026	5
				99.509	6	1.26	7
				100.41	3	0.093	13
				129.0650	10	2.42	9
				135.54	5	0.018	4
				137.91	5	0.024	5
				141.02	3	0.050	8

Nuclide name	Half-life	Uncertainty of half-life	Half-life unit	γ-ray energy (keV)	Uncertainty of γ-ray energy(keV)	Emission rate (%)	Uncertainty of emission rate(%)
†^{228}Ac	6.15	2	H	145.849	10	0.158	8
				153.977	10	0.722	21
				168.65	10	0.010	3
				173.964	13	0.035	5
				184.540	20	0.070	8
				191.353	10	0.123	8
				199.407	10	0.315	5
				204.026	10	0.112	15
				209.253	6	3.89	7
				214.85	10	0.029	4
				214.85	5	0.76	11
				223.85	10	0.054	5
				231.42	10	0.025	4
				257.52	10	0.030	3
				263.58	10	0.040	4
				270.2450	20	3.46	6
				278.95	5	0.160	21
				278.95	5	0.031	5
				282.00	3	0.072	19
				321.646	8	0.226	11
				326.04	20	0.033	5
				327.4		0.12	4
				328.000	6	2.95	12
				332.370	4	0.40	4
				338.320	3	11.27	19
				340.96	5	0.369	21
				356.94	10	0.0170	18
				377.99	10	0.025	3
				389.12	15	0.0103	15
				397.94	10	0.027	3
				399.62	10	0.029	3
				409.462	6	1.92	4
				416.30	20	0.0132	21
				419.42	10	0.021	3
				440.44	5	0.121	8
				449.15	5	0.048	5
				452.47	10	0.015	5
				457.17	15	0.0150	23
				463.004	6	4.40	7
				466.40	10	0.029	3
				470.25	20	0.013	3
				471.76	15	0.033	3
				474.75	10	0.022	3
				478.33	5	0.209	15
				480.94	20	0.023	5
				490.33	15	0.0111	23
				492.37	10	0.0235	23
				503.823	13	0.182	12
				508.959	17	0.45	5
				515.06	10	0.049	5
				520.151	16	0.067	5
				523.131	16	0.103	8
				540.76	10	0.026	3
				546.47	5	0.201	13
				548.73	15	0.023	3
				555.12	10	0.046	5
				562.500	4	0.87	3
				570.91	10	0.182	24
				572.14	8	0.150	16
				583.41	5	0.111	10

Nuclide name	Half-life	Uncertainty of half-life	Half-life unit	γ-ray energy (keV)	Uncertainty of γ-ray energy(keV)	Emission rate (%)	Uncertainty of emission rate(%)
† ^{228}Ac	6.15	2	H	590.4		0.017	3
				610.64	10	0.023	5
				616.22	3	0.080	5
				620.38	5	0.080	5
				623.27	20	0.011	3
				627.23	20	0.014	3
				629.40	5	0.045	5
				634.18	10	0.0106	21
				640.34	3	0.054	5
				648.84	10	0.022	22
				648.84	10	0.022	22
				651.51	3	0.090	8
				663.82	10	0.028	6
				666.45	10	0.057	6
				672.00	15	0.026	8
				674.2		0.05	6
				674.8		2.1	7
				677.11	10	0.062	5
				684.0		0.019	5
				688.10	5	0.067	5
				688.10	5	0.067	5
				699.08	15	0.037	5
				701.747	14	0.173	10
				707.41	5	0.155	15
				718.48	15	0.019	4
				726.863	15	0.62	8
				737.72	5	0.037	4
				755.315	4	1.00	3
				772.291	5	1.49	3
				774.10	20	0.06000	
				776.56	10	0.019	6
				778.2		0.022	6
				782.142	5	0.485	19
				791.5	3	0.013	3
				791.5	3	0.010	3
				792.8		0.08000	
				794.947	5	4.25	7
				816.71	10	0.030	3
				824.934	23	0.050	5
				830.486	8	0.540	21
				835.710	6	1.61	6
				840.377	7	0.91	4
				870.46	4	0.044	4
				873.17	15	0.031	6
				874.44	7	0.047	10
				877.46	10	0.014	3
				887.33	10	0.027	3
				901.23	15	0.016	3
				904.20	4	0.77	3
				911.204	4	25.8	4
				918.97	10	0.027	3
				944.196	14	0.095	8
				947.982	11	0.106	8
				958.61	4	0.28	4
				964.766	10	4.99	9
				968.971	17	15.8	3
				975.96	5	0.050	5
				979.48	10	0.026	3
				987.71	20	0.077	13
				988.63	20	0.077	13

Nuclide name	Half-life	Uncertainty of half-life	Half-life unit	γ-ray energy (keV)	Uncertainty of γ-ray energy(keV)	Emission rate (%)	Uncertainty of emission rate(%)
† ^{228}Ac	6.15	2	H	1016.44	15	0.011	11
				1016.44	15	0.011	11
				1019.86	10	0.021	4
				1033.248	9	0.201	13
				1039.65	15	0.044	9
				1040.92	15	0.044	9
				1053.09	20	0.013	4
				1054.11	20	0.018	5
				1062.55	15	0.010	3
				1065.18	4	0.132	10
				1074.71	15	0.010	3
				1095.679	20	0.129	10
				1103.41	10	0.0150	23
				1110.610	10	0.285	23
				1110.610	10	0.019	10
				1117.63	10	0.054	8
				1142.85	15	0.0103	21
				1153.52	4	0.139	10
				1164.50	8	0.065	5
				1175.31	10	0.024	3
				1217.03	10	0.021	3
				1245.05	20	0.095	18
				1247.08	4	0.50	3
				1250.04	10	0.062	5
				1276.69	10	0.014	3
				1286.27	20	0.050	10
				1287.68	20	0.080	15
				1309.71	20	0.019	6
				1315.34	10	0.015	3
				1347.50	15	0.015	3
				1357.78	15	0.020	4
				1365.70	15	0.014	3
				1374.19	10	0.014	4
				1385.39	10	0.0106	21
				1401.49	10	0.012	3
				1415.66	10	0.021	4
				1430.95	10	0.035	7
				1451.40	15	0.0106	21
				1459.138	15	0.83	8
				1469.71	15	0.020	4
				1480.37	15	0.016	3
				1495.910	20	0.86	4
				1501.57	5	0.46	3
				1529.05	10	0.057	6
				1537.89	10	0.047	5
				1548.65	4	0.038	4
				1557.11	4	0.178	13
				1559.85	20	0.020	4
				1573.26	5	0.033	3
				1580.53	3	0.60	4
				1588.20	3	3.22	8
				1625.06	5	0.255	18
				1630.627	10	1.51	4
				1638.281	10	0.47	3
				1666.523	13	0.178	13
				1677.67	3	0.054	5
				1684.01	20	0.015	5
				1686.09	7	0.095	8
				1700.59	20	0.0101	23
				1702.43	5	0.048	5

Nuclide name	Half-life	Uncertainty of half-life	Half-life unit	γ-ray energy (keV)	Uncertainty of γ-ray energy(keV)	Emission rate (%)	Uncertainty of emission rate(%)
† ^{228}Ac	6.15	2	H	1724.21	4	0.029	3
				1738.2	3	0.018	4
				1740.4	3	0.011	3
				1758.11	10	0.035	4
				1823.22	10	0.044	4
				1835.43	10	0.038	4
				1842.13	10	0.042	4
				1870.83	10	0.0243	23
				1887.10	5	0.090	8
				1907.18	20	0.0119	10
				1929.78	20	0.0199	21
				1952.33	15	0.059	5
				1965.24	20	0.0204	18
† ^{228}Th	1.9125	9	Y	84.373	3	1.19	4
				131.613	4	0.127	4
				166.410	4	0.101	4
				205.93	5	0.0191	8
				215.983	5	0.247	8
† ^{231}Th	25.52	1	H	9.200		0.0330	15
				10.25		0.0502	23
				17.20		0.23	8
				18.07		0.011	11
				19.10		0.244	12
				25.640	20	14.1	10
				42.86	7	0.059	3
				58.5700	24	0.462	25
				63.86	3	0.023	4
				72.751	3	0.252	14
				81.2280	14	0.90	6
				82.0870	14	0.42	3
				84.2140	13	6.6	4
				89.950	20	1.00	6
				93.02	4	0.047	6
				99.278	3	0.131	9
				102.2700	13	0.436	24
				106.61	3	0.0176	11
				116.820	20	0.0222	17
				124.914	17	0.058	3
				134.030	20	0.0250	14
				135.664	11	0.079	5
				145.940	20	0.0317	20
				163.101	5	0.154	9
				174.150	20	0.0178	11
				183.500	20	0.0330	20
				217.94	3	0.0396	20
† ^{231}Pa	3.276E+4	11	Y	16.50	10	0.221	9
				19.60		0.35	10
				25.48	6	0.119	14
				27.360	20	10.5	5
				29.970	20	0.097	6
				35.83	3	0.0162	11
				38.200	20	0.145	6
				39.980	20	0.016	4
				44.140	20	0.055	5
				46.340	20	0.186	11
				52.71	3	0.077	5
				54.600	20	0.070	5
				57.19	3	0.0328	23
				63.64	3	0.0445	17
				74.15	4	0.0223	9

Nuclide name	Half-life	Uncertainty of half-life	Half-life unit	γ-ray energy (keV)	Uncertainty of γ-ray energy(keV)	Emission rate (%)	Uncertainty of emission rate(%)
† ^{231}Pa	3.276E+4	11	Y	77.34	3	0.0572	19
				96.84	3	0.084	3
				100.85	6	0.0228	9
				144.40	8	0.0115	10
				243.08	9	0.0336	24
				246.04	9	0.012	4
				255.78	7	0.1059	20
				260.19	8	0.182	4
				273.15	6	0.0577	13
				277.22	7	0.0679	15
				283.682	16	1.65	3
				286.58	10	0.0104	6
				300.066	10	2.41	5
				302.667	9	0.17	5
				302.667	9	2.3	4
				312.92	5	0.0986	20
				327.14	7	0.0359	9
				330.055	15	1.36	3
				340.71	6	0.177	4
				354.48	5	0.0961	21
				357.11	8	0.168	4
				379.35	7	0.0496	12
				407.81	3	0.0355	8
† ^{234}Th	24.10	3	D	62.860	20	0.016	3
				63.290	20	3.7	4
				73.920	20	0.0130	15
				83.30	5	0.060	6
				87.02	6	0.015	3
				92.380	10	2.13	21
				92.800	20	2.10	20
				112.81	5	0.210	23
				184.8		0.010	5
† ^{234m}Pa	1.159	16	M	73.920	20	0.013	4
		11		258.227	3	0.0764	22
				740.10	8	0.0109	17
				742.813	5	0.1066	23
				766.42	10	0.317	5
				786.28	10	0.0544	9
				921.72	10	0.01278	16
				945.940	20	0.0101	9
				1001.03	10	0.842	9
				1193.73	12	0.01358	17
				1510.21	10	0.01305	21
				1737.75	10	0.0213	3
				1831.36	10	0.01742	24
† ^{235}U	703.8E+6	5	Y	19.55	5	63	3
				31.60	5	0.017	6
				34.70	10	0.0370	4
				41.4	3	0.030	10
				41.96	15	0.060	10
				51.21	5	0.034	7
				54.25	5	0.015	15
				64.45	5	0.013	12
				72.70	20	0.1200	12
				73.72	5	0.01000	10
				74.94	3	0.051	6
				96.090	20	0.091	12
				109.19	7	1.66	14
				115.45	5	0.030	10
				120.35	5	0.0260	3

Nuclide name	Half-life	Uncertainty of half-life	Half-life unit	γ-ray energy (keV)	Uncertainty of γ-ray energy(keV)	Emission rate (%)	Uncertainty of emission rate(%)
†^{235}U	703.8E+6	5	Y	136.55	5	0.01200	12
				140.760	20	0.200	20
				143.760	20	10.96	14
				150.930	20	0.090	10
				163.356	3	5.08	7
				182.62	5	0.39	5
				185.715	5	57.0	7
				194.940	10	0.630	12
				198.900	20	0.036	6
				202.120	10	1.080	23
				205.316	10	5.02	6
				215.28	4	0.029	3
				221.386	14	0.118	7
				233.50	3	0.038	4
				240.88	4	0.074	6
				246.830	20	0.055	3
				251.50	10	0.020	20
				275.35	15	0.051	6
				275.49	6	0.0320	4
				279.50	5	0.270	3
				291.65	3	0.040	6
				345.92	3	0.040	6
				387.84	3	0.040	6
^{239}Np	2.356	3	D	4.200		2.600	
				44.660	20	0.130	10
				49.410	20	0.120	20
				57.28		0.036	
				57.30		0.090	
				61.4600	20	1.300	20
				67.860	20	0.10	3
				106.1230	20	25.34	17
				106.47	4	0.049	8
				124.4		0.010	
				166.39	6	0.016	7
				181.70	3	0.082	3
				209.7530	20	3.363	20
				226.380	20	0.259	16
				227.8		0.5100	
				228.1830	10	10.73	9
				254.40	3	0.1092	22
				272.84	3	0.0766	19
				277.5990	10	14.51	8
				285.4600	20	0.794	7
				315.880	3	1.600	12
				334.3100	20	2.056	13
				434.7	5	0.013	
^{241}Am	432.6	6	Y	26.34460	20	2.27	13
				32.18		0.0174	5
				33.1960	10	0.126	4
				43.420	3	0.073	8
				55.560	20	0.0181	18
				59.54091	10	35.9	4
				98.970	20	0.0203	5
				102.980	20	0.0195	5

Table D5.2 Nuclear data in the energy order.

γ-ray energy (keV)	Nuclide name	Half-life	Half-life unit	Emission rate (%)	γ-ray energy (keV)	Nuclide name	Half-life	Half-life unit	Emission rate (%)
4.2	^{239}Np	2.356	D	2.600	61.1	^{127}Sb	3.85	D	1.44
9.4	^{157}Eu	15.18	H	1.7	61.5	^{239}Np	2.356	D	1.300
13.8	^{140}Ba	12.751	D	1.22	62.5	†^{227}Th	18.68	D	0.11
16.5	†^{231}Pa	3.276E+4	Y	0.221	62.5	†^{227}Th	18.68	D	0.11
17.2	†^{231}Th	25.52	H	0.23	62.9	^{151}Pm	28.40	H	0.207
19.1	†^{231}Th	25.52	H	0.244	63.3	†^{234}Th	24.10	D	3.7
19.6	†^{235}U	703.8E+6	Y	63	63.8	†^{232}Th	14.0E+9	Y	0.263
19.6	†^{231}Pa	3.276E+4	Y	0.35	63.9	^{157}Eu	15.18	H	23
20.3	†^{227}Th	18.68	D	0.24	64.4	^{157}Eu	15.18	H	0.13
20.9	^{133m}Te	55.4	M	0.32	64.8	^{237}U	6.75	D	1.282
25.5	†^{231}Pa	3.276E+4	Y	0.119	64.9	^{151}Pm	28.40	H	1.89
25.6	†^{231}Th	25.52	H	14.1	65.7	^{182}Ta	114.74	D	3.01
25.7	^{151}Pm	28.40	H	0.97	65.8	^{151}Pm	28.40	H	1.15
26.3	^{241}Am	432.6	Y	2.27	66.0	*^{75}Ge	82.78	M	0.114
26.3	^{237}U	6.75	D	2.43	66.1	^{75}Se	119.78	D	1.111
26.5	^{155}Eu	4.753	Y	0.316	66.9	^{136}Cs	13.01	D	4.79
27.4	†^{231}Pa	3.276E+4	Y	10.5	67.7	^{182}Ta	114.74	D	42.9
27.5	^{88}Kr	2.825	H	1.94	67.9	^{239}Np	2.356	D	0.10
27.8	^{129}Te	69.6	M	16.3	69.7	^{153}Sm	46.50	H	4.73
30.0	^{140}Ba	12.751	D	14.1	69.7	^{151}Pm	28.40	H	0.47
30.6	^{201}Tl	3.0421	D	0.253	71.1	^{117}Cd	2.49	H	0.39
31.7	^{182}Ta	114.74	D	0.874	72.0	^{187}W	24.000	H	13.55
32.2	^{201}Tl	3.0421	D	0.258	72.5	^{145}Pr	5.984	H	0.261
33.2	^{237}U	6.75	D	0.130	72.7	†^{235}U	703.8E+6	Y	0.1200
33.2	^{241}Am	432.6	Y	0.126	72.8	†^{231}Th	25.52	H	0.252
33.6	^{144}Ce	284.91	D	0.200	72.8	^{149}Nd	1.728	H	0.60
33.6	†^{223}Ra	11.43	D	0.10	72.8	Pb(Kα2)			
35.5	^{125}Sb	2.75856	Y	4.37	74.1	^{133m}Te	55.4	M	0.30
35.5	^{125m}Te	57.40	D	7.30	74.3	^{149}Nd	1.728	H	1.11
38.2	†^{231}Pa	3.276E+4	Y	0.145	74.7	^{149}Nd	1.728	H	0.98
39.6	^{129}I	1.57E+7	Y	7.51	75.0	Pb(Kα1)			
39.9	†^{212}Bi	60.55	M	1.06	75.4	^{153}Sm	46.50	H	0.19
39.9	^{133m}Te	55.4	M	0.146	75.7	^{149}Nd	1.728	H	0.228
40.6	^{99}Mo	65.924	H	1.04	76.2	^{151}Pm	28.40	H	0.203
41.0	^{144}Ce	284.91	D	0.257	76.8	^{134}Te	41.8	M	0.274
42.7	^{182}Ta	114.74	D	0.268	76.9	^{157}Eu	15.18	H	0.20
43.8	†^{227}Th	18.68	D	0.213	77.1	^{149}Nd	1.728	H	0.61
44.7	^{239}Np	2.356	D	0.130	77.1	Bi(Kα1)			
45.3	^{155}Eu	4.753	Y	1.31	77.4	^{197}Hg	64.14	H	18.7
46.3	†^{231}Pa	3.276E+4	Y	0.186	79.1	^{108m}Ag	438	Y	6.6
46.5	†^{210}Pb	22.20	Y	4.25	79.2	^{131m}Te	33.25	H	0.123
47.5	^{133m}Te	55.4	M	0.177	79.4	^{134}Te	41.8	M	20.9
49.4	^{239}Np	2.356	D	0.120	79.6	^{133}Xe	5.2475	D	0.44
49.7	^{132}Te	3.204	D	15.0	79.7	†^{227}Th	18.68	D	1.95
49.8	†^{227}Th	18.68	D	0.43	80.1	^{144}Ce	284.91	D	1.36
50.1	†^{227}Th	18.68	D	8.4	80.2	^{131}I	8.0252	D	2.62
51.0	^{237}U	6.75	D	0.340	80.3	^{149}Nd	1.728	H	0.451
51.8	^{157}Eu	15.18	H	0.76	81.0	^{133}Xe	5.2475	D	36.9
53.2	†^{214}Pb	26.8	M	1.075	81.1	^{131m}Te	33.25	H	3.92
53.3	^{103}Ru	39.247	D	0.443	81.2	†^{231}Th	25.52	H	0.90
53.4	^{144}Ce	284.91	D	0.100	81.6	^{133m}Te	55.4	M	0.26
54.5	^{157}Eu	15.18	H	3.8	82.1	†^{231}Th	25.52	H	0.42
57.4	^{143}Ce	33.039	H	11.7	83.4	^{153}Sm	46.50	H	0.192
57.8	†^{228}Ac	6.15	H	0.47	84.2	†^{231}Th	25.52	H	6.6
58.5	^{149}Nd	1.728	H	1.42	84.4	†^{228}Th	1.9125	Y	1.19
58.6	†^{231}Th	25.52	H	0.462	84.7	^{182}Ta	114.74	D	2.654
58.9	^{149}Nd	1.728	H	1.30	84.9	Pb(Kβ1)			
59.5	^{237}U	6.75	D	34.5	86.1	^{155}Eu	4.753	Y	0.154
59.5	^{241}Am	432.6	Y	35.9	86.4	^{136}Cs	13.01	D	5.9
60.0	^{155}Eu	4.753	Y	1.22	86.4	^{131m}Te	33.25	H	0.142

γ-ray energy (keV)	Nuclide name	Half-life	Half-life unit	Emission rate (%)	γ-ray energy (keV)	Nuclide name	Half-life	Half-life unit	Emission rate (%)
86.5	^{155}Eu	4.753	Y	30.7	120.5	^{147}Nd	10.98	D	0.376
87.3	Bi(Kβ1)				121.1	^{75}Se	119.78	D	17.20
88.1	^{133m}Te	55.4	M	1.06	121.8	^{152}Eu	13.517	Y	28.53
89.0	^{156}Eu	15.19	D	8.4	122.3	^{88}Kr	2.825	H	0.197
89.5	^{153}Sm	46.50	H	0.158	122.3	†^{223}Ra	11.43	D	1.209
89.7	^{117}Cd	2.49	H	3.26	122.4	^{149}Nd	1.728	H	0.256
90.0	†^{231}Th	25.52	H	1.00	123.1	^{154}Eu	8.601	Y	40.4
91.1	^{147}Nd	10.98	D	28.1	126.6	^{149}Nd	1.728	H	0.111
91.3	^{67}Ga	3.2617	D	3.11	129.1	†^{228}Ac	6.15	H	2.42
92.2	^{82}Br	35.282	H	0.719	129.6	^{105m}Rh	40	S	20.00
92.3	^{133m}Te	55.4	M	0.16	129.8	^{105}Ru	4.44	H	5.68
92.4	†^{234}Th	24.10	D	2.13	129.8	^{85m}Kr	4.480	H	0.301
92.8	†^{234}Th	24.10	D	2.10	130.6	†^{219}Rn	3.96	S	0.13
93.3	^{67}Ga	3.2617	D	38.81	131.1	^{134}Te	41.8	M	0.18
93.9	†^{227}Th	18.68	D	1.51	131.1	^{140}La	1.67858	D	0.467
95.0	^{133m}Te	55.4	M	2.30	131.6	†^{228}Th	1.9125	Y	0.127
96.7	^{75}Se	119.78	D	3.449	132.7	^{140}Ba	12.751	D	0.202
97.0	^{149}Nd	1.728	H	1.45	133.0	^{181}Hf	42.39	D	43.3
97.4	^{153}Sm	46.50	H	0.772	133.5	^{144}Ce	284.91	D	11.09
97.7	^{117m}Cd	3.36	H	1.05	134.2	^{187}W	24.000	H	10.36
97.8	^{133m}Te	55.4	M	0.106	134.6	^{131}Sb	23.03	M	2.5
98.1	^{151}Pm	28.40	H	0.36	134.9	^{131m}Te	33.25	H	0.68
99.3	†^{231}Th	25.52	H	0.131	135.3	^{201}Tl	3.0421	D	2.565
99.4	^{117m}Cd	3.36	H	0.10	135.4	^{134}I	52.5	M	4.3
99.5	†^{228}Ac	6.15	H	1.26	136.0	^{75}Se	119.78	D	58.5
100.0	^{151}Pm	28.40	H	2.54	136.3	^{181}Hf	42.39	D	5.85
100.1	^{182}Ta	114.74	D	14.20	136.4	^{192}Ir	73.829	D	0.199
101.4	^{134}Te	41.8	M	0.38	136.6	^{133m}Te	55.4	M	0.12
101.6	^{131m}Te	33.25	H	0.164	136.9	^{181}Hf	42.39	D	0.86
101.9	^{151}Pm	28.40	H	1.28	138.1	^{138}Cs	32.5	M	1.49
102.1	^{131m}Te	33.25	H	7.66	139.0	^{134}I	52.5	M	0.76
102.3	†^{231}Th	25.52	H	0.436	139.2	^{149}Nd	1.728	H	0.51
102.8	^{128}Sb	9.05	H	0.40	139.3	^{151}Pm	28.40	H	0.50
103.2	^{153}Sm	46.50	H	29.25	139.7	⁎^{75m}Ge	47.7	S	39.5
104.8	^{151}Pm	28.40	H	3.5	140.5	^{99m}Tc	6.0072	H	89
105.3	^{155}Eu	4.753	Y	21.1	140.8	†^{235}U	703.8E+6	Y	0.200
105.5	^{129m}Te	33.6	D	0.14	141.1	^{201}Tl	3.0421	D	0.28
105.9	^{142}La	91.1	M	0.1422	142.7	^{59}Fe	44.490	D	1.02
106.1	^{239}Np	2.356	D	25.34	143.2	^{151}Pm	28.40	H	0.214
109.2	†^{235}U	703.8E+6	Y	1.66	143.8	†^{235}U	703.8E+6	Y	10.96
109.3	^{125m}Te	57.40	D	0.280	144.2	†^{223}Ra	11.43	D	3.27
109.4	^{140}La	1.67858	D	0.219	145.4	^{141}Ce	32.511	D	48.4
109.7	^{136}Cs	13.01	D	0.409	145.8	†^{228}Ac	6.15	H	0.158
110.4	^{182}Ta	114.74	D	0.107	147.4	^{132}I	2.295	H	0.237
111.8	^{132}Te	3.204	D	1.74	147.5	^{151}Pm	28.40	H	0.153
112.5	^{138}Cs	32.5	M	0.130	149.1	^{105}Ru	4.44	H	1.75
112.5	^{149}Nd	1.728	H	0.119	149.7	^{131m}Te	33.25	H	4.9
112.8	†^{234}Th	24.10	D	0.210	150.8	^{133m}Te	55.4	M	0.27
113.1	†^{227}Th	18.68	D	0.155	150.8	^{133m}Te	55.4	M	0.53
113.1	†^{227}Th	18.68	D	0.54	151.2	^{85m}Kr	4.480	H	75.2
113.7	^{182}Ta	114.74	D	1.871	152.0	^{134}I	52.5	M	0.106
114.3	^{149}Nd	1.728	H	19.2	152.4	^{182}Ta	114.74	D	7.02
115.2	†^{212}Pb	10.64	H	0.596	152.6	^{128}Sb	9.05	H	0.50
116.3	^{132}Te	3.204	D	1.96	153.2	^{136}Cs	13.01	D	7.7
116.4	^{182}Ta	114.74	D	0.444	154.0	†^{228}Ac	6.15	H	0.722
116.4	^{133m}Te	55.4	M	0.22	154.2	†^{223}Ra	11.43	D	5.70
116.9	^{149}Nd	1.728	H	0.11	154.3	^{127}Sb	3.85	D	0.15
117.0	^{125}Sb	2.75856	Y	0.263	155.9	^{149}Nd	1.728	H	5.9
117.2	†^{227}Th	18.68	D	0.199	156.2	^{151}Pm	28.40	H	0.149
118.4	^{128}Sb	9.05	H	0.60	156.4	^{77}Ge	11.211	H	0.69

γ-ray energy (keV)	Nuclide name	Half-life	Half-life unit	Emission rate (%)	γ-ray energy (keV)	Nuclide name	Half-life	Half-life unit	Emission rate (%)
156.4	^{182}Ta	114.74	D	2.671	185.7	†^{235}U	703.8E+6	Y	57.0
158.2	^{135}Xe	9.14	H	0.289	186.2	†^{226}Ra	1600	Y	3.64
158.6	†^{223}Ra	11.43	D	0.695	186.6	^{151}Pm	28.40	H	0.180
159.7	^{131m}Te	33.25	H	0.123	187.3	^{136}Cs	13.01	D	0.54
159.9	^{131}Sb	23.03	M	0.47	188.1	^{131m}Te	33.25	H	0.205
160.6	^{133}Xe	5.2475	D	0.1066	188.2	^{154}Eu	8.601	Y	0.2400
160.8	^{117}Cd	2.49	H	0.25	188.5	^{134}I	52.5	M	0.77
162.5	^{134}I	52.5	M	0.29	188.6	^{149}Nd	1.728	H	1.79
162.7	^{140}Ba	12.751	D	6.22	189.8	^{131m}Te	33.25	H	0.49
162.9	^{151}Pm	28.40	H	0.88	190.3	^{114m}In	49.51	D	15.56
163.1	†^{231}Th	25.52	H	0.154	190.5	^{81m}Kr	13.10	S	67.6983
163.4	†^{235}U	703.8E+6	Y	5.08	190.5	^{131m}Te	33.25	H	0.112
163.5	^{105}Ru	4.44	H	0.156	191.4	†^{228}Ac	6.15	H	0.123
163.6	^{151}Pm	28.40	H	1.55	191.4	^{197}Hg	64.14	H	0.632
163.9	^{136}Ba	0.3084	S	31.25	192.0	^{138}Cs	32.5	M	0.50
163.9	^{136}Cs	13.01	D	4.69	192.0	^{149}Nd	1.728	H	0.57
163.9	^{131m}Xe	11.86	D	1.95	192.3	^{59}Fe	44.490	D	3.08
164.4	^{133m}Te	55.4	M	0.77	193.4	^{133m}Te	55.4	M	0.47
164.6	^{237}U	6.75	D	1.86	193.9	^{138}Cs	32.5	M	0.328
165.9	^{139}Ba	82.93	M	23.7	194.7	^{77}Ge	11.211	H	1.67
165.9	^{201}Tl	3.0421	D	0.155	194.9	†^{235}U	703.8E+6	Y	0.630
166.0	^{88}Kr	2.825	H	3.10	196.3	^{88}Kr	2.825	H	26.0
166.4	†^{228}Th	1.9125	Y	0.101	196.6	^{147}Nd	10.98	D	0.190
166.6	^{136}Cs	13.01	D	0.63	198.2	^{133m}Te	55.4	M	0.13
167.4	^{201}Tl	3.0421	D	10.00	198.4	^{182}Ta	114.74	D	1.465
167.8	^{151}Pm	28.40	H	8.3	198.6	⫲^{75}Ge	82.78	M	1.19
168.4	^{151}Pm	28.40	H	0.92	198.6	^{75}Se	119.78	D	1.496
168.6	^{117m}Cd	3.36	H	0.29	198.9	^{149}Nd	1.728	H	1.39
169.0	^{133m}Te	55.4	M	4.2	199.2	^{156}Eu	15.19	D	0.74
171.3	^{111}In	2.8047	D	90.7	199.4	†^{228}Ac	6.15	H	0.315
172.7	^{125}Sb	2.75856	Y	0.191	200.6	^{131m}Te	33.25	H	7.28
173.5	^{140}La	1.67858	D	0.127	200.7	^{133m}Te	55.4	M	0.35
174.2	^{78}As	90.7	M	0.18	201.0	^{133m}Te	55.4	M	0.13
176.3	^{125}Sb	2.75856	Y	6.84	201.2	^{134}Te	41.8	M	8.9
176.5	^{151}Pm	28.40	H	0.86	201.3	^{192}Ir	73.829	D	0.471
176.6	^{136}Cs	13.01	D	13.7	202.0	^{151}Pm	28.40	H	0.88
176.9	^{133m}Te	55.4	M	0.18	202.1	†^{235}U	703.8E+6	Y	1.080
177.2	^{151}Pm	28.40	H	3.8	202.5	^{90m}Y	3.19	H	97.3
177.2	^{133m}Te	55.4	M	0.18	204.0	†^{228}Ac	6.15	H	0.112
177.2	^{131}I	8.0252	D	0.269	204.1	^{95m}Nb	3.61	D	2.30
177.3	^{77}Ge	11.211	H	0.13	204.1	^{125}Sb	2.75856	Y	0.317
177.8	^{149}Nd	1.728	H	0.155	204.1	†^{227}Th	18.68	D	0.23
178.1	^{133m}Te	55.4	M	0.27	204.2	^{151}Pm	28.40	H	0.131
178.3	^{142}La	91.1	M	0.19	204.4	^{128}Sb	9.05	H	1.00
179.4	^{117}Cd	2.49	H	0.10	205.0	†^{227}Th	18.68	D	0.16
179.4	^{182}Ta	114.74	D	3.119	205.3	†^{235}U	703.8E+6	Y	5.02
179.5	†^{223}Ra	11.43	D	0.153	205.8	^{192}Ir	73.829	D	3.31
180.4	^{129}Sb	4.366	H	2.84	206.1	†^{227}Th	18.68	D	0.25
180.9	^{134}Te	41.8	M	18.3	206.2	^{187}W	24.000	H	0.153
181.1	^{99}Mo	65.924	H	6.05	208.0	^{237}U	6.75	D	21.2
182.3	^{131m}Te	33.25	H	0.71	208.1	^{125}Sb	2.75856	Y	0.248
182.3	^{131m}Te	33.25	H	0.992	208.1	^{149}Nd	1.728	H	2.55
182.3	^{130}Sb	39.5	M	65	208.6	^{157}Eu	15.18	H	0.150
182.6	†^{235}U	703.8E+6	Y	0.39	208.8	^{77}Ge	11.211	H	1.12
183.1	^{134}Te	41.8	M	0.6	209.0	^{67}Ga	3.2617	D	2.460
183.1	^{131m}Te	33.25	H	0.149	209.0	^{129}Te	69.6	M	0.180
183.6	^{132}I	2.295	H	0.138	209.0	^{151}Pm	28.40	H	1.73
184.6	^{67}Ga	3.2617	D	21.410	209.3	†^{228}Ac	6.15	H	3.89
184.6	^{133m}Te	55.4	M	0.13	209.8	^{239}Np	2.356	D	3.363
185.5	^{149}Nd	1.728	H	0.104	210.5	^{134}Te	41.8	M	22.7

γ-ray energy (keV)	Nuclide name	Half-life	Half-life unit	Emission rate (%)	γ-ray energy (keV)	Nuclide name	Half-life	Half-life unit	Emission rate (%)
210.6	†^{227}Th	18.68	D	1.25	240.1	^{151}Pm	28.40	H	3.8
211.0	^{77}Ge	11.211	H	30.0	240.2	^{149}Nd	1.728	H	3.94
211.3	^{149}Nd	1.728	H	25.9	240.7	^{88}Kr	2.825	H	0.253
211.4	†^{208}Tl	3.053	M	0.180	240.9	^{133m}Te	55.4	M	0.27
212.3	^{138}Cs	32.5	M	0.175	240.9	^{131m}Te	33.25	H	7.32
213.5	^{133m}Te	55.4	M	1.73	241.0	†^{224}Ra	3.66	D	4.10
213.9	^{149}Nd	1.728	H	0.40	241.6	^{92}Sr	2.611	H	2.93
214.0	^{131m}Te	33.25	H	0.411	241.9	^{140}La	1.67858	D	0.414
214.0	^{133m}Te	55.4	M	0.18	242.0	†^{214}Pb	26.8	M	7.251
214.8	^{128}Sb	9.05	H	1.00	244.4	^{133m}Te	55.4	M	0.27
214.9	†^{228}Ac	6.15	H	0.76	244.5	^{129}Sb	4.366	H	0.403
215.5	^{77}Ge	11.211	H	27.9	244.7	^{152}Eu	13.517	Y	7.55
216.0	†^{228}Th	1.9125	Y	0.247	245.4	^{111}In	2.8047	D	94.1
217.0	^{134}I	52.5	M	0.23	245.5	^{149}Nd	1.728	H	0.21
218.9	^{97}Zr	16.749	H	0.168	245.7	^{149}Nd	1.728	H	0.80
219.1	^{77}Ge	11.211	H	0.14	246.2	^{187}W	24.000	H	0.136
220.5	^{135}I	6.58	H	1.75	247.9	^{154}Eu	8.601	Y	6.89
220.9	^{117}Cd	2.49	H	1.17	249.7	^{128}Sb	9.05	H	0.60
220.9	^{117m}Cd	3.36	H	0.24	249.8	^{135}Xe	9.14	H	90
221.1	^{133m}Te	55.4	M	0.19	250.3	†^{227}Th	18.68	D	0.45
221.4	†^{235}U	703.8E+6	Y	0.118	250.6	^{129}Te	69.6	M	0.38
221.5	^{82}Br	35.282	H	2.28	251.5	^{133m}Te	55.4	M	0.22
222.1	^{182}Ta	114.74	D	7.57	252.4	^{127}Sb	3.85	D	8.5
224.2	^{133m}Te	55.4	M	0.13	252.5	†^{227}Th	18.68	D	0.111
225.1	^{105}Ru	4.44	H	0.123	252.6	†^{208}Tl	3.053	M	0.780
226.4	^{239}Np	2.356	D	0.259	253.2	^{131m}Te	33.25	H	0.627
226.8	^{149}Nd	1.728	H	0.163	254.2	^{97}Zr	16.749	H	1.15
227.2	^{151}Pm	28.40	H	0.34	254.3	^{151}Pm	28.40	H	0.169
227.3	^{128}Sb	9.05	H	1.5	254.4	^{239}Np	2.356	D	0.1092
227.8	^{138}Cs	32.5	M	1.51	254.6	†^{227}Th	18.68	D	0.71
227.8	^{239}Np	2.356	D	0.5100	254.7	^{77}Ge	11.211	H	0.197
227.9	^{125}Sb	2.75856	Y	0.1311	255.1	^{132}I	2.295	H	0.237
228.2	^{132}Te	3.204	D	88	255.1	^{113}Sn	115.09	D	2.11
228.2	^{239}Np	2.356	D	10.73	255.4	^{131m}Te	33.25	H	0.299
229.3	^{182}Ta	114.74	D	3.644	255.8	†^{231}Pa	3.276E+4	Y	0.1059
229.6	^{149}Nd	1.728	H	0.482	256.2	†^{227}Th	18.68	D	7.0
229.7	^{135}I	6.58	H	0.241	257.8	^{133m}Te	55.4	M	0.35
230.1	^{133m}Te	55.4	M	0.22	258.0	^{130}Sb	39.5	M	3.9
230.2	^{84}Br	31.76	M	0.30	258.1	^{149}Nd	1.728	H	0.376
230.7	^{131m}Te	33.25	H	0.187	258.1	^{151}Pm	28.40	H	0.56
231.4	^{115}Cd	53.46	H	0.740	258.8	^{113}Ag	5.37	H	1.64
231.6	^{143}Ce	33.039	H	2.05	258.8	⁎^{74}Ga	8.12	M	0.11
232.4	^{151}Pm	28.40	H	1.03	258.9	†^{214}Pb	26.8	M	0.531
233.2	⁎^{74}Ga	8.12	M	0.16	259.8	^{134}Te	41.8	M	0.44
233.2	^{133}I	20.83	H	0.294	260.2	†^{231}Pa	3.276E+4	Y	0.182
233.2	^{133m}Xe	2.198	D	10.12	260.9	^{115}Cd	53.46	H	1.94
233.4	†^{208}Tl	3.053	M	0.310	261.2	^{91}Sr	9.65	H	0.449
234.8	†^{227}Th	18.68	D	0.45	261.6	^{133m}Te	55.4	M	6.3
235.0	^{128}Sb	9.05	H	0.30	262.7	^{133}I	20.83	H	0.359
235.0	^{133m}Te	55.4	M	0.13	262.8	^{105}Ru	4.44	H	6.57
235.5	^{134}I	52.5	M	2.13	262.9	†^{227}Th	18.68	D	0.107
235.7	^{95}Zr	64.032	D	0.270	262.9	^{132}I	2.295	H	1.28
235.7	^{95m}Nb	3.61	D	24.8	264.1	^{182}Ta	114.74	D	3.612
236.0	†^{227}Th	18.68	D	12.9	264.3	^{135}I	6.58	H	0.184
236.6	^{151}Pm	28.40	H	0.160	264.5	^{77}Ge	11.211	H	53.3
236.7	^{151}Pm	28.40	H	0.19	264.6	⁎^{75}Ge	82.78	M	11.4
237.1	^{151}Pm	28.40	H	0.52	264.7	^{75}Se	119.78	D	58.9
238.6	^{149}Nd	1.728	H	0.89	266.5	^{140}La	1.67858	D	0.466
238.6	†^{212}Pb	10.64	H	43.6	266.9	^{93}Y	10.18	H	7.4
239.1	^{187}W	24.000	H	0.100	267.2	^{133}I	20.83	H	0.117

γ-ray energy (keV)	Nuclide name	Half-life	Half-life unit	Emission rate (%)	γ-ray energy (keV)	Nuclide name	Half-life	Half-life unit	Emission rate (%)
267.5	^{237}U	6.75	D	0.712	290.8	^{127}Sb	3.85	D	2.02
267.7	^{149}Nd	1.728	H	6.0	292.1	^{117}Cd	2.49	H	0.64
268.1	^{77}Ge	11.211	H	0.3	292.1	^{117m}Cd	3.36	H	0.10
268.5	^{129}Sb	4.366	H	0.214	293.3	^{143}Ce	33.039	H	42.8
269.5	†^{223}Ra	11.43	D	13.9	293.3	^{127}Sb	3.85	D	0.29
270.2	^{149}Nd	1.728	H	10.7	294.8	^{149}Nd	1.728	H	0.57
270.2	†^{228}Ac	6.15	H	3.46	294.8	^{133m}Te	55.4	M	0.18
270.6	^{125}Sn	9.64	D	0.11	295.0	^{103}Ru	39.247	D	0.288
271.2	†^{219}Rn	3.96	S	10.8	295.2	†^{214}Pb	26.8	M	18.42
272.4	^{97}Zr	16.749	H	0.23	295.3	^{129}Sb	4.366	H	0.828
272.6	^{91}Sr	9.65	H	0.26	295.7	^{131}Sb	23.03	M	1.6
272.9	†^{227}Th	18.68	D	0.51	295.9	^{152}Eu	13.517	Y	0.440
273.2	^{149}Nd	1.728	H	0.18	296.0	^{192}Ir	73.829	D	28.71
273.3	^{117}Cd	2.49	H	27.9	296.5	†^{227}Th	18.68	D	0.44
273.5	^{82}Br	35.282	H	0.803	298.6	^{113}Ag	5.37	H	10.00
273.6	^{136}Cs	13.01	D	12.66	299.5	^{117m}Cd	3.36	H	0.45
273.8	†^{214}Bi	19.9	M	0.128	300.0	†^{227}Th	18.68	D	2.21
274.3	^{131}Sb	23.03	M	1.2	300.1	†^{231}Pa	3.276E+4	Y	2.41
274.7	^{91}Sr	9.65	H	1.04	300.1	†^{212}Pb	10.64	H	3.30
274.8	†^{214}Pb	26.8	M	0.355	300.2	^{67}Ga	3.2617	D	16.64
275.2	^{151}Pm	28.40	H	6.8	301.1	^{149}Nd	1.728	H	0.376
275.4	^{147}Nd	10.98	D	0.910	301.3	^{131}Sb	23.03	M	2.4
275.4	^{149}Nd	1.728	H	0.65	302.0	⁎^{74}Ga	8.12	M	0.11
276.0	^{81}Kr	2.29E5	Y	0.298	302.7	†^{231}Pa	3.276E+4	Y	2.3
277.0	^{149}Nd	1.728	H	0.342	302.7	†^{231}Pa	3.276E+4	Y	0.17
277.4	†^{208}Tl	3.053	M	6.6	303.3	^{130}Sb	39.5	M	5.8
277.6	^{239}Np	2.356	D	14.51	303.9	^{75}Se	119.78	D	1.315
278.0	^{134}Te	41.8	M	21.2	304.5	†^{227}Th	18.68	D	1.15
278.0	^{133m}Te	55.4	M	0.44	304.8	^{140}Ba	12.751	D	4.29
278.3	^{128}Sb	9.05	H	0.60	304.9	^{85m}Kr	4.480	H	14.0
278.4	^{129}Te	69.6	M	0.57	306.1	^{105}Rh	35.36	H	5.1
278.6	^{131m}Te	33.25	H	1.72	306.7	^{151}Pm	28.40	H	0.239
278.8	^{134}I	52.5	M	0.144	307.9	^{133m}Te	55.4	M	0.22
279.0	†^{228}Ac	6.15	H	0.160	308.5	^{192}Ir	73.829	D	29.70
279.2	^{203}Pb	51.92	H	80.9	309.5	^{131m}Te	33.25	H	0.36
279.5	†^{235}U	703.8E+6	Y	0.270	310.0	^{127}Sb	3.85	D	0.26
279.5	^{75}Se	119.78	D	25.02	310.3	^{117m}Cd	3.36	H	0.50
279.8	^{117}Cd	2.49	H	0.11	311.0	^{149}Nd	1.728	H	0.510
280.1	^{151}Pm	28.40	H	0.232	311.7	^{88}Kr	2.825	H	0.107
280.1	^{105}Rh	35.36	H	0.166	312.1	^{133m}Te	55.4	M	1.77
280.4	^{127}Sb	3.85	D	0.66	312.6	^{42}K	12.355	H	0.336
281.3	^{129}Te	69.6	M	0.165	312.7	†^{227}Th	18.68	D	0.52
282.5	^{149}Nd	1.728	H	0.62	314.1	^{128}Sb	9.05	H	61
283.2	^{131m}Te	33.25	H	0.37	314.2	^{133m}Te	55.4	M	0.31
283.3	^{192}Ir	73.829	D	0.266	314.4	^{129}Sb	4.366	H	0.123
283.7	†^{231}Pa	3.276E+4	Y	1.65	314.9	†^{227}Th	18.68	D	0.3
284.3	^{131}I	8.0252	D	6.12	314.9	†^{227}Th	18.68	D	0.3
284.8	^{133m}Te	55.4	M	0.18	315.9	^{239}Np	2.356	D	1.600
284.9	^{132}I	2.295	H	0.71	316.3	^{113}Ag	5.37	H	1.343
285.5	^{239}Np	2.356	D	0.794	316.4	^{105}Ru	4.44	H	11.1
285.5	^{130}Sb	39.5	M	3.5	316.5	^{192}Ir	73.829	D	82.86
286.0	^{149}Pm	53.08	H	3.10	316.7	^{132}I	2.295	H	0.128
286.1	†^{227}Th	18.68	D	1.74	317.7	^{128}Sb	9.05	H	3.0
288.2	†^{223}Ra	11.43	D	0.160	318.4	^{129}Sb	4.366	H	0.227
288.2	^{149}Nd	1.728	H	0.69	318.7	^{157}Eu	15.18	H	2.9
288.2	†^{212}Bi	60.55	M	0.337	318.8	^{133m}Te	55.4	M	0.18
288.5	^{135}I	6.58	H	3.10	318.9	^{105}Rh	35.36	H	19.1
289.6	†^{227}Th	18.68	D	1.9	319.4	^{147}Nd	10.98	D	2.13
290.3	^{135}I	6.58	H	0.304	319.8	^{134}I	52.5	M	0.46
290.8	^{151}Pm	28.40	H	0.83	319.9	^{136}Cs	13.01	D	0.50

γ-ray energy (keV)	Nuclide name	Half-life	Half-life unit	Emission rate (%)	γ-ray energy (keV)	Nuclide name	Half-life	Half-life unit	Emission rate (%)
320.1	$_{51}Cr$	27.704	D	9.910	344.5	^{117}Cd	2.49	H	17.9
321.0	^{125}Sb	2.75856	Y	0.416	344.9	^{151}Pm	28.40	H	2.12
321.6	†^{228}Ac	6.15	H	0.226	345.4	^{133}I	20.83	H	0.104
322.3	^{128}Sb	9.05	H	3.0	345.6	^{133m}Te	55.4	M	0.18
323.8	^{131}Sb	23.03	M	1.2	345.9	^{181}Hf	42.39	D	15.12
323.9	†^{223}Ra	11.43	D	3.99	346.8	†^{223}Ra	11.43	D	0.181
323.9	^{151}Pm	28.40	H	1.22	347.3	^{133m}Te	55.4	M	0.53
324.9	^{138}Cs	32.5	M	0.290	347.8	^{149}Nd	1.728	H	0.161
325.3	^{117m}Cd	3.36	H	0.13	348.9	†^{214}Bi	19.9	M	0.104
325.8	^{131}I	8.0252	D	0.273	349.2	^{149}Nd	1.728	H	1.38
325.8	^{151}Pm	28.40	H	0.106	349.8	^{151}Pm	28.40	H	0.142
326.0	^{133m}Te	55.4	M	0.22	350.0	^{105}Ru	4.44	H	0.289
326.1	^{105}Ru	4.44	H	1.06	350.2	^{105}Ru	4.44	H	1.02
326.2	$_{131}Sb$	23.03	M	1.2	350.5	†^{227}Th	18.68	D	0.110
326.6	^{149}Nd	1.728	H	4.56	350.6	^{143}Ce	33.039	H	3.23
327.4	†^{228}Ac	6.15	H	0.12	351.0	^{125}Sn	9.64	D	0.26
328.0	†^{228}Ac	6.15	H	2.95	351.1	†^{211}Bi	2.14	M	13.02
328.0	†^{212}Bi	60.55	M	0.125	351.1	^{134}I	52.5	M	0.42
328.4	†^{223}Ra	11.43	D	0.209	351.1	^{78}As	90.7	M	0.162
328.8	^{140}La	1.67858	D	20.3	351.3	^{131m}Te	33.25	H	0.202
329.4	^{152}Eu	13.517	Y	0.1213	351.6	^{149}Nd	1.728	H	1.17
329.8	^{151}Pm	28.40	H	0.221	351.9	†^{214}Pb	26.8	M	35.60
329.9	†^{227}Th	18.68	D	2.9	353.3	^{151}Pm	28.40	H	0.106
330.1	†^{231}Pa	3.276E+4	Y	1.36	354.3	$_{78}As$	90.7	M	1.9
330.4	^{97}Zr	16.749	H	0.143	354.7	^{131m}Te	33.25	H	0.220
330.9	^{105}Ru	4.44	H	0.67	354.7	^{84}Br	31.76	M	0.30
330.9	^{130}Sb	39.5	M	78	355.4	^{97}Zr	16.749	H	2.09
332.1	^{125}Sn	9.64	D	1.4	355.4	^{133m}Te	55.4	M	0.52
332.4	^{237}U	6.75	D	1.200	357.0	^{128}Sb	9.05	H	1.5
332.4	†^{228}Ac	6.15	H	0.40	357.1	†^{231}Pa	3.276E+4	Y	0.168
333.1	^{113}Ag	5.37	H	0.598	358.4	^{135}Xe	9.14	H	0.221
333.2	^{129}Sb	4.366	H	0.171	358.9	^{157}Eu	15.18	H	0.31
334.0	†^{223}Ra	11.43	D	0.101	359.2	^{129}Sb	4.366	H	2.39
334.2	^{133m}Te	55.4	M	2.7	360.1	^{149}Nd	1.728	H	0.153
334.3	^{133m}Te	55.4	M	6.8	360.3	^{127}Te	9.35	H	0.135
334.3	^{131m}Te	33.25	H	9.22	361.1	^{133}I	20.83	H	0.11
334.3	^{239}Np	2.356	D	2.056	361.9	^{135}I	6.58	H	0.187
334.4	†^{227}Th	18.68	D	1.14	362.2	^{88}Kr	2.825	H	2.25
334.4	^{157}Eu	15.18	H	0.84	363.1	^{133m}Te	55.4	M	0.40
334.7	^{88}Kr	2.825	H	0.145	363.3	^{132}I	2.295	H	0.49
334.8	^{59}Fe	44.490	D	0.270	363.9	^{138}Cs	32.5	M	0.244
335.4	^{131m}Te	33.25	H	0.131	364.2	$_{129}Sb$	4.366	H	0.305
336.2	^{115}Cd	53.46	H	1.000	364.4	^{113}Ag	5.37	H	0.140
336.2	^{115m}In	4.486	H	45.8	364.5	^{131}I	8.0252	D	81.5
337.5	^{77}Ge	11.211	H	0.21	365.0	^{131m}Te	33.25	H	1.16
338.3	†^{223}Ra	11.43	D	2.84	365.3	$_{138}Cs$	32.5	M	0.191
338.3	†^{228}Ac	6.15	H	11.27	366.1	^{128}Sb	9.05	H	1.5
338.5	†^{214}Bi	19.9	M	0.11	366.3	^{65}Ni	2.51719	H	4.81
338.6	^{77}Ge	11.211	H	0.72	366.4	^{99}Mo	65.924	H	1.200
339.4	^{113}Ag	5.37	H	0.638	366.6	^{149}Nd	1.728	H	0.54
340.1	^{151}Pm	28.40	H	22.5	366.9	^{117m}Cd	3.36	H	3.33
340.5	^{136}Cs	13.01	D	46.8	367.3	^{142}La	91.1	M	0.1422
340.7	†^{231}Pa	3.276E+4	Y	0.177	367.5	^{77}Ge	11.211	H	14.5
341.0	†^{228}Ac	6.15	H	0.369	367.8	^{152}Eu	13.517	Y	0.859
342.6	†^{227}Th	18.68	D	0.35	367.9	^{133m}Te	55.4	M	0.18
342.8	^{133m}Te	55.4	M	0.40	370.5	^{157}Eu	15.18	H	11.2
342.9	†^{223}Ra	11.43	D	0.222	370.9	^{237}U	6.75	D	0.1073
342.9	^{131m}Te	33.25	H	0.37	371.7	†^{223}Ra	11.43	D	0.487
344.3	^{152}Eu	13.517	Y	26.59	374.5	$_{192}Ir$	73.829	D	0.727
344.4	^{133m}Te	55.4	M	0.58	376.8	^{133m}Te	55.4	M	0.18

γ-ray energy (keV)	Nuclide name	Half-life	Half-life unit	Emission rate (%)	γ-ray energy (keV)	Nuclide name	Half-life	Half-life unit	Emission rate (%)
379.9	^{151}Pm	28.40	H	0.95	416.4	^{77}Ge	11.211	H	22.7
379.9	^{91}Sr	9.65	H	0.147	416.5	^{192}Ir	73.829	D	0.670
379.9	^{157}Eu	15.18	H	0.27	416.8	^{132}I	2.295	H	0.47
380.5	^{125}Sb	2.75856	Y	1.517	417.4	^{131m}Te	33.25	H	0.269
382.0	^{84}Br	31.76	M	0.56	417.6	^{133}I	20.83	H	0.154
382.1	^{113}Ag	5.37	H	0.145	417.6	^{135}I	6.58	H	3.53
383.9	^{131m}Te	33.25	H	0.19	417.9	^{127}Te	9.35	H	0.99
384.0	^{133m}Te	55.4	M	0.13	417.9	$_{130}$I	12.36	H	34.2
384.7	^{149}Nd	1.728	H	0.267	419.1	⁎^{75}Ge	82.78	M	0.185
386.8	†^{214}Bi	19.9	M	0.295	419.7	^{77}Ge	11.211	H	1.22
387.9	$_{132}$I	2.295	H	0.17	419.8	$_{117}$Cd	2.49	H	0.18
387.9	^{132}I	2.295	H	0.17	420.1	^{157}Eu	15.18	H	0.94
387.9	^{132}I	2.295	H	0.17	420.2	^{142}La	91.1	M	0.237
388.0	^{117}Cd	2.49	H	0.31	421.6	^{138}Cs	32.5	M	0.427
388.9	†^{214}Bi	19.9	M	0.402	422.9	^{133}I	20.83	H	0.311
390.5	^{88}Kr	2.825	H	0.64	423.6	^{149}Nd	1.728	H	7.4
391.0	^{78}As	90.7	M	0.124	423.7	^{140}Ba	12.751	D	3.10
391.7	^{113}Sn	115.09	D	64.97	425.2	^{149}Nd	1.728	H	0.272
391.8	^{127}Sb	3.85	D	0.96	427.1	†^{211}Pb	36.1	M	1.76
392.4	^{133m}Te	55.4	M	0.142	427.4	^{157}Eu	15.18	H	0.162
393.4	^{105}Ru	4.44	H	3.77	427.9	^{125}Sb	2.75856	Y	29.6
393.4	^{157}Eu	15.18	H	0.124	429.0	^{133m}Te	55.4	M	1.77
393.5	^{67}Ga	3.2617	D	4.56	429.9	^{135}I	6.58	H	0.304
393.6	^{142}La	91.1	M	0.1896	430.5	^{92}Sr	2.611	H	3.28
397.0	^{133m}Te	55.4	M	0.58	431.8	^{132}I	2.295	H	0.47
397.2	^{117}Cd	2.49	H	0.20	432.4	^{131m}Te	33.25	H	0.64
398.2	^{147}Nd	10.98	D	0.912	432.5	$_{140}$La	1.67858	D	2.90
399.0	^{157}Eu	15.18	H	1.34	433.0	^{143}Ce	33.039	H	0.159
399.0	^{77}Ge	11.211	H	0.105	433.3	^{142}La	91.1	M	0.379
400.3	^{124}Sb	60.20	D	0.139	433.4	^{134}I	52.5	M	4.15
400.4	^{97}Zr	16.749	H	0.245	433.7	^{135}I	6.58	H	0.554
400.7	^{75}Se	119.78	D	11.41	433.8	^{131}Sb	23.03	M	2.0
401.3	^{154}Eu	8.601	Y	0.188	433.9	^{108m}Ag	438	Y	90.5
401.3	^{203}Pb	51.92	H	3.35	434.2	^{117}Cd	2.49	H	9.8
401.8	†^{219}Rn	3.96	S	6.6	434.4	^{157}Eu	15.18	H	0.36
402.6	^{87}Kr	76.3	M	50	434.4	$_{156}$Eu	15.19	D	0.209
403.0	^{135}I	6.58	H	0.232	434.7	^{129}Sb	4.366	H	0.1113
404.3	^{128}Sb	9.05	H	1.00	435.0	^{129}Sb	4.366	H	0.212
404.6	^{129}Sb	4.366	H	1.172	435.1	^{134}Te	41.8	M	18.9
404.9	†^{211}Pb	36.1	M	3.78	435.3	^{133m}Te	55.4	M	0.97
405.5	^{134}I	52.5	M	7.37	437.6	^{140}Ba	12.751	D	1.929
405.7	†^{214}Bi	19.9	M	0.169	439.4	^{117}Cd	2.49	H	0.11
406.0	^{133m}Te	55.4	M	0.31	439.4	^{117m}Cd	3.36	H	0.18
407.0	^{151}Pm	28.40	H	0.187	439.5	^{77}Ge	11.211	H	0.207
408.0	^{135}Xe	9.14	H	0.358	439.9	^{147}Nd	10.98	D	1.28
408.1	^{125}Sb	2.75856	Y	0.184	440.4	†^{228}Ac	6.15	H	0.121
409.0	^{138}Cs	32.5	M	4.66	440.9	^{151}Pm	28.40	H	1.51
409.1	^{157}Eu	15.18	H	2.72	441.0	^{127}Sb	3.85	D	0.7
409.5	†^{228}Ac	6.15	H	1.92	443.6	^{149}Nd	1.728	H	1.15
409.7	^{129}Sb	4.366	H	0.231	443.6	^{125}Sb	2.75856	Y	0.306
410.5	^{147}Nd	10.98	D	0.150	443.8	^{103}Ru	39.247	D	0.339
410.7	^{157}Eu	15.18	H	17.8	444.0	^{152}Eu	13.517	Y	2.827
411.0	^{134}I	52.5	M	0.57	444.0	^{152}Eu	13.517	Y	0.298
411.1	^{152}Eu	13.517	Y	2.237	444.1	^{124}Sb	60.20	D	0.1889
411.8	^{198}Au	2.6941	D	95.62	444.5	^{154}Eu	8.601	Y	0.547
412.1	^{127}Sb	3.85	D	3.8	444.9	^{133m}Te	55.4	M	1.64
413.2	^{133m}Te	55.4	M	0.53	445.0	† $_{223}$Ra	11.43	D	1.29
413.5	^{105}Ru	4.44	H	2.27	445.1	^{127}Sb	3.85	D	4.3
414.8	^{135}I	6.58	H	0.301	445.7	^{151}Pm	28.40	H	4.0
416.0	^{152}Eu	13.517	Y	0.1088	445.7	$_{128}$Sb	9.05	H	1.5

γ-ray energy (keV)	Nuclide name	Half-life	Half-life unit	Emission rate (%)	γ-ray energy (keV)	Nuclide name	Half-life	Half-life unit	Emission rate (%)
446.2	^{132}I	2.295	H	0.60	479.5	^{90m}Y	3.19	H	90.74
446.8	^{110m}Ag	249.83	D	3.70	479.5	^{187}W	24.000	H	26.6
448.5	^{92}Y	3.54	H	2.3	480.4	†^{214}Pb	26.8	M	0.337
449.9	⁎^{63}Zn	38.47	M	0.236	482.2	^{181}Hf	42.39	D	80.5
450.8	^{157}Eu	15.18	H	1.24	483.6	^{130}Sb	39.5	M	2.2
451.0	^{127}Sb	3.85	D	0.18	484.6	^{192}Ir	73.829	D	3.19
451.4	^{151}Pm	28.40	H	0.29	484.8	^{117m}Cd	3.36	H	1.02
451.6	^{135}I	6.58	H	0.316	484.9	⁎^{74}Ga	8.12	M	1.06
452.3	^{131m}Te	33.25	H	1.5	487.0	^{140}La	1.67858	D	45.5
453.0	†^{212}Bi	60.55	M	0.363	487.1	†^{214}Pb	26.8	M	0.432
453.4	^{129}Sb	4.366	H	0.538	487.4	^{129}Te	69.6	M	1.42
454.5	^{128}Sb	9.05	H	1.5	487.4	^{133m}Te	55.4	M	0.44
454.8	†^{214}Bi	19.9	M	0.292	488.0	^{132}I	2.295	H	0.23
455.4	^{130}Sb	39.5	M	4.8	488.0	^{132}I	2.295	H	0.23
456.0	^{127}Sb	3.85	D	0.11	488.7	^{152}Eu	13.517	Y	0.414
456.7	^{131}Sb	23.03	M	0.7	488.9	^{134}I	52.5	M	1.45
457.8	^{130}I	12.36	H	0.237	489.1	^{192}Ir	73.829	D	0.438
458.9	^{134}I	52.5	M	1.31	489.2	^{147}Nd	10.98	D	0.155
459.5	^{128}Sb	9.05	H	1.5	489.5	^{105}Ru	4.44	H	0.55
459.6	^{129}Te	69.6	M	7.7	490.3	^{151}Pm	28.40	H	0.126
460.9	^{157}Eu	15.18	H	0.99	490.3	^{156}Eu	15.19	D	0.160
460.9	^{117m}Cd	3.36	H	1.62	490.4	^{143}Ce	33.039	H	2.16
461.0	^{134}Te	41.8	M	9.7	491.3	^{92}Sr	2.611	H	0.27
461.4	^{77}Ge	11.211	H	1.33	492.4	^{115}Cd	53.46	H	8.03
462.0	†^{214}Pb	26.8	M	0.212	492.6	^{92}Y	3.54	H	0.49
462.2	^{78}As	90.7	M	0.59	493.0	^{133m}Te	55.4	M	0.62
462.2	^{133m}Te	55.4	M	1.24	493.0	⁎^{74}Ga	8.12	M	5.0
462.5	^{130}Sb	39.5	M	0.80	495.0	^{133m}Te	55.4	M	0.155
462.8	^{138}Cs	32.5	M	30.7	497.0	^{78}As	90.7	M	0.18
462.9	^{131m}Te	33.25	H	1.76	497.1	^{103}Ru	39.247	D	91.0
463.0	†^{228}Ac	6.15	H	4.40	497.6	⁎^{74}Ga	8.12	M	0.96
463.0	^{117}Cd	2.49	H	0.75	497.8	^{117}Cd	2.49	H	0.11
463.4	^{125}Sb	2.75856	Y	10.49	499.3	^{105}Ru	4.44	H	2.0
464.0	^{133m}Te	55.4	M	0.22	500.0	^{129}Sb	4.366	H	0.430
464.6	^{134}Te	41.8	M	4.7	500.1	^{105}Ru	4.44	H	0.55
465.5	^{134}I	52.5	M	0.36	502.8	^{127}Sb	3.85	D	0.8
468.0	^{130}Sb	39.5	M	18.0	503.0	^{131}I	8.0252	D	0.359
468.1	^{192}Ir	73.829	D	47.84	503.5	^{152}Eu	13.517	Y	0.1524
468.2	^{131m}Te	33.25	H	0.30	503.7	^{78}As	90.7	M	0.42
468.8	⁎^{75}Ge	82.78	M	0.223	503.8	†^{228}Ac	6.15	H	0.182
469.4	^{105}Ru	4.44	H	17.5	504.7	⁎^{74}Ga	8.12	M	0.10
469.8	†^{214}Bi	19.9	M	0.132	505.3	^{129}Sb	4.366	H	0.518
469.9	^{125}Sn	9.64	D	1.5	505.8	^{132}I	2.295	H	4.94
470.1	^{105}Ru	4.44	H	0.184	506.7	^{130}Sb	39.5	M	2.0
470.4	^{157}Eu	15.18	H	0.202	507.2	^{136}Cs	13.01	D	1.00
471.1	⁎ ^{74}Ga	8.12	M	0.39	507.2	^{133m}Te	55.4	M	0.35
471.8	^{88}Kr	2.825	H	0.73	507.6	^{97}Zr	16.749	H	5.03
471.9	^{133m}Te	55.4	M	0.66	507.9	^{65}Ni	2.51719	H	0.293
472.7	^{156}Eu	15.19	D	0.145	509.0	†^{228}Ac	6.15	H	0.45
473.0	^{127}Sb	3.85	D	25.8	510.5	^{130}I	12.36	H	0.85
473.6	^{132}I	2.295	H	0.17	510.5	^{133}I	20.83	H	1.83
474.6	^{157}Eu	15.18	H	2.56	510.8	†^{208}Tl	3.053	M	22.60
475.4	^{134}Cs	2.0652	Y	1.477	511.8	^{187}W	24.000	H	0.807
475.5	^{77}Ge	11.211	H	1.07	511.9	^{106}Rh	30.07	S	20.4
476.0	^{181}Hf	42.39	D	0.703	513.4	^{97}Zr	16.749	H	0.55
477.6	† ^{7}Be	53.22	D	10.44	513.7	^{105}Ru	4.44	H	0.20
478.2	^{132}I	2.295	H	0.17	514.0	^{85}Kr	10.739	Y	0.434
478.2	^{154}Eu	8.601	Y	0.2250	514.4	^{134}I	52.5	M	2.24
478.3	†^{228}Ac	6.15	H	0.209	514.4	^{129}Sb	4.366	H	0.147
478.6	^{133m}Te	55.4	M	0.75	514.7	^{142}La	91.1	M	0.14

γ-ray energy (keV)	Nuclide name	Half-life	Half-life unit	Emission rate (%)	γ-ray energy (keV)	Nuclide name	Half-life	Half-life unit	Emission rate (%)
516.3	^{151}Pm	28.40	H	0.194	563.2	^{134}Cs	2.0652	Y	8.338
516.7	^{138}Cs	32.5	M	0.43	564.0	^{152}Eu	13.517	Y	0.494
519.7	^{133m}Te	55.4	M	0.22	564.2	^{122}Sb	2.7238	D	70.67
520.6	^{77}Ge	11.211	H	0.28	564.4	^{117m}Cd	3.36	H	14.7
521.0	⁎^{74}Ga	8.12	M	0.12	565.0	^{151}Pm	28.40	H	0.353
522.7	^{132}I	2.295	H	16.0	565.5	^{134}I	52.5	M	0.95
523.1	^{129}Sb	4.366	H	1.55	566.0	^{134}Te	41.8	M	18.6
523.1	†^{228}Ac	6.15	H	0.103	566.4	^{152}Eu	13.517	Y	0.131
524.8	^{131m}Te	33.25	H	0.131	567.0	^{129}Sb	4.366	H	0.136
524.8	^{157}Eu	15.18	H	0.31	567.6	^{157}Eu	15.18	H	0.148
525.2	^{129}Sb	4.366	H	0.1644	569.3	^{134}Cs	2.0652	Y	15.373
525.5	^{124}Sb	60.20	D	0.138	569.4	^{77}Ge	11.211	H	0.15
525.6	^{133m}Te	55.4	M	0.22	569.7	^{207}Bi	31.55	Y	97.75
526.5	^{128}Sb	9.05	H	45	570.8	^{134}I	52.5	M	0.31
526.6	^{135m}Xe	15.29	M	80.6	570.9	†^{228}Ac	6.15	H	0.182
527.0	^{117}Cd	2.49	H	0.14	570.9	^{157}Eu	15.18	H	1.59
527.9	^{115}Cd	53.46	H	27.5	571.5	^{76}As	26.24	H	0.140
529.9	^{133}I	20.83	H	87.0	572.1	†^{228}Ac	6.15	H	0.150
530.7	^{131m}Te	33.25	H	0.101	574.1	^{133m}Te	55.4	M	0.58
531.0	^{147}Nd	10.98	D	13.4	574.1	^{133m}Te	55.4	M	0.97
531.6	^{142}La	91.1	M	0.1422	575.0	^{151}Pm	28.40	H	0.117
532.4	^{133m}Te	55.4	M	0.71	575.1	^{105}Ru	4.44	H	0.85
533.7	†^{214}Pb	26.8	M	0.181	576.0	^{135}I	6.58	H	0.129
534.9	^{133m}Te	55.4	M	0.84	578.1	^{142}La	91.1	M	1.33
535.4	^{132}I	2.295	H	0.51	580.1	†^{214}Pb	26.8	M	0.370
536.1	^{130}I	12.36	H	99.00	581.4	^{133m}Te	55.4	M	0.40
537.3	^{140}Ba	12.751	D	24.39	582.0	^{154}Eu	8.601	Y	0.893
539.1	^{130}I	12.36	H	1.40	582.0	^{187}W	24.000	H	0.1308
539.3	^{105}Ru	4.44	H	0.114	582.6	^{77}Ge	11.211	H	0.80
540.3	^{133m}Te	55.4	M	0.22	582.9	^{128}Sb	9.05	H	1.00
540.5	^{149}Nd	1.728	H	6.6	583.2	†^{208}Tl	3.053	M	85.0
540.8	^{134}I	52.5	M	7.66	583.4	†^{228}Ac	6.15	H	0.111
540.9	⁎^{74}Ga	8.12	M	0.16	584.0	^{113}Ag	5.37	H	0.21
541.4	^{131m}Te	33.25	H	0.108	584.2	^{127}Sb	3.85	D	0.33
543.3	^{127}Sb	3.85	D	2.9	586.0	^{130}I	12.36	H	1.69
544.6	^{129}Sb	4.366	H	15.42	586.3	^{152}Eu	13.517	Y	0.455
545.0	^{117m}Cd	3.36	H	0.16	586.3	^{131m}Te	33.25	H	1.90
545.3	^{78}As	90.7	M	3.0	586.4	^{133m}Te	55.4	M	0.22
546.5	†^{228}Ac	6.15	H	0.201	587.2	^{143}Ce	33.039	H	0.267
546.6	^{135}I	6.58	H	7.15	588.6	^{192}Ir	73.829	D	4.522
547.0	^{138}Cs	32.5	M	10.8	589.1	^{187}W	24.000	H	0.150
547.2	^{132}I	2.295	H	1.14	591.1	^{157}Eu	15.18	H	0.160
551.6	^{187}W	24.000	H	6.14	591.8	^{154}Eu	8.601	Y	4.95
551.8	⁎^{74}Ga	8.12	M	0.11	594.3	^{128}Sb	9.05	H	1.00
551.8	^{78}As	90.7	M	0.17	594.8	^{147}Nd	10.98	D	0.283
553.9	^{130}I	12.36	H	0.66	595.4	^{134}I	52.5	M	11.1
554.4	^{82}Br	35.282	H	71.7	595.5	^{130}Sb	39.5	M	1.00
555.6	^{91m}Y	49.71	M	95.0	595.8	⁎^{74}As	17.77	D	59
555.9	^{149}Nd	1.728	H	0.59	595.9	⁎^{74}Ga	8.12	M	91.80
556.7	^{129m}Te	33.6	D	0.118	597.3	^{117m}Cd	3.36	H	0.131
556.8	^{149}Nd	1.728	H	0.44	599.5	^{156}Eu	15.19	D	2.08
557.1	^{103}Ru	39.247	D	0.841	600.6	^{125}Sb	2.75856	Y	17.65
557.5	^{154}Eu	8.601	Y	0.269	601.5	^{133m}Te	55.4	M	0.102
557.9	^{77}Ge	11.211	H	16.8	602.1	^{131m}Te	33.25	H	0.30
558.4	^{114m}In	49.51	D	4.4	602.4	^{97}Zr	16.749	H	1.38
559.1	^{76}As	26.24	H	45.0	602.7	^{124}Sb	60.20	D	97.8
559.2	^{105}Ru	4.44	H	0.109	603.0	^{128}Sb	9.05	H	1.7
561.1	^{92}Y	3.54	H	2.4	603.5	^{127}Sb	3.85	D	4.5
562.5	†^{228}Ac	6.15	H	0.87	603.5	^{130}I	12.36	H	0.61
563.2	^{76}As	26.24	H	1.20	604.2	⁎^{74}Ga	8.12	M	2.85

γ-ray energy (keV)	Nuclide name	Half-life	Half-life unit	Emission rate (%)	γ-ray energy (keV)	Nuclide name	Half-life	Half-life unit	Emission rate (%)
604.4	^{192}Ir	73.829	D	8.216	634.8	⁎^{74}As	17.77	D	15.4
604.7	^{134}Cs	2.0652	Y	97.62	635.7	^{130}Sb	39.5	M	1.6
604.8	^{84}Br	31.76	M	1.7	636.0	^{125}Sb	2.75856	Y	11.22
605.1	^{133m}Te	55.4	M	1.02	636.2	^{128}Sb	9.05	H	36
606.2	^{129}Sb	4.366	H	0.146	636.2	^{151}Pm	28.40	H	1.42
606.4	^{82}Br	35.282	H	1.229	636.3	^{134}Te	41.8	M	1.68
606.7	^{125}Sb	2.75856	Y	4.98	636.5	^{133m}Te	55.4	M	0.18
607.3	^{133m}Te	55.4	M	0.13	637.0	^{131}I	8.0252	D	7.16
608.2	^{135}Xe	9.14	H	2.90	637.1	^{78}As	90.7	M	0.21
608.4	⁎^{74}Ga	8.12	M	14.4	637.8	^{127}Sb	3.85	D	0.44
608.4	⁎^{74}As	17.77	D	0.552	638.7	^{105}Ru	4.44	H	0.222
609.3	†^{214}Bi	19.9	M	45.49	639.0	⁎^{74}Ga	8.12	M	0.83
609.4	^{131m}Te	33.25	H	0.134	641.3	^{142}La	91.1	M	47.4
609.5	^{65}Ni	2.51719	H	0.155	642.3	^{131}Sb	23.03	M	24
610.3	^{103}Ru	39.247	D	5.76	642.3	^{133m}Te	55.4	M	0.71
612.1	^{103}Ru	39.247	D	0.105	642.7	^{131}I	8.0252	D	0.217
612.5	^{192}Ir	73.829	D	5.34	645.4	^{134}Te	41.8	M	0.89
613.8	^{78}As	90.7	M	54	645.9	^{124}Sb	60.20	D	7.42
614.3	^{108m}Ag	438	Y	89.8	646.2	^{142}La	91.1	M	0.14
614.4	^{77}Ge	11.211	H	0.53	646.3	^{156}Eu	15.19	D	6.3
615.2	^{181}Hf	42.39	D	0.233	647.5	^{133m}Te	55.4	M	15.5
616.2	^{106}Rh	30.07	S	0.75	647.9	^{129}Sb	4.366	H	0.124
617.5	^{117m}Cd	3.36	H	0.34	649.9	^{135}I	6.58	H	0.46
617.7	⁎^{75}Ge	82.78	M	0.114	650.5	^{132}I	2.295	H	2.57
618.0	^{133}I	20.83	H	0.544	650.8	^{92}Sr	2.611	H	0.37
618.4	^{187}W	24.000	H	7.57	652.3	^{127}Sb	3.85	D	0.37
619.1	^{82}Br	35.282	H	43.7	652.3	^{91}Sr	9.65	H	2.98
619.3	^{157}Eu	15.18	H	3.6	652.7	^{105}Ru	4.44	H	0.31
619.8	^{131}Sb	23.03	M	1.6	652.9	^{91}Sr	9.65	H	8.0
620.1	^{91}Sr	9.65	H	1.78	653.0	^{91}Sr	9.65	H	0.37
620.4	^{110m}Ag	249.83	D	2.73	653.3	^{133m}Te	55.4	M	0.49
620.9	^{132}I	2.295	H	0.39	654.2	^{128}Sb	9.05	H	17.0
621.2	^{132}I	2.295	H	1.58	654.3	^{151}Pm	28.40	H	0.241
621.3	^{133m}Te	55.4	M	0.40	654.3	^{129}Sb	4.366	H	2.97
621.8	^{134}I	52.5	M	10.6	654.7	^{130}Sb	39.5	M	2.00
621.9	^{106}Rh	30.07	S	9.93	654.8	^{149}Nd	1.728	H	8.0
622.8	^{157}Eu	15.18	H	0.99	655.6	^{157}Eu	15.18	H	0.188
623.3	^{133m}Te	55.4	M	0.22	656.2	^{105}Ru	4.44	H	2.1
624.8	^{77}Ge	11.211	H	0.190	656.5	^{152}Eu	13.517	Y	0.1441
625.3	^{154}Eu	8.601	Y	0.316	657.1	^{76}As	26.24	H	6.2
625.5	^{187}W	24.000	H	1.314	657.8	^{110m}Ag	249.83	D	95.61
625.7	^{131}Sb	23.03	M	2.4	657.9	^{78}As	90.7	M	0.27
626.3	^{110m}Ag	249.83	D	0.217	657.9	^{131}Sb	23.03	M	4
626.7	^{130}Sb	39.5	M	2.8	657.9	^{97}Nb	72.1	M	98.23
627.0	^{117}Cd	2.49	H	0.11	658.2	^{130}Sb	39.5	M	1.7
627.3	^{117m}Cd	3.36	H	0.236	659.0	^{132}I	2.295	H	0.10
628.0	^{134}I	52.5	M	2.22	660.8	^{117}Cd	2.49	H	0.11
628.7	^{157}Eu	15.18	H	0.101	660.9	^{91}Sr	9.65	H	0.101
628.7	^{128}Sb	9.05	H	31	661.7	^{137m}Ba	2.552	M	89.90
629.0	^{133m}Te	55.4	M	0.27	661.7	^{137}Cs	30.08	Y	85.10
630.2	^{132}I	2.295	H	13.3	663.5	^{117m}Cd	3.36	H	0.68
630.2	^{149}Nd	1.728	H	0.189	664.6	^{143}Ce	33.039	H	5.69
631.3	^{91}Sr	9.65	H	0.556	665.1	^{131m}Te	33.25	H	4.18
631.8	^{117m}Cd	3.36	H	2.80	665.3	^{76}As	26.24	H	0.36
631.9	^{77}Ge	11.211	H	7.4	665.4	†^{214}Bi	19.9	M	1.531
632.0	^{133m}Te	55.4	M	0.22	665.9	^{134}Te	41.8	M	1.18
632.3	^{105}Ru	4.44	H	0.151	667.1	^{128}Sb	9.05	H	2.5
632.5	^{124}Sb	60.20	D	0.1046	667.5	^{127}Sb	3.85	D	0.74
633.7	^{129}Sb	4.366	H	2.53	667.7	^{132}I	2.295	H	98.70
634.4	^{77}Ge	11.211	H	2.14	668.5	^{130}I	12.36	H	96

γ-ray energy (keV)	Nuclide name	Half-life	Half-life unit	Emission rate (%)	γ-ray energy (keV)	Nuclide name	Half-life	Half-life unit	Emission rate (%)
668.7	^{151}Pm	28.40	H	0.36	697.8	^{129}Sb	4.366	H	0.254
669.0	^{131}Sb	23.03	M	1.9	698.1	^{133m}Te	55.4	M	0.75
669.2	^{151}Pm	28.40	H	0.29	698.4	^{82}Br	35.282	H	28.4
669.2	^{130}Sb	39.5	M	1.10	698.5	^{127}Sb	3.85	D	3.64
669.6	⁎^{63}Zn	38.47	M	8.2	698.6	^{77}Ge	11.211	H	0.231
669.8	^{132}I	2.295	H	4.6	699.2	^{97}Zr	16.749	H	0.101
670.3	^{129}Sb	4.366	H	0.96	699.6	^{117}Cd	2.49	H	0.24
671.3	^{151}Pm	28.40	H	0.90	700.9	^{157}Eu	15.18	H	0.30
671.4	^{132}I	2.295	H	3.5	701.5	⁎^{74}Ga	8.12	M	0.77
671.4	^{125}Sb	2.75856	Y	1.791	701.7	†^{228}Ac	6.15	H	0.173
672.3	^{113}Ag	5.37	H	0.87	702.5	^{131m}Te	33.25	H	0.377
673.1	^{77}Ge	11.211	H	0.53	702.7	^{94}Nb	2.03E+4	Y	100.0
673.1	^{77}Ge	11.211	H	0.132	702.9	^{133m}Te	55.4	M	1.95
673.8	^{87}Kr	76.3	M	1.89	703.1	†^{214}Bi	19.9	M	0.472
674.6	^{152}Eu	13.517	Y	0.169	703.8	^{97}Zr	16.749	H	1.01
674.8	†^{228}Ac	6.15	H	2.1	704.2	^{151}Pm	28.40	H	0.34
675.8	^{145}Pr	5.984	H	0.514	704.6	†^{211}Pb	36.1	M	0.462
675.9	^{198}Au	2.6941	D	0.805	705.3	^{77}Ge	11.211	H	0.108
676.4	^{105}Ru	4.44	H	15.7	706.6	^{133}I	20.83	H	1.51
676.6	^{110m}Ag	249.83	D	0.143	706.7	^{134}I	52.5	M	0.83
676.6	^{154}Eu	8.601	Y	0.1672	706.7	^{110m}Ag	249.83	D	16.69
677.3	^{134}I	52.5	M	7.9	707.1	^{129}Sb	4.366	H	0.138
677.3	^{88}Kr	2.825	H	0.235	707.4	†^{228}Ac	6.15	H	0.155
677.6	^{110m}Ag	249.83	D	10.70	707.9	^{135}I	6.58	H	0.66
678.6	^{152}Eu	13.517	Y	0.473	708.1	^{110m}Ag	249.83	D	0.23
680.2	^{93}Y	10.18	H	0.67	709.3	^{151}Pm	28.40	H	0.137
680.2	^{133}I	20.83	H	0.650	709.3	^{124}Sb	60.20	D	1.353
680.5	^{203}Pb	51.92	H	0.75	709.9	^{156}Eu	15.19	D	0.88
680.6	^{113}Ag	5.37	H	0.695	710.4	^{133m}Te	55.4	M	0.58
680.9	^{130}Sb	39.5	M	6.5	712.3	^{77}Ge	11.211	H	0.86
681.8	^{90m}Y	3.19	H	0.32	712.7	^{117m}Cd	3.36	H	1.00
682.3	^{127}Sb	3.85	D	0.6	712.7	^{117}Cd	2.49	H	0.56
682.8	^{129}Sb	4.366	H	5.76	713.0	^{134}Te	41.8	M	4.7
683.2	^{157}Eu	15.18	H	0.24	713.1	^{131m}Te	33.25	H	1.38
683.6	^{138}Cs	32.5	M	0.108	713.8	^{124}Sb	60.20	D	2.276
683.9	^{128}Sb	9.05	H	3.0	714.4	^{77}Ge	11.211	H	7.5
684.2	^{129}Sb	4.366	H	0.622	715.0	⁎^{74}Ga	8.12	M	0.22
685.7	^{127}Sb	3.85	D	36.8	715.8	^{154}Eu	8.601	Y	0.187
685.8	^{187}W	24.000	H	33.2	716.4	^{117}Cd	2.49	H	0.20
685.9	^{147}Nd	10.98	D	0.886	717.7	^{151}Pm	28.40	H	4.1
685.9	^{131m}Te	33.25	H	0.149	718.9	^{133m}Te	55.4	M	0.66
686.1	^{130}I	12.36	H	1.07	719.3	^{152}Eu	13.517	Y	0.250
686.3	^{78}As	90.7	M	0.92	719.9	†^{214}Bi	19.9	M	0.392
686.6	^{130}Sb	39.5	M	3.2	721.9	^{143}Ce	33.039	H	5.39
687.0	^{110m}Ag	249.83	D	6.53	722.0	†^{208}Tl	3.053	M	0.24
687.5	^{78}As	90.7	M	0.65	722.2	^{127}Sb	3.85	D	1.88
687.5	^{157}Eu	15.18	H	1.20	722.4	^{78}As	90.7	M	0.146
688.6	^{129}Sb	4.366	H	0.164	722.8	^{124}Sb	60.20	D	10.76
688.7	^{152}Eu	13.517	Y	0.856	722.9	^{108m}Ag	438	Y	90.8
690.1	^{135}I	6.58	H	0.129	722.9	^{131}I	8.0252	D	1.77
690.5	^{97}Zr	16.749	H	0.183	723.3	^{154}Eu	8.601	Y	20.06
692.4	^{154}Eu	8.601	Y	1.777	723.5	^{156}Eu	15.19	D	5.4
692.7	^{122}Sb	2.7238	D	3.85	723.5	^{133m}Te	55.4	M	0.22
692.9	^{128}Sb	9.05	H	2.0	724.2	^{95}Zr	64.032	D	44.27
694.8	^{129}Sb	4.366	H	0.403	724.3	^{105}Ru	4.44	H	47.3
694.9	^{78}As	90.7	M	16.7	725.2	^{114m}In	49.51	D	4.4
695.6	^{131m}Te	33.25	H	0.38	726.3	^{131}Sb	23.03	M	4.1
695.9	^{129m}Te	33.6	D	3.0	726.9	†^{228}Ac	6.15	H	0.62
696.3	^{149}Nd	1.728	H	0.171	727.0	^{132}I	2.295	H	2.2
696.5	^{144}Pr	17.28	M	1.342	727.2	^{132}I	2.295	H	3.2

γ-ray energy (keV)	Nuclide name	Half-life	Half-life unit	Emission rate (%)	γ-ray energy (keV)	Nuclide name	Half-life	Half-life unit	Emission rate (%)
727.3	†^{212}Bi	60.55	M	6.67	767.2	^{134}Te	41.8	M	29.5
727.6	^{128}Sb	9.05	H	4.0	768.4	†^{214}Bi	19.9	M	4.894
728.4	^{132}I	2.295	H	1.6	768.4	^{133}I	20.83	H	0.460
728.6	^{117}Cd	2.49	H	0.24	769.0	^{129}Sb	4.366	H	0.321
729.6	^{129m}Te	33.6	D	0.70	769.1	^{151}Pm	28.40	H	0.106
730.7	^{134}I	52.5	M	1.83	770.6	^{65}Ni	2.51719	H	0.104
730.8	^{117m}Cd	3.36	H	0.1048	771.7	^{76}As	26.24	H	0.122
731.9	^{133m}Te	55.4	M	0.49	772.0	^{97}Zr	16.749	H	0.24
732.0	^{130}Sb	39.5	M	22.0	772.3	†^{228}Ac	6.15	H	1.49
733.5	^{56}Co	77.236	D	0.191	772.6	^{132}I	2.295	H	75.6
733.9	⁎^{74}Ga	8.12	M	0.110	772.8	^{151}Pm	28.40	H	0.90
734.0	^{133m}Te	55.4	M	1.42	772.9	^{187}W	24.000	H	5.02
736.1	^{151}Pm	28.40	H	0.47	773.3	^{138}Cs	32.5	M	0.233
736.5	^{84}Br	31.76	M	1.29	773.4	^{129}Sb	4.366	H	2.82
737.1	^{129}Sb	4.366	H	0.444	773.7	^{131m}Te	33.25	H	36.8
739.2	^{134}I	52.5	M	0.69	773.7	^{128}Sb	9.05	H	1.5
739.5	^{99}Mo	65.924	H	12.20	774.1	^{131m}Te	33.25	H	0.52
739.5	^{130}I	12.36	H	82	775.0	^{97}Zr	16.749	H	0.1862
739.8	^{133m}Te	55.4	M	0.49	776.5	^{82}Br	35.282	H	83.6
740.1	^{76}As	26.24	H	0.117	777.9	^{99}Mo	65.924	H	4.31
742.6	^{134}Te	41.8	M	15.3	778.9	^{152}Eu	13.517	Y	12.93
742.8	†^{234m}Pa	1.159	M	0.1066	779.7	^{133m}Te	55.4	M	1.42
742.9	^{133m}Te	55.4	M	0.31	780.0	^{132}I	2.295	H	1.18
743.3	^{128}Sb	9.05	H	100	781.3	^{77}Ge	11.211	H	1.07
743.4	^{97m}Nb	58.7	S	97.90	782.1	^{138}Cs	32.5	M	0.33
743.4	^{97}Zr	16.749	H	93.09	782.1	^{133m}Te	55.4	M	0.27
743.6	^{77}Ge	11.211	H	0.190	782.1	†^{228}Ac	6.15	H	0.485
744.2	^{131m}Te	33.25	H	1.53	782.5	^{131m}Te	33.25	H	7.51
744.3	^{110m}Ag	249.83	D	4.77	783.7	^{127}Sb	3.85	D	15.1
745.2	^{187}W	24.000	H	0.368	784.3	⁎^{74}Ga	8.12	M	0.67
745.8	^{77}Ge	11.211	H	1.03	784.4	^{132}I	2.295	H	0.38
745.9	^{127}Sb	3.85	D	0.15	784.8	^{77}Ge	11.211	H	1.38
748.1	^{117}Cd	2.49	H	0.56	785.1	^{151}Pm	28.40	H	0.221
748.1	^{117m}Cd	3.36	H	4.5	785.4	†^{212}Bi	60.55	M	1.102
748.3	^{145}Pr	5.984	H	0.525	785.5	^{135}I	6.58	H	0.152
749.8	^{91}Sr	9.65	H	23.7	786.0	†^{214}Pb	26.8	M	1.06
749.9	^{77}Ge	11.211	H	0.93	786.4	†^{214}Bi	19.9	M	0.32
751.6	^{140}La	1.67858	D	4.33	786.4	^{129}Sb	4.366	H	1.071
752.6	^{157}Eu	15.18	H	0.26	787.2	^{129}Sb	4.366	H	1.74
752.8	^{151}Pm	28.40	H	1.28	787.7	^{56}Co	77.236	D	0.311
752.9	†^{214}Bi	19.9	M	0.128	788.2	^{117m}Cd	3.36	H	0.50
753.3	^{133m}Te	55.4	M	0.27	788.3	^{88}Kr	2.825	H	0.53
754.0	^{128}Sb	9.05	H	100	789.0	^{77}Ge	11.211	H	0.101
755.3	†^{228}Ac	6.15	H	1.00	789.7	^{133m}Te	55.4	M	0.35
756.7	^{95}Zr	64.032	D	54.38	790.3	^{88}Kr	2.825	H	0.125
756.8	^{133m}Te	55.4	M	0.27	790.7	^{124}Sb	60.20	D	0.739
756.8	^{154}Eu	8.601	Y	4.52	793.4	^{130}Sb	39.5	M	100
761.1	^{129}Sb	4.366	H	4.32	793.8	^{131m}Te	33.25	H	13.4
761.4	^{91}Sr	9.65	H	0.576	794.4	^{77}Ge	11.211	H	0.30
762.7	^{157}Eu	15.18	H	0.37	794.7	^{133m}Te	55.4	M	0.84
762.7	^{117m}Cd	3.36	H	1.73	794.9	†^{228}Ac	6.15	H	4.25
763.1	†^{208}Tl	3.053	M	1.79	795.9	^{134}Cs	2.0652	Y	85.46
763.9	^{110m}Ag	249.83	D	22.60	797.7	^{135}I	6.58	H	0.17
764.9	^{152}Eu	13.517	Y	0.189	797.7	^{156}Eu	15.19	D	0.109
765.8	^{95}Nb	34.991	D	99.808	800.2	^{130}I	12.36	H	0.101
766.1	^{138}Cs	32.5	M	0.146	800.3	^{125}Sn	9.64	D	1.1
766.4	†^{234m}Pa	1.159	M	0.317	800.5	^{133m}Te	55.4	M	0.89
766.5	†^{211}Pb	36.1	M	0.617	802.0	^{134}Cs	2.0652	Y	8.688
766.7	^{134}I	52.5	M	4.15	802.1	^{129}Te	69.6	M	0.192
766.8	^{77}Ge	11.211	H	0.83	802.2	^{84}Br	31.76	M	6.0

γ-ray energy (keV)	Nuclide name	Half-life	Half-life unit	Emission rate (%)	γ-ray energy (keV)	Nuclide name	Half-life	Half-life unit	Emission rate (%)
802.7	^{128}Sb	9.05	H	1.20	839.5	^{130}Sb	39.5	M	100
803.1	†^{210}Po	138.376	D	0.00103	840.2	^{117}Cd	2.49	H	0.81
803.1	†^{206}Tl	4.202	M	0.0050	840.4	†^{228}Ac	6.15	H	0.91
804.5	^{97}Zr	16.749	H	0.61	841.2	^{156}Eu	15.19	D	0.208
805.1	^{133m}Te	55.4	M	0.13	841.5	^{78}As	90.7	M	0.16
805.6	^{97}Zr	16.749	H	0.2793	841.6	^{152}Eu	13.517	Y	0.168
806.2	†^{214}Bi	19.9	M	1.264	842.6	^{78}As	90.7	M	1.08
807.9	^{151}Pm	28.40	H	0.56	843.2	^{77}Ge	11.211	H	0.216
808.3	^{130}I	12.36	H	0.236	844.1	^{134}Te	41.8	M	1.2
808.8	^{149}Nd	1.728	H	0.189	844.3	^{92}Y	3.54	H	1.25
809.3	⁎^{74}Ga	8.12	M	0.29	844.9	^{131m}Te	33.25	H	0.15
809.5	^{132}I	2.295	H	2.6	845.4	^{154}Eu	8.601	Y	0.568
810.4	^{77}Ge	11.211	H	2.38	845.4	^{87}Kr	76.3	M	7.3
810.5	^{152}Eu	13.517	Y	0.317	845.8	^{128}Sb	9.05	H	2.5
810.8	^{58}Co	70.86	D	99.450	845.9	^{105}Ru	4.44	H	0.63
811.8	^{156}Eu	15.19	D	9.7	846.8	⁎^{56}Mn	2.5789	H	98.85
812.0	^{132}I	2.295	H	5.5	846.8	^{56}Co	77.236	D	99.9399
813.0	^{129}Sb	4.366	H	48.2	847.0	^{134}I	52.5	M	96
813.4	^{77}Ge	11.211	H	0.139	848.7	^{151}Pm	28.40	H	0.281
813.6	^{128}Sb	9.05	H	13.0	850.3	^{88}Kr	2.825	H	0.173
814.3	^{87}Kr	76.3	M	0.164	850.7	^{154}Eu	8.601	Y	0.243
815.5	^{154}Eu	8.601	Y	0.511	850.7	^{117}Cd	2.49	H	0.12
815.8	^{140}La	1.67858	D	23.28	852.0	^{105}Ru	4.44	H	0.156
816.3	^{133m}Te	55.4	M	0.62	852.2	^{131m}Te	33.25	H	19.9
816.4	^{134}I	52.5	M	0.62	852.2	^{131m}Te	33.25	H	0.37
817.0	^{127}Sb	3.85	D	0.40	854.6	^{131}Sb	23.03	M	3.3
817.7	^{151}Pm	28.40	H	0.17	854.9	^{97}Zr	16.749	H	0.357
818.0	^{110m}Ag	249.83	D	7.43	855.7	^{130}Sb	39.5	M	1.6
818.5	^{136}Cs	13.01	D	99.70	856.1	^{131m}Te	33.25	H	0.60
818.5	^{136}Ba	0.3084	S	99.706	856.3	^{133}I	20.83	H	1.24
819.3	^{133m}Te	55.4	M	0.13	857.3	^{134}I	52.5	M	6.70
819.5	^{129}Sb	4.366	H	1.39	858.4	^{156}Eu	15.19	D	0.205
820.4	^{156}Eu	15.19	D	0.169	859.5	^{149}Pm	53.08	H	0.109
820.5	^{133}I	20.83	H	0.155	860.4	^{117m}Cd	3.36	H	7.9
820.6	^{127}Sb	3.85	D	0.22	860.6	†^{208}Tl	3.053	M	12.50
820.8	^{91}Sr	9.65	H	0.161	860.8	^{128}Sb	9.05	H	0.40
821.2	†^{214}Bi	19.9	M	0.161	861.3	^{117}Cd	2.49	H	0.28
822.0	^{105}Ru	4.44	H	0.21	861.6	^{142}La	91.1	M	1.66
822.5	^{125}Sn	9.64	D	4.3	862.3	^{88}Kr	2.825	H	0.67
822.8	^{131m}Te	33.25	H	5.90	862.6	^{117}Cd	2.49	H	0.61
823.0	^{99}Mo	65.924	H	0.134	863.0	^{132}I	2.295	H	0.56
823.3	^{77}Ge	11.211	H	0.63	864.0	^{58}Co	70.86	D	0.686
824.9	^{131}Sb	23.03	M	2.6	864.0	^{133m}Te	55.4	M	12.5
826.5	†^{214}Bi	19.9	M	0.117	864.0	^{134}I	52.5	M	0.19
827.1	^{133m}Te	55.4	M	0.44	864.6	^{187}W	24.000	H	0.409
827.6	^{117m}Cd	3.36	H	0.26	865.1	^{131m}Te	33.25	H	0.19
827.8	^{82}Br	35.282	H	24.2	865.8	^{156}Eu	15.19	D	0.188
828.1	^{78}As	90.7	M	8.1	866.0	^{131}Sb	23.03	M	0.47
829.8	^{97}Zr	16.749	H	0.239	867.0	^{156}Eu	15.19	D	1.33
829.8	^{130}Sb	39.5	M	1.8	867.4	^{152}Eu	13.517	Y	4.23
830.5	†^{228}Ac	6.15	H	0.540	867.6	^{76}As	26.24	H	0.131
831.8	^{117}Cd	2.49	H	2.26	867.8	⁎^{74}Ga	8.12	M	8.7
832.0	†^{211}Pb	36.1	M	3.52	867.8	^{140}La	1.67858	D	5.50
834.8	^{88}Kr	2.825	H	13.0	871.1	^{94}Nb	2.03E+4	Y	100.0
834.8	^{54}Mn	312.20	D	99.9760	871.7	^{138}Cs	32.5	M	5.11
835.7	†^{228}Ac	6.15	H	1.61	873.2	^{154}Eu	8.601	Y	12.08
835.8	^{128}Sb	9.05	H	1.0	873.5	^{106}Rh	30.07	S	0.439
836.4	^{87}Kr	76.3	M	0.77	874.9	^{129}Sb	4.366	H	0.534
836.8	^{135}I	6.58	H	6.69	875.2	^{77}Ge	11.211	H	0.82
839.1	†^{214}Pb	26.8	M	0.583	875.3	^{133}I	20.83	H	4.51

γ-ray energy (keV)	Nuclide name	Half-life	Half-life unit	Emission rate (%)	γ-ray energy (keV)	Nuclide name	Half-life	Half-life unit	Emission rate (%)
875.9	^{105}Ru	4.44	H	2.50	919.3	^{152}Eu	13.517	Y	0.419
876.6	^{132}I	2.295	H	1.04	919.6	^{140}La	1.67858	D	2.66
876.7	^{129}Sb	4.366	H	2.75	920.6	^{131m}Te	33.25	H	1.16
877.4	^{130}I	12.36	H	0.191	920.7	^{145}Pr	5.984	H	0.146
877.7	^{151}Pm	28.40	H	0.101	922.6	^{134}I	52.5	M	0.14
878.0	^{128}Sb	9.05	H	3.5	923.1	^{77}Ge	11.211	H	0.74
878.2	^{105}Ru	4.44	H	0.47	923.4	^{131m}Te	33.25	H	0.112
878.2	^{142}La	91.1	M	0.1896	923.9	^{149}Nd	1.728	H	0.101
879.4	^{187}W	24.000	H	0.171	924.4	^{127}Sb	3.85	D	0.52
879.7	^{91}Sr	9.65	H	0.188	925.2	^{140}La	1.67858	D	6.90
880.5	^{143}Ce	33.039	H	1.031	925.5	^{77}Ge	11.211	H	0.71
880.7	^{117}Cd	2.49	H	3.96	925.6	^{134}Te	41.8	M	1.48
880.7	^{117m}Cd	3.36	H	0.7	925.8	^{91}Sr	9.65	H	3.85
880.8	^{138}Cs	32.5	M	0.11	926.0	^{130}Sb	39.5	M	0.40
881.6	^{84}Br	31.76	M	42	926.3	^{152}Eu	13.517	Y	0.272
882.0	^{78}As	90.7	M	0.19	927.4	^{132}I	2.295	H	0.41
882.7	^{133m}Te	55.4	M	1.77	927.6	†^{208}Tl	3.053	M	0.125
883.3	^{130}Sb	39.5	M	1.2	928.0	^{182}Ta	114.74	D	0.614
883.6	^{113}Ag	5.37	H	0.282	928.9	^{77}Ge	11.211	H	1.09
884.1	^{134}I	52.5	M	65.1	929.3	^{117m}Cd	3.36	H	0.79
884.5	^{192}Ir	73.829	D	0.292	931.4	^{117m}Cd	3.36	H	3.64
884.7	^{110m}Ag	249.83	D	75.0	933.1	^{131}Sb	23.03	M	26.4
884.8	^{133m}Te	55.4	M	0.80	934.1	†^{214}Bi	19.9	M	3.107
884.8	^{133m}Te	55.4	M	0.80	934.5	^{92}Y	3.54	H	13.9
884.9	^{78}As	90.7	M	0.46	934.6	^{125}Sn	9.64	D	0.21
886.0	^{117m}Cd	3.36	H	0.39	934.9	^{130}Sb	39.5	M	19.0
886.7	⁎^{74}Ga	8.12	M	0.34	935.0	^{138}Cs	32.5	M	0.181
887.7	^{67}Ga	3.2617	D	0.148	937.5	^{110m}Ag	249.83	D	35.0
888.5	^{133m}Te	55.4	M	0.66	939.4	^{77}Ge	11.211	H	0.304
888.7	^{78}As	90.7	M	2.1	939.5	^{129}Sb	4.366	H	0.1918
889.3	^{46}Sc	83.79	D	99.9840	940.5	^{129}Sb	4.366	H	0.77
889.9	^{133m}Te	55.4	M	0.22	941.3	^{131m}Te	33.25	H	0.75
891.4	^{133m}Te	55.4	M	0.84	942.5	⁎^{74}Ga	8.12	M	1.27
892.8	^{154}Eu	8.601	Y	0.521	943.4	^{131}Sb	23.03	M	47.1
893.4	^{125}Sn	9.64	D	0.29	944.4	^{156}Eu	15.19	D	1.33
893.4	†^{212}Bi	60.55	M	0.378	944.9	^{88}Kr	2.825	H	0.294
894.9	^{142}La	91.1	M	8.34	945.2	^{133m}Te	55.4	M	0.49
896.0	^{134}Te	41.8	M	0.44	945.7	^{117}Cd	2.49	H	1.53
896.5	^{77}Ge	11.211	H	0.126	946.7	^{87}Kr	76.3	M	0.129
897.8	^{207}Bi	31.55	Y	0.128	947.1	^{93}Y	10.18	H	2.1
898.0	^{88}Rb	17.773	M	14.40	947.5	^{156}Eu	15.19	D	0.292
900.7	^{77}Ge	11.211	H	0.107	947.5	^{84}Br	31.76	M	0.35
903.2	^{129}Sb	4.366	H	0.140	947.9	^{134}I	52.5	M	4.01
904.1	^{154}Eu	8.601	Y	0.889	948.0	†^{228}Ac	6.15	H	0.106
904.2	†^{228}Ac	6.15	H	0.77	948.7	^{151}Pm	28.40	H	0.35
907.0	^{77}Ge	11.211	H	1.00	949.2	^{133m}Te	55.4	M	0.53
907.6	^{105}Ru	4.44	H	0.53	949.6	^{117}Cd	2.49	H	0.22
908.8	^{128}Sb	9.05	H	1.0	951.0	^{140}La	1.67858	D	0.519
909.7	^{133}I	20.83	H	0.214	952.0	^{82}Br	35.282	H	0.378
910.0	^{131m}Te	33.25	H	3.17	952.1	†^{212}Bi	60.55	M	0.17
910.1	^{132}I	2.295	H	0.93	952.3	^{117}Cd	2.49	H	0.14
911.0	^{131}Sb	23.03	M	0.71	953.3	^{92}Sr	2.611	H	3.52
911.2	†^{228}Ac	6.15	H	25.8	954.6	^{132}I	2.295	H	17.6
912.7	^{133m}Te	55.4	M	44	957.2	^{117m}Cd	3.36	H	0.39
912.8	^{92}Y	3.54	H	0.63	958.6	^{131}Sb	23.03	M	0.61
913.9	^{77}Ge	11.211	H	0.39	958.6	†^{228}Ac	6.15	H	0.28
914.8	^{133m}Te	55.4	M	8.8	959.0	^{78}As	90.7	M	0.46
914.9	^{130}Sb	39.5	M	1.8	959.7	^{182}Ta	114.74	D	0.350
915.0	^{129}Sb	4.366	H	23.3	960.5	^{156}Eu	15.19	D	1.45
915.6	^{125}Sn	9.64	D	4.1	961.0	⁎^{74}Ga	8.12	M	1.62

γ-ray energy (keV)	Nuclide name	Half-life	Half-life unit	Emission rate (%)	γ-ray energy (keV)	Nuclide name	Half-life	Half-life unit	Emission rate (%)
961.0	^{156}Eu	15.19	D	0.15	1005.7	^{84}Br	31.76	M	0.46
961.4	^{135}I	6.58	H	0.15	1006.7	^{142}La	91.1	M	0.237
962.1	⁎^{63}Zn	38.47	M	6.5	1007.5	^{133m}Te	55.4	M	0.53
962.2	^{142}La	91.1	M	0.38	1007.6	^{82}Br	35.282	H	1.304
963.1	^{117}Cd	2.49	H	0.61	1009.8	^{138}Cs	32.5	M	29.8
963.4	^{152}Eu	13.517	Y	0.140	1011.4	^{142}La	91.1	M	3.93
964.1	^{152}Eu	13.517	Y	14.51	1011.9	^{156}Eu	15.19	D	0.31
964.1	†^{214}Bi	19.9	M	0.365	1015.9	^{84}Br	31.76	M	6.2
964.8	†^{228}Ac	6.15	H	4.99	1017.4	^{125}Sn	9.64	D	0.32
966.8	^{129}Sb	4.366	H	8.96	1017.5	^{105}Ru	4.44	H	0.32
966.9	^{134}I	52.5	M	0.39	1018.1	^{97}Zr	16.749	H	0.3724
967.0	^{130}I	12.36	H	0.88	1018.7	^{78}As	90.7	M	0.14
968.2	^{124}Sb	60.20	D	1.882	1021.2	^{97}Zr	16.749	H	1.01
968.2	^{78}As	90.7	M	0.16	1022.8	^{149}Nd	1.728	H	0.104
969.0	†^{228}Ac	6.15	H	15.8	1024.3	⁎^{74}Ga	8.12	M	0.14
969.3	^{117}Cd	2.49	H	0.45	1024.3	^{91}Sr	9.65	H	33.5
969.4	^{105}Ru	4.44	H	2.10	1024.4	^{97}Nb	72.1	M	1.09
969.8	^{156}Eu	15.19	D	0.37	1026.7	^{97}Zr	16.749	H	0.2793
970.5	^{133m}Te	55.4	M	0.27	1027.0	^{134}Te	41.8	M	0.44
971.3	^{97}Zr	16.749	H	0.278	1027.4	^{156}Eu	15.19	D	0.128
972.0	^{135}I	6.58	H	0.89	1029.1	^{117m}Cd	3.36	H	11.7
972.3	^{128}Sb	9.05	H	1.0	1029.9	^{133m}Te	55.4	M	0.97
972.6	^{135}I	6.58	H	1.21	1030.7	^{129}Sb	4.366	H	15.13
972.6	^{133m}Te	55.4	M	0.44	1030.7	^{130}Sb	39.5	M	1.5
974.7	^{134}I	52.5	M	4.78	1033.2	†^{228}Ac	6.15	H	0.201
975.1	⁎^{74}Ga	8.12	M	0.27	1035.0	^{132}I	2.295	H	0.51
977.4	^{56}Co	77.236	D	1.421	1035.4	^{131m}Te	33.25	H	0.101
978.3	^{133m}Te	55.4	M	3.9	1035.6	^{117}Cd	2.49	H	0.24
979.0	^{145}Pr	5.984	H	0.256	1037.3	^{129}Sb	4.366	H	0.307
980.3	^{133m}Te	55.4	M	1.19	1037.8	^{56}Co	77.236	D	14.05
982.7	†^{208}Tl	3.053	M	0.205	1038.6	^{134}Cs	2.0652	Y	0.990
984.2	^{132}I	2.295	H	0.59	1038.8	^{135}I	6.58	H	7.9
985.7	^{157}Eu	15.18	H	0.146	1039.6	^{88}Kr	2.825	H	0.48
985.8	^{77}Ge	11.211	H	0.112	1040.3	^{134}I	52.5	M	2.03
985.8	^{88}Kr	2.825	H	1.31	1040.4	^{156}Eu	15.19	D	0.50
987.3	^{84}Br	31.76	M	0.79	1043.7	^{142}La	91.1	M	2.70
987.8	^{131m}Te	33.25	H	0.149	1044.0	^{82}Br	35.282	H	27.6
988.4	^{113}Ag	5.37	H	0.423	1044.4	^{182}Ta	114.74	D	0.239
990.1	^{88}Kr	2.825	H	0.142	1045.1	^{124}Sb	60.20	D	1.833
991.5	^{131}Sb	23.03	M	1.4	1047.5	^{128}Sb	9.05	H	3.5
992.1	^{130}Sb	39.5	M	1.9	1048.1	^{136}Cs	13.01	D	80
992.7	^{129}Sb	4.366	H	0.105	1048.1	^{136}Ba	0.3084	S	99.820
993.6	⁎^{74}Ga	8.12	M	0.64	1049.5	^{88}Kr	2.825	H	0.142
995.1	^{133m}Te	55.4	M	0.40	1050.4	^{131}Sb	23.03	M	0.7
995.1	^{135}I	6.58	H	0.15	1050.4	^{106}Rh	30.07	S	1.56
996.1	^{133m}Te	55.4	M	0.31	1051.4	^{145}Pr	5.984	H	0.175
996.3	^{154}Eu	8.601	Y	10.48	1051.7	^{117}Cd	2.49	H	3.79
996.5	^{129}Sb	4.366	H	0.176	1052.0	†^{214}Bi	19.9	M	0.313
996.6	^{77}Ge	11.211	H	0.109	1052.3	^{133}I	20.83	H	0.556
996.9	^{56}Co	77.236	D	0.111	1052.7	^{117}Cd	2.49	H	0.73
997.2	^{110m}Ag	249.83	D	0.130	1053.7	^{133m}Te	55.4	M	0.13
999.2	^{131m}Te	33.25	H	0.164	1054.3	^{138}Cs	32.5	M	0.159
999.9	⁎^{74}Ga	8.12	M	0.13	1054.6	^{91}Sr	9.65	H	0.224
999.9	⁎^{74}Ga	8.12	M	0.13	1058.8	^{134}I	52.5	M	0.10
1000.2	^{130}Sb	39.5	M	2.3	1059.7	^{131m}Te	33.25	H	1.49
1001.0	†^{234m}Pa	1.159	M	0.842	1060.1	^{133}I	20.83	H	0.138
1001.7	^{182}Ta	114.74	D	2.086	1061.8	^{77}Ge	11.211	H	0.161
1004.8	^{154}Eu	8.601	Y	18.01	1061.9	^{133m}Te	55.4	M	1.33
1005.1	^{78}As	90.7	M	0.32	1063.7	^{207}Bi	31.55	Y	74.5
1005.3	^{152}Eu	13.517	Y	0.659	1065.1	^{156}Eu	15.19	D	4.9

γ-ray energy (keV)	Nuclide name	Half-life	Half-life unit	Emission rate (%)	γ-ray energy (keV)	Nuclide name	Half-life	Half-life unit	Emission rate (%)
1065.2	†^{228}Ac	6.15	H	0.132	1123.7	⁎^{63}Zn	38.47	M	0.111
1066.0	^{117m}Cd	3.36	H	23.1	1124.0	^{135}I	6.58	H	3.62
1067.1	^{125}Sn	9.64	D	10	1125.0	^{77}Ge	11.211	H	0.126
1070.0	†^{214}Bi	19.9	M	0.272	1125.1	^{117}Cd	2.49	H	0.45
1072.6	^{134}I	52.5	M	14.9	1125.5	^{131m}Te	33.25	H	11.0
1075.5	^{130}Sb	39.5	M	0.40	1126.6	^{129}Sb	4.366	H	0.120
1076.0	^{156}Eu	15.19	D	0.34	1128.0	^{131m}Te	33.25	H	0.93
1077.0	^{86}Rb	18.642	D	8.64	1128.1	^{106}Rh	30.07	S	0.404
1078.1	^{133m}Te	55.4	M	0.13	1128.6	^{154}Eu	8.601	Y	0.300
1078.6	^{128}Sb	9.05	H	2.0	1129.5	^{156}Eu	15.19	D	0.135
1078.6	†^{212}Bi	60.55	M	0.564	1129.6	^{128}Sb	9.05	H	0.80
1079.2	^{156}Eu	15.19	D	4.6	1129.9	^{76}As	26.24	H	0.126
1079.6	^{133m}Te	55.4	M	0.44	1130.6	^{142}La	91.1	M	0.47
1079.8	^{78}As	90.7	M	1.62	1131.5	^{135}I	6.58	H	22.6
1080.8	^{77}Ge	11.211	H	0.27	1131.5	⁎^{74}Ga	8.12	M	0.87
1081.3	^{82}Br	35.282	H	0.644	1132.4	^{92}Y	3.54	H	0.24
1082.6	^{84}Br	31.76	M	0.14	1133.7	†^{214}Bi	19.9	M	0.2512
1083.9	^{129}Te	69.6	M	0.49	1134.2	^{130}Sb	39.5	M	0.40
1084.0	^{152}Eu	13.517	Y	0.245	1134.5	⁎^{74}Ga	8.12	M	0.19
1085.2	^{77}Ge	11.211	H	6.4	1134.5	⁎^{74}Ga	8.12	M	0.19
1085.8	^{152}Eu	13.517	Y	10.11	1134.9	^{133m}Te	55.4	M	0.27
1087.7	^{198}Au	2.6941	D	0.1589	1136.0	^{132}I	2.295	H	3.01
1087.7	^{125}Sn	9.64	D	1.2	1136.2	^{134}I	52.5	M	9.1
1088.0	^{129}Sb	4.366	H	0.411	1137.3	^{133m}Te	55.4	M	0.22
1089.2	^{125}Sn	9.64	D	4.6	1137.6	^{130}Sb	39.5	M	0.30
1089.5	^{130}Sb	39.5	M	3.7	1140.4	^{56}Co	77.236	D	0.132
1089.7	^{152}Eu	13.517	Y	1.734	1140.5	^{156}Eu	15.19	D	0.283
1089.9	^{142}La	91.1	M	0.1422	1140.7	^{122}Sb	2.7238	D	0.76
1093.9	†^{208}Tl	3.053	M	0.430	1140.7	^{154}Eu	8.601	Y	0.237
1095.7	†^{228}Ac	6.15	H	0.129	1140.8	^{91}Sr	9.65	H	0.127
1096.5	^{130}I	12.36	H	0.552	1141.3	^{88}Kr	2.825	H	1.28
1096.5	^{130}Sb	39.5	M	0.80	1141.4	^{130}Sb	39.5	M	2.0
1098.4	^{133m}Te	55.4	M	0.71	1141.6	^{127}Sb	3.85	D	0.37
1099.2	^{59}Fe	44.490	D	56.5	1142.4	^{92}Sr	2.611	H	2.79
1100.1	^{134}I	52.5	M	0.69	1142.4	^{117}Cd	2.49	H	1.67
1101.3	⁎^{74}Ga	8.12	M	5.42	1142.7	^{133m}Te	55.4	M	1.06
1101.6	^{135}I	6.58	H	1.61	1143.3	^{132}I	2.295	H	1.35
1103.2	^{134}I	52.5	M	0.80	1143.5	^{117}Cd	2.49	H	0.14
1103.3	^{143}Ce	33.039	H	0.415	1145.1	^{78}As	90.7	M	1.67
1104.5	^{129}Sb	4.366	H	0.341	1146.2	^{130}Sb	39.5	M	0.60
1109.2	^{152}Eu	13.517	Y	0.189	1147.2	^{138}Cs	32.5	M	1.24
1109.5	†^{211}Pb	36.1	M	0.115	1147.8	^{132}I	2.295	H	0.27
1110.6	†^{228}Ac	6.15	H	0.285	1148.0	^{97}Zr	16.749	H	2.62
1111.6	^{129}Te	69.6	M	0.191	1148.9	^{131m}Te	33.25	H	1.5
1112.1	^{152}Eu	13.517	Y	13.67	1148.9	^{131m}Te	33.25	H	0.24
1112.7	^{128}Sb	9.05	H	2.0	1150.3	^{145}Pr	5.984	H	0.194
1113.4	^{182}Ta	114.74	D	0.445	1150.9	^{131m}Te	33.25	H	0.63
1114.9	^{77}Ge	11.211	H	0.111	1151.2	^{125}Sn	9.64	D	0.11
1115.5	^{65}Ni	2.51719	H	15.43	1151.9	^{77}Ge	11.211	H	0.201
1115.5	^{65}Zn	243.93	D	50.04	1153.5	†^{228}Ac	6.15	H	0.139
1116.6	^{117}Cd	2.49	H	1.03	1153.7	^{156}Eu	15.19	D	6.8
1118.3	^{154}Eu	8.601	Y	0.113	1154.1	^{156}Eu	15.19	D	4.7
1119.1	^{84}Br	31.76	M	0.14	1155.2	†^{214}Bi	19.9	M	1.633
1120.0	^{117m}Cd	3.36	H	0.13	1156.0	^{156}Eu	15.19	D	0.131
1120.1	^{117}Cd	2.49	H	0.24	1157.0	^{182}Ta	114.74	D	0.73
1120.3	†^{214}Bi	19.9	M	14.92	1157.4	^{130}I	12.36	H	11.3
1120.5	^{46}Sc	83.79	D	99.9870	1158.1	^{182}Ta	114.74	D	0.29
1121.3	^{182}Ta	114.74	D	35.24	1158.2	^{128}Sb	9.05	H	1.5
1122.2	^{130}I	12.36	H	0.253	1159.1	^{136}Cs s			
1123.6	^{131}Sb	23.03	M	8.9	1159.1	^{134}I	52.5	M	0.34

γ-ray energy (keV)	Nuclide name	Half-life	Half-life unit	Emission rate (%)	γ-ray energy (keV)	Nuclide name	Half-life	Half-life unit	Emission rate (%)
1159.9	^{135}I	6.58	H	0.103	1221.4	^{182}Ta	114.74	D	27.23
1160.2	^{142}La	91.1	M	1.71	1222.6	^{130}I	12.36	H	0.179
1160.3	⁎^{74}Ga	8.12	M	0.63	1223.6	^{182}Ta	114.74	D	0.24
1164.0	^{134}I	52.5	M	0.13	1227.5	^{133m}Te	55.4	M	0.13
1165.5	^{131m}Te	33.25	H	0.134	1228.1	^{78}As	90.7	M	0.11
1168.0	^{129}Sb	4.366	H	0.253	1228.5	^{76}As	26.24	H	1.22
1168.0	^{134}Cs	2.0652	Y	1.790	1229.1	^{117}Cd	2.49	H	0.61
1169.0	^{135}I	6.58	H	0.88	1229.6	^{133m}Te	55.4	M	0.18
1169.1	^{156}Eu	15.19	D	0.266	1230.7	^{156}Eu	15.19	D	8.0
1169.5	^{78}As	90.7	M	0.12	1231.0	^{182}Ta	114.74	D	11.62
1170.7	^{117m}Cd	3.36	H	0.66	1232.3	^{117}Cd	2.49	H	0.28
1172.9	^{132}I	2.295	H	1.09	1233.1	^{142}La	91.1	M	1.90
1173.2	^{60}Co	1925.28	D	99.85	1233.8	^{131}Sb	23.03	M	2.3
1173.3	^{125}Sn	9.64	D	0.18	1234.6	^{117m}Cd	3.36	H	11.0
1174.0	^{133m}Te	55.4	M	0.31	1235.4	^{136}Cs	13.01	D	20.0
1174.1	^{134}Cs s				1236.4	^{133}I	20.83	H	1.51
1175.1	^{56}Co	77.236	D	2.252	1237.3	^{131m}Te	33.25	H	0.63
1175.4	^{87}Kr	76.3	M	1.11	1237.8	^{129}Sb	4.366	H	0.241
1176.4	^{142}La	91.1	M	0.1422	1238.1	†^{214}Bi	19.9	M	5.834
1177.4	⁎^{74}Ga	8.12	M	0.24	1238.3	^{56}Co	77.236	D	66.46
1179.5	^{88}Kr	2.825	H	1.00	1239.0	^{130}Sb	39.5	M	1.8
1181.6	^{128}Sb	9.05	H	4.5	1239.0	^{134}I	52.5	M	0.21
1183.4	^{117}Cd	2.49	H	0.13	1240.3	^{78}As	90.7	M	5.9
1184.4	⁎^{74}Ga	8.12	M	0.28	1240.5	^{135}I	6.58	H	0.90
1185.0	^{88}Kr	2.825	H	0.69	1241.3	^{154}Eu	8.601	Y	0.1226
1185.0	^{84}Br	31.76	M	0.108	1242.0	^{142}La	91.1	M	0.237
1189.0	^{182}Ta	114.74	D	16.49	1242.2	^{77}Ge	11.211	H	0.42
1190.0	^{134}I	52.5	M	0.35	1242.4	^{156}Eu	15.19	D	6.6
1190.4	^{132}I s				1245.2	^{88}Kr	2.825	H	0.363
1191.1	^{142}La	91.1	M	0.379	1246.1	^{154}Eu	8.601	Y	0.856
1191.9	^{131}Sb	23.03	M	0.6	1247.1	†^{228}Ac	6.15	H	0.50
1191.9	^{131}Sb	23.03	M	0.6	1247.9	^{117}Cd	2.49	H	1.20
1193.3	^{77}Ge	11.211	H	2.68	1249.1	^{131}Sb	23.03	M	0.52
1194.6	^{113}Ag	5.37	H	0.378	1249.9	^{152}Eu	13.517	Y	0.187
1196.2	^{117m}Cd	3.36	H	0.39	1250.5	^{128}Sb	9.05	H	1.0
1198.0	^{133m}Te	55.4	M	0.18	1250.7	^{88}Kr	2.825	H	1.12
1199.1	^{78}As	90.7	M	0.70	1252.0	^{133m}Te	55.4	M	0.27
1199.2	^{138}Cs	32.5	M	0.17	1256.9	^{117m}Cd	3.36	H	0.18
1203.3	^{93}Y	10.18	H	0.109	1256.9	^{122}Sb	2.7238	D	0.81
1203.7	^{138}Cs	32.5	M	0.40	1257.4	^{182}Ta	114.74	D	1.509
1204.2	^{133m}Te	55.4	M	0.18	1258.4	^{129}Sb	4.366	H	0.402
1204.2	⁎^{74}Ga	8.12	M	7.62	1258.5	^{130}Sb	39.5	M	1.00
1204.4	⁎^{74}As	17.77	D	0.285	1259.5	^{128}Sb	9.05	H	1.0
1204.8	^{91}Y	58.51	D	0.26	1260.0	^{117}Cd	2.49	H	1.14
1205.5	^{117m}Cd	3.36	H	0.13	1260.4	^{135}I	6.58	H	28.7
1206.6	^{131m}Te	33.25	H	9.41	1263.3	^{129}Sb	4.366	H	0.910
1207.4	^{131}Sb	23.03	M	4.1	1263.9	^{77}Ge	11.211	H	0.90
1207.7	†^{214}Bi	19.9	M	0.451	1264.9	^{138}Cs	32.5	M	0.137
1209.0	^{117m}Cd	3.36	H	0.18	1267.6	^{131}Sb	23.03	M	3.0
1209.0	^{117m}Cd	3.36	H	0.13	1268.6	^{97}Nb	72.1	M	0.147
1209.0	^{129}Sb	4.366	H	0.940	1269.5	^{134}I	52.5	M	0.56
1209.8	^{88}Kr	2.825	H	0.14	1272.1	^{130}I	12.36	H	0.748
1211.9	^{129}Sb	4.366	H	0.38	1272.7	^{117}Cd	2.49	H	0.73
1212.7	^{88}Kr	2.825	H	0.14	1272.8	^{132}I	2.295	H	0.168
1212.9	^{76}As	26.24	H	1.44	1273.1	^{129}Sb	4.366	H	0.164
1212.9	^{152}Eu	13.517	Y	1.415	1273.7	^{182}Ta	114.74	D	0.660
1213.3	^{84}Br	31.76	M	2.6	1274.4	^{154}Eu	8.601	Y	34.8
1215.4	^{77}Ge	11.211	H	0.134	1274.5	^{22}Na	2.6018	Y	99.940
1216.1	^{76}As	26.24	H	3.42	1276.1	^{97}Zr	16.749	H	0.94
1220.9	^{125}Sn	9.64	D	0.27	1276.1	^{129}Sb	4.366	H	0.103

γ-ray energy (keV)	Nuclide name	Half-life	Half-life unit	Emission rate (%)	γ-ray energy (keV)	Nuclide name	Half-life	Half-life unit	Emission rate (%)
1277.4	^{156}Eu	15.19	D	2.89	1339.8	^{128}Sb	9.05	H	1.0
1280.0	^{77}Ge	11.211	H	0.183	1342.7	^{182}Ta	114.74	D	0.2565
1280.9	^{91}Sr	9.65	H	0.93	1343.6	^{138}Cs	32.5	M	1.14
1281.0	†^{214}Bi	19.9	M	1.434	1348.9	^{133m}Te	55.4	M	1.19
1281.7	^{129}Sb	4.366	H	0.559	1350.4	^{133}I	20.83	H	0.150
1284.7	^{131}Sb	23.03	M	0.3	1352.3	^{88}Kr	2.825	H	0.159
1284.7	^{131}Sb	23.03	M	0.3	1352.6	^{134}I	52.5	M	0.41
1287.5	^{129}Sb	4.366	H	0.100	1354.5	^{141}La	3.92	H	1.64
1289.1	^{182}Ta	114.74	D	1.372	1355.2	^{124}Sb	60.20	D	1.038
1290.3	^{127}Sb	3.85	D	0.37	1357.9	⁎^{74}Ga	8.12	M	0.16
1290.6	^{78}As	90.7	M	0.10	1360.2	^{56}Co	77.236	D	4.283
1290.8	^{132}I	2.295	H	1.13	1360.3	^{131}Sb	23.03	M	0.9
1291.0	^{117}Cd	2.49	H	0.67	1361.0	^{97}Zr	16.749	H	0.6516
1291.6	^{59}Fe	44.490	D	43.2	1362.4	^{117}Cd	2.49	H	0.24
1292.3	^{130}Sb	39.5	M	3.7	1362.7	^{97}Zr	16.749	H	1.02
1292.8	^{152}Eu	13.517	Y	0.101	1363.0	^{142}La	91.1	M	2.13
1293.6	^{41}Ar	109.61	M	99.160	1365.2	^{134}Cs	2.0652	Y	3.017
1293.9	⁎^{74}Ga	8.12	M	0.25	1365.5	^{117m}Cd	3.36	H	1.65
1295.1	^{132}I	2.295	H	1.88	1366.3	^{88}Rb	17.773	M	0.113
1297.9	^{132}I	2.295	H	0.89	1366.4	^{156}Eu	15.19	D	1.57
1298.2	^{133}I	20.83	H	2.35	1367.9	^{135}I	6.58	H	0.61
1298.7	^{129}Sb	4.366	H	0.12	1368.2	^{124}Sb	60.20	D	2.624
1299.1	^{152}Eu	13.517	Y	1.633	1368.5	^{77}Ge	11.211	H	3.19
1299.2	^{133m}Te	55.4	M	0.13	1368.6	^{24}Na	14.997	H	99.9936
1301.5	^{129}Sb	4.366	H	0.202	1368.7	^{130}Sb	39.5	M	1.10
1303.3	^{117}Cd	2.49	H	18.4	1369.5	^{88}Kr	2.825	H	1.48
1303.8	†^{214}Bi	19.9	M	0.107	1372.1	^{132}I	2.295	H	2.47
1307.2	^{133m}Te	55.4	M	0.31	1372.3	^{133m}Te	55.4	M	0.22
1308.7	^{78}As	90.7	M	13.0	1373.5	^{78}As	90.7	M	4.8
1309.3	^{77}Ge	11.211	H	0.51	1373.8	^{182}Ta	114.74	D	0.2224
1312.8	^{77}Ge	11.211	H	0.373	1376.1	^{124}Sb	60.20	D	0.483
1312.8	⁎^{74}Ga	8.12	M	0.62	1377.7	†^{214}Bi	19.9	M	3.988
1314.7	^{117}Cd	2.49	H	0.59	1378.0	^{128}Sb	9.05	H	1.8
1315.2	^{131m}Te	33.25	H	0.67	1381.2	^{78}As	90.7	M	0.76
1317.5	^{82}Br	35.282	H	26.9	1382.5	^{88}Rb	17.773	M	0.784
1317.9	^{132}I	2.295	H	0.118	1382.6	^{87}Kr	76.3	M	0.288
1318.2	^{132}I s				1383.9	^{92}Sr	2.611	H	90
1318.3	^{129}Sb	4.366	H	0.462	1384.3	^{110m}Ag	249.83	D	25.1
1319.7	^{77}Ge	11.211	H	0.295	1385.0	^{129}Sb	4.366	H	0.100
1321.3	^{105}Ru	4.44	H	0.203	1385.3	†^{214}Bi	19.9	M	0.793
1322.4	^{134}I	52.5	M	0.11	1388.6	^{136}Cs s			
1323.2	^{142}La	91.1	M	0.33	1389.3	^{142}La	91.1	M	0.43
1325.0	^{88}Kr	2.825	H	0.16	1389.9	^{87}Kr	76.3	M	0.119
1325.5	^{124}Sb	60.20	D	1.580	1392.0	^{131}Sb	23.03	M	0.8
1327.0	^{129}Sb	4.366	H	0.695	1393.0	^{142}La	91.1	M	0.1422
1331.8	^{131}Sb	23.03	M	0.85	1394.8	^{131m}Te	33.25	H	0.105
1332.1	⁎^{74}Ga	8.12	M	1.74	1394.9	^{132}I s			
1332.5	^{60}Co	1925.28	D	99.9826	1398.6	^{132}I	2.295	H	7.01
1334.0	^{133m}Te	55.4	M	0.22	1398.9	^{131}Sb	23.03	M	1.37
1334.3	^{110m}Ag	249.83	D	0.143	1400.6	^{134}Cs s			
1335.4	^{56}Co	77.236	D	0.1224	1401.5	†^{214}Bi	19.9	M	1.330
1336.0	^{134}I	52.5	M	0.14	1402.2	^{142}La	91.1	M	0.1422
1337.2	⁎^{74}Ga	8.12	M	0.8	1403.9	^{130}I	12.36	H	0.345
1337.2	⁎^{74}Ga	8.12	M	0.8	1404.4	^{117}Cd	2.49	H	0.12
1337.5	^{132}I s				1405.4	^{92}Y	3.54	H	4.8
1337.6	^{117}Cd	2.49	H	1.62	1406.7	^{134}Cs s			
1338.0	^{87}Kr	76.3	M	0.63	1406.9	^{88}Kr	2.825	H	0.218
1339.0	^{78}As	90.7	M	0.39	1408.0	†^{214}Bi	19.9	M	2.394
1339.1	^{132}I s				1408.0	^{152}Eu	13.517	Y	20.87
1339.3	^{117m}Cd	3.36	H	2.07	1408.7	^{117}Cd	2.49	H	1.28

γ-ray energy (keV)	Nuclide name	Half-life	Half-life unit	Emission rate (%)	γ-ray energy (keV)	Nuclide name	Half-life	Half-life unit	Emission rate (%)
1412.1	⁎^{63}Zn	38.47	M	0.75	1479.0	^{77}Ge	11.211	H	0.126
1413.4	^{91}Sr	9.65	H	0.98	1479.7	^{132}I s			
1414.3	^{134}I	52.5	M	0.22	1480.9	^{129}Sb	4.366	H	0.373
1415.7	^{138}Cs	32.5	M	0.37	1481.8	^{65}Ni	2.51719	H	23.59
1417.6	⁎^{74}Ga	8.12	M	0.110	1488.4	^{130}Sb	39.5	M	0.60
1419.3	^{130}Sb	39.5	M	1.20	1488.9	^{124}Sb	60.20	D	0.672
1419.4	^{129}Sb	4.366	H	0.394	1489.2	^{144}Pr	17.28	M	0.278
1419.7	^{125}Sn	9.64	D	0.49	1489.4	⁎^{74}Ga	8.12	M	2.88
1420.5	^{139}Ba	82.93	M	0.261	1494.0	^{154}Eu	8.601	Y	0.698
1421.7	^{110m}Ag s				1494.1	^{142}La	91.1	M	0.1422
1422.3	^{117}Cd	2.49	H	0.33	1495.6	^{138}Cs	32.5	M	0.18
1425.4	^{93}Y	10.18	H	0.25	1495.6	^{77}Ge	11.211	H	0.53
1428.2	^{134}I	52.5	M	0.17	1495.9	†^{228}Ac	6.15	H	0.86
1431.0	^{117}Cd	2.49	H	0.558	1499.6	^{130}Sb	39.5	M	0.40
1431.4	^{134}I	52.5	M	0.17	1499.8	^{132}I s			
1432.9	^{117m}Cd	3.36	H	13.4	1501.6	†^{228}Ac	6.15	H	0.46
1433.5	^{117}Cd	2.49	H	0.11	1502.8	^{135}I	6.58	H	1.08
1435.8	^{138}Cs	32.5	M	76.3	1505.0	^{110m}Ag	249.83	D	13.33
1436.6	^{124}Sb	60.20	D	1.217	1505.5	^{134}I	52.5	M	0.11
1437.5	^{129}Sb	4.366	H	0.316	1506.2	^{133m}Te	55.4	M	0.22
1439.1	^{76}As	26.24	H	0.279	1509.2	†^{214}Bi	19.9	M	2.130
1440.3	^{132}I s				1510.2	⁎^{74}Ga	8.12	M	0.23
1440.9	^{78}As	90.7	M	0.32	1512.7	†^{212}Bi	60.55	M	0.29
1442.2	^{207}Bi	31.55	Y	0.1310	1515.7	^{97}Nb	72.1	M	0.122
1442.6	^{132}I	2.295	H	1.40	1516.3	^{133m}Te	55.4	M	1.02
1442.7	^{56}Co	77.236	D	0.180	1516.3	^{142}La	91.1	M	0.43
1443.4	⁎^{74}Ga	8.12	M	1.8	1517.2	^{131}Sb	23.03	M	1.22
1443.4	⁎^{74}Ga	8.12	M	1.8	1518.4	^{88}Kr	2.825	H	2.15
1443.7	^{130}Sb	39.5	M	2.5	1521.1	^{130}Sb	39.5	M	0.80
1445.0	^{138}Cs	32.5	M	0.97	1524.6	^{142}La	91.1	M	0.47
1445.1	^{124}Sb	60.20	D	0.330	1524.6	^{42}K	12.355	H	18.08
1445.5	^{142}La	91.1	M	0.1422	1526.3	^{124}Sb	60.20	D	0.409
1448.4	^{135}I	6.58	H	0.32	1526.8	^{129}Sb	4.366	H	0.548
1450.2	^{117}Cd	2.49	H	0.61	1528.1	^{152}Eu	13.517	Y	0.279
1450.5	^{93}Y	10.18	H	0.33	1529.8	^{88}Kr	2.825	H	10.9
1452.7	^{77}Ge	11.211	H	0.127	1530.0	^{78}As	90.7	M	2.5
1453.6	^{76}As	26.24	H	0.108	1531.2	^{87}Kr	76.3	M	0.36
1455.0	^{133m}Te	55.4	M	0.58	1533.7	^{130}Sb	39.5	M	0.90
1455.1	^{131}Sb	23.03	M	0.47	1534.7	^{84}Br	31.76	M	0.100
1455.2	^{134}I	52.5	M	2.30	1538.0	^{131}Sb	23.03	M	0.5
1457.6	^{135}I	6.58	H	8.7	1538.1	^{136}Cs	13.01	D	0.100
1457.6	^{152}Eu	13.517	Y	0.497	1538.5	†^{214}Bi	19.9	M	0.398
1458.9	^{133m}Te	55.4	M	0.13	1538.8	^{77}Ge	11.211	H	0.150
1459.1	†^{228}Ac	6.15	H	0.83	1540.2	^{142}La	91.1	M	0.47
1460.0	^{207}Bi	31.55	Y	1.61	1541.5	^{134}I	52.5	M	0.51
1460.8	†^{40}K	1.248E+9	Y	10.66	1542.4	^{110m}Ag s			
1461.2	^{142}La	91.1	M	0.95	1543.3	†^{214}Bi	19.9	M	0.303
1463.8	^{84}Br	31.76	M	2.0	1544.2	^{131}Sb	23.03	M	0.9
1464.8	^{88}Kr	2.825	H	0.114	1545.8	^{142}La	91.1	M	2.99
1470.0	^{134}I	52.5	M	0.76	1547.0	⁎^{63}Zn	38.47	M	0.122
1470.3	^{131}Sb	23.03	M	1.55	1552.0	^{133m}Te	55.4	M	0.13
1471.7	⁎^{74}Ga	8.12	M	0.193	1553.5	^{131}Sb	23.03	M	0.6
1473.1	^{130}Sb	39.5	M	0.60	1555.3	^{138}Cs	32.5	M	0.366
1473.8	^{91}Sr	9.65	H	0.168	1557.1	†^{228}Ac	6.15	H	0.178
1474.9	^{82}Br	35.282	H	16.39	1559.0	^{131}Sb	23.03	M	0.42
1475.5	^{117}Cd	2.49	H	0.42	1561.6	^{130}Sb	39.5	M	0.60
1475.8	^{110m}Ag	249.83	D	4.08	1562.2	^{117}Cd	2.49	H	1.42
1476.6	^{77}Ge	11.211	H	0.253	1562.3	^{106}Rh	30.07	S	0.163
1476.7	^{132}I	2.295	H	0.130	1562.3	^{110m}Ag	249.83	D	1.22
1478.2	⁎^{74}Ga	8.12	M	0.30	1566.4	^{135}I	6.58	H	1.29

γ-ray energy (keV)	Nuclide name	Half-life	Half-life unit	Emission rate (%)	γ-ray energy (keV)	Nuclide name	Half-life	Half-life unit	Emission rate (%)
1570.1	^{129}Sb	4.366	H	0.872	1674.7	^{58}Co	70.86	D	0.517
1570.3	⁎^{74}Ga	8.12	M	0.97	1676.8	⁎^{74}Ga	8.12	M	0.73
1573.5	^{133m}Te	55.4	M	0.22	1678.0	^{135}I	6.58	H	9.6
1573.5	^{131}Sb	23.03	M	1.04	1682.1	^{117}Cd	2.49	H	0.70
1573.7	^{77}Ge	11.211	H	0.70	1682.1	^{156}Eu	15.19	D	0.272
1576.6	^{117}Cd	2.49	H	11.2	1683.2	^{133m}Te	55.4	M	3.3
1578.0	^{87}Kr	76.3	M	0.129	1684.0	†^{214}Bi	19.9	M	0.214
1578.1	^{84}Br	31.76	M	0.67	1685.6	^{88}Kr	2.825	H	0.66
1578.4	^{117}Cd	2.49	H	0.14	1685.7	^{128}Sb	9.05	H	0.50
1579.8	^{124}Sb	60.20	D	0.38	1688.6	^{142}La	91.1	M	0.237
1580.5	†^{228}Ac	6.15	H	0.60	1691.0	^{124}Sb	60.20	D	47.57
1581.0	^{133m}Te	55.4	M	0.13	1704.4	^{133m}Te	55.4	M	0.58
1581.9	^{130}Sb	39.5	M	1.9	1706.5	^{135}I	6.58	H	4.10
1583.2	†^{214}Bi	19.9	M	0.705	1706.9	^{117}Cd	2.49	H	1.00
1587.7	^{133m}Te	55.4	M	1.15	1707.9	^{128}Sb	9.05	H	0.30
1588.2	†^{228}Ac	6.15	H	3.22	1709.9	^{77}Ge	11.211	H	0.325
1591.4	^{110m}Ag s				1713.4	^{78}As	90.7	M	1.78
1593.2	^{128}Sb	9.05	H	0.50	1717.1	^{138}Cs	32.5	M	0.107
1594.8	†^{214}Bi	19.9	M	0.267	1719.7	^{77}Ge	11.211	H	0.410
1595.2	^{110m}Ag s				1721.0	^{78}As	90.7	M	0.32
1596.2	^{140}La	1.67858	D	95.4	1721.8	^{131}Sb	23.03	M	2.45
1596.5	^{154}Eu	8.601	Y	1.797	1722.7	^{142}La	91.1	M	1.52
1599.4	†^{214}Bi	19.9	M	0.324	1723.1	^{117}Cd	2.49	H	2.01
1600.1	^{129}Sb	4.366	H	0.579	1724.0	^{91}Sr	9.65	H	0.161
1602.0	⁎^{74}Ga	8.12	M	0.29	1724.3	^{129}Sb	4.366	H	0.133
1603.8	^{88}Kr	2.825	H	0.46	1724.9	^{65}Ni	2.51719	H	0.399
1607.6	^{84}Br	31.76	M	0.40	1727.2	^{132}I s			
1608.8	^{131}Sb	23.03	M	1.4	1727.2	^{77}Ge	11.211	H	0.152
1611.2	^{87}Kr	76.3	M	0.114	1727.7	^{138}Cs	32.5	M	0.111
1613.8	^{134}I	52.5	M	4.31	1729.6	†^{214}Bi	19.9	M	2.878
1614.1	^{138}Cs	32.5	M	0.137	1737.2	^{78}As	90.7	M	0.11
1617.0	^{130}Sb	39.5	M	0.90	1738.2	^{129}Sb	4.366	H	7.45
1617.2	⁎^{74}Ga	8.12	M	0.129	1739.1	^{117}Cd	2.49	H	0.13
1618.2	^{142}La	91.1	M	0.284	1740.5	^{87}Kr	76.3	M	2.04
1620.5	†^{212}Bi	60.55	M	1.47	1741.2	^{84}Br	31.76	M	1.6
1622.3	^{132}I s				1741.5	^{134}I	52.5	M	2.56
1622.5	^{129}Sb	4.366	H	0.208	1744.9	⁎^{74}Ga	8.12	M	4.82
1623.4	^{65}Ni	2.51719	H	0.498	1749.8	^{130}Sb	39.5	M	0.30
1625.1	†^{228}Ac	6.15	H	0.255	1750.2	^{97}Zr	16.749	H	1.09
1626.6	^{130}Sb	39.5	M	0.60	1756.1	^{131}Sb	23.03	M	1.13
1629.2	^{134}I	52.5	M	0.19	1756.4	^{142}La	91.1	M	2.70
1630.6	†^{228}Ac	6.15	H	1.51	1757.4	^{132}I	2.295	H	0.30
1638.3	†^{228}Ac	6.15	H	0.47	1762.6	^{130}Sb	39.5	M	2.5
1642.0	^{78}As	90.7	M	0.16	1764.5	†^{214}Bi	19.9	M	15.30
1643.3	^{134}Cs s				1768.2	^{142}La	91.1	M	0.24
1643.6	^{133m}Te	55.4	M	0.27	1770.2	^{207}Bi	31.55	Y	6.87
1644.3	^{134}I	52.5	M	0.39	1770.8	^{142}La	91.1	M	0.19
1644.3	^{142}La	91.1	M	0.237	1771.4	^{56}Co	77.236	D	15.41
1646.0	^{131m}Te	33.25	H	1.20	1773.2	^{133m}Te	55.4	M	0.53
1646.2	^{133m}Te	55.4	M	0.22	1778.3	^{138}Cs	32.5	M	0.137
1650.3	^{82}Br	35.282	H	0.739	1779.6	^{82}Br	35.282	H	0.1112
1651.4	^{91}Sr	9.65	H	0.291	1779.9	^{88}Rb	17.773	M	0.238
1652.1	^{117}Cd	2.49	H	0.28	1785.5	^{128}Sb	9.05	H	0.40
1652.2	^{117m}Cd	3.36	H	0.47	1787.7	^{76}As	26.24	H	0.293
1655.2	^{134}I	52.5	M	0.23	1791.2	^{135}I	6.58	H	7.72
1655.6	^{130}Sb	39.5	M	0.80	1791.9	^{78}As	90.7	M	0.97
1656.1	^{129}Sb	4.366	H	1.311	1797.5	^{133m}Te	55.4	M	0.14
1661.3	†^{214}Bi	19.9	M	1.047	1803.7	^{132}I s			
1666.5	†^{228}Ac	6.15	H	0.178	1806.5	⁎^{74}Ga	8.12	M	0.28
1669.5	^{117m}Cd	3.36	H	0.63	1806.7	^{125}Sn	9.64	D	0.15

γ-ray energy (keV)	Nuclide name	Half-life	Half-life unit	Emission rate (%)	γ-ray energy (keV)	Nuclide name	Half-life	Half-life unit	Emission rate (%)
1806.8	^{134}I	52.5	M	5.55	1961.5	^{142}La	91.1	M	0.1422
1810.7	⁎^{56}Mn	2.5789	H	26.9	1962.8	^{132}I s			
1810.8	^{56}Co	77.236	D	0.640	1963.7	^{56}Co	77.236	D	0.707
1811.0	^{132}I s				1965.8	^{131}Sb	23.03	M	1.3
1818.7	^{84}Br	31.76	M	0.24	1966.0	^{156}Eu	15.19	D	3.9
1821.2	^{131}Sb	23.03	M	1.22	1967.8	^{133m}Te	55.4	M	0.13
1822.2	^{110m}Ag s				1969.9	^{134}Cs s			
1829.8	⁎^{74}Ga	8.12	M	1.90	1971.0	⁎^{74}Ga	8.12	M	0.20
1830.7	^{135}I	6.58	H	0.58	1981.3	^{138}Cs	32.5	M	0.14
1835.7	^{78}As	90.7	M	1.46	1984.6	^{131}Sb	23.03	M	0.42
1836.0	^{88}Rb	17.773	M	22.81	1995.6	^{78}As	90.7	M	1.35
1838.4	†^{214}Bi	19.9	M	0.350	1997.3	^{117m}Cd	3.36	H	26.2
1840.6	^{132}I s				1997.4	^{130}Sb	39.5	M	2.10
1842.6	^{87}Kr	76.3	M	0.139	1999.3	⁎^{74}Ga	8.12	M	0.40
1846.5	^{77}Ge	11.211	H	0.177					
1847.3	^{92}Y	3.54	H	0.36					
1847.4	†^{214}Bi	19.9	M	2.025					
1851.6	^{97}Zr	16.749	H	0.31					
1854.3	^{131}Sb	23.03	M	4.2					
1854.4	^{131}Sb	23.03	M	4.2					
1856.4	^{117}Cd	2.49	H	0.25					
1857.4	^{156}Eu	15.19	D	0.240					
1866.6	^{136}Cs s								
1867.3	^{117}Cd	2.49	H	0.11					
1870.8	^{133m}Te	55.4	M	0.44					
1871.6	^{129}Sb	4.366	H	0.356					
1873.2	†^{214}Bi	19.9	M	0.214					
1877.0	^{156}Eu	15.19	D	1.51					
1877.5	^{84}Br	31.76	M	1.12					
1881.2	^{133m}Te	55.4	M	0.18					
1884.4	^{130}Sb	39.5	M	0.70					
1885.6	^{133m}Te	55.4	M	0.80					
1887.3	^{142}La	91.1	M	0.14					
1887.7	^{131m}Te	33.25	H	1.31					
1892.8	^{88}Kr	2.825	H	0.14					
1893.0	^{133m}Te	55.4	M	0.12					
1894.0	^{78}As	90.7	M	0.29					
1896.1	†^{214}Bi	19.9	M	0.149					
1897.6	^{84}Br	31.76	M	14.6					
1901.3	^{142}La	91.1	M	7.16					
1908.7	^{88}Kr	2.825	H	0.100					
1915.7	^{131}Sb	23.03	M	1.0					
1917.8	^{93}Y	10.18	H	1.57					
1921.0	^{78}As	90.7	M	0.81					
1921.1	^{132}I	2.295	H	1.23					
1923.3	^{142}La	91.1	M	0.19					
1923.5	^{78}As	90.7	M	0.76					
1925.9	^{134}I	52.5	M	0.18					
1927.3	^{135}I	6.58	H	0.296					
1933.6	^{142}La	91.1	M	0.1422					
1937.7	^{156}Eu	15.19	D	1.94					
1940.6	⁎^{74}Ga	8.12	M	5.4					
1945.5	^{132}I s								
1946.3	^{156}Eu	15.19	D	0.165					
1948.0	^{130}Sb	39.5	M	1.20					
1949.4	^{142}La	91.1	M	0.38					
1956.4	^{131}Sb	23.03	M	0.8					
1957.5	^{117m}Cd	3.36	H	0.16					

Table D5.3 Nuclear data for each nuclide (nuclides used for calibration).

Nuclide name	Half-life	Uncertainty of half-life	Half-life unit	γ-ray energy (keV)	Uncertainty of γ-ray energy(keV)	Emission rate (%)	Uncertainty of emission rate(%)
^{51}Cr	27.704	3	D	320.0824	4	9.910	10
^{54}Mn	312.20	20	D	834.848	3	99.9760	10
^{57}Co	271.74	6	D	14.4129	6	9.16	15
				122.06067	12	85.60	17
				136.4736	3	10.68	8
				570.09	20	0.0158	10
				692.41	7	0.149	10
^{59}Fe	44.490	9	D	142.6510	20	1.02	5
				192.343	5	3.08	12
				334.80	20	0.270	12
				382.0	4	0.018	3
				1099.245	3	56.5	19
				1291.590	6	43.2	14
				1481.70	20	0.059	7
^{60}Co	1925.28	14	D	1173.228	3	99.85	3
				1332.492	4	99.9826	6
^{65}Zn	243.93	9	D	1115.5391	20	50.04	10
^{85}Sr	64.849	7	D	514.0049	22	96	4
				868.06	5	0.0120	7
^{88}Y	106.627	21	D	850.6	8	0.065	13
				898.042	3	93.7	3
				1382.2	10	0.021	6
				1836.063	12	99.2	3
^{109}Cd	461.9	4	D	88.0336	10	3.644	16
^{113}Sn	115.09	3	D	255.134	10	2.11	8
				391.698	3	64.97	17
^{125}Sb	2.75856	25	Y	19.80	6	0.0204	10
				35.489	5	4.37	5
				58.43	5	0.012	6
				116.955	11	0.263	4
				172.719	8	0.191	8
				176.3140	20	6.84	7
				178.842	5	0.0337	24
				198.654	11	0.0128	6
				204.138	10	0.317	7
				208.077	5	0.248	5
				209.32	9	0.045	3
				227.891	10	0.1311	23
				321.04	4	0.416	5
				380.452	8	1.517	17
				408.065	10	0.184	3
				427.874	4	29.6	3
				443.555	9	0.306	4
				463.365	4	10.49	11
				600.5970	20	17.65	19
				606.713	3	4.98	6
				635.950	3	11.22	15
				671.441	6	1.791	19
^{133}Ba	10.551	11	Y	53.1622	6	2.14	4
				79.6142	12	2.65	5
				80.9979	11	32.9	4
				160.6120	16	0.638	6
				223.2368	13	0.453	4
				276.3989	12	7.16	5
				302.8508	5	18.34	13
				356.0129	7	62.05	19
				383.8485	12	8.94	7
^{134}Cs	2.0652	4	Y	242.738	8	0.027	3
				326.589	13	0.0162	10
				475.3650	20	1.477	7

Nuclide name	Half-life	Uncertainty of half-life	Half-life unit	γ-ray energy (keV)	Uncertainty of γ-ray energy(keV)	Emission rate (%)	Uncertainty of emission rate(%)
^{134}Cs	2.0652	4	Y	563.246	5	8.338	14
				569.331	3	15.373	17
				604.7210	20	97.62	11
				795.864	4	85.46	6
				801.953	4	8.688	16
				1038.610	7	0.990	3
				1167.968	5	1.790	5
				1365.185	7	3.017	8
^{137}Cs	30.08	9	Y	661.657	3	85.10	20
^{139}Ce	137.641	20	D	165.8575	11	79.90	
^{152}Eu	13.517	14	Y	121.7817	3	28.53	16
				148.00	5	0.0205	11
				212.43	11	0.0207	6
				244.6974	8	7.55	5
				251.633	9	0.0670	19
				271.08	4	0.0715	19
				275.42	4	0.0346	9
				295.9387	17	0.440	5
				315.10	3	0.0399	11
				316.13	13	0.0101	5
				324.83	3	0.0681	19
				329.41	5	0.1213	25
				340.46	10	0.0266	8
				344.2785	12	26.59	21
				351.66	5	0.0106	8
				367.7892	20	0.859	6
				411.1165	12	2.237	13
				416.02	3	0.1088	20
				443.9607	16	2.827	15
				444.01	17	0.298	11
				482.33	5	0.0247	8
				488.6793	20	0.414	4
				493.54	4	0.0303	14
				503.467	9	0.1524	20
				520.24	4	0.0534	17
				523.13	5	0.0153	7
				526.88	5	0.0120	8
				534.25	5	0.0410	11
				556.48	10	0.0177	7
				562.98	14	0.0202	19
				563.986	5	0.494	5
				566.438	6	0.131	4
				586.265	3	0.455	4
				595.61	12	0.032	11
				656.489	5	0.1441	23
				671.155	14	0.024	5
				674.64	14	0.169	4
				675.0		0.0213	8
				678.623	5	0.473	4
				686.60	5	0.0203	7
				688.670	5	0.856	7
				696.87	19	0.016	8
				712.83	5	0.0955	25
				719.346	7	0.250	8
				719.36	14	0.095	4
				728.04	4	0.0111	4
				764.88	4	0.189	5
				768.96	4	0.082	5
				778.9046	24	12.93	9
				794.78	5	0.0263	16

Nuclide name	Half-life	Uncertainty of half-life	Half-life unit	γ-ray energy (keV)	Uncertainty of γ-ray energy(keV)	Emission rate (%)	Uncertainty of emission rate(%)
^{152}Eu	13.517	14	Y	805.71	9	0.0152	6
				810.451	5	0.317	3
				839.36	4	0.0177	6
				841.574	5	0.168	3
				867.380	3	4.23	3
				896.59	9	0.0670	22
				901.19	5	0.0854	25
				919.337	4	0.419	5
				926.31	5	0.272	4
				930.59	5	0.0729	19
				958.63	5	0.0197	11
				963.367	7	0.140	7
				964.057	5	14.51	7
				974.09	5	0.0136	8
				990.18	5	0.0314	14
				1005.27	5	0.659	11
				1084.0	10	0.245	8
				1084.38	11	0.0106	8
				1085.837	10	10.11	5
				1089.737	5	1.734	12
				1109.18	5	0.189	7
				1112.076	3	13.67	9
				1170.97	9	0.0372	16
				1206.09	16	0.0130	14
				1212.948	11	1.415	9
				1249.94	5	0.187	3
				1261.35	5	0.0335	14
				1292.78	5	0.101	3
				1299.142	8	1.633	11
				1348.10	7	0.0173	8
				1363.78	5	0.0258	6
				1408.013	3	20.87	10
				1457.643	11	0.497	5
				1528.10	4	0.279	4
^{203}Hg	46.594	12	D	279.1952	10	81.56	5
^{241}Am	432.6	6	Y	26.34460	20	2.27	13
				32.18		0.0174	5
				33.1960	10	0.126	4
				43.420	3	0.073	8
				55.560	20	0.0181	18
				59.54091	10	35.9	4
				98.970	20	0.0203	5
				102.980	20	0.0195	5

Table D5.4 Nuclear data in the energy order (nuclides used for calibration)

γ-ray energy (keV)	Nuclide name	Half-life	Half-life unit	Emission rate (%)	γ-ray energy (keV)	Nuclide name	Half-life	Half-life unit	Emission rate (%)
14.4	^{57}Co	271.74	D	9.16	636.0	^{125}Sb	2.75856	Y	11.22
26.3	^{241}Am	432.6	Y	2.27	656.5	^{152}Eu	13.517	Y	0.1441
33.2	^{241}Am	432.6	Y	0.126	661.7	^{137}Cs	30.08	Y	85.10
35.5	^{125}Sb	2.75856	Y	4.37	671.4	^{125}Sb	2.75856	Y	1.791
53.2	^{133}Ba	10.551	Y	2.14	674.6	^{152}Eu	13.517	Y	0.169
59.5	^{241}Am	432.6	Y	35.9	678.6	^{152}Eu	13.517	Y	0.473
79.6	^{133}Ba	10.551	Y	2.65	688.7	^{152}Eu	13.517	Y	0.856
81.0	^{133}Ba	10.551	Y	32.9	692.4	^{57}Co	271.74	D	0.149
88.0	^{109}Cd	461.9	D	3.644	719.3	^{152}Eu	13.517	Y	0.250
117.0	^{125}Sb	2.75856	Y	0.263	764.9	^{152}Eu	13.517	Y	0.189
121.8	^{152}Eu	13.517	Y	28.53	778.9	^{152}Eu	13.517	Y	12.93
122.1	^{57}Co	271.74	D	85.60	795.9	^{134}Cs	2.0652	Y	85.46
136.5	^{57}Co	271.74	D	10.68	802.0	^{134}Cs	2.0652	Y	8.688
142.7	^{59}Fe	44.490	D	1.02	810.5	^{152}Eu	13.517	Y	0.317
160.6	^{133}Ba	10.551	Y	0.638	834.8	^{54}Mn	312.20	D	99.9760
165.9	^{139}Ce	137.641	D	79.90	841.6	^{152}Eu	13.517	Y	0.168
172.7	^{125}Sb	2.75856	Y	0.191	867.4	^{152}Eu	13.517	Y	4.23
176.3	^{125}Sb	2.75856	Y	6.84	898.0	^{88}Y	106.627	D	93.7
192.3	^{59}Fe	44.490	D	3.08	919.3	^{152}Eu	13.517	Y	0.419
204.1	^{125}Sb	2.75856	Y	0.317	926.3	^{152}Eu	13.517	Y	0.272
208.1	^{125}Sb	2.75856	Y	0.248	963.4	^{152}Eu	13.517	Y	0.140
223.2	^{133}Ba	10.551	Y	0.453	964.1	^{152}Eu	13.517	Y	14.51
227.9	^{125}Sb	2.75856	Y	0.1311	1005.3	^{152}Eu	13.517	Y	0.659
244.7	^{152}Eu	13.517	Y	7.55	1038.6	^{134}Cs	2.0652	Y	0.990
255.1	^{113}Sn	115.09	D	2.11	1084.0	^{152}Eu	13.517	Y	0.245
276.4	^{133}Ba	10.551	Y	7.16	1085.8	^{152}Eu	13.517	Y	10.11
279.2	^{203}Hg	46.594	D	81.56	1089.7	^{152}Eu	13.517	Y	1.734
295.9	^{152}Eu	13.517	Y	0.440	1099.2	^{59}Fe	44.490	D	56.5
302.9	^{133}Ba	10.551	Y	18.34	1109.2	^{152}Eu	13.517	Y	0.189
320.1	^{51}Cr	27.704	D	9.910	1112.1	^{152}Eu	13.517	Y	13.67
321.0	^{125}Sb	2.75856	Y	0.416	1115.5	^{65}Zn	243.93	D	50.04
329.4	^{152}Eu	13.517	Y	0.1213	1168.0	^{134}Cs	2.0652	Y	1.790
334.8	^{59}Fe	44.490	D	0.270	1173.2	^{60}Co	1925.28	D	99.85
344.3	^{152}Eu	13.517	Y	26.59	1212.9	^{152}Eu	13.517	Y	1.415
356.0	^{133}Ba	10.551	Y	62.05	1249.9	^{152}Eu	13.517	Y	0.187
367.8	^{152}Eu	13.517	Y	0.859	1291.6	^{59}Fe	44.490	D	43.2
380.5	^{125}Sb	2.75856	Y	1.517	1292.8	^{152}Eu	13.517	Y	0.101
383.8	^{133}Ba	10.551	Y	8.94	1299.1	^{152}Eu	13.517	Y	1.633
391.7	^{113}Sn	115.09	D	64.97	1332.5	^{60}Co	1925.28	D	99.9826
408.1	^{125}Sb	2.75856	Y	0.184	1365.2	^{134}Cs	2.0652	Y	3.017
411.1	^{152}Eu	13.517	Y	2.237	1408.0	^{152}Eu	13.517	Y	20.87
416.0	^{152}Eu	13.517	Y	0.1088	1457.6	^{152}Eu	13.517	Y	0.497
427.9	^{125}Sb	2.75856	Y	29.6	1528.1	^{152}Eu	13.517	Y	0.279
443.6	^{125}Sb	2.75856	Y	0.306	1836.1	^{88}Y	106.627	D	99.2
444.0	^{152}Eu	13.517	Y	2.827					
444.0	^{152}Eu	13.517	Y	0.298					
463.4	^{125}Sb	2.75856	Y	10.49					
475.4	^{134}Cs	2.0652	Y	1.477					
488.7	^{152}Eu	13.517	Y	0.414					
503.5	^{152}Eu	13.517	Y	0.1524					
514.0	^{85}Sr	64.849	D	96					
563.2	^{134}Cs	2.0652	Y	8.338					
564.0	^{152}Eu	13.517	Y	0.494					
566.4	^{152}Eu	13.517	Y	0.131					
569.3	^{134}Cs	2.0652	Y	15.373					
586.3	^{152}Eu	13.517	Y	0.455					
600.6	^{125}Sb	2.75856	Y	17.65					
604.7	^{134}Cs	2.0652	Y	97.62					
606.7	^{125}Sb	2.75856	Y	4.98					

Reference

1. ISO 11929-1:2019, Determination of the characteristic limits (decision threshold, detection limit and limits of the coverage interval) for measurements of ionizing radiation — Fundamentals and application — Part1: Elementary applications. ISO. 2019, ISO 11929-1.
2. ISO 20042:2019, Measurement of radioactivity - Gamma-ray emitting radionuclides - Generic test method using gamma-ray spectrometry. ISO. 2019.
3. Masayasu Noguchi, Hiroshi Tominaga, Radiation application measurement From fundamentals to application (2004). Nikkan Kogyo Shimbun, Ltd.
4. Masaki Uesugi, *et al*., The Determination of ^{210}Pb in Lead, Radioisotopes 31, 131-134 (1982).
5. Masaki Uesugi, *et al*., Improvements on the method for determining of ^{210}Pb and ^{210}Po in lead, Journal of Radioanalytical and Nuclear Chemistry 283, 577-584 (2010).
6. M.C. Lepy, *et al.*, Transfer of Ge detectors efficiency calibration from point source geometry to other geometries, EUROMET action 428 (2000).
7. L. Moens, *et al*., Calculation of the absolute peak efficiency of gamma-ray detectors for different counting geometries, Nuclear Instruments and Methods in Physics Research 187, 451-472 (1981).
8. T. Vidmar, *et al*., Testing efficiency transfer codes for equivalence, Applied Radiation and Isotopes 68, 355-359 (2010).
9. Tim Vidmar, EFFTRAN — A Monte Carlo efficiency transfer code for gamma-ray spectrometry, Nuclear Instruments and Methods in Physics Research Section A 550, 603-608 (2005).
10. Hidetaka Imai (ed.) Handbook on [GUM]; Expression of uncertainty in measurement 2018, Japanese Standards Association.
11. Octavian Sima, Marie Christine Lépy, Application of GUM Supplement 1 to uncertainty of Monte Carlo computed efficiency in gamma-ray spectrometry, Applied Radiation and Isotopes 109, 493-499 (2016).
12. J.A. Cooper, Factors determining the ultimate detection sensitivity of Ge(Li) gamma-ray spectrometers, Nuclear Instruments and Methods 82, 273-277 (1970).
13. H. Kaiser, Zum Problem der Nachweisgrenze, Analytisehe Chemie 209, 1-18 (1965).
14. L.A. Currie, Limits for qualitative detection and quantitative determination Application to Radiochemistry, Analytical Chemistry 40, 586-593 (1968).
15. ISO 11929:2010, Determination of the characteristic limits (decision threshold, detection limit and limits of the confidence interval) for measurements of ionizing radiation — Fundamentals and application. ISO. 2010, ISO 11929:2010.
16. Determination and interpretation of characteristic limits for radioactivity measurements decision threshold, detection limit and limits of the confidence interval. IAEA. 2017, IAEA Analytical Quality in Nuclear Applications Series No. 48.
17. Yoshihiko Mizumoto, Toshio Kusakabe, Shiro Iwata, Ratio of peak to total efficiencies for germanium detectors, Radioisotopes 36, 20-23 (1987).
18. Masayasu Noguchi, Takashi Komine, Masakazu Akiyama, Correction methods of γ-ray self-absorption in bulk sample, Radioisotopes 49, 189-198 (2000).
19. K. Sato, *et al*., Determination of attenuation coefficient for self-absorption correction in routine gamma ray spectrometry of environmental bulk sample, Journal of Radioanalytical and Nuclear Chemistry Articles 84, 431-440 (1984).
20. Masayasu Noguchi, Empirical equations for photon interaction cross section and mass attenuation coefficient, Radioisotopes 36, 49-56 (1987).
21. Kaneaki Satoh *et al.*, Determination of γ-ray peak efficiency including self - absorption correction for bulk environmental samples, Radioisotopes 32, 1-6 (1983).

22. Junta Yanai, Tatsuro Okada, Hidekazu Yamada, Elemental composition of agricultural soils in Japan in relation to soil type, land use, and region, Japanese Journal of Soil Science and Plant Nutrition 83, 673-680 (2012).
23. JCGM 101:2008, Evaluation of measurement data – Supplement 1 to the "Guide to the expression of uncertainty in measurement" ― Propagation of distributions using a Monte Carlo method. JCGM. 2008, JCGM 2008.
24. Chushiro Yonezawa, *et al*., Results of a collaborative experiment on a correction of (2018).
25. Chushiro Yonezawa, Katsuhiro Shirono, Tomoko Haraga, Analysis of ^{134}Cs, ^{137}Cs and ^{40}K in the certified reference material of brown rice by gamma-ray spectrometry using a Ge detector — Part 2: Uncertainty evaluation, Bunseki Kagaku 66, 27-37 (2017).
26. Katsuhiro Shirono, *et al*., A practical evaluation of measurement uncertainty in gamma-ray efficiency curve determination through an analytical approach, Applied Radiation and Isotopes 121, 131-141 (2017).
27. Alessia Ceccatelli, *et al*., Calculation spreadsheet for uncertainty estimation of measurement results in gamma-ray spectrometry and its validation for quality assurance purpose, Applied Radiation and Isotopes 124, 7-15 (2017).
28. 19 Confirmation Committee Report 011Report on the Inspection (Location Prefecture) Project of Radioactivity Analysis and Confirmation, Ministry of Education, Culture, Sports, Science and Technology, 2007.
29. Environmental radioactivity analysis training -Method for measurement using germanium semiconductor detector, Japan Chemical Analysis Center, 2019.